THE NEUROVASCULAR UNIT AS A POTENTIAL BIOMARKER AND THERAPEUTIC TARGET IN CEREBROVASCULAR DISEASE

EDITED BY: Shereen Nizari, Cheryl Hawkes, Anusha Mishra and Yorito Hattori

PUBLISHED IN: Frontiers in Aging Neuroscience

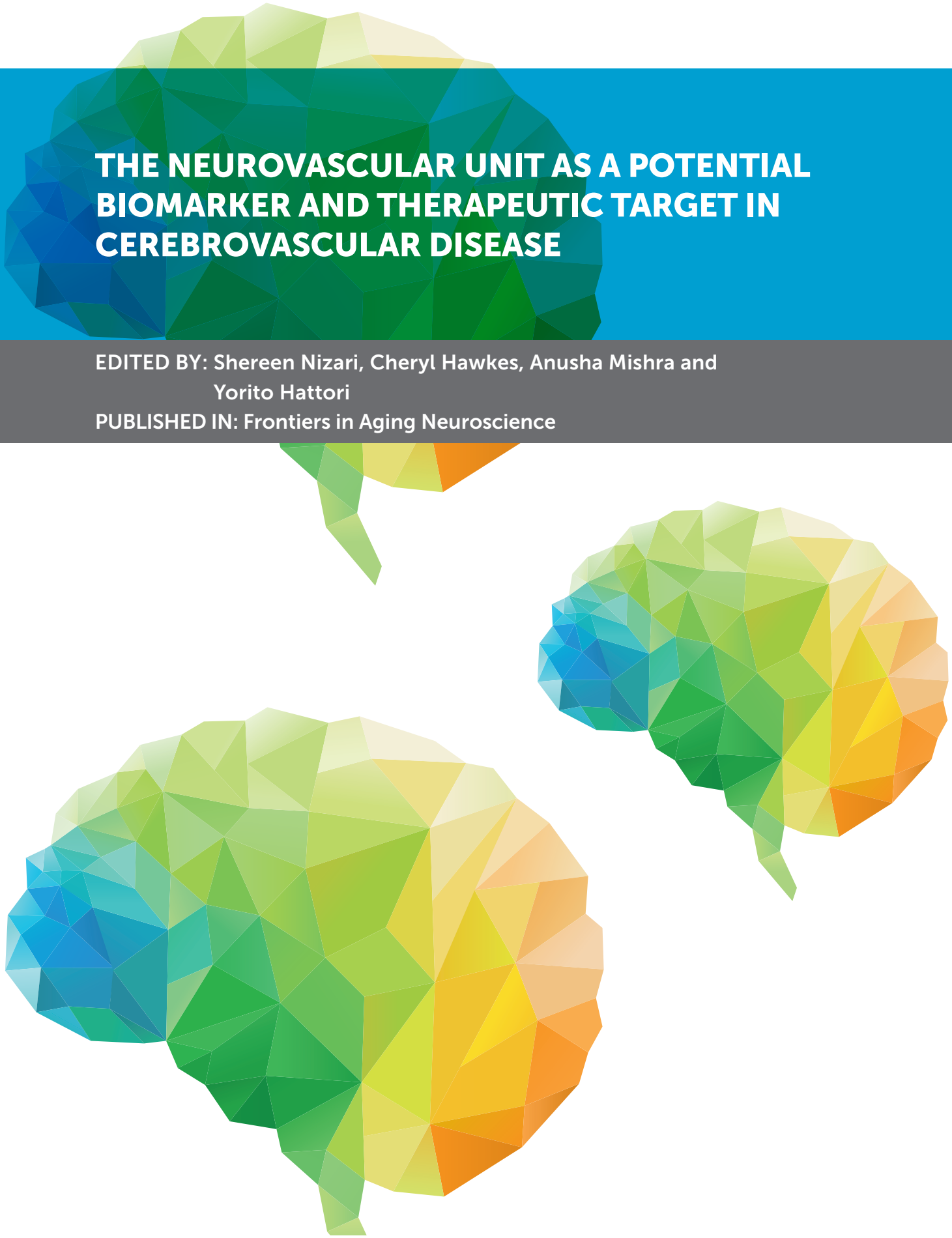

frontiers Research Topics

ISSN 1664-8714
ISBN 978-2-88976-238-5
DOI 10.3389/978-2-88976-238-5

About Frontiers

Frontiers is more than just an open-access publisher of scholarly articles: it is a pioneering approach to the world of academia, radically improving the way scholarly research is managed. The grand vision of Frontiers is a world where all people have an equal opportunity to seek, share and generate knowledge. Frontiers provides immediate and permanent online open access to all its publications, but this alone is not enough to realize our grand goals.

Frontiers Journal Series

The Frontiers Journal Series is a multi-tier and interdisciplinary set of open-access, online journals, promising a paradigm shift from the current review, selection and dissemination processes in academic publishing. All Frontiers journals are driven by researchers for researchers; therefore, they constitute a service to the scholarly community. At the same time, the Frontiers Journal Series operates on a revolutionary invention, the tiered publishing system, initially addressing specific communities of scholars, and gradually climbing up to broader public understanding, thus serving the interests of the lay society, too.

Dedication to Quality

Each Frontiers article is a landmark of the highest quality, thanks to genuinely collaborative interactions between authors and review editors, who include some of the world's best academicians. Research must be certified by peers before entering a stream of knowledge that may eventually reach the public - and shape society; therefore, Frontiers only applies the most rigorous and unbiased reviews.
Frontiers revolutionizes research publishing by freely delivering the most outstanding research, evaluated with no bias from both the academic and social point of view. By applying the most advanced information technologies, Frontiers is catapulting scholarly publishing into a new generation.

What are Frontiers Research Topics?

Frontiers Research Topics are very popular trademarks of the Frontiers Journals Series: they are collections of at least ten articles, all centered on a particular subject. With their unique mix of varied contributions from Original Research to Review Articles, Frontiers Research Topics unify the most influential researchers, the latest key findings and historical advances in a hot research area! Find out more on how to host your own Frontiers Research Topic or contribute to one as an author by contacting the Frontiers Editorial Office: frontiersin.org/about/contact

THE NEUROVASCULAR UNIT AS A POTENTIAL BIOMARKER AND THERAPEUTIC TARGET IN CEREBROVASCULAR DISEASE

Topic Editors:
Shereen Nizari, University College London, United Kingdom
Cheryl Hawkes, Lancaster University, United Kingdom
Anusha Mishra, Oregon Health and Science University, United States
Yorito Hattori, National Cerebral and Cardiovascular Center (Japan), Japan

Citation: Nizari, S., Hawkes, C., Mishra, A., Hattori, Y., eds. (2022). The Neurovascular Unit as a Potential Biomarker and Therapeutic Target in Cerebrovascular Disease. Lausanne: Frontiers Media SA. doi: 10.3389/978-2-88976-238-5

Table of Contents

frontiers | Frontiers in Aging Neuroscience

EDITORIAL
published: 05 May 2022
doi: 10.3389/fnagi.2022.908716

Editorial: The Neurovascular Unit as a Potential Biomarker and Therapeutic Target in Cerebrovascular Disease

Shereen Nizari[1,2]*, *Cheryl A. Hawkes*[3], *Yorito Hattori*[4] and *Anusha Mishra*[5,6]

[1] Centre for Advanced Biomedical Imaging, Division of Medicine, University College London, London, United Kingdom, [2] Centre for Cardiovascular and Metabolic Neuroscience, Department of Neuroscience, Physiology & Pharmacology, University College London, London, United Kingdom, [3] Department of Biomedical and Life Sciences, Lancaster University, Lancaster, United Kingdom, [4] Department of Neurology, National Cerebral and Cardiovascular Center, Suita, Japan, [5] Knight Cardiovascular Institute, Oregon Health & Science University, Portland, OR, United States, [6] Department of Neurology, Jungers Center for Neurosciences Research, Oregon Health & Science University, Portland, OR, United States

Keywords: neurovascular unit (NVU), cerebrovascular disease, biomarker, cerebral blood flow (CBF), therapeutic target

Editorial on the Research Topic

The Neurovascular Unit as a Potential Biomarker and Therapeutic Target in Cerebrovascular Disease

INTRODUCTION

The brain is one of the most metabolically demanding organs—it requires 20% of the body's energy supply yet forms only 2% of the body's weight. Therefore, brain activity is supported by a dynamically regulated supply of blood and, hence, energy substrates through the cerebrovascular network. Furthermore, the post-mitotic nature of neurons and their longevity makes the brain very sensitive to extracellular perturbations. Thus, the cerebrovasculature also has to be specialized to minimize perturbations of the brain microenvironment, a property mediated by the blood-brain barrier that is formed by the neurovascular unit (NVU).

The NVU is a multicellular structure formed by neurons, glia and vascular cells. The NVU is fundamental to the distribution of cerebral blood flow, regulation of extracellular homeostasis and, as recently shown, waste clearance from the brain. Therefore, the NVU represents a pivotal point of vulnerability for the brain. In this Research Topic, 12 contributing articles address the potential of the NVU and provide evidence demonstrating the importance of the NVU as a biomarker and therapeutic target for cerebrovascular disease.

PHYSIOLOGICAL PARAMETERS OF THE NVU AS BIOMARKERS AND TARGETS FOR THERAPEUTIC INTERVENTION

It is important to first understand the structure and function of the healthy NVU to identify abnormal events and therapeutic targets. Shaw et al. provide a thorough and detailed characterization of the cerebrovascular bed, highlighting differences in its structure and function as it branches from penetrating arterioles to capillaries. Using immunohistochemistry and by assessing vasomotion along the vascular tree in awake mice *via* two-photon microscopy, they provide novel data characterizing points of contractility, angiogenic capacity, and vasodilatory potential across the vascular tree and branch points (Shaw et al.). The differences in vasodilatory response across the vascular tree are also highlighted in the study by Rosehart et al., in which they show that stimulation of capillaries with prostaglandin E2 elicits vasodilation of upstream arterioles. This was blunted in a model of small vessel disease, suggesting a reduction in capillary-to-arteriole signal propagation as a potential mechanism for the pathologies associated with cerebral small vessel disease, while also suggesting a new biomarker for NVU dysfunction (Rosehart et al.).

OPEN ACCESS

Edited and reviewed by:
Jun Wang,
Icahn School of Medicine at Mount Sinai, United States

***Correspondence:**
Shereen Nizari
shereen.nizari@gmail.com

Specialty section:
This article was submitted to Neuroinflammation and Neuropathy, a section of the journal Frontiers in Aging Neuroscience

Received: *30 March 2022*
Accepted: *19 April 2022*
Published: *05 May 2022*

Citation:
Nizari S, Hawkes CA, Hattori Y and Mishra A (2022) Editorial: The Neurovascular Unit as a Potential Biomarker and Therapeutic Target in Cerebrovascular Disease. Front. Aging Neurosci. 14:908716. doi: 10.3389/fnagi.2022.908716

Specific modifiable physiological parameters of the NVU are also highlighted within this Research Topic. Inhibitors of carbonic anhydrases, the pH regulating enzymes, can protect the NVU in stroke and Alzheimer's disease, as reviewed by Lemon et al. Hayes et al. provide novel data on another parameter, the neuroprotective hormone insulin-like growth factor-1 (IGF-1), demonstrating a difference in vulnerability to glutamate-induced toxicity across different cell types of the NVU when IGF-1 is inhibited.

Together, these data highlight multiple structural and functional points within the NVU that may potentially serve as targets for therapeutic intervention. The differential regulation at the various vascular segments and the transitional zones between them in the vascular tree is also noteworthy; each segment could be differently affected during disease, or be targeted for therapy.

NVU RISK FACTORS AND BIOMARKERS ACROSS THE LIFESPAN

The biomarker and target potential of the NVU across the lifespan is another key focus of this topic. In an opinion piece, Beishon and Panerai emphasize the importance of mid-life therapeutic targeting and lifestyle alterations targeting known risk factors for dementia. The comprehensive review by Ouellette and Lacoste highlights the shared vascular abnormalities associated with neurodevelopmental and neurodegenerative disorders, despite their distinct clinical presentation at different life stages.

Lecordier et al. provide a detailed review of early risk factor events for NVU dysfunction leading to dementia, highlighting triggering pathological events. They specifically underscore the importance of air pollution as a risk factor for dementia, and provide a detailed summary of its impact on NVU components (Lecordier et al.). Exercise is suggested to reduce cerebrovascular disease and alleviate the risk for developing dementia. Ohtomo et al. report that, in a model of chronic hypoperfusion, exercise was able to alleviate fewer behavioral deficits in middle aged mice compared to their previous study on young mice, suggesting the value of early lifestyle interventions. Altogether, these reports showcase the potential of the NVU as a biomarker and the importance of protecting NVU function across the lifespan.

CLINICAL BIOMARKERS OF DISEASE OUTCOME AND PROGRESSION

The significance of using the NVU, or the pathologies associated with it, as a biomarker and therapeutic target in the clinical setting is also emphasized in this Research Topic. A systematic meta-analysis by Wang et al. demonstrates the role of cerebral small vessel disease in negative prognosis following intravenous thrombolysis treatment for acute ischemic stroke, highlighting the value of NVU pathology in predicting treatment outcomes.

In addition, Monteiro et al. report a reduction in neurovascular coupling in patients with hypertension while hypercapnic hyperemia is preserved, prior to detectable cerebral small vessel disease. This impairment was further exacerbated when hypertension was comorbid with diabetes, suggesting that NVU dysfunction may contribute to the cerebral effects of chronic hypertension and diabetes (Monteiro et al.). Staszewski et al. provide further support for the NVU as a biomarker for disease progression, demonstrating that decreases in cerebrovascular reactivity are measurable over a 24 month follow-up period in patients with small vessel disease, irrespective of initial radiological disease assessment.

Lastly, Ren et al. suggest that disruptions in the glymphatic system, a hypothesized route of paravascular waste clearance, may be the cause of, and serve as a biomarker for, peri-operative neurocognitive disorder. Their review highlight anesthesia choice and management as potentially modifiable risk factors for peri-operative neurocognitive disorder (Ren et al.).

CONCLUSION AND FUTURE DIRECTIONS

This Research Topic provides both preclinical and clinical evidence of the importance of the NVU as a contributor to cerebrovascular disease and, thus, a therapeutically targetable fulcrum, while underscoring its value as an accessible biomarker for disease etiology and progression. The additional targeting of co-morbidities and detrimental lifestyle risk factors that lead to NVU dysfunction, which change over the lifespan, are also essential for disease management. It is clear that further characterization of the NVU, including its functions in health and different pathological contexts, and how it is modified by lifestyle choices and comorbid conditions, are all important avenues for future work. Findings from such studies may suggest potential therapeutic targets for cerebrovascular diseases, and may even be applicable to related dementia conditions.

AUTHOR CONTRIBUTIONS

All authors listed have made a substantial, direct, and intellectual contribution to the work and approved it for publication.

ACKNOWLEDGMENTS

The guest editors would like to thank all authors for their contribution, reviewers for their time, and the Frontiers editorial team for their support.

Conflict of Interest: The authors declare that the research was conducted in the absence of any commercial or financial relationships that could be construed as a potential conflict of interest.

frontiers in Aging Neuroscience

REVIEW
published: 07 June 2021
doi: 10.3389/fnagi.2021.659457

Dysfunction of the Glymphatic System as a Potential Mechanism of Perioperative Neurocognitive Disorders

*Xuli Ren[1], Shan Liu[2], Chuang Lian[3], Haixia Li[2], Kai Li[1], Longyun Li[1] and Guoqing Zhao[1,4]**

[1] Department of Anaesthesiology, China-Japan Union Hospital of Jilin University, Changchun, China, [2] Department of Neurology, First Affiliated Hospital of Jilin University, Changchun, China, [3] Department of Anaesthesiology, Jilin City People's Hospital, Jilin, China, [4] Jilin University, Changchun, China

Perioperative neurocognitive disorder (PND) frequently occurs in the elderly as a severe postoperative complication and is characterized by a decline in cognitive function that impairs memory, attention, and other cognitive domains. Currently, the exact pathogenic mechanism of PND is multifaceted and remains unclear. The glymphatic system is a newly discovered glial-dependent perivascular network that subserves a pseudo-lymphatic function in the brain. Recent studies have highlighted the significant role of the glymphatic system in the removal of harmful metabolites in the brain. Dysfunction of the glymphatic system can reduce metabolic waste removal, leading to neuroinflammation and neurological disorders. We speculate that there is a causal relationship between the glymphatic system and symptomatic progression in PND. This paper reviews the current literature on the glymphatic system and some perioperative factors to discuss the role of the glymphatic system in PND.

Keywords: glymphatic system, postoperative complications, postoperative neuropathy, postoperative cognitive dysfunction, perioperative neurocognitive disorders

OPEN ACCESS

Edited by:
Shereen Nizari, University College London, United Kingdom

Reviewed by:
Humberto Mestre, University of Rochester, United States

***Correspondence:**
Guoqing Zhao
guoqing@jlu.edu.cn

Received: *27 January 2021*
Accepted: *18 May 2021*
Published: *07 June 2021*

Citation:
Ren X, Liu S, Lian C, Li H, Li K, Li L and Zhao G (2021) Dysfunction of the Glymphatic System as a Potential Mechanism of Perioperative Neurocognitive Disorders. Front. Aging Neurosci. 13:659457. doi: 10.3389/fnagi.2021.659457

INTRODUCTION

Perioperative neurocognitive disorder (PND), which encompasses delirium and postoperative cognitive dysfunction, commonly occurs in the elderly after anesthesia and surgery. Previously, all forms of postoperative cognitive impairments were called "postoperative cognitive dysfunction," but more recently, the use of "perioperative neurocognitive disorder" is recommended as an overarching term for cognitive impairment identified in the preoperative or postoperative period (Evered et al., 2018a). This change aligns PND with the phenotypically similar neurocognitive diagnoses listed in the Diagnostic and Statistical Manual of Mental Disorders, version 5, such as Alzheimer's disease (AD) (Evered et al., 2018a). Furthermore, PND has emerged as a significant global public health issue that leads to more extended in-hospital stays, higher hospitalization costs, and higher mortality rates (Yang and Terrando, 2019). The risk factors for PND are multifaceted, which might be related to anesthetic management, tissue damage, surgery duration, psychological stress, and genetic susceptibilities (Subramaniyan and Terrando, 2019; Eckenhoff et al., 2020). As the elderly population continues to increase, the number of cases of PND will continue to rise. The incrementally growing prevalence forces researchers to explore the mechanisms underlying the pathogenesis of PND and to seek optimal prevention and treatment measures (Evered and Silbert, 2018; Berger et al., 2019).

Preclinical and clinical studies support the notion that neuroinflammation plays a significant role in the pathogenesis of PND (Nathan, 2019; Yang et al., 2019, 2020). Trauma experienced during surgery triggers the release of endogenous factors known as damage-associated molecular

patterns that can activate immune cells such as neutrophils and monocytes, promote pro-inflammatory cytokines, and subsequently cause systemic inflammation (Huber-Lang et al., 2018). Uncontrolled systemic inflammation is associated with a compromised blood-brain barrier (BBB). BBB impairment promotes immune cell movement and pro-inflammatory cytokines from the blood into the brain parenchyma, triggering neuroinflammation and ultimately leading to postoperative cognitive impairment (Abrahamov et al., 2017; Yang et al., 2017, 2020). Microglia, the resident immune cells of the central nervous system (CNS), perform "immune surveillance," and survey their assigned brain regions (Kettenmann et al., 2011). In addition, with prolonged systemic inflammation, microglia start to develop an activated phenotype characterized by an increase in pro-inflammatory mediators, such as interferon-γ, interleukin (IL)-1β, tumor necrosis factor (TNF)-α, and reactive oxygen species (Liu L. R. t al., 2020). Pro-inflammatory factors released by microglia such as IL-1α and TNF contribute to the subsequent activation of astrocytes and further promote neuroinflammation (Liddelow et al., 2017; Liu L. R. t al., 2020). Complement system activation is another essential inflammatory response that is activated by surgically triggered damaged-associated molecular patterns. For example, the deposition of the C-reactive protein, a biomarker for delirium, can activate and regulate the classical complement pathway, thereby contributing to dysregulated inflammation. Blocking the complement cascade (e.g., complement C3 gene deficiency and selective complement inhibitor for complement C3) improves neuroinflammation and functional outcomes of PND (Alawieh et al., 2018) also suggests the contribution of neuroinflammation in PND.

Several studies have shown that the pathological mechanism of PND is similar to that of AD (Evered et al., 2016; Gerlach and Chaney, 2018). It was also demonstrated that a significant accumulation of amyloid-β (Aβ) and tau in the brain parenchyma after anesthesia and surgery (Terrando et al., 2011). Moreover, increased Aβ and tau in the cerebrospinal fluid (CSF) have been reported in patients after surgery (Evered et al., 2018b), which are risk factors for PND (Xie Z. et al., 2013; Evered et al., 2016; Cunningham et al., 2019). The accumulation of Aβ and tau induces neuroinflammation, leading to glial activation, pro-inflammatory factor release, and neuronal damage (Calsolaro and Edison, 2016).

The glymphatic system is a recently discovered waste removal system that utilizes a unique perivascular channel system formed by astrocytes (Iliff et al., 2012; Benveniste et al., 2017; Zhang C. et al., 2018). Although the glymphatic system contributes to the delivery of nutrients, specifically glucose, its most influential and recognized function is to clear extracellular metabolites and waste products from the parenchyma into the CSF (Abbott et al., 2018; Nedergaard, 2013; Simon and Iliff, 2016). Since its discovery, researchers have proposed that waste or protein aggregates induced by glymphatic dysfunction are associated with neurodegenerative diseases, including AD (Tarasoff-Conway et al., 2015; Harrison et al., 2020; Nedergaard and Goldman, 2020). Given the characteristics of the glymphatic system and the complexity of possible changes during the perioperative stage, we herein speculate a causal relationship between the glymphatic system and symptomatic progression in PND. Glymphatic dysfunction in the perioperative period, which leads to waste accumulation, could trigger or exacerbate neuroinflammation and eventually lead to cognitive dysfunction. Through this review, we discuss the function and driving mechanism of the glymphatic system, outline the current evidence to illustrate the impact of anesthesia and surgery on the glymphatic system, and emphasize the viewpoint that glymphatic dysfunction is involved in the pathogenesis of PND.

GLYMPHATIC PATHWAY

The glymphatic system is a perivascular network that subserves a pseudo-lymphatic function throughout the brain (**Figure 1**). Iliff et al. named this brain-wide fluid transport pathway the glial-associated lymphatic system or glymphatic system due to its dependence on glial water flux and the lymphatic function of the brain (Iliff et al., 2012). As the macroscopic waste clearance system of the CNS, the glymphatic system's fundamental role is to eliminate soluble proteins and metabolites, including Aβ and tau, based on the evidence that 40%−80% of neurotoxic compounds can be cleared from the CNS via this system (Iliff et al., 2012). The neurotoxic compound clearance process within the glymphatic system is described as a 3-step serial process (Benveniste et al., 2019b). First, CSF is continuously transported from the subarachnoid space and Virchow-Robin space to the peri-arterial spaces in a bulk-flow driven manner; subsequently, CSF is propelled from the peri-arterial compartment into the interstitial fluid (ISF) space. The convection and mixing of CSF and ISF are facilitated by aquaporin 4 (AQP4) in the dense and complex brain parenchyma. Ultimately, CSF-ISF fluid mixes with interstitial waste solutes and is subsequently transported to the perivenous space, from the meningeal lymphatic vessels to the lymphatic vessels and circulatory system (Plog and Nedergaard, 2018).

AQP4 is required to maintain the glymphatic function and is abundantly expressed in the end-feet of astrocytes that surround arteries and veins. It is also anchored to the astrocyte membrane by the carboxyl terminus of α-syntrophin. Syntrophin-dependent AQP4 mediates the bidirectional transport of water across the brain-blood interface (Amiry-Moghaddam et al., 2003). As a bidirectional channel, the effects of AQP4 on glymphatic function may be diverse and require further investigation. Although the role of AQP4 in promoting ISF clearance is debated, a large body of evidence suggests that it facilitates CSF movement from perivascular spaces into the interstitial space and activates flushing of ISF (Smith et al., 2017). Studies on different strains of AQP4-knockout mice have suggested that AQP4 is necessary for the rapid movement of CSF from the perivascular space into the ISF and through the brain (Mestre et al., 2018a). Moreover, AQP4 reduces the resistance to CSF movement from the periarterial space into the interstitium and subsequently from the interstitium into the perivenous space (Groothuis et al., 2007). The flow of CSF via the glymphatic pathway is an essential part of the CNS that eliminates metabolic waste products, such as Aβ and lactic acid, from deep inside the brain and delivers

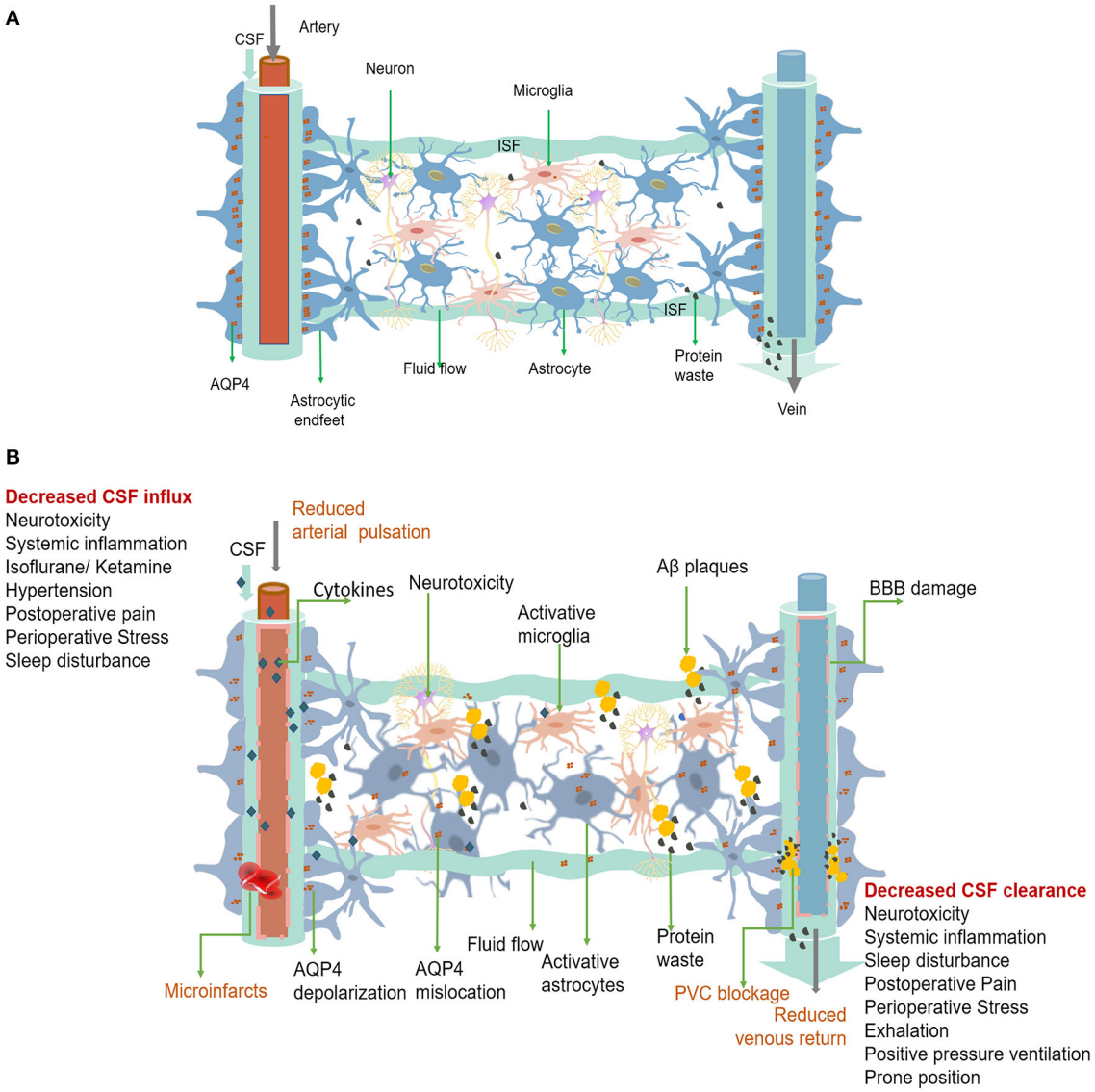

FIGURE 1 | (A) The glymphatic system is a perivascular channel formed by astrocyte end-feet throughout the brain. CSF enters the brain parenchyma through the periarterial space, exchanges with ISF, and finally exits through the perivenous space. Rapid exchange of CSF within ISF is facilitated by AQP4, which is anchored to the astrocytic end-feet. Interstitial solutes, including protein waste, are drained from the brain with CSF through the perivenous space and via the meninges and cervical lymphatics. **(B)** Dysfunction of the perioperative glymphatic system. Perioperative anesthetic drugs can cause hemodynamic changes that reduce arterial pulsation mechanism change and decrease the inflow of the glymphatic system. Surgically induced systemic inflammation can cause blood-brain barrier opening and glymphatic system damage, leading to neuroinflammation and decreased waste clearance. Both the entry of peripheral inflammatory substances and the accumulation of protein wastes in the brain, such as Aβ accumulation and folding, can activate astrocytes and microglia and trigger neuroinflammation. Neuroinflammation can worsen the damage to the function and structure of the glymphatic system. Forceful expiration, positive pressure ventilation, and prone position can cause a decrease in venous return, leading to a decrease in CSF clearance. Pain, preoperative stress, and sleep disturbances can affect both CSF inflow and clearance. Glymphatic dysfunction can lead to a more significant accumulation of protein and waste products, which can trigger neuroinflammation and lead to PND. PVC, Perivascular space.

nutrients, such as glucose, or therapeutic drugs to the brain parenchyma. This CSF circulation differs from typical lymphatic vessels and acts as a pseudo-lymphatic drainage within the CNS. Therefore, more recently, alternative CSF circulation in the brain has been proposed as a glymphatic circulation (Benveniste et al., 2019b).

THE DRIVING MECHANISM OF GLYMPHATIC SYSTEM

Arterial Vascular Pulsation

Unlike other peripheral organs, limited tissue compliance of the rigid skull facilitates the propagation of arterial pressure

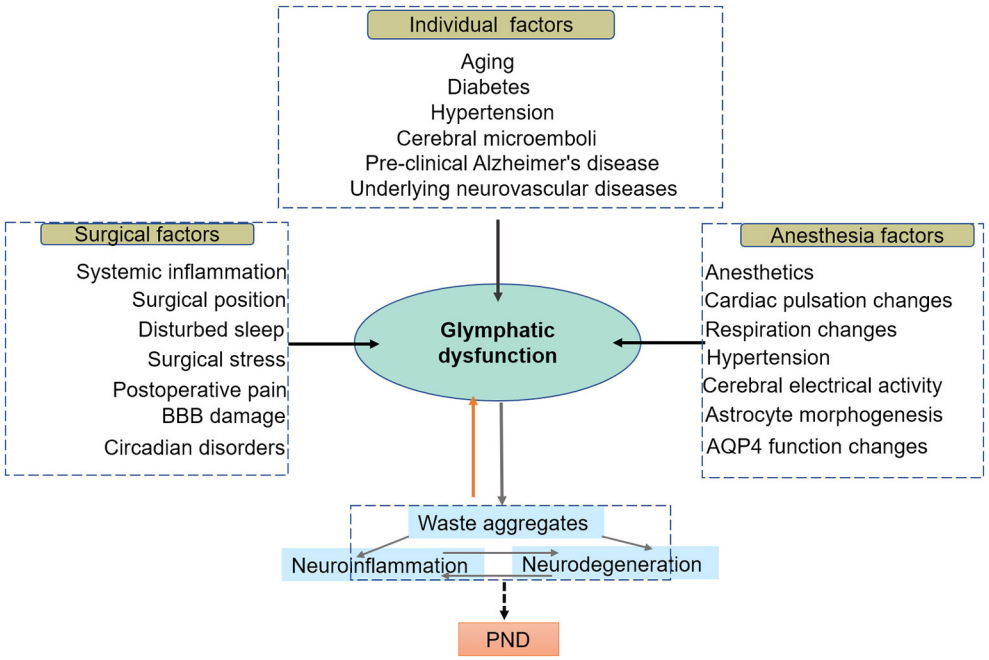

FIGURE 2 | In this model, the glymphatic system resides at the intersection of a broad scope of perioperative risk factors, which share an association with diminished brain waste clearance. Individual factors are preexisting impairments in glymphatic function prior to surgery; anesthetic and surgical factors are associated with a dramatic decline in perioperative glymphatic function, compromising the glymphatic system and exacerbating the progression of preexisting disease. Glymphatic system dysfunction, in turn, contributes to protein aggregation and misfolding, leading to neuroinflammation, neurodegeneration, and ultimately PND.

pulsations throughout the brain, resulting in measurable pulsatile blood flow and venous outflow in the microvasculature (Shi et al., 2020). This cardiac pulsation along the entire vascular bed is believed to be the most critical physical mechanism for glymphatic propulsion, facilitating CSF movement in the glymphatic system (Kyrtsos and Baras, 2015; Kiviniemi et al., 2016; Hablitz et al., 2020). Cardiovascular pulsation is also the fastest driving mechanism of the glymphatic system, originating in the basal peri-arterial spaces around the Willis's circle and extending centrifugally toward the cerebral cortex (Kiviniemi et al., 2016). The dynamic source is mainly due to the oscillation of the arterial wall caused by the heartbeat, which produces a net flow consistent with the blood flow direction and the same frequency as the cardiac cycle (Iliff et al., 2013; Kiviniemi et al., 2016). Each cardiac cycle involves a fast expansion of the artery wall, followed by a slow contraction. The bulk flow rate of CSF, calculated by CSF viscosity and the shape, cross-sectional area, and length of the vessels, is proportional to the hydraulic pressure drop along the vessels and inversely proportional to the hydraulic resistance (Thomas, 2019). The combined effects of diffusion and advection also play a role in clearing solutes from the brain (Thomas, 2019). The arterial wall pressure generates the hydraulic pressure of the CSF, which allows CSF to be delivered to the brain via the glymphatic system, a process in which the contractility of the vessel wall or the slow wave of vasomotor tension also plays an important role (Kiviniemi et al., 2016). Any reduction in vessel wall contractibility or slow contraction in vasomotor tone increases backflow and decreases net flow in the glymphatic system (Mestre et al., 2018b). CSF flow may be mechanically regulated by pressure differences, which may be a neurophysiological regulatory mechanism. For example, astrocyte calcium activity has been shown to propagate along blood vessels as waveforms and regulate water permeability and ion exchange in the perivascular space (Rangroo Thrane et al., 2013). Additionally, intracranial pressure and heart rate are related to cardiac pulsation and affect glymphatic function. Increased intracranial pressure (ICP) decreases the mean arterial pressure and impairs the function of the glymphatic system (Chen et al., 2018), while glymphatic influx correlates negatively with heart rate (Hablitz et al., 2019).

Research has shown that the glymphatic cross-section is a non-concentric elliptical space outside the vessel, which provides the least hydraulic resistance (Tithof et al., 2019). This cross-section model is quite different from the usual circular annulus models, which assume that the small arteries are located in the center of the space (Mestre et al., 2018b; Thomas, 2019). Moreover, Mestre et al. have shown that the glymphatic system infrastructure around pial arteries is 10 times larger *in vivo* than previous estimates after fixation based on electron microscope images (Tithof et al., 2019). As such, the glymphatic system offers much less viscous resistance to CSF flow than previously thought. These results also demonstrate the importance of further *in vivo* studies on the glymphatic system.

Respiratory Forces

Advances in imaging and computational techniques have demonstrated that the respiratory mechanism is another important process that dominates the perivenous space (Kiviniemi et al., 2016). Although the respiratory force is not the primary driver of CSF flow, it is a modulating factor that supplements cardiac pulsation (Dreha-Kulaczewski et al., 2015). Respiratory dynamics are related to extreme low-frequency vasomotor oscillations during perivenous fluid movements (Kiviniemi et al., 2016). A study using magnetic resonance spin labeling in humans showed that CSF movement was enhanced during deep inhalation and was inhibited during deep exhalation (Yamada et al., 2013). A possible explanation is that forced inspiration causes blood to be drawn from the brain through the veins into the thorax, resulting in a decrease in intracerebral venous pressure, an expansion of the perivenous space, and an increase in CSF outflow from the perivenous space into the brain. Moreover, small but rapid CSF movement was observed during breath-holding, which is thought to reflect cardiac pulsations (Yamada et al., 2013). Alternatively, exhalation reduces venous outflow from the brain in a low-pressure venous drainage system (Kiviniemi et al., 2016). Additionally, respiration produces lower-frequency ICP oscillations and hydraulic pressure changes (Dreha-Kulaczewski et al., 2015).

Circadian Regulation

Sleep is essential for the maintenance of healthy brain functions. Hence, early research suggests that glymphatic clearance is mainly associated with the sleep-wake cycle (Xie L. et al., 2013). Studies in rodents have shown that CSF absorption in the perivascular space and ISF flushing increase during sleep (Xie L. et al., 2013). Glymphatic activity is regulated by circadian regulation, with a daily rhythm that peaks at midday when mice are mostly likely to sleep (Hablitz et al., 2020). Similarly, glymphatic activity was more significant at night than during the day in patients administered with gadolinium as a CSF tracer to evaluate glymphatic function (Eide and Ringstad, 2019). The mechanism by which the circadian rhythm of the brain regulates glymphatic activity remains unclear. Circadian neural activities can be detected with an electroencephalogram (EEG) device (Dijk, 1999). Overnight EEG has shown that delta (1–4 Hz) power and sigma (12–15 Hz) power are high during non-rapid eye movement (NREM) sleep and low during rapid eye movement (REM) sleep. In contrast, beta (23–30 Hz) power is higher in REM sleep than in NREM sleep, except for an artifactual peak during cycle 2. EEG activity that resembles sleep or wakefulness tightly correlates to the glymphatic influx (Hablitz et al., 2019). The brain's waste clearance mainly occurs during the NREM stage, while the CSF influx was strongly suppressed during wakefulness (Hablitz et al., 2019, 2020). Sigma power during NREM fluctuates reciprocally with delta, becoming high when delta is low and low when delta is high (Campbell, 2009). It has been demonstrated that either high delta rhythm or slow oscillation (<1 Hz), which is a characteristic of NREM sleep, is positively correlated with the glymphatic function, while beta power that resembles wakefulness is negatively correlated with the glymphatic function (Hablitz et al., 2019). The underlying relationships between EEG power and glymphatic activity remains unclear. A recent study has revealed a coherent pattern of oscillating electrophysiological, hemodynamic, and CSF dynamics during NREM sleep (Fultz et al., 2019). These results suggest that neural activity may affect the function of the glymphatic system through hemodynamic circadian rhythms (**Figure 2**). Lactate concentration in the brain also closely corresponds to EEG activity and is considered the best metabolic biomarker of the sleep-wake cycle (Lundgaard et al., 2017). Lactate concentration decreases during the transition from wakefulness to sleep, leading to an expansion of the extracellular space and a decrease in intra-tissue resistance results, contributing to faster CSF influx into the interstitium and finally solute efflux.

GLYMPHATIC FUNCTION AFFECTED BY ANESTHETICS

Currently, most animal experiments on glymphatic function are performed by applying anesthetic drugs to simulate the sleep state. The effect of anesthetics cannot be ignored when studying the effect of sleep on glymphatic function. Currently, limited research has been conducted to investigate the effects of anesthetics or sedatives on the rodent glymphatic system. A study demonstrated that inhaled isoflurane (2–2.5%) inhibited CSF circulation and waste clearance in the brain (Gakuba et al., 2018). This result indicates that inhaled isoflurane inhibited glymphatic function, especially at a high dose (3%) (Gakuba et al., 2018). This research also showed that ketamine, a common intravenous anesthetic, also inhibited glymphatic activity at an intraperitoneal dose of 150 $mg{\cdot}kg^{-1}$ in mouse models (Gakuba et al., 2018). The inhibitory effect of ketamine on glymphatic function could be reversed using a combination of ketamine and 10 $mg{\cdot}kg^{-1}$ of xylazine (Gakuba et al., 2018). However, Xie et al. previously found that ketamine (100 $mg{\cdot}kg^{-1}$) combined with xylazine (20 $mg{\cdot}kg^{-1}$) significantly increased the influx of the CSF tracer in all mice analyzed (Xie L. et al., 2013). The opposite effects of the two different anesthetic regimens require further study. One possible explanation is whether ketamine inhibits or increases lymphatic inflow, depending on the dose of ketamine and its combination with xylazine, an α_2-adrenergic agonist and an analog of clonidine used as a sedative and analgesic in animals. Xylazine increases glymphatic CSF influx and may remedy the impairment of ketamine use in the glymphatic system (Gakuba et al., 2018).

Dexmedetomidine (DEXM) is another α_2-adrenergic agonist widely used for anesthesia or sedation in clinics and has also been shown to enhance glymphatic function in animal research (Lilius et al., 2019a). Recently, Ozturk et al. reported that DEXM supplemented with low-dose isoflurane increased glymphatic transport compared to that of isoflurane only (Ozturk et al., 2021). DEXM has also been shown to increase the delivery of intrathecally administered drugs, such as oxycodone and naloxone, by increasing glymphatic flow (Lilius et al., 2019b).

Propofol is a widely used intravenous anesthetic in humans with anti-inflammatory (Ren et al., 2014) and neuroprotective

properties (Miller et al., 2018). Recent studies have found that propofol can increase glymphatic activity (Gakuba et al., 2018). Pentobarbital has also been shown to significantly increase glymphatic function in animal models (Hablitz et al., 2019), although benzodiazepines have mainly been replaced by human anesthesia. Other anesthetics used in animal anesthesia such as α-chloralose and avertin inhibit CSF tracer influx in the glymphatic pathway (Hablitz et al., 2019). Therefore, glymphatic function is affected by the dose, type, and combination of anesthetics. Although the exact mechanisms underlying these preclinical experiments remain unclear, they may provide valuable information for studying the functional effects of the glymphatic system during clinical anesthesia (**Table 1**).

Interestingly, these animal studies on glymphatic dysfunction agree with those of clinical studies on PND. Anesthetics are a risk factor for postoperative cognitive decline or neuropathological changes (Schenning et al., 2016). It has been confirmed that inhaled anesthetics, such as isoflurane or sevoflurane, have more chance of causing postoperative cognitive dysfunction (Ologunde and Ma, 2011; Hu et al., 2014), whereas some intravenous anesthetics, such as DEXM and propofol, cause slight harm or even improve perioperative cognitive function (Miller et al., 2018). Anesthetics that have a significant inhibitory effect on the glymphatic system are more likely to cause perioperative cognitive impairment, whereas some anesthetics that enhance glymphatic function are less likely to cause cognitive impairment. The effects of ketamine on the glymphatic system and postoperative cognition have been controversial (Morrison et al., 2018). DEXM enhances glymphatic function and has also been shown to prevent postoperative delirium and cognitive dysfunction caused by inhaled anesthetics in elderly patients (Zhang et al., 2018). Therefore, anesthetics may affect postoperative brain function by affecting the glymphatic function. Currently, the mechanisms underlying the effects of anesthetics on glymphatic function remain unclear. Further clinical research is necessary to determine the optimal variety, dose, and combination of anesthetics and drugs to reduce glymphatic function impairment during anesthesia.

THE UNDERLYING MECHANISM OF ALTERED GLYMPHATIC FUNCTION DURING INTRAOPERATIVE ANESTHESIA MANAGEMENT

The mechanisms that regulate glymphatic function under normal physiological conditions include arterial pulsatility, respiration, and neural activity. However, these mechanisms may be disrupted during anesthesia, including general anesthesia and spinal anesthesia (Scott, 2018). During clinical anesthesia, the heart rate, blood pressure, and arterial pulsation are significantly changed, and spontaneous negative pressure respiration is replaced with positive pressure ventilation. The arousal mechanism is also significantly suppressed during general anesthesia (Schiff, 2020). Anesthesia-induced pathological processes, such as the breakdown of glymphatic CSF-ISF exchange, have been linked to disease initiation and progression. As a result, the impact of anesthesia on glymphatic function needs to be considered.

Cardiac Pulsation Mechanism Change

The sympathetic, stellate ganglion, and subcutaneous sympathetic nerves are all suppressed by most anesthesia types, including general, neuraxial, epidural, and lumbar anesthesia. Anesthesia suppresses blood pressure and heart rate by causing dose-dependent vasodilation or vasoplegia. Hypotension occurs due to anesthesia-induced reduction in heart rate, vasodilation, reduced afterload, and circulating volume. Furthermore, a lower heart rate has a strong positive association with glymphatic influx (Hablitz et al., 2019). Currently, there is no research on the relationship between hypotension and glymphatic activity. Mestre et al. found that the jerky and irregular reversal of microparticle flow caused by increased arteriole stiffness and pulsation amplitude in distal vessels during hypertension reduced perivascular pump dynamics and decreased net CSF flow and waste clearance in the perivascular space (Mestre et al., 2018b). Additionally, CSF production is related to sympathetic or adrenergic receptor activity. Increased sympathetic tone inhibits carbonic anhydrase associated with the choroidal epithelium and likely reduces CSF production and glymphatic circulation (Damkier et al., 2013; Benveniste et al., 2017). Recently, Liu et al. also reported that CSF production was increased by a combination of α_1-, α_2-, and non-selective β-adrenergic receptor antagonists, as well as some anesthetics, including isoflurane, ketamine, and xylazine (Liu G. et al., 2020).

Perioperative hemodynamic optimization is crucial for improving outcomes after surgery and anesthesia. Anesthesia management often includes the administration of catecholamine vasoactive drugs such as norepinephrine, dopamine, and phenylephrine to maintain stable hemodynamics throughout surgery (Foss and Kehlet, 2019). Norepinephrine, a central regulator, also inhibits glymphatic transport (Jessen et al., 2015). However, Iliff et al. demonstrated that dobutamine increased the pulsatility of the penetrating artery by 60% and enhanced the glymphatic influx (Iliff et al., 2013). Furthermore, catecholamines can modulate astrocyte function and signaling to regulate the glymphatic system (Fuxe et al., 2015). The astrocytic dopamine and adrenergic receptor subtypes are significant drug targets in neurological and psychiatric diseases (Fuxe et al., 2015). Norepinephrine and dobutamine also work together to affect glymphatic function by acting on fluid availability and convective fluxes through various mechanisms. Therefore, catecholamines may be the primary regulators of solute clearance from the brain.

Theoretically, any changes in cardiovascular parameters induced by anesthesia can impair the cardiac pulsation mechanism, resulting in waste accumulation. Hence, understanding the processes contributing to pulsatility and how these components drive waste clearance by the glymphatic system continues to evolve. Further research is needed to determine the most appropriate management of glymphatic function during clinical anesthesia.

TABLE 1 | The effect of verified factors on glymphatic system.

Classification	Perioperative factors	Glymphatic function	Classification	Perioperative factors	Glymphatic function
Anesthetic factors	Neurotoxicity	Impair (Rangroo Thrane et al., 2013)	Cardiovascular factors	Acute hypertension	Impair (Mestre et al., 2018b)
				Chronic hypertension	Impair (Mortensen et al., 2019; Koundal et al., 2020)
	Isoflurane (2–2.5%)	Inhibit (2–2.5%) (Gakuba et al., 2018)		Heart rate	Negative correlation (Hablitz et al., 2019)
	Sevoflurane	Enhance (2.5%) (Gao et al., 2019)		Dobutamine	Enhance (Iliff et al., 2013; Yamada et al., 2013)
	Dexmedetomidine	Enhance (20 mg.kg^{-1}; ip) (Hablitz et al., 2019; Lilius et al., 2019a)		Norepinephrine	Inhibit (Jessen et al., 2015)
	Xylazine	Enhance (Hablitz et al., 2019)	Surgical factors	Neuroinflammation	Impair (Yu et al., 2019)
	Ketamine	Inhibit (150 mg.kg^{-1}) (with xylazine, 10 mg.kg^{-1}) (Gakuba et al., 2018)		Position	lateral > supine > prone (Lee et al., 2015)
		Enhance (100 mg.kg^{-1}) (with xylazine 20 mg.kg^{-1}) (Hablitz et al., 2019)		Sleep disturb	Impair (Nedergaard and Goldman, 2020).
	Propofol	Enhance (Gakuba et al., 2018)		BBB damage	Impair (Meng et al., 2019; Yu et al., 2019)
	Pentobarbital	Enhance (60 mg.kg^{-1}; ip) (Hablitz et al., 2019)		Postoperative Pain	Impair (Chouchou et al., 2014)
	α-chloralose	Inhibit (80 mg.kg^{-1}; ip) (xylazine Hablitz et al., 2019)		Perioperative Stress	Impair (Wei et al., 2019)
	Avertin	Inhibit (120 mg.kg^{-1}; ip) (Hablitz et al., 2019)	Individual factors	Preclinical stage of AD	Impair (Masters et al., 2015)
Arouse stage	Wake	Inhibit (Xie L. et al., 2013; Eide and Ringstad, 2019)		Neurovascular diseases	Impair (Riba-Llena et al., 2018)
	Sleep	Enhance (Xie L. et al., 2013; Alawieh et al., 2018)		Aging	Impair (Iliff et al., 2013)
	EEG	Beta power inhibit (Hablitz et al., 2019)		Apo E gene	Impair (Mentis et al., 2020)
		Delta power enhance (Hablitz et al., 2019)		AQP4 gene	Impair (Hubbard et al., 2018).
Respiration	Free breathing	N/A		Chronic hypertension	Impair (Mestre et al., 2018b; Riba-Llena et al., 2018)
	Deep inhalation	Enhanced (Dreha-Kulaczewski et al., 2015)		Diabetes	Impair (Zhang et al., 2014; Jiang et al., 2017)
	Mechanical ventilation	N/A	Other factors	Intracranial pressure	Increase will impair (Dreha-Kulaczewski et al., 2015)

Respiration Changes

During experimental testing in mouse or rat models described above, spontaneous respiration was inhibited but still preserved in research involving the glymphatic system. Spontaneous respiration in anesthetized animals is very different from that in controlled or assisted respiration under clinical anesthesia. During clinical anesthesia, positive-pressure mechanical ventilation is often used to replace spontaneous respiration. Mechanical ventilation differs from spontaneous breathing in terms of physiology, and its effect on glymphatic system transport in the brain is currently unknown. Ventilators are inspiratory assist devices that deliver tidal breath under positive pressure. Positive pressure ventilation, including positive end-expiratory pressure, may increase intrathoracic pressure and reduce venous return, subsequently causing increased ICP (Chen et al., 2018). Positive pressure ventilation also reduces cerebral perfusion pressure due to increased ICP and decreased mean arterial pressure (Chen et al., 2018). It has been hypothesized that ventilation impairs respiration, causing waste accumulation in the brain.

Although the administration of local anesthetics through the spinal or epidural canal can provide anesthesia without the need

for mechanical ventilation, there are still additional effects on the sympathetic nervous system, parasympathetic nervous system, and motor control, resulting in respiratory impairment (Wink et al., 2016). Theoretically, these changes impair the function of the glymphatic system. Some respiratory parameters, such as tidal volume, frequency, and airway pressure, have not been studied in relation to glymphatic activity.

Preclinical and clinical evidence suggests that mechanical ventilation induces adverse neurocognitive effects (Wang et al., 2015). It is estimated that 70–100% of critically ill patients have cognitive impairment after mechanical ventilation, and 20% of patients still have cognitive impairment 5 years later (Herridge et al., 2016; Bilotta et al., 2019). In patients with COVID-19, delirium/neurological disorders are clearly correlated with prolonged mechanical ventilation (Alonso-Lana et al., 2020; Helms et al., 2020). However, the mechanism by which mechanical ventilation affects the incidence of postoperative cognitive disorder remains unclear. The discovery of this novel glymphatic pathway may provide clues for future research. Evaluating perioperative glymphatic function might provide new insights for understanding the pathophysiological mechanisms underlying cognitive decline during clinical anesthesia and surgery.

Arousal Regulation Mechanism Altered by Anesthesia

Some studies have demonstrated that arousal state correlates with the glymphatic system (Hablitz et al., 2019), while the arousal state also reflects "depth of anesthesia" in clinical settings (Shalbaf et al., 2015). The arousal state is closely related to hemodynamic rhythms such as blood pressure, heart rate, and blood oxygenation level-dependent signals, which affect glymphatic function (Fultz et al., 2019). The depth of anesthesia can affect not only the hemodynamics but also the arousal mechanism. Therefore, there may be a relationship between anesthesia depth and glymphatic function (Shalbaf et al., 2015). General anesthesia is characterized by the suppression of central arousal controlled by the locus coeruleus and noradrenergic tone (Brown et al., 2010). Norepinephrine release is reduced when anesthesia suppresses sympathetic nerve activity. It has been confirmed that noradrenergic blockade or reduction produces the same changes in ISF volume fraction in the glymphatic system (Xie L. et al., 2013).

However, accurate estimation of the depth of anesthesia remains an important issue in clinical or animal anesthesia. Non-invasive EEG or evoked potential indices, such as the bispectral index, narcotrend index, state entropy, and response entropy, for monitoring anesthesia depth are widely used in clinical research. High EEG delta power is positively associated with glymphatic activity, while beta power is negatively corelated in animal models (Hablitz et al., 2019). When bispectral index-guided deep anesthesia is used in geriatric anesthesia, postoperative delirium and cognitive decline in elderly surgical patients are reduced (Deschamps et al., 2019; Miao et al., 2019). Therefore, intraoperative indicators for monitoring anesthesia depth are clinically significant for research about the relationship between glymphatic function and PND. Insufficient anesthesia can cause physiological and psychological injuries, whereas overdose anesthesia may induce hemodynamic disturbances. Therefore, monitoring the depth of anesthesia may also prevent impairment of the glymphatic system and cognition due to inadequate or excessive anesthesia.

Astrocytes and AQP4 Function Changes

The use of *in vivo* two-photon imaging demonstrated that calcium signaling in astrocytes is associated with the selective transport of small lipophilic molecules and rapid ISF movement throughout the glymphatic system (Rangroo Thrane et al., 2013). A recent study found that glymphatic flow is regulated by fluid shear stress produced by perivascular CSF or ISF dynamics, which are capable of mechanically opening NMDA receptors and producing increased Ca^{2+} currents in cultured astrocytes (Maneshi et al., 2017). General anesthetics, especially ketamine, inhibit NMDA receptors and reduce Ca^{2+} signaling (Duman et al., 2019), likely to regulate glymphatic function through this mechanism. The anesthetic sevoflurane induces changes in astrocyte morphogenesis by downregulating ezrin, an actin-binding membrane-bound protein, in addition to disrupting astrocyte Ca^{2+} currents acutely and chronically (Zhou et al., 2019). Moreover, brain surgery such as cisterna magna puncture can cause spontaneous frequent but asynchronous astrocytic Ca^{2+} signaling and impair glymphatic lipid transport, consequently increasing intracellular lipid accumulation (Rangroo Thrane et al., 2013).

AQP4 colocalizes the inwardly rectifying potassium channel Kir4.1 and contributes to the coupled influx of water and K^+ after neuronal activity (Jo et al., 2015). Accordingly, some anesthetics can impair AQP4 function by blocking potassium channels (Ou et al., 2020), leading to glymphatic function changes. In recent studies, 2.5% sevoflurane has also been shown to increase glymphatic function by upregulating AQP4 expression in astrocytes (Gao et al., 2019). Changes in AQP4 expression and depolarization are functionally relevant to the glymphatic system and cognition (Hubbard et al., 2018).

GLYMPHATIC FUNCTION AFFECTED BY SURGERY

Persistent systemic inflammation caused by surgery can disrupt the integrity of the BBB (Vacas et al., 2014; Hughes et al., 2016; Bi et al., 2017; Wang et al., 2017; Ni et al., 2018; Verheggen et al., 2018). The BBB is a complex functional and anatomical system that prevents the entry of neurotoxic plasma elements, blood cells, and pathogens into the brain. It is comprised of endothelial cells, perivascular microglia, pericytes, neurons, and astrocytic end-feet (Sweeney et al., 2019). Tight junction proteins located between adjacent endothelial cells include claudins, tricellulin, occludin, and zonula occludens (Sweeney et al., 2019). Acute endothelial dysfunction caused by surgically induced systemic inflammation may lead to BBB disorders (Plog et al., 2015; Ekeloef et al., 2017). Inflammation after laparotomy can decrease the levels of tight junction

proteins such as claudin, β-catenin, occludins, and ZO-1, all of which can contribute to tight junctions and BBB permeability (Yang et al., 2017). Moreover, astrocytes are easily activated by postoperative inflammatory cytokines such as TNF-α, IL-1β, IL-6, complement C3, and high mobility group box-1, which can subsequently damage the integrity of the BBB, especially in the hippocampus (He et al., 2012; Jin et al., 2014; Xiong et al., 2018). Activated astrocytes can also encourage tissue proliferation, resulting in scar-like perivascular barriers (Voskuhl et al., 2009). The endothelial cell membrane and the BBB close junctions comprise the vascular components of the glymphatic system, while the avascular components consist of astrocyte end-feet integrated with glia-line boundaries between the neuropil and axon tract regions (Plog and Nedergaard, 2018). Therefore, systemic inflammation influences the function of the glymphatic system based on the evidence that the structure and function of the glymphatic system are closely related to that of the BBB (Verheggen et al., 2018). Notably, a recent study found that lipopolysaccharide-induced systemic inflammation reduced perivascular CSF tracer flow and penetration into the parenchyma (Manouchehrian et al., 2021). These observations may be beneficial for our understanding of the role of systemic inflammation in glymphatic clearance.

How the Surgical Position Influences Glymphatic Transport

Researchers have studied the effects of body position on glymphatic function and Aβ clearance using optical imaging, CSF radiotracers, and fluorescent tracers in the brains of anesthetized rodents. According to previous studies, glymphatic transport is most effective in the lateral position, inferior in the supine position, and least efficient in the prone position (Lee et al., 2015). Thus, it is clear that postural or gravitational factors also exert regulatory control over the glymphatic pathway. Thus, we speculate that in postures with the head down, minor changes in CSF pressure, such as ICP and hydrostatic pressure, increase due to gravity; tissue pressure or vascular function could alter the shape of perivascular spaces and accelerate glymphatic drainage problems, impairing cognitive function.

Although PND was initially described as a complication after cardiac surgery, many recent studies have found that some patients undergoing non-cardiac surgeries, such as orthopedic surgery, also suffered cognitive decline (Evered and Silbert, 2018). Due to the various types of surgery, surgical posture may be an essential but overlooked factor in these studies. Some prone surgeries, particularly spine surgery, may cause postoperative cognitive impairment (Kim et al., 2016; Ezhevskaya et al., 2019). Furthermore, Trendelenburg, a supine position used in laparoscopic surgery in which the patient's head is lower than the feet, can result in postoperative cognitive decline. This position could increase intra-abdominal pressure, reduce cerebral venous outflow, and impair lymphatic function, similar to positive pressure ventilation or positive end-expiratory pressure (Maerz et al., 2017). Some studies have even demonstrated that sleeping in the supine position has been shown to reduce cognitive function in healthy volunteers, while sleeping in the upright position did not affect the participants (Muehlhan et al., 2014). According to studies on posture and glymphatic function, the surgical position can worsen the cognitive impairment, especially in prolonged surgeries, including cardiac surgery. Understanding the effects of different body postures on the glymphatic clearance pathway may be necessary for interpreting the procedure of PND.

Perioperative Sleep Disorder Leads to Glymphatic Dysfunction

The clearance of the glymphatic system is closely related to the sleep-wake cycle, with sleep promoting faster metabolite removal (Xie L. et al., 2013). However, perioperative sleep is frequently disrupted by many factors, including postoperative pain, environmental and surgical stress, anesthesia, and other factors that lead to discomfort (Whitlock et al., 2017; Su and Wang, 2018). Postoperative sleep disruptions manifest as sleep fragmentation and reduced slow-wave and REM sleep durations (Chouchou et al., 2014). In particular, REM sleep disorder may significantly negatively affect postoperative cognition (Lazic et al., 2017). Subsequently, the glymphatic system is impaired and degrades with sleep disturbances (Nedergaard and Goldman, 2020). After a night of sleep deprivation, protein Aβ levels in the thalamus and medial temporal structures are also elevated in healthy individuals (Shokri-Kojori et al., 2018). Moreover, sleep disruption increases the neuronal activity and generates more waste products, including lactate, which are exported via glymphatic fluid transport (Lundgaard et al., 2017).

Postoperative pain remains a significant health care issue that disturbs sleep in the postoperative period, and sleep disturbances may, in turn, exacerbate postoperative pain (Chouchou et al., 2014). Anesthesia is substantially different from natural sleep, sometimes interfering with the circadian rhythm and disrupting the sleep cycle, subsequently affecting glymphatic clearance (Lazic et al., 2017). Additionally, surgical and environmental stress appears to be a significant cause of sleep disruptions during peri-operation (Xu et al., 2016), and chronic stress via glucocorticoid signaling impairs AQP4-mediated glymphatic transport (Wei et al., 2019). This evidence suggests that cognitive decline in patients with sleep disorders may be caused by decreased waste removal and increased waste accumulation in the brain due to glymphatic dysfunction.

Currently, in animal models of glymphatic function, sleep is simulated by anesthesia or sleep deprivation. Owing to technical limitations, it is difficult to perform such experiments on naturally sleeping mice (Xie L. et al., 2013). According to some studies, the effects of sleep and general anesthesia on the glymphatic system are equivalent (Xie L. et al., 2013; Benveniste et al., 2019a). However, anesthesia and natural sleep outcomes remain markedly different; anesthesia can affect hemodynamics, interfere with the biological clock, and disrupt the sleep cycle (Lazic et al., 2017). Thus, the impact of anesthesia on the glymphatic system needs to be investigated further.

WHY SOME PATIENTS ARE SUSCEPTIBLE TO PND

Notably, the adverse cerebral effects of anesthesia were primarily reported in the elderly (Bedford, 1955; Berger et al., 2015). It is not yet fully understood why elderly patients are highly susceptible to PND, while young people who undergo surgery rarely develop it (Hu et al., 2020). Researchers have discovered some PND-susceptible patients with preoperative disease, such as preclinical AD (Xu et al., 2014), hyperglycemia (Zhang et al., 2014), cerebral microemboli (Wang et al., 2020), and other underlying neurovascular diseases or neurodegeneration (Wang et al., 2020). These preoperative diseases may share common underlying mechanisms and contribute to neurocognitive dysfunction or dementia. With advances in imaging technology, it has been found that these diseases have glymphatic impairment (Gaberel et al., 2014; Kress et al., 2014; Kyrtsos and Baras, 2015; Jiang et al., 2017; Hadjihambi et al., 2019). A theory states that susceptible patients with PND and aging have preexisting glymphatic dysfunction but progresses slowly without significant cognitive impairment (Bolte et al., 2020). Perioperative risk factors exacerbate the preexisting glymphatic damage beyond the compensatory limit, resulting in significant cognitive changes in these individuals. AD is a progressive neurodegenerative disorder characterized by gradual cognitive decline, which is characteristic of extracellular Aβ deposition and intracellular accumulation of hyperphosphorylated tau (Long and Holtzman, 2019). Patients in the preclinical stage of AD, particularly those with APOE4 genetic risk factors (Mentis et al., 2020), already have Aβ accumulation and impaired glymphatic clearance, but no clinically detectable symptoms of cognitive impairment (Masters et al., 2015). Moreover, aging is associated with degenerative changes in the brain's structure and function, such as reduced cerebrovascular pulsatility, depolarized or downregulated AQP4, and sleep deprivation, which impair glymphatic function (Zeppenfeld et al., 2017). Glymphatic dysfunction may result in the deposition of toxic solutes (including amyloid) in the aging brain, which exacerbates glymphatic dysfunction and creates a vicious cycle (Iliff et al., 2013). Vascular dementia is caused by many neurovascular diseases, including hypertension, ischemic stroke, traumatic brain injury, and microinfarcts, which significantly impair arterial CSF pulsation and glymphatic clearance (Riba-Llena et al., 2018). Diabetes can also impair cardiac pulsation due to pathological changes in the vascular endothelium (Jiang et al., 2017).

Due to technical limitations, few previous studies have used non-invasive methods to investigate glymphatic function in humans, particularly hospitalized surgical patients susceptible to PND. Recent advances in imaging, such as real-time MRI (Ding et al., 2018), ultra-fast MRI (Kiviniemi et al., 2016), and gadolinium-based contrast agents enhanced MRI (Ringstad et al., 2018; Deike-Hofmann et al., 2019), will provide a sensitive and non-invasive tool for assessing glymphatic function in clinical trials. Notably, it is essential to develop intraoperative monitoring tools for glymphatic function. A new method of measuring human glymphatic function that uses near-infrared spectroscopy has been developed for long-term monitoring of brain function, which is highly compatible with perioperative monitoring (Myllylä et al., 2018). These non-invasive methods may help translate glymphatic measurements from the laboratory to the clinic (Jiang, 2019). Advances in technology will yield new and valuable information about the glymphatic system, providing a quantitative map for the diagnosis, monitoring, and prognosis of neurological disorders, including PND.

CONCLUSION AND PERSPECTIVE

Recent discoveries concerning the glymphatic system anatomy and mechanisms have contributed to a better understanding of CSF circulation and waste removal. Furthermore, the glymphatic system has an immune function and may affect the onset and progression of PND, either directly or indirectly. Because clinical research on perioperative glymphatic changes is still lacking, scientists and clinicians, particularly gerontologists, neurologists, psychiatrists, anesthesiologists, and surgeons, can collaborate to uncover the etiological mechanisms of perioperative glymphatic changes. The glymphatic concept may provide a strategic breakthrough in rethinking, treating, and, most importantly, preventing PND.

Human studies exploring the physiological and pathological mechanisms between the glymphatic system and brain cognition over time have greatly improved our knowledge; however, some key issues still need to be addressed by future research. First, the definition of normal or healthy glymphatic function may be one of the biggest challenges. A simpler and quicker intraoperative monitoring method remains to be developed. A better description of glymphatic dynamics will help demarcate "normal" and "abnormal" glymphatic function in humans and identify preventive strategies for PND. Second, perioperative factors such as anesthetic type, intraoperative hemodynamics, surgery position, surgical inflammation, and previous health status may confound research on the glymphatic system and PND. Cross-sectional clinical studies have demonstrated specific changes in the glymphatic transport of patients susceptible to neurological diseases, which is helpful in predicting the incidence of PND. Third, more clinical studies should be conducted instead of purely animal studies. Although association analysis may provide critical information for cause-effect deductions, correlation does not necessarily mean causation. Fourth, basic research targeting the perioperative glymphatic system in PND merits optimization; specifically, appropriate model systems should be carefully selected. Finally, the translation of basic research results into clinically relevant effects in humans should be expedited. Most data on the role of the glymphatic system are based on animal studies. Preclinical animal studies frequently result in unexpected failures during clinical transition due to unidentified reasons. Alternatively, future therapeutic interventions will likely be based on individual factors due to significant differences in anatomical variation and disease complexity among human populations.

AUTHOR CONTRIBUTIONS

XR, GZ, LL, and CL contributed significantly to conception of the review and edited the review. XR undertook the literature, drafted, and corrected most of the manuscript and tables. SL, KL, and HL assisted with part of the pictures and manuscript. CL contributed to the sections of glymphatic system and anaesthetics. All authors contributed to the article and approved the submitted version.

REFERENCES

Abbott, N., J., Pizzo, M., E., Preston, J., E., Janigro, D., and Thorne, R., G. (2018). The role of brain barriers in fluid movement in the CNS: is there a 'glymphatic' system? *Acta Neuropatol.* 135, 387–407. doi: 10.1007/s00401-018-1812-4

Abrahamov, D., Levran, O., Naparstek, S., Refaeli, Y., Kaptson, S., Abu Salah, M., et al. (2017). Blood-brain barrier disruption after cardiopulmonary bypass: diagnosis and correlation to cognition. *Ann. Thorac. Surg.* 104, 161–169. doi: 10.1016/j.athoracsur.2016.10.043

Alawieh, A., Langley, E. F., and Tomlinson, S. (2018). Targeted complement inhibition salvages stressed neurons and inhibits neuroinflammation after stroke in mice. *Sci. Transl. Med.* 10:eaao6459. doi: 10.1126/scitranslmed.aao6459

Alonso-Lana, S., Marquié, M., Ruiz, A., and Boada, M. (2020). Cognitive and neuropsychiatric manifestations of COVID-19 and effects on elderly individuals with dementia. *Front. Aging Neurosci.* 12:588872. doi: 10.3389/fnagi.2020.588872

Amiry-Moghaddam, M., Otsuka, T., Hurn, P. D., Traystman, R. J., Haug, F. M., Froehner, S. C., et al. (2003). An alpha-syntrophin-dependent pool of AQP4 in astroglial end-feet confers bidirectional water flow between blood and brain. *Proc. Natl. Acad. Sci. U.S.A.* 100, 2106–2111. doi: 10.1073/pnas.0437946100

Bedford, P. D. (1955). Adverse cerebral effects of anaesthesia on old people. *Lancet* 269, 259–263. doi: 10.1016/S0140-6736(55)92689-1

Benveniste, H., Heerdt, P. M., Fontes, M., Rothman, D. L., and Volkow, N. D. (2019a). Glymphatic system function in relation to anesthesia and sleep states. *Anesth. Analg.* 128, 747–758. doi: 10.1213/ANE.0000000000004069

Benveniste, H., Lee, H., and Volkow, N. D. (2017). The glymphatic pathway: waste removal from the CNS via cerebrospinal fluid transport. *Neuroscientist* 23, 454–465. doi: 10.1177/1073858417691030

Benveniste, H., Liu, X., Koundal, S., Sanggaard, S., Lee, H., and Wardlaw, J. (2019b). The glymphatic system and waste clearance with brain aging: a review. *Gerontology* 65, 106–119. doi: 10.1159/000490349

Berger, M., Nadler, J. W., Browndyke, J., Terrando, N., Ponnusamy, V., Cohen, H. J., et al. (2015). Postoperative cognitive dysfunction: minding the gaps in our knowledge of a common postoperative complication in the elderly. *Anesthesiol. Clin.* 33, 517–550. doi: 10.1016/j.anclin.2015.05.008

Berger, M., Oyeyemi, D., Olurinde, M. O., Whitson, H. E., Weinhold, K. J., Woldorff, M. G., et al. (2019). The INTUIT study: investigating neuroinflammation underlying postoperative cognitive dysfunction. *J. Am. Geriatr. Soc.* 67, 794–798. doi: 10.1111/jgs.15770

Bi, J., Shan, W., Luo, A., and Zuo, Z. (2017). Critical role of matrix metallopeptidase 9 in postoperative cognitive dysfunction and age-dependent cognitive decline. *Oncotarget* 8, 51817–51829. doi: 10.18632/oncotarget.15545

Bilotta, F., Giordano, G., Sergi, P. G., and Pugliese, F. (2019). Harmful effects of mechanical ventilation on neurocognitive functions. *Crit. Care* 23:273. doi: 10.1186/s13054-019-2546-y

Bolte, A. C., Dutta, A. B., Hurt, M. E., Smirnov, I., Kovacs, M. A., McKee, C. A., et al. (2020). Meningeal lymphatic dysfunction exacerbates traumatic brain injury pathogenesis. *Nat. Commun.* 11:4524. doi: 10.1038/s41467-020-18113-4

Brown, E. N., Lydic, R., and Schiff, N. D. (2010). General anesthesia, sleep, and coma. *N. Engl. J. Med.* 363, 2638–2650. doi: 10.1056/NEJMra0808281

Calsolaro, V., and Edison, P. (2016). Neuroinflammation in Alzheimer's disease: current evidence and future directions. *Alzheimers Dement.* 12, 719–732. doi: 10.1016/j.jalz.2016.02.010

Campbell, I. G. (2009). EEG recording and analysis for sleep research. *Curr. Protoc. Neurosci.* Chapter 10, Unit10.12. doi: 10.1002/0471142301.ns1002s49

Chen, H., Chen, K., Xu, J. Q., Zhang, Y. R., Yu, R. G., and Zhou, J. X. (2018). Intracranial pressure responsiveness to positive end-expiratory pressure is influenced by chest wall elastance: a physiological study in patients with aneurysmal subarachnoid hemorrhage. *BMC Neurol.* 18:124. doi: 10.1186/s12883-018-1132-2

Chouchou, F., Khoury, S., Chauny, J. M., Denis, R., and Lavigne, G. J. (2014). Postoperative sleep disruptions: a potential catalyst of acute pain? *Sleep Med. Rev.* 18, 273–282. doi: 10.1016/j.smrv.2013.07.002

Cunningham, E. L., McGuinness, B., McAuley, D. F., Toombs, J., Mawhinney, T., O'Brien, S., et al. (2019). CSF Beta-amyloid 1-42 concentration predicts delirium following elective arthroplasty surgery in an observational cohort study. *Ann. Surg.* 269, 1200–1205. doi: 10.1097/SLA.0000000000002684

Damkier, H. H., Brown, P. D., and Praetorius, J. (2013). Cerebrospinal fluid secretion by the choroid plexus. *Physiol. Rev.* 93, 1847–1892. doi: 10.1152/physrev.00004.2013

Deike-Hofmann, K., Reuter, J., Haase, R., Paech, D., Gnirs, R., Bickelhaupt, S., et al. (2019). Glymphatic pathway of gadolinium-based contrast agents through the brain: overlooked and misinterpreted. *Invest. Radiol.* 54, 229–237. doi: 10.1097/RLI.0000000000000533

Deschamps, A., Saha, T., El-Gabalawy, R., Jacobsohn, E., Overbeek, C., Palermo, J., et al. (2019). Protocol for the electroencephalography guidance of anesthesia to alleviate geriatric syndromes (ENGAGES-Canada) study: a pragmatic, randomized clinical trial. *F1000Res.* 8:1165. doi: 10.12688/f1000research.19213.1

Dijk, D. J. (1999). Circadian variation of EEG power spectra in NREM and REM sleep in humans: dissociation from body temperature. *J. Sleep Res.* 8, 189–195. doi: 10.1046/j.1365-2869.1999.00159.x

Ding, G., Chopp, M., Li, L., Zhang, L., Davoodi-Bojd, E., Li, Q., et al. (2018). MRI investigation of glymphatic responses to Gd-DTPA infusion rates. *J. Neurosci. Res.* 96, 1876–1886. doi: 10.1002/jnr.24325

Dreha-Kulaczewski, S., Joseph, A. A., Merboldt, K. D., Ludwig, H. C., Gärtner, J., and Frahm, J. (2015). Inspiration is the major regulator of human CSF flow. *J. Neurosci.* 35, 2485–2491. doi: 10.1523/JNEUROSCI.3246-14.2015

Duman, R. S., Shinohara, R., Fogaça, M. V., and Hare, B. (2019). Neurobiology of rapid-acting antidepressants: convergent effects on GluA1-synaptic function. *Mol. Psychiatry* 24, 1816–1832. doi: 10.1038/s41380-019-0400-x

Eckenhoff, R. G., Maze, M., Xie, Z., Culley, D. J., Goodlin, S. J., Zuo, Z., et al. (2020). Perioperative neurocognitive disorder: state of the preclinical science. *Anesthesiology* 132, 55–68. doi: 10.1097/ALN.0000000000002956

Eide, P. K., and Ringstad, G. (2019). Delayed clearance of cerebrospinal fluid tracer from entorhinal cortex in idiopathic normal pressure hydrocephalus: a glymphatic magnetic resonance imaging study. *J. Cereb. Blood Flow Metab.* 39, 1355–1368. doi: 10.1177/0271678X18760974

Ekeloef, S., Larsen, M. H., Schou-Pedersen, A. M., Lykkesfeldt, J., Rosenberg, J., and Gögenür, I. (2017). Endothelial dysfunction in the early postoperative period after major colon cancer surgery. *Br. J. Anaesth.* 118, 200–206. doi: 10.1093/bja/aew410

Evered, L., Silbert, B., Knopman, D. S., Scott, D. A., DeKosky, S. T., Rasmussen, L. S., et al. (2018a). Recommendations for the nomenclature of cognitive change associated with anaesthesia and surgery-2018. *Anesthesiology* 129, 872–879. doi: 10.1097/ALN.0000000000002334

Evered, L., Silbert, B., Scott, D. A., Ames, D., Maruff, P., and Blennow, K. (2016). Cerebrospinal fluid biomarker for Alzheimer disease predicts postoperative cognitive dysfunction. *Anesthesiology* 124, 353–361. doi: 10.1097/ALN.0000000000000953

Evered, L., Silbert, B., Scott, D. A., Zetterberg, H., and Blennow, K. (2018b). Association of changes in plasma neurofilament light and tau levels with anesthesia and surgery: results from the CAPACITY and ARCADIAN studies. *JAMA Neurol.* 75, 542–547. doi: 10.1001/jamaneurol.2017.4913

Evered, L. A., and Silbert, B. S. (2018). Postoperative cognitive dysfunction and noncardiac surgery. *Anesth. Analg.* 127, 496–505. doi: 10.1213/ANE.0000000000003514

Ezhevskaya, A. A., Ovechkin, A. M., Prusakova, Z. B., Zagrekov, V. I., Mlyavykh, S. G., and Anderson, D. G. (2019). Relationship among anesthesia technique, surgical stress, and cognitive dysfunction following spinal surgery: a randomized trial. *J. Neurosurg. Spine*. doi: 10.3171/2019.4.SPINE184. [Epub ahead of print].

Foss, N. B., and Kehlet, H. (2019). Perioperative haemodynamics and vasoconstriction: time for reconsideration? *Br. J. Anaesth.* 123, 100–103. doi: 10.1016/j.bja.2019.04.052

Fultz, N. E., Bonmassar, G., Setsompop, K., Stickgold, R. A., Rosen, B. R., Polimeni, J. R., et al. (2019). Coupled electrophysiological, hemodynamic, and cerebrospinal fluid oscillations in human sleep. *Science* 366, 628–631. doi: 10.1126/science.aax5440

Fuxe, K., Agnati, L. F., Marcoli, M., and Borroto-Escuela, D. O. (2015). Volume transmission in central dopamine and noradrenaline neurons and its astroglial targets. *Neurochem. Res.* 40, 2600–2614. doi: 10.1007/s11064-015-1574-5

Gaberel, T., Gakuba, C., Goulay, R., Martinez De Lizarrondo, S., Hanouz, J. L., Emery, E., et al. (2014). Impaired glymphatic perfusion after strokes revealed by contrast-enhanced MRI: a new target for fibrinolysis? *Stroke* 45, 3092–3096. doi: 10.1161/STROKEAHA.114.006617

Gakuba, C., Gaberel, T., Goursaud, S., Bourges, J., Di Palma, C., Quenault, A., et al. (2018). General anesthesia inhibits the activity of the "glymphatic system". *Theranostics* 8, 710–722. doi: 10.7150/thno.19154

Gao, X., Ming, J., Liu, S., Lai, B., Fang, F., and Cang, J. (2019). Sevoflurane enhanced the clearance of Aβ1-40 in hippocampus under surgery via up-regulating AQP-4 expression in astrocyte. *Life Sci.* 221, 143–151. doi: 10.1016/j.lfs.2019.02.024

Gerlach, R. M., and Chaney, M. A. (2018). Postoperative cognitive dysfunction related to Alzheimer disease? *J. Thorac. Cardiovasc. Surg.* 155, 968–969. doi: 10.1016/j.jtcvs.2017.10.113

Groothuis, D. R., Vavra, M. W., Schlageter, K. E., Kang, E. W., Itskovich, A. C., Hertzler, S., et al. (2007). Efflux of drugs and solutes from brain: the interactive roles of diffusional transcapillary transport, bulk flow and capillary transporters. *J. Cereb. Blood Flow Metab.* 27, 43–56. doi: 10.1038/sj.jcbfm.9600315

Hablitz, L. M., Plá, V., Giannetto, M., Vinitsky, H. S., Stæger, F. F., Metcalfe, T., et al. (2020). Circadian control of brain glymphatic and lymphatic fluid flow. *Nat. Commun.* 11:4411. doi: 10.1038/s41467-020-18115-2

Hablitz, L. M., Vinitsky, H. S., Sun, Q., Stæger, F. F., Sigurdsson, B., Mortensen, K. N., et al. (2019). Increased glymphatic influx is correlated with high EEG delta power and low heart rate in mice under anesthesia. *Sci. Adv.* 5:eaav5447. doi: 10.1126/sciadv.aav5447

Hadjihambi, A., Harrison, I. F., Costas-Rodríguez, M., Vanhaecke, F., Arias, N., Gallego-Durán, R., et al. (2019). Impaired brain glymphatic flow in experimental hepatic encephalopathy. *J. Hepatol.* 70, 40–49. doi: 10.1016/j.jhep.2018.08.021

Harrison, I. F., Ismail, O., Machhada, A., Colgan, N., Ohene, Y., Nahavandi, P., et al. (2020). Impaired glymphatic function and clearance of tau in an Alzheimer's disease model. *Brain* 143, 2576–2593. doi: 10.1093/brain/awaa179

He, H. J., Wang, Y., Le, Y., Duan, K. M., Yan, X. B., Liao, Q., et al. (2012). Surgery upregulates high mobility group box-1 and disrupts the blood-brain barrier causing cognitive dysfunction in aged rats. *CNS Neurosci. Therap.* 18, 994–1002. doi: 10.1111/cns.12018

Helms, J., Kremer, S., Merdji, H., Schenck, M., Severac, F., Clere-Jehl, R., et al. (2020). Delirium and encephalopathy in severe COVID-19: a cohort analysis of ICU patients. *Crit. Care* 24:491. doi: 10.1186/s13054-020-03200-1

Herridge, M. S., Moss, M., Hough, C. L., Hopkins, R. O., Rice, T. W., Bienvenu, O. J., et al. (2016). Recovery and outcomes after the acute respiratory distress syndrome (ARDS) in patients and their family caregivers. *Intensive Care Med.* 42, 725–738. doi: 10.1007/s00134-016-4321-8

Hu, N., Guo, D., Wang, H., Xie, K., Wang, C., Li, Y., et al. (2014). Involvement of the blood-brain barrier opening in cognitive decline in aged rats following orthopedic surgery and high concentration of sevoflurane inhalation. *Brain Res.* 1551, 13–24. doi: 10.1016/j.brainres.2014.01.015

Hu, Z., Zhang, F., Liao, Q., and Ouyang, W. (2020). The glymphatic system: a potential pathophysiological focus for perioperative neurocognitive disorder. *Explor. Res. Hypothesis Med.* 6, 24–27. doi: 10.14218/ERHM.2020.00041

Hubbard, J. A., Szu, J. I., and Binder, D. K. (2018). The role of aquaporin-4 in synaptic plasticity, memory and disease. *Brain Res. Bull.* 136, 118–129. doi: 10.1016/j.brainresbull.2017.02.011

Huber-Lang, M., Lambris, J. D., and Ward, P. A. (2018). Innate immune responses to trauma. *Nat. Immunol.* 19, 327–341. doi: 10.1038/s41590-018-0064-8

Hughes, C. G., Pandharipande, P. P., Thompson, J. L., Chandrasekhar, R., Ware, L. B., Ely, E. W., et al. (2016). Endothelial activation and blood-brain barrier injury as risk factors for delirium in critically ill patients. *Crit. Care Med.* 44, e809–e817. doi: 10.1097/CCM.0000000000001739

Iliff, J. J., Wang, M., Liao, Y., Plogg, B. A., Peng, W., Gundersen, G. A., et al. (2012). A paravascular pathway facilitates CSF flow through the brain parenchyma and the clearance of interstitial solutes, including amyloid β. *Sci. Transl. Med.* 4:147ra111. doi: 10.1126/scitranslmed.3003748

Iliff, J. J., Wang, M., Zeppenfeld, D. M., Venkataraman, A., Plog, B. A., Liao, Y., et al. (2013). Cerebral arterial pulsation drives paravascular CSF-interstitial fluid exchange in the murine brain. *J. Neurosci.* 33, 18190–18199. doi: 10.1523/JNEUROSCI.1592-13.2013

Jessen, N. A., Munk, A. S., Lundgaard, I., and Nedergaard, M. (2015). The glymphatic system: a beginner's guide. *Neurochem. Res.* 40, 2583–2599. doi: 10.1007/s11064-015-1581-6

Jiang, Q. (2019). MRI and glymphatic system. *Stroke Vasc. Neurol.* 4, 75–77. doi: 10.1136/svn-2018-000197

Jiang, Q., Zhang, L., Ding, G., Davoodi-Bojd, E., Li, Q., Li, L., et al. (2017). Impairment of the glymphatic system after diabetes. *J. Cereb. Blood Flow Metab.* 37, 1326–1337. doi: 10.1177/0271678X16654702

Jin, W. J., Feng, S. W., Feng, Z., Lu, S. M., Qi, T., and Qian, Y. N. (2014). Minocycline improves postoperative cognitive impairment in aged mice by inhibiting astrocytic activation. *Neuroreport* 25, 1–6. doi: 10.1097/WNR.0000000000000082

Jo, A. O., Ryskamp, D. A., Phuong, T. T., Verkman, A. S., Yarishkin, O., MacAulay, N., et al. (2015). TRPV4 and AQP4 channels synergistically regulate cell volume and calcium homeostasis in retinal müller glia. *J. Neurosci.* 35, 13525–13537. doi: 10.1523/JNEUROSCI.1987-15.2015

Kettenmann, H., Hanisch, U. K., Noda, M., and Verkhratsky, A. (2011). Physiology of microglia. *Physiol. Rev.* 91, 461–553. doi: 10.1152/physrev.00011.2010

Kim, J., Shim, J. K., Song, J. W., Kim, E. K., and Kwak, Y. L. (2016). Postoperative cognitive dysfunction and the change of regional cerebral oxygen saturation in elderly patients undergoing spinal surgery. *Anesth. Analg.* 123, 436–444. doi: 10.1213/ANE.0000000000001352

Kiviniemi, V., Wang, X., Korhonen, V., Keinänen, T., Tuovinen, T., Autio, J., et al. (2016). Ultra-fast magnetic resonance encephalography of physiological brain activity - Glymphatic pulsation mechanisms? *J. Cereb. Blood Flow Metab.* 36, 1033–1045. doi: 10.1177/0271678X15622047

Koundal, S., Elkin, R., Nadeem, S., Xue, Y., Constantinou, S., Sanggaard, S., et al. (2020). Optimal mass transport with lagrangian workflow reveals advective and diffusion driven solute transport in the glymphatic system. *Sci. Rep.* 10:1990. doi: 10.1038/s41598-020-60586-2

Kress, B. T., Iliff, J. J., Xia, M., Wang, M., Wei, H. S., Zeppenfeld, D., et al. (2014). Impairment of paravascular clearance pathways in the aging brain. *Ann. Neurol.* 76, 845–861. doi: 10.1002/ana.24271

Kyrtsos, C. R., and Baras, J. S. (2015). Modeling the role of the glymphatic pathway and cerebral blood vessel properties in Alzheimer's disease pathogenesis. *PLoS ONE* 10:e0139574. doi: 10.1371/journal.pone.0139574

Lazic, K., Petrovic, J., Ciric, J., Kalauzi, A., and Saponjic, J. (2017). REM sleep disorder following general anesthesia in rats. *Physiol. Behav.* 168, 41–54. doi: 10.1016/j.physbeh.2016.10.013

Lee, H., Xie, L., Yu, M., Kang, H., Feng, T., Deane, R., et al. (2015). The effect of body posture on brain glymphatic transport. *J. Neurosci.* 35, 11034–11044. doi: 10.1523/JNEUROSCI.1625-15.2015

Liddelow, S. A., Guttenplan, K. A., Clarke, L. E., Bennett, F. C., Bohlen, C. J., Schirmer, L., et al. (2017). Neurotoxic reactive astrocytes are induced by activated microglia. *Nature* 541, 481–487. doi: 10.1038/nature21029

Lilius, T. O., Blomqvist, K., Hauglund, N. L., Liu, G., Stæger, F. F., Bærentzen, S., et al. (2019b). Dexmedetomidine enhances glymphatic brain delivery of intrathecally administered drugs. *J. Controlled Release* 304, 29–38.

Lilius, T. O., Blomqvist, K., Hauglund, N. L., Liu, G., Staeger, F. F., Baerentzen, S., et al. (2019a). Dexmedetomidine enhances glymphatic brain delivery of intrathecally administered drugs. *J. Controlled Release* 304, 29–38. doi: 10.1016/j.jconrel.2019.05.005

Liu, G., Mestre, H., Sweeney, A. M., Sun, Q., Weikop, P., Du, T., et al. (2020). Direct measurement of cerebrospinal fluid production in mice. *Cell Rep.* 33:108524. doi: 10.1016/j.celrep.2020.108524

Liu, L. R., Liu, J. C., Bao, J. S., Bai, Q. Q., and Wang, G. Q. (2020). Interaction of microglia and astrocytes in the neurovascular unit. *Front. Immunol.*11:1024. doi: 10.3389/fimmu.2020.01024

Long, J. M., and Holtzman, D. M. (2019). Alzheimer disease: an update on pathobiology and treatment strategies. *Cell* 179, 312–339. doi: 10.1016/j.cell.2019.09.001

Lundgaard, I., Lu, M. L., Yang, E., Peng, W., Mestre, H., Hitomi, E., et al. (2017). Glymphatic clearance controls state-dependent changes in brain lactate concentration. *J. Cereb. Blood Flow Metab.* 37, 2112–2124. doi: 10.1177/0271678X16661202

Maerz, D. A., Beck, L. N., Sim, A. J., and Gainsburg, D. M. (2017). Complications of robotic-assisted laparoscopic surgery distant from the surgical site. *Br. J. Anaesth.* 118, 492–503. doi: 10.1093/bja/aex003

Maneshi, M. M., Maki, B., Gnanasambandam, R., Belin, S., Popescu, G. K., Sachs, F., et al. (2017). Mechanical stress activates NMDA receptors in the absence of agonists. *Sci. Rep.* 7:39610. doi: 10.1038/srep39610

Manouchehrian, O., Ramos, M., Bachiller, S., Lundgaard, I., and Deierborg, T. (2021). Acute systemic LPS-exposure impairs perivascular CSF distribution in mice. *J. Neuroinflammation* 18:34. doi: 10.1186/s12974-021-02082-6

Masters, C. L., Bateman, R., Blennow, K., Rowe, C. C., Sperling, R. A., and Cummings, J. L. (2015). Alzheimer's disease. *Nat. Rev. Dis. Primers* 1:15056. doi: 10.1038/nrdp.2015.56

Meng, Y., Abrahao, A., Heyn, C. C., Bethune, A. J., Huang, Y., Pople, C. B., et al. (2019). Glymphatics visualization after focused ultrasound-induced blood-brain barrier opening in humans. *Ann. Neurol.* 86, 975–980. doi: 10.1002/ana.25604

Mentis, A. A., Dardiotis, E., and Chrousos, G. P. (2020). Apolipoprotein E4 and meningeal lymphatics in Alzheimer disease: a conceptual framework. *Mol. Psychiatry* 26, 1075–1097. doi: 10.1038/s41380-020-0731-7

Mestre, H., Hablitz, L. M., Xavier, A. L., Feng, W., Zou, W., Pu, T., et al. (2018a). Aquaporin-4-dependent glymphatic solute transport in the rodent brain. *eLife* 7:e40070. doi: 10.7554/eLife.40070

Mestre, H., Tithof, J., Du, T., Song, W., Peng, W., Sweeney, A. M., et al. (2018b). Flow of cerebrospinal fluid is driven by arterial pulsations and is reduced in hypertension. *Nat. Commun.* 9:4878. doi: 10.1038/s41467-018-07318-3

Miao, M., Xu, Y., Sun, M., Chang, E., Cong, X., and Zhang, J. (2019). BIS index monitoring and perioperative neurocognitive disorders in older adults: a systematic review and meta-analysis. *Aging Clin. Exp. Res.* 32, 2449–2458. doi: 10.1007/s40520-019-01433-x

Miller, D., Lewis, S. R., Pritchard, M. W., Schofield-Robinson, O. J., Shelton, C. L., Alderson, P., et al. (2018). Intravenous versus inhalational maintenance of anaesthesia for postoperative cognitive outcomes in elderly people undergoing non-cardiac surgery. *Cochrane Database Syst. Rev.* 8:Cd012317. doi: 10.1002/14651858.CD012317.pub2

Morrison, R. L., Fedgchin, M., Singh, J., Van Gerven, J., Zuiker, R., Lim, K. S., et al. (2018). Effect of intranasal esketamine on cognitive functioning in healthy participants: a randomized, double-blind, placebo-controlled study. *Psychopharmacology* 235, 1107–1119. doi: 10.1007/s00213-018-4828-5

Mortensen, K. N., Sanggaard, S., Mestre, H., Lee, H., Kostrikov, S., Xavier, A. L. R., et al. (2019). Impaired glymphatic transport in spontaneously hypertensive rats. *J. Neurosci.* 39, 6365–6377. doi: 10.1523/JNEUROSCI.1974-18.2019

Muehlhan, M., Marxen, M., Landsiedel, J., Malberg, H., and Zaunseder, S. (2014). The effect of body posture on cognitive performance: a question of sleep quality. *Front. Hum. Neurosci.* 8:171. doi: 10.3389/fnhum.2014.00171

Myllylä, T., Harju, M., Korhonen, V., Bykov, A., Kiviniemi, V., and Meglinski, I. (2018). Assessment of the dynamics of human glymphatic system by near-infrared spectroscopy. *J. Biophotonics* 11:e201700123. doi: 10.1002/jbio.201700123

Nathan, N. (2019). Inflamed in the membrane: neuroinflammation and perioperative neurocognitive disorders. *Anesth. Analg.* 128:604. doi: 10.1213/ANE.0000000000004098

Nedergaard, M. (2013). Neuroscience. Garbage truck of the brain. *Science* 340, 1529–1530. doi: 10.1126/science.1240514

Nedergaard, M., and Goldman, S. A. (2020). Glymphatic failure as a final common pathway to dementia. *Science* 370, 50–56. doi: 10.1126/science.abb8739

Ni, P., Dong, H., Wang, Y., Zhou, Q., Xu, M., Qian, Y., et al. (2018). IL-17A contributes to perioperative neurocognitive disorders through blood-brain barrier disruption in aged mice. *J. Neuroinflammation* 15:332. doi: 10.1186/s12974-018-1374-3

Ologunde, R., and Ma, D. (2011). Do inhalational anesthetics cause cognitive dysfunction? *Acta Anaesthesiol. Taiwan.* 49, 149–153. doi: 10.1016/j.aat.2011.11.001

Ou, M., Kuo, F. S., Chen, X., Kahanovitch, U., Olsen, M. L., Du, G., et al. (2020). Isoflurane inhibits a Kir4.1/5.1-like conductance in neonatal rat brainstem astrocytes and recombinant Kir4.1/5.1 channels in a heterologous expression system. *J. Neurophysiol.* 124, 740–749. doi: 10.1152/jn.00358.2020

Ozturk, B. O., Monte, B., Koundal, S., Dai, F., Benveniste, H., and Lee, H. (2021). Disparate volumetric fluid shifts across cerebral tissue compartments with two different anesthetics. *Fluids Barriers of the CNS* 18:1. doi: 10.1186/s12987-020-00236-x

Plog, B. A., Dashnaw, M. L., Hitomi, E., Peng, W., Liao, Y., Lou, N., et al. (2015). Biomarkers of traumatic injury are transported from brain to blood via the glymphatic system. *J. Neurosci.* 35, 518–526. doi: 10.1523/JNEUROSCI.3742-14.2015

Plog, B. A., and Nedergaard, M. (2018). The glymphatic system in central nervous system health and disease: past, present, and future. *Annu. Rev. Pathol.* 13, 379–394. doi: 10.1146/annurev-pathol-051217-111018

Rangroo Thrane, V., Thrane, A. S., Plog, B. A., Thiyagarajan, M., Iliff, J. J., Deane, R., et al. (2013). Paravascular microcirculation facilitates rapid lipid transport and astrocyte signaling in the brain. *Sci. Rep.* 3:2582. doi: 10.1038/srep02582

Ren, X., Lv, F., Fang, B., Liu, S., Lv, H., He, G., et al. (2014). Anesthetic agent propofol inhibits myeloid differentiation factor 88-dependent and independent signaling and mitigates lipopolysaccharide-mediated reactive oxygen species production in human neutrophils *in vitro*. *Eur. J. Pharmacol.* 744, 164–172. doi: 10.1016/j.ejphar.2014.10.030

Riba-Llena, I., Jiménez-Balado, J., Castañé, X., Girona, A., López-Rueda, A., Mundet, X., et al. (2018). Arterial stiffness is associated with basal ganglia enlarged perivascular spaces and cerebral small vessel disease load. *Stroke* 49, 1279–1281. doi: 10.1161/STROKEAHA.118.020163

Ringstad, G., Valnes, L. M., Dale, A. M., Pripp, A. H., Vatnehol, S. S., Emblem, K. E., et al. (2018). Brain-wide glymphatic enhancement and clearance in humans assessed with MRI. *JCI Insight* 3:e121537. doi: 10.1172/jci.insight.121537

Schenning, K. J., Murchison, C. F., Mattek, N. C., Silbert, L. C., Kaye, J. A., and Quinn, J. F. (2016). Surgery is associated with ventricular enlargement as well as cognitive and functional decline. *Alzheimers Dement.* 12, 590–597. doi: 10.1016/j.jalz.2015.10.004

Schiff, N. D. (2020). Central lateral thalamic nucleus stimulation awakens cortex via modulation of cross-regional, laminar-specific activity during general anesthesia. *Neuron* 106, 1–3. doi: 10.1016/j.neuron.2020.02.016

Scott, D. H. T. (2018). Non-invasive blood pressure measurement displays. *Anaesthesia* 73:1299. doi: 10.1111/anae.14433

Shalbaf, R., Behnam, H., and Jelveh Moghadam, H. (2015). Monitoring depth of anesthesia using combination of EEG measure and hemodynamic variables. *Cogn. Neurodyn.* 9, 41–51. doi: 10.1007/s11571-014-9295-z

Shi, Y., Thrippleton, M. J., Blair, G. W., Dickie, D. A., Marshall, I., Hamilton, I., et al. (2020). Small vessel disease is associated with altered cerebrovascular pulsatility but not resting cerebral blood flow. *J. Cereb. Blood Flow Metab.* 40, 85–99. doi: 10.1177/0271678X18803956

Shokri-Kojori, E., Wang, G. J., Wiers, C. E., Demiral, S. B., Guo, M., Kim, S. W., et al. (2018). β-Amyloid accumulation in the human brain after one night of sleep deprivation. *Proc. Natl. Acad. Sci. U.S.A.* 115, 4483–4488. doi: 10.1073/pnas.1721694115

Simon, M. J., and Iliff, J. J. (2016). Regulation of cerebrospinal fluid (CSF) flow in neurodegenerative, neurovascular and neuroinflammatory disease. *Biochim. Biophys. Acta* 1862, 442–451. doi: 10.1016/j.bbadis.2015.10.014

Smith, A. J., Yao, X., Dix, J. A., Jin, B. J., and Verkman, A. S. (2017). Test of the 'glymphatic' hypothesis demonstrates diffusive and aquaporin-4-independent solute transport in rodent brain parenchyma. *eLife* 6:e27679 doi: 10.7554/eLife.27679.019

Su, X., and Wang, D. X. (2018). Improve postoperative sleep: what can we do? *Curr. Opin. Anaesthesiol.* 31, 83–88. doi: 10.1097/ACO.0000000000000538

Subramaniyan, S., and Terrando, N. (2019). Neuroinflammation and perioperative neurocognitive disorders. *Anesth. Analg.* 128, 781–788. doi: 10.1213/ANE.0000000000004053

Sweeney, M. D., Zhao, Z., Montagne, A., Nelson, A. R., and Zlokovic, B. V. (2019). Blood-brain barrier: from physiology to disease and back. *Physiol. Rev.* 99, 21–78. doi: 10.1152/physrev.00050.2017

Tarasoff-Conway, J. M., Carare, R. O., Osorio, R. S., Glodzik, L., Butler, T., Fieremans, E., et al. (2015). Clearance systems in the brain-implications for Alzheimer disease. *Nat. Rev. Neurol.* 11, 457–470. doi: 10.1038/nrneurol.2015.119

Terrando, N., Eriksson, L. I., Ryu, J. K., Yang, T., Monaco, C., Feldmann, M., et al. (2011). Resolving postoperative neuroinflammation and cognitive decline. *Ann. Neurol.*70, 986–995. doi: 10.1002/ana.22664

Thomas, J. H. (2019). Fluid dynamics of cerebrospinal fluid flow in perivascular spaces. *J. R. Soc. Interface* 16:20190572. doi: 10.1098/rsif.2019.0572

Tithof, J., Kelley, D. H., Mestre, H., Nedergaard, M., and Thomas, J. H. (2019). Hydraulic resistance of periarterial spaces in the brain. *Fluids Barriers CNS* 16:19. doi: 10.1186/s12987-019-0140-y

Vacas, S., Degos, V., Tracey, K. J., and Maze, M. (2014). High-mobility group box 1 protein initiates postoperative cognitive decline by engaging bone marrow-derived macrophages. *Anesthesiology* 120, 1160–1167. doi: 10.1097/ALN.0000000000000045

Verheggen, I. C. M., Van Boxtel, M. P. J., Verhey, F. R. J., Jansen, J. F. A., and Backes, W. H. (2018). Interaction between blood-brain barrier and glymphatic system in solute clearance. *Neurosci. Biobehav. Rev.* 90, 26–33. doi: 10.1016/j.neubiorev.2018.03.028

Voskuhl, R. R., Peterson, R. S., Song, B., Ao, Y., Morales, L. B., Tiwari-Woodruff, S., et al. (2009). Reactive astrocytes form scar-like perivascular barriers to leukocytes during adaptive immune inflammation of the CNS. *J. Neurosci.* 29, 11511–11522. doi: 10.1523/JNEUROSCI.1514-09.2009

Wang, B., Li, S., Cao, X., Dou, X., Li, J., Wang, L., et al. (2017). Blood-brain barrier disruption leads to postoperative cognitive dysfunction. *Curr. Neurovasc. Res.* 14, 359–367. doi: 10.2174/1567202614666171009105825

Wang, P., Velagapudi, R., Kong, C., Rodriguiz, R. M., Wetsel, W. C., Yang, T., et al. (2020). Neurovascular and immune mechanisms that regulate postoperative delirium superimposed on dementia. *Alzheimers Dement.* 16, 734–749. doi: 10.1002/alz.12064

Wang, R., Chen, J., and Wu, G. (2015). Variable lung protective mechanical ventilation decreases incidence of postoperative delirium and cognitive dysfunction during open abdominal surgery. *Int. J. Clin. Exp. Med.* 8, 21208–21214.

Wei, F., Song, J., Zhang, C., Lin, J., Xue, R., Shan, L. D., et al. (2019). Chronic stress impairs the aquaporin-4-mediated glymphatic transport through glucocorticoid signaling. *Psychopharmacology* 236, 1367–1384. doi: 10.1007/s00213-018-5147-6

Whitlock, E. L., Diaz-Ramirez, L. G., Glymour, M. M., Boscardin, W. J., Covinsky, K. E., and Smith, A. K. (2017). Association between persistent pain and memory decline and dementia in a longitudinal cohort of elders. *JAMA Intern. Med.* 177, 1146–1153. doi: 10.1001/jamainternmed.2017.1622

Wink, J., de Wilde, R. B., Wouters, P. F., van Dorp, E. L., Veering, B. T., Versteegh, M. I., et al. (2016). Thoracic epidural anesthesia reduces right ventricular systolic function with maintained ventricular-pulmonary coupling. *Circulation* 134, 1163–1175. doi: 10.1161/CIRCULATIONAHA.116.022415

Xie, L., Kang, H., Xu, Q., Chen, M. J., Liao, Y., Thiyagarajan, M., et al. (2013). Sleep drives metabolite clearance from the adult brain. *Science* 342, 373–377. doi: 10.1126/science.1241224

Xie, Z., McAuliffe, S., Swain, C. A., Ward, S. A., Crosby, C. A., Zheng, H., et al. (2013). Cerebrospinal fluid aβ to tau ratio and postoperative cognitive change. *Ann. Surg.* 258, 364–369. doi: 10.1097/SLA.0b013e318298b077

Xiong, C., Liu, J., Lin, D., Zhang, J., Terrando, N., and Wu, A. (2018). Complement activation contributes to perioperative neurocognitive disorders in mice. *J. Neuroinflammation* 15:254. doi: 10.1186/s12974-018-1292-4

Xu, T., Wick, E. C., and Makary, M. A. (2016). Sleep deprivation and starvation in hospitalised patients: how medical care can harm patients. *BMJ Qual. Saf.* 25, 311–314. doi: 10.1136/bmjqs-2015-004395

Xu, Z., Dong, Y., Wang, H., Culley, D. J., Marcantonio, E. R., Crosby, G., et al. (2014). Age-dependent postoperative cognitive impairment and Alzheimer-related neuropathology in mice. *Sci. Rep.* 4:3766. doi: 10.1038/srep03766

Yamada, S., Miyazaki, M., Yamashita, Y., Ouyang, C., Yui, M., Nakahashi, M., et al. (2013). Influence of respiration on cerebrospinal fluid movement using magnetic resonance spin labeling. *Fluids Barriers CNS* 10:36. doi: 10.1186/2045-8118-10-36

Yang, S., Gu, C., Mandeville, E. T., Dong, Y., Esposito, E., Zhang, Y., et al. (2017). Anesthesia and surgery impair blood-brain barrier and cognitive function in mice. *Front. Immunol.* 8:902. doi: 10.3389/fimmu.2017.00902

Yang, T., and Terrando, N. (2019). The evolving role of specialized pro-resolving mediators in modulating neuroinflammation in perioperative neurocognitive disorders. *Adv. Exp. Med. Biol.* 1161, 27–35. doi: 10.1007/978-3-030-21735-8_4

Yang, T., Velagapudi, R., and Terrando, N. (2020). Neuroinflammation after surgery: from mechanisms to therapeutic targets. *Nat. Immunol.* 21, 1319–1326. doi: 10.1038/s41590-020-00812-1

Yang, T., Xu, G., Newton, P. T., Chagin, A. S., Mkrtchian, S., Carlström, M., et al. (2019). Maresin 1 attenuates neuroinflammation in a mouse model of perioperative neurocognitive disorders. *Br. J. Anaesth.* 122, 350–360. doi: 10.1016/j.bja.2018.10.062

Yu, P., Venkat, P., Chopp, M., Zacharek, A., Shen, Y., Liang, L., et al. (2019). Deficiency of tPA exacerbates white matter damage, neuroinflammation, glymphatic dysfunction and cognitive dysfunction in aging mice. *Aging Dis.* 10, 770–783. doi: 10.14336/AD.2018.0816

Zeppenfeld, D. M., Simon, M., Haswell, J. D., D'Abreo, D., Murchison, C., Quinn, J. F., et al. (2017). Association of perivascular localization of Aquaporin-4 with cognition and Alzheimer disease in aging brains. *JAMA Neurol.* 74, 91–99. doi: 10.1001/jamaneurol.2016.4370

Zhang, C., Lin, J., Wei, F., Song, J., Chen, W., Shan, L., et al. (2018). Characterizing the glymphatic influx by utilizing intracisternal infusion of fluorescently conjugated cadaverine. *Life Sci.* 201, 150–160. doi: 10.1016/j.lfs.2018.03.057

Zhang, H., Wu, Z., Zhao, X., and Qiao, Y. (2018). Role of dexmedetomidine in reducing the incidence of postoperative cognitive dysfunction caused by sevoflurane inhalation anesthesia in elderly patients with esophageal carcinoma. *J. Cancer Res. Therap.* 14, 1497–1502. doi: 10.4103/jcrt.JCRT_164_18

Zhang, X., Yan, X., Gorman, J., Hoffman, S. N., Zhang, L., and Boscarino, J. A. (2014). Perioperative hyperglycemia is associated with postoperative neurocognitive disorders after cardiac surgery. *Neuropsychiatr. Dis. Treat.* 10, 361–370. doi: 10.2147/NDT.S57761

Zhou, B., Chen, L., Liao, P., Huang, L., Chen, Z., Liao, D., et al. (2019). Astroglial dysfunctions drive aberrant synaptogenesis and social behavioral deficits in mice with neonatal exposure to lengthy general anesthesia. *PLoS Biol.* 17:e3000086. doi: 10.1371/journal.pbio.3000086

Conflict of Interest: The authors declare that the research was conducted in the absence of any commercial or financial relationships that could be construed as a potential conflict of interest.

frontiers in Aging Neuroscience

SYSTEMATIC REVIEW
published: 13 July 2021
doi: 10.3389/fnagi.2021.692942

Neuroimaging Markers of Cerebral Small Vessel Disease on Hemorrhagic Transformation and Functional Outcome After Intravenous Thrombolysis in Patients With Acute Ischemic Stroke: A Systematic Review and Meta-Analysis

Yiqiao Wang[1], Xiaoting Yan[1], Jie Zhan[2], Peiming Zhang[1], Guangming Zhang[1], Shuqi Ge[1], Hao Wen[3], Lin Wang[1], Nenggui Xu[1] and Liming Lu[1]**

[1] South China Research Center for Acupuncture and Moxibustion, Medical College of Acu-Moxi and Rehabilitation, Guangzhou University of Chinese Medicine, Guangzhou, China, [2] Postdoctoral Programme, The Second Affiliated Hospital of Guangzhou University of Chinese Medicine, Guangzhou, China, [3] Department of Neurology, The Sun Yat-sen Memorial Hospital of Sun Yat-sen University, Guangzhou, China

OPEN ACCESS

Edited by:
Cheryl Hawkes,
Lancaster University, United Kingdom

Reviewed by:
Sami Curtze,
University of Helsinki, Finland
Yuchuan Ding,
Wayne State University, United States

***Correspondence:**
Nenggui Xu
ngxu8018@163.com
Liming Lu
lulimingleon@126.com

Received: 09 April 2021
Accepted: 11 June 2021
Published: 13 July 2021

Citation:
Wang Y, Yan X, Zhan J, Zhang P, Zhang G, Ge S, Wen H, Wang L, Xu N and Lu L (2021) Neuroimaging Markers of Cerebral Small Vessel Disease on Hemorrhagic Transformation and Functional Outcome After Intravenous Thrombolysis in Patients With Acute Ischemic Stroke: A Systematic Review and Meta-Analysis. Front. Aging Neurosci. 13:692942. doi: 10.3389/fnagi.2021.692942

Objective: The aim of this study was to perform a systematic review and meta-analysis to assess whether cerebral small vessel disease (CSVD) on neuroimaging of patients with acute ischemic stroke (AIS) treated with intravenous thrombolysis (IVT) is associated with an increased risk of hemorrhagic transformation (HT), symptomatic intracranial hemorrhage (sICH), and poor functional outcome (PFO).

Methods: A thorough search of several databases was carried out to identify relevant studies up to December 2020. We included studies of patients with AIS and neuroimaging markers of CSVD treated with IVT. The primary outcome was HT, and the secondary outcomes were sICH and 3-month PFO. The quality of the studies involved was evaluated using the Newcastle–Ottawa Scale (NOS). The meta-analysis with the fixed effects model was performed.

Results: Twenty-four eligible studies (n = 9,419) were pooled in the meta-analysis. All included studies were regarded as high quality with the NOS scores of at least 6 points. The meta-analysis revealed associations between the presence of CSVD and HT, sICH, and the 3-month PFO after IVT. Compared with no CSVD, the presence of CSVD was associated with an increased risk of HT (OR: 1.81, 95% CI: 1.52–2.16), sICH (OR: 2.42, 95% CI: 1.76–3.33), and 3-month PFO (OR: 2.15, 95% CI: 1.89–2.44). For patients with AIS complicated with CSVD, compared with a CSVD score of 0–1, a CSVD score of 2–4 was associated with an increased risk of HT (OR: 3.10, 95% CI: 1.67–5.77), sICH (OR: 2.86, 95% CI: 1.26–6.49), and 3-month PFO (OR: 4.58, 95% CI: 2.97–7.06).

Conclusion: Patients with AIS complicated with neuroimaging markers of CSVD are at increased risk of HT and 3-month PFO after IVT. However, it is still necessary to clarify the exact role of CSVD in the occurrence, development, and prognosis of AIS.

Systematic Review Registration: www.ClinicalTrials.gov, identifier CRD42021233900.

Keywords: cerebral small vessel disease, acute ischemic stroke, intravenous thrombolysis, hemorrhagic transformation, neuroimaging markers

INTRODUCTION

Stroke is the second leading cause of death worldwide, leading to death in 5.5 million people and affecting 13.7 million each year. Ischemic stroke accounts for 70% of all patients with stroke. The 2016 Global Burden of Disease Study data that were published in 2019 suggest that one in four adults is reported to be at risk of having a stroke in their lifetime (GBD 2016 Stroke Collaborators, 2019; Lindsay et al., 2019).

Cerebral small vessel disease (CSVD) is a widespread cerebrovascular disease with specific neuroimaging characteristics (Chen et al., 2019). With the development of neuroimaging technology, the brain imaging of more patients with acute ischemic stroke (AIS) has detected the neuroimaging markers of CSVD such as cerebral microbleed (CMB), white matter hyperintensity (WMH), lacunar infarction (LI), and enlarged perivascular space (EPVS) (Curtze et al., 2016; Chen et al., 2019). CSVD accounts for 25% of cases of AIS, and it affects cognitive function, gait disturbance, swallowing, and other functions (Pantoni, 2010).

Studies have shown that CSVD may be a risk factor for intracranial hemorrhage, but none of these studies have a clear determinism (Emberson et al., 2014; Jickling et al., 2014; Pang et al., 2019). Hemorrhagic transformation (HT) occurs in 10–40% of patients with ischemic stroke and is a major complication of intravenous thrombolysis (IVT) (Terruso et al., 2009; Beslow et al., 2011; Jickling et al., 2014). HT can be divided into symptomatic and asymptomatic according to the deterioration of neurological function, both of which worsen the prognosis of stroke, especially in cognitive and neurological functions (Dzialowski et al., 2007; Park et al., 2012). Most patients with AIS complicated with CSVD have no obvious clinical symptoms at the initial stage, which are easy to be ignored by doctors. Therefore, for patients with AIS complicated with CSVD, HT, symptomatic intracranial hemorrhage (sICH), and poor functional outcome (PFO) after IVT have gradually attached the attention of medical researchers (Liu X.Y. et al., 2019). Different subtypes of CSVD may have different effects on HT and clinical prognosis after IVT in patients with AIS, and different subtypes of CSVD often coexist in the same patients with AIS.

Several recent studies have explored the relationship between these neuroimaging markers of CSVD and clinical outcomes after IVT in patients with AIS (Drelon et al., 2020; Liu X. et al., 2020). Previous meta-analyses have investigated the increased risk of CSVD for HT and PFO in patients with AIS (Charidimou et al., 2016; Tsivgoulis et al., 2016; Wang et al., 2017). However, these studies are mainly limited to a particular subtype of CSVD, and some patients receive endovascular treatment. Whether the existence of neuroimaging markers of CSVD affects the HT, sICH, and PFO of patients with AIS after IVT is still a controversial issue. Therefore, we performed a systematic review and meta-analysis to evaluate whether CSVD on neuroimaging of patients with AIS treated with IVT is associated with an increased risk of HT, sICH, and PFO.

METHODS

This systematic review and meta-analysis was performed in accordance with the Preferred Reporting Items for Systematic reviews and Meta-Analyses (PRISMA) guidelines.

Search Strategy

We systematically searched the MEDLINE, Cochrane Library, Embase, CNKI, VIP, and WANFANG databases from inception to December 2020 to find relevant studies. The articles were not restricted based on the language of publication. The details of the search strategy are presented in **Supplementary Appendix 1**. Two authors (i.e., WYQ and YXT) scanned the titles and abstracts to find the articles that were most relevant to this study; then, the full texts of the relevant articles were examined, and the final decision on inclusion was made by consensus.

Selection Criteria

Types of Studies

We included cohort studies (i.e., prospective and retrospective) in which patients with AIS or suspected AIS were treated with IVT. The relationship between neuroimaging markers of CSVD and clinical outcomes was assessed. All eligible trials were published in full text without language restrictions.

Types of Participants

We considered trials that included IVT-treated patients with AIS or patients who were treated with IVT for suspected ischemic stroke. The diagnosis of AIS meets the WHO diagnostic criteria (No authors listed, 1989), and participants were confirmed by CT or MRI. The diagnosis points of AIS are as follows: (1) acute onset, (2) focal neurological deficit, (3) responsible lesions appearing on imaging or symptoms lasting more than 24 h, and (4) excluding cerebral hemorrhage by brain CT/MRI. Trials involving patients treated with endovascular therapy were excluded. Cerebral imaging had to be performed for the

visualization of CSVD. CMB, WMH, LI, and EPVS can all be detected on MRI (Chen et al., 2019). CMB is defined as a small, round, or oval hypointense lesion that can be shown on T2*-weighted gradient recalled echo (GRE) and susceptibility-weighted imaging (SWI) (Wardlaw et al., 2013). WMH is an imaging description of white matter demyelination, it is hyperintense on T2-weighted image (T2WI) and fluid-attenuated inversion recovery (FLAIR) sequences on MRI, and it can also be shown on CT, but the range of lesions shown on CT may not be ideal (Wardlaw et al., 2013; van Leijsen et al., 2018). LI is a hyperintense area with the largest lesion diameter less than 20 mm on the axial plane of the FLAIR sequence (Wardlaw et al., 2013). Generally, the diameter of the perivascular space is less than 2 mm, the EPVS can extend to a diameter of 2–4 mm, and it can be detected on MRI (Chen et al., 2019). To expand the scope of the study, WMH detected on CT is also included (Charidimou et al., 2016).

Primary Outcome Assessments

The primary outcome for the systematic review was the occurrence of HT. There are many types of HT diagnostic criteria, such as the European Cooperative Acute Stroke Studies (ECASS) (Fiorelli et al., 1999; Larrue et al., 2001; Hacke et al., 2008) and the National Institute of Neurological Disorders and Stroke (NINDS) (No authors listed, 1997). The diagnosis points of ECASS are as follows: (1) hemorrhagic infarction (HI): there was a small spot-like hemorrhage along the edge of the infarct and sheet-like non-massive bleeding or multiple fused spot-like hemorrhages in the infarct area and (2) parenchymal hematoma (PH): hematoma, i.e., bleeding with slight or obvious space-occupying effect or bleeding away from the infarct. The main points of the diagnosis of NINDS are as follows: (1) HI: different low-density/high-density foci with punctate or blurred borders in the acute infarct can be tested on CT and (2) PH: typical homogeneous high-density lesions with clear boundaries, with or without cerebral edema or space-occupying effects, can be tested on CT.

Secondary Outcome Assessments

The secondary outcomes included the occurrence of sICH, and sICH was defined by the scores on the ECASS (Fiorelli et al., 1999; Larrue et al., 2001; Hacke et al., 2008), NINDS (No authors listed, 1997), and Safe Implementation of Thrombolysis in Stroke-Monitoring Study (SITS-MOST) (Rha et al., 2014). The 3-month PFO was defined as a Modified Rankin Scale (mRS) score > 2. The relationships among HT, sICH, 3-month PFO, and the total burden of CSVD (by using the Total Burden Rating Scale of CSVD) were also examined. The diagnosis points of ECASS are as follows: bleeding is seen on CT, and the increase in the National Institute of Health Stroke Scale (NIHSS) score is ≥ 4 points. The diagnosis points of NINDS are as follows: bleeding on CT, accompanied by neurological decline. The main points of diagnosis of SITS-MOST are as follows: the infarct area or remote area PH is seen on CT, the NIHSS score increased by 4 points or more compared with the minimum level of 24 h after admission, and bleeding caused death. The mRS can assess the complete independent living ability of patients with stroke, where a score of 0 means asymptomatic and the higher scores indicate a worse prognosis (i.e., a score of 6 indicates death). The concept of the total burden of CSVD was proposed by Staals et al. (2014), who developed a scale to quantitatively evaluate the cumulative effect of CSVD throughout the whole brain. The total score of the scale ranges from 0 to 4 points, and the higher the score, the more serious the CSVD.

Data Extraction

We used a preset electronic collection form to extract the basic characteristics of the studies, such as study design, first author, year of publication, country, sample size, age, sex, imaging method, type of neuroimaging markers of CSVD (i.e., CMB, WMH, LI, and EPVS), the definition of HT and sICH, the total burden of CSVD, and clinical outcome. The number of patients with neuroimaging markers of CSVD and the number of outcome events in each study were extracted, and conversion was performed when studies were reported as a percentage. When a study reported the relationship between different subtypes of CSVD and outcomes, the data were extracted separately.

Quality Assessment

Two reviewers independently assessed each study for quality using the Newcastle–Ottawa Scale (NOS) (Wells et al., 2013), which mainly contains three domains as follows: (1) selection, (2) comparability, and (3) outcome. The selection domain included the representativeness of the exposed cohort, selection of non-exposed cohort, ascertainment of exposure, and demonstration that the outcome of interest was not present at the beginning of the study. The comparability domain included the comparability of cohorts based on the design or analysis. Outcomes included the assessment, long enough follow-up for outcomes to occur, and adequacy of follow-up of cohorts. The maximum score of the NOS was 9 points, and a score ≥ 6 indicated a high-quality study. Disagreements in the studies were resolved by senior researchers. The details of the quality assessment can be found in **Supplementary Appendix 2**.

Statistical Analyses

We used RevMan software version 5.3 and Stata MP software version 14.0 for all the statistical analyses. The meta-analysis was used to calculate the combined odds ratio (OR) and the corresponding 95% CI to quantify the strength of the association between the presence and severity of CSVD and HT, sICH, and 3-month PFO after IVT. The total burden of CSVD was divided into two groups, namely, 0–1 and 2–4 points. We tested for heterogeneity between trial results using the I^2 statistic (Higgins et al., 2003) (when $P \leq 0.1$ and $I^2 \leq 25\%$ indicated low heterogeneity, $25\% < I^2 \leq 50\%$ indicated moderate heterogeneity, and $I^2 > 50\%$ indicated significant heterogeneity). The fixed effects model was used when heterogeneity between studies was not detected; otherwise, the random effects model was used.

To explore the factors associated with heterogeneity, the subgroup analysis according to different types of CSVD (i.e., CMB, WMH, LI, and EPVS) was performed to explore the impact of different types on the outcome. The sensitivity analysis was used to analyze whether the conclusion was stable, and we

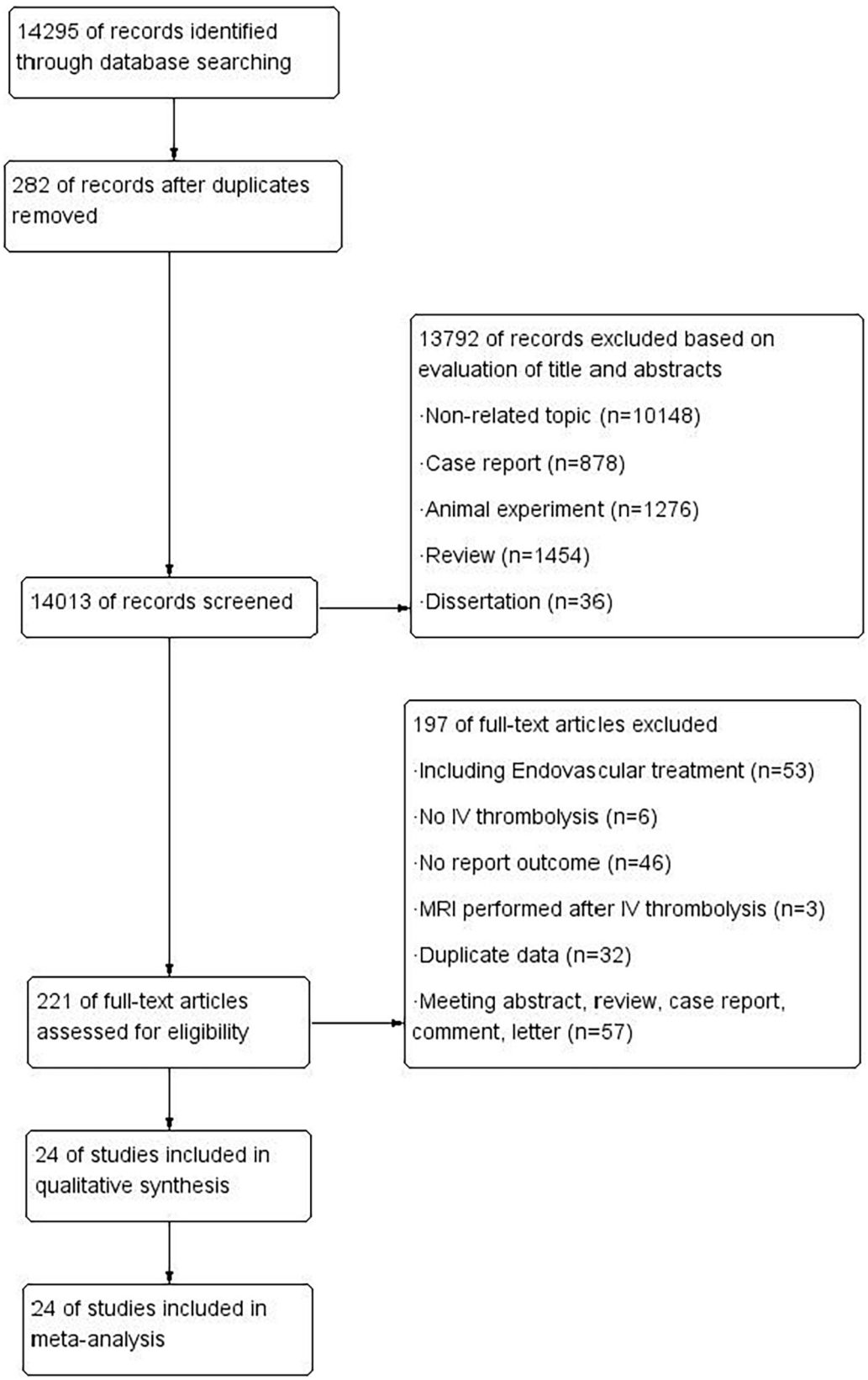

FIGURE 1 | Flow diagram of the search process and study selection.

TABLE 1 | Characteristics of the studies in the meta-analysis.

Author (year)	Period	Country	Study design	Sample	Mean/Median Age(y)	Gender (Female/male)	CVSD	Clinical outcomes	Imaging method	Time-HT/sICH	NOS
Moriya et al. (2013)	2007.11–2011.12	Japan	Prospective	71	73 ± 10	21/50	CMB	HT(NINDS)	T2*-GRE(1.5T), FLAIR, DWI, T1WI, T2WI	Between days 4 and 7 after admission	6
Capuana et al. (2020)	NA	Italy	Retrospective	434	68.3 ± 13.5	170/264	CMB	HT(ECASS **II**) sICH(ECASS)	T2*-GRE(1.5T), T1WI, T2WI, FLAIR, DWI, PWI, 3d-TOF-MRA	Within 24 h after IVT	8
Liu et al. (2019b)	2016.08–2018.07	China	Prospective	218	65.79 ± 11.99	144/74	The total burden of CSVD, WMH	PFO	T2*-GRE (-), FLAIR, T2WI, T1WI, DWI, 3d-TOF-MRA	/	8
Wen et al. (2019)	2016.09–2019.01	China	Retrospective	326	Good outcome:65 ± 12 Poor outcome: 70 ± 12	117/209	WMH	PFO	T1WI, T2WI, FLAIR	/	8
Liu L. et al. (2019)	2017.01–2019.01	China	Retrospective	175	67 ± 11	62/113	The total burden of CSVD	PFO, HT (ECASSII), sICH (ECASSII)	DWI, FLAIR, SWI, MRA	Within 24 h after IVT	8
Liu X.Y. et al. (2019)	2016.08–2018.01	China	Retrospective	154	66.00 (59.00, 74.25) **(**Median;Interquartile range)	51/103	The total burden of CSVD, CMB, Li, CMB, LI	HT(ECASSII), sICH(NINDS)	T1WI, T2WI, FLAIR, DWI	Within 24 h after IVT	6
Chacon-Portillo et al. (2018)	2011.01–2015.12	America	Retrospective	292	62.8 ± 15.3	151/141	CMB	sICH (NINDS), HT(ECASSII)	T1WI, T2WI, DWI, SWI	Within 24 h after IVT	6
Nagaraja et al. (2018)	2009.01–2013.12	America	Retrospective	366	67 ± 15	168/198	CMB	HT (ECASSI)	T2*-GRE(1.5T), DWI, FLAIR, CT (HT)	At 18–36 h after IVT	6
Liu et al. (2018)	2013.06–2017.05	China	Retrospective	97	66.6 ± 9.1	29/68	WMH	PFO, HT(ECASSII)	DWL, FLAIR, MRA-, CT (HT)	Within 24 h after IVT	8
Liu et al. (2017)	2014.01–2017.03	China	Retrospective	78	WMH: 73.7 ± 6.7 No WMH:61.3±10.6	24/54	WMH, LI	PFO, HT(ECASSII), sICH (ECASSII)	T1WI, FLAIR, DWI, MRA	Within 24 h after IVT	8
Yan et al. (2015a)	2009.06–2015.06	China	Retrospective	449	66.8 ± 12.9 SICH: 73 (64, 79)	151/298	CMB	PFO, HT(ECASSII), sICH(ECASSII)	SWI	Within 24 h after IVT	7
Curtze et al. (2015a)	2001.12–2014.02	UK	Retrospective	2481	No SICH:69 (60, 77) (Median; Interquartile range)	1,074/1,407	WMH	sICH(ECASSII)	CT	At 24 h post IVT	6
Dannenberg et al. (2014)	2008.01–2013.08	Germany	Prospective	326	76 (68, 84) (Median; Interquartile range)	167/159	CMB	sICH(ECASSIII)	T2*-GRE(3T), DWI	Within 36 h after IVT	8

(Continued)

TABLE 1 | Continued

Author (year)	Period	Country	Study design	Sample	Mean/Median Age(y)	Gender (Female/male)	CVSD	Clinical outcomes	Imaging method	Time-HT/sICH	NOS
Yan et al. (2014)	2009.06–2013.05	China	Retrospective	225	66.29 ± 13.01	73/152	CMB	HT(ECASSII)	FLAIR, DWI, PWI, SWI, MRA	Within 24 h after IVT	8
Zheng et al. (2012)	2006.07–2011.10	China	Retrospective	175	68 ± 10	70/105	WMH	HT(ECASSII)	CT, T2WI, FLAIR	Within 24 h after IVT	7
Kakuda et al. (2005)	2001.04–2005.01	America, Canada, Belgium	Prospective	70	71 ± 29	39/31	CMB	HT(ECASS) sICH(ECASS)	GRE(1.5T), DWI, PWI, MRA, T1WI	At 3–6 h after IVT and at day 30	8
Derex et al. (2004)	2001.05–2002.08	France	Retrospective	44	63.2 ± 14.1	21/23	CMB	HT(NINDS), sICH(NINDS)	T2*-GRE(1.5T), CT(HT, SICH)	At day 7	6
Yan et al. (2015a)	2009.06–2014.02	China	Retrospective	333	66.15 ± 13.02	110/223	CMB	HT(ECASSII), PFO	GRE(3.0T), DWI, SWI	At 24 hours post IVT	6
Dong and Xia (2018)	2015.01–2016.12	China	Prospective	56	69.26 ± 2.25	25/31	CMB	HT(ECASS)	T1WI, T2WI, T2FLAIR, DWI, MRA, SWI	At 24 hours post IVT	6
Zhang and Zhang (2018)	2015.07–2016.07	China	Retrospective	206	CMB: 63.2 ± 9.5 NO CMB: 61.5 ± 9.0	83/123	CMB	sICH(SITS-MOST), PFO	T2*-GRE(-), T1WI, T2WI, DWI	NA	6
Huang (2017)	2010.01–2016.01	China	Retrospective	100	18–80	42/58	CMB	HT(ECASSI)	SWI, CT(HT)	At 24 hours post IVT	6
Zhuo et al. (2020)	2012.03–2018.01	China	Retrospective	178	62.3 ± 10.5	53/125	CMB, LI	PFO	T1WI, T2WI, DWI, FLAIR, SWI	/	8
Xue et al. (2017)	2012.01–2015.06	China	Prospective	80	56 ± 12	22/58	CMB	HT(ECASSII)	DWI, MRA, SWI	At 24 ± 12 hours post IVT	6
Curtze et al. (2015b)	2001.12–2014.02	UK	Retrospective	2485	78 (72–83)	1076/1409	WMH	PFO	CT	/	6

CMB, cerebral microbleed; WMH, white matter hyperintensity; LI, lacunar infarction; The total burden of CSVD, the total burden of cerebral small vessel disease; NA not available; HT, hemorrhagic transformation; sICH, symptomatic intracranial hemorrhage; PFO, poor functional outcome; ECASS, European Cooperative Acute Stroke Studies; SITS-MOST, safe implementation of thrombolysis in stroke-monitoring study; NINDS, the National Institute of Neurological Disorders and Stroke; T1WI, T1 Weighted Image; T2WI, T2 Weighted Image; FLAIR, Fluid attenuated inversion recovery; SWI, susceptibility-weighted imaging; T2-GRE, T2*-weighted gradient-recalled echo; DWI, Diffusion-Weighted Imaging; PWI, Perfusion-Weighted Imaging; CT, Computed Tomography; MRA, Magnetic Resonance Angiography; 3d-TOF-MRA, 3D time-of-flight Magnetic Resonance Angiography; CT (HT, sICH), CT was used to detected HT, sICH.*

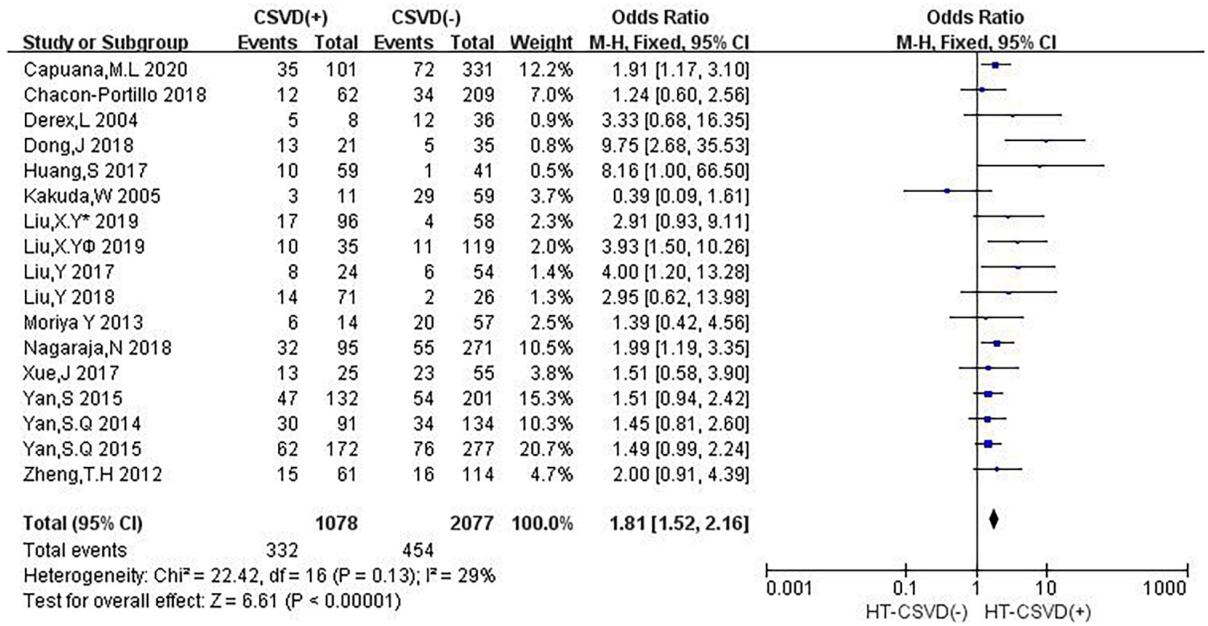

FIGURE 2 | Forest plot showing the Impact of CSVD on HT (Liu, XY$^{\Psi}$ 2019 and Liu, XY$^{\Phi}$ 2019 are from Liu et al. (2019a); Liu, XY$^{¥}$ 2019 represents the data of LI in this study, and Liu, Y* 2019 represents the data of CMB in this study).

eliminated each study one by one to explore its influence on the conclusion. We planned to use funnel plots to visually observe the possibility of reporting bias and combined the Egger's test to detect publication bias (Egger et al., 1997). Two-sided $P \leq 0.05$ was considered statistically significant.

RESULTS

Review of the Literature

Our initial search yielded 14,295 potentially related studies. Of note, 282 studies were excluded because they were duplicates, 13,792 were excluded based on titles and abstracts, and 197 were excluded after a full-text reading revealed that the studies did not meet the inclusion criteria. Finally, for a total of 9,419 patients, 24 studies (Derex et al., 2004; Kakuda et al., 2005; Zheng et al., 2012; Moriya et al., 2013; Dannenberg et al., 2014; Yan et al., 2014, 2015a,b; Curtze et al., 2015a,b; Liu et al., 2017, 2018; Huang, 2017; Xue et al., 2017; Chacon-Portillo et al., 2018; Nagaraja et al., 2018; Dong and Xia, 2018; Zhang and Zhang, 2018; Liu L. et al., 2019; Liu et al., 2019a; Liu L. et al., 2019; Wen et al., 2019; Capuana et al., 2020; Zhuo et al., 2020) meeting the criteria were included. The selection process is shown in **Figure 1**. These studies were cohort studies published from the year 2004 to 2020 and included 6 prospective and 18 retrospective studies. Among them, 17 studies evaluated HT, 11 studies mentioned sICH, and 10 studies assessed 3-month PFO. Three of these studies reported separate associations with the total burden of CSVD. In the included studies, the neuroimaging markers of CSVD included cerebral CMB, WMH, and LI, and no studies related to EPVS were found. The characteristics of these studies are shown in **Table 1**.

Neuroimaging Markers of CSVD and HT

Sixteen studies evaluated the relationship between neuroimaging markers of CSVD and HT. The pooled overall rate of HT after IVT was 24.9% in the entire population. The pooled rate was 30.8% of patients in the CSVD presence group vs. 21.9% of patients in the group without CSVD presence. The total number of participants was 3,155 patients. Compared with no CSVD, the presence of CSVD was associated with an increased risk of HT (OR: 1.81, 95% CI: 1.52–2.16) (**Figure 2**). The heterogeneity between studies was not significant (I^2 = 29%, P = 0.13). The risk of HT after IVT was higher in patients with CSVD than in patients without CSVD on neuroimaging.

In subgroup analyses, the influence of CSVD on HT showed a few changes when the studies were stratified according to the type of CSVD (**Figure 3**). Twelve studies (50%) reported the relationship between CMB and HT, three studies (12.5%) evaluated the association between WMH and HT, and one study (4.2%) mentioned the relationship between CMB and HT as well as LI and HT. Compared with no CMB, the presence of CMB was associated with an increased risk of HT (OR: 1.72, 95% CI: 1.43–2.08), and moderate heterogeneity was observed (I^2 = 38%, P = 0.08). Compared with no WMH, the presence of WMH was associated with an increased risk of HT (OR: 2.54, 95% CI: 1.39–4.64), and there was no heterogeneity (I^2 = 0, P = 0.62). An estimate specific for LI and HT was provided in only one study (OR: 2.91, 95% CI: 0.93–9.11).

We performed the sensitivity analyses to explore whether the change in the inclusion criteria of studies influenced the robustness of the combined results. We recalculated the pooled OR by excluding each individual study in turn. The range of the combined ORs was from 1.75 (95% CI: 1.46–2.09) to 1.89

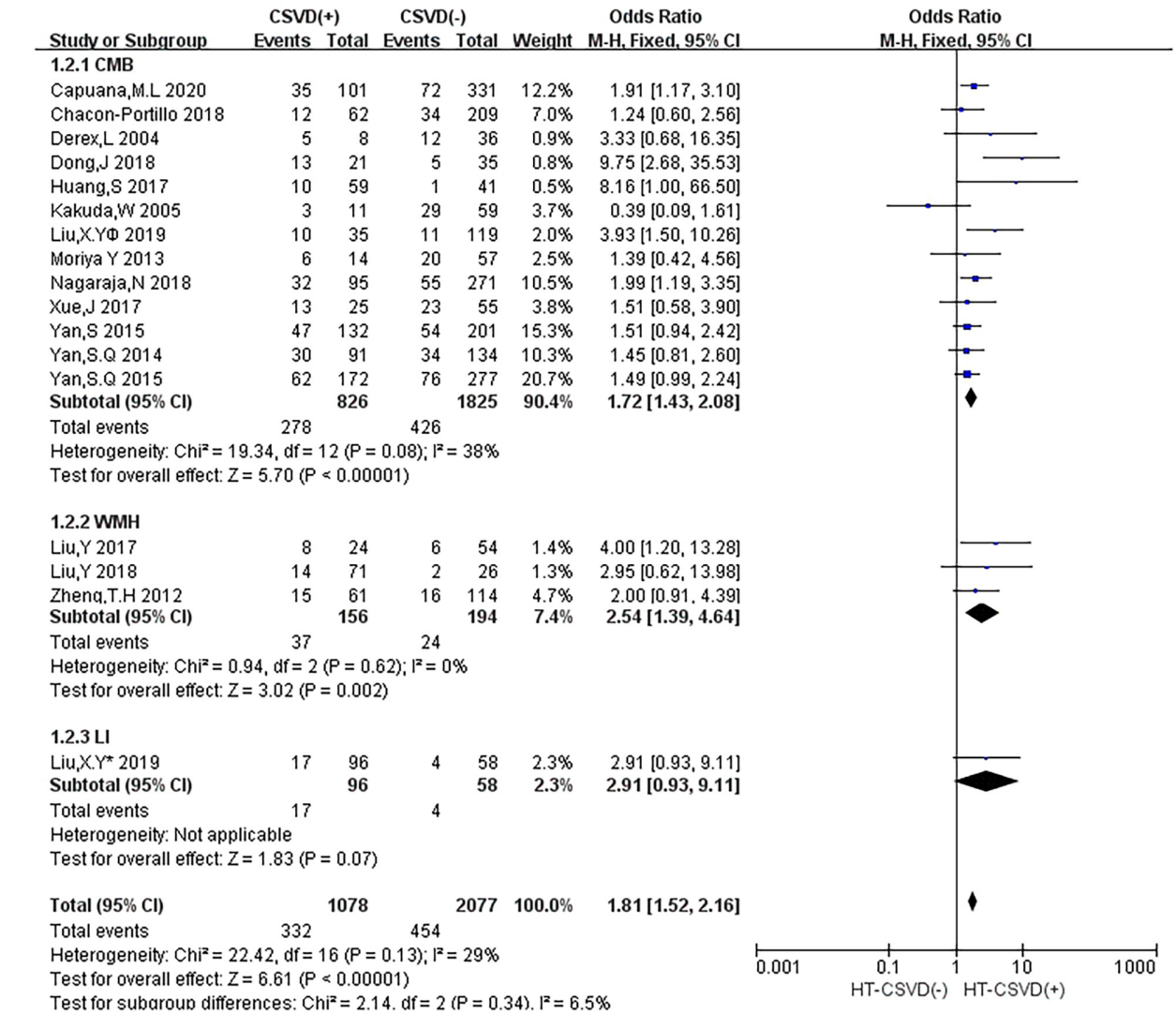

FIGURE 3 | Forest plot of subgroup analysis showing the impact of subtypes of CSVD on HT.

(95% CI: 1.56–2.30) when the studies of Dong and Xia (2018) and Yan et al. (2015a) were excluded. The results showed that no individual study significantly affected the pooled effect size. Furthermore, the funnel plots (**Figure 4**) and the Egger's test ($t = 1.88$, $P = 0.079$) indicated no publication bias.

Neuroimaging Markers of CSVD and sICH

Nine studies reported the relationship between neuroimaging markers of CSVD and sICH. The pooled overall rate of sICH after IVT was 4.3% in the entire population. The pooled rate was 6.4% of patients in the CSVD presence group vs. 2.7% of patients in the group without CSVD presence. The total number of participants was 4,285 patients. Compared with no CSVD, the presence of CSVD was associated with an increased risk of sICH (OR: 2.42, 95% CI: 1.76–3.33) (**Figure 5**). The heterogeneity was not detected ($I^2 = 0\%$, $P = 0.49$). The risk of sICH after IVT was found to be higher in patients with evidence of CSVD than in patients without CSVD on neuroimaging.

In subgroup analyses, different types of CSVD had slightly different effects on sICH (**Figure 6**). Seven studies (29.2%) reported the relationship between CMB and sICH, only two studies (8.3%) evaluated the association between WMH and sICH, and no study mentioned the correlation between LI and sICH. Compared with no CMB, the presence of CMB was associated with an increased risk of HT (OR: 2.86, 95% CI: 1.63–5.02), and low heterogeneity was observed ($I^2 = 5\%$, $P = 0.39$). Compared with no WMH, the presence of WMH was associated with an increased risk of sICH (OR: 2.27, 95% CI: 1.54–3.33), and there was no heterogeneity ($I^2 = 0\%$, $P = 0.61$).

We performed the sensitivity analyses to explore whether the outcome was stable. We recalculated the pooled OR by excluding each individual study in turn. The range of the combined OR

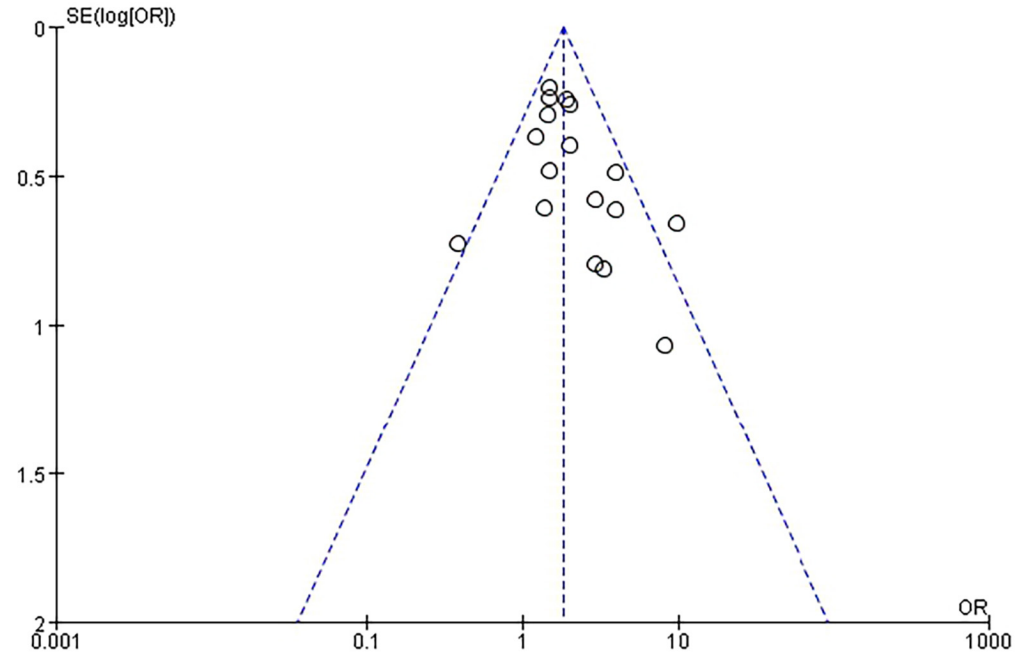

Egger's test

Std_Eff	Coeff	Standard Error	*t*	$p > \|t\|$	[95% Confidence	Interval]
Slope	.1967596	.2299342	0.86	0.406	-.2933335	.6868527
bias	1.15107	.6117395	1.88	0.079	-.1528215	2.454962

FIGURE 4 | Funnel plot and Egger's test of studies evaluating the association between CSVD and HT.

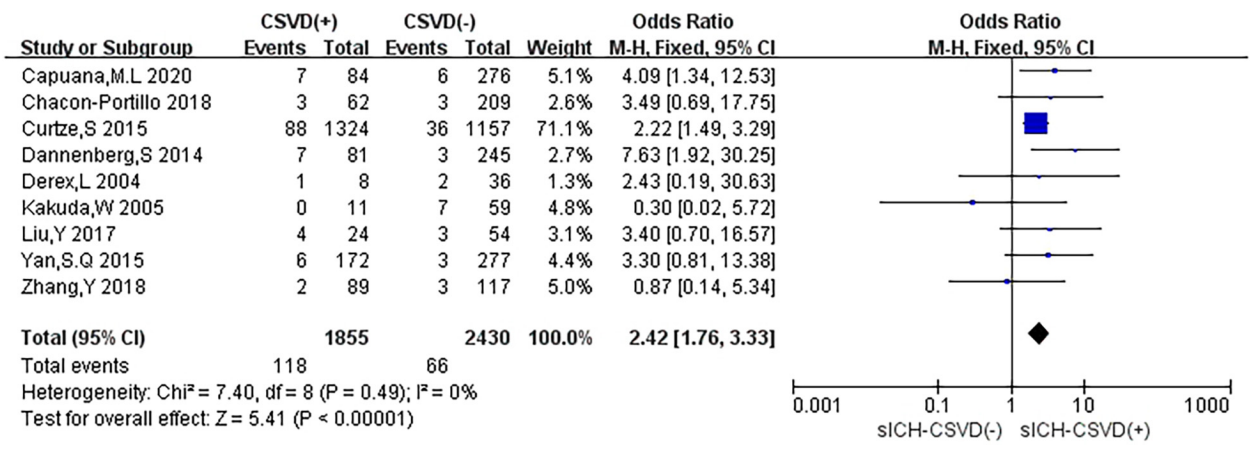

FIGURE 5 | Forest plot showing the impact of CSVD on sICH.

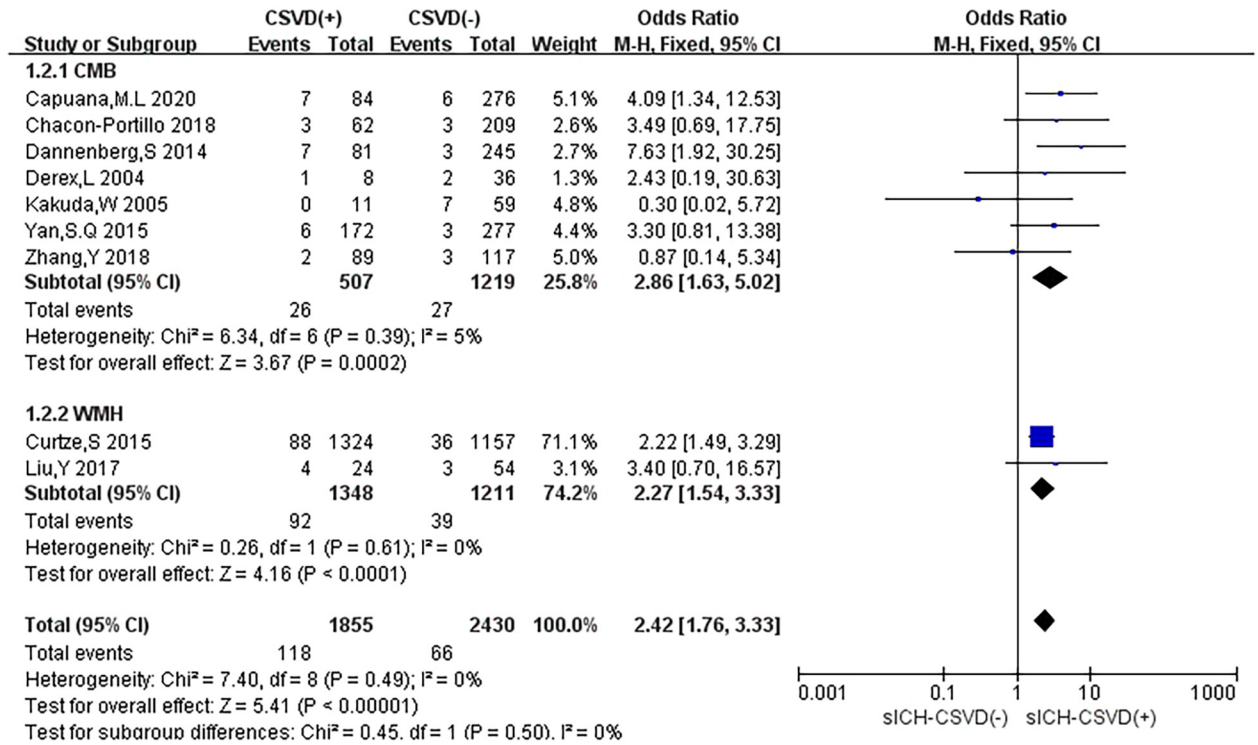

FIGURE 6 | Forest plot of subgroup analysis showing the impact of subtypes of CSVD on sICH.

was from 2.28 (95% CI: 1.64–3.16) to 2.92 (95% CI: 1.72–4.96) when the studies of Dannenberg et al. (2014) and Curtze et al. (2015a) were excluded. The results suggested that no individual study significantly affected the pooled effect size. The funnel plots (**Figure 7**) and the Egger's test ($t = 0.22$, $P = 0.833$) indicated no evidence of publication bias.

Neuroimaging Markers of CSVD and 3-Month PFO

Nine studies investigated the relation between neuroimaging markers of CSVD and PFO. The pooled overall rate of 3-month PFO after IVT was 38.8% in the entire population. The pooled rate was 45.8% of patients in the CSVD presence group vs. 31.6% of patients in the group without CSVD presence. The total number of participants was 4,626, and compared with no CSVD, the presence of CSVD was associated with an increased risk of 3-month PFO (OR: 2.15, 95% CI: 1.89–2.44) (**Figure 8**). The heterogeneity between studies was moderate ($I^2 = 40\%$, $P = 0.08$). The results showed that patients with evidence of CSVD were at higher risk for PFO after IVT than patients without neuroimaging evidence of CSVD.

In subgroup analyses, the influence of CSVD on PFO showed some changes when studies were stratified according to the type of CSVD (**Figure 9**). Three studies (12.5%) reported the relationship between CMB and PFO, four studies (16.7%) evaluated the association between WMH and PFO, one study (4.2%) mentioned the relationship between CMB and PFO as well as LI and PFO, and one study (4.2%) reported the association between WMH and PFO as well as between LI and PFO. Compared with no CMB, the presence of CMB was associated with an increased risk of 3-month PFO (OR: 1.65, 95% CI: 1.29–2.10), and no heterogeneity was observed ($I^2 = 0\%$, $P = 0.83$). Compared with no WMH, the presence of WMH was associated with an increased risk of 3-month PFO (OR: 2.32, 95% CI: 1.99–2.71), and there was significant heterogeneity ($I^2 = 55\%$, $P = 0.07$). Compared with no LI, the presence of LI was associated with an increased risk of 3-month PFO (OR: 3.18, 95% CI: 1.74–5.83). There was no evidence of substantial heterogeneity among studies ($I^2 = 0\%$, $P = 0.74$).

The sensitivity analysis was carried out to explore the robustness of our analysis, and we recalculated the pooled OR by excluding each individual study in turn. The range of the combined ORs was from 2.06 (95% CI: 1.69–2.52) to 2.21 (95% CI: 1.93–2.52) when the studies of Curtze et al. (2015b) and Yan et al. (2015a) were excluded. The results showed that no individual study significantly affected the pooled effect size. The funnel plots (**Figure 10**) and the Egger's test ($t = 0.69$, $P = 0.508$) showed no evidence of publication bias.

The Total Burden of CSVD

Three studies were related to the total burden of CSVD, among which one explored the relationship between the total burden of CSVD and HT, sICH, and PFO (**Figure 11**). One study (4.2%) reported the relationship between the total burden of CSVD and HT as well as sICH, and one study (4.2%) investigated the association between the total burden of CSVD and PFO. We

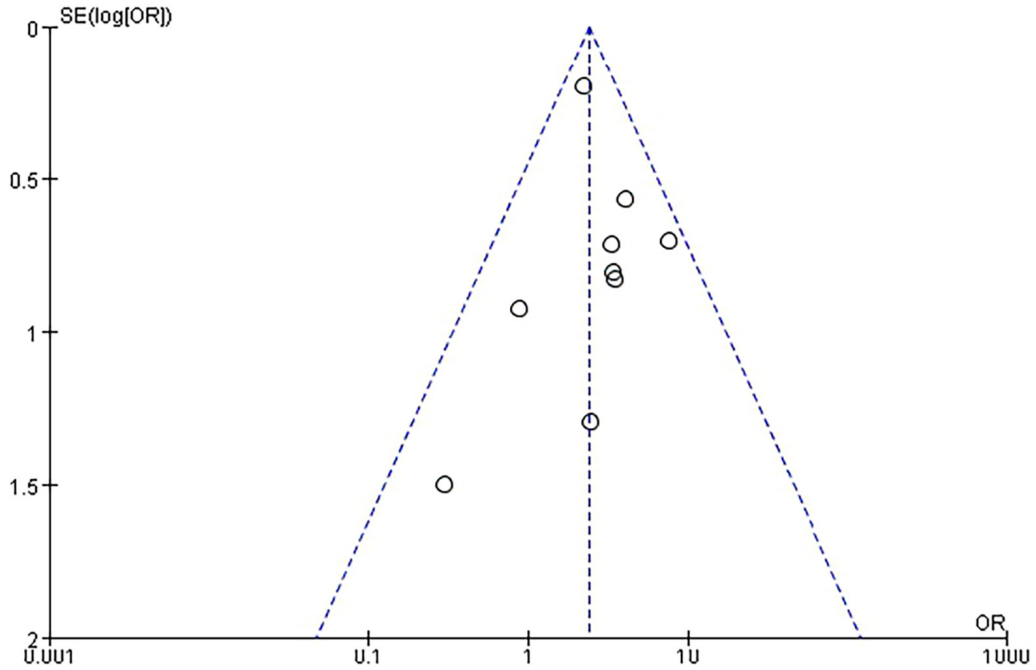

Egger's test

Std_Eff	Coeff	Standard Error	t	p>|t|	[95% Confidence	Interval]
Slope	.8714415	.2789136	3.12	0.017	.2119156	1.530967
bias	.123372	.563507	0.22	0.833	-1.20911	1.455854

FIGURE 7 | Funnel plot and Egger's test of studies evaluating the association between CSVD and sICH.

calculated pooled ORs of HT, sICH, and PFO for 2–4 CSVD scores vs. 0–1 CSVD scores. Compared with a CSVD score of 0–1, a CSVD score of 2–4 was associated with an increased risk of HT (OR: 3.10, 95% CI: 1.67–5.77), and no heterogeneity could be found (I^2 = 0%, P = 0.80). Compared with a CSVD score of 0–1, a CSVD score of 2–4 was associated with an increased risk of sICH (OR: 2.86, 95% CI: 1.26–6.49), and there was no heterogeneity (I^2 = 0%, P = 0.52). Compared with a CSVD score of 0–1, a CSVD score of 2–4 was associated with an increased risk of 3-month PFO (OR: 4.58, 95% CI: 2.97–7.06), and there was no evidence of substantial heterogeneity among studies (I^2 = 0%, P = 0.44).

DISCUSSION

By using the systematic review and meta-analysis of these studies on the evidence of neuroimaging markers of CSVD, we observed that neuroimaging markers of CSVD (i.e., CMB, WMH, LI, and EPVS) represented an important indicator of a higher risk of HT, sICH, and 3-month PFO after IVT in patients with AIS. In addition, we found that a CSVD score of 2–4 (i.e., the Total Burden Rating Scale of CSVD) was a potential risk indicator for incidents. Our meta-analysis confirmed the association between the presence of neuroimaging markers of CSVD and the risk of HT and PFO after IVT. At present, there are many reports on the relationship between various subtypes of CSVD and HT and clinical prognosis after IVT in patients with AIS, but no definite conclusion has been reached. To the best of our knowledge, our study is the first to systematically evaluate the risk of HT and clinical prognosis in patients with AIS combined with neuroimaging markers of CSVD after IVT.

Cerebral small vessel disease is a widespread cerebrovascular disease that mainly manifests in CMB, WMH, LI, and EPVS on imaging. It mainly affects the perforation of small arteries, capillaries, and venules. The increased risk of HT and PFO in patients with AIS with CSVD after IVT may be related to the following mechanisms: First, the changes in blood pressure variability may have an effect on the increased risk. Studies

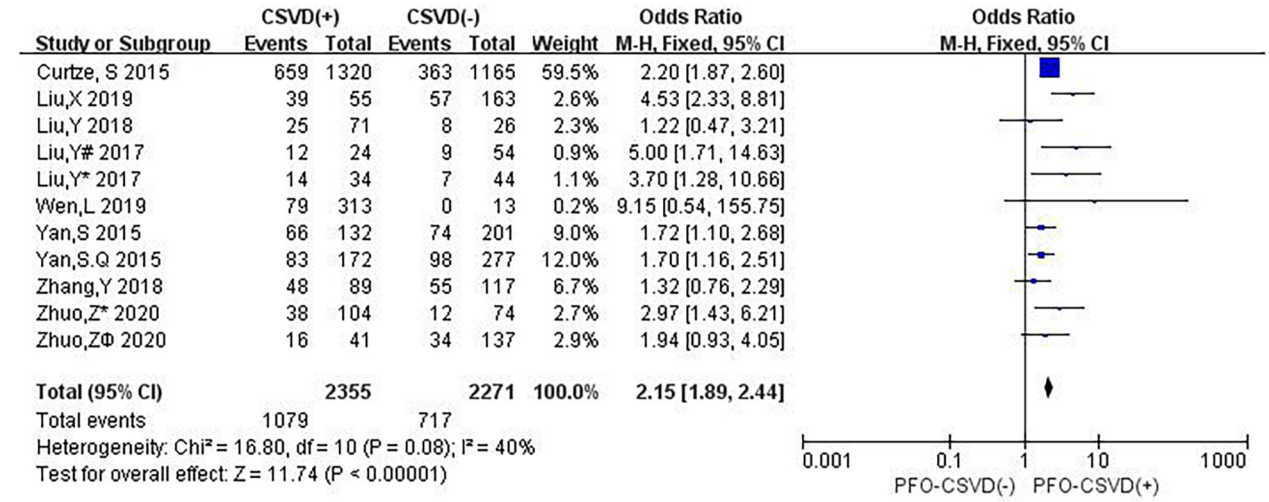

FIGURE 8 | Forest plot showing the impact of CSVD on 3-month PFO. (Liu, Y$^{\#}$ 2017 and Liu, Y* 2017 are from Liu, Y 2017 (Liu et al., 2017); Liu, Y$^{\#}$ 2017 represents the data of WMH in this study, and Liu, Y* 2017 represents the data of LI in this study; both Zhuo *Z** 2020 and Zhuo Z$^{\Phi}$ 2020 are from Zhuo et al. (2020); Zhuo Z* 2020 represents the data of LI in this study, and Zhuo Z$^{\Phi}$ 2020 represents the data of CMB in this study).

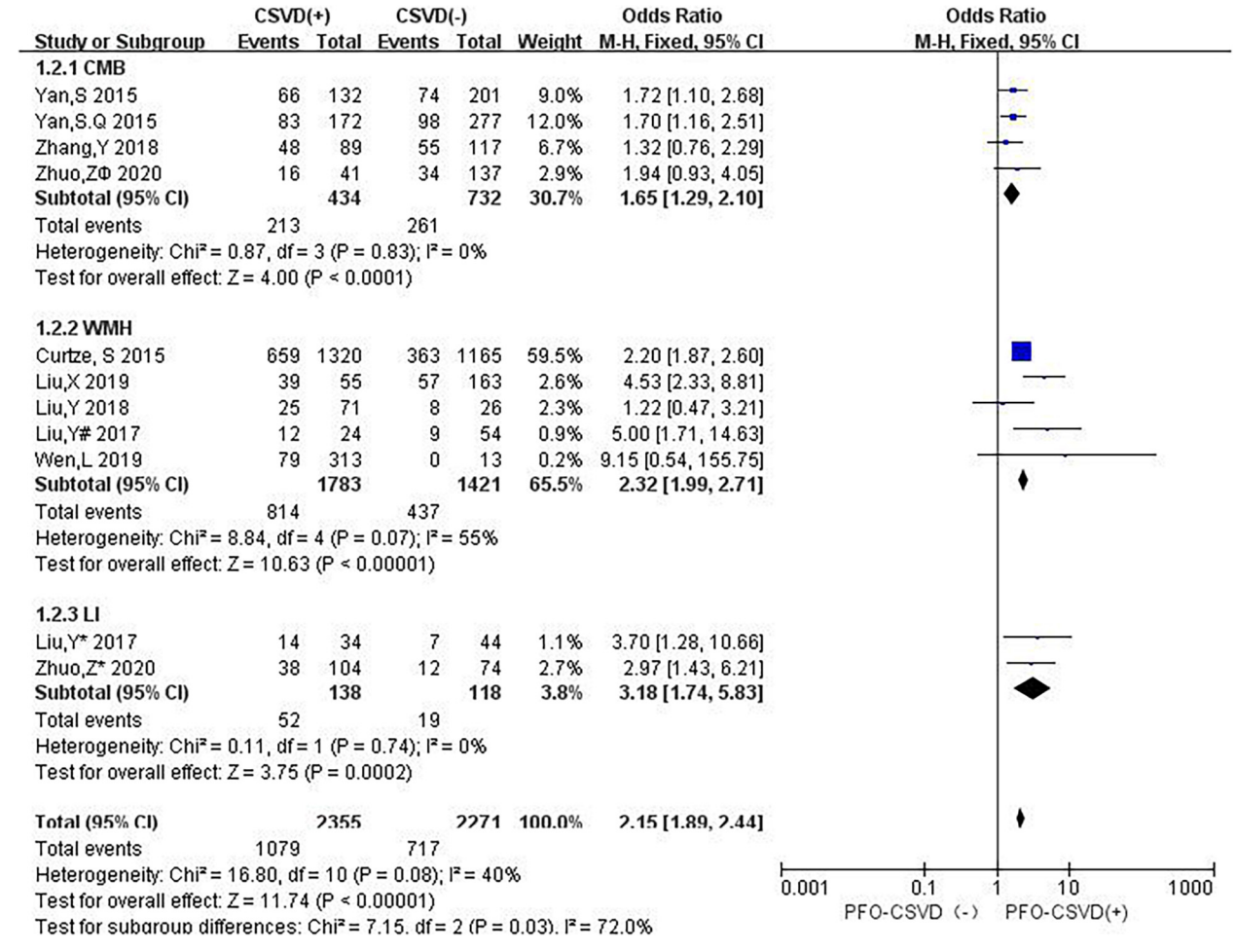

FIGURE 9 | Forest plot of subgroup analysis showing the impact of subtypes of CSVD on 3-month PFO.

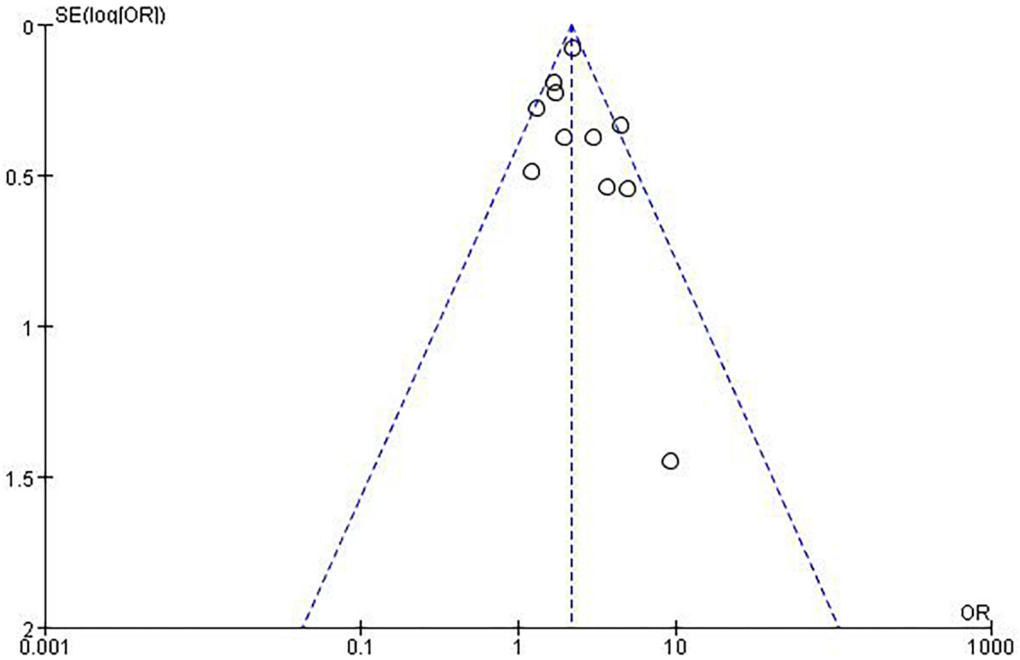

Egger's test

Std_Eff	Coef.	Standard. Error.	t	p> |t|	[95% Confidence	Interval]
Slope	.6822478	.1392509	4.90	0.001	.3672403	.9972553
bias	.4431912	.6421661	0.69	0.508	-1.009489	1.895872

FIGURE 10 | Funnel plot and Egger's test of studies evaluating the association between CSVD and 3-month PFO.

have shown that increased blood pressure variability is closely related to the progression of CSVD, and increased blood pressure variability means increased blood pressure fluctuations, which increases the difficulty of maintaining the steady state of blood supply to the brain. The occurrence of hypoperfusion is more frequent (de Heus et al., 2020), which may be related to the occurrence of HT. Second, the destruction of the permeability of the blood–brain barrier, neuroimaging, and cerebrospinal fluid analysis indicate that leakage of the blood–brain barrier is a common feature of CSVD (Farrall and Wardlaw, 2009). When the permeability of the blood–brain barrier is broken, serum proteins and toxic effects will penetrate brain tissue, which may explain the complicated brain edema and poor functional prognosis in patients with AIS after IVT. Finally, the decrease in cerebral blood flow and vascular reactivity, the decrease in cerebral blood flow, and the decrease in vascular reactivity are related to CMB, WMH, LI, and EPVS (Gregg et al., 2015; Blair et al., 2016; Staszewski et al., 2019; Wang et al., 2020; Zhang et al., 2020). A previous meta-analysis of the cross-sectional studies revealed that patients with WMH had decreased cerebral blood flow (Shi et al., 2016), which may explain the PFO of patients with AIS after IVT. However, It is worth noting that IVT is still the standard treatment for patients with AIS within 4.5 h of onset (Powers et al., 2019). Although there is a 2–7% risk of sICH after IVT treatment, the risk of disability or death is absolutely reduced by 10% at 3 months (Turc et al., 2014). There is currently no research to prove that CSVD is an absolute contraindication for IVT in the treatment of AIS, several studies have shown that LI will benefit from IVT (Eggers et al., 2017; Matusevicius et al., 2019). Therefore, we cannot arbitrarily regard the neuroimaging markers of CSVD as an absolute contraindication for IVT based on the results obtained in our study.

Different subtypes of CSVD may have different effects on HT and the clinical prognosis of patients with AIS after IVT. Several meta-analyses have studied the prognosis of patients with CMB and WMH. Our results are consistent with a recent meta-analysis including 11 studies, which reported that WMH significantly increased the incidence of sICH after IVT and showed that the combined incidence of WMH and sICH was 1.55, and the OR for WMH and 3- to 6-month PFO was 2.02 (Charidimou et al., 2016). However, a previous updated meta-analysis on a similar topic was performed by Wang et al. (2017) including 11 studies with 2,702 patients and showed that CMB presence was not significantly associated with an increased risk of sICH.

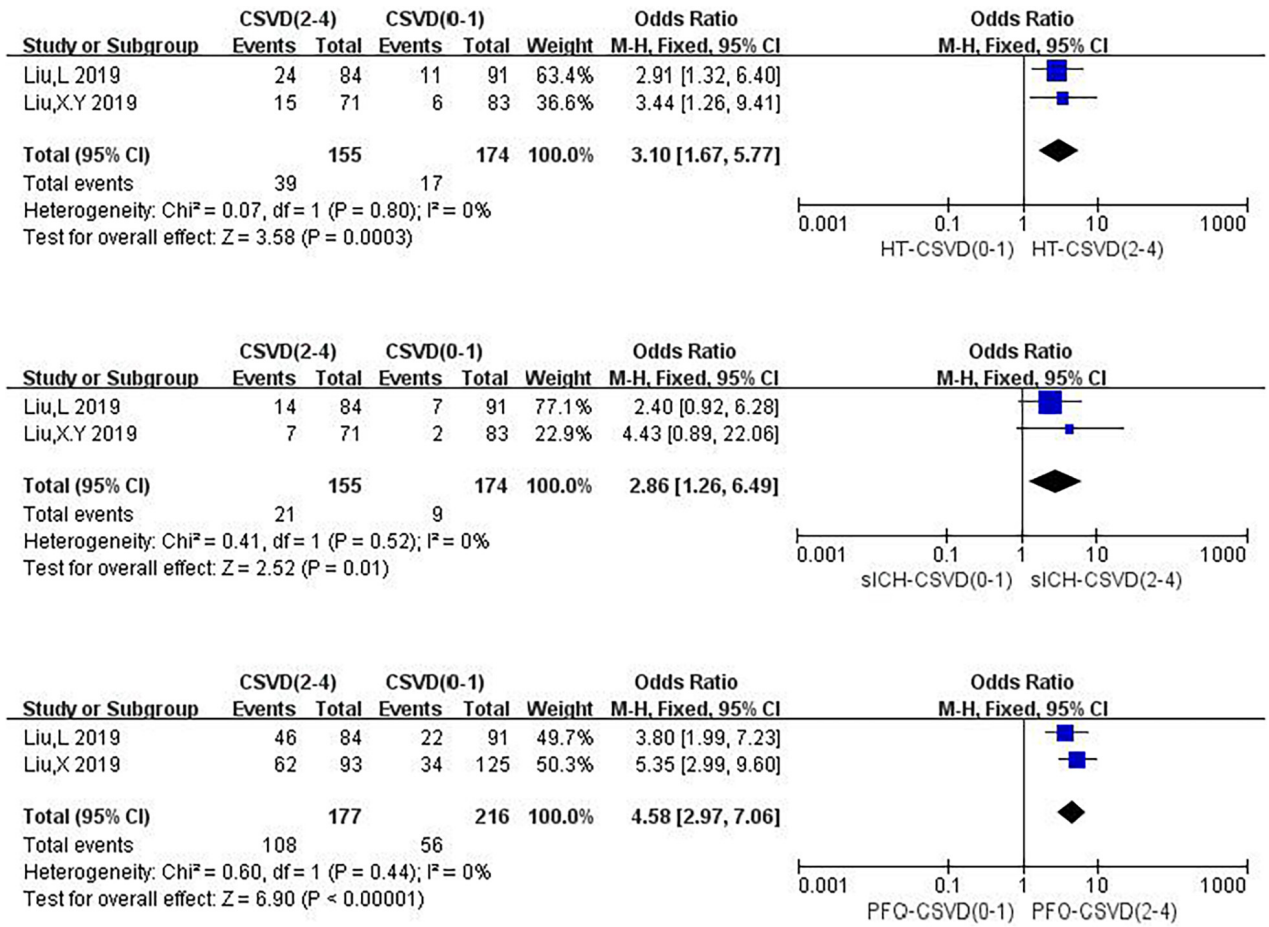

FIGURE 11 | Forest plot showing the impact of CSVD score on HT, sICH and 3-months PFO.

Compared with the previous meta-analysis, our results did not find such a connection. There are three possible reasons for this difference in the results. First, our study has a large sample size, including 24 articles (9,419 patients), and strict inclusion and exclusion criteria, while the earlier study only included 11 articles (2,702 patients). Second, in our study, the included patients with neuroimaging markers of CSVD could be tested by a variety of imaging methods, such as T1-weighted image (T1WI), T2WI, diffusion-weighted imaging (DWI), SWI, T2*-GRE, while in a previous study (Wang et al., 2017), only SWI and T2*-GRE were included in the imaging methods. Third, our results had low heterogeneity compared with previous studies (Charidimou et al., 2016; Wang et al., 2017).

Our study has the following strengthens. First, our study is the earliest to systematically evaluate the risk of HT and PFO in patients with AIS combined with the neuroimaging markers of CSVD after IVT. Second, we applied rigorous methodological standards, performed a systematic search, included a large sample size, and conducted an in-depth analysis of different subgroups. Our study also has some limitations as follows. First, there are differences in neuroimaging methods, both CT and MRI, which may affect the diagnosis of CSVD. Although the range of lesions shown on CT may not be ideal to expand the sample size, CT is also used to detect WMH. This may have a slight impact on the results of our study. However, we found that in previous studies, the application of CT to detect WMH was also be used for research (Charidimou et al., 2016). Second, the IVT protocol is different, and the baseline characteristics of the patient, such as previous use of anticoagulant drugs and repeated strokes, will affect the outcome. Third, the definitions of HT and sICH are different in each study. Although all we included are defined by standard criteria, they may still affect the results. However, in previous studies, the different definitions of HT and sICH, respectively, were combined for analysis (Charidimou et al., 2016; Wang et al., 2017). Fourth, in our study, in the subgroup analysis of CSVD and 3-month PFO, the presence of WMH was associated with the increased risk of 3-month PFO, and there was a significant heterogeneity. We found that the heterogeneity was observed from the study of Liu L. et al. (2019) probably due to the inclusion of participants, they excluded patients who had a premorbid mRS score > 2. Finally, there were no studies with EPVS, and only three studies mentioned the overall burden of CSVD.

CONCLUSION

Our results indicate that patients with AIS complicated with the neuroimaging markers of CSVD are at an increased risk of HT and 3-month PFO after IVT. Our study strengthened the correlation between the neuroimaging markers of CSVD and the adverse outcome of AIS after IVT. However, it is undeniable that these patients can still benefit from IVT in some aspects. Therefore, it cannot be simply considered that the neuroimaging markers of CSVD are a contraindication for IVT in patients with AIS. It is still necessary to clarify the exact role of CSVD in the occurrence, development, and prognosis of AIS.

DATA AVAILABILITY STATEMENT

The original contributions presented in the study are included in the article/**Supplementary Material**, further inquiries can be directed to the corresponding author/s.

AUTHOR CONTRIBUTIONS

YW and LL were responsible for conception and design of this systematic review. YW drafted the manuscript. LL and NX revised the manuscript. YW, JZ, and SG designed the search strategies. YW, XY, and PZ conducted the electronic search. YW and XY extracted the data. YW and GZ assessed the risk of bias. YW, HW, and LW analyzed and interpreted the data. LL arbitrated any disagreements in the process of systematic review. All authors approved this manuscript.

FUNDING

This study was funded by the special project of "Lingnan modernization of traditional Chinese medicine" in 2019 Guangdong Provincial R&D Program (No. 2020B1111100008), the Chinese Medicine Innovation Team Project of the State Administration of Traditional Chinese Medicine, the Youth Scientific Research Training Project of Guangzhou University of Chinese Medicine (No. 2019QNPY02), the Guangdong Provincial Key Fields of Higher Education (New Generation Information Technology) in 2020 (No. 2020ZDZX3024), the General Program of the National Natural Science Foundation of China (No. 81774406), the National Key R&D Program of China (Nos. 2019YFC1709100; 2019YFC1709102), the Qi-Huang Scholar of National Traditional Chinese Medicine Leading Talents Support Program (2018), the Opening Operation Program of Key Laboratory of Acupuncture and Moxibustion of Traditional Chinese Medicine in Guangdong (No. 2017B030314143), the Youth Program of the National Natural Science Foundation of China (No. 81904297), and the Elite Youth Education Program' of Guangzhou University of Chinese Medicine (No. QNYC20190106). The funders had no influence on study design, data collection and analysis, decision to publish, or preparation of the manuscript.

SUPPLEMENTARY MATERIAL

The Supplementary Material for this article can be found online at: https://www.frontiersin.org/articles/10.3389/fnagi.2021.692942/full#supplementary-material

REFERENCES

Beslow, L. A., Smith, S. E., Vossough, A., Licht, D. J., Kasner, S. E., Favilla, C. G., et al. (2011). Hemorrhagic transformation of childhood arterial ischemic stroke. *Stroke* 42, 941–946. doi: 10.1161/strokeaha.110.604199

Blair, G. W., Doubal, F. N., Thrippleton, M. J., Marshall, I., and Wardlaw, J. M. (2016). Magnetic resonance imaging for assessment of cerebrovascular reactivity in cerebral small vessel disease: a systematic review. *J. Cereb. Blood Flow Metab.* 36, 833–841. doi: 10.1177/0271678x16631756

Capuana, M. L., Lorenzano, S., Caselli, M. C., Paciaroni, M., and Toni, D. (2020). Hemorrhagic risk after intravenous thrombolysis for ischemic stroke in patients with cerebral microbleeds and white matter disease. *Neurol. Sci.* 42, 1969–1976. doi: 10.1007/s10072-020-04720-y

Chacon-Portillo, M. A., Llinas, R. H., and Marsh, E. B. (2018). Cerebral microbleeds shouldn't dictate treatment of acute stroke: a retrospective cohort study evaluating risk of intracerebral hemorrhage. *BMC Neurol.* 18:33.

Charidimou, A., Pasi, M., Fiorelli, M., Shams, S., von Kummer, R., Pantoni, L., et al. (2016). Leukoaraiosis, cerebral hemorrhage, and outcome after intravenous thrombolysis for acute ischemic stroke: a meta-analysis (v1). *Stroke* 47, 2364–2372. doi: 10.1161/strokeaha.116.014096

Chen, X., Wang, J., Shan, Y., Cai, W., Liu, S., Hu, M., et al. (2019). Cerebral small vessel disease: neuroimaging markers and clinical implication. *J. Neurol.* 266, 2347–2362. doi: 10.1007/s00415-018-9077-3

Curtze, S., Haapaniemi, E., Melkas, S., Mustanoja, S., Putaala, J., Sairanen, T., et al. (2015a). White matter lesions double the risk of post-thrombolytic intracerebral hemorrhage. *Stroke* 46, 2149–2155. doi: 10.1161/strokeaha.115.009318

Curtze, S., Melkas, S., Sibolt, G., Haapaniemi, E., Mustanoja, S., Putaala, J., et al. (2015b). Cerebral computed tomography-graded white matter lesions are associated with worse outcome after thrombolysis in patients with stroke. *Stroke* 46, 1554–1560. doi: 10.1161/strokeaha.115.008941

Curtze, S., Putaala, J., Sibolt, G., Melkas, S., Mustanoja, S., Haapaniemi, E., et al. (2016). Cerebral white matter lesions and post-thrombolytic remote parenchymal hemorrhage. *Ann. Neurol.* 80, 593–599. doi: 10.1002/ana.24760

Dannenberg, S., Scheitz, J. F., Rozanski, M., Erdur, H., Brunecker, P., Werring, D. J., et al. (2014). Number of cerebral microbleeds and risk of intracerebral hemorrhage after intravenous thrombolysis. *Stroke* 45, 2900–2905. doi: 10.1161/strokeaha.114.006448

de Heus, R., Reumers, S., van der Have, A., Tumelaire, M., Tully, P. J., and Claassen, J. A. H. R. (2020). Day-to-Day home blood pressure variability is associated with cerebral small vessel disease burden in a memory clinic population. *J. Alzheimers Dis.* 74, 463–472. doi: 10.3233/jad-191134

Derex, L., Nighoghossian, N., Hermier, M., Adeleine, P., Philippeau, F., Honnorat, J., et al. (2004). Thrombolysis for ischemic stroke in patients with old microbleeds on pretreatment MRI. *Cerebrovasc. Dis.* 17, 238–241. doi: 10.1159/000076123

Dong, J., and Xia, Y. J. (2018). The application value of magnetic resonance SWI in the diagnosis and treatment of acute cerebral infraction. *J. Med. Imaging* 28, 1423–1426.

Drelon, A., Kuchcinski, G., Caparros, F., Dequatre-Ponchelle, N., Moulin, S., Cordonnier, C., et al. (2020). Remote brain hemorrhage after IV thrombolysis: role of preexisting lesions. *Neurology* 94, e961–e967.

Dzialowski, I., Pexman, J. H., Barber, P. A., Demchuk, A. M., Buchan, A. M., Hill, M. D., et al. (2007). Asymptomatic hemorrhage after thrombolysis may not be benign: prognosis by hemorrhage type in the Canadian alteplase for stroke effectiveness study registry. *Stroke* 38, 75–79. doi: 10.1161/01.str.0000251644.76546.62

Egger, M., Davey, S. G., Schneider, M., and Minder, C. (1997). Bias in meta-analysis detected by a simple, graphical test. *BMJ* 315, 629–634. doi: 10.1136/bmj.315.7109.629

Eggers, C., Bocksrucker, C., and Seyfang, L. (2017). The efficacy of thrombolysis in lacunar stroke – evidence from the Austrian Stroke Unit Registry. *Eur. J. Neurol.* 24, 780–787. doi: 10.1111/ene.13288

Emberson, J., Lees, K. R., Lyden, P., Blackwell, L., Albers, G., Bluhmki, E., et al. (2014). Effect of treatment delay, age, and stroke severity on the effects of intravenous thrombolysis with alteplase for acute ischaemic stroke: a meta-analysis of individual patient data from randomised trials. *Lancet* 384, 1929–1935. doi: 10.1016/s0140-6736(14)60584-5

Farrall, A. J., and Wardlaw, J. M. (2009). Blood-brain barrier: ageing and microvascular disease–systematic review and meta-analysis. *Neurobiol. Aging* 30, 337–352. doi: 10.1016/j.neurobiolaging.2007.07.015

Fiorelli, M., Bastianello, S., von Kummer, R., del Zoppo, G. J., Larrue, V., Lesaffre, E., et al. (1999). Hemorrhagic transformation within 36 hours of a cerebral infarct: relationships with early clinical deterioration and 3-month outcome in the European Cooperative Acute Stroke Study I (ECASS I) cohort. *Stroke* 30, 2280–2284. doi: 10.1161/01.str.30.11.2280

GBD 2016 Stroke Collaborators (2019). Global, regional, and national burden of stroke, 1990-2016: a systematic analysis for the Global Burden of Disease Study 2016. *Lancet Neurol.* 18, 439–458.

Gregg, N. M., Kim, A. E., Gurol, M. E., Lopez, O. L., Aizenstein, H. J., Price, J. C., et al. (2015). Incidental cerebral microbleeds and cerebral blood flow in elderly individuals. *JAMA Neurol.* 72, 1021–1028. doi: 10.1001/jamaneurol.2015.1359

Hacke, W., Kaste, M., Bluhmki, E., Brozman, M., Dávalos, A., and Guidetti, D. (2008). Thrombolysis with alteplase 3 to 4.5 hours after acute ischemic stroke. *N. Engl. J. Med.* 359, 1317–1329.

Higgins, J. P., Thompson, S. G., Deeks, J. J., and Altman, D. G. (2003). Measuring inconsistency in meta-analyses. *BMJ* 327, 557–560. doi: 10.1136/bmj.327.7414.557

Huang, S. S. (2017). Cerebral microhemorrhage foci are associated with hemorrhage transformation and prognosis of patients with acute cerebral infarction after intravenous thrombolysis. *Med. J. Commun.* 31, 63–65.

Jickling, G. C., Liu, D., Stamova, B., Ander, B. P., Zhan, X., Lu, A., et al. (2014). Hemorrhagic transformation after ischemic stroke in animals and humans. *J. Cereb. Blood Flow Metab.* 34, 185–199. doi: 10.1038/jcbfm.2013.203

Kakuda, W., Thijs, V. N., Lansberg, M. G., Bammer, R., Wechsler, L., Kemp, S., et al. (2005). Clinical importance of microbleeds in patients receiving IV thrombolysis. *Neurology* 65, 1175–1178. doi: 10.1212/01.wnl.0000180519.27680.0f

Larrue, V., von Kummer, R. R., Müller, A., and Bluhmki, E. (2001). Risk factors for severe hemorrhagic transformation in ischemic stroke patients treated with recombinant tissue plasminogen activator: a secondary analysis of the European-Australasian Acute Stroke Study (ECASS II). *Stroke* 32, 438–441. doi: 10.1161/01.str.32.2.438

Lindsay, M. P., Norrving, B., Sacco, R. L., Brainin, M., Hacke, W., Martins, S., et al. (2019). World Stroke Organization (WSO): global stroke fact sheet 2019. *Int. J. Stroke* 14, 806–817. doi: 10.1177/1747493019881353

Liu, L., Luo, H., Liu, H., et al. (2019). Influence of cerebral small vessel disease overall burden on clinical outcome of acute stroke patients after intravenous thrombolysis. *Chin. J. Cerebrovasc. Dis.* 16, 393–399.

Liu, X., Li, T., Diao, S., Cai, X., Kong, Y., Zhang, L., et al. (2019a). The global burden of cerebral small vessel disease related to neurological deficit severity and clinical outcomes of acute ischemic stroke after IV rt-PA treatment. *Neurol. Sci.* 40, 1157–1166. doi: 10.1007/s10072-019-03790-x

Liu, X., Li, T., Wang, Z., et al. (2019b). Relationship between total cerebral small vessel disease burden and hemorrhagic transformation of acute ischemic stroke patients after intravenous thrombolysis. *Chin. J. Neurol.* 52, 209–215.

Liu, X., Zhang, J., Tian, C., and Wang, J. (2020). The relationship of leukoaraiosis, haemorrhagic transformation and prognosis at 3 months after intravenous thrombolysis in elderly patients aged >= 60 years with acute cerebral infarction. *Neurol. Sci.* 41, 3195–3200. doi: 10.1007/s10072-020-04398-2

Liu, X. Y., Li, T., Mei, C. H., et al. (2019). Recent advances in hemorrhage transformation and clinical prognoses after intravenous thrombolysis in acute ischemic stroke with cerebral small vessel disease. *Chin. J. Neuromed.* 18, 481–486.

Liu, Y., Zhang, M., Chen, Y., Gao, P., Yun, W., and Zhou, X. (2018). The degree of leukoaraiosis predicts clinical outcomes and prognosis in patients with middle cerebral artery occlusion after intravenous thrombolysis. *Brain Res.* 1681, 28–33. doi: 10.1016/j.brainres.2017.12.033

Liu, Y., Zhang, M., Yun, W., Zhang, Z. X., Zhou, X. J., and Yun, W. W. (2017). Influence of moderate to severe leukoaraiosis on hemorrhagic transformation and prognosis of acute ischemic stroke patients after intravenous thrombolysis. *Chin. J. Neurol.* 50, 885–891.

Matusevicius, M., Paciaroni, M., Caso, V., Bottai, M., Khurana, D., de Bastos, M., et al. (2019). Outcome after intravenous thrombolysis in patients with acute lacunar stroke: an observational study based on SITS international registry and a meta-analysis. *Int. J. Stroke* 14, 878–886. doi: 10.1177/1747493019840947

Moriya, Y., Takahashi, W., Kijima, C., Yutani, S., Iijima, E., Mizuma, A., et al. (2013). Predictors for hemorrhagic transformation with intravenous tissue plasminogen activator in acute ischemic stroke. *Tokai J. Exp. Clin. Med.* 38, 24–27.

Nagaraja, N., Tasneem, N., Shaban, A., Dandapat, S., Ahmed, U., Policeni, B., et al. (2018). Cerebral microbleeds are an independent predictor of hemorrhagic transformation following intravenous alteplase administration in acute ischemic stroke. *J. Stroke Cerebrovasc. Dis.* 27, 1403–1411. doi: 10.1016/j.jstrokecerebrovasdis.2017.12.044

No authors listed (1989). Stroke–1989. Recommendations on stroke prevention, diagnosis, and therapy. Report of the WHO task force on stroke and other cerebrovascular disorders. *Stroke* 20, 1407–1431. doi: 10.1161/01.str.20.10.1407

No authors listed (1997). Intracerebral hemorrhage after intravenous t-PA therapy for ischemic stroke. The NINDS t-PA Stroke Study Group. *Stroke* 28, 2109–2118. doi: 10.1161/01.str.28.11.2109

Pang, J., Zhang, J. H., and Jiang, Y. (2019). Delayed recanalization in acute ischemic stroke patients: late is better than never? *J. Cereb. Blood Flow Metab.* 39, 2536–2538. doi: 10.1177/0271678x19881449

Pantoni, L. (2010). Cerebral small vessel disease: from pathogenesis and clinical characteristics to therapeutic challenges. *Lancet Neurol.* 9, 689–701. doi: 10.1016/s1474-4422(10)70104-6

Park, J. H., Ko, Y., Kim, W. J., Jang, M. S., Yang, M. H., Han, M.-K., et al. (2012). Is asymptomatic hemorrhagic transformation really innocuous? *Neurology* 78, 421–426. doi: 10.1212/wnl.0b013e318245d22c

Powers, W. J., Rabinstein, A. A., Ackerson, T., Adeoye, O. M., Bambakidis, N. C., Becker, K., et al. (2019). Guidelines for the early management of patients with acute ischemic stroke: 2019 update to the 2018 guidelines for the early management of acute ischemic stroke: a guideline for healthcare professionals from the American Heart Association/American Stroke Association. *Stroke* 50, e344–e418.

Rha, J. H., Shrivastava, V. P., Wang, Y., Lee, K. E., Ahmed, N., Bluhmki, E., et al. (2014). Thrombolysis for acute ischaemic stroke with alteplase in an Asian population: results of the multicenter, multinational safe implementation of thrombolysis in Stroke-Non-European Union World (SITS-NEW). *Int. J. Stroke* 9(Suppl. A100), 93–101. doi: 10.1111/j.1747-4949.2012.00895.x

Shi, Y., Thrippleton, M. J., Makin, S. D., Marshall, I., Geerlings, M. I., de Craen, A. J. M., et al. (2016). Cerebral blood flow in small vessel disease: a systematic review and meta-analysis. *J. Cereb. Blood Flow Metab.* 36, 1653–1667. doi: 10.1177/0271678x16662891

Staals, J., Makin, S. D., Doubal, F. N., Dennis, M. S., and Wardlaw, J. M. (2014). Stroke subtype, vascular risk factors, and total MRI brain small-vessel disease burden. *Neurology* 83, 1228–1234. doi: 10.1212/wnl.0000000000000837

Staszewski, J., Skrobowska, E., Piusińska-Macoch, R., Brodacki, B., and Stępień, A. (2019). Cerebral and extracerebral vasoreactivity in patients with different clinical manifestations of cerebral small-vessel disease: data from the significance of hemodynamic and hemostatic factors in the course of different manifestations of cerebral small-vessel disease study. *J. Ultrasound Med.* 38, 975–987. doi: 10.1002/jum.14782

Terruso, V., D'Amelio, M., Di Benedetto, N., Lupo, I., Saia, V., Famoso, G., et al. (2009). Frequency and determinants for hemorrhagic transformation of cerebral infarction. *Neuroepidemiology* 33, 261–265. doi: 10.1159/000229781

Tsivgoulis, G., Zand, R., Katsanos, A. H., Turc, G., Nolte, C. H., Jung, S., et al. (2016). Risk of symptomatic intracerebral hemorrhage after intravenous thrombolysis in patients with acute ischemic stroke and high cerebral microbleed burden: a meta-analysis. *JAMA Neurol.* 73, 675–683. doi: 10.1001/jamaneurol.2016.0292

Turc, G., Isabel, C., and Calvet, D. (2014). Intravenous thrombolysis for acute ischemic stroke. *Diagn. Interv. Imaging* 95, 1129–1133.

van Leijsen, E., Bergkamp, M. I., van Uden, I., Ghafoorian, M., van der Holst, H. M., Norris, D. G., et al. (2018). Progression of white matter hyperintensities preceded by heterogeneous decline of microstructural integrity. *Stroke* 49, 1386–1393. doi: 10.1161/strokeaha.118.020980

Wang, H., Nie, Z. Y., Liu, M., Li, R. R., Huang, L. H., Lu, Z., et al. (2020). Clinical characteristics of perivascular space and brain CT perfusion in stroke-free patients with intracranial and extracranial atherosclerosis of different extents. *Ann. Transl. Med.* 8:215. doi: 10.21037/atm.2020.01.35

Wang, S., Lv, Y., Zheng, X., Qiu, J., and Chen, H. S. (2017). The impact of cerebral microbleeds on intracerebral hemorrhage and poor functional outcome of acute ischemic stroke patients treated with intravenous thrombolysis: a systematic review and meta-analysis. *J. Neurol.* 264, 1309–1319.

Wardlaw, J. M., Smith, E. E., Biessels, G. J., Cordonnier, C., Fazekas, F., Frayne, R., et al. (2013). Neuroimaging standards for research into small vessel disease and its contribution to ageing and neurodegeneration. *Lancet Neurol.* 12, 822–838.

Wells, G. A., Shea, B., Higgins, J. P., Sterne, J., Tugwell, P., and Reeves, B. C. (2013). Checklists of methodological issues for review authors to consider when including non-randomized studies in systematic reviews. *Res. Synth. Methods* 4, 63–77. doi: 10.1002/jrsm.1077

Wen, L., Guofang, C., Yixin, L., Weitvei, L., Lei, P., Shengku, Z., et al. (2019). White matter hyperintensities and prognosis of patients with acute cerebral infarction treated by intravenous thrombolysis with alteplasejan analysis of influencing factors. *Chin. J. Cerebrovasc. Dis.* 16, 508–513.

Xue, J., Wang, H., Gao, P. Y., et al. (2017). Study on correlation between cerebral microbleeds and hemorrhagic transformation after thrombolytic therapy in acute ischemic stroke. *Chin. J. Stroke* 12, 477–483.

Yan, S., Jin, X., Zhang, X., Zhang, S., Liebeskind, D. S., and Lou, M. (2015a). Extensive cerebral microbleeds predict parenchymal haemorrhage and poor outcome after intravenous thrombolysis. *J. Neurol. Neurosurg. Psychiatry* 86, 1267–1272. doi: 10.1136/jnnp-2014-309857

Yan, S., Mao, Y., Zhong, G., Zhang, S., and Lou, M. (2015b). Safety of intravenous thrombolysis in cerebral microbleeds patients with prior antiplatelet therapy. *Zhejiang Da Xue Xue Bao Yi Xue Ban* 44, 618–624.

Yan, S. Q., Wan, J. P., Guo, Y., Zhang, S., and Lou, M. (2014). [Impact of cerebral microbleeds on outcomes of acute ischemic stroke treated with intravenous thrombolysis]. *Zhejiang Da Xue Xue Bao Yi Xue Ban* 43, 20–27.

Zhang, D. P., Yin, S., Zhang, H. L., Li, D., Song, B., and Liang, J. X. (2020). Association between intracranial arterial dolichoectasia and cerebral small vessel disease and its underlying mechanisms. *J. Stroke* 22, 173–184. doi: 10.5853/jos.2019.02985

Zhang, Y. X., and Zhang, P. L. (2018). Safety of intravenous thrombolytic therapy with alteplase in patients with acute cerebral ischemic stroke complicated with cerebral microbleeds. *J. Apoplexy Nerv. Dis.* 34, 314–316.

Zheng, T. H., Hao, J. J., Zhou, X. Y., et al. (2012). Analysis of related factors of early intracranial hemorrhage after intravenous rt-PA thrombolysis in advance-aged patients with cerebral infarction. *Chin. J. Cerebrovasc. Dis.* 9:362.

Zhuo, Z. L., Nie, Z. Y., Liu, Y. H., et al. (2020). Correlation between total burden of cerebral small vessel disease and outcome after intravenous thrombolysis in acute ischemic stroke patients. *Chin. J. Stroke* 15, 734–739.

Conflict of Interest: The authors declare that the research was conducted in the absence of any commercial or financial relationships that could be construed as a potential conflict of interest.

frontiers in Aging Neuroscience

OPINION
published: 28 July 2021
doi: 10.3389/fnagi.2021.721937

The Neurovascular Unit in Dementia: An Opinion on Current Research and Future Directions

Lucy Beishon[1]* *and Ronney B. Panerai*[1,2]

[1] Department of Cardiovascular Sciences, University of Leicester, Leicester, United Kingdom, [2] National Institute for Health Research Leicester Biomedical Research Centre, British Heart Foundation Cardiovascular Research Centre, Glenfield Hospital, Leicester, United Kingdom

Keywords: Alzheimer's disease, mild cognitive impairment, cerebrovascular disease, cognitive dysfunction, neurovascular coupling

INTRODUCTION

Dementia is a burgeoning public health crisis, with 50 million people currently affected worldwide (Prince et al., 2015). As the population ages, this figure is set to rise dramatically by 40% over the next 12 years (Prince et al., 2015). Dementia is an umbrella term for several disorders which result in the progressive loss of memory or other cognitive functions (Scott and Barrett, 2007). It remains an incurable disease, and current therapeutics have limited efficacy at slowing disease progression for one third of patients (Rockwood et al., 2008). Of the dementia sub-types, Alzheimer's disease (AD) remains the most prevalent, accounting for ∼60–70% cases (Alzheimer's-Society, 2016). Vascular dementia (VaD) is the second most common form and is responsible for ∼20% of cases, with a further 10% being a combination of these two diseases (Alzheimer's-Society, 2016). However, in practise these distinctions are somewhat arbitrary given the significant overlap in altered vascular structure and function in both of these major sub-types (Kalaria and Ballard, 1999). At least 30% of patients with AD have evidence of cerebrovascular disease on post-mortem examination, and almost all have evidence of cerebral amyloid angiopathy, microvascular degeneration, and white matter lesions (Kalaria and Ballard, 1999). Similarly, one-third of patients with VaD exhibit pathology consistent with AD (e.g., hippocampal or temporal lobe atrophy) (Kalaria and Ballard, 1999). Longitudinal studies have demonstrated that vascular risk factors (e.g., hypertension), significantly increase the risk of both AD and VaD (Rius-Pérez et al., 2018). In genetically at-risk individuals positive for apolipoprotein E4 (APOE4), atherosclerosis can increase the risk of AD by three-fold (Hoffmann et al., 2010). This article provides an opinion on the current evidence on the role of the neurovascular unit in dementia, for further information, several recent reviews are available on this topic (Nelson et al., 2016; Kisler et al., 2017).

AMYLOID CASCADE HYPOTHESIS

A number of mechanistic models have been proposed to understand the pathological basis of AD. The amyloid cascade hypothesis gained increasing traction over the last few decades, having dominated the research sphere (Morris et al., 2014). Amyloid-based biomarkers have been incorporated into a number of diagnostic guidelines (Jack et al., 2018), and the histopathological (gold standard) diagnosis of AD includes the presence of amyloid plaque and neurofibrillatory tangles (Deture and Dickson, 2019). However, despite decades of research into this hypothesis, and several large trials of amyloid based drugs, none have demonstrated efficacy warranting their widespread use in clinical practise (Morris et al., 2014). Only tramiprosate, a selective anti-oligomer agent, has demonstrated potential benefit for a sub-group of APOE4 positive individuals with early AD and is currently under investigation in a phase three trial (Tolar et al., 2020). These

OPEN ACCESS

Edited by:
Shereen Nizari, University College London, United Kingdom

Reviewed by:
Amy Renee Nelson, University of South Alabama, United States

***Correspondence:**
Lucy Beishon
Lb330@le.ac.uk

Received: *07 June 2021*
Accepted: *06 July 2021*
Published: *28 July 2021*

Citation:
Beishon L and Panerai RB (2021) The Neurovascular Unit in Dementia: An Opinion on Current Research and Future Directions. Front. Aging Neurosci. 13:721937. doi: 10.3389/fnagi.2021.721937

findings have raised several questions around the amyloid cascade hypothesis. Firstly, the lack of efficacy for amyloid-based targets may suggest amyloid is a by-product rather than causative agent of the disease process. This is supported by the finding that amyloid deposition commonly occurs in cognitively healthy older adults, and plaque burden does not correlate well with the level of cognitive deficit (Morris et al., 2014). In contrast, synaptic loss, microglial activation, neurofibrillatory tangles, and cerebral blood flow correlate better with disease severity in AD (Rius-Pérez et al., 2018). Secondly, the potential efficacy in a subgroup of early AD (Tolar et al., 2020) suggests that amyloid is a late occurrence in the disease process, at which stage irrevocable damage and cognitive decline has ensued. Furthermore, only patients with a strong genetic risk may benefit from these therapies (Tolar et al., 2020), limiting the wider applicability of these drugs. These unanswered questions have thus stimulated the search for earlier potential therapeutic targets, particularly those which are identifiable at earlier stages, preceding the development of cognitive decline and amyloid deposition.

VASCULAR CASCADE HYPOTHESIS

The vascular cascade hypothesis postulates that early disruption of vascular mechanisms as a result of sustained vascular risk factors and poor lifestyle habits, results in a state of chronic hypoperfusion (Rius-Pérez et al., 2018). This leads to the development of blood brain barrier breakdown, tau hyperphosphorylation, and amyloid deposition (Nelson et al., 2016). The blood brain barrier is essential to maintain a tightly controlled environment, and contributes to the clearance of amyloid-beta (Rius-Pérez et al., 2018). BBB dysfunction has been demonstrated to occur in the hippocampus with normal ageing (Montagne et al., 2015), early AD (Nation et al., 2019), and in APOE4 positive individuals (Montagne et al., 2020). As a result, amyloid deposition damages the cerebrovasculature, both structurally and functionally, therefore worsening hypoperfusion in a cyclical fashion (Nelson et al., 2016). These findings led to the development of the two-hit hypothesis, where the vascular insult represents the first "hit" to the system, followed by the amyloid or second "hit," with the two processes subsequently interacting in a dynamic manner to worsen hypoperfusion, increase tau hyperphosphorylation, and promote amyloid deposition (Nelson et al., 2016). Importantly, the vascular hit is thought to occur earlier in the disease process (Hays et al., 2016). This notion is supported by longitudinal studies of ageing demonstrating that alterations in cerebral haemodynamics are detectable in cognitively intact older adults, and are predictive of future dementia risk (Wolters et al., 2017).

THE NEUROVASCULAR UNIT IN DEMENTIA

The neurovascular unit is formed by the neurone and its supporting cells (astrocytes, endothelial cells, pericytes, and smooth muscle cells) (Iadecola, 2017). They are closely related both structurally and functionally to ensure the tight coupling of neuronal activity and cerebral blood flow, termed neurovascular coupling (NVC) (Iadecola, 2017). This is achieved through feedforward and feedback mechanisms as a result of the release of active metabolites and chemical mediators (Hosford and Gourine, 2019). De-coupling of these processes has been shown to occur in animal models of AD (Girouard and Iadecola, 2006). Human studies have demonstrated conflicting findings of both increased (Corriveau-Lecavalier et al., 2019), and decreased (Beishon et al., 2018) vascular responses to cognitive stimulation. These opposing findings may reflect compensatory mechanisms occurring early in the disease process, vs. the failure of these mechanisms at later stages (Merlo et al., 2019).

Therefore, deficiencies occurring in one or more components of the NVU threaten this tightly coordinated system. Inadequate matching of perfusion to neuronal activity will fail to clear the active metabolites generated by a resource intensive process, the accumulation of which can result in neurotoxicity (Girouard and Iadecola, 2006). Furthermore, inadequate perfusion will limit the provision of oxygen and glucose, essential for optimal neuronal function and cell signalling, thus limiting the capacity for cognitive function (Girouard and Iadecola, 2006).

THE NVU AS A BIOMARKER AND THERAPEUTIC TARGET IN DEMENTIA

As a result of these findings, increasing interest in the NVU as both a biomarker and therapeutic target has emerged. A number of neuroimaging based methods have been used to detect abnormalities in cerebral haemodynamics occurring in healthy, mildly impaired, or established dementia (Hays et al., 2016). A number of neuroimaging based biomarkers have been investigated, and can be broadly divided into portable and non-portable based techniques. Portable techniques have the advantage of providing a simple, bedside measurement with excellent temporal resolution and continuous monitoring of haemodynamic measures (Panerai, 2009; Balardin et al., 2017). Studies measuring metabolic changes, as a proxy for perfusion, have demonstrated good sensitivity and specificity to differentiate stable and progressive forms of mild cognitive impairment (MCI) (Henderson, 2012; Marcus et al., 2014). However, many of these techniques remain confined to the research domain, and are only recommended where the diagnosis remains uncertain (National Institute for Health Care Excellence, 2018).

In terms of vascular targets, the majority of research has focussed on currently available treatments to modify vascular risk, such as antihypertensive drugs (Bhat, 2015). Given the extensive evidence supporting a role for vascular mechanisms in the development of AD, modification of vascular risk is an attractive and amenable target. However, to gain benefit, these factors are likely to need controlling in mid-life given that these risks translate into cognitive decline over a sustained and longer period (Livingston et al., 2020). Furthermore, the role for vascular risk, and particularly blood pressure reduction, remains uncertain for people with established dementia (Harrison et al., 2016). A recent Cochrane review found limited evidence to support antihypertensive withdrawal in dementia, and may

result in increased cardiovascular events (Jongstra et al., 2016). Data from observational studies suggest cerebral autoregulation remains intact in MCI and dementia (De Heus et al., 2018), and a recent study demonstrated improved hippocampal CBF in patients with dementia treated with nilvadipine (Jong et al., 2019). The RADAR trial is currently ongoing, and will investigate the effects of losartan in mild to moderate AD on brain atrophy, white matter hyper intensities, and cerebral blood flow (Kehoe et al., 2018). Recently, interest has been gaining momentum on the effects of lifestyle interventions (exercises, diet, cognitive intervention) on cerebrovascular function, and whether multi-modal interventions can promote vascular brain health. In two recent systematic reviews (Beishon et al., 2020), cognitive training has been demonstrated to alter brain volumes and functional connectivity in MCI and dementia, but few studies have specifically investigated their effects on vascular mechanisms. Finally, novel therapeutic targets have been proposed around the various components of the NVU (Zlokovic, 2011). Vasculoprotective agents that target blood brain barrier function (e.g., activated protein C) and promote integrity are promising (Zlokovic, 2011). Similarly, mediators that promote angiogenesis (vascular endothelial growth factor) or improve amyloid-beta clearance (insulin like growth factor) may also be beneficial (Zlokovic, 2011).

DISCUSSION

In summary, vascular mechanisms play a key role in development and progression of cognitive dysfunction. Importantly, disruption to vascular physiology occurs early in the disease process, providing a potential target to prevent or delay the onset of dementia. Despite this breadth of evidence demonstrating both structural and functional damage to the cerebrovascular system in early dementia, few vascular targets have been the subject of large-scale randomised controlled trials. Disappointingly, in a recent review, few trials employed agents or targets of vascular dysfunction (Huang et al., 2020). This suggests more work is needed in both animal models to identify potential targets, and in patients to take these targets to clinical trials. Importantly, the identification of new targets has been hampered by a lack of translation between animal models and clinical trials (Cavanaugh et al., 2014). Current transgenic animal models of AD most closely represent inherited forms of AD, which are not the dominant phenotype seen in clinical practise (Cavanaugh et al., 2014). These models will have a bias towards amyloid-based pathology, and may not reflect the alterations to vascular structure and function seen in humans, particularly with late-onset AD. Furthermore, the amyloid pathology in animal models does not correlate well with that seen in humans, suggesting there are key differences in the pathological basis of AD development between species (Cavanaugh et al., 2014). BBB dysfunction has been demonstrated in animal models of AD (Montagne et al., 2017), but amongst genetic-based models which may be pathologically distinct from late onset AD seen clinically. In addition to drug-based targets, research is urgently needed to clarify the role of lifestyle interventions on cerebrovascular disease in dementia risk reduction and treatment. Lifestyle interventions are resource intensive, and can be physically and mentally demanding for people with dementia to undertake. The Finnish Geriatric Intervention Study to Prevent Cognitive Impairment and Disability (FINGER) randomised at-risk older adults to an intensive programme of diet, exercise, cognitive training, and vascular risk monitoring, lasting 2 years (Ngandu et al., 2015). The trial found small benefits to cognitive function in the intervention group, with a drop-out rate of ∼12% (Ngandu et al., 2015). Given that benefits to cognitive function tend to be small, and the long trajectory to cognitive decline, cerebrovascular biomarkers as a surrogate for clinical outcome measures could be beneficial in reducing the durations required for clinical trials to demonstrate effectiveness. However, limited information is available on the effects of such multi-modal interventions on cerebrovascular function, and their relationship to longer term clinical outcomes. Future trials of lifestyle interventions would benefit from the addition of cerebrovascular outcomes to understand the effects on vascular structure and function, which could contribute to the identification of novel therapeutic targets.

AUTHOR CONTRIBUTIONS

LB and RP jointly drafted the manuscript. All authors contributed to the article and approved the submitted version.

FUNDING

LB was a research training fellow supported by the Dunhill Medical trust (RTF\1806\27).

REFERENCES

Alzheimer's-Society (2016). *Demography [Online]*. London: Alzheimer's Society. Available online at: https://www.alzheimers.org.uk/info/20091/position_statements/93/demography (accessed February 12, 2017).

Balardin, J. B., Zimeo Morais, G. A., Furucho, R. A., Trambaiolli, L., Vanzella, P., Biazoli, C. Jr., et al. (2017). Imaging brain function with functional near-infrared spectroscopy in unconstrained environments. *Front. Hum. Neurosci.* 11:258. doi: 10.3389/fnhum.2017.00258

Beishon, L., Intharakham, K., Swienton, D., Panerai, R. B., Robinson, T. G., and Haunton, V. J. (2020). Neuroimaging outcomes in studies of cognitive training in mild cognitive impairment and early Alzheimer's disease: a systematic review. *Curr. Alzheimer Res.* 17, 472–486. doi: 10.2174/1567205017666200624202425

Beishon, L., Panerai, R. B., Robinson, T. G., Subramaniam, H., and Haunton, V. J. (2018). The assessment of cerebrovascular response to a language task from the Addenbrooke's cognitive examination in cognitive impairment: a feasibility functional transcranial Doppler ultrasonography study. *J. Alzheimers Dis. Rep.* 2, 153–164. doi: 10.3233/ADR-180068

Bhat, N. R. (2015). Vasculoprotection as a convergent, multi-targeted mechanism of anti-AD therapeutics and interventions. *J. Alzheimers Dis.* 46, 581–591. doi: 10.3233/JAD-150098

Cavanaugh, S. E., Pippin, J. J., and Barnard, N. D. (2014). Animal models of Alzheimer disease: historical pitfalls and a path forward. *Altex* 31, 279–302. doi: 10.14573/altex.1310071

Corriveau-Lecavalier, N., Mellah, S., Clément, F., and Belleville, S. (2019). Evidence of parietal hyperactivation in individuals with mild cognitive impairment

who progressed to dementia: a longitudinal fMRI study. *NeuroImage Clin.* 24:101958. doi: 10.1016/j.nicl.2019.101958

De Heus, R. A. A., De Jong, D. L. K., Sanders, M. L., Van Spijker, G. J., Oudegeest-Sander, M. H., Hopman, M. T., et al. (2018). Dynamic regulation of cerebral blood flow in patients with Alzheimer disease. *Hypertension* 72, 139–150. doi: 10.1161/HYPERTENSIONAHA.118.10900

Deture, M. A., and Dickson, D. W. (2019). The neuropathological diagnosis of Alzheimer's disease. *Mol. Neurodegener.* 14:32. doi: 10.1186/s13024-019-0333-5

Girouard, H., and Iadecola, C. (2006). Neurovascular coupling in the normal brain and in hypertension, stroke, and Alzheimer disease. *J. Appl. Physiol.* 100, 328–335. doi: 10.1152/japplphysiol.00966.2005

Harrison, J. K., Van Der Wardt, V., Conroy, S. P., Stott, D. J., Dening, T., Gordon, A. L., et al. (2016). New horizons: the management of hypertension in people with dementia. *Age Ageing* 45, 740–746. doi: 10.1093/ageing/afw155

Hays, C. C., Zlatar, Z. Z., and Wierenga, C. E. (2016). The utility of cerebral blood flow as a biomarker of preclinical Alzheimer's disease. *Cell. Mol. Neurobiol.* 36, 167–179. doi: 10.1007/s10571-015-0261-z

Henderson, T. A. (2012). The diagnosis and evaluation of dementia and mild cognitive impairment with emphasis on SPECT perfusion neuroimaging. *CNS Spectr.* 17, 176–206. doi: 10.1017/S1092852912000636

Hoffmann, T., Bennett, S., Koh, C.-L., and Mckenna, K. (2010). A systematic review of cognitive interventions to improve functional ability in people who have cognitive impairment following stroke. *Top. Stroke Rehabil.* 17, 99–107. doi: 10.1310/tsr1702-99

Hosford, P. S., and Gourine, A. V. (2019). What is the key mediator of the neurovascular coupling response? *Neurosci. Biobehav. Rev.* 96, 174–181. doi: 10.1016/j.neubiorev.2018.11.011

Huang, L.-K., Chao, S.-P., and Hu, C.-J. (2020). Clinical trials of new drugs for Alzheimer disease. *J. Biomed. Sci.* 27:18. doi: 10.1186/s12929-019-0609-7

Iadecola, C. (2017). The neurovascular unit coming of age: a journey through neurovascular coupling in health and disease. *Neuron* 96, 17–42. doi: 10.1016/j.neuron.2017.07.030

Jack, C. R., Bennett, D. A., Blennow, K., Carrillo, M. C., Dunn, B., Haeberlein, S. B., et al. (2018). NIA-AA research framework: toward a biological definition of Alzheimer's disease. *Alzheimers Dement.* 14, 535–562. doi: 10.1016/j.jalz.2018.02.018

Jong, D. L. K. D., Heus, R. A. A. D., Rijpma, A., Donders, R., Rikkert, M. G. M. O., Günther, M., et al. (2019). Effects of nilvadipine on cerebral blood flow in patients with Alzheimer disease. *Hypertension* 74, 413–420. doi: 10.1161/HYPERTENSIONAHA.119.12892

Jongstra, S., Harrison, J. K., Quinn, T. J., and Richard, E. (2016). Antihypertensive withdrawal for the prevention of cognitive decline. *Cochrane Database Syst. Rev.* 11:CD011971. doi: 10.1002/14651858.CD011971.pub2

Kalaria, R. N., and Ballard, C. (1999). Overlap between pathology of Alzheimer disease and vascular dementia. *Alzheimer Dis. Assoc. Disord.* 13(Suppl. 3), S115–S123. doi: 10.1097/00002093-199912003-00017

Kehoe, P. G., Blair, P. S., Howden, B., Thomas, D. L., Malone, I. B., Horwood, J., et al. (2018). The rationale and design of the reducing pathology in Alzheimer's disease through angiotensin targeting (RADAR) trial. *J. Alzheimers Dis.* 61, 803–814. doi: 10.3233/JAD-170101

Kisler, K., Nelson, A. R., Montagne, A., and Zlokovic, B. V. (2017). Cerebral blood flow regulation and neurovascular dysfunction in Alzheimer disease. *Nat. Rev. Neurosci.* 18, 419–434. doi: 10.1038/nrn.2017.48

Livingston, G., Huntley, J., Sommerlad, A., Ames, D., Ballard, C., Banerjee, S., et al. (2020). Dementia prevention, intervention, and care: 2020 report of the Lancet Commission. *Lancet* 396, 413–446. doi: 10.1016/S0140-6736(20)30367-6

Marcus, C., Mena, E., and Subramaniam, R. M. (2014). Brain PET in the diagnosis of Alzheimer's disease. *Clin. Nucl. Med.* 39, e413–e422. doi: 10.1097/RLU.0000000000000547

Merlo, S., Spampinato, S. F., and Sortino, M. A. (2019). Early compensatory responses against neuronal injury: a new therapeutic window of opportunity for Alzheimer's Disease? *CNS Neurosci. Ther.* 25, 5–13. doi: 10.1111/cns.13050

Montagne, A., Barnes, S. R., Sweeney, M. D., Halliday, M. R., Sagare, A. P., Zhao, Z., et al. (2015). Blood-brain barrier breakdown in the aging human hippocampus. *Neuron* 85, 296–302. doi: 10.1016/j.neuron.2014.12.032

Montagne, A., Nation, D. A., Sagare, A. P., Barisano, G., Sweeney, M. D., Chakhoyan, A., et al. (2020). APOE4 leads to blood–brain barrier dysfunction predicting cognitive decline. *Nature* 581, 71–76. doi: 10.1038/s41586-020-2247-3

Montagne, A., Zhao, Z., and Zlokovic, B. V. (2017). Alzheimer's disease: a matter of blood-brain barrier dysfunction? *J. Exp. Med.* 214, 3151–3169. doi: 10.1084/jem.20171406

Morris, G. P., Clark, I. A., and Vissel, B. (2014). Inconsistencies and controversies surrounding the amyloid hypothesis of Alzheimer's disease. *Acta Neuropathol. Commun.* 2:135. doi: 10.1186/s40478-014-0135-5

Nation, D. A., Sweeney, M. D., Montagne, A., Sagare, A. P., D'orazio, L. M., Pachicano, M., et al. (2019). Blood–brain barrier breakdown is an early biomarker of human cognitive dysfunction. *Nat. Med.* 25, 270–276. doi: 10.1038/s41591-018-0297-y

National Institute for Health and Care Excellence (2018). *Dementia [Online]*. Available online at: https://pathways.nice.org.uk/pathways/dementia (accessed March 07, 2018).

Nelson, A. R., Sweeney, M. D., Sagare, A. P., and Zlokovic, B. V. (2016). Neurovascular dysfunction and neurodegeneration in dementia and Alzheimer's disease. *Biochim. Biophys. Acta* 1862, 887–900. doi: 10.1016/j.bbadis.2015.12.016

Ngandu, T., Lehtisalo, J., Solomon, A., Levälahti, E., Ahtiluoto, S., Antikainen, R., et al. (2015). A 2 year multidomain intervention of diet, exercise, cognitive training, and vascular risk monitoring versus control to prevent cognitive decline in at-risk elderly people (FINGER): a randomised controlled trial. *Lancet* 385, 2255–2263. doi: 10.1016/S0140-6736(15)60461-5

Panerai, R. B. (2009). Transcranial Doppler for evaluation of cerebral autoregulation. *Clin. Auton. Res.* 19, 197–211. doi: 10.1007/s10286-009-0011-8

Prince, M., Wimo, A., Guerchet, M., Ali, G.-C., Wu, Y.-T., and Prina, M. (2015). *World Alzheimer Report 2015. The Global Impact of Dementia. An Analysis of the Prevalence, Incidence, Costs, and Trends*. Alzheimer's Disease International.

Rius-Pérez, S., Tormos, A. M., Pérez, S., and Taléns-Visconti, R. (2018). Vascular pathology: cause or effect in Alzheimer disease? *Neurología* 33, 112–120. doi: 10.1016/j.nrleng.2015.07.008

Rockwood, K., Dai, D., and Mitnitski, A. (2008). Patterns of decline and evidence of subgroups in patients with Alzheimer's disease taking galantamine for up to 48 months. *Int. J. Geriatr. Psychiatry* 23, 207–214. doi: 10.1002/gps.1864

Scott, K. R., and Barrett, A. M. (2007). Dementia syndromes: evaluation and treatment. *Expert Rev. Neurother.* 7, 407–422. doi: 10.1586/14737175.7.4.407

Tolar, M., Abushakra, S., Hey, J. A., Porsteinsson, A., and Sabbagh, M. (2020). Aducanumab, gantenerumab, BAN2401, and ALZ-801—the first wave of amyloid-targeting drugs for Alzheimer's disease with potential for near term approval. *Alzheimers Res. Ther.* 12:95. doi: 10.1186/s13195-020-00663-w

Wolters, F. J., Zonneveld, H. I., Hofman, A., Van Der Lugt, A., Koudstaal, P. J., Vernooij, M. W., et al. (2017). Cerebral perfusion and the risk of dementia: a population-based study. *Circulation* 136, 719–728. doi: 10.1161/CIRCULATIONAHA.117.027448

Zlokovic, B. V. (2011). Neurovascular pathways to neurodegeneration in Alzheimer's disease and other disorders. *Nat. Rev. Neurosci.* 12, 723–738. doi: 10.1038/nrn3114

Conflict of Interest: The authors declare that the research was conducted in the absence of any commercial or financial relationships that could be construed as a potential conflict of interest.

Publisher's Note: All claims expressed in this article are solely those of the authors and do not necessarily represent those of their affiliated organizations, or those of the publisher, the editors and the reviewers. Any product that may be evaluated in this article, or claim that may be made by its manufacturer, is not guaranteed or endorsed by the publisher.

frontiers in Aging Neuroscience

ORIGINAL RESEARCH
published: 13 August 2021
doi: 10.3389/fnagi.2021.695965

Prostaglandin E_2 Dilates Intracerebral Arterioles When Applied to Capillaries: Implications for Small Vessel Diseases

*Amanda C. Rosehart[1], Thomas A. Longden[2], Nick Weir[2], Jackson T. Fontaine[1], Anne Joutel[3,4] and Fabrice Dabertrand[1,5]**

[1] Department of Anesthesiology, University of Colorado Anschutz Medical Campus, Aurora, CO, United States, [2] Department of Physiology, School of Medicine, University of Maryland, Baltimore, Baltimore, MD, United States, [3] INSERM, UMR 1266, GHU Paris Psychiatrie et Neurosciences, Institute of Psychiatry and Neuroscience of Paris, University of Paris, Paris, France, [4] Department of Pharmacology, Larner College of Medicine, University of Vermont, Burlington, VT, United States, [5] Department of Pharmacology, University of Colorado Anschutz Medical Campus, Aurora, CO, United States

Prostaglandin E_2 (PGE_2) has been widely proposed to mediate neurovascular coupling by dilating brain parenchymal arterioles through activation of prostanoid EP4 receptors. However, our previous report that direct application of PGE_2 induces an EP1-mediated constriction strongly argues against its direct action on arterioles during neurovascular coupling, the mechanisms sustaining functional hyperemia. Recent advances have highlighted the role of capillaries in sensing neuronal activity and propagating vasodilatory signals to the upstream penetrating parenchymal arteriole. Here, we examined the effect of capillary stimulation with PGE_2 on upstream arteriolar diameter using an *ex vivo* capillary-parenchymal arteriole preparation and *in vivo* cerebral blood flow measurements with two-photon laser-scanning microscopy. We found that PGE_2 caused upstream arteriolar dilation when applied onto capillaries with an EC_{50} of 70 nM. The response was inhibited by EP1 receptor antagonist and was greatly reduced, but not abolished, by blocking the strong inward-rectifier K^+ channel. We further observed a blunted dilatory response to capillary stimulation with PGE_2 in a genetic mouse model of cerebral small vessel disease with impaired functional hyperemia. This evidence casts previous findings in a different light, indicating that capillaries are the locus of PGE_2 action to induce upstream arteriolar dilation in the control of brain blood flow, thereby providing a paradigm-shifting view that nonetheless remains coherent with the broad contours of a substantial body of existing literature.

Keywords: functional hyperemia, cerebral small vessel diseases, CADASIL, microcirculation, neurovascular coupling, potassium channel, prostaglandin E_2, epidermal growth factor receptor

OPEN ACCESS

Edited by:
Anusha Mishra, Oregon Health and Science University, United States

Reviewed by:
Cam Ha Tran, University of Nevada, Reno, United States
George C. Wellman, University of Vermont, United States
Eric Newman, University of Minnesota, United States

****Correspondence:***
Fabrice Dabertrand
Fabrice.Dabertrand@CUAnschutz.edu

Received: *15 April 2021*
Accepted: *15 June 2021*
Published: *13 August 2021*

Citation:
Rosehart AC, Longden TA, Weir N, Fontaine JT, Joutel A and Dabertrand F (2021) Prostaglandin E_2 Dilates Intracerebral Arterioles When Applied to Capillaries: Implications for Small Vessel Diseases. Front. Aging Neurosci. 13:695965. doi: 10.3389/fnagi.2021.695965

INTRODUCTION

As a leading cause of stroke and dementia, cerebral small vessel diseases (SVDs) pose a horrendous threat to the elderly population (Pantoni, 2010; Wardlaw et al., 2019). Despite their major contribution to age-related vascular cognitive impairment and disability (Iadecola et al., 2019), the disease processes and key biological mechanisms underlying these disorders remain largely

unknown. Moreover, there are no specific treatments outside the management of vascular risk factors and use of anti-platelets after ischemic stroke. However, accumulating experimental evidence suggests that functional alterations in the cerebral microcirculation have early and deleterious consequences on functional hyperemia—the ability of the brain to increase local blood flow in response to local increases in neuronal activity (Huneau et al., 2018; Iadecola et al., 2019).

Cerebral Autosomal Dominant Arteriopathy with Subcortical Infarcts and Leukoencephalopathy (CADASIL) is the most common genetic form of cerebral SVDs. Remarkably, CADASIL includes all clinical and MRI manifestations of sporadic SVDs, hence offering a lens through which to view more common forms of sporadic SVDs (Chabriat et al., 2009). Both CADASIL patients and the *TgNotch3*^{R169C} mouse model, hereafter referred to as SVD mice, exhibit deficits in functional hyperemia at an early stage of the disease progression (Joutel et al., 2010; Huneau et al., 2018). We have recently demonstrated that activation of the epidermal growth factor receptor (EGFR) by its ligand heparin-binding EGF-like growth factor (HB-EGF) ameliorates the cerebral vascular deficits of the SVD mouse—including impaired functional hyperemia (Capone et al., 2016; Dabertrand et al., 2021). Part of this effect is mediated by reenabling capillary-to-arteriole signaling during the neurovascular coupling that underpins functional hyperemia (Dabertrand et al., 2021). In physiological conditions, action potentials increase extracellular K^+ concentration which activates the strong inward-rectifier K^+ (Kir2.1) channel in capillary endothelial cells (cECs). This creates a hyperpolarizing signal that rapidly propagates to upstream arterioles, driving vasodilation and local hyperemia (Longden et al., 2017; Harraz et al., 2018a; Moshkforoush et al., 2020). This mechanism is vulnerable to pathology, and we recently demonstrated that SVD lowers the synthesis of the phospholipid PIP_2, which prevents Kir2.1 channels from acting as sensors of increases in external K^+ (Dabertrand et al., 2021). Strikingly, we showed that both HB-EGF and systemic injection of exogenous PIP_2 improved functional hyperemia deficits in SVD mice by restoring capillary-to-arteriole signaling.

Functional hyperemia is a vital process controlled by multiple mechanisms that provide layers of redundancy, and thus neurovascular coupling agents other than K^+ ions have been postulated (Attwell et al., 2010; Kaplan et al., 2020). Among these, prostaglandin E_2 (PGE_2), produced by cyclooxygenase-2 (COX-2) from arachidonic acid, has been widely proposed to be released from excitatory neurons to relax arteriolar smooth muscle cells (SMCs) by activation of the G_S protein-coupled prostanoid EP4 receptor and subsequent cyclic adenosine monophosphate-dependent pathway (Zonta et al., 2002; Takano et al., 2005; Gordon et al., 2008; Attwell et al., 2010; Lacroix et al., 2015). Yet, this interpretation appears incompatible with our previous demonstration that PGE_2 causes constriction, rather than dilation, when applied directly to isolated cortical arterioles—an effect that occurs via activation of the G_q protein-coupled prostanoid EP1 receptor (Dabertrand et al., 2013). Consistent with these observations, the EP1 receptor is robustly expressed not only in the arteriolar SMCs, but also in cECs of the brain microcirculation (Vanlandewijck et al., 2018). We therefore hypothesized that PGE_2 contributes to neurovascular coupling by initiating a vasodilatory signal from the capillaries to the upstream parenchymal arterioles, rather than by targeting SMCs directly. Using a combination of *ex vivo* and *in vivo* approaches, we report that capillary stimulation with PGE_2 induces upstream arteriolar dilation and increases blood flow *in vivo*. Consistent with defective functional hyperemia, we further show that PGE_2-induced capillary-to-arteriole signaling is blunted in the SVD mouse model and can be rescued by HB-EGF.

MATERIALS AND METHODS

Animals

All experimental protocols used in this study were approved by the Institutional Animal Care and Use Committee (IACUC) of the University of Colorado, Anschutz Medical Campus. Adult (2–3 months old) male C57/BL6J mice (Jackson Laboratories, United States), were housed on a 12-h light:dark cycle with environmental enrichment and free access to food and water. *TgNotch3*^{WT} (WT) and *TgNotch3*^{R169C} (SVD) lines have been previously described (Joutel et al., 2010) and were used at 6 months of age in order for the *TgNotch3*^{R169C} mice to develop the SVD phenotype, and for consistency with our previous studies (Dabertrand et al., 2015, 2021; Capone et al., 2016; Fontaine et al., 2020). All mice were euthanized by i.p. injection of sodium pentobarbital (100 mg/kg) followed by rapid decapitation.

Ex vivo Capillary-Parenchymal Arteriole Preparation

The CaPA preparation was obtained as previously described (Longden et al., 2017; Rosehart et al., 2019) by dissecting intracerebral arterioles arising from the M1 region of the middle cerebral artery, leaving the attached capillary bed intact. Arteriolar segments were cannulated on glass micropipettes with one end occluded by a tie and pressurized using a Living Systems Instrumentation (United States) pressure servo controller with a mini peristaltic pump. The ends of the capillaries were then sealed by the downward pressure of an overlying glass micropipette. CaPA preparations were superfused (4 mL/min) with prewarmed (36°C ± 1°C), gassed (5% CO_2, 20% O_2, and 75% N_2) artificial cerebrospinal fluid (aCSF) for at least 30 min. The composition of aCSF was 125 mM NaCl, 3 mM KCl, 26 mM $NaHCO_3$, 1.25 mM NaH_2PO_4, 1 mM $MgCl_2$, 4 mM glucose, 2 mM $CaCl_2$, pH 7.3 (after aeration with 5% CO_2). Application of pressure (40 mmHg) to the cannulated parenchymal arteriole segment in this preparation pressurized the entire tree and induced myogenic tone in the arteriolar segment. Only viable CaPA preparations, defined as those that developed pressure-induced myogenic tone greater than 15%, were used in subsequent experiments. Arteriolar viability was validated by bath-applying NS309 (1 μM), which causes an endothelial-dependent vasodilation through activation of small- and intermediate-conductance, Ca^{2+}-sensitive K^+ (SK and IK, respectively) channels, or the thromboxane receptor agonist U46619 (1 μM), which causes robust vasoconstriction.

Dilatory responses of the attached arteriole segment to K^+ and PGE_2 were obtained by applying aCSF containing 10 mM K^+ or PGE_2 onto capillary extremities by pressure ejection from a glass micropipette (tip diameter, ∼5 μm) attached to a Picospritzer III (Parker, United States) at ∼5 psi for 20 s. The dose-responses were performed using pipettes filled with the different concentrations of PGE_2 and testing them sequentially starting with the lowest concentration. Contrary to arteriolar endothelial cells, cECs do not express functional IK and SK channels and spatial restriction of the drugs applied onto the capillary ends was validated by the lack of response to local stimulation with NS309 (1 μM), as previously described (Rosehart et al., 2019). In some control experiments, K^+ and PGE_2 were applied directly to the arteriole segment and the other drugs were applied via the bath perfusion. The luminal diameter of the parenchymal arteriole was acquired at 15 Hz using a CCD camera and IonWizard 6.2 edge-detection software (IonOptix, United States). Two regions were simultaneously recorded, zone 1 where the capillary tree sprouted from of the arteriole and zone 2 located 250 μm upstream of this, and diameter from both of these sites was averaged unless noted otherwise. Changes in arteriolar diameter were calculated from the average luminal diameter measured over the last 10 s of stimulation and were normalized to the maximum dilatory responses in 0 mM Ca^{2+} bath solution at the end of each experiment using the following equation: [(change in diameter)/(maximal diameter-initial diameter)] × 100.

In vivo Imaging of Cerebral Hemodynamics

As previously described (Longden et al., 2017), mice were anesthetized with isoflurane (5% induction and 2% maintenance) during the surgical procedure. The skull was exposed, cleaned, and a stainless-steel head plate was attached with a mixture of dental cement and superglue. Isoflurane was replaced with α-chloralose (50 mg/kg) and urethane (750 mg/kg) during recording. FITC-dextran (2000 kDa) was injected via the retro-orbital sinus to visualize the cerebral vasculature and for contrast imaging of RBCs. A penetrating arteriole, identified by the direction of the RBCs flowing into the brain, was followed and a downstream capillary was selected for study in cortical layers 2 or 3. A pipette was then maneuvered into the brain and positioned adjacent to the capillary under study, and aCSF containing, or not, 1 μM PGE_2 was ejected (200–300 ms, 8 ± 1 psi, ∼4 picoliters). The ejected volume was monitored by including 0.2 mg/mL tetramethylrhodamine isothiocyanate (TRITC; 150 kDa)-labeled dextran in the pipette (**Figure 1E**). RBC flux data were collected by line scanning at 5 kHz. Images were acquired using a Zeiss LSM-7 multiphoton microscope (Zeiss, United States) equipped with a 20x Plan Apochromat 1.0 N.A. DIC VIS-IR water-immersion objective and coupled to a Coherent Chameleon Vision II Titanium-Sapphire pulsed infrared laser (Coherent, United States). FITC and TRITC were excited at 820 nm, and emitted fluorescence was separated through 500–550 and 570–610 nm bandpass filters, respectively.

Reagents

HC030031, HC067047, PGE_2, NS309, and SC51322 were purchased from Tocris Bioscience (United States); All other chemicals and reagents were obtained from Sigma-Aldrich (United States). The vehicle for HB-EGF solutions was 0.2-μm–filtered PBS containing 0.1% BSA.

Statistical Analysis

Data in figures and text are presented as means ± standard error of the mean (SEM). Statistical testing was performed using GraphPad Prism 8 software. All data passed the Kolmogorov–Smirnov test for normality. Statistical significance was determined using one-way analysis of variance (ANOVA) followed by Tukey's *post hoc* test, unless otherwise stated.

RESULTS

To investigate the effect of capillary stimulation with PGE_2 on upstream arteriolar diameter, we used our previously developed *ex vivo* capillary-parenchymal arteriole (CaPA) preparation that allows to apply vasoactive substances at specific points along the arteriole-capillary continuum by pressure ejection (Longden et al., 2017; Rosehart et al., 2019). Consistent with our previous report that PGE_2 acts as a vasoconstrictor (Dabertrand et al., 2013), local application of 1 μM PGE_2 directly on the arteriolar segment caused a decrease in diameter (**Figures 1A–C**). In contrast, and as expected (Longden et al., 2017; Dabertrand et al., 2021), 10 mM K^+ also applied on the arteriole caused a robust dilation. Interestingly, either 10 mM K^+ or 1 μM PGE_2 caused upstream dilations when applied onto capillary extremities and the amplitudes of these were virtually identical (56.2% ± 3.9% and 47.8% ± 4.2%, respectively) (**Figures 1A–C** and **Supplementary Movie 1**). However, the kinetics of the responses appear significantly different with slower onset (5.27 ± 1.35 s) and time to peak (9.65 ± 1.5 s) for PGE_2 compared to K^+ responses, (1.7 ± 0.4 s and 3.87 ± 1.13 s, respectively).

We next tested the effect of increasing concentrations of PGE_2 locally applied to the arteriolar segment and observed a concentration-dependent constriction with a calculated EC_{50} of 145 nM (**Figure 1D**). The arteriolar dilation in response to capillary stimulations with PGE_2 was also concentration-dependent with a calculated EC_{50} of 70 nM and a maximal response at 1 μM, and thus we chose to use the latter concentration throughout the study for capillary stimulation (**Figure 1E** and **Supplementary Movie 1**). Finally, we tested the effect of a modest concentration of PGE_2 (500 nM) applied via the bath perfusion, hence stimulating both the capillary ends and the arteriolar segment, and measured a small but clear constriction (**Figures 1F,G**).

In our initial report of capillary-to-arteriole electrical signaling (Longden et al., 2017), we identified the cEC strong inward-rectifier K^+ channel, Kir2.1, as the molecular cornerstone of the capillary-to-arteriole electrical mechanism elicited by capillary stimulation with 10 mM K^+. Increasing extracellular K^+ concentration from 3 to 10 mM activates Kir2.1 channels in cECs, which induces a regenerative hyperpolarization that

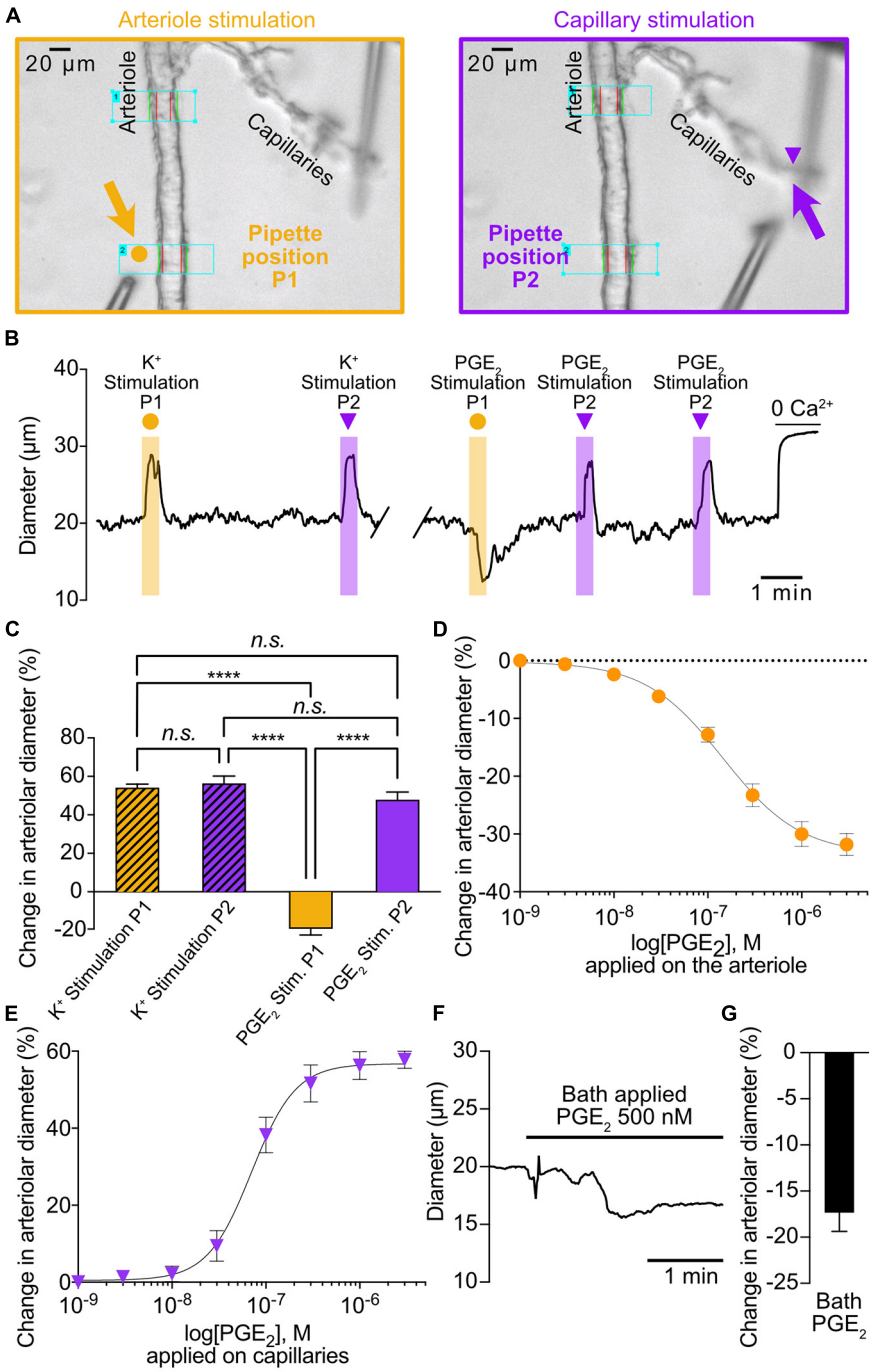

FIGURE 1 | PGE_2 causes upstream arteriolar dilation when applied onto capillaries. **(A)** Pipette positions for arteriole stimulation (left, 5 orange arrow) and capillary stimulation (right, purple arrow) in CaPA preparations. **(B)** Representative trace of arteriolar diameter showing effects of pressure ejection of 10 mM K^+ or 1 µM PGE_2 onto arteriole (P1, orange dot) and capillaries (P2, purple triangle). **(C)** Summary data from 6 mice (*n.s.*, not significant; $^{****}P < 0.0001$, one-way ANOVA, Tukey's test). **(D)** Concentration-response curve produced by locally applying PGE_2 to the arteriolar segment over a concentration range of 1 nM to 3 µM (5 mice). An EC_{50} of 145 nM was calculated from the non-linear regression curve. **(E)** Concentration-response curve produced by locally applying PGE_2 to capillary extremities over a concentration range of 1 nM to 3 µM (8 mice). An EC_{50} of 70 nM was calculated from the non-linear regression curve. **(F)** Representative trace of arteriolar diameter showing effects of bath application of 500 nM PGE_2. **(G)** Summary data from 5 mice.

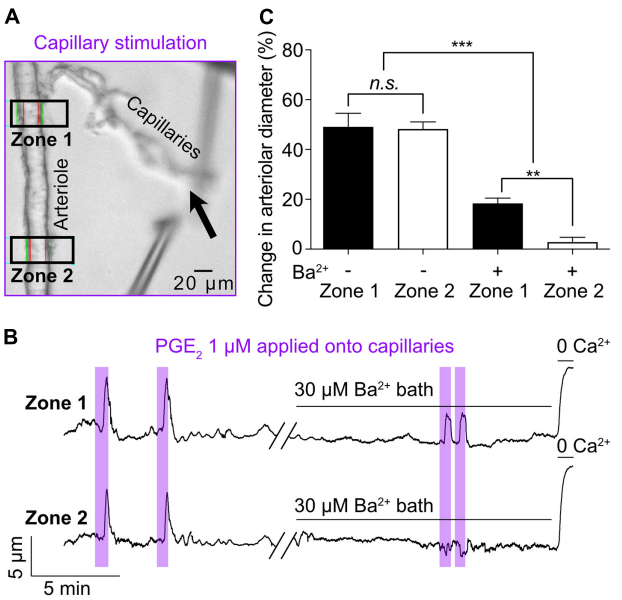

FIGURE 2 | Kir channel blocker Ba^{2+} (30 μM) inhibits the propagation, not the initiation, of the PGE_2-induced upstream arteriolar dilation. **(A)** Micrograph showing Zone 1 and Zone 2 positions for arteriolar diameter recording during capillaries stimulation (black arrow) with 1 μM PGE_2. **(B)** Representative traces of arteriolar diameter at zone 1 and zone 2 showing the effect of 30 μM bath-applied Ba^{2+} on PGE_2-induced upstream dilation. **(C)** Summary data from 5 mice (*n.s.*, not significant; $^{**}P < 0.01$, $^{***}P < 0.001$, one-way ANOVA, Tukey's test).

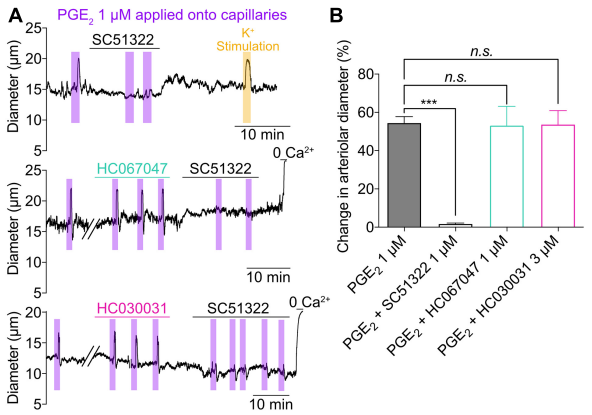

FIGURE 3 | Activation of capillary EP1 receptor initiates PGE_2-induced upstream dilation independently of TRPV4 and TRPA1 channels. **(A)** Representative traces of arteriolar diameter showing effects of pressure ejection of PGE_2 1 μM onto capillaries in absence or presence of SC51322 (1 μM, EP1 antagonist), HC067047 (1 μM, TRPV4 antagonist), and HC030031 (3 μM, TRPA1 antagonist). **(B)** Summary data from 5 to 8 mice (*n.s.*, not significant; $^{***}P < 0.001$, one-way ANOVA, Dunnett's test).

travels retrogradely to dilate the upstream arteriole. Consistent with this model, 30 μM Ba^{2+}—which, among the inward rectifier K^+ channels expressed in the microcirculation, preferentially blocks Kir2 channels (Longden and Nelson, 2015)—completely abolished the arteriolar dilation in response to capillary-applied 10 mM K^+. Therefore, we tested the effect of Ba^{2+} on arteriolar dilation induced by capillary stimulation with PGE_2. Arteriolar diameter was recorded at two distinct zones: zone 1 was placed at the branching of the transitional segment from the arteriole and zone 2 was located 250 μm upstream of this (**Figure 2A**). PGE_2 locally applied onto capillaries led to similar dilatory responses in zone 1 (49.1% ± 5.5%) and zone 2 (48.2% ± 2.9%) (**Figures 2B,C**). Remarkably, bath application of 30 μM Ba^{2+} decreased upstream arteriolar dilation at zone 1 in response to capillary stimulation with PGE_2 by 63% and virtually eliminated dilation at zone 2. The onset of the remnant dilation observed at zone 1 was unchanged by Ba^{2+} (5.27 ± 1.35 s 6.49 ± 2.81 s). Taken together, these data suggest that the Kir2.1 channel is not required to initiate PGE_2-induced upstream arteriolar dilation, but rather participates in the amplification and propagation of the vasodilatory signal, as evidenced by the difference between zone 1 and zone 2.

To investigate the mechanistic underpinnings of the capillary-to-arteriole signaling induced by PGE_2, we first superfused the *ex vivo* CaPA preparation with 1 μM SC51322, a prostanoid receptor antagonist specific for the EP1 receptor. SC51322 abolished the response to PGE_2, while the dilation induced by 10 mM K^+ remained intact (**Figures 3A,B**). This observation suggests that PGE_2 acts through activation of G protein-coupled receptors of the $G_{q/11}$ subtype (G_qPCR) and subsequent Ca^{2+} signaling. Depletion of plasma membrane phosphatidylinositol 4,5-bisphosphate (PIP_2) following G_qPCR activation is known to stimulate transient receptor potential (TRP) channels, a major pathway for extracellular Ca^{2+} influx (Kim et al., 2008; Harraz et al., 2018b). Moreover, recent work by Thakore et al. (2021) has revealed that activation of TRPA1 channel in cECs can initiate a biphasic, propagating retrograde signal that dilates upstream parenchymal arterioles during functional hyperemia. However, the TRPA1 antagonist HC030031 at 3 μM had no effect on the dilation induced by capillary stimulation with PGE_2 (**Figures 3A,B**). Inhibition of TRPV4, another Ca^{2+}-permeable TRP channel expressed by cECs (Harraz et al., 2018b), with 1 μM HC067047 also did not impact the effect of PGE_2 (**Figures 3A,B**). These results suggest that PGE_2 induces upstream arteriole dilation via activation of the EP1 receptor but independently of TRPV4 and TRPA1 channels.

We then tested the ability of PGE_2 to dilate upstream arterioles *in vivo* by measuring capillary red blood cell (RBC) flux with two-photon laser-scanning microscopy. Fluorescein isothiocyanate (FITC)-labeled dextran was used to visualize the cortical microcirculation and a pipette containing 1 μM PGE_2 was maneuvered into the brain through a cranial window and positioned next to a capillary of interest (**Figure 4A**). Pressure ejection (8 ± 1 psi) for up to 300 ms of PGE_2 evoked a significant increase in capillary RBC flux (Δ = 12 ± 4 RBCs/s) consistent with the notion that the mechanisms we observed in CaPA preparations are also at play in the intact system (**Figures 4B–D**). In contrast, ejection of aCSF vehicle had no effect on capillary RBC flux (**Figure 4E**). To determine whether PGE_2 also causes upstream dilation we next performed experiments in which we imaged at the parenchymal arteriole-transitional zone junction

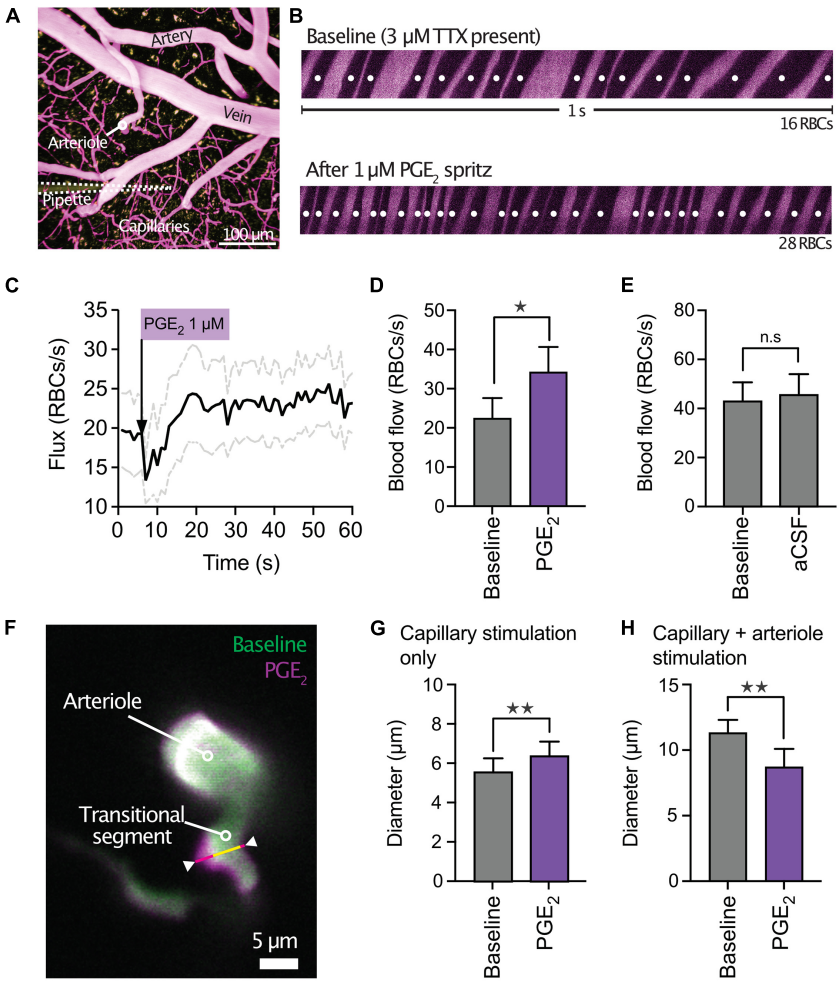

FIGURE 4 | PGE_2 causes capillary hyperemia *in vivo*. **(A)** Micrograph of mouse cortical vasculature showing a micropipette containing PGE_2 and TRITC-dextran (yellow) in close apposition to a capillary (FITC-dextran, purple). **(B)** Red blood cell (RBC) flux was measured by high-frequency line scanning over a period of 1 min at baseline (top panel) and after application of 1 µM PGE_2 (lower panel) onto a capillary. RBCs appear as black streaks in plasma (purple). **(C)** Average traces (black line) plus SEM (gray lines) showing the increase in RBC flux to PGE_2. The dip immediately following the ejection of PGE_2 is caused by momentary pressure on the capillary wall. **(D)** Summary data of RBC flux showing significant hyperemia following capillary stimulation with 1 µM PGE_2 (n = 14 experiments, 6 mice, $^*P < 0.05$, paired Student's t-test). **(E)** In contrast, ejection of aCSF vehicle onto capillaries had no effect on RBC flux (n = 9 experiments, 5 mice, $P > 0.05$, paired Student's t-test). **(F)** Overlay showing the diameter of a penetrating arteriole and the transitional segment to the capillary bed at baseline (green) and after PGE_2 ejection onto a downstream capillary (magenta). The upstream dilation was most prominent in the region highlighted by the white arrowheads. **(G)** Summary data showing upstream dilation to capillary ejection of PGE_2 (n = 5 experiments, 4 mice, $^{**}P < 0.01$, paired Student's t-test). **(H)** In contrast, simultaneous stimulation of both capillaries and arterioles with PGE_2 *in vivo* led to constriction (n = 7 experiments, 3 mice, $^{**}P < 0.01$, paired Student's t-test).

(**Figure 4F**). Here, we found that ejection of 1 µM PGE_2 selectively onto capillaries routinely produced a small upstream dilation (**Figures 4F,G** and **Supplementary Movie 2**). In contrast, if we applied PGE_2 onto both capillaries and arterioles *in vivo* by increasing the duration of ejection, causing spread of the ejected solution to the upstream arteriole along a paravascular route, we observed constriction (**Figure 4H**), consistent with our *ex vivo* data. As expected, ejection of aCSF vehicle alone had no effect on upstream arteriolar diameter (12.95 ± 0.57 µm baseline diameter vs. 12.96 ± 0.8 µm after aCSF ejection, n = 6 experiments, 3 mice, P = 0.97, paired Student's t-test).

Finally, we investigated the effect of SVD on PGE_2-initiated capillary-to-arteriole signaling. *Ex vivo* stimulation of capillaries from SVD mice with PGE_2 induced an upstream arteriolar dilation that was 58% smaller at Zone 1 and 64.8% smaller at Zone 2 compared with that in *TgNotch3*^{WT} control (WT) mice, revealing attenuated PGE_2-mediated signaling (**Figure 5**). The difference between zone 1 and 2 dilations were not significant. We previously reported that activation of the epidermal growth factor receptor (EGFR) by its ligand heparin-binding EGF-like growth factor (HB-EGF) ameliorates the cerebral vascular deficits of the SVD mouse—including neurovascular coupling and functional hyperemia deficits (Capone et al., 2016; Dabertrand et al., 2021). We then directly tested the effect of HB-EGF on PGE_2-induced upstream vasodilation in *ex vivo* preparations from SVD mice. Bath-applied 30 ng/mL HB-EGF dramatically enhanced the upstream arteriolar dilation induced by capillary stimulation with PGE_2, increasing the average dilation from 19.8% ± 1% to

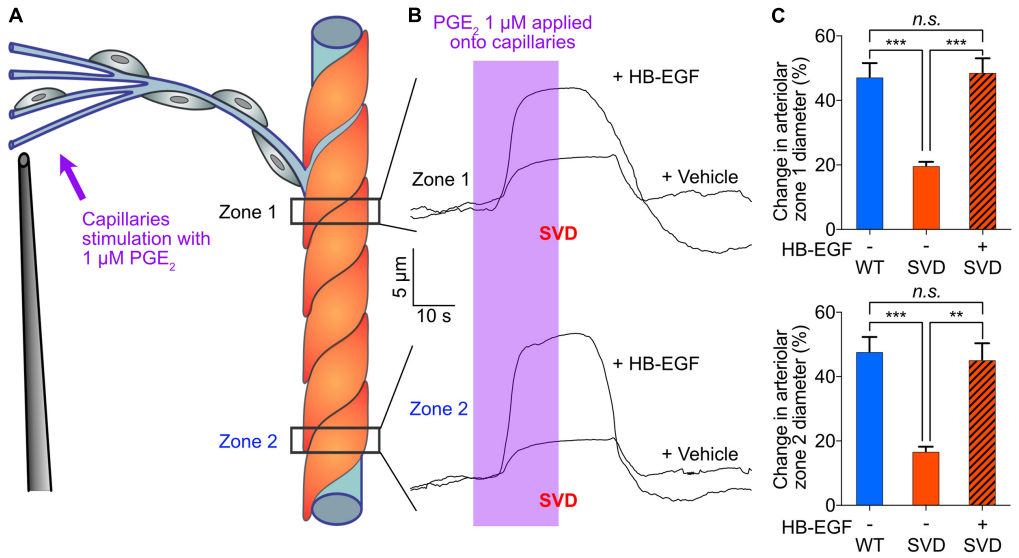

FIGURE 5 | In the SVD mouse model, blunted upstream arteriolar dilation in response to capillary stimulation with PGE_2 is completely restored by bath application of 30 ng/ml HB-EGF. **(A)** Cartoon showing Zone 1 and Zone 2 positions for arteriolar diameter recording during capillaries stimulation with 1 μM PGE2. **(B)** Representative traces of arteriolar diameter showing the effect of pressure ejection of PGE_2 1 μM onto capillaries in absence or presence of 30 ng/ml HB-EGF in a preparation from SVD mouse model. **(C)** Summary data from 5 to 6 mice (*n.s.*, not significant; $^{**}P < 0.01$, $^{***}P < 0.001$, one-way ANOVA Dunnett's test).

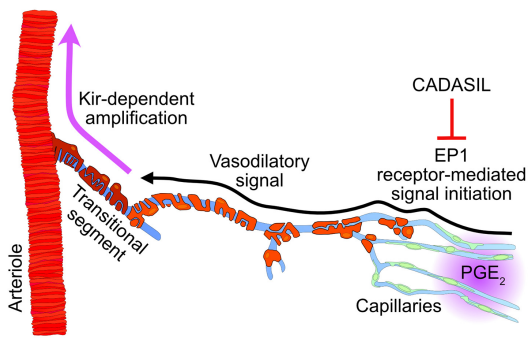

FIGURE 6 | Proposed mechanism involving PGE_2 during functional hyperemia and its inhibition in cerebral small vessel disease (CADASIL). Intracellular increases in Ca^{2+} caused by phospholipase C activation during EP1 signaling triggers a propagating vasodilatory signal that is amplified by Kir channel in the transitional segment region. CADASIL, which lowers the pool of phospholipase C substrate PIP_2, would limit the synthesis of the second messenger IP_3, resulting in a reduced PGE_2-evoked upstream dilation during functional hyperemia.

48.7% ± 4.3% at Zone 1, and from 16.8% ± 1.4% to 45.3% ± 5.1% at Zone 2 (**Figure 5** and **Supplementary Movie 3**). HB-EGF completely restored PGE_2-induced upstream dilation, abolishing the differences measured between WT and SVD animals.

DISCUSSION

Our progress in understanding functional hyperemia in health and disease has been hampered by large gaps in our comprehension of the mechanism underlying this basic physiological response—and persistent controversies surrounding it (Kaplan et al., 2020). Our recent work identified Kir2.1 channels in cECs as the molecular cornerstone initiating and propagating a retrograde hyperpolarizing vasodilatory signal from capillaries to arterioles (Longden et al., 2017; Harraz et al., 2018a; Moshkforoush et al., 2020; Dabertrand et al., 2021). The present study extends this capillary-based paradigm, providing support for a new signaling modality that posits a central role for the G_qPCR EP1 receptor in mediating PGE_2-induced vasodilatory signal that propagates upstream to cause dilation of feeding parenchymal arterioles (**Figure 6**). Importantly, these findings hold the promise of resolving controversies surrounding how PGE_2, a widely proposed mediator of neurovascular coupling (Zonta et al., 2002; Takano et al., 2005; Gordon et al., 2008; Attwell et al., 2010; Watkins et al., 2014), can promote functional hyperemia despite evidence that it directly constricts arterioles (Dabertrand et al., 2013).

Our observations raise the immediate question of which effect of PGE_2, capillary-mediated vasodilation or direct arteriolar constriction, predominates during neurovascular coupling. We calculated an EC_{50} of 145 nM for the PGE_2-induced constriction of the parenchymal arteriole, while the vasodilation induced by capillary stimulation displayed an EC_{50} of 70 nM. In our experimental conditions, a simultaneous stimulation of capillaries and the arteriole with 500 nM PGE_2 led to a constriction, suggesting that the arteriolar effect prevails when both vascular segments are exposed to PGE_2. A possible explanation for these observations is that the microvascular response to PGE_2 has a kinetic component in which the fast constriction predominates over the slower capillary-mediated response. However, this stimulation via the bath perfusion likely does not reflect *in vivo* conditions. Accordingly, we tested the

effect of increasing our ejection duration *in vivo* such that PGE_2 not only stimulated the targeted capillaries but also spread upstream to the arteriole. Here too this maneuver produced arteriolar constriction, again suggesting that this response will predominate when the arteriole is exposed directly to PGE_2. Since the dense capillary network within the brain lies in close proximity to all neurons (Nishimura et al., 2007; Blinder et al., 2013), it is expected that cECs are the primary sensors of neuronal activity and any neurally derived PGE_2. Therefore, the vasodilatory effect would be expected to predominate during neurovascular coupling in physiological conditions and our data suggest that this occurs through local exposure of the capillaries to PGE_2. However, a variety of brain conditions, including ischemia and neurodegeneration (Minghetti, 2004), are known to up-regulate COX-2 expression in excitatory neurons which results in an EP1-dependent neurotoxicity of PGE_2 (Kawano et al., 2006). In this pathological situation, higher PGE_2 concentrations could lead to arteriolar constriction and then contribute to PGE_2 neurotoxicity by limiting local blood supply.

Neuronal activation leads to rapid increases in blood flow within, and on the surface, of the brain. Hillman and colleagues elegantly provided evidence for involvement of the endothelium in stimulus-evoked, conducted vasodilation from the brain parenchyma to arterioles and pial arteries *in vivo* (Chen et al., 2014). Our previous study on neurovascular coupling demonstrated how capillary endothelium is capable of transmitting an electrical signal to cause upstream vasodilation in support of functional hyperemia (Longden et al., 2017). We showed that activation of the Kir2.1 channel in cECs by extracellular K^+ ions propagates a regenerative hyperpolarization from cell-to-cell up to the feeding arteriole to cause vasodilation (Longden et al., 2017; Harraz et al., 2018a; MacMillan and Evans, 2018). Interestingly, recent work from Thakore et al. (2021) showed that 4-hydroxynonenal (4-HNE), an endogenous product of lipid peroxidation, activates transient receptor potential ankyrin 1 (TRPA1) channel in cECs to cause upstream arteriolar dilation during functional hyperemia. These recent findings introduce the concept that a slowly propagating short-range Ca^{2+} signal is initiated in the capillary endothelium and converted into the fast-propagating hyperpolarization that causes dilation of upstream arterioles. The conversion is proposed to occur in the transitional region between the capillaries and the arteriole (Ratelade et al., 2020) by activation of the small- and intermediate-conductance Ca^{2+}-activated K^+ channels (SK and IK, respectively) and amplification of the hyperpolarization by Kir channel (Thakore et al., 2021). The transitional region refers to the first segment sprouting out of the arteriole, visible on **Figure 1** micrographs, while local stimulations are applied onto the 3rd and 4th order capillary branches after the transitional region. A vast body of literature reports (de Wit et al., 1999; Domeier and Segal, 2007; Bagher and Segal, 2011) supports the concept that a propagating Ca^{2+} signal is capable of acting through IK/SK channels, which are not present in cECs (Longden et al., 2017) but are expressed by transitional and arteriolar ECs (Hannah et al., 2011; Thakore et al., 2021). The generated hyperpolarizing signal is further amplified via Kir channel activation (Sonkusare et al., 2016) and conveyed through myoendothelial junctions to adjacent SMCs. In the dilation induced by capillary stimulation with PGE_2, inhibition of the Kir2.1 channel with Ba^{2+} had a profound effect, particularly measurable on the propagation of the dilation, which is consistent with the biphasic propagative model proposed by Thakore et al. (2021). Interestingly, inhibition of TRPA1 channels did not prevent PGE_2 from causing upstream dilation, suggesting a different initiation mechanism, likely involving G_q protein activation and inositol trisphosphate (IP_3)-mediated Ca^{2+} release, as opposed to direct Ca^{2+} entry across the plasma membrane. Our previous work also highlighted the role of G_qPCR activation in breaking down phosphatidylinositol 4,5-bisphosphate (PIP_2), resulting in decreased Kir2.1 channel activity and increased open probability of the Ca^{2+}/Na^+-permeable TRPV4 channel (Harraz et al., 2018a,b, 2020). However, blocking TRPV4 channels had no effect on the dilation induced by PGE_2 either. Given these data, we propose that EP1-initiated IP_3-dependent Ca^{2+} signals arriving in the transitional segment activate endothelial IK/SK channels, and the ensuing membrane potential hyperpolarization activates Kir channels, converting the incoming Ca^{2+} signal into a Kir-dependent hyperpolarizing signal. The characterization of such a Ca^{2+} signal will require more extensive investigation, but the vasodilation induced by capillary stimulation with PGE_2 is clearly central to the postulated role of this molecule as a neurovascular coupling agent.

Cerebral SVDs have emerged as a central link between two major co-morbidities. They account for more than 30% of strokes worldwide and at least 40% of dementia cases (Pantoni, 2010; Iadecola, 2013). CADASIL is caused by dominant mutations in the NOTCH3 receptor, expressed by SMCs and pericytes, that stereotypically lead to the extracellular deposition of the NOTCH3 ectodomain ($NOTCH3^{ECD}$), which recruits and aggregates other proteins on vessels, ultimately forming deposits termed granular osmiophilic material (GOM) (Joutel et al., 2000, 2016; Chabriat et al., 2009). One of these proteins is the tissue inhibitor of metalloproteinases 3 (TIMP3), which directly complexes with $NOTCH^{ECD}$ and abnormally accumulates in the extra cellular matrix of brain vessels in patients and mice with CADASIL (Monet-Leprêtre et al., 2013). A deficit in CBF hemodynamics, including functional hyperemia, is an early disease manifestation in patients (Chabriat et al., 2000; Pfefferkorn et al., 2001; Liem et al., 2009; Huneau et al., 2018) and a prominent feature of the well-established $TgNotch3^{R169C}$ CADASIL mouse model used in the present study (Joutel et al., 2010; Capone et al., 2016; Dabertrand et al., 2021). Our recent work indicates that TIMP3 effects on cerebrovascular reactivity are attributable to inhibition of ADAM17 and subsequent suppression of EGFR signaling by inhibition of ectodomain shedding of its ligand HB-EGF (Dabertrand et al., 2015, 2021; Capone et al., 2016).

Consistent with this model, we previously found that EGFR activation with exogenous soluble HB-EGF restores cerebral arterial tone and functional hyperemia (Dabertrand et al., 2015, 2021; Capone et al., 2016). Here, we

found that PGE_2-induced dilation was impaired in the CADASIL mouse model and fully restored by HB-EGF.

We previously identified two downstream consequences of the suppressed TIMP3-ADAM17-EGFR signaling module: (i) the upregulation of voltage gated K^+ ($K_V1.5$) channels in the arteriolar SMCs (Dabertrand et al., 2015; Capone et al., 2016); and (ii) the partial inhibition of Kir2.1 channels in cECs, but not in arteriolar ECs and SMCs (Dabertrand et al., 2021). Here, we report a third consequence: the disruption of PGE_2-induced capillary-to-arteriole signaling, reinforcing the concept that extracellular matrix alterations have profound impacts on cerebrovascular dynamics in SVDs. Using computational modeling, we previously investigated the impact of K_V channel upregulation on membrane potential dynamics in the context of concurrent activation of myocyte Kir channels (Koide et al., 2018). Interestingly, while these analyses showed that a higher K_V channel current density would reduce the membrane potential range over which Kir channels can be activated to cause and propagate dilation, the more hyperpolarized resting membrane potential (9 mV) actually facilitates Kir channel activation. Thus, arterioles from the CADASIL mouse model would still hyperpolarize and dilate in response to Kir channel opening, as observed experimentally (Dabertrand et al., 2015; Koide et al., 2018), but at the cost of a smaller vasodilatory reserve. At the capillary level, we previously described, and modeled, how a 50% reduction in cECs Kir2.1 current is sufficient to completely abolish the capillary-to-arteriole electrical signaling in response to 10 mM K^+ (Harraz et al., 2018a; Moshkforoush et al., 2020), and then strongly reduces functional hyperemia in the CADASIL mouse model (Dabertrand et al., 2021). We attributed this endothelial dysfunction to a reduced cEC metabolism caused by inhibition of the EGFR pathway (Dabertrand et al., 2021). The resulting lower ATP/ADP ratio in CADASIL compared to WT cECs decreases the synthesis of PIP_2 and its availability to act as an essential cofactor for Kir2.1 channel—hence reducing the channel activity (Huang et al., 1998; Hansen et al., 2011; Harraz et al., 2018a, 2020). Of particular note, PIP_2 is also a substrate for phospholipase C during EP1 signaling, and a reduced pool of PIP_2 would certainly limit the synthesis of the second messenger IP_3, which mobilizes Ca^{2+} from endoplasmic reticulum stores through its action on its cognate receptor. The observation that HB-EGF restores both Kir2.1- and PGE_2-initiated signaling is consistent with this concept. The impact of CADASIL on neurovascular coupling is thus multifaceted, involving disruption of two different propagating signals sharing connections to the EGFR pathway in cECs, and Kir channel activation in the transitional and arteriolar segments.

We have made major progress in establishing potential contributing mechanisms to cerebral hemodynamics impairment observed at an early stage of CADASIL, a Mendelian paradigm of SVDs (Chabriat et al., 2009) and the most common hereditary cause of stroke (Pantoni, 2010) and dementia (Schmidt et al., 2012). Here we demonstrate that functional hyperemia deficits in this SVD involve a PGE_2-initiated capillary-to-arteriole signal that is normally regulated by the TIMP3-ADAM17-EGFR signaling module. Furthermore, the evidence that PGE_2 induces arteriolar dilation via capillary stimulation has the potential to reconcile disparate findings in neurovascular studies. Our mechanistic studies thus lay the groundwork for novel targeted strategies for treating CADASIL and other cerebrovascular diseases.

DATA AVAILABILITY STATEMENT

The original contributions presented in the study are included in the article/**Supplementary Material**, further inquiries can be directed to the corresponding author.

ETHICS STATEMENT

The animal study was reviewed and approved by the Institutional Animal Care and Use Committee (IACUC) of the University of Colorado, Anschutz Medical Campus.

AUTHOR CONTRIBUTIONS

AR, JF, and FD performed *ex vivo* experiments, data collection, and analysis. TL and NW performed *in vivo* experiments, data collection, and analysis. AJ contributed to the study design. FD designed and directed the research and wrote the manuscript. All authors edited the manuscript and approved its submission.

FUNDING

This study was supported by the National Institute on Aging R01AG066645 to TL, and National Institute of Neurological Disorders and Stroke DP2OD02944801 to TL, a grant from the National Research Agency, France (ANR-16-RHUS-0004) to AJ, awards from the CADASIL Together We Have Hope Non-profit Organization, a research grant from the Center for Women's Health Research located at the University of Colorado Anschutz Medical Campus, a research grant from the University of Pennsylvania Orphan Disease Center in partnership with the cureCADASIL, and National Heart, Lung, and Blood Institute R01HL136636 to FD.

SUPPLEMENTARY MATERIAL

The Supplementary Material for this article can be found online at: https://www.frontiersin.org/articles/10.3389/fnagi.2021.695965/full#supplementary-material

Supplementary Movie 1 | Capillary stimulation with PGE2 1 μM evokes upstream arterial dilation in *ex vivo* CaPA preparation.

Supplementary Movie 2 | Capillary stimulation with PGE_2 causes upstream dilation of the arteriole and transitional segment *in vivo*.

Supplementary Movie 3 | Exogenous application of 30 ng/ml HB-EGF fully restores upstream arterial dilation in response to capillary stimulation with 1 μM PGE_2 in CaPA preparation from a SVD mouse.

REFERENCES

Attwell, D., Buchan, A. M., Charpak, S., Lauritzen, M., MacVicar, B. A., and Newman, E. A. (2010). Glial and neuronal control of brain blood flow. *Nature* 468, 232–243. doi: 10.1038/nature09613

Bagher, P., and Segal, S. S. (2011). Regulation of blood flow in the microcirculation: role of conducted vasodilation. *Acta Physiol.* 202, 271–284. doi: 10.1111/j.1748-1716.2010.02244.x

Blinder, P., Tsai, P. S., Kaufhold, J. P., Knutsen, P. M., Suhl, H., and Kleinfeld, D. (2013). The cortical angiome: an interconnected vascular network with noncolumnar patterns of blood flow. *Nat. Neurosci.* 16, 889–897. doi: 10.1038/nn.3426

Capone, C., Dabertrand, F., Baron-Menguy, C., Chalaris, A., Ghezali, L., Domenga-Denier, V., et al. (2016). Mechanistic insights into a TIMP3-sensitive pathway constitutively engaged in the regulation of cerebral hemodynamics. *Elife* 5:e17536. doi: 10.7554/eLife.17536

Chabriat, H., Joutel, A., Dichgans, M., Tournier-Lasserve, E., and Bousser, M.-G. (2009). CADASIL. *Lancet Neurol.* 8, 643–653. doi: 10.1016/S1474-4422(09)70127-9

Chabriat, H., Pappata, S., Ostergaard, L., Clark, C. A., Pachot-Clouard, M., Vahedi, K., et al. (2000). Cerebral hemodynamics in CADASIL before and after acetazolamide challenge assessed with MRI bolus tracking. *Stroke* 31, 1904–1912. doi: 10.1161/01.str.31.8.1904

Chen, B. R., Kozberg, M. G., Bouchard, M. B., Shaik, M. A., and Hillman, E. M. C. (2014). A critical role for the vascular endothelium in functional neurovascular coupling in the brain. *J. Am. Heart Assoc.* 3:e000787. doi: 10.1161/JAHA.114.000787

Dabertrand, F., Hannah, R. M., Pearson, J. M., Hill-Eubanks, D. C., Brayden, J. E., and Nelson, M. T. (2013). Prostaglandin E_2, a postulated astrocyte-derived neurovascular coupling agent, constricts rather than dilates parenchymal arterioles. *J. Cereb. Blood Flow Metab.* 33, 479–482. doi: 10.1038/jcbfm.2013.9

Dabertrand, F., Harraz, O. F., Koide, M., Longden, T. A., Rosehart, A. C., Hill-Eubanks, D. C., et al. (2021). PIP_2 corrects cerebral blood flow deficits in small vessel disease by rescuing capillary Kir2.1 activity. *Proc. Natl. Acad. Sci. U. S. A.* 118:e2025998118. doi: 10.1073/pnas.2025998118/pnas.1420765112

Dabertrand, F., Krøigaard, C., Bonev, A. D., Cognat, E., Dalsgaard, T., Domenga-Denier, V., et al. (2015). Potassium channelopathy-like defect underlies early-stage cerebrovascular dysfunction in a genetic model of small vessel disease. *Proc. Natl. Acad. Sci. U. S. A.* 112, E796–E805. doi: 10.1073/pnas.1420765112

de Wit, C., Esser, N., Lehr, H. A., Bolz, S. S., and Pohl, U. (1999). Pentobarbital-sensitive EDHF comediates ACh-induced arteriolar dilation in the hamster microcirculation. *Am. J. Physiol.* 276, H1527–H1534. doi: 10.1152/ajpheart.1999.276.5.H1527

Domeier, T. L., and Segal, S. S. (2007). Electromechanical and pharmacomechanical signalling pathways for conducted vasodilatation along endothelium of hamster feed arteries. *J. Physiol.* 579, 175–186. doi: 10.1113/jphysiol.2006.124529

Fontaine, J. T., Rosehart, A. C., Joutel, A., and Dabertrand, F. (2020). HB-EGF depolarizes hippocampal arterioles to restore myogenic tone in a genetic model of small vessel disease. *Mech. Ageing Dev.* 192:111389. doi: 10.1016/j.mad.2020.111389

Gordon, G. R. J., Choi, H. B., Rungta, R. L., Ellis-Davies, G. C. R., and MacVicar, B. A. (2008). Brain metabolism dictates the polarity of astrocyte control over arterioles. *Nature* 456, 745–749. doi: 10.1038/nature07525

Hannah, R. M., Dunn, K. M., Bonev, A. D., and Nelson, M. T. (2011). Endothelial SK(Ca) and IK(Ca) channels regulate brain parenchymal arteriolar diameter and cortical cerebral blood flow. *J. Cereb. Blood Flow Metab.* 31, 1175–1186. doi: 10.1038/jcbfm.2010.214

Hansen, S. B., Tao, X., and MacKinnon, R. (2011). Structural basis of PIP_2 activation of the classical inward rectifier K^+ channel Kir2.2. *Nature* 477, 495–498. doi: 10.1038/nature10370

Harraz, O. F., Hill-Eubanks, D., and Nelson, M. T. (2020). PIP_2: a critical regulator of vascular ion channels hiding in plain sight. *Proc. Natl. Acad. Sci. U. S. A.* 117, 20378–20389. doi: 10.1073/pnas.2006737117

Harraz, O. F., Longden, T. A., Dabertrand, F., Hill-Eubanks, D., and Nelson, M. T. (2018a). Endothelial G_qPCR activity controls capillary electrical signaling and brain blood flow through PIP_2 depletion. *Proc. Natl. Acad. Sci. U. S. A.* 115, E3569–E3577. doi: 10.1073/pnas.1800201115

Harraz, O. F., Longden, T. A., Hill-Eubanks, D., and Nelson, M. T. (2018b). PIP_2 depletion promotes TRPV4 channel activity in mouse brain capillary endothelial cells. *Elife* 7:351. doi: 10.7554/eLife.38689

Huang, C. L., Feng, S., and Hilgemann, D. W. (1998). Direct activation of inward rectifier potassium channels by PIP_2 and its stabilization by Gbetagamma. *Nature* 391, 803–806. doi: 10.1038/35882

Huneau, C., Houot, M., Joutel, A., Béranger, B., Giroux, C., Benali, H., et al. (2018). Altered dynamics of neurovascular coupling in CADASIL. *Ann. Clin. Transl. Neurol.* 5, 788–802. doi: 10.1002/acn3.574

Iadecola, C. (2013). The pathobiology of vascular dementia. *Neuron* 80, 844–866. doi: 10.1016/j.neuron.2013.10.008

Iadecola, C., Duering, M., Hachinski, V., Joutel, A., Pendlebury, S. T., Schneider, J. A., et al. (2019). Vascular cognitive impairment and dementia: JACC scientific expert panel. *J. Am. Coll. Cardiol.* 73, 3326–3344. doi: 10.1016/j.jacc.2019.04.034

Joutel, A., Andreux, F., Gaulis, S., Domenga, V., Cecillon, M., Battail, N., et al. (2000). The ectodomain of the Notch3 receptor accumulates within the cerebrovasculature of CADASIL patients. *J. Clin. Invest.* 105, 597–605. doi: 10.1172/JCI8047

Joutel, A., Haddad, I., Ratelade, J., and Nelson, M. T. (2016). Perturbations of the cerebrovascular matrisome: a convergent mechanism in small vessel disease of the brain? *J. Cereb. Blood Flow Metab.* 36, 143–157. doi: 10.1038/jcbfm.2015.62

Joutel, A., Monet-Leprêtre, M., Gosele, C., Baron-Menguy, C., Hammes, A., Schmidt, S., et al. (2010). Cerebrovascular dysfunction and microcirculation rarefaction precede white matter lesions in a mouse genetic model of cerebral ischemic small vessel disease. *J. Clin. Invest.* 120, 433–445. doi: 10.1172/JCI39733DS1

Kaplan, L., Chow, B. W., and Gu, C. (2020). Neuronal regulation of the blood–brain barrier and neurovascular coupling. *Nat. Rev. Neurosci.* 21, 1–17. doi: 10.1038/s41583-020-0322-2

Kawano, T., Anrather, J., Zhou, P., Park, L., Wang, G., Frys, K. A., et al. (2006). Prostaglandin E2 EP1 receptors: downstream effectors of COX-2 neurotoxicity. *Nat. Med.* 12, 225–229. doi: 10.1038/nm1362

Kim, D., Cavanaugh, E. J., and Simkin, D. (2008). Inhibition of transient receptor potential A1 channel by phosphatidylinositol-4,5-bisphosphate. *Am. J. Physiol. Cell Physiol.* 295, C92–C99. doi: 10.1152/ajpcell.00023.2008

Koide, M., Moshkforoush, A., Tsoukias, N. M., Hill-Eubanks, D. C., Wellman, G. C., Nelson, M. T., et al. (2018). The yin and yang of K_V channels in cerebral small vessel pathologies. *Microcirculation* 25, 1–10. doi: 10.1111/micc.12436

Lacroix, A., Toussay, X., Anenberg, E., Lecrux, C., Ferreiros, N., Karagiannis, A., et al. (2015). COX-2-derived prostaglandin E2 produced by pyramidal neurons contributes to neurovascular coupling in the rodent cerebral cortex. *J. Neurosci.* 35, 11791–11810. doi: 10.1523/JNEUROSCI.0651-15.2015

Liem, M. K., Lesnik Oberstein, S. A. J., Haan, J., Boom, R. V. D., Ferrari, M. D., Buchem, M. A. V., et al. (2009). cerebrovascular reactivity is a main determinant of white matter hyperintensity progression in CADASIL. *Am. J. Neuroradiol.* 30, 1244–1247. doi: 10.3174/ajnr.A1533

Longden, T. A., Dabertrand, F., Koide, M., Gonzales, A. L., Tykocki, N. R., Brayden, J. E., et al. (2017). Capillary K^+-sensing initiates retrograde hyperpolarization to increase local cerebral blood flow. *Nat. Neurosci.* 20, 717–726. doi: 10.1038/nn.4533

Longden, T. A., and Nelson, M. T. (2015). Vascular inward rectifier K^+ channels as external K^+ sensors in the control of cerebral blood flow. *Microcirculation* 22, 183–196. doi: 10.1111/micc.12190

MacMillan, S., and Evans, A. M. (2018). AMPK-α1 or AMPK-α2 Deletion in smooth muscles does not affect the hypoxic ventilatory response or systemic arterial blood pressure regulation during hypoxia. *Front. Physiol.* 9:655. doi: 10.3389/fphys.2018.00655

Minghetti, L. (2004). Cyclooxygenase-2 (COX-2) in inflammatory and degenerative brain diseases. *J. Neuropathol. Exp. Neurol.* 63, 901–910. doi: 10.1093/jnen/63.9.901

Monet-Leprêtre, M., Haddad, I., Baron-Menguy, C., Fouillot-Panchal, M., Riani, M., Domenga-Denier, V., et al. (2013). Abnormal recruitment of extracellular matrix proteins by excess Notch3ECD: a new pathomechanism in CADASIL. *Brain* 136, 1830–1845. doi: 10.1093/brain/awt092

Moshkforoush, A., Ashenagar, B., Harraz, O. F., Dabertrand, F., Longden, T. A., Nelson, M. T., et al. (2020). The capillary Kir channel as sensor and

amplifier of neuronal signals: modeling insights on K^+-mediated neurovascular communication. *Proc. Natl. Acad. Sci. U. S. A.* 117, 16626–16637. doi: 10.1073/pnas.2000151117

Nishimura, N., Schaffer, C. B., Friedman, B., Lyden, P. D., and Kleinfeld, D. (2007). Penetrating arterioles are a bottleneck in the perfusion of neocortex. *Proc. Natl. Acad. Sci. U. S. A.* 104, 365–370. doi: 10.1073/pnas.0609551104

Pantoni, L. (2010). Cerebral small vessel disease: from pathogenesis and clinical characteristics to therapeutic challenges. *Lancet Neurol.* 9, 689–701. doi: 10.1016/S1474-4422(10)70104-6

Pfefferkorn, T., von Stuckrad-Barre, S., Herzog, J., Gasser, T., Hamann, G. F., and Dichgans, M. (2001). Reduced cerebrovascular CO_2 reactivity in CADASIL: a transcranial Doppler sonography study. *Stroke* 32, 17–21. doi: 10.1161/01.str.32.1.17

Ratelade, J., Klug, N. R., Lombardi, D., Angelim, M. K. S. C., Dabertrand, F., Domenga-Denier, V., et al. (2020). Reducing hypermuscularization of the transitional segment between arterioles and capillaries protects against spontaneous intracerebral hemorrhage. *Circulation* 141, 2078–2094. doi: 10.1161/CIRCULATIONAHA.119.040963

Rosehart, A. C., Johnson, A. C., and Dabertrand, F. (2019). Ex vivo pressurized hippocampal capillary-parenchymal arteriole preparation for functional study. *J. Vis. Exp.* 1–7. doi: 10.3791/60676

Schmidt, H., Freudenberger, P., Seiler, S., and Schmidt, R. (2012). Genetics of subcortical vascular dementia. *Exp. Gerontol.* 47, 873–877. doi: 10.1016/j.exger.2012.06.003

Sonkusare, S. K., Dalsgaard, T., Bonev, A. D., and Nelson, M. T. (2016). Inward rectifier potassium (Kir2.1) channels as end-stage boosters of endothelium-dependent vasodilators. *J. Physiol.* 594, 3271–3285. doi: 10.1113/JP271652

Takano, T., Tian, G.-F., Peng, W., Lou, N., Libionka, W., Han, X., et al. (2005). Astrocyte-mediated control of cerebral blood flow. *Nat. Neurosci.* 9, 260–267. doi: 10.1038/nn1623

Thakore, P., Alvarado, M. G., Ali, S., Mughal, A., Pires, P. W., Yamasaki, E., et al. (2021). Brain endothelial cell TRPA1 channels initiate neurovascular coupling. *Elife* 10:e63040. doi: 10.7554/eLife.63040

Vanlandewijck, M., He, L., Mäe, M. A., Andrae, J., Ando, K., Del Gaudio, F., et al. (2018). A molecular atlas of cell types and zonation in the brain vasculature. *Nature* 554, 475–480. doi: 10.1038/nature25739

Wardlaw, J. M., Smith, C., and Dichgans, M. (2019). Small vessel disease: mechanisms and clinical implications. *Lancet Neurol.* 18, 684–696. doi: 10.1016/S1474-4422(19)30079-1

Watkins, S., Robel, S., Kimbrough, I. F., Robert, S. M., Ellis-Davies, G., and Sontheimer, H. (2014). Disruption of astrocyte-vascular coupling and the blood-brain barrier by invading glioma cells. *Nat. Commun.* 5:4196. doi: 10.1038/ncomms5196

Zonta, M., Angulo, M. C., Gobbo, S., Rosengarten, B., Hossmann, K.-A., Pozzan, T., et al. (2002). Neuron-to-astrocyte signaling is central to the dynamic control of brain microcirculation. *Nat. Neurosci.* 6, 43–50. doi: 10.1038/nn980

Conflict of Interest: The authors declare that the research was conducted in the absence of any commercial or financial relationships that could be construed as a potential conflict of interest.

The reviewer GW declared a shared affiliation, with no collaboration, with one of the authors AJ to the handling editor at the time of the review.

Publisher's Note: All claims expressed in this article are solely those of the authors and do not necessarily represent those of their affiliated organizations, or those of the publisher, the editors and the reviewers. Any product that may be evaluated in this article, or claim that may be made by its manufacturer, is not guaranteed or endorsed by the publisher.

frontiers in Aging Neuroscience

REVIEW
published: 10 September 2021
doi: 10.3389/fnagi.2021.727590

Neurovascular Alterations in Vascular Dementia: Emphasis on Risk Factors

Sarah Lecordier[1,2], *Daniel Manrique-Castano*[1,2], *Yara El Moghrabi*[1,2] *and Ayman ElAli*[1,2]*

[1]Neuroscience Axis, Research Center of CHU de Québec-Université Laval, Québec City, QC, Canada, [2]Department of Psychiatry and Neuroscience, Faculty of Medicine, Université Laval, Québec City, QC, Canada

Vascular dementia (VaD) constitutes the second most prevalent cause of dementia in the world after Alzheimer's disease (AD). VaD regroups heterogeneous neurological conditions in which the decline of cognitive functions, including executive functions, is associated with structural and functional alterations in the cerebral vasculature. Among these cerebrovascular disorders, major stroke, and cerebral small vessel disease (cSVD) constitute the major risk factors for VaD. These conditions alter neurovascular functions leading to blood-brain barrier (BBB) deregulation, neurovascular coupling dysfunction, and inflammation. Accumulation of neurovascular impairments over time underlies the cognitive function decline associated with VaD. Furthermore, several vascular risk factors, such as hypertension, obesity, and diabetes have been shown to exacerbate neurovascular impairments and thus increase VaD prevalence. Importantly, air pollution constitutes an underestimated risk factor that triggers vascular dysfunction *via* inflammation and oxidative stress. The review summarizes the current knowledge related to the pathological mechanisms linking neurovascular impairments associated with stroke, cSVD, and vascular risk factors with a particular emphasis on air pollution, to VaD etiology and progression. Furthermore, the review discusses the major challenges to fully elucidate the pathobiology of VaD, as well as research directions to outline new therapeutic interventions.

Keywords: vascular dementia (VaD), stroke, cerebral small vessel disease (cSVD), neurovascular abnormalities, blood-brain barrier, neuroinflammation, air pollution

OPEN ACCESS

Edited by:
Shereen Nizari, University College London, United Kingdom

Reviewed by:
Scott Edward Counts, Michigan State University, United States
Marcus O. W. Grimm, Saarland University, Germany

***Correspondence:**
Ayman ElAli
ayman.el-ali@crchudequebec.ulaval.ca

Received: *19 June 2021*
Accepted: *05 August 2021*
Published: *10 September 2021*

Citation:
Lecordier S, Manrique-Castano D, El Moghrabi Y and ElAli A (2021) Neurovascular Alterations in Vascular Dementia: Emphasis on Risk Factors. Front. Aging Neurosci. 13:727590. doi: 10.3389/fnagi.2021.727590

INTRODUCTION

Dementia affects nearly 50 million people worldwide, and the World Health Organization (WHO) estimates that this number will triple by 2050 (Patterson, 2018). Dementia is a heterogeneous neurodegenerative pathology that encompasses Alzheimer's disease (AD), vascular dementia (VaD), Lewy body dementia (LBD), frontotemporal dementia (FTD), and Parkinson's disease (PD). Although the overall prevalence of dementia is higher in aging men, its severity is more pronounced in aging females, a disparity that might implicate sex hormones (Appelros et al., 2009; Podcasy and Epperson, 2016; Poorthuis et al., 2017). VaD comes just after AD as a main cause of dementia, accounting for approximately 15–20% of dementia cases in the Western countries and could reach up to 30% in Asia and developing countries (Rizzi et al., 2014). Vascular deficiencies are now considered relevant contributors to mixed dementia (MxD), which accounts for 25–35% of all dementia cases (Jellinger, 2007; Rosa et al., 2020).

The Vascular Impairment of Cognition Classification Consensus Study (VICCCS) defines VaD as "clinically significant deficits in at least one cognitive domain comprising sensation, perception, motor skills and construction, attention and concentration, memory, executive functioning, processing speed and language/verbal speed, that are of sufficient severity to cause severe disruption of activities of daily living" (Sachdev et al., 2006; Andrianopoulos et al., 2017; Skrobot et al., 2018). The cognitive functions are assessed through the Montreal Cognitive Assessment Test which evaluates five cognitive domains; executive function, attention, memory, language, and visuospatial function (Pendlebury et al., 2012; Skrobot et al., 2018; Iadecola et al., 2019). Diagnosis of VaD is divided into two major research fields; cognitive tests and neuroimaging. Indeed, the diagnosis does not rely only on memory impairments, but it is supported by the presence of diverse cognitive deficits accompanied by diagnostic imaging evidencing cerebrovascular abnormalities such as brain atrophy, white matter hyperintensities, infarcts, and hemorrhages. Accordingly, four different subtypes arise: post-stroke dementia (PSD) in which dementia appears 6 months after stroke, subcortical ischemic vascular dementia (SIVaD), multi-infarct dementia, and MxD (Skrobot et al., 2018). The cognitive deficits associated with VaD are caused by structural and functional vascular abnormalities that are exacerbated with age. These abnormalities promote the emergence of chronic alterations in the neurovascular functions that underlie the etiology of cognitive decline observed in VaD (**Figure 1**).

VaD is tightly associated with several risk factors that can be categorized into four groups, which comprise: (i) cerebrovascular disease-related factors; (ii) atherosclerotic factors, such as smoking, myocardial infarction, diabetes mellitus, and hyperlipidemia; (iii) demographic factors, such as age, biological sex and education; and (iv) genetic factors, such as the emergence of mutations leading to vascular encephalopathies (Ritchie and Lovestone, 2002; Gorelick, 2004). Noteworthy, these vascular risk factors are now being recognized as clinical risk factors for AD pathology (O'Brien and Markus, 2014; **Figure 1**).

The cerebrovascular disease-related factors include cerebral tissue loss volume, bilateral cerebral infarction, strategic infarction, and white matter disease (WMD; Ritchie and Lovestone, 2002; Gorelick, 2004). Furthermore, hypertension was shown to be associated with larger white matter and smaller brain volumes, silent or strategical subcortical or cortical infarcts, and loss of volume in the thalamus or temporal lobe that are critical for cognitive functions (Ritchie and Lovestone, 2002; Gorelick, 2004). While age remains a principal risk factor for dementia, the presence of familial dementia history, and the epsilon 4 allele of apolipoprotein E (ApoE)4 susceptibility gene were recognized as an important risk factor for VaD (Ritchie and Lovestone, 2002; Gorelick, 2004). In addition, variables such as the female sex, various types of infection of lipid concentrations, history of head injury, head circumference, hormone replacement therapy (HRT), as well as thyroid dysfunction and preceding history of depression could interact with ApoE genotype and hence increase the risk of dementia (Ritchie and Lovestone, 2002; Gorelick, 2004). The genetic factors include vascular encephalopathies such as cerebral autosomal dominant arteriopathy with subcortical infarcts and leukoencephalopathy (CADASIL), autosomal recessive cerebral arteriopathy with subcortical infarcts and leukoencephalopathy (CARASIL), and potentially ApoE4 (Ritchie and Lovestone, 2002; Gorelick, 2004). Recently, environmental factors, namely air pollution, have been shown to constitute an important, yet underestimated, risk factor for dementia, inducing VaD and AD (Azarpazhooh and Hachinski, 2018; Béjot et al., 2018). Indeed, numerous studies have demonstrated that the elevated levels of air pollutants are directly linked to brain chronic inflammation and neurodegenerative diseases (Campbell et al., 2005; Schwartz et al., 2005; Calderón-Garcidueñas et al., 2007; Hartz et al., 2008; Block and Calderón-Garcidueñas, 2009; Mills et al., 2009; Rozemuller et al., 2012; Paul et al., 2019). Among air pollutants, ultrafine particles (UFPs) are particularly deleterious due to their ability to reach the brain where they act as inflammatory triggers and neurotoxins (Block and Calderón-Garcidueñas, 2009; Hameed et al., 2020).

As mentioned, VaD prevalence is strongly linked to cerebrovascular diseases, which essentially include stroke and cerebral small vessel disease (cSVD; Grinberg and Thal, 2010; Gorelick et al., 2011; Jellinger, 2013). Indeed, one patient in 10 has a stroke before developing a form of dementia that is not related to AD. In turn, cSVD was found in up to 62% of patients diagnosed with VaD, outlining a strong correlation between these pathologies (Gorelick et al., 2011; Venkat et al., 2015; van Veluw et al., 2017; Shih et al., 2018; Iadecola et al., 2019). Stroke and cSVD are characterized by the dysfunction of the neurovascular unit, which anatomically comprises sealed endothelial cells forming the blood-brain barrier (BBB), perivascular cells that include pericytes, and vascular smooth muscle cells (VSMCs), astrocytes, microglia, and neurons (Hermann and ElAli, 2012). The neurovascular unit integrates signals from the different neighboring cells to generate critical functions that include BBB maintenance, neurovascular coupling, vascular stability, and immunomodulation (Zlokovic, 2011; Hermann and ElAli, 2012). Neurovascular functions are impaired after stroke and cSVD leading to BBB dysfunction, neurovascular uncoupling, hypoperfusion, inflammation, and loss of neurons (Zlokovic, 2008, 2011; Guo and Lo, 2009; Moskowitz et al., 2010). These pathological events are at the origin of ischemic and hemorrhagic lesions, which strongly correlate with the cognitive deficits observed in VaD.

Despite being the second most common form of dementia after AD, little is known about the molecular and cellular mechanisms underlying the pathobiology of VaD. This gap in the literature is mainly due to disease heterogeneity in the clinical setup and the lack of an optimal experimental model that can accurately replicate most of the pathological events underlying the etiology and progression of the different forms of VaD. It is now established that accumulation of brain lesions over time mediated by neurovascular impairments constitutes a major contributor to the pathobiology of VaD in the elderly (Venkat et al., 2015; Corrada et al., 2016; Ince et al., 2017; Summers et al., 2017; van Veluw et al., 2017; Shih et al., 2018). The review summarizes the current knowledge related to the

pathological mechanisms underlying the pathobiology of VaD with an emphasis on stroke, cSVD and risk factors with a focus on air pollution. We will discuss the challenges and research directions that might help in a better understanding of VaD pathobiology, thereby outlining new therapeutic interventions.

MAJOR RISK FACTOR-MEDIATED MECHANISMS IMPLICATED IN VAD PATHOBIOLOGY

Stroke-Related Dementia

Ischemic or hemorrhagic strokes trigger major pathophysiological mechanisms that underlay VaD (Mijajlović et al., 2017). Indeed, epidemiological studies indicate that stroke history doubles the risk of dementia in the elderly (<65 years) and increases the incidence of early mortality (Savva and Stephan, 2010). Approximately 10% of patients exhibit signs of dementia before their first cerebrovascular accident, and another 10% manifest cognitive deficits soon after their first event (Desmond et al., 2002; Pendlebury and Rothwell, 2009). Particularly, recurrent stroke events raise the prevalence of dementia to 30%, constituting the most prominent causal factor of the disease (Pendlebury and Rothwell, 2009). Noteworthy, an examination of the association between stroke rates and dementia in the frame of the National Long-Term Care Survey (NLTCS) between 1984–2001 reported that the elevated incidence of post-stroke dementia is related to increased patient survival, due to clinical improvements in stroke management (Ukraintseva et al., 2006). Assessment of the neuropsychological parameters revealed that deterioration of the executive functions, abstraction, visual memory, and visuoconstruction constitute some of the most critical long-term cognitive disabilities observed in stroke patients (Sachdev et al., 2004). In contrast, praxis-gnosis, working memory, and language have been shown to be impacted to a lesser extent (Sachdev et al., 2004). The Sydney Stroke Study disclosed that in 50–85 years old patients diagnosed with VaD, the stroke volume and premorbid function were the most significant determinants of cognitive deterioration following the initial insult (Sachdev et al., 2006). It is remarkable to notice that in the last decade, stroke incidence increased by 23% in young adults aged between 35 and 50 years, especially because of the unhealthy lifestyle that meaningfully increased the rate of risk factors in this population, including smoking, hypertension, and obesity (Ekker et al., 2019; George, 2020). Due to the advances in acute stroke care, young stroke patients live longer and thus are at high risk of developing dementia at later stages (Pinter et al., 2019).

BBB Dysfunction

Hallmark of stroke pathophysiology (Yang et al., 2019), BBB dysfunction constitutes a pivotal factor implicated in the initiation and exacerbation of the cascade of events leading to dementia (Zlokovic, 2011; Sachdev et al., 2014; Noe et al., 2020). Following primary injury, BBB breakdown allows the uncontrolled infiltration into the brain of blood-borne molecules, including plasma proteins, metabolites, neurotoxic compounds, and peripheral immune cells that contribute to secondary injury progression *via* edema formation, neuroinflammation, and glial reactivity (Halder and Milner, 2019; Koizumi et al., 2019) that aggravate the initial neurological deficits (Khanna et al., 2014; Jiang et al., 2018). The experimental findings indicate that acute BBB impairment is widely mediated by early inflammatory mediators, such as cytokines and chemokines, as well as oxidative stress, including reactive oxygen species (ROS) and reactive nitrosative species (RNS; Yang et al., 2019). The action of these substrates is further potentiated by matricellular proteins, proteoglycans, and metalloproteinases (MMPs) secreted in the extracellular space (Jones and Bouvier, 2014). Experimental and clinical studies revealed that MMP-9 significantly contributes to long-term BBB breakdown in several brain disorders, namely stroke and neurodegenerative diseases (Barr et al., 2010; Montagne et al., 2017; Underly et al., 2017; **Figure 2**).

Upon ischemic stroke, MMP-9 is secreted by the cells forming the neurovascular unit *via* regulation of the extracellular signal-regulated kinase-(ERK)-1/2) and the signal transducer and activator of transcription (STAT)-3 pathways, leading to the degradation of basal lamina/extracellular matrix (ECM) proteins, and the recruitment and extravasation of peripheral immune cells (Nishikawa et al., 2018; Jäkel et al., 2020). Interestingly, human brain studies showed that MMP-9 is implicated in the degradation of type IV collagen at the basal lamina, resulting in hemorrhagic transformations (Rosell et al., 2006, 2008), enhanced leukocyte infiltration, and poor neurological outcomes (Kim et al., 2016). In parallel, studies employing MMP-9$^{-/-}$ mice showed that leukocyte-derived MMP-9 plays an essential role in mediating BBB dysfunction and is associated with elevated leukocyte transmigration that exacerbates the inflammatory signaling in the acute phase of stroke (Gidday et al., 2005). Furthermore, photothrombotic mouse models of cerebral ischemia have reported that BBB permeability at the level of the capillary is governed by pericytes exhibiting MMP-9 activation, which was later neutralized by specific MMP-9 inhibition (Underly et al., 2017). Elevated MMP-9 activity has been also reported to be associated with increased brain edema and IgG extravasation after ischemia in hyperlipidemic mice (ElAli et al., 2011). These observations indicate that hyperlipidemia exacerbates stroke-mediated BBB dysfunction, which could eventually aggravate dementia (**Figure 2**).

On an important note, stroke-induced MMP-9 expression has risen as an informative prognostic marker for a poor neurological outcome, increased mortality, and the emergence of typical signs of dementia (Zhong et al., 2017). Clinical investigations disclosed that high MMPs expression correlates with increased levels of albumin cerebrospinal fluid (CSF) in patients with vascular cognitive impairment (VCI) derived from SIVD, multiple strokes, and leukoaraiosis (Candelario-Jalil et al., 2011). In parallel, independently of the presence of vascular risk factors, elevated serum MMP-9 levels are associated with mild (25.6% of patients) and severe (27.4%) cognitive impairment 3 months following stroke according to the Mini-Mental State Examination and Montreal Cognitive Assessment (Zhong et al., 2018). Moreover, high MMP-9 levels in patients with cardioembolic

stroke involving the middle cerebral artery (MCA) territory are related to large infarct volumes and poor behavioral scores based on the National Institutes of Health Stroke Scale (NIHSS; Montaner et al., 2001). Otherwise, the strong correlation between MMP-9 expression and the hyperintense acute reperfusion injury marker (HARM) has led to consider this protein as a revealing marker for BBB disruption (Barr et al., 2010). Furthermore, increased MMP-9 activity has been detected in the frontal and parietal cortex of postmortem human brains diagnosed with AD and patients exhibiting cognitive deficits (Bruno et al., 2009). MMP-9 enhanced expression is also notable in the CSF of AD patients, directly correlated with T-tau and P-tau levels (Stomrud et al., 2010). Importantly, a longitudinal study (4–10 years) enrolling AD and VaD patients revealed higher MMP-9 levels in the CSF of VaD patients compared to AD or controls (Adair et al., 2004). These findings imply that assessment of MMP-9 levels might constitute a potential strategy to distinguish between the different types of dementia.

Cell-based assays have demonstrated that exposure of pericytes to amyloid-β ($A\beta)_{42}$ induced MMP-9 activity, which in turn ameliorated protein aggregation (Schultz et al., 2014). This outlines the presence of a direct pathological link between the molecular markers of dementia and MMP-9 activity, even though MMP-9 is an active substrate for Aβ degradation (Hernandez-Guillamon et al., 2015). Overall, current evidence suggests that MMP-9-mediated BBB dysfunction following stroke may constitute an early pathological mechanism that initiates the neurodegenerative cascades leading to cognitive deficits over time. Although MMP-9 inhibition has been proposed as a therapeutic strategy to attenuate BBB breakdown after cerebral ischemia (Dong et al., 2009; Chaturvedi and Kaczmarek, 2014), animal studies showed that MMP-9 is required for neurovascular remodeling and adaptation in the chronic phase after stroke (Zhao et al., 2006). Furthermore, MMP-9 is implicated in the clearance of various misfolded proteins involved in several neurodegenerative diseases, such as Aβ (Hernandez-Guillamon et al., 2015). The current knowledge implies that MMP-9 impact on BBB breakdown and neurodegeneration is time and context-dependent, which entails a contextualized modulation of protein expression/activity to preserve BBB integrity and attenuate cognitive deficits associated with stroke.

Post-stroke Neuroinflammation

Evidence obtained from AD studies outlined an important pathological link among chronic neuroinflammation, vascular damage, and cognitive decline in aged patients (Rhodin and Thomas, 2001; Kinney et al., 2018). Importantly, the neuroinflammatory responses associated with AD could be observed as well in other forms of dementia, including frontotemporal dementia (FTD; Bevan-Jones et al., 2020), PD (Caggiu et al., 2019), and VaD (Iadecola, 2013). Neuroinflammation plays a critical role in modulating tissue injury and repair after stroke. This process integrates various molecular and cellular mechanisms that comprise the release of inflammatory and oxidative stress mediators, glial reactivity, and peripheral immune cell activation and extravasation (Guruswamy and ElAli, 2017; Dzyubenko et al., 2018; Jayaraj et al., 2019). In this regard, uncontrolled microglial activation and the subsequent release of proinflammatory cytokines after stroke (Zhao et al., 2017) are strongly associated with demyelination and axonal loss (Sachdev et al., 2004).

It has been reported that in a rodent model of cerebral hypoperfusion, microglial activation *via* the complement (C)3-C3aR pathway, which is implicated in myelin phagocytosis, resulted in learning and memory deficits (Zhang et al., 2020). Interestingly, the cognitive impairments were attenuated by the genetic deletion of *c3ar1* or *via* the administration of SB290157, a potent C3aR antagonist (Zhang et al., 2020). Similarly, experimental investigations using cerebral ischemia have shown that fingolimod (FTY720), a potent agonist of sphingosine 1 phosphate (S1P), induced a microglial anti-inflammatory phenotype (M2 phenotype) through the activation of STAT-3 signaling pathway (Qin et al., 2017). Modulating microglial activation to adopt a protective M2 phenotype resulted in enhanced oligodendrocytogenesis and white matter integrity, and reduced cognitive deficiencies associated with working memory (Qin et al., 2017). Induction of severe chronic cerebral hypoperfusion (SCCH) in APP/PS1 mice that overproduced Aβ accelerated spatial learning and memory decline in 4-month adult animals. This was correlated to the accumulation of parenchymal Aβ plaques in the hippocampus and diminished activity of the ERK-1/2 pathway. APP/PS1 mice subjected to SCCH had higher levels of patrolling monocytes in peripheral blood. Interestingly, this model revealed that SCCH reduces microglial interaction with Aβ plaques in the hippocampus, denoting a reduced capacity for Aβ clearing in the brain parenchyma (Bordeleau et al., 2016). Alternatively, the release of prostaglandins, which act as inflammatory mediators upon stroke, has been shown to be associated with exacerbated Aβ-mediated cognitive decline and impaired synaptic plasticity (Kotilinek et al., 2008; **Figure 2**).

Loss of white matter integrity by hyper-reactive ramified and amoeboid microglia was also found in the posterior cingulate cortex of post-mortem brains of patients diagnosed with Down syndrome who are at higher risk of developing AD neuropathology (Martini et al., 2020). Furthermore, microglia in post-mortem AD brains exhibit accelerated aging and transcriptional alterations associated with the isoforms of ApoE, a protein broadly related to both dementia and cardiovascular disease (Srinivasan et al., 2020). In this regard, findings from subarachnoid hemorrhage in mice indicate that ApoE mediates protective effects following injury by inducing M1 microglial quiescence (Pang et al., 2018), suggesting that adequate lipid metabolism modulates neuroinflammation. Functional human brain investigations using positron emission tomography (PET) coupled to 11C-PK11195, which is an *in vivo* marker of activated microglia, have unraveled a progressive microglial activation and neuroinflammation, which were correlated with long-term (14 to 16 months) cognitive decline in AD patients (Malpetti et al., 2020). In this regard, activated microglia exhibiting a pro-inflammatory neurotoxic phenotype (M1 phenotype) trigger the activation of pro-inflammatory astrocytes (A1 astrocytes) *via* tumor necrosis factor (TNF)-α, interleukin (IL)-1α, and C1q cytokines (Liddelow et al., 2017). In turn, A1 reactive

astrocytes exacerbate oligodendrocyte and neuronal death (Liddelow et al., 2017).

In line with these findings, an exaggerated astrocyte reactivity has been related to dementia and cognitive decline (Jo et al., 2014; Csipo et al., 2020). The evidence suggests that morbid neuroinflammatory responses maintained by A1 reactive astrocytes could result in mediating brain injury or age-related neurodegeneration and cognitive deficits. For instance, hippocampal astrocytes are susceptible to the upregulation of inflammatory-related genes and pathways, such as C3 and C4b, C-X-C motif chemokine ligand (CXCL)-10, and the peptidase inhibitor serine protease inhibitor A3N (SERPINA3N; Clarke et al., 2018). Interestingly, in a mouse model of familial Danish dementia (FDD), abundant A1 reactive astrocytes were detected in the brain, which correlated with the appearance of cerebral amyloid angiopathy (CAA), a disease characterized by the deposition of Aβ within the cerebral vasculature and a major risk of VaD. In this context, an increased number of astrocytes was observed in perivascular zones, accompanied by numerous cell branches and enhanced glial fibrillary acid protein (GFAP) expression (Taylor et al., 2020; **Figure 2**).

Several approaches have demonstrated that the usage of anti-inflammatory strategies could attenuate cognitive deficits associated with dementia. For instance, activation of the cannabinoid receptor 2 (CB_2R) using different agonists promoted memory restitution through the reduction of oxidative stress and mitochondrial dysfunction (Jayant and Sharma, 2016). In line with these findings, cell-based assays have shown that CB_2R activation stimulated the microglial release of IL-10, a key anti-inflammatory cytokine, *via* activation of ERK1/2, c-Jun N-terminal kinase (JNK), and mitogen-activated protein kinases (MAPKs) pathways, accompanied by the inhibition of the nuclear factor-κB (NF-κB) pathway (Correa et al., 2010). Likewise, administration of the CB_2R agonist paeoniflorin (PF) ameliorated memory and learning deficits in mice, accompanied by induction of M2 cells and the release of anti-inflammatory mediators, such as transforming growth factor (TGF)-β1, and IL-10, instead of pro-inflammatory ones, such as TNF-α, IL-1β, and IL-6. This phenotypic switch is driven by the enhanced activity of phosphoinositide-3-kinase (PI3K/AKT) anti-inflammatory pathway and the inhibition of the mammalian target of rapamycin (mTOR)/NF-κB pro-inflammatory signaling (Luo et al., 2018). Experimental findings indicate that the inhibition of mTOR attenuated cognitive deficits, which were accompanied by a restoration of M1/M2 microglia phenotypic switch following cerebral hypoperfusion (Chen et al., 2016).

Remarkably, in a rodent model of VaD, it has been shown that acupuncture could attenuate inflammation by reducing TNF-α and Toll-like receptor (TLR)4 expression in microglia, and suppressing the myeloid differentiation factor (MyD88)/NF-κB pathway (Wang et al., 2020). Furthermore, pharmacological administration of PLX5622, a potent inhibitor of colony stimulating factor-1 receptor (CSF-1R) that is required for microglial cell survival, improved short-term memory in a rodent model of induced hypertension. This effect was accompanied by controlled microglia reactivity and preservation of BBB integrity (Kerkhofs et al., 2020). It has also been demonstrated that depletion of microglia *via* CSF1R inhibition prevented Aβ plaque development in the hippocampus of a mouse model of AD (Spangenberg et al., 2019). Attenuation of microglial reactivity *via* blockage of CCL-5 signaling also preserved BBB integrity in the context of systemic inflammation (Haruwaka et al., 2019). Taken together, there is strong evidence associating chronic uncontrolled neuroinflammatory responses after stroke to the emergence of long-term cognitive disabilities and dementia, mediated essentially by microglial reactivity. Therefore, strategies aiming to modulate microglial response by stimulating a protective phenotype might constitute a potential approach to attenuate VaD occurrence after stroke.

Stroke-Mediated Proteinopathies

Accumulation of Aβ in the brain constitutes a hallmark of AD pathogenesis (Chen et al., 2017). Early studies using human post-mortem brains revealed that amyloid precursor protein (APP) is not implicated exclusively in AD pathology, and its expression is as well induced in the brain after stroke (Cochran et al., 1991; Jendroska et al., 1997). For instance, mutant mice overexpressing APP exhibited a substantial reduction of cerebral blood flow (CBF) accompanied by larger infarcts after stroke, suggesting that APP exacerbated ischemic injury by impairing structural and functional vascular integrity (Zhang et al., 1997). Moreover, it has been shown that cerebral ischemia promotes APP deposition in the lesion core, the perilesional regions, as well as in the white matter areas exhibiting myelin loss (Nihashi et al., 2001; Zhan et al., 2015).

Endothelin (ET)-1 is a powerful vasoconstrictor synthesized by endothelial cells and reactive astrocytes, which have been shown to be implicated in ischemic stroke pathobiology as well as Aβ deposition. Examination of post-mortem human brains showed strong ET-1 expression in reactive astrocytes surrounding Aβ plaques (Hung et al., 2015). Furthermore, ET-1 overexpression in the acute phase after stroke has been involved in BBB disruption, glial reactivity, and neuronal death. Indeed, mutant mice exhibiting astrocytic ET-1 overexpression (GET-1 mice) experience severe memory and spatial learning deficits, associated with the upregulation of cleaved caspase-3, TNF-α, and IL-1β (Thiel et al., 2014; Hung et al., 2015). Using cell-based assays, ET-1 overexpression in reactive astrocytes has been shown to amplify Aβ production (Hung et al., 2015). Aβ accretion contributes to the development of cognitive deficits by impairing the receptor for advanced glycation endproducts (RAGE)-mediated Aβ clearance, which exacerbates inflammation, oxidative stress, and neurodegeneration (Min et al., 2020). These findings indicate that ET-1 upregulation after ischemic stroke is tightly associated with Aβ production and deposition and has considerable effects on excitotoxicity and BBB integrity. Furthermore, comorbid models of Aβ toxicity and cerebral ischemia have reported that Aβ deposition exacerbates ischemic damage. This condition leads to ventricular enlargement and striatal atrophy, morphological alterations in microglia, increased production of inflammatory mediators and enhanced glial communication *via* the gap junction proteins connexin (CX)-43. These observations are particularly important as ventricular enlargement was associated with deposition of

neurofibrillary tangles and Aβ plaques, directly implicated in the pathogenesis of various forms of dementia (Amtul et al., 2015). Furthermore, evidence indicates that the interactions among lipoprotein-associated triggering receptor expressed on myeloid cells (TREM) 2 and apolipoproteins are involved in modulating microglia-mediated Aβ phagocytosis (Yeh et al., 2016), thus suggesting that Aβ clearance is associated with lipid metabolism (**Figure 2**). Likewise, it has been shown that exogenous administration of Aβ triggers tau phosphorylation and magnifies learning and memory deficits in animals subjected to cerebral ischemia (Song et al., 2013).

Finally, the generation of RNS, including peroxynitrite, revealed by the formation of 3-nitrotyrosine (3-NT), is increased in perivascular astrocytes and microglial cells after $A\beta_{42}$ injection, strongly correlating with BBB leakage (Ryu and McLarnon, 2006). These findings suggest that Aβ pathology could trigger the release of reactive nitrogen species in astrocytes, directly undermining cerebrovascular integrity. Moreover, it has been demonstrated that Aβ binding to RAGE induces ROS production leading to loss of the tight junction proteins claudin-5, occludin, and zonula occludens (ZO)-1, as well as deficient endothelial cell function (Carrano et al., 2011). Overall, this bidirectional pathological crosstalk implies that exacerbated cognitive decline strongly emerges when cerebral injury and Aβ toxicity occur comorbidly.

cSVD

cSVD comprises numerous pathologies impacting cerebral arteries, arterioles, venules, and capillaries, which are associated with diverse pathological and etiological processes (Østergaard et al., 2016; Staszewski et al., 2017; Li et al., 2018; Parkes et al., 2018). Six different types of cSVD are classified according to their etiology (Pantoni, 2010; Li et al., 2018). Atherosclerosis and sporadic and hereditary CAA are the most frequent forms. Recent reports outlined a significant increase in the number of genetic microangiopathies distinct from CAA such as CADASIL or Fabry's disease (Razvi and Bone, 2006; Ballabio et al., 2007; Dichgans, 2007; Hara et al., 2009). Microangiopathies caused by inflammation or mediated by immunity are rare and characterized by the presence of inflammatory cells within the vasculature (Jennette and Falk, 1997), generally caused by mechanisms associated with systemic pathologies. Venous collagenosis is a pathologic thickening of the wall of veins and venules that are located near the lateral ventricles, thus leading to a smaller lumen and sometimes to an occlusion (**Figure 2**). Finally, post-radiation angiopathies are a side effect of cerebral irradiation that appears a few months to years after treatment. These angiopathies mainly affect small vessels of the white matter associated with fibrinoid necrosis, resulting in an increased thickness of the walls accompanied by a reduced diameter, which jointly could lead to a thrombotic occlusion (Dropcho, 1991).

cSVD Associated Parenchymal Pathology

cSVD refers to various and complex pathological and etiological processes. Therefore, the clinical manifestations depend on both the cause of the pathology and the affected brain territory. Among the most common symptoms are stroke-related manifestations, progressive cognitive deterioration, VaD, gait disturbance, sphincter dysfunction, and psychiatric disorders (van der Flier et al., 2005; Pantoni, 2010; Del Bene et al., 2013; Li et al., 2018; de Laat et al., 2011). cSVD is thought to constitute the major cause of vascular cognitive deficits and are responsible for up to 45% of dementia cases (Shi and Wardlaw, 2016; Li et al., 2018). Cognitive deficits are associated with impaired executive functions, decline in memory and attention, regression in verbal fluency, and delayed recall. These symptoms are accompanied by others that are not specific, including dizziness, trouble sleeping, tinnitus, and hearing loss. Moreover, neuropsychiatric symptoms can be observed, including hallucinations, agitation, depression, anxiety, disinhibition, apathy, irritability, and changes in appetite. Most of these manifestations are often accompanied by brain microbleeds. Cerebral microangiopathies are accountable for up to 20–30% of ischemic stroke as well as a considerable proportion of hemorrhage and encephalopathies caused by emboli, thrombosis, or stenosis of the vessel (Cai et al., 2015; Shi and Wardlaw, 2016; Regenhardt et al., 2019).

In addition to the cerebrovascular pathologies, cSVD exhibits a unique parenchymal pathology characterized by small subcortical infarcts, lacunar stroke, microbleeds, white matter hyperintensities (WMH), enlarged perivascular spaces, and brain atrophy detectable in imaging (van der Flier et al., 2005; de Laat et al., 2011; Del Bene et al., 2013; Wardlaw et al., 2013; Li et al., 2018; Regenhardt et al., 2018; Das et al., 2019). Small subcortical ischemic stroke is the result of severe tissue ischemia caused by the occlusion of a perforating arteriole. Patients either have typical stroke symptoms or a lesion visible only using neuroimaging approaches (Wardlaw et al., 2013; Li et al., 2018). Lesions can be anywhere in the brain and are round or ovoid and less than 20 mm in diameter (Smith et al., 2012; Brundel et al., 2012; van Veluw et al., 2017; Hartmann et al., 2018). They appear hyperintense in a diffusion-weighted image (DWI), hypointense on the map of apparent diffusion coefficients, and normal to hyperintense in fluid-attenuated inversion recovery (FLAIR)/T2 imaging (Okazaki et al., 2015; Potter et al., 2015; Li et al., 2018). DWI is the most sensitive technique currently used to detect ischemia a few hours after stroke onset. Recent infarcts will form a cavity characterized by morphological changes that include a reduction in volume and diameter within 90 days of the onset of the infarction (Moreau et al., 2012; Potter et al., 2015; Li et al., 2018). These infarcts can evolve in three different ways, namely lacuna, WMH without cavitation T2-weighted sequence, and finally, they could disappear without visible consequences in conventional magnetic resonance imaging (MRI). When a recent small subcortical ischemic stroke resolves into lacuna, it actually forms a fluid-filled cavity called a lacunar stroke and represents 40% of acute ischemic strokes. Lacunar insults are divided in two different categories; cavitated old infarcts and incomplete infarcts (Fisher, 1965; Lammie et al., 1998; Regenhardt et al., 2018). Old infarcts are pan-necrotic cavitation with scattered macrophages whereas incomplete infarcts are described as exhibiting loss of neurons and oligodendrocytes associated with invading $CD68^+$ macrophages and reactive microglia in addition to reactive astrocytes that are found inside and around the lesion site

(Merino and Hachinski, 2000; Brundel et al., 2012; Regenhardt et al., 2018).

The vascular damage can also develop into BBB leakage or cerebral microbleeds, which appear as small, round, and homogeneous hypointense foci on T2-weighted MRI and are mostly asymptomatic. They originate essentially from the rupture of a precapillary arteriole and are usually associated with vascular risk factor exposition or vascular Aβ deposition (Cordonnier et al., 2007; De Silva and Faraci, 2016; Shi and Wardlaw, 2016; Toth et al., 2017). The rupture is caused by various factors such as age, hypertension, cerebral ischemia, dementia, and cerebral amyloid angiopathy (CAA), and participates in cognitive deficits, dementia, and transient neurological deficits (Martinez-Ramirez et al., 2014; Shi and Wardlaw, 2016; Li et al., 2018). Microbleeds trigger proliferation and migration of microglia and astrocytes as well as monocyte recruitment (Liddelow et al., 2017). The immune cells release various inflammatory factors that impair neuronal function, as well as neurotransmitters that may be neurotoxic and interfere with neuronal circuitry to promote cognitive decline (Tancredi et al., 2000; Beattie et al., 2002; Rosidi et al., 2011; Donzis and Tronson, 2014).

The cerebral white matter is composed of myelinated axons, myelinating oligodendrocytes, oligodendrocyte precursor cells (OPCs), astrocytes, and microglia (Hase et al., 2018). WMH is common in older people and is a typical feature of cerebral microangiopathies, which are associated with BBB disruption, small white matter infarcts, glial activation, loss of oligodendrocytes, and demyelination caused by chronic diffuse hypoperfusion associated with a reduced CBF (Prins and Scheltens, 2015; Li et al., 2018). WMH is generally located within the white matter including the pons and brainstem but also in the deep gray matter. It is distributed symmetrically and bilaterally and appears hyperintense on FLAIR or T2 MRI. Importantly, WMH triples the risk of stroke, doubles the risk of dementia, and substantially increases the risk of death (Debette and Markus, 2010; Pantoni, 2010; Shi and Wardlaw, 2016). Symptoms develop insidiously and are associated essentially with cognitive impairments, dementia, and depression (Debette and Markus, 2010; Pantoni, 2010; Shi and Wardlaw, 2016).

The perivascular space is an extension of the subarachnoid space that surrounds the brain microvasculature. It is a liquid-filled space that cannot be detected by conventional imaging in a physiological context. When this space is widened, it often appears hyperintense on T2 MRI, hypointensity on T1 weighting, and sometimes hypointense on FLAIR (Aribisala et al., 2013; Shi and Wardlaw, 2016; Li et al., 2018). Finally, brain atrophy refers to a diminished brain volume on neuroimaging characterized by symmetrical or asymmetrical decreased total volume, increased ventricular volumes, enlarged superficial sulci, and decreased specific gray or white matter volumes (Mok et al., 2011). One main region affected is the hippocampus and is associated with cognitive decline (Muller et al., 2011; Jokinen et al., 2012).

Atherosclerosis

Atherosclerosis is an age-related condition that constitutes a major risk factor for cerebral microangiopathies. As its severity is increased by diabetes and hypertension, it is also called hypertensive microangiopathy (Tan et al., 2017; Li et al., 2018; Ter Telgte et al., 2018). The risk factors for atherosclerosis are also hyperlipidemia, smoking, and moderate to severe sleep apnea (Østergaard et al., 2016; Cannistraro et al., 2019). Atherosclerosis is characterized by a chronic inflammation associated with the deposition of low-density lipoproteins (LDL) within the vasculature, leading to its internalization by endothelial cells (Tabas et al., 2015), and resulting in the thickening and hardening of the arterial walls (Lusis, 2000; Shabir et al., 2018). Upon deposition, LDL undergoes oxidation by ROS to form oxidized (ox)-LDL, which further exacerbates the inflammatory response within the vasculature (Tabas et al., 2007). Indeed, by binding to vascular cell adhesion molecule (VCAM)-1 and P-selectin, monocytes can infiltrate the intima and differentiate into macrophages to engulf ox-LDL (Chistiakov et al., 2016). Macrophages, which are now called foam-cells due to the intracellular accumulation of lipids (Spann et al., 2012), accumulate and form stable fatty-streaks into the intima, and cells can calcify over time to slowly occlude the vessel (Alexander and Owens, 2012; Chistiakov et al., 2017). These pathological events occur in large to medium size arteries and lead to microbleeds, microinfarcts, as well as lipohyalinosis, characterized by the deposition of hyaline into the walls of connective tissue (Gorelick et al., 2011). This aspect is specific to the brain due to inflammation caused by ROS, ox-LDL, and gliosis involving astrocytes, OPCs, and microglia (Caplan, 2015). Lipohyalinosis fosters the infiltration of monocytes and T helper (TH)-1 lymphocytes that amplify the production of inflammatory mediators, such as TNF-α and interferon (INF)-γ (Stemme et al., 1995; Frostegård et al., 1999). Moreover, the assembly of inflammasomes can be promoted through the activation of nucleotide-binding oligomerization domain (NOD)-like receptor protein (NLRP)-3, stimulated by the formation of cholesterol crystals, caspase-1 and apoptosis-associated speck-like protein containing (ASC), caspase activation and recruitment domain (CARD; Weber and Noels, 2011). This results in IL-1β release, which in turn stimulates the release of IL-6 and C-reactive protein (CRP), implicated in the pathogenesis of atherosclerosis and thrombosis (Ridker et al., 2017; **Figure 2**).

Besides, the elevated levels of LDL combined with the low levels of high-density lipoprotein (HDL) play an important role in the pathogenesis of atherosclerosis and constitute as well a major risk factor for VaD (Hao and Friedman, 2014; Georgakis et al., 2020). Indeed, HDL exerts a protective role through its antioxidant properties and mediates beneficial effects on platelets and endothelial function, thus on coagulation and inflammation (Bandeali and Farmer, 2012). Furthermore, HDL interacts with triglyceride-rich lipoproteins, attenuating their deferential effects (Bandeali and Farmer, 2012). Moreover, it could contribute to the removal of cholesterol excess from the brain microvasculature through ApoE and heparin sulfate proteoglycans (Mulder and Terwel, 1998). HDL counteracts the inhibition of vessel relaxation caused by ox-LDL and decreases LDL peroxidation which affects cellular function and impairs membrane-bound receptors and enzymes (Braughler

and Hall, 1992; Matsuda et al., 1993). Importantly, the impact of hyperlipidemia seems to be differentially modulated depending upon biological sex. Indeed, a recent study shows that females exhibit greater expression of genes related to neuroprotection in response to lipid stress compared to age-matching males (Nuthikattu et al., 2020). Finally, lipid derivatives are now being under the scope of researchers who are trying to unravel novel biomarkers to better understand and diagnose VaD pathology. Indeed, in an interesting recent study that aimed to discover lipid biomarkers in the context of VaD, it has been reported that patients with dementia exhibit low levels for ceramides, cholesterol esters, and phospholipids, and high levels of glycerides compared to controls (Liu et al., 2020). These observations indicate that lipid derivatives could indeed be used as novel diagnostic and prognostic biomarkers in VaD. However, more research is needed in this direction to validate the use of lipid derivatives as diagnostic and prognostic biomarkers in VaD.

Vascular damage caused by atherosclerosis can lead to microatheromas, microaneurysms, and even stenosis or obstruction of the vessel, impairing the mechanisms of blood flow autoregulation and leading to chronic cerebral hypoperfusion (Pantoni, 2010; Li et al., 2018). Importantly, occlusion of the cerebral arteries results in local ischemia or lacunar infarction (Kraft et al., 2017; Ter Telgte et al., 2018), while stenosis and hypoperfusion in the white matter cause incomplete ischemia lesions evidenced by neuroimaging as white matter hyperintensity (Rigsby et al., 2007). When the pathology affects the cerebral arterioles <50 μm in diameter, it is called small cerebrovascular atherosclerosis (Li et al., 2018).

Sporadic and Hereditary CAA

CAA is a chronic degenerative disease characterized by the loss of VSMCs and the accumulation into the vessel wall of eosinophilic hyaline material composed of soluble $A\beta_{40}$ (Attems et al., 2011; Charidimou et al., 2017). CAA affects 50–60% of the elderly population affected by dementia, including 85–95% of AD cases (Sacco, 2000; Jellinger, 2002; Thal et al., 2003; Keage et al., 2009; Charidimou et al., 2017; Zhang et al., 2017; Li et al., 2018). The initial cognitive deficits associated with VaD could be explained by the particular sensitivity of the hippocampus and the cortex to CAA (Arvanitakis et al., 2011; Li et al., 2018). CAA is associated with changes in basal membrane (BM) composition and morphology that could predispose Aβ accumulation in the vessel even though the mechanism is not yet fully understood (Perlmutter et al., 1990, 1991; Su et al., 1992; Morris et al., 2014; Howe et al., 2020). Among the reported changes are BM thickening and degeneration, abnormal heparan sulfate proteoglycans (HSPGs) deposits, and irregular vasculature accompanied by increased collagen IV, fibronectin, agrin, and perlecan expression (Berzin et al., 2000; Farkas et al., 2000; Bourasset et al., 2009; Gama Sosa et al., 2010; Keable et al., 2016; Lepelletier et al., 2017; Magaki et al., 2018; Singh-Bains et al., 2019). Furthermore, vascular functional impairments are featured by BBB dysfunction caused by loss of endothelial cells, deregulation of mural cells mediated by oligomeric Aβ accumulation, as well as induction of astrocytosis with dystrophic endfeet surrounding BM Aβ deposits (Shimizu et al., 2009; de Jager et al., 2013; Giannoni et al., 2016; Yang et al., 2017; Magaki et al., 2018; Nortley et al., 2019). Two possible mechanisms for Aβ deposition have been proposed: (i) release of vascular Aβ from VSMCs directly into the vessel wall; and (ii) release of parenchymal Aβ by neurons which deposits afterward into the vessel wall (Davis et al., 2004; Herzig et al., 2004; Vidal et al., 2009; ElAli et al., 2013). In both cases, the protein accumulates due to a poor clearance towards the periphery (Davis et al., 2004; Herzig et al., 2004; Vidal et al., 2009; ElAli et al., 2013). Insufficient Aβ clearance can impair perivascular drainage pathways or diminish the ATP binding cassette subfamily B member-1 (ABCB1) and low-density lipoprotein receptor-related protein (LRP)1, a specialized endothelial-mediated active transport system implicated in Aβ mobilization from the brain into the blood circulation, namely (Deane et al., 2004; Herzig et al., 2006; Weller et al., 2008; Hawkes et al., 2011). Interestingly, LRP1 plays an important role in protecting against neurodegeneration. Indeed, LRP1 downregulation doesn't only affect Aβ clearance but causes as well BBB breakdown through activation of MMP-9, thus leading to loss of neurons and cognitive deficits (Nikolakopoulou et al., 2021). Furthermore, recent evidence reveals that vascular Aβ could be engulfed and eliminated by circulating patrolling monocytes, which act as the housekeeper vascular homeostasis by surveying endothelial cells (Auffray et al., 2007; Carlin et al., 2013; Michaud et al., 2013; Thériault et al., 2015). In this regard, it has been demonstrated that patrolling monocytes located at the luminal wall internalize Aβ microaggregates that are diffusing from the parenchyma into the blood. Unfortunately, patrolling monocyte ability to phagocyte vascular Aβ in AD is defective, resulting in an overall increase of highly toxic $A\beta_{40}$ and $A\beta_{42}$ oligomers (Hallé et al., 2015; Gu et al., 2016). Moreover, chronic mild cerebral hypoperfusion impairs BBB functional properties and promotes the accumulation of circulating Aβ into the vessel wall, which initiates the cascade of parenchymal Aβ deposition (ElAli et al., 2013). Aβ accumulation and BM rearrangement trigger BBB breakdown, endorsing the formation of perivascular edema and the infiltration of toxic blood-derived substrates into the brain, which in turn contribute to the exacerbation of localized injuries and enlargement of the perivascular space (Holland et al., 2008; Hartz et al., 2012; Wardlaw et al., 2013; Li et al., 2018; **Figure 2**).

The overwhelming evidence is suggesting that the here mentioned vascular abnormalities leading to dementia reported in CAA occur as well in different forms of dementia, including AD and LBD (Salat et al., 2006; Okamoto et al., 2010; Soontornniyomkij et al., 2010; Arvanitakis et al., 2011; Love et al., 2014; Martinez-Ramirez et al., 2014; Reijmer et al., 2016; Li et al., 2018). This form of cSVD can be sporadic or of a genetic origin. For instance, a syndrome called hereditary brain hemorrhage with amyloidosis (HBHA) is associated with a mutation in the *APP* gene. This syndrome results in the deposition of misfolded amyloid fibrils in the walls of cerebral arterioles, which in turn activates a cascade of events leading to the development of CAA. The clinical phenotype develops between the ages of 45–65 years and is associated with intracerebral hemorrhages, WMH, multifocal lesions of a hemorrhagic and ischemic nature (Kamp et al., 2014; Marini et al., 2020). The presence of *ApoE4*

allele, which constitutes the main risk factor for AD, has also been demonstrated to constitute an important risk factor for this form of cSVD (Hermann and ElAli, 2012). ApoE4 is a lipid-binding protein which plays an important role in lipoprotein metabolism as well as transport of triglycerides and cholesterol (Hirsch-Reinshagen et al., 2009). It binds to LDL, very-low-density lipoprotein (VLDL) debris, and some HDL *via* LRP (Bu, 2009; Leduc et al., 2010). ApoE4 can form complexes with Aβ and impairs Aβ through LRP thus attenuating its clearance and subsequently leading to its accumulation in the brain (Cho et al., 2001; Verghese et al., 2013). Moreover, ApoE4 increases the formation of Aβ oligomers, which are now well established to constitute the most neurotoxic form of Aβ (Hashimoto et al., 2012; Youmans et al., 2012). Interestingly, human pericytes of the prefrontal cortex and hippocampus of ApoE4 carriers exhibit increased activation of nuclear factor of activated T-cells (NFAT), which might account for CAA occurrence (Blanchard et al., 2020; **Figure 2**).

Moreover, non-APP sources of CAA exist and are caused by mutations of the BRI2 [i.e., integral membrane protein (ITM)2B] gene, essentially a codon stop mutation. Indeed, processing of the mutated form of BRI2 protein leads to the generation of 34-mer amyloid Bri (ABri) and amyloid Dan (ADan) peptides that accumulate in the brain, either to the ABri amyloid subunit or the AD amyloidogenic fragment. ABri and ADan are responsible for the Familial British (FBD) and Danish (FDD) dementia characterized among other pathological features by severe CAA (Vidal et al., 1999, 2000; Yamada and Naiki, 2012).

Genetic cSVD

Mutations in specific genes constitute the third most common cause of cSVD, among which the mutation of the *neurogenic locus notch homolog protein (NOTCH)3* gene is the better characterized (Cannistraro et al., 2019; Marini et al., 2020). NOTCH3 is a member of the transmembrane receptor NOTCH family, which is critically involved in developmental patterning, cell fate decisions, regulation of cell survival, and proliferation (Kopan and Ilagan, 2009; Bray, 2016; Baron, 2017; Hosseini-Alghaderi and Baron, 2020). During adulthood, NOTCH3 regulates stem cells and their lineages to promote tissue maintenance and repair. NOTCH3 is expressed by VSMCs and pericytes and plays a key role in regulating the crosstalk between the mural and endothelial cells. It controls the vascular tone and flow-mediated dilation *via* the modulation of the Ras homolog family member A (RHOA)/ Rho-associated protein kinase (ROCK) pathway in cerebral arteries (Joutel et al., 2000; Belin de Chantemèle et al., 2008; Li et al., 2009; Marini et al., 2020). However, the role of NOTCH3 is not restricted to the vasculature, since it is expressed in neural stem cells and is implicated in neuronal differentiation (Alunni et al., 2013; Kawai et al., 2017).

A mutation in the *NOTCH 3 gene* is responsible for CADASIL, the most common autosomal dominant inherited cSVD (Louvi et al., 2006; Di Donato et al., 2017; Hosseini-Alghaderi and Baron, 2020; Marini et al., 2020). *NOTCH3* gene is affected essentially by missense mutations that lead to an odd number of cysteine residues located in the extracellular domain of the encoded receptor, and is associated with an early accumulation of the receptor's extracellular domain containing aggregates in small vessels (Joutel et al., 2000, 2001; Monet-Leprêtre et al., 2013; Yamamoto et al., 2013). The function and activity of the NOTCH3 receptor are differently impacted by the mutations. However, the accumulation of extracellular domain containing aggregates in small vessels leads to mural cell degeneration *via* apoptosis or impaired proliferation (Joutel et al., 2000, 2001; Monet-Leprêtre et al., 2013; Yamamoto et al., 2013). Furthermore, the mutation itself causes profound morphological changes in pericytes, associated with dysfunctional mitochondria that could lead to oxidative and phosphorylation deficiencies, secondary lysosomes, and large cytoplasmic vesicles that result in cellular injury and autophagic apoptosis (de la Peña et al., 2001; Gu et al., 2012). This cascade of events cause neurovascular unit dysfunction characterized by detachment of astrocytic endfeet, destabilization of the vasculature, deregulation of vascular contractility, leakage of the BBB, and infiltration of toxic blood-born components into the brain parenchyma due to the decreased endothelial adherens junction protein, thus jointly resulting in diminished reactivity to CO_2 (Ghosh et al., 2015; **Figure 2**).

Pericytes and endothelial cells are intimately interconnected through peg-and-socket junctions, which degenerate upon *NOTCH3* mutations. For instance, endothelial cells exhibit degenerative features, such as selective death or swelling, causing vessel stenosis or occlusion (Dziewulska and Lewandowska, 2012). Deregulation of pericyte-endothelial cells crosstalk causes cerebrovascular dysfunction that comprises reduced vascular density and impaired CBF (Tuominen et al., 2004; Lacombe et al., 2005; Miao et al., 2006; Gu et al., 2012; De Guio et al., 2014; Liu X.-Y. et al., 2015; Ihara and Yamamoto, 2016; Ping et al., 2019). Moreover, chronic cerebral hypoperfusion resulting from cerebrovascular dysfunction exacerbates pericyte degeneration, reduces pericyte coverage for the capillaries, and subsequently increases BBB permeability leading to white matter impairments and neuronal loss (Ueno et al., 2002; Bell et al., 2010; Montagne et al., 2018; Liu et al., 2019; Nikolakopoulou et al., 2019). BBB breakdown allows the infiltration into the parenchyma of toxic blood-born metabolites that accumulate around the vasculature, thus inducing macrophage, microglia, and T-cells activation and recruitment, which jointly promote axonal degeneration (Davalos et al., 2012; Ryu et al., 2015). Neuronal loss is mainly provoked by the secretion of pro-inflammatory mediators and the generation of ROS and RNS by pericytes within the perivascular space, which further exacerbates leukocyte adhesion and infiltration as well as microglial cell activation (Matsumoto et al., 2018; Erdener and Dalkara, 2019). Finally, the structural lesions within the white matter are worsened by the release of pericyte-derived bone morphogenetic protein (BMP)-4, which promotes astrogliosis (Uemura et al., 2018, 2020). Evidence of these pathological events could be detected using imaging approaches that indicate WMH, ischemic manifestations, subcortical hemorrhages, and microbleeds. A new sensitive assay was recently developed allowing pericyte injury detection in the CSF, a new technology that could serve as a diagnostic tool for WMD (Sweeney et al., 2020).

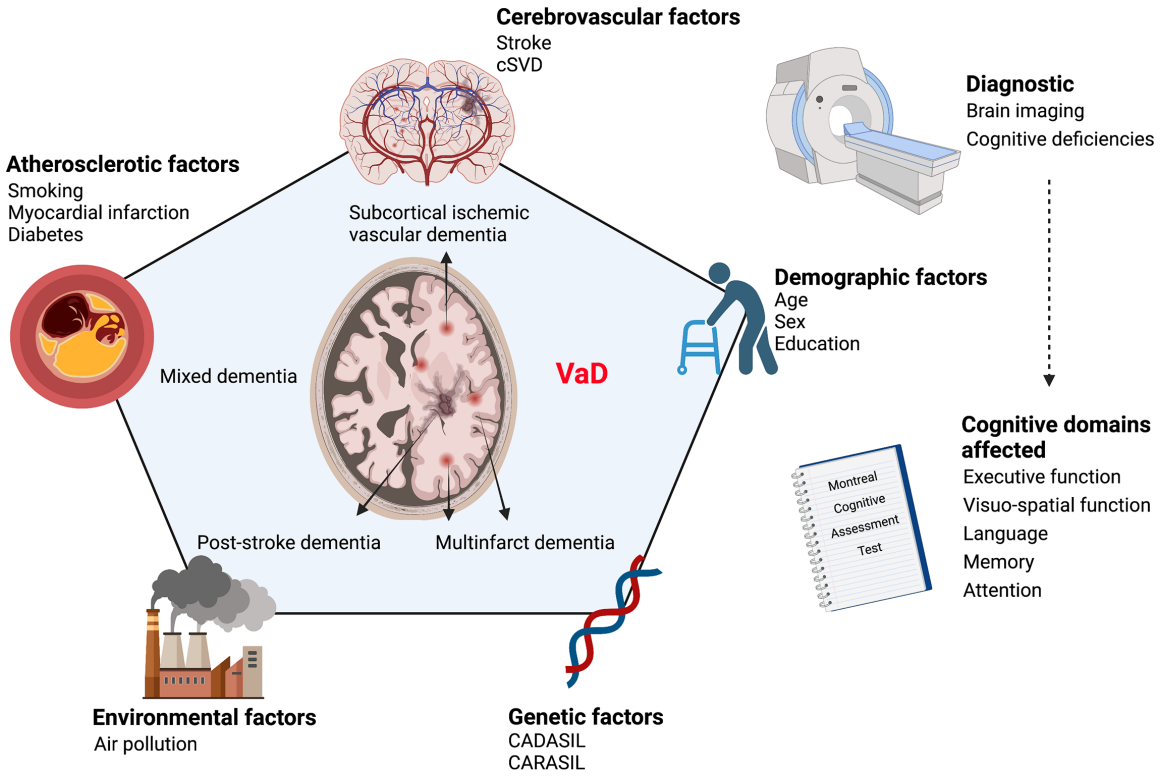

FIGURE 1 | Scheme illustrating the continuum of risk factors that contribute to VaD etiology. VaD emerges as a conjunction of various risk factors affecting vascular homeostasis, namely cerebrovascular diseases, atherosclerosis, genetic and environmental factors. VaD diagnosis is based on the evaluation of cognitive deficiencies combined with neuroimaging to detect underlying vascular alterations. VaD, vascular dementia; CADASIL, cerebral autosomal dominant arteriopathy with subcortical infarcts and leukoencephalopathy; CARASIL, cerebral autosomal recessive arteriopathy with subcortical infarcts and leukoencephalopathy; cSVD, cerebral small vessel disease. Created with BioRender.com.

CADASIL develops gradually over time and the earliest symptoms appear on average around 30 years of age, usually 10 years earlier in women than men, and are manifested as migraines with aura (Guey et al., 2016; Di Donato et al., 2017). The migraine could also manifest with atypical attacks with basilar, hemiplegic, or prolonged aura and a few patients can even develop very severe attacks leading to confusion, fever, meningitis, or even coma that can mimic encephalopathy (Schon et al., 2003; Vahedi et al., 2004; Ragno et al., 2013; Tan and Markus, 2016; Drazyk et al., 2019). Adults between the age of 20 and 65 years are subject to transient ischemic attacks and stroke (Lesnik Oberstein et al., 2001). CADASIL is associated as well with some psychiatric manifestations, which include mood disturbances, severe depression, and schizophrenia (Lågas and Juvonen, 2001; Valenti et al., 2008, 2011; Noh et al., 2014; Ho and Mondry, 2015; Di Donato et al., 2017). Finally, 40% of symptomatic cases report apathy which drastically impacts the quality of life of CADASIL patients (Reyes et al., 2009). The final stage of CADASIL progression is dementia, but cognitive decline starts years before (Brookes et al., 2016).

A recessive form of CADASIL exists under the name of CARASIL. This form of hereditary cSVD is caused by the mutation of the *high-temperature requirement A serine peptidase 1* (*HTRA1*) gene which has two major functions, degrading various substrates and inhibiting TGF-β1 signaling pathway that is involved in various processes namely angiogenesis and BBB formation *via* pericyte-endothelial cell crosstalk (Oka et al., 2004; Hara et al., 2009; Shiga et al., 2011; Akhtar-Schaefer et al., 2019; Kandasamy et al., 2020). HTRA1 is expressed in various brain cells comprising endothelial cells and VSMCs (De Luca et al., 2003; Oka et al., 2004; Campioni et al., 2010; Tennstaedt et al., 2012; Tiaden and Richards, 2013). Loss of HTRA1 function results in increased TGF-β1 availability and thereby signaling, leading to vascular fibrosis and extracellular matrix synthesis, which jointly cause microvascular degeneration, CBF reduction, and neurogenesis alterations (Wyss-Coray et al., 2000; Tarkowski et al., 2002; Gaertner et al., 2005; Yamamoto et al., 2011; Zhang et al., 2012; Martinez-Canabal et al., 2013; Beaufort et al., 2014; Friedrich et al., 2015). Moreover, the mutation has been shown to be associated with impaired pericyte proliferation, accumulation of protein within the vessel walls, MMPs activity, and BBB permeability (Joutel et al., 2016; Baron-Menguy et al., 2017; Ikawati et al., 2018; Marini et al., 2020). Cognitive decline begins early compared with CADASIL, as well as gait disturbances, lower back, pain and alopecia (Shiga et al., 2011; Marini et al., 2020).

Fabry's disease is an X-inherited rare disorder that belongs to the family of lysosomal storage diseases and is caused by a

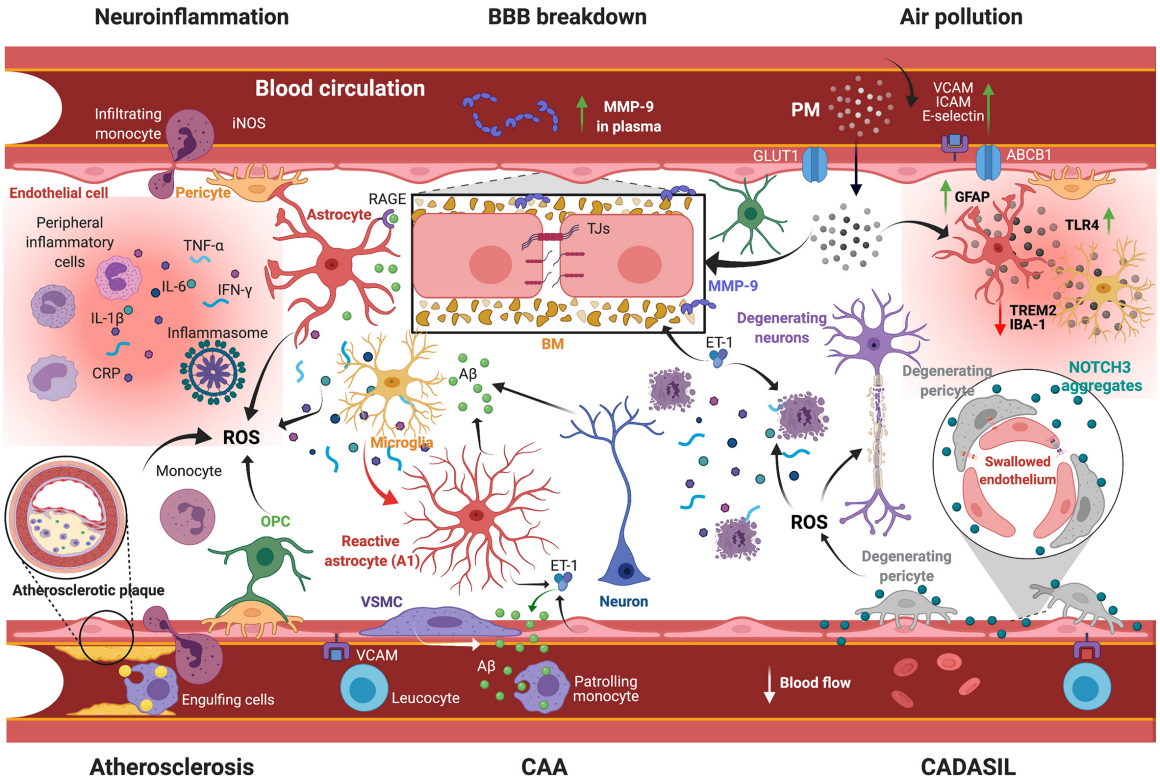

FIGURE 2 | Scheme illustrating the mechanisms underlying VaD pathobiology. Several vascular risk factors are implicated in orchestrating pathological responses leading to VaD: (i) BBB breakdown involves the impairment of TJs and degradation of BM formed by ECM proteins *via* MMP-9 activity. Plasma MMP-9 levels constitute an effective prognostic marker for a poor neurological outcome; (ii) Post-stroke neuroinflammation comprises extravasation of peripheral immune cells and secretion of inflammatory mediators (e.g., CRP, TNF-α, IL-1β, IL-6, IFN-γ), as well as ROS generation and glial activation, accompanied by cerebral Aβ aggregation; (iii) Atherosclerosis comprises the accumulation of lipids and the calcification of immune cells into the intima, leading to vessel occlusion and hypoperfusion. This condition is associated with the generation of ROS that causes chronic inflammation; (iv) CAA is associated with the degeneration of VSMCs and vascular Aβ aggregation due to impaired clearance; (v) CADASIL is associated with NOTCH3 aggregation, causing endothelial cell swelling and pericyte degeneration and subsequently CBF impairment; and (vi) Exposure to air pollution, which implies PM infiltration into the brain, exacerbates BBB breakdown and neuroinflammation. VaD, vascular dementia; BBB, blood-brain barrier; TJs, tight junctions; BM, basement membrane; ECM, extracellular matrix proteins; MMP-9, matrix metalloproteinase-9; CRP, C-reactive protein; TNF-α, tumor necrosis factor-α; IL-1β/6, interleukin-1β/6; IFN-γ, interferon-γ; ROS, reactive oxygen species; Aβ, amyloid-β; CAA, cerebral amyloid angiopathy; VSMCs, vascular smooth muscle cell; CADASIL, cerebral autosomal dominant arteriopathy with subcortical infarcts and leukoencephalopathy; NOTCH3, neurogenic locus notch homolog protein-3; CBF, cerebral blood flow; PM, particulate matter; GLUT1, glucose transporter-1; ABCB1, ATP binding cassette subfamily B member-1; VCAM, vascular cell adhesion protein; ICAM, intercellular adhesion molecule; TLR4, Toll like receptor-4; TREM2, triggering receptor expressed on myeloid cells-2; GFAP, glial fibrillary acidic protein; RAGE, receptor for advanced glycation endproducts; ET-1, endothelin-1; iNOS, inducible nitric oxide synthase; OPC, oligodendrocyte progenitor cell. Created with BioRender.com.

mutation in the α-*galactosidase (GAL)A* gene that encodes for α-GAL enzyme that plays a key role in sphingolipid metabolism (El-Abassi et al., 2014). The mutation causes deficiencies in α-GAL activity that results in the accumulation of sphingolipids in various organs and tissues including the vessels (Rolfs et al., 2013). The cerebrovascular complications in Fabry's disease arise from peripheral neuropathy and are associated with mild to severe headache, vertigo, transient ischemic attacks, ischemic stroke, intracerebral hemorrhage, and VaD (Okeda and Nisihara, 2008). Furthermore, deposition of toxic metabolites within the vasculature and VSMCs lead to ischemia, vessel stenosis, occlusion, and dilation with local changes in CBF (Shimotori et al., 2008). The disease is more severe in men compared to women and is often present with infantile neuropathy, gastrointestinal symptoms, corneal opacity, hearing loss, and angiokeratoma (Sims et al., 2009; Schiffmann, 2015; Marini et al., 2020). Brain structural damage and symptoms exacerbate with age.

Collagen IV, which exists as a heterodimer derived from the transcription of *COL4A1* and *COL4A2* genes, is an essential component of the vascular BM. Mutations in these two genes are associated with microangiopathies in several organs (Germain et al., 2019; Marini et al., 2020). More precisely, *COL4A1* mutation is responsible for ocular, renal, muscular, and cerebral deficits (Vahedi and Alamowitch, 2011; Marini et al., 2020). Furthermore, cerebral microangiopathies have been shown to affect half of the carriers of this mutation. WMH, dilation of the perivascular spaces, lacunar infarctions, and microbleeds have been reported as well (Vahedi and Alamowitch, 2011). Pontine autosomal dominant microangiopathy and

leukoencephalopathy (PADMAL) syndrome is a specific form of cerebral microangiopathies associated with the *COL4A1* mutation (Verdura et al., 2016), and is associated with an overexpression of the gene with the absence of protein misfolding. Patients with this syndrome have dysarthria, ataxia, and stroke as well as mood disorders and dementia. On the other hand, *COL4A2* mutation is associated with an increased prevalence of lacunar ischemic stroke and deep intracerebral hemorrhages (Verdura et al., 2016). In contrast to *COL4A1* mutation, *COL4A2* mutation impairs the trimerization of collagen IV due to defects in the α-helix structure, which cause BM instability, loss of vascular wall integrity, and increased BBB permeability, mediated by the intra- and extracellular accumulation of deficient collagen IV (Kuo et al., 2012; Meuwissen et al., 2015; Verdura et al., 2016; Zhang et al., 2017; Malik et al., 2018; Germain et al., 2019).

Forkhead Box C1 (FOXC1) is highly expressed in pericytes. Its expression plays an important role in controlling endothelial cell proliferation and vascular stability. *FOXC1* mutation reproduces some of the events reported upon *COL4A1* mutation, especially the ischemic infarctions, and cerebral microangiopathies that lead to WMH, which are visible in neuroimaging (French et al., 2014). The retinal vasculopathy with cerebral leukodystrophy (RVCL) syndrome includes three pathological conditions: (i) cerebral retinal vasculopathy (CRV); (ii) hereditary vascular retinopathy (HRV); and (iii) hereditary endotheliopathy with retinopathy, nephropathy, and stroke (HERNS). Patients with these syndromes possess a mutation in three prime repair exonuclease (TREX)-1 that encodes for a DNA exonuclease (Stam et al., 2016). This mutation causes a defect in apoptosis and INF signaling (Rice et al., 2015; Marini et al., 2020). All characteristics of the cerebral microangiopathies are found in RVCL patients who report the following symptoms: neurological deficits, migraines, cognitive deficits, psychiatric disorders, and seizures (Stam et al., 2016; Marini et al., 2020).

Environmental Risk Factors: Air Pollution

The increasing interaction with the environmental risk factors associated with human activities has a significant impact on health due to the exposure to various hazardous pollutants. Currently, environmental factors are directly implicated in the etiology and progression of diverse pathologies, including brain diseases. Indoor and outdoor air pollution is among the environmental factors that play a particularly important role in the deterioration of vascular health (Block and Calderón-Garcidueñas, 2009). Indeed, air pollution, which is defined as the release of an amalgam of pollutants into the atmosphere, has been reported to increase the prevalence of cardiovascular, cerebrovascular, and respiratory diseases, as well as cancer (Campbell et al., 2005; Schwartz et al., 2005; Calderón-Garcidueñas et al., 2007; Hartz et al., 2008; Block and Calderón-Garcidueñas, 2009; Mills et al., 2009; Rozemuller et al., 2012; Cho et al., 2018; Paul et al., 2019). Epidemiological studies have indicated that nearly one-third of the global stroke burden and about one-fifth of the global dementia burden, including VaD, are attributable to air pollution (Feigin et al., 2016; Azarpazhooh and Hachinski, 2018; Béjot et al., 2018). Furthermore, numerous studies have outlined a link between high levels of air pollutants, chronic brain inflammation, and neurodegeneration (Campbell et al., 2005; Schwartz et al., 2005; Calderón-Garcidueñas et al., 2007; Hartz et al., 2008; Block and Calderón-Garcidueñas, 2009; Mills et al., 2009; Rozemuller et al., 2012; Paul et al., 2019). These effects are mainly attributable to the exposure to fine particulate matter (PM), and more precisely to PM of 2.5 microns or less in diameter ($PM_{2.5}$). Indeed, the experimental findings have indicated that UFPs could reach the brain through different routes, including the intranasal cavity, where they act as an inflammatory mediators, thus deregulating the function of cells forming the neurovascular unit (Oberdörster et al., 2004; Peters et al., 2006). In particular, exposure to PM leads to impaired olfactory function, one of the initial atypical symptoms that emerge in individuals affected by different forms of dementia (Campbell et al., 2005; Schwartz et al., 2005; Calderón-Garcidueñas et al., 2007; Hartz et al., 2008; Block and Calderón-Garcidueñas, 2009; Mills et al., 2009; Rozemuller et al., 2012; Paul et al., 2019). The correlation between air pollution and dementia, including VaD and AD, was highlighted in various epidemiological studies relying mostly on cohort studies in polluted regions (Åström et al., 2021). The Betula cohort revealed an association of dementia incidence, AD in particular, with traffic-related air pollution (TRAP; Oudin et al., 2019). Moreover, studies have found that exposure of the elderly to air pollution, notably PM_{10} and $PM_{2.5}$ was associated with cognitive decline (Wu et al., 2015). In an interesting case-control study, it was reported that elevated long-term PM_{10} levels were associated with a significantly increased risk of AD and VaD prevalence in the elderly. A dose-response relationship between PM_{10} exposure and the risk of AD and VaD was reported (Wu et al., 2015).

Impact on Endothelial Functions

Various studies have investigated the impact of air pollutants, and more specifically PM, on endothelial functions. For instance, exposure of isolated rat brain capillaries to diesel exhaust particles (DEP) altered BBB function through oxidative stress generation and proinflammatory cytokine production, which jointly induced the expression of adhesion molecules that exacerbate infiltration of immune cells into the brain (Hartz et al., 2008). Exposure to DEP deregulated the expression of several transporters and receptors that are critically involved in BBB functionality namely ABCB1, multidrug-resistance associated proteins (MRP)1, MRP2, MRP4, breast cancer resistance protein (BCRP), glucose transporter (GLUT)1, and the metabolizing enzyme glutathione S-transferase (GST)π (Hartz et al., 2008). Several reports have demonstrated an increased BBB permeability following exposure to a mixed vehicular emission, translated essentially by deregulation of the TJs (Rojas et al., 2011; Oppenheim et al., 2013; Bernardi et al., 2021). For instance, human brain microvascular endothelial cells in culture exposed to nanoparticles of aluminum oxide exhibit reduced cell viability, altered mitochondrial function, increased oxidative stress, and diminished expression of the TJs proteins claudin-5 and occludin (Chen et al., 2008; Block and Calderón-Garcidueñas, 2009). Interestingly, epidemiological studies have outlined a strong correlation between air pollution

and neuroinflammation in highly exposed residents (Calderón-Garcidueñas et al., 2008). Indeed, these studies reported an upregulation of some inflammatory markers, such as expression of cyclooxygenase (COX)-2 and IL-1β, as well as infiltration of immune cells into the olfactory bulb (OB), frontal cortex, substantia nigrae, and vagus nerves (Calderón-Garcidueñas et al., 2008). Importantly, most of the inflammatory responses were concentrated at the vasculature translated by activation of NF-κB pathway in brain endothelial cells, accompanied by oxidative stress, $A\beta_{42}$ immunoreactivity, trafficking of inflammatory cells into the perivascular space, and an altered BBB (Calderón-Garcidueñas et al., 2008). In line with these observations, direct exposure of brain endothelial cells in culture to $PM_{2.5}$ deregulated TJs and increased permeability and monocyte transmigration across the endothelial monolayer (Liu F. et al., 2015). In addition, exposure to both $PM_{2.5}$ and PM_{10} induced the activation of endothelial cells accompanied by an enhanced adhesion of U937 monocytic cells to the endothelial monolayer (Montiel-Dávalos et al., 2007). Interestingly, exposure to $PM_{2.5}$ also induced ICAM-1 expression, whereas exposure to PM_{10} induced expression of E-selectin and P-selectin (Montiel-Dávalos et al., 2007; **Figure 2**).

In vivo experiments in which mice were exposed to a mixed vehicular emission, a combination of gasoline and diesel engine exhausts, the animals exhibited altered BBB integrity through the deregulation of the TJs protein, namely claudin-5 and occludin (Oppenheim et al., 2013). This was accompanied by an augmentation of inducible nitric oxide synthase (iNOS) levels, an increase in the production of IL-1β in the parenchyma, and deregulation of ABCB1 transport activity (Oppenheim et al., 2013). Moreover, exposure to PM *in vitro* and *in vivo* has been shown to stimulate the re-localization of the TJs protein ZO-1 from the cell membrane and reduce its protein level (Wang et al., 2012). Importantly, PM mediated the intracellular mobilization of calcium (Ca^{2+}) dependently upon ROS, activating calpain that is implicated in ZO-1 degradation and disruption of the endothelial barrier (Wang et al., 2012). Using a 3D human *in vitro* BBB model, indoor nanoscale particulate matter (INPM) was shown to translocate across the BBB and accentuate inflammation by inducing ROS (Li et al., 2020). This induction was followed by abnormal nuclear reactor factor (NRF)-2 expression and a disruption of the kelch ECH associating protein (KEAP)-1/antioxidant response elements (ARE) pathway which is involved in supporting cells to overcome stress (Li et al., 2020). Interestingly, exposure of rodents to urban PM increased the levels of ET-1 mRNA and reduced TNF-α mRNA levels in the cerebral hemisphere and the pituitary gland. These results suggest that the cerebrovascular effects of urban pollutants are associated with the modulation of gene expression involved in the regulation of vasoconstriction in the brain and pituitary gland (Benatti et al., 1993; Thomson et al., 2007).

Exposure to $PM_{2.5}$ has been shown to increase the prevalence of carotid artery stenosis (CAS), a well-established risk factor for ischemic stroke, correlating with an increased BBB permeability (Newman et al., 2015; Szarmach et al., 2017). In line with these observations, a strong association between air pollution with systemic brain inflammation was revealed in children living in polluted areas, associated with short-term memory deficits, prefrontal WMH, and BBB disruption (Calderón-Garcidueñas et al., 2016). The same study reported a leaking vascular network, degeneration of pericytes, VSMCs, and endothelial cells, thickening of the BM, and reduced perivascular astroglial coverage in the prefrontal white matter of dog brains (Calderón-Garcidueñas et al., 2016). Exposure to $PM_{2.5}$ has been demonstrated as well to accelerate atherosclerosis development through induction of vascular dysfunction as well as promotion of coagulopathies, which were accompanied by a strong inflammatory response and lipid abnormalities (Liang et al., 2020). Finally, exposure of ApoE-deficient mice to TRAP, mixed vehicle emissions, induced the cerebral expression of ICAM-1 and the release of pro-inflammatory mediators, such as TNF-α and IL-1β (Adivi et al., 2021).

Impact on the Dynamics of Astrocytes and Oligodendrocytes

Evidence indicates that astrocytes respond to PM in a context-dependent manner (Allen et al., 2014). For instance, early postnatal exposure to ambient UFPs decreased GFAP immunoreactivity in male subjects and increased GFAP expression as well as other neuroinflammation markers in females (Allen et al., 2014). Exposure of male and female rodents during gestation and early postnatal development to TRAP attenuated astrogliosis specifically in the dentate gyrus (DG) associated with reduced GFAP immunoreactivity, which remained unchanged in CA1 and CA3 regions (Patten et al., 2020). Previous findings have shown that maternal exposure to carbon black nanoparticles (CB-NP) induced astrogliosis in the cortex of rodents, affecting the interaction of the astrocyte endfeet with the endothelium and perivascular macrophages (Onoda et al., 2017). Interestingly, intranasal delivery of $PM_{2.5}$ to male rodents subjected to ischemic stroke exacerbated astrocytic reactivity *via* GFAP activation and iNOS induction, aggravating post-stroke neurobehavioral impairments (Chen et al., 2016). In line with these results, rodents exposed to PM for a prolonged period exhibited altered neuronal and astrocytic functions *via* impairment of mitochondrial activity (Araújo et al., 2019). Likewise, exposure of rodents to natural air pollution sources, such as volcanic-derived particles, increased GFAP immunoreactivity in astrocytes (Camarinho et al., 2019; Navarro et al., 2021). Moreover, exposure of rodents to low doses of CB-NP induced endoplasmic reticulum (ER) stress in perivascular macrophages and reactive astrocytes, specifically around the vasculature of offspring animals, associated with the accumulation of β-sheet rich misfolded proteins (Onoda et al., 2020). Cell-based assays have shown that exposure of astrocytes to PM activated janus kinase (JAK)-2/STAT-3 and p38/JNK/ERK pathways in reactive astrocytes triggering iNOS induction and IL-1β production (Li et al., 2016). In this regard, PM has been reported to increase the expression and release of proinflammatory mediators through activation of the NF-κB signaling pathway (Li et al., 1999; Gómez-Budia et al., 2020).

Furthermore, exposure to UFPs altered adult OPCs turnover and survival of mature oligodendrocytes (OLs), accompanied by increased oxidative stress and decreased total antioxidant

capacities (TAC) that impair the remyelination capacity of the brain (Kim J. Y. et al., 2020). Furthermore, prenatal exposure to concentrated ambient particles (CAPs), which were defined as UFPs, promoted a premature maturational shift in OLs in the corpus callosum (CC), followed by hypermyelination (Klocke et al., 2018). Interestingly, females showed significant alterations in oligodendrocytogenesis in the CC (Klocke et al., 2018). Finally, in a mouse model of lysolecithin-induced demyelination of the subcortical white matter, exposure to $PM_{2.5}$ hampered remyelination and disrupted oligodendroglia differentiation (Parolisi et al., 2021).

Impact on Microglial Reactivity and Consequences on Neurons

In response to air pollution, microglia are activated through the upregulation of several proinflammatory mediators that affect neuronal function (Gómez-Budia et al., 2020). Microglia respond to air pollution by adopting an amoeboid shape *in vitro* (Cole et al., 2016; Roqué et al., 2016; Mumaw et al., 2017), as well as *in vivo* (Araújo et al., 2019). Indeed, mice exposed to DEP exhibited reduced adult neurogenesis through activation of microglia (Coburn et al., 2018). In contrast, attenuating microglial reactivity hampered neuroinflammation and oxidative stress (Coburn et al., 2018). Cell-based assays showed that exposure of BV-2 immortalized microglial cell to $PM_{2.5}$ increased mRNA expression of various proinflammatory markers, namely IL-6, IL-1β, TNF-α, iNOS, COX-2, TREM2, and TLR2/4, while reducing mRNA expression of key anti-inflammatory markers, such as IL-10 and Arginase (ARG)-1 (Kim R.-E. et al., 2020). In parallel, exposure of rodents to DEP for a long period triggered the activation of microglia in the nuclei of the solitary tract (NTS), accompanied by ER dilation and mitochondrial vacuolization in the medulla, hence outlining structural alterations of the neuronal network (Chen et al., 2021). Interestingly, rodents exposed to DEP for a long period showed an induced ionized calcium-binding adaptor molecule (IBA)-1 expression in the brain (Levesque et al., 2011). Interestingly, microglial reactivity was accompanied by an increased mRNA expression of TNF-α, IL-6, and macrophage inflammatory protein (MCP)-1α in the midbrain, cortex, and OB, while IL-1β was expressed particularly in the midbrain (Levesque et al., 2011). Mice exposed to PM also triggered the induction of mRNA expression of TLR4, MyD88, TNF-α, and tumor necrosis factor receptor (TNFR)-2 in microglia (Woodward et al., 2017a). Activation of the latter was further confirmed through an increased intracellular expression of inflammatory mediators, such as COX-2, NF-κB, prostaglandin E2 (PGE2), and iNOS both *in vitro* and *in vivo* (Babadjouni et al., 2018; Chen et al., 2018). Using cell-based assays, TNF-α induction in microglia upon PM exposure inhibited neurite outgrowth (Cheng et al., 2016). Inhibition of NRF-2 activity prior to exposure of BV-2 microglial cells to $PM_{2.5}$ attenuated cell viability, induced ROS generation, and stimulated NF-κB pathway, outlining NRF-2 role in mitigating PM deleterious effects (Chen et al., 2018).

Importantly, *in vivo* experiments showed that exposure to DEP in $TREM2^{-/-}$ mice accentuated IL-1β expression (Greve et al., 2020). PM has been demonstrated to impact neuron-glial crosstalk. Acute exposure of adult mice to $PM_{2.5}$ increased the levels of lipoperoxidation and proinflammatory cytokines in the brain and activated microglia, accompanied by reduced neurogenesis in the subgranular zone (SGZ) and subventricular zone (SVZ; Bernardi et al., 2021). Neuronal cell cultures exhibited reduced viability upon exposure to $PM_{2.5}$ associated with increased release of glutamate (Liu F. et al., 2015). Prior treatment of cells with the *N*-methyl-D-aspartate (NMDA) receptor mitigated $PM_{2.5}$-mediated neuronal loss (Liu F. et al., 2015). Moreover, neuronal cultures displayed dopaminergic neurotoxicity upon exposure to DEP only in presence of microglia, which was associated with elevated levels of ROS (Block et al., 2004). Co-culture of neurons and microglia exposed to $PM_{2.5}$ in presence of oligomeric oAβ exacerbated IL-1β and ROS release aggravating oAβ-induced neuronal injury and inflammation (Wang et al., 2018). PM have been shown to directly impact neuronal function. For instance, exposure of rodents to nano PM caused hippocampal neurite atrophy and decreased expression of myelin basic protein (MBP), accompanied by increased TNF-α mRNA expression (Woodward et al., 2017b). In this regard, epidemiological studies have outlined a strong correlation between the levels of PM in air and neuronal chromatolysis and satellitosis in exposed dogs, associated with cortical neurons degeneration, and neurofibrillary tangle formation (Calderón-Garcidueñas et al., 2002).

Interestingly, epidemiological studies comprising elderly women revealed that residence in places contaminated with high levels of fine PM increases the risks for global cognitive decline and all-cause of dementia by 81 and 92%, respectively, with stronger adverse effects in ApoE4 carriers (Cacciottolo et al., 2017). Experimental findings obtained from female AD mouse models (5xFAD; Familial AD) expressing either ApoE3 or ApoE4 mice that were exposed to urban nano PM for 15 weeks showed increased Aβ plaques and soluble Aβ oligomers, which were associated with neuronal changes in the hippocampus (Cacciottolo et al., 2017). These findings were confirmed *in vitro* upon exposure of neuroblastoma cells (N2a-APP/swe) to nano PM translated by an enhanced pro-amyloidogenic processing of the APP, explaining the elevated cerebral Aβ production (Cacciottolo et al., 2017). Furthermore, long-term exposure to ambient air pollution was found to be associated with rapid cognitive decline in aged adults, where ApoE4 carriers exhibited the fastest cognitive decline (Kulick et al., 2020; **Figure 2**).

Further *in vivo* experimental investigations implicating exposure to TRAP nano PM showed an increased production of Aβ peptides, associated with oxidative damage (Cacciottolo et al., 2020). Indeed, exposure of J20-APPswe mice, an AD mouse model, to nano PM for 150 h revealed exacerbated lipid oxidation and pro-amyloidogenic processing of APP in lipid raft fractions compared to controls (Cacciottolo et al., 2020). These observations were further confirmed *in vitro* using N2a-APPswe cells exposed to nano PM (Cacciottolo et al., 2020). Importantly, the link between air pollution and HDL was highlighted in the Multi-Ethnic Study of Atherosclerosis Air Pollution (MESA Air) study showing that exposure to air pollution was significantly associated with low levels of

HDL (Bell et al., 2017). In this regard, ApoE-deficient mice exposed for 2 weeks to DEP, exhibited high systemic pro-oxidant effects associated with dysfunctional HDL (Yin et al., 2013). These observations would indicate that PM exposure could be responsible for the attenuated HDL protective effects against atherosclerosis (Yin et al., 2013).

CONCLUSION AND PERSPECTIVES

Through this review, we aimed to highlight the structural and functional neurovascular alterations underlying VaD pathobiology. The epidemiological, clinical, and experimental investigations are indicating that the long-term outcomes of early pathophysiological events impacting neurovascular functions upon cerebrovascular disorders have major consequences on imitating a cascade of events that lead to VaD. Moreover, the recent findings are outlining air pollution as a major vascular risk factor that is directly implicated in promoting neurovascular impairments associated with VaD. Given the heterogeneity of cerebrovascular disorders, which include stroke, genetic and sporadic microangiopathies, combined with the diverse effects of environmental factors, a better understating of the short- and long-term remodeling processes at the neurovascular unit is urgently required to allow getting new insights into VaD pathobiology. Such knowledge will allow the identification of key "targetable" mechanisms for therapeutic purposes.

Recent findings are suggesting that BBB disruption occurs in some cases for a prolonged period beyond the acute and subacute phases after stroke (Bernardo-Castro et al., 2020). A prolonged, yet subtle, disruption of the BBB could trigger a cascade of events that lead to VaD. For instance, high expression levels of MMPs, the main mediator of BBB disruption, are significantly associated with cognitive deficits (Yang and Rosenberg, 2011). However, targeting MMPs is a double-edged sword as while preserving the BBB in the acute and sub-acute phase, its inhibition impairs neurovascular adaptation in the chronic phase, thus impeding brain plasticity (Yang and Rosenberg, 2011). More promising appears to be the inhibition of beta-site APP cleaving enzyme (BACE)1 that seems to protect endothelial cell integrity in the context of CADASIL and AD (Chacón-Quintero et al., 2021). In the same way, rodent models of aging suggest that the mitochondrial overexpression of catalase improves diminish vascular impairment and benefits neurovascular coupling (Csiszar et al., 2019).

On the other hand, uncontrolled post-stroke neuroinflammation, especially excessive microglial activation, is associated with cognitive deficits (Guruswamy and ElAli, 2017; Gefen et al., 2019; Jayaraj et al., 2019; Zhang et al., 2021). In this regard, strategies aiming to mitigate neuroinflammation *via* modulation of microglia could attenuate cognitive decline related to stroke (Guruswamy and ElAli, 2017; Dzyubenko et al., 2018; Jayaraj et al., 2019). In this regard, evidence suggests that the prominent microglial regulator, insulin-like growth factor (IGF)-1, reduces gliosis while preserving brain volume and myelination, as well as motor performance and memory when administered intranasally in aged mice (Farias Quipildor et al., 2019). Efficient immunomodulatory approaches capable of fine-tuning microglial activation are still to be developed.

Importantly, the emergence and turnover of stroke-mediated proteinopathies are associated with BBB disruption and neuroinflammation. Although the role of cSVD is critically important in the etiology of VaD, there is still a huge gap in the literature as to our understanding of the underlying mechanisms. This is due to the fact that the current knowledge is obtained either from genetic or non-clinically relevant sporadic animal models. Indeed, the majority of cSVD cases are sporadic and associated with diverse risk factors, as such, it is critically important to develop animal models that replicate some of the pathological features associated with VaD. However, the overwhelming findings indicate the loss-of-function on the local cerebrovascular network caused a central role in initiating a pathological cascade of events that lead to altered neuro-glial functions, and thus subsequently dementia (Rouhl et al., 2012; Shoamanesh et al., 2015; Fu and Yan, 2018; Li et al., 2018; Jian et al., 2020).

Air pollution has emerged as a significant risk factor for cerebrovascular and neurodegenerative disorders (Wu et al., 2015; Åström et al., 2021). It is becoming clear that exposure to PM, one of the most deleterious air pollutants, increases the risk of chronic neuroinflammation that leads to dementia (Wu et al., 2015; Åström et al., 2021). Cell-based assays have demonstrated that PM acts as a powerful inflammatory and oxidative stress mediator in various brain cell types. Interestingly, PM exposure seems to amplify the pathological responses underlying VaD pathobiology. Although the impact of PM on neurovascular functions is evidenced *in vitro*, little is known about its role in mediating neurovascular impairments *in vivo*. Future studies should consider investigating the consequences of PM exposure as a comorbid condition in the design of preclinical experiments.

As previously mentioned, besides PM, various modifiable vascular risk factors are recognized to impact VaD. For instance, stroke and cSVD share common risk factors such as hypertension, atherosclerosis, obesity, atrial fibrillation, diabetes, dyslipidemia, high homocysteine, metabolic syndrome, smoking, as well as cardiac and carotid arterial disease (Barnes and Yaffe, 2011; O'Brien and Thomas, 2015; Kalaria et al., 2016; Tariq and Barber, 2018). Given their central role, various preventive approaches have been developed and adopted to attenuate the impact of this triad of vascular on VaD. Such approaches are exemplified by the landmark multidomain Finnish Geriatric Intervention Study to Prevent Cognitive Impairment and Disability (FINGER), which has been shown to enhance all cognitive sub-domains through a multidomain lifestyle intervention that include dietary counseling, physical exercise, cognitive training, and vascular and metabolic risk monitoring for a period of 2 years (Ngandu et al., 2015; Kivipelto et al., 2020). Furthermore, knowing the detrimental role of high blood pressure in VaD prevalence, the Systolic Blood Pressure Intervention Trial (SPRINT) and its sub-study the Memory and Cognition in Decreased Hypertension (MIND) were established with an emphasis on investigating the consequences of lowering systolic blood pressure. Although the incidence of dementia was not

improved, the trial reported a reduction of mild cognitive impairment (MCI) and MCI composite in subjects with lower blood pressure. Interestingly, these observations were associated with a reduction of WM lesion volumes (Kjeldsen et al., 2018; Peters et al., 2019). Despite that, each trial discloses important limitations, yet the impact of modifying main VaD risk factors was shown to allow the development of efficient interventions. Further research is needed for longer periods with a more representative population to lessen the limitations and improve the efficiency of interventions aiming to attenuate dementia prevalence.

Finally, a deep analysis of the current scientific knowledge outlines brain pericytes as a major effector in the pathobiology of VaD. Through their spatial localization, pericytes play a central role in integrating and processing signals from their milieu to generate critical neurovascular functions, which include BBB maintenance, CBF modulation, vascular stabilization, and immunomodulation (Zlokovic, 2011; Hermann and ElAli, 2012). Following a stroke, pericytes undergo cell death at the ischemic core and get activated in the peri-lesion site where they detach from the vasculature (Zlokovic, 2011; Hermann and ElAli, 2012). Importantly, it has been reported that even after successful recanalization, pericytes located at the peri-lesion site remain contracted impeding the capillary microcirculation, which leads to vascular constriction and chronic hypoperfusion (Dalkara, 2019). Moreover, microcirculation of the white matter was disrupted upon pericyte degeneration leading to the accumulation of toxic blood-derived fibrotic deposits within the vasculature, which promotes vascular fibrosis, accompanied by a reduction in the regional CBF (Montagne et al., 2018). These changes are supposed to be directly implicated in the pathogenesis of diffuse WMD associated with loss of oligodendrocytes and subsequently myelinated axons (Montagne et al., 2018). The findings indicate that pericyte degeneration plays a major role in the pathogenesis, and thereby therapies, of WMD associated with cSVD (Montagne et al., 2018). Furthermore, the generation of pericytes is translated by elevated levels of the soluble-platelet derived growth factor receptor (PDGFR)β (sPDGFRβ) in the CSF, strongly correlating with BBB breakdown, CBF reduction, and cognitive decline (Sweeney et al., 2020). Therefore, decoding the pericyte reactivity to stressors related to the vascular risk factors constitutes a promising avenue that might lead to achieving major breakthroughs in getting new mechanistic insights in the pathobiology of VaD and in developing novel therapeutic interventions.

AUTHOR CONTRIBUTIONS

The authors contributed to the review as follows: SL wrote, edited, and finalized the draft as well as prepared the figures. DM-C wrote, edited, and finalized the draft as well as prepared the figures. YE wrote the section related to air pollution. AEA conceptualized, wrote, and finalized the draft. All authors contributed to the article and approved the submitted version.

FUNDING

This work was supported by grants from the Natural Sciences and Engineering Research Council of Canada (NSERC; #RGPIN-2017-06119), the *Fonds de recherche du Québec—Santé* (FRQS; #35170), Heart and Stroke Foundation of Canada (HSFC; #G-18-0022118), and the Canadian Institutes of Health Research (CIHR; #169062; all to AEA). AEA holds a CIHR Tier 2 Canada Research Chair in molecular and cellular neurovascular interactions.

REFERENCES

Adair, J. C., Charlie, J., Dencoff, J. E., Kaye, J. A., Quinn, J. F., Camicioli, R. M., et al. (2004). Measurement of gelatinase B (MMP-9) in the cerebrospinal fluid of patients with vascular dementia and Alzheimer disease. *Stroke* 35, e159–e162. doi: 10.1161/01.STR.0000127420.10990.76

Adivi, A., Lucero, J., Simpson, N., McDonald, J. D., and Lund, A. K. (2021). Exposure to traffic-generated air pollution promotes alterations in the integrity of the brain microvasculature and inflammation in female ApoE$^{-/-}$ mice. *Toxicol. Lett.* 339, 39–50. doi: 10.1016/j.toxlet.2020.12.016

Akhtar-Schaefer, I., Reuten, R., Koch, M., Pietsch, M., and Langmann, T. (2019). AMD-associated HTRA1 variants do not influence TGF-β signaling in microglia. *Adv. Exp. Med. Biol.* 1185, 3–7. doi: 10.1007/978-3-030-27378-1_1

Alexander, M. R., and Owens, G. K. (2012). Epigenetic control of smooth muscle cell differentiation and phenotypic switching in vascular development and disease. *Annu. Rev. Physiol.* 74, 13–40. doi: 10.1146/annurev-physiol-012110-142315

Allen, J. L., Liu, X., Weston, D., Prince, L., Oberdörster, G., Finkelstein, J. N., et al. (2014). Developmental exposure to concentrated ambient ultrafine particulate matter air pollution in mice results in persistent and sex-dependent behavioral neurotoxicity and glial activation. *Toxicol. Sci.* 140, 160–178. doi: 10.1093/toxsci/kfu059

Alunni, A., Krecsmarik, M., Bosco, A., Galant, S., Pan, L., Moens, C. B., et al. (2013). Notch3 signaling gates cell cycle entry and limits neural stem cell amplification in the adult pallium. *Development* 140, 3335–3347. doi: 10.1242/dev.095018

Amtul, Z., Whitehead, S. N., Keeley, R. J., Bechberger, J., Fisher, A. L., McDonald, R. J., et al. (2015). Comorbid rat model of ischemia and β-amyloid toxicity: striatal and cortical degeneration. *Brain Pathol.* 25, 24–32. doi: 10.1111/bpa.12149

Andrianopoulos, V., Gloeckl, R., Vogiatzis, I., and Kenn, K. (2017). Cognitive impairment in COPD: should cognitive evaluation be part of respiratory assessment? *Breathe* 13, e1–e9. doi: 10.1183/20734735.001417

Appelros, P., Stegmayr, B., and Terént, A. (2009). Sex differences in stroke epidemiology: a systematic review. *Stroke* 40, 1082–1090. doi: 10.1161/STROKEAHA.108.540781

Araújo, J. E., Jorge, S., Santos, H. M., Chiechi, A., Galstyan, A., Lodeiro, C., et al. (2019). Proteomic changes driven by urban pollution suggest particulate matter as a deregulator of energy metabolism, mitochondrial activity, and oxidative pathways in the rat brain. *Sci. Total Environ.* 687, 839–848. doi: 10.1016/j.scitotenv.2019.06.102

Aribisala, B. S., Valdés Hernández, M. C., Royle, N. A., Morris, Z., Muñoz Maniega, S., Bastin, M. E., et al. (2013). Brain atrophy associations with white matter lesions in the ageing brain: the Lothian Birth Cohort 1936. *Eur. Radiol.* 23, 1084–1092. doi: 10.1007/s00330-012-2677-x

Arvanitakis, Z., Leurgans, S. E., Wang, Z., Wilson, R. S., Bennett, D. A., and Schneider, J. A. (2011). Cerebral amyloid angiopathy pathology and cognitive domains in older persons. *Ann. Neurol.* 69, 320–327. doi: 10.1002/ana.22112

Åström, D. O., Adolfsson, R., Segersson, D., Forsberg, B., and Oudin, A. (2021). Local contrasts in concentration of ambient particulate air pollution (PM2.5) and incidence of Alzheimer's disease and dementia: results from the betula cohort in northern sweden. *J. Alzheimers Dis.* 81, 83–85. doi: 10.3233/JAD-201538

Attems, J., Jellinger, K., Thal, D. R., and Van Nostrand, W. (2011). Review: sporadic cerebral amyloid angiopathy. *Neuropathol. Appl. Neurobiol.* 37, 75–93. doi: 10.1111/j.1365-2990.2010.01137.x

Auffray, C., Fogg, D., Garfa, M., Elain, G., Join-Lambert, O., Kayal, S., et al. (2007). Monitoring of blood vessels and tissues by a population of monocytes with patrolling behavior. *Science* 317, 666–670. doi: 10.1126/science.1142883

Azarpazhooh, M. R., and Hachinski, V. (2018). Air pollution: a silent common killer for stroke and dementia. *Int. J. Stroke* 13, 667–668. doi: 10.1177/1747493018784476

Babadjouni, R., Patel, A., Liu, Q., Shkirkova, K., Lamorie-Foote, K., Connor, M., et al. (2018). Nanoparticulate matter exposure results in neuroinflammatory changes in the corpus callosum. *PLoS One* 13:e0206934. doi: 10.1371/journal.pone.0206934

Ballabio, E., Bersano, A., Bresolin, N., and Candelise, L. (2007). Monogenic vessel diseases related to ischemic stroke: a clinical approach. *J. Cereb. Blood Flow Metab.* 27, 1649–1662. doi: 10.1038/sj.jcbfm.9600520

Bandeali, S., and Farmer, J. (2012). High-density lipoprotein and atherosclerosis: the role of antioxidant activity. *Curr. Atheroscler. Rep.* 14, 101–107. doi: 10.1007/s11883-012-0235-2

Barnes, D. E., and Yaffe, K. (2011). The projected effect of risk factor reduction on Alzheimer's disease prevalence. *Lancet Neurol.* 10, 819–828. doi: 10.1016/S1474-4422(11)70072-2

Baron, M. (2017). Combining genetic and biophysical approaches to probe the structure and function relationships of the notch receptor. *Mol. Membr. Biol.* 34, 33–49. doi: 10.1080/09687688.2018.1503742

Baron-Menguy, C., Domenga-Denier, V., Ghezali, L., Faraci, F. M., and Joutel, A. (2017). Increased notch3 activity mediates pathological changes in structure of cerebral arteries. *Hypertension* 69, 60–70. doi: 10.1161/HYPERTENSIONAHA.116.08015

Barr, T. L., Latour, L. L., Lee, K.-Y., Schaewe, T. J., Luby, M., Chang, G. S., et al. (2010). Blood-brain barrier disruption in humans is independently associated with increased matrix metalloproteinase-9. *Stroke* 41, e123–e128. doi: 10.1161/STROKEAHA.109.570515

Beattie, E. C., Stellwagen, D., Morishita, W., Bresnahan, J. C., Ha, B. K., Von Zastrow, M., et al. (2002). Control of synaptic strength by glial TNFα. *Science* 295, 2282–2285. doi: 10.1126/science.1067859

Beaufort, N., Scharrer, E., Kremmer, E., Lux, V., Ehrmann, M., Huber, R., et al. (2014). Cerebral small vessel disease-related protease HtrA1 processes latent TGF-β binding protein 1 and facilitates TGF-β signaling. *Proc. Natl. Acad. Sci. U S A* 111, 16496–16501. doi: 10.1073/pnas.1418087111

Béjot, Y., Reis, J., Giroud, M., and Feigin, V. (2018). A review of epidemiological research on stroke and dementia and exposure to air pollution. *Int. J. Stroke* 13, 687–695. doi: 10.1177/1747493018772800

Belin de Chantemèle, E. J., Retailleau, K., Pinaud, F., Vessières, E., Bocquet, A., Guihot, A. L., et al. (2008). Notch3 is a major regulator of vascular tone in cerebral and tail resistance arteries. *Arterioscler. Thromb. Vasc. Biol.* 28, 2216–2224. doi: 10.1161/ATVBAHA.108.171751

Bell, G., Mora, S., Greenland, P., Tsai, M., Gill, E., and Kaufman, J. D. (2017). Association of air pollution exposures with high-density lipoprotein cholesterol and particle number: the multi-ethnic study of atherosclerosis. *Arterioscler. Thromb. Vasc. Biol.* 37, 976–982. doi: 10.1161/ATVBAHA.116.308193

Bell, R. D., Winkler, E. A., Sagare, A. P., Singh, I., LaRue, B., Deane, R., et al. (2010). Pericytes control key neurovascular functions and neuronal phenotype in the adult brain and during brain aging. *Neuron* 68, 409–427. doi: 10.1016/j.neuron.2010.09.043

Benatti, L., Bonecchi, L., Cozzi, L., and Sarmientos, P. (1993). Two preproendothelin 1 mRNAs transcribed by alternative promoters. *J. Clin. Invest.* 91, 1149–1156. doi: 10.1172/JCI116274

Bernardi, R. B., Zanchi, A. C. T., Damaceno-Rodrigues, N. R., Veras, M. M., Saldiva, P. H. N., Barros, H. M. T., et al. (2021). The impact of chronic exposure to air pollution over oxidative stress parameters and brain histology. *Environ. Sci. Pollut. Res. Int.* doi: 10.1007/s11356-021-14023-0. [Epub ahead of print].

Bernardo-Castro, S., Sousa, J. A., Brás, A., Cecília, C., Rodrigues, B., Almendra, L., et al. (2020). Pathophysiology of blood-brain barrier permeability throughout the different stages of ischemic stroke and its implication on hemorrhagic transformation and recovery. *Front. Neurol.* 11:594672. doi: 10.3389/fneur.2020.594672

Berzin, T. M., Zipser, B. D., Rafii, M. S., Kuo-Leblanc, V., Yancopoulos, G. D., Glass, D. J., et al. (2000). Agrin and microvascular damage in Alzheimer's disease. *Neurobiol. Aging* 21, 349–355. doi: 10.1016/s0197-4580(00)00121-4

Bevan-Jones, W. R., Cope, T. E., Jones, P. S., Kaalund, S. S., Passamonti, L., Allinson, K., et al. (2020). Neuroinflammation and protein aggregation co-localize across the frontotemporal dementia spectrum. *Brain* 143, 1010–1026. doi: 10.1093/brain/awaa033

Blanchard, J. W., Bula, M., Davila-Velderrain, J., Akay, L. A., Zhu, L., Frank, A., et al. (2020). Reconstruction of the human blood-brain barrier *in vitro* reveals a pathogenic mechanism of APOE4 in pericytes. *Nat. Med.* 26, 952–963. doi: 10.1038/s41591-020-0886-4

Block, M. L., and Calderón-Garcidueñas, L. (2009). Air pollution: mechanisms of neuroinflammation and CNS disease. *Trends Neurosci.* 32, 506–516. doi: 10.1016/j.tins.2009.05.009

Block, M. L., Wu, X., Pei, Z., Li, G., Wang, T., Qin, L., et al. (2004). Nanometer size diesel exhaust particles are selectively toxic to dopaminergic neurons: the role of microglia, phagocytosis, and NADPH oxidase. *FASEB J.* 18, 1618–1620. doi: 10.1096/fj.04-1945fje

Bordeleau, M., ElAli, A., and Rivest, S. (2016). Severe chronic cerebral hypoperfusion induces microglial dysfunction leading to memory loss in APPswe/PS1 mice. *Oncotarget* 7, 11864–11880. doi: 10.18632/oncotarget.7689

Bourasset, F., Ouellet, M., Tremblay, C., Julien, C., Do, T. M., Oddo, S., et al. (2009). Reduction of the cerebrovascular volume in a transgenic mouse model of Alzheimer's disease. *Neuropharmacology* 56, 808–813. doi: 10.1016/j.neuropharm.2009.01.006

Braughler, J. M., and Hall, E. D. (1992). Involvement of lipid peroxidation in CNS injury. *J. Neurotrauma* 9, S1–S7.

Bray, S. J. (2016). Notch signalling in context. *Nat. Rev. Mol. Cell Biol.* 17, 722–735. doi: 10.1038/nrm.2016.94

Brookes, R. L., Hollocks, M. J., Tan, R. Y. Y., Morris, R. G., and Markus, H. S. (2016). Brief screening of vascular cognitive impairment in patients with cerebral autosomal-dominant arteriopathy with subcortical infarcts and leukoencephalopathy without dementia. *Stroke* 47, 2482–2487. doi: 10.1161/STROKEAHA.116.013761

Brundel, M., de Bresser, J., van Dillen, J. J., Kappelle, L. J., and Biessels, G. J. (2012). Cerebral microinfarcts: a systematic review of neuropathological studies. *J. Cereb. Blood Flow Metab.* 32, 425–436. doi: 10.1038/jcbfm.2011.200

Bruno, M. A., Mufson, E. J., Wuu, J., and Cuello, A. C. (2009). Increased matrix metalloproteinase 9 activity in mild cognitive impairment. *J. Neuropathol. Exp. Neurol.* 68, 1309–1318. doi: 10.1097/NEN.0b013e3181c22569

Bu, G. (2009). Apolipoprotein E and its receptors in Alzheimer's disease: pathways, pathogenesis and therapy. *Nat. Rev. Neurosci.* 10, 333–344. doi: 10.1038/nrn2620

Cacciottolo, M., Morgan, T. E., Saffari, A. A., Shirmohammadi, F., Forman, H. J., Sioutas, C., et al. (2020). Traffic-related air pollutants (TRAP-PM) promote neuronal amyloidogenesis through oxidative damage to lipid rafts. *Free Radic. Biol. Med.* 147, 242–251. doi: 10.1016/j.freeradbiomed.2019.12.023

Cacciottolo, M., Wang, X., Driscoll, I., Woodward, N., Saffari, A., Reyes, J., et al. (2017). Particulate air pollutants, APOE alleles and their contributions to cognitive impairment in older women and to amyloidogenesis in experimental models. *Transl. Psychiatry* 7:e1022. doi: 10.1038/tp.2016.280

Caggiu, E., Arru, G., Hosseini, S., Niegowska, M., Sechi, G., Zarbo, I. R., et al. (2019). Inflammation, infectious triggers, and parkinson's disease. *Front. Neurol.* 10:122. doi: 10.3389/fneur.2019.00122

Cai, Z., Wang, C., He, W., Tu, H., Tang, Z., Xiao, M., et al. (2015). Cerebral small vessel disease and Alzheimer's disease. *Clin. Interv. Aging* 10, 1695–1704. doi: 10.2147/CIA.S90871

Calderón-Garcidueñas, L., Azzarelli, B., Acuna, H., Garcia, R., Gambling, T. M., Osnaya, N., et al. (2002). Air pollution and brain damage. *Toxicol. Pathol.* 30, 373–389. doi: 10.1080/01926230252929954

Calderón-Garcidueñas, L., Reynoso-Robles, R., Vargas-Martínez, J., Gómez-Maqueo-Chew, A., Pérez-Guillé, B., Mukherjee, P. S., et al. (2016). Prefrontal white matter pathology in air pollution exposed Mexico City young urbanites and their potential impact on neurovascular unit dysfunction and the development of Alzheimer's disease. *Environ. Res.* 146, 404–417. doi: 10.1016/j.envres.2015.12.031

Calderón-Garcidueñas, L., Solt, A. C., Henríquez-Roldán, C., Torres-Jardón, R., Nuse, B., Herritt, L., et al. (2008). Long-term air pollution exposure is associated with neuroinflammation, an altered innate immune response, disruption of the blood-brain barrier, ultrafine particulate deposition, and accumulation of amyloid β-42 and α-synuclein in children and young adults. *Toxicol. Pathol.* 36, 289–310. doi: 10.1177/0192623307313011

Calderón-Garcidueñas, L., Vincent, R., Mora-Tiscareño, A., Franco-Lira, M., Henríquez-Roldán, C., Barragán-Mejía, G., et al. (2007). Elevated plasma endothelin-1 and pulmonary arterial pressure in children exposed to air pollution. *Environ. Health Perspect.* 115, 1248–1253. doi: 10.1289/ehp.9641

Camarinho, R., Garcia, P. V., Choi, H., and Rodrigues, A. S. (2019). Overproduction of TNF-α and lung structural remodelling due to chronic exposure to volcanogenic air pollution. *Chemosphere* 222, 227–234. doi: 10.1016/j.chemosphere.2019.01.138

Campbell, A., Oldham, M., Becaria, A., Bondy, S. C., Meacher, D., Sioutas, C., et al. (2005). Particulate matter in polluted air may increase biomarkers of inflammation in mouse brain. *Neurotoxicology* 26, 133–140. doi: 10.1016/j.neuro.2004.08.003

Campioni, M., Severino, A., Manente, L., Tuduce, I. L., Toldo, S., Caraglia, M., et al. (2010). The serine protease HtrA1 specifically interacts and degrades the tuberous sclerosis complex 2 protein. *Mol. Cancer Res.* 8, 1248–1260. doi: 10.1158/1541-7786.MCR-09-0473

Candelario-Jalil, E., Thompson, J., Taheri, S., Grossetete, M., Adair, J. C., Edmonds, E., et al. (2011). Matrix metalloproteinases are associated with increased blood-brain barrier opening in vascular cognitive impairment. *Stroke* 42, 1345–1350. doi: 10.1161/STROKEAHA.110.600825

Cannistraro, R. J., Badi, M., Eidelman, B. H., Dickson, D. W., Middlebrooks, E. H., and Meschia, J. F. (2019). CNS small vessel disease: a clinical review. *Neurology* 92, 1146–1156. doi: 10.1212/WNL.0000000000007654

Caplan, L. R. (2015). Lacunar infarction and small vessel disease: pathology and pathophysiology. *J. Stroke* 17, 2–6. doi: 10.5853/jos.2015.17.1.2

Carlin, L. M., Stamatiades, E. G., Auffray, C., Hanna, R. N., Glover, L., Vizcay-Barrena, G., et al. (2013). Nr4a1-dependent Ly6C(low) monocytes monitor endothelial cells and orchestrate their disposal. *Cell* 153, 362–375. doi: 10.1016/j.cell.2013.03.010

Carrano, A., Hoozemans, J. J. M., van der Vies, S. M., Rozemuller, A. J. M., van Horssen, J., and de Vries, H. E. (2011). Amyloid β induces oxidative stress-mediated blood-brain barrier changes in capillary amyloid angiopathy. *Antioxid. Redox Signal.* 15, 1167–1178. doi: 10.1089/ars.2011.3895

Chacón-Quintero, M. V., Pineda-López, L. G., Villegas-Lanau, C. A., Posada-Duque, R., and Cardona-Gómez, G. P. (2021). β-secretase 1 underlies reactive astrocytes and endothelial disruption in neurodegeneration. *Front. Cell. Neurosci.* 15:656832. doi: 10.3389/fncel.2021.656832

Charidimou, A., Boulouis, G., Gurol, M. E., Ayata, C., Bacskai, B. J., Frosch, M. P., et al. (2017). Emerging concepts in sporadic cerebral amyloid angiopathy. *Brain* 140, 1829–1850. doi: 10.1093/brain/awx047

Chaturvedi, M., and Kaczmarek, L. (2014). Mmp-9 inhibition: a therapeutic strategy in ischemic stroke. *Mol. Neurobiol.* 49, 563–573. doi: 10.1007/s12035-013-8538-z

Chen, Z., Chen, F., Fang, Z., Zhao, H., Zhan, C., Li, C., et al. (2021). Glial activation and inflammation in the NTS in a rat model after exposure to diesel exhaust particles. *Environ. Toxicol. Pharmacol.* 83:103584. doi: 10.1016/j.etap.2021.103584

Chen, X., Liu, S., Zhang, W., Wu, C., Liu, H., Zhang, F., et al. (2018). Nrf2 deficiency exacerbates PM2.5-induced olfactory bulb injury. *Biochem. Biophys. Res. Commun.* 505, 1154–1160. doi: 10.1016/j.bbrc.2018.10.057

Chen, G.-F., Xu, T.-H., Yan, Y., Zhou, Y.-R., Jiang, Y., Melcher, K., et al. (2017). Amyloid β: structure, biology and structure-based therapeutic development. *Acta Pharmacol. Sin.* 38, 1205–1235. doi: 10.1038/aps.2017.28

Chen, L., Yokel, R. A., Hennig, B., and Toborek, M. (2008). Manufactured aluminum oxide nanoparticles decrease expression of tight junction proteins in brain vasculature. *J. Neuroimmune Pharmacol.* 3, 286–295. doi: 10.1007/s11481-008-9131-5

Chen, L., Zhang, Y., Li, D., Zhang, N., Liu, R., Han, B., et al. (2016). Everolimus (RAD001) ameliorates vascular cognitive impairment by regulating microglial function *via* the mTORC1 signaling pathway. *J. Neuroimmunol.* 299, 164–171. doi: 10.1016/j.jneuroim.2016.09.008

Cheng, H., Davis, D. A., Hasheminassab, S., Sioutas, C., Morgan, T. E., and Finch, C. E. (2016). Urban traffic-derived nanoparticulate matter reduces neurite outgrowth *via* TNFα *in vitro*. *J. Neuroinflammation* 13:19. doi: 10.1186/s12974-016-0480-3

Chistiakov, D. A., Bobryshev, Y. V., and Orekhov, A. N. (2016). Macrophage-mediated cholesterol handling in atherosclerosis. *J. Cell. Mol. Med.* 20, 17–28. doi: 10.1111/jcmm.12689

Chistiakov, D. A., Myasoedova, V. A., Melnichenko, A. A., Grechko, A. V., and Orekhov, A. N. (2017). Calcifying matrix vesicles and atherosclerosis. *Biomed Res. Int.* 2017:7463590. doi: 10.1155/2017/7463590

Cho, C.-C., Hsieh, W.-Y., Tsai, C.-H., Chen, C.-Y., Chang, H.-F., and Lin, C.-S. (2018). *In vitro* and *in vivo* experimental studies of PM2.5 on disease progression. *Int. J. Environ. Res. Public Health* 15:1380. doi: 10.3390/ijerph15071380

Cho, H. S., Hyman, B. T., Greenberg, S. M., and Rebeck, G. W. (2001). Quantitation of apoE domains in Alzheimer disease brain suggests a role for apoE in Aβ aggregation. *J. Neuropathol. Exp. Neurol.* 60, 342–349. doi: 10.1093/jnen/60.4.342

Clarke, L. E., Liddelow, S. A., Chakraborty, C., Münch, A. E., Heiman, M., and Barres, B. A. (2018). Normal aging induces A1-like astrocyte reactivity. *Proc. Natl. Acad. Sci. U S A* 115, E1896–E1905. doi: 10.1073/pnas.1800165115

Coburn, J. L., Cole, T. B., Dao, K. T., and Costa, L. G. (2018). Acute exposure to diesel exhaust impairs adult neurogenesis in mice: prominence in males and protective effect of pioglitazone. *Arch. Toxicol.* 92, 1815–1829. doi: 10.1007/s00204-018-2180-5

Cochran, E., Bacci, B., Chen, Y., Patton, A., Gambetti, P., and Autilio-Gambetti, L. (1991). Amyloid precursor protein and ubiquitin immunoreactivity in dystrophic axons is not unique to Alzheimer's disease. *Am. J. Pathol.* 139, 485–489.

Cole, T. B., Coburn, J., Dao, K., Roqué, P., Chang, Y.-C., Kalia, V., et al. (2016). Sex and genetic differences in the effects of acute diesel exhaust exposure on inflammation and oxidative stress in mouse brain. *Toxicology* 374, 1–9. doi: 10.1016/j.tox.2016.11.010

Cordonnier, C., Al-Shahi Salman, R., and Wardlaw, J. (2007). Spontaneous brain microbleeds: systematic review, subgroup analyses and standards for study design and reporting. *Brain* 130, 1988–2003. doi: 10.1093/brain/awl387

Corrada, M. M., Sonnen, J. A., Kim, R. C., and Kawas, C. H. (2016). Microinfarcts are common and strongly related to dementia in the oldest-old: the 90+ study. *Alzheimers Dement.* 12, 900–908. doi: 10.1016/j.jalz.2016.04.006

Correa, F., Hernangómez, M., Mestre, L., Loría, F., Spagnolo, A., Docagne, F., et al. (2010). Anandamide enhances IL-10 production in activated microglia by targeting CB(2) receptors: roles of ERK1/2, JNK, and NF-κB. *Glia* 58, 135–147. doi: 10.1002/glia.20907

Csipo, T., Lipecz, A., Ashpole, N. M., Balasubramanian, P., and Tarantini, S. (2020). Astrocyte senescence contributes to cognitive decline. *Geroscience* 42, 51–55. doi: 10.1007/s11357-019-00140-9

Csiszar, A., Yabluchanskiy, A., Ungvari, A., Ungvari, Z., and Tarantini, S. (2019). Overexpression of catalase targeted to mitochondria improves neurovascular coupling responses in aged mice. *Geroscience* 41, 609–617. doi: 10.1007/s11357-019-00111-0

Dalkara, T. (2019). Pericytes: a novel target to improve success of recanalization therapies. *Stroke* 50, 2985–2991. doi: 10.1161/STROKEAHA.118.023590

Das, A. S., Regenhardt, R. W., Feske, S. K., and Gurol, M. E. (2019). Treatment approaches to lacunar stroke. *J. Stroke Cerebrovasc. Dis.* 28, 2055–2078. doi: 10.1016/j.jstrokecerebrovasdis.2019.05.004

Davalos, D., Ryu, J. K., Merlini, M., Baeten, K. M., Le Moan, N., Petersen, M. A., et al. (2012). Fibrinogen-induced perivascular microglial clustering is required for the development of axonal damage in neuroinflammation. *Nat. Commun.* 3:1227. doi: 10.1038/ncomms2230

Davis, J., Xu, F., Deane, R., Romanov, G., Previti, M. L., Zeigler, K., et al. (2004). Early-onset and robust cerebral microvascular accumulation of amyloid β-protein in transgenic mice expressing low levels of a vasculotropic Dutch/Iowa mutant form of amyloid β-protein precursor. *J. Biol. Chem.* 279, 20296–20306. doi: 10.1074/jbc.M312946200

De Guio, F., Vignaud, A., Ropele, S., Duering, M., Duchesnay, E., Chabriat, H., et al. (2014). Loss of venous integrity in cerebral small vessel disease: a 7-T MRI study in cerebral autosomal-dominant arteriopathy with subcortical infarcts and leukoencephalopathy (CADASIL). *Stroke* 45, 2124–2126. doi: 10.1161/STROKEAHA.114.005726

de Jager, M., van der Wildt, B., Schul, E., Bol, J. G. J. M., van Duinen, S. G., Drukarch, B., et al. (2013). Tissue transglutaminase colocalizes with extracellular matrix proteins in cerebral amyloid angiopathy. *Neurobiol. Aging* 34, 1159–1169. doi: 10.1016/j.neurobiolaging.2012.10.005

de la Peña, P., Bornstein, B., del Hoyo, P., Fernández-Moreno, M. A., Martín, M. A., Campos, Y., et al. (2001). Mitochondrial dysfunction associated with a mutation in the Notch3 gene in a CADASIL family. *Neurology* 57, 1235–1238. doi: 10.1212/wnl.57.7.1235

de Laat, K. F., Tuladhar, A. M., van Norden, A. G. W., Norris, D. G., Zwiers, M. P., and de Leeuw, F.-E. (2011). Loss of white matter integrity is associated with gait disorders in cerebral small vessel disease. *Brain* 134, 73–83. doi: 10.1093/brain/awq343

De Luca, A., De Falco, M., Severino, A., Campioni, M., Santini, D., Baldi, F., et al. (2003). Distribution of the serine protease HtrA1 in normal human tissues. *J. Histochem. Cytochem.* 51, 1279–1284. doi: 10.1177/00221554030 5101004

De Silva, T. M., and Faraci, F. M. (2016). Microvascular dysfunction and cognitive impairment. *Cell. Mol. Neurobiol.* 36, 241–258. doi: 10.1007/s10571-015 -0308-1

Deane, R., Wu, Z., Sagare, A., Davis, J., Du Yan, S., Hamm, K., et al. (2004). LRP/amyloid β-peptide interaction mediates differential brain efflux of Aβ isoforms. *Neuron* 43, 333–344. doi: 10.1016/j.neuron.2004.07.017

Debette, S., and Markus, H. S. (2010). The clinical importance of white matter hyperintensities on brain magnetic resonance imaging: systematic review and meta-analysis. *BMJ* 341:c3666. doi: 10.1136/bmj.c3666

Del Bene, A., Makin, S. D. J., Doubal, F. N., Inzitari, D., and Wardlaw, J. M. (2013). Variation in risk factors for recent small subcortical infarcts with infarct size, shape, and location. *Stroke* 44, 3000–3006. doi: 10.1161/STROKEAHA. 113.002227

Desmond, D. W., Moroney, J. T., Sano, M., and Stern, Y. (2002). Incidence of dementia after ischemic stroke: results of a longitudinal study. *Stroke* 33, 2254–2260. doi: 10.1161/01.str.0000028235.91778.95

Di Donato, I., Bianchi, S., De Stefano, N., Dichgans, M., Dotti, M. T., Duering, M., et al. (2017). Cerebral Autosomal Dominant Arteriopathy with Subcortical Infarcts and Leukoencephalopathy (CADASIL) as a model of small vessel disease: update on clinical, diagnostic, and management aspects. *BMC Med.* 15:41. doi: 10.1186/s12916-017-0778-8

Dichgans, M. (2007). Genetics of ischaemic stroke. *Lancet Neurol.* 6, 149–161. doi: 10.1016/S1474-4422(07)70028-5

Dong, X., Song, Y.-N., Liu, W.-G., and Guo, X.-L. (2009). Mmp-9, a potential target for cerebral ischemic treatment. *Curr. Neuropharmacol.* 7, 269–275. doi: 10.2174/157015909790031157

Donzis, E. J., and Tronson, N. C. (2014). Modulation of learning and memory by cytokines: signaling mechanisms and long term consequences. *Neurobiol. Learn. Mem.* 115, 68–77. doi: 10.1016/j.nlm.2014.08.008

Drazyk, A. M., Tan, R. Y. Y., Tay, J., Traylor, M., Das, T., and Markus, H. S. (2019). Encephalopathy in a large cohort of british cerebral autosomal dominant arteriopathy with subcortical infarcts and leukoencephalopathy patients. *Stroke* 50, 283–290. doi: 10.1161/STROKEAHA.118.023661

Dropcho, E. J. (1991). Central nervous system injury by therapeutic irradiation. *Neurol. Clin.* 9, 969–988. doi: 10.1016/s0733-8619(18)30260-3

Dziewulska, D., and Lewandowska, E. (2012). Pericytes as a new target for pathological processes in CADASIL. *Neuropathology* 32, 515–521. doi: 10.1111/j.1440-1789.2011.01290.x

Dzyubenko, E., Manrique-Castano, D., Kleinschnitz, C., Faissner, A., and Hermann, D. M. (2018). Role of immune responses for extracellular matrix remodeling in the ischemic brain. *Ther. Adv. Neurol. Disord.* 11:1756286418818092. doi: 10.1177/1756286418 818092

Ekker, M. S., Verhoeven, J. I., Vaartjes, I., van Nieuwenhuizen, K. M., Klijn, C. J. M., and de Leeuw, F.-E. (2019). Stroke incidence in young adults according to age, subtype, sex, and time trends. *Neurology* 92, e2444–e2454. doi: 10.1212/WNL.0000000000007533

El-Abassi, R., Singhal, D., and England, J. D. (2014). Fabry's disease. *J. Neurol. Sci.* 344, 5–19. doi: 10.1016/j.jns.2014.06.029

ElAli, A., Doeppner, T. R., Zechariah, A., and Hermann, D. M. (2011). Increased blood-brain barrier permeability and brain edema after focal cerebral ischemia induced by hyperlipidemia: role of lipid peroxidation and calpain-1/2, matrix metalloproteinase-2/9 and RhoA overactivation. *Stroke* 42, 3238–3244. doi: 10.1161/STROKEAHA.111.615559

ElAli, A., Thériault, P., Préfontaine, P., and Rivest, S. (2013). Mild chronic cerebral hypoperfusion induces neurovascular dysfunction, triggering peripheral β-amyloid brain entry and aggregation. *Acta Neuropathol. Commun.* 1:75. doi: 10.1186/2051-5960-1-75

Erdener, S. E., and Dalkara, T. (2019). Small vessels are a big problem in neurodegeneration and neuroprotection. *Front. Neurol.* 10:889. doi: 10.3389/fneur.2019.00889

Farias Quipildor, G. E., Mao, K., Hu, Z., Novaj, A., Cui, M.-H., Gulinello, M., et al. (2019). Central IGF-1 protects against features of cognitive and sensorimotor decline with aging in male mice. *Geroscience* 41, 185–208. doi: 10.1007/s11357-019-00065-3

Farkas, E., De Jong, G. I., de Vos, R. A., Jansen Steur, E. N., and Luiten, P. G. (2000). Pathological features of cerebral cortical capillaries are doubled in Alzheimer's disease and Parkinson's disease. *Acta Neuropathol.* 100, 395–402. doi: 10.1007/s004010000195

Feigin, V. L., Roth, G. A., Naghavi, M., Parmar, P., Krishnamurthi, R., Chugh, S., et al. (2016). Global burden of stroke and risk factors in 188 countries, during 1990–2013: a systematic analysis for the Global Burden of Disease Study 2013. *Lancet Neurol.* 15, 913–924. doi: 10.1016/S1474-4422(16) 30073-4

Fisher, C. M. (1965). Lacunes: small, deep cerebral infarcts. *Neurology* 15, 774–784. doi: 10.1212/wnl.15.8.774

French, C. R., Seshadri, S., Destefano, A. L., Fornage, M., Arnold, C. R., Gage, P. J., et al. (2014). Mutation of FOXC1 and PITX2 induces cerebral small-vessel disease. *J. Clin. Invest.* 124, 4877–4881. doi: 10.1172/JCI 75109

Friedrich, U., Datta, S., Schubert, T., Plössl, K., Schneider, M., Grassmann, F., et al. (2015). Synonymous variants in HTRA1 implicated in AMD susceptibility impair its capacity to regulate TGF-β signaling. *Hum. Mol. Genet.* 24, 6361–6373. doi: 10.1093/hmg/ddv346

Frostegård, J., Ulfgren, A. K., Nyberg, P., Hedin, U., Swedenborg, J., Andersson, U., et al. (1999). Cytokine expression in advanced human atherosclerotic plaques: dominance of pro-inflammatory (Th1) and macrophage-stimulating cytokines. *Atherosclerosis* 145, 33–43. doi: 10.1016/s0021-9150(99) 00011-8

Fu, Y., and Yan, Y. (2018). Emerging role of immunity in cerebral small vessel disease. *Front. Immunol.* 9:67. doi: 10.3389/fimmu.2018.00067

Gaertner, R. F., Wyss-Coray, T., Von Euw, D., Lesné, S., Vivien, D., and Lacombe, P. (2005). Reduced brain tissue perfusion in TGF-β 1 transgenic mice showing Alzheimer's disease-like cerebrovascular abnormalities. *Neurobiol. Dis.* 19, 38–46. doi: 10.1016/j.nbd.2004.11.008

Gama Sosa, M. A., Gasperi, R. D., Rocher, A. B., Wang, A. C.-J., Janssen, W. G. M., Flores, T., et al. (2010). Age-related vascular pathology in transgenic mice expressing presenilin 1-associated familial Alzheimer's disease mutations. *Am. J. Pathol.* 176, 353–368. doi: 10.2353/ajpath.2010.090482

Gefen, T., Kim, G., Bolbolan, K., Geoly, A., Ohm, D., Oboudiyat, C., et al. (2019). Activated microglia in cortical white matter across cognitive aging trajectories. *Front. Aging Neurosci.* 11:94. doi: 10.3389/fnagi.2019.00094

Georgakis, M. K., Malik, R., Anderson, C. D., Parhofer, K. G., Hopewell, J. C., and Dichgans, M. (2020). Genetic determinants of blood lipids and cerebral small vessel disease: role of high-density lipoprotein cholesterol. *Brain* 143, 597–610. doi: 10.1093/brain/awz413

George, M. G. (2020). Risk factors for ischemic stroke in younger adults: a focused update. *Stroke* 51, 729–735. doi: 10.1161/STROKEAHA.119.024156

Germain, D. P., Elliott, P. M., Falissard, B., Fomin, V. V., Hilz, M. J., Jovanovic, A., et al. (2019). The effect of enzyme replacement therapy on clinical outcomes in male patients with Fabry disease: a systematic literature review by a European panel of experts. *Mol. Genet. Metab. Rep.* 19:100454. doi: 10.1016/j.ymgmr. 2019.100454

Ghosh, M., Balbi, M., Hellal, F., Dichgans, M., Lindauer, U., and Plesnila, N. (2015). Pericytes are involved in the pathogenesis of cerebral autosomal

dominant arteriopathy with subcortical infarcts and leukoencephalopathy. *Ann. Neurol.* 78, 887–900. doi: 10.1002/ana.24512

Giannoni, P., Arango-Lievano, M., Neves, I. D., Rousset, M.-C., Baranger, K., Rivera, S., et al. (2016). Cerebrovascular pathology during the progression of experimental Alzheimer's disease. *Neurobiol. Dis.* 88, 107–117. doi: 10.1016/j.nbd.2016.01.001

Gidday, J. M., Gasche, Y. G., Copin, J.-C., Shah, A. R., Perez, R. S., Shapiro, S. D., et al. (2005). Leukocyte-derived matrix metalloproteinase-9 mediates blood-brain barrier breakdown and is proinflammatory after transient focal cerebral ischemia. *Am. J. Physiol. Heart Circ. Physiol.* 289, H558–H568. doi: 10.1152/ajpheart.01275.2004

Gómez-Budia, M., Konttinen, H., Saveleva, L., Korhonen, P., Jalava, P. I., Kanninen, K. M., et al. (2020). Glial smog: interplay between air pollution and astrocyte-microglia interactions. *Neurochem. Int.* 136:104715. doi: 10.1016/j.neuint.2020.104715

Gorelick, P. B. (2004). Risk factors for vascular dementia and Alzheimer disease. *Stroke* 35, 2620–2622. doi: 10.1161/01.STR.0000143318.70292.47

Gorelick, P. B., Scuteri, A., Black, S. E., DeCarli, C., Greenberg, S. M., Iadecola, C., et al. (2011). Vascular contributions to cognitive impairment and dementia. *Stroke* 42, 2672–2713. doi: 10.1161/STR.0b013e3182299496

Greve, H. J., Mumaw, C. L., Messenger, E. J., Kodavanti, P. R. S., Royland, J. L., Kodavanti, U. P., et al. (2020). Diesel exhaust impairs TREM2 to dysregulate neuroinflammation. *J. Neuroinflammation* 17:351. doi: 10.1186/s12974-020-02017-7

Grinberg, L. T., and Thal, D. R. (2010). Vascular pathology in the aged human brain. *Acta Neuropathol.* 119, 277–290. doi: 10.1007/s00401-010-0652-7

Gu, B. J., Huang, X., Ou, A., Rembach, A., Fowler, C., Avula, P. K., et al. (2016). Innate phagocytosis by peripheral blood monocytes is altered in Alzheimer's disease. *Acta Neuropathol.* 132, 377–389. doi: 10.1007/s00401-016-1596-3

Gu, X., Liu, X.-Y., Fagan, A., Gonzalez-Toledo, M. E., and Zhao, L.-R. (2012). Ultrastructural changes in cerebral capillary pericytes in aged Notch3 mutant transgenic mice. *Ultrastruct. Pathol.* 36, 48–55. doi: 10.3109/01913123.2011.620220

Guey, S., Mawet, J., Hervé, D., Duering, M., Godin, O., Jouvent, E., et al. (2016). Prevalence and characteristics of migraine in CADASIL. *Cephalalgia* 36, 1038–1047. doi: 10.1177/0333102415620909

Guo, S., and Lo, E. H. (2009). Dysfunctional cell-cell signaling in the neurovascular unit as a paradigm for central nervous system disease. *Stroke* 40, S4–S7. doi: 10.1161/STROKEAHA.108.534388

Guruswamy, R., and ElAli, A. (2017). Complex roles of microglial cells in ischemic stroke pathobiology: new insights and future directions. *Int. J. Mol. Sci.* 18:496. doi: 10.3390/ijms18030496

Halder, S. K., and Milner, R. (2019). A critical role for microglia in maintaining vascular integrity in the hypoxic spinal cord. *Proc. Natl. Acad. Sci. U S A* 116, 26029–26037. doi: 10.1073/pnas.1912178116

Hallé, M., Tribout-Jover, P., Lanteigne, A.-M., Boulais, J., St-Jean, J. R., Jodoin, R., et al. (2015). Methods to monitor monocytes-mediated amyloid-β uptake and phagocytosis in the context of adjuvanted immunotherapies. *J. Immunol. Methods* 424, 64–79. doi: 10.1016/j.jim.2015.05.002

Hameed, S., Zhao, J., and Zare, R. N. (2020). Ambient PM particles reach mouse brain, generate ultrastructural hallmarks of neuroinflammation, and stimulate amyloid deposition, tangles, and plaque formation. *Talanta Open* 2:100013. doi: 10.1016/j.talo.2020.100013

Hao, W., and Friedman, A. (2014). The LDL-HDL profile determines the risk of atherosclerosis: a mathematical model. *PLoS One* 9:e90497. doi: 10.1371/journal.pone.0090497

Hara, K., Shiga, A., Fukutake, T., Nozaki, H., Miyashita, A., Yokoseki, A., et al. (2009). Association of HTRA1 mutations and familial ischemic cerebral small-vessel disease. *N. Engl. J. Med.* 360, 1729–1739. doi: 10.1056/NEJMoa0801560

Hartmann, D. A., Hyacinth, H. I., Liao, F.-F., and Shih, A. Y. (2018). Does pathology of small venules contribute to cerebral microinfarcts and dementia? *J. Neurochem.* 144, 517–526. doi: 10.1111/jnc.14228

Hartz, A. M. S., Bauer, B., Block, M. L., Hong, J.-S., and Miller, D. S. (2008). Diesel exhaust particles induce oxidative stress, proinflammatory signaling, and P-glycoprotein up-regulation at the blood-brain barrier. *FASEB J.* 22, 2723–2733. doi: 10.1096/fj.08-106997

Hartz, A. M. S., Bauer, B., Soldner, E. L. B., Wolf, A., Boy, S., Backhaus, R., et al. (2012). Amyloid-β contributes to blood-brain barrier leakage in transgenic human amyloid precursor protein mice and in humans with cerebral amyloid angiopathy. *Stroke* 43, 514–523. doi: 10.1161/STROKEAHA.111.627562

Haruwaka, K., Ikegami, A., Tachibana, Y., Ohno, N., Konishi, H., Hashimoto, A., et al. (2019). Dual microglia effects on blood brain barrier permeability induced by systemic inflammation. *Nat. Commun.* 10:5816. doi: 10.1038/s41467-019-13812-z

Hase, Y., Horsburgh, K., Ihara, M., and Kalaria, R. N. (2018). White matter degeneration in vascular and other ageing-related dementias. *J. Neurochem.* 144, 617–633. doi: 10.1111/jnc.14271

Hashimoto, T., Serrano-Pozo, A., Hori, Y., Adams, K. W., Takeda, S., Banerji, A. O., et al. (2012). Apolipoprotein E, especially apolipoprotein E4, increases the oligomerization of amyloid β peptide. *J. Neurosci.* 32, 15181–15192. doi: 10.1523/JNEUROSCI.1542-12.2012

Hawkes, C. A., Härtig, W., Kacza, J., Schliebs, R., Weller, R. O., Nicoll, J. A., et al. (2011). Perivascular drainage of solutes is impaired in the ageing mouse brain and in the presence of cerebral amyloid angiopathy. *Acta Neuropathol.* 121, 431–443. doi: 10.1007/s00401-011-0801-7

Hermann, D. M., and ElAli, A. (2012). The abluminal endothelial membrane in neurovascular remodeling in health and disease. *Sci. Signal.* 5:re4. doi: 10.1126/scisignal.2002886

Hernandez-Guillamon, M., Mawhirt, S., Blais, S., Montaner, J., Neubert, T. A., Rostagno, A., et al. (2015). Sequential amyloid-β degradation by the matrix metalloproteases MMP-2 and MMP-9. *J. Biol. Chem.* 290, 15078–15091. doi: 10.1074/jbc.M114.610931

Herzig, M. C., Van Nostrand, W. E., and Jucker, M. (2006). Mechanism of cerebral β-amyloid angiopathy: murine and cellular models. *Brain Pathol.* 16, 40–54. doi: 10.1111/j.1750-3639.2006.tb00560.x

Herzig, M. C., Winkler, D. T., Burgermeister, P., Pfeifer, M., Kohler, E., Schmidt, S. D., et al. (2004). Aβ is targeted to the vasculature in a mouse model of hereditary cerebral hemorrhage with amyloidosis. *Nat. Neurosci.* 7, 954–960. doi: 10.1038/nn1302

Hirsch-Reinshagen, V., Burgess, B. L., and Wellington, C. L. (2009). Why lipids are important for Alzheimer disease? *Mol. Cell. Biochem.* 326, 121–129. doi: 10.1007/s11010-008-0012-2

Ho, C. S. H., and Mondry, A. (2015). CADASIL presenting as schizophreniform organic psychosis. *Gen. Hosp. Psychiatry* 37, 273.e11–273.e13. doi: 10.1016/j.genhosppsych.2015.02.006

Holland, C. M., Smith, E. E., Csapo, I., Gurol, M. E., Brylka, D. A., Killiany, R. J., et al. (2008). Spatial distribution of white-matter hyperintensities in Alzheimer disease, cerebral amyloid angiopathy, and healthy aging. *Stroke* 39, 1127–1133. doi: 10.1161/STROKEAHA.107.497438

Hosseini-Alghaderi, S., and Baron, M. (2020). Notch3 in development, health and disease. *Biomolecules* 10:485. doi: 10.3390/biom10030485

Howe, M. D., McCullough, L. D., and Urayama, A. (2020). The role of basement membranes in cerebral amyloid angiopathy. *Front. Physiol.* 11:601320. doi: 10.3389/fphys.2020.601320

Hung, V. K. L., Yeung, P. K. K., Lai, A. K. W., Ho, M. C. Y., Lo, A. C. Y., Chan, K. C., et al. (2015). Selective astrocytic endothelin-1 overexpression contributes to dementia associated with ischemic stroke by exaggerating astrocyte-derived amyloid secretion. *J. Cereb. Blood Flow Metab.* 35, 1687–1696. doi: 10.1038/jcbfm.2015.109

Iadecola, C. (2013). The pathobiology of vascular dementia. *Neuron* 80, 844–866. doi: 10.1016/j.neuron.2013.10.008

Iadecola, C., Duering, M., Hachinski, V., Joutel, A., Pendlebury, S. T., Schneider, J. A., et al. (2019). Vascular cognitive impairment and dementia: JACC scientific expert panel. *J. Am. Coll. Cardiol.* 73, 3326–3344. doi: 10.1016/j.jacc.2019.04.034

Ihara, M., and Yamamoto, Y. (2016). Emerging evidence for pathogenesis of sporadic cerebral small vessel disease. *Stroke* 47, 554–560. doi: 10.1161/STROKEAHA.115.009627

Ikawati, M., Kawaichi, M., and Oka, C. (2018). Loss of HtrA1 serine protease induces synthetic modulation of aortic vascular smooth muscle cells. *PLoS One* 13:e0196628. doi: 10.1371/journal.pone.0196628

Ince, P. G., Minett, T., Forster, G., Brayne, C., Wharton, S. B., and Medical Research Council Cognitive Function and Ageing Neuropathology Study. (2017). Microinfarcts in an older population-representative brain donor cohort (MRC CFAS): prevalence, relation to dementia, and mobility and implications

for the evaluation of cerebral Small Vessel Disease. *Neuropathol. Appl. Neurobiol.* 43, 409–418. doi: 10.1111/nan.12363

Jäkel, L., Kuiperij, H. B., Gerding, L. P., Custers, E. E. M., van den Berg, E., Jolink, W. M. T., et al. (2020). Disturbed balance in the expression of MMP9 and TIMP3 in cerebral amyloid angiopathy-related intracerebral haemorrhage. *Acta Neuropathol. Commun.* 8:99. doi: 10.1186/s40478-020-00972-z

Jayant, S., and Sharma, B. (2016). Selective modulator of cannabinoid receptor type 2 reduces memory impairment and infarct size during cerebral hypoperfusion and vascular dementia. *Curr. Neurovasc. Res.* 13, 289–302. doi: 10.2174/1567202613666160902102007

Jayaraj, R. L., Azimullah, S., Beiram, R., Jalal, F. Y., and Rosenberg, G. A. (2019). Neuroinflammation: friend and foe for ischemic stroke. *J. Neuroinflammation* 16:142. doi: 10.1186/s12974-019-1516-2

Jellinger, K. A. (2002). Alzheimer disease and cerebrovascular pathology: an update. *J. Neural Transm.* 109, 813–836. doi: 10.1007/s007020200068

Jellinger, K. A. (2007). The enigma of mixed dementia. *Alzheimers Dement.* 3, 40–53. doi: 10.1016/j.jalz.2006.09.002

Jellinger, K. A. (2013). Pathology and pathogenesis of vascular cognitive impairment-a critical update. *Front. Aging Neurosci.* 5:17. doi: 10.3389/fnagi.2013.00017

Jendroska, K., Hoffmann, O. M., and Patt, S. (1997). Amyloid β peptide and precursor protein (APP) in mild and severe brain ischemia. *Ann. N Y Acad. Sci.* 826, 401–405. doi: 10.1111/j.1749-6632.1997.tb48492.x

Jennette, J. C., and Falk, R. J. (1997). Small-vessel vasculitis. *N. Engl. J. Med.* 337, 1512–1523. doi: 10.1056/NEJM199711203372106

Jian, B., Hu, M., Cai, W., Zhang, B., and Lu, Z. (2020). Update of immunosenescence in cerebral small vessel disease. *Front. Immunol.* 11:585655. doi: 10.3389/fimmu.2020.585655

Jiang, X., Andjelkovic, A. V., Zhu, L., Yang, T., Bennett, M. V. L., Chen, J., et al. (2018). Blood-brain barrier dysfunction and recovery after ischemic stroke. *Prog. Neurobiol.* 163–164, 144–171. doi: 10.1016/j.pneurobio.2017.10.001

Jo, W. K., Law, A. C. K., and Chung, S. K. (2014). The neglected co-star in the dementia drama: the putative roles of astrocytes in the pathogeneses of major neurocognitive disorders. *Mol. Psychiatry* 19, 159–167. doi: 10.1038/mp.2013.171

Jokinen, H., Lipsanen, J., Schmidt, R., Fazekas, F., Gouw, A. A., van der Flier, W. M., et al. (2012). Brain atrophy accelerates cognitive decline in cerebral small vessel disease: the LADIS study. *Neurology* 78, 1785–1792. doi: 10.1212/WNL.0b013e3182583070

Jones, E. V., and Bouvier, D. S. (2014). Astrocyte-secreted matricellular proteins in CNS remodelling during development and disease. *Neural Plast.* 2014:321209. doi: 10.1155/2014/321209

Joutel, A., Andreux, F., Gaulis, S., Domenga, V., Cecillon, M., Battail, N., et al. (2000). The ectodomain of the Notch3 receptor accumulates within the cerebrovasculature of CADASIL patients. *J. Clin. Invest.* 105, 597–605. doi: 10.1172/JCI8047

Joutel, A., Favrole, P., Labauge, P., Chabriat, H., Lescoat, C., Andreux, F., et al. (2001). Skin biopsy immunostaining with a Notch3 monoclonal antibody for CADASIL diagnosis. *Lancet* 358, 2049–2051. doi: 10.1016/S0140-6736(01)07142-2

Joutel, A., Haddad, I., Ratelade, J., and Nelson, M. T. (2016). Perturbations of the cerebrovascular matrisome: a convergent mechanism in small vessel disease of the brain? *J. Cereb. Blood Flow Metab.* 36, 143–157. doi: 10.1038/jcbfm.2015.62

Kalaria, R. N., Akinyemi, R., and Ihara, M. (2016). Stroke injury, cognitive impairment and vascular dementia. *Biochim. Biophys. Acta* 1862, 915–925. doi: 10.1016/j.bbadis.2016.01.015

Kamp, J. A., Moursel, L. G., Haan, J., Terwindt, G. M., Lesnik Oberstein, S. A. M. J., van Duinen, S. G., et al. (2014). Amyloid β in hereditary cerebral hemorrhage with amyloidosis-Dutch type. *Rev. Neurosci.* 25, 641–651. doi: 10.1515/revneuro-2014-0008

Kandasamy, M., Anusuyadevi, M., Aigner, K. M., Unger, M. S., Kniewallner, K. M., de Sousa, D. M. B., et al. (2020). TGF-β signaling: a therapeutic target to reinstate regenerative plasticity in vascular dementia? *Aging Dis.* 11, 828–850. doi: 10.14336/AD.2020.0222

Kawai, H., Kawaguchi, D., Kuebrich, B. D., Kitamoto, T., Yamaguchi, M., Gotoh, Y., et al. (2017). Area-specific regulation of quiescent neural stem cells by Notch3 in the adult mouse subependymal zone. *J. Neurosci.* 37, 11867–11880. doi: 10.1523/JNEUROSCI.0001-17.2017

Keable, A., Fenna, K., Yuen, H. M., Johnston, D. A., Smyth, N. R., Smith, C., et al. (2016). Deposition of amyloid β in the walls of human leptomeningeal arteries in relation to perivascular drainage pathways in cerebral amyloid angiopathy. *Biochim. Biophys. Acta* 1862, 1037–1046. doi: 10.1016/j.bbadis.2015.08.024

Keage, H. A. D., Carare, R. O., Friedland, R. P., Ince, P. G., Love, S., Nicoll, J. A., et al. (2009). Population studies of sporadic cerebral amyloid angiopathy and dementia: a systematic review. *BMC Neurol.* 9:3. doi: 10.1186/1471-2377-9-3

Kerkhofs, D., van Hagen, B. T., Milanova, I. V., Schell, K. J., van Essen, H., Wijnands, E., et al. (2020). Pharmacological depletion of microglia and perivascular macrophages prevents vascular cognitive impairment in Ang II-induced hypertension. *Theranostics* 10, 9512–9527. doi: 10.7150/thno.44394

Khanna, A., Kahle, K. T., Walcott, B. P., Gerzanich, V., and Simard, J. M. (2014). Disruption of ion homeostasis in the neurogliovascular unit underlies the pathogenesis of ischemic cerebral edema. *Transl. Stroke Res.* 5, 3–16. doi: 10.1007/s12975-013-0307-9

Kim, J. Y., Kim, J.-H., Kim, Y.-D., and Seo, J. H. (2020). High vulnerability of oligodendrocytes to oxidative stress induced by ultrafine urban particles. *Antioxidants* 10:4. doi: 10.3390/antiox10010004

Kim, J. Y., Park, J., Chang, J. Y., Kim, S.-H., and Lee, J. E. (2016). Inflammation after ischemic stroke: the role of leukocytes and glial cells. *Exp. Neurobiol.* 25, 241–251. doi: 10.5607/en.2016.25.5.241

Kim, R.-E., Shin, C. Y., Han, S.-H., and Kwon, K. J. (2020). Astaxanthin suppresses PM2.5-induced neuroinflammation by regulating Akt phosphorylation in BV-2 microglial cells. *Int. J. Mol. Sci.* 21:7227. doi: 10.3390/ijms21197227

Kinney, J. W., Bemiller, S. M., Murtishaw, A. S., Leisgang, A. M., Salazar, A. M., and Lamb, B. T. (2018). Inflammation as a central mechanism in Alzheimer's disease. *Alzheimers Dement.* 4, 575–590. doi: 10.1016/j.trci.2018.06.014

Kivipelto, M., Mangialasche, F., Snyder, H. M., Allegri, R., Andrieu, S., Arai, H., et al. (2020). World-wide FINGERS network: a global approach to risk reduction and prevention of dementia. *Alzheimers Dement.* 16, 1078–1094. doi: 10.1002/alz.12123

Kjeldsen, S. E., Narkiewicz, K., Burnier, M., and Oparil, S. (2018). Intensive blood pressure lowering prevents mild cognitive impairment and possible dementia and slows development of white matter lesions in brain: the SPRINT Memory and Cognition IN Decreased Hypertension (SPRINT MIND) study. *Blood Press.* 27, 247–248. doi: 10.1080/08037051.2018.1507621

Klocke, C., Allen, J. L., Sobolewski, M., Blum, J. L., Zelikoff, J. T., and Cory-Slechta, D. A. (2018). Exposure to fine and ultrafine particulate matter during gestation alters postnatal oligodendrocyte maturation, proliferation capacity and myelination. *Neurotoxicology* 65, 196–206. doi: 10.1016/j.neuro.2017.10.004

Koizumi, T., Taguchi, K., Mizuta, I., Toba, H., Ohigashi, M., Onishi, O., et al. (2019). Transiently proliferating perivascular microglia harbor M1 type and precede cerebrovascular changes in a chronic hypertension model. *J. Neuroinflammation* 16:79. doi: 10.1186/s12974-019-1467-7

Kopan, R., and Ilagan, M. X. G. (2009). The canonical Notch signaling pathway: unfolding the activation mechanism. *Cell* 137, 216–233. doi: 10.1016/j.cell.2009.03.045

Kotilinek, L. A., Westerman, M. A., Wang, Q., Panizzon, K., Lim, G. P., Simonyi, A., et al. (2008). Cyclooxygenase-2 inhibition improves amyloid-β-mediated suppression of memory and synaptic plasticity. *Brain* 131, 651–664. doi: 10.1093/brain/awn008

Kraft, P., Schuhmann, M. K., Garz, C., Jandke, S., Urlaub, D., Mencl, S., et al. (2017). Hypercholesterolemia induced cerebral small vessel disease. *PLoS One* 12:e0182822. doi: 10.1371/journal.pone.0182822

Kulick, E. R., Elkind, M. S. V., Boehme, A. K., Joyce, N. R., Schupf, N., Kaufman, J. D., et al. (2020). Long-term exposure to ambient air pollution, APOE-ϵ4 status and cognitive decline in a cohort of older adults in northern Manhattan. *Environ. Int.* 136:105440. doi: 10.1016/j.envint.2019.105440

Kuo, D. S., Labelle-Dumais, C., and Gould, D. B. (2012). COL4A1 and COL4A2 mutations and disease: insights into pathogenic mechanisms and potential therapeutic targets. *Hum. Mol. Genet.* 21, R97–R110. doi: 10.1093/hmg/dds346

Lacombe, P., Oligo, C., Domenga, V., Tournier-Lasserve, E., and Joutel, A. (2005). Impaired cerebral vasoreactivity in a transgenic mouse model of cerebral autosomal dominant arteriopathy with subcortical infarcts and

leukoencephalopathy arteriopathy. *Stroke* 36, 1053–1058. doi: 10.1161/01.STR.0000163080.82766.eb

Lågas, P. A., and Juvonen, V. (2001). Schizophrenia in a patient with cerebral autosomally dominant arteriopathy with subcortical infarcts and leucoencephalopathy (CADASIL disease). *Nord. J. Psychiatry* 55, 41–42. doi: 10.1080/080394801750093724

Lammie, G. A., Brannan, F., and Wardlaw, J. M. (1998). Incomplete lacunar infarction (Type Ib lacunes). *Acta Neuropathol.* 96, 163–171. doi: 10.1007/s004010050877

Leduc, V., Jasmin-Bélanger, S., and Poirier, J. (2010). APOE and cholesterol homeostasis in Alzheimer's disease. *Trends Mol. Med.* 16, 469–477. doi: 10.1016/j.molmed.2010.07.008

Lepelletier, F.-X., Mann, D. M. A., Robinson, A. C., Pinteaux, E., and Boutin, H. (2017). Early changes in extracellular matrix in Alzheimer's disease. *Neuropathol. Appl. Neurobiol.* 43, 167–182. doi: 10.1111/nan.12295

Lesnik Oberstein, S. A., van den Boom, R., van Buchem, M. A., van Houwelingen, H. C., Bakker, E., Vollebregt, E., et al. (2001). Cerebral microbleeds in CADASIL. *Neurology* 57, 1066–1070. doi: 10.1212/wnl.57.6.1066

Levesque, S., Taetzsch, T., Lull, M. E., Kodavanti, U., Stadler, K., Wagner, A., et al. (2011). Diesel exhaust activates and primes microglia: air pollution, neuroinflammation, and regulation of dopaminergic neurotoxicity. *Environ. Health Perspect.* 119, 1149–1155. doi: 10.1289/ehp.1002986

Li, Z. W., Chu, W., Hu, Y., Delhase, M., Deerinck, T., Ellisman, M., et al. (1999). The IKKβ subunit of IκB kinase (IKK) is essential for nuclear factor κB activation and prevention of apoptosis. *J. Exp. Med.* 189, 1839–1845. doi: 10.1084/jem.189.11.1839

Li, Q., Yang, Y., Reis, C., Tao, T., Li, W., Li, X., et al. (2018). Cerebral small vessel disease. *Cell Transplant.* 27, 1711–1722. doi: 10.1177/0963689718795148

Li, X., Zhang, X., Leathers, R., Makino, A., Huang, C., Parsa, P., et al. (2009). Notch3 signaling promotes the development of pulmonary arterial hypertension. *Nat. Med.* 15, 1289–1297. doi: 10.1038/nm.2021

Li, Y., Liu, Y., Hu, C., Chang, Q., Deng, Q., Yang, X., et al. (2020). Study of the neurotoxicity of indoor airborne nanoparticles based on a 3D human blood-brain barrier chip. *Environ. Int.* 143:105598. doi: 10.1016/j.envint.2020.105598

Li, T., Zhao, J., Ge, J., Yang, J., Song, X., Wang, C., et al. (2016). Particulate matter facilitates C6 glioma cells activation and the release of inflammatory factors through MAPK and JAK2/STAT3 pathways. *Neurochem. Res.* 41, 1969–1981. doi: 10.1007/s11064-016-1908-y

Liang, S., Zhang, J., Ning, R., Du, Z., Liu, J., Batibawa, J. W., et al. (2020). The critical role of endothelial function in fine particulate matter-induced atherosclerosis. *Part. Fibre Toxicol.* 17:61. doi: 10.1186/s12989-020-00391-x

Liddelow, S. A., Guttenplan, K. A., Clarke, L. E., Bennett, F. C., Bohlen, C. J., Schirmer, L., et al. (2017). Neurotoxic reactive astrocytes are induced by activated microglia. *Nature* 541, 481–487. doi: 10.1038/nature21029

Liu, Y., Chan, D. K. Y., Thalamuthu, A., Wen, W., Jiang, J., Paradise, M., et al. (2020). Plasma lipidomic biomarker analysis reveals distinct lipid changes in vascular dementia. *Comput. Struct. Biotechnol. J.* 18, 1613–1624. doi: 10.1016/j.csbj.2020.06.001

Liu, F., Huang, Y., Zhang, F., Chen, Q., Wu, B., Rui, W., et al. (2015). Macrophages treated with particulate matter PM2.5 induce selective neurotoxicity through glutaminase-mediated glutamate generation. *J. Neurochem.* 134, 315–326. doi: 10.1111/jnc.13135

Liu, X.-Y., Gonzalez-Toledo, M. E., Fagan, A., Duan, W.-M., Liu, Y., Zhang, S., et al. (2015). Stem cell factor and granulocyte colony-stimulating factor exhibit therapeutic effects in a mouse model of CADASIL. *Neurobiol. Dis.* 73, 189–203. doi: 10.1016/j.nbd.2014.09.006

Liu, Q., Radwanski, R., Babadjouni, R., Patel, A., Hodis, D. M., Baumbacher, P., et al. (2019). Experimental chronic cerebral hypoperfusion results in decreased pericyte coverage and increased blood-brain barrier permeability in the corpus callosum. *J. Cereb. Blood Flow Metab.* 39, 240–250. doi: 10.1177/0271678X17743670

Louvi, A., Arboleda-Velasquez, J. F., and Artavanis-Tsakonas, S. (2006). CADASIL: a critical look at a Notch disease. *Dev. Neurosci.* 28, 5–12. doi: 10.1159/000090748

Love, S., Chalmers, K., Ince, P., Esiri, M., Attems, J., Jellinger, K., et al. (2014). Development, appraisal, validation and implementation of a consensus protocol for the assessment of cerebral amyloid angiopathy in post-mortem brain tissue. *Am. J. Neurodegener. Dis.* 3, 19–32.

Luo, X.-Q., Li, A., Yang, X., Xiao, X., Hu, R., Wang, T.-W., et al. (2018). Paeoniflorin exerts neuroprotective effects by modulating the M1/M2 subset polarization of microglia/macrophages in the hippocampal CA1 region of vascular dementia rats *via* cannabinoid receptor 2. *Chin. Med.* 13:14. doi: 10.1186/s13020-018-0173-1

Lusis, A. J. (2000). Atherosclerosis. *Nature* 407, 233–241. doi: 10.1038/35025203

Magaki, S., Tang, Z., Tung, S., Williams, C. K., Lo, D., Yong, W. H., et al. (2018). The effects of cerebral amyloid angiopathy on integrity of the blood-brain barrier. *Neurobiol. Aging* 70, 70–77. doi: 10.1016/j.neurobiolaging.2018.06.004

Malik, R., Rannikmäe, K., Traylor, M., Georgakis, M. K., Sargurupremraj, M., Markus, H. S., et al. (2018). Genome-wide meta-analysis identifies 3 novel loci associated with stroke. *Ann. Neurol.* 84, 934–939. doi: 10.1002/ana.25369

Malpetti, M., Kievit, R. A., Passamonti, L., Jones, P. S., Tsvetanov, K. A., Rittman, T., et al. (2020). Microglial activation and tau burden predict cognitive decline in Alzheimer's disease. *Brain* 143, 1588–1602. doi: 10.1093/brain/awaa088

Marini, S., Anderson, C. D., and Rosand, J. (2020). Genetics of cerebral small vessel disease. *Stroke* 51, 12–20. doi: 10.1161/STROKEAHA.119.024151

Martinez-Canabal, A., Wheeler, A. L., Sarkis, D., Lerch, J. P., Lu, W.-Y., Buckwalter, M. S., et al. (2013). Chronic over-expression of TGFβ1 alters hippocampal structure and causes learning deficits. *Hippocampus* 23, 1198–1211. doi: 10.1002/hipo.22159

Martinez-Ramirez, S., Greenberg, S. M., and Viswanathan, A. (2014). Cerebral microbleeds: overview and implications in cognitive impairment. *Alzheimers Res. Ther.* 6:33. doi: 10.1186/alzrt263

Martini, A. C., Helman, A. M., McCarty, K. L., Lott, I. T., Doran, E., Schmitt, F. A., et al. (2020). Distribution of microglial phenotypes as a function of age and Alzheimer's disease neuropathology in the brains of people with Down syndrome. *Alzheimers Dement. Transl. Res. Clin. Interv.* 12:e12113. doi: 10.1002/dad2.12113

Matsuda, Y., Hirata, K., Inoue, N., Suematsu, M., Kawashima, S., Akita, H., et al. (1993). High density lipoprotein reverses inhibitory effect of oxidized low density lipoprotein on endothelium-dependent arterial relaxation. *Circ. Res.* 72, 1103–1109. doi: 10.1161/01.res.72.5.1103

Matsumoto, J., Dohgu, S., Takata, F., Machida, T., Bölükbaşi Hatip, F. F., Hatip-Al-Khatib, I., et al. (2018). TNF-α-sensitive brain pericytes activate microglia by releasing IL-6 through cooperation between IκB-NFκB and JAK-STAT3 pathways. *Brain Res.* 1692, 34–44. doi: 10.1016/j.brainres.2018.04.023

Merino, J. G., and Hachinski, V. (2000). Leukoaraiosis: reifying rarefaction. *Arch. Neurol.* 57, 925–926. doi: 10.1001/archneur.57.7.925

Meuwissen, M. E. C., Halley, D. J. J., Smit, L. S., Lequin, M. H., Cobben, J. M., de Coo, R., et al. (2015). The expanding phenotype of COL4A1 and COL4A2 mutations: clinical data on 13 newly identified families and a review of the literature. *Genet. Med.* 17, 843–853. doi: 10.1038/gim.2014.210

Miao, Q., Paloneva, T., Tuisku, S., Roine, S., Poyhonen, M., Viitanen, M., et al. (2006). Arterioles of the lenticular nucleus in CADASIL. *Stroke* 37, 2242–2247. doi: 10.1161/01.STR.0000236838.84150.c2

Michaud, J.-P., Bellavance, M.-A., Préfontaine, P., and Rivest, S. (2013). Real-time *in vivo* imaging reveals the ability of monocytes to clear vascular amyloid β. *Cell Rep.* 5, 646–653. doi: 10.1016/j.celrep.2013.10.010

Mijajlović, M. D., Pavlović, A., Brainin, M., Heiss, W.-D., Quinn, T. J., Ihle-Hansen, H. B., et al. (2017). Post-stroke dementia—a comprehensive review. *BMC Med.* 15:11. doi: 10.1186/s12916-017-0779-7

Mills, N. L., Donaldson, K., Hadoke, P. W., Boon, N. A., MacNee, W., Cassee, F. R., et al. (2009). Adverse cardiovascular effects of air pollution. *Nat. Clin. Pract. Cardiovasc. Med.* 6, 36–44. doi: 10.1038/ncpcardio1399

Min, L.-J., Iwanami, J., Shudou, M., Bai, H.-Y., Shan, B.-S., Higaki, A., et al. (2020). Deterioration of cognitive function after transient cerebral ischemia with amyloid-β infusion-possible amelioration of cognitive function by AT2 receptor activation. *J. Neuroinflammation* 17:106. doi: 10.1186/s12974-020-01775-8

Mok, V., Wong, K. K., Xiong, Y., Wong, A., Schmidt, R., Chu, W., et al. (2011). Cortical and frontal atrophy are associated with cognitive impairment in age-related confluent white-matter lesion. *J. Neurol. Neurosurg. Psychiatry* 82, 52–57. doi: 10.1136/jnnp.2009.201665

Monet-Leprêtre, M., Haddad, I., Baron-Menguy, C., Fouillot-Panchal, M., Riani, M., Domenga-Denier, V., et al. (2013). Abnormal recruitment of extracellular matrix proteins by excess Notch3 ECD: a new pathomechanism in CADASIL. *Brain* 136, 1830–1845. doi: 10.1093/brain/awt092

Montagne, A., Nikolakopoulou, A. M., Zhao, Z., Sagare, A. P., Si, G., Lazic, D., et al. (2018). Pericyte degeneration causes white matter dysfunction in the mouse central nervous system. *Nat. Med.* 24, 326–337. doi: 10.1038/nm.4482

Montagne, A., Zhao, Z., and Zlokovic, B. V. (2017). Alzheimer's disease: a matter of blood-brain barrier dysfunction? *J. Exp. Med.* 214, 3151–3169. doi: 10.1084/jem.20171406

Montaner, J., Alvarez-Sabín, J., Molina, C., Anglés, A., Abilleira, S., Arenillas, J., et al. (2001). Matrix metalloproteinase expression after human cardioembolic stroke: temporal profile and relation to neurological impairment. *Stroke* 32, 1759–1766. doi: 10.1161/01.str.32.8.1759

Montiel-Dávalos, A., Alfaro-Moreno, E., and López-Marure, R. (2007). PM2.5 and PM10 induce the expression of adhesion molecules and the adhesion of monocytic cells to human umbilical vein endothelial cells. *Inhal. Toxicol.* 19, 91–98. doi: 10.1080/08958370701495212

Moreau, F., Patel, S., Lauzon, M. L., McCreary, C. R., Goyal, M., Frayne, R., et al. (2012). Cavitation after acute symptomatic lacunar stroke depends on time, location, and MRI sequence. *Stroke* 43, 1837–1842. doi: 10.1161/STROKEAHA.111.647859

Morris, A. W. J., Carare, R. O., Schreiber, S., and Hawkes, C. A. (2014). The cerebrovascular basement membrane: role in the clearance of β-amyloid and cerebral amyloid angiopathy. *Front. Aging Neurosci.* 6:251. doi: 10.3389/fnagi.2014.00251

Moskowitz, M. A., Lo, E. H., and Iadecola, C. (2010). The science of stroke: mechanisms in search of treatments. *Neuron* 67, 181–198. doi: 10.1016/j.neuron.2010.07.002

Mulder, M., and Terwel, D. (1998). Possible link between lipid metabolism and cerebral amyloid angiopathy in Alzheimer's disease: a role for high-density lipoproteins? *Haemostasis* 28, 174–194. doi: 10.1159/000022429

Muller, M., Appelman, A. P. A., van der Graaf, Y., Vincken, K. L., Mali, W. P. T. M., and Geerlings, M. I. (2011). Brain atrophy and cognition: interaction with cerebrovascular pathology? *Neurobiol. Aging* 32, 885–893. doi: 10.1016/j.neurobiolaging.2009.05.005

Mumaw, C. L., Surace, M., Levesque, S., Kodavanti, U. P., Kodavanti, P. R. S., Royland, J. E., et al. (2017). Atypical microglial response to biodiesel exhaust in healthy and hypertensive rats. *Neurotoxicology* 59, 155–163. doi: 10.1016/j.neuro.2016.10.012

Navarro, A., García, M., Rodrigues, A. S., Garcia, P. V., Camarinho, R., and Segovia, Y. (2021). Reactive astrogliosis in the dentate gyrus of mice exposed to active volcanic environments. *J. Toxicol. Environ. Health Part A* 84, 213–226. doi: 10.1080/15287394.2020.1850381

Newman, J. D., Thurston, G. D., Cromar, K., Guo, Y., Rockman, C. B., Fisher, E. A., et al. (2015). Particulate air pollution and carotid artery stenosis. *J. Am. Coll. Cardiol.* 65, 1150–1151. doi: 10.1016/j.jacc.2014.12.052

Ngandu, T., Lehtisalo, J., Solomon, A., Levälahti, E., Ahtiluoto, S., Antikainen, R., et al. (2015). A 2 year multidomain intervention of diet, exercise, cognitive training, and vascular risk monitoring versus control to prevent cognitive decline in at-risk elderly people (FINGER): a randomised controlled trial. *Lancet* 385, 2255–2263. doi: 10.1016/S0140-6736(15)60461-5

Nihashi, T., Inao, S., Kajita, Y., Kawai, T., Sugimoto, T., Niwa, M., et al. (2001). Expression and distribution of β amyloid precursor protein and β amyloid peptide in reactive astrocytes after transient middle cerebral artery occlusion. *Acta Neurochir.* 143, 287–295. doi: 10.1007/s007010170109

Nikolakopoulou, A. M., Montagne, A., Kisler, K., Dai, Z., Wang, Y., Huuskonen, M. T., et al. (2019). Pericyte loss leads to circulatory failure and pleiotrophin depletion causing neuron loss. *Nat. Neurosci.* 22, 1089–1098. doi: 10.1038/s41593-019-0434-z

Nikolakopoulou, A. M., Wang, Y., Ma, Q., Sagare, A. P., Montagne, A., Huuskonen, M. T., et al. (2021). Endothelial LRP1 protects against neurodegeneration by blocking cyclophilin A. *J. Exp. Med.* 218:e20202207. doi: 10.1084/jem.20202207

Nishikawa, H., Liu, L., Nakano, F., Kawakita, F., Kanamaru, H., Nakatsuka, Y., et al. (2018). Modified citrus pectin prevents blood-brain barrier disruption in mouse subarachnoid hemorrhage by inhibiting galectin-3. *Stroke* 49, 2743–2751. doi: 10.1161/STROKEAHA.118.021757

Noe, C. R., Noe-Letschnig, M., Handschuh, P., Noe, C. A., and Lanzenberger, R. (2020). Dysfunction of the blood-brain barrier-a key step in neurodegeneration and dementia. *Front. Aging Neurosci.* 12:185. doi: 10.3389/fnagi.2020.00185

Noh, S.-M., Chung, S. J., Kim, K.-K., Kang, D.-W., Lim, Y.-M., Kwon, S. U., et al. (2014). Emotional disturbance in CADASIL: its impact on quality of life and caregiver burden. *Cerebrovasc. Dis.* 37, 188–194. doi: 10.1159/000357798

Nortley, R., Korte, N., Izquierdo, P., Hirunpattarasilp, C., Mishra, A., Jaunmuktane, Z., et al. (2019). Amyloid β oligomers constrict human capillaries in Alzheimer's disease *via* signaling to pericytes. *Science* 365:eaav9518. doi: 10.1126/science.aav9518

Nuthikattu, S., Milenkovic, D., Rutledge, J. C., and Villablanca, A. C. (2020). Sex-dependent molecular mechanisms of lipotoxic injury in brain microvasculature: implications for dementia. *Int. J. Mol. Sci.* 21:8146. doi: 10.3390/ijms21218146

O'Brien, J. T., and Markus, H. S. (2014). Vascular risk factors and Alzheimer's disease. *BMC Med.* 12:218. doi: 10.1186/s12916-014-0218-y

O'Brien, J. T., and Thomas, A. (2015). Vascular dementia. *Lancet* 386, 1698–1706. doi: 10.1016/S0140-6736(15)00463-8

Oberdörster, G., Sharp, Z., Atudorei, V., Elder, A., Gelein, R., Kreyling, W., et al. (2004). Translocation of inhaled ultrafine particles to the brain. *Inhal. Toxicol.* 16, 437–445. doi: 10.1080/08958370490439597

Oka, C., Tsujimoto, R., Kajikawa, M., Koshiba-Takeuchi, K., Ina, J., Yano, M., et al. (2004). HtrA1 serine protease inhibits signaling mediated by Tgfβ family proteins. *Development* 131, 1041–1053. doi: 10.1242/dev.00999

Okamoto, Y., Ihara, M., Tomimoto, H., Taylor Kimberly, W., and Greenberg, S. M. (2010). Silent ischemic infarcts are associated with hemorrhage burden in cerebral amyloid angiopathy. *Neurology* 74:93; author reply 93. doi: 10.1212/WNL.0b013e3181c77627

Okazaki, S., Hornberger, E., Griebe, M., Gass, A., Hennerici, M. G., and Szabo, K. (2015). MRI characteristics of the evolution of supratentorial recent small subcortical infarcts. *Front. Neurol.* 6:118. doi: 10.3389/fneur.2015.00118

Okeda, R., and Nisihara, M. (2008). An autopsy case of Fabry disease with neuropathological investigation of the pathogenesis of associated dementia. *Neuropathology* 28, 532–540. doi: 10.1111/j.1440-1789.2008.00883.x

Onoda, A., Kawasaki, T., Tsukiyama, K., Takeda, K., and Umezawa, M. (2020). Carbon nanoparticles induce endoplasmic reticulum stress around blood vessels with accumulation of misfolded proteins in the developing brain of offspring. *Sci. Rep.* 10:10028. doi: 10.1038/s41598-020-66744-w

Onoda, A., Takeda, K., and Umezawa, M. (2017). Dose-dependent induction of astrocyte activation and reactive astrogliosis in mouse brain following maternal exposure to carbon black nanoparticle. *Part. Fibre Toxicol.* 14:4. doi: 10.1186/s12989-017-0184-6

Oppenheim, H. A., Lucero, J., Guyot, A.-C., Herbert, L. M., McDonald, J. D., Mabondzo, A., et al. (2013). Exposure to vehicle emissions results in altered blood brain barrier permeability and expression of matrix metalloproteinases and tight junction proteins in mice. *Part. Fibre Toxicol.* 10:62. doi: 10.1186/1743-8977-10-62

Østergaard, L., Engedal, T. S., Moreton, F., Hansen, M. B., Wardlaw, J. M., Dalkara, T., et al. (2016). Cerebral small vessel disease: capillary pathways to stroke and cognitive decline. *J. Cereb. Blood Flow Metab.* 36, 302–325. doi: 10.1177/0271678X15606723

Oudin, A., Andersson, J., Sundström, A., Nordin Adolfsson, A., Oudin Åström, D., Adolfsson, R., et al. (2019). Traffic-related air pollution as a risk factor for dementia: no clear modifying effects of APOEε4 in the betula cohort. *J. Alzheimers Dis.* 71, 733–740. doi: 10.3233/JAD-181037

Patterson, C. (2018). *World Alzheimer Report 2018. The State of the Art of Dementia Research: New Frontiers*. London, UK: Alzheimer's Disease International.

Pang, J., Peng, J., Matei, N., Yang, P., Kuai, L., Wu, Y., et al. (2018). Apolipoprotein E exerts a whole-brain protective property by promoting M1? Microglia quiescence after experimental subarachnoid hemorrhage in mice. *Transl. Stroke Res.* 9, 654–668. doi: 10.1007/s12975-018-0665-4

Pantoni, L. (2010). Cerebral small vessel disease: from pathogenesis and clinical characteristics to therapeutic challenges. *Lancet Neurol.* 9, 689–701. doi: 10.1016/S1474-4422(10)70104-6

Parkes, I., Chintawar, S., and Cader, M. Z. (2018). Neurovascular dysfunction in dementia—human cellular models and molecular mechanisms. *Clin. Sci.* 132, 399–418. doi: 10.1042/CS20160720

Parolisi, R., Montarolo, F., Pini, A., Rovelli, S., Cattaneo, A., Bertolotto, A., et al. (2021). Exposure to fine particulate matter (PM2.5) hampers myelin repair in a mouse model of white matter demyelination. *Neurochem. Int.* 145:104991. doi: 10.1016/j.neuint.2021.104991

Patten, K. T., González, E. A., Valenzuela, A., Berg, E., Wallis, C., Garbow, J. R., et al. (2020). Effects of early life exposure to traffic-related air pollution on brain development in juvenile Sprague-Dawley rats. *Transl. Psychiatry* 10:166. doi: 10.1038/s41398-020-0845-3

Paul, K. C., Haan, M., Mayeda, E. R., and Ritz, B. R. (2019). Ambient air pollution, noise and late-life cognitive decline and dementia risk. *Annu. Rev. Public Health* 40, 203–220. doi: 10.1146/annurev-publhealth-040218-044058

Pendlebury, S. T., Mariz, J., Bull, L., Mehta, Z., and Rothwell, P. M. (2012). MoCA, ACE-R, and MMSE versus the national institute of neurological disorders and stroke-canadian stroke network vascular cognitive impairment harmonization standards neuropsychological battery after TIA and stroke. *Stroke* 43, 464–469. doi: 10.1161/STROKEAHA.111.633586

Pendlebury, S. T., and Rothwell, P. M. (2009). Prevalence, incidence, and factors associated with pre-stroke and post-stroke dementia: a systematic review and meta-analysis. *Lancet Neurol.* 8, 1006–1018. doi: 10.1016/S1474-4422(09)70236-4

Perlmutter, L. S., Barrón, E., Saperia, D., and Chui, H. C. (1991). Association between vascular basement membrane components and the lesions of Alzheimer's disease. *J. Neurosci. Res.* 30, 673–681. doi: 10.1002/jnr.490300411

Perlmutter, L. S., Chui, H. C., Saperia, D., and Athanikar, J. (1990). Microangiopathy and the colocalization of heparan sulfate proteoglycan with amyloid in senile plaques of Alzheimer's disease. *Brain Res.* 508, 13–19. doi: 10.1016/0006-8993(90)91111-s

Peters, A., Veronesi, B., Calderón-Garcidueñas, L., Gehr, P., Chen, L. C., Geiser, M., et al. (2006). Translocation and potential neurological effects of fine and ultrafine particles a critical update. *Part. Fibre Toxicol.* 3:13. doi: 10.1186/1743-8977-3-13

Peters, R., Warwick, J., Anstey, K. J., and Anderson, C. S. (2019). Blood pressure and dementia: what the SPRINT-MIND trial adds and what we still need to know. *Neurology* 92, 1017–1018. doi: 10.1212/WNL.0000000000007543

Ping, S., Qiu, X., Kyle, M., Hughes, K., Longo, J., and Zhao, L.-R. (2019). Stem cell factor and granulocyte colony-stimulating factor promote brain repair and improve cognitive function through VEGF-A in a mouse model of CADASIL. *Neurobiol. Dis.* 132:104561. doi: 10.1016/j.nbd.2019.104561

Pinter, D., Enzinger, C., Gattringer, T., Eppinger, S., Niederkorn, K., Horner, S., et al. (2019). Prevalence and short-term changes of cognitive dysfunction in young ischaemic stroke patients. *Eur. J. Neurol.* 26, 727–732. doi: 10.1111/ene.13879

Podcasy, J. L., and Epperson, C. N. (2016). Considering sex and gender in Alzheimer disease and other dementias. *Dialogues Clin. Neurosci.* 18, 437–446. doi: 10.31887/DCNS.2016.18.4/cepperson

Poorthuis, M. H. F., Algra, A. M., Algra, A., Kappelle, L. J., and Klijn, C. J. M. (2017). Female- and male-specific risk factors for stroke: a systematic review and meta-analysis. *JAMA Neurol.* 74, 75–81. doi: 10.1001/jamaneurol.2016.3482

Potter, G. M., Doubal, F. N., Jackson, C. A., Chappell, F. M., Sudlow, C. L., Dennis, M. S., et al. (2015). Enlarged perivascular spaces and cerebral small vessel disease. *Int. J. Stroke* 10, 376–381. doi: 10.1111/ijs.12054

Prins, N. D., and Scheltens, P. (2015). White matter hyperintensities, cognitive impairment and dementia: an update. *Nat. Rev. Neurol.* 11, 157–165. doi: 10.1038/nrneurol.2015.10

Qin, C., Fan, W.-H., Liu, Q., Shang, K., Murugan, M., Wu, L.-J., et al. (2017). Fingolimod protects against ischemic white matter damage by modulating microglia toward M2 polarization *via* STAT3 pathway. *Stroke* 48, 3336–3346. doi: 10.1161/STROKEAHA.117.018505

Ragno, M., Pianese, L., Morroni, M., Cacchiò, G., Manca, A., Di Marzio, F., et al. (2013). "CADASIL coma" in an Italian homozygous CADASIL patient: comparison with clinical and MRI findings in age-matched heterozygous patients with the same G528C NOTCH3 mutation. *Neurol. Sci.* 34, 1947–1953. doi: 10.1007/s10072-013-1418-5

Razvi, S. S. M., and Bone, I. (2006). Single gene disorders causing ischaemic stroke. *J. Neurol.* 253, 685–700. doi: 10.1007/s00415-006-0048-8

Regenhardt, R. W., Das, A. S., Lo, E. H., and Caplan, L. R. (2018). Advances in understanding the pathophysiology of lacunar stroke: a review. *JAMA Neurol.* 75, 1273–1281. doi: 10.1001/jamaneurol.2018.1073

Regenhardt, R. W., Das, A. S., Ohtomo, R., Lo, E. H., Ayata, C., and Gurol, M. E. (2019). Pathophysiology of lacunar stroke: history's mysteries and modern interpretations. *J. Stroke Cerebrovasc. Dis.* 28, 2079–2097. doi: 10.1016/j.jstrokecerebrovasdis.2019.05.006

Reijmer, Y. D., van Veluw, S. J., and Greenberg, S. M. (2016). Ischemic brain injury in cerebral amyloid angiopathy. *J. Cereb. Blood Flow Metab.* 36, 40–54. doi: 10.1038/jcbfm.2015.88

Reyes, S., Viswanathan, A., Godin, O., Dufouil, C., Benisty, S., Hernandez, K., et al. (2009). Apathy: a major symptom in CADASIL. *Neurology* 72, 905–910. doi: 10.1212/01.wnl.0000344166.03470.f8

Rhodin, J. A., and Thomas, T. O. M. (2001). A vascular connection to alzheimer's disease. *Microcirculation* 8, 207–220. doi: 10.1038/sj/mn/7800086

Rice, G. I., Rodero, M. P., and Crow, Y. J. (2015). Human disease phenotypes associated with mutations in TREX1. *J. Clin. Immunol.* 35, 235–243. doi: 10.1007/s10875-015-0147-3

Ridker, P. M., Everett, B. M., Thuren, T., MacFadyen, J. G., Chang, W. H., Ballantyne, C., et al. (2017). Antiinflammatory therapy with canakinumab for atherosclerotic disease. *N. Engl. J. Med.* 377, 1119–1131. doi: 10.1056/NEJMoa1707914

Rigsby, C. S., Pollock, D. M., and Dorrance, A. M. (2007). Spironolactone improves structure and increases tone in the cerebral vasculature of male spontaneously hypertensive stroke-prone rats. *Microvasc. Res.* 73, 198–205. doi: 10.1016/j.mvr.2006.12.001

Ritchie, K., and Lovestone, S. (2002). The dementias. *Lancet* 360, 1759–1766. doi: 10.1016/S0140-6736(02)11667-9

Rizzi, L., Rosset, I., and Roriz-Cruz, M. (2014). Global epidemiology of dementia: Alzheimer's and vascular types. *Biomed Res. Int.* 2014:908915. doi: 10.1155/2014/908915

Rojas, H., Ritter, C., and Pizzol, F. D. (2011). Mechanisms of dysfunction of the blood-brain barrier in critically ill patients: emphasis on the role of matrix metalloproteinases. *Rev. Bras. Ter. Intensiva* 23, 222–227. doi: 10.1590/S0103-507X2011000200016

Rolfs, A., Fazekas, F., Grittner, U., Dichgans, M., Martus, P., Holzhausen, M., et al. (2013). Acute cerebrovascular disease in the young: the Stroke in Young Fabry Patients study. *Stroke* 44, 340–349. doi: 10.1161/STROKEAHA.112.663708

Roqué, P. J., Dao, K., and Costa, L. G. (2016). Microglia mediate diesel exhaust particle-induced cerebellar neuronal toxicity through neuroinflammatory mechanisms. *Neurotoxicology* 56, 204–214. doi: 10.1016/j.neuro.2016.08.006

Rosa, G., Giannotti, C., Martella, L., Massa, F., Serafini, G., Pardini, M., et al. (2020). Brain aging, cardiovascular diseases, mixed dementia, and frailty in the oldest old: from brain phenotype to clinical expression. *J. Alzheimers Dis.* 75, 1083–1103. doi: 10.3233/JAD-191075

Rosell, A., Cuadrado, E., Ortega-Aznar, A., Hernández-Guillamon, M., Lo, E. H., and Montaner, J. (2008). MMP-9-positive neutrophil infiltration is associated to blood-brain barrier breakdown and basal lamina type IV collagen degradation during hemorrhagic transformation after human ischemic stroke. *Stroke* 39, 1121–1126. doi: 10.1161/STROKEAHA.107.500868

Rosell, A., Ortega-Aznar, A., Alvarez-Sabín, J., Fernández-Cadenas, I., Ribó, M., Molina, C. A., et al. (2006). Increased brain expression of matrix

metalloproteinase-9 after ischemic and hemorrhagic human stroke. *Stroke* 37, 1399–1406. doi: 10.1161/01.STR.0000223001.06264.af

Rosidi, N. L., Zhou, J., Pattanaik, S., Wang, P., Jin, W., Brophy, M., et al. (2011). Cortical microhemorrhages cause local inflammation but do not trigger widespread dendrite degeneration. *PLoS One* 6:e26612. doi: 10.1371/journal.pone.0026612

Rouhl, R. P. W., Damoiseaux, J. G. M. C., Lodder, J., Theunissen, R. O. M. F. I. H., Knottnerus, I. L. H., Staals, J., et al. (2012). Vascular inflammation in cerebral small vessel disease. *Neurobiol. Aging* 33, 1800–1806. doi: 10.1016/j.neurobiolaging.2011.04.008

Rozemuller, A. J. M., Jansen, C., Carrano, A., van Haastert, E. S., Hondius, D., van der Vies, S. M., et al. (2012). Neuroinflammation and common mechanism in Alzheimer's disease and prion amyloidosis: amyloid-associated proteins, neuroinflammation and neurofibrillary degeneration. *Neurodegener. Dis.* 10, 301–304. doi: 10.1159/000335380

Ryu, J. K., and McLarnon, J. G. (2006). Minocycline or iNOS inhibition block 3-nitrotyrosine increases and blood-brain barrier leakiness in amyloid β-peptide-injected rat hippocampus. *Exp. Neurol.* 198, 552–557. doi: 10.1016/j.expneurol.2005.12.016

Ryu, J. K., Petersen, M. A., Murray, S. G., Baeten, K. M., Meyer-Franke, A., Chan, J. P., et al. (2015). Blood coagulation protein fibrinogen promotes autoimmunity and demyelination *via* chemokine release and antigen presentation. *Nat. Commun.* 6:8164. doi: 10.1038/ncomms9164

Sacco, R. L. (2000). Lobar intracerebral hemorrhage. *N. Engl. J. Med.* 342, 276–279. doi: 10.1056/NEJM200001273420410

Sachdev, P. S., Blacker, D., Blazer, D. G., Ganguli, M., Jeste, D. V., Paulsen, J. S., et al. (2014). Classifying neurocognitive disorders: the DSM-5 approach. *Nat. Rev. Neurol.* 10, 634–642. doi: 10.1038/nrneurol.2014.181

Sachdev, P. S., Brodaty, H., Valenzuela, M. J., Lorentz, L., Looi, J. C. L., Berman, K., et al. (2006). Clinical determinants of dementia and mild cognitive impairment following ischaemic stroke: the Sydney Stroke Study. *Dement. Geriatr. Cogn. Disord.* 21, 275–283. doi: 10.1159/000091434

Sachdev, P. S., Brodaty, H., Valenzuela, M. J., Lorentz, L., Looi, J. C. L., Wen, W., et al. (2004). The neuropsychological profile of vascular cognitive impairment in stroke and TIA patients. *Neurology* 62, 912–919. doi: 10.1212/01.wnl.0000115108.65264.4b

Salat, D. H., Smith, E. E., Tuch, D. S., Benner, T., Pappu, V., Schwab, K. M., et al. (2006). White matter alterations in cerebral amyloid angiopathy measured by diffusion tensor imaging. *Stroke* 37, 1759–1764. doi: 10.1161/01.STR.0000227328.86353.a7

Savva, G. M., Stephan, B. C. M., and Alzheimer's Society Vascular Dementia Systematic Review Group. (2010). Epidemiological studies of the effect of stroke on incident dementia: a systematic review. *Stroke* 41, e41–e46. doi: 10.1161/STROKEAHA.109.559880

Schiffmann, R. (2015). Fabry disease. *Handb. Clin. Neurol.* 132, 231–248. doi: 10.1016/B978-0-444-62702-5.00017-2

Schon, F., Martin, R. J., Prevett, M., Clough, C., Enevoldson, T. P., and Markus, H. S. (2003). "CADASIL coma": an underdiagnosed acute encephalopathy. *J. Neurol. Neurosurg. Psychiatry* 74, 249–252. doi: 10.1136/jnnp.74.2.249

Schultz, N., Nielsen, H. M., Minthon, L., and Wennström, M. (2014). Involvement of matrix metalloproteinase-9 in amyloid-β 1–42-induced shedding of the pericyte proteoglycan NG2. *J. Neuropathol. Exp. Neurol.* 73, 684–692. doi: 10.1097/NEN.0000000000000084

Schwartz, J., Litonjua, A., Suh, H., Verrier, M., Zanobetti, A., Syring, M., et al. (2005). Traffic related pollution and heart rate variability in a panel of elderly subjects. *Thorax* 60, 455–461. doi: 10.1136/thx.2004.024836

Shabir, O., Berwick, J., and Francis, S. E. (2018). Neurovascular dysfunction in vascular dementia, Alzheimer's and atherosclerosis. *BMC Neurosci.* 19:62. doi: 10.1186/s12868-018-0465-5

Shi, Y., and Wardlaw, J. M. (2016). Update on cerebral small vessel disease: a dynamic whole-brain disease. *Stroke Vasc. Neurol.* 1, 83–92. doi: 10.1136/svn-2016-000035

Shiga, A., Nozaki, H., Yokoseki, A., Nihonmatsu, M., Kawata, H., Kato, T., et al. (2011). Cerebral small-vessel disease protein HTRA1 controls the amount of TGF-β1 *via* cleavage of proTGF-β1. *Hum. Mol. Genet.* 20, 1800–1810. doi: 10.1093/hmg/ddr063

Shih, A. Y., Hyacinth, H. I., Hartmann, D. A., and van Veluw, S. J. (2018). Rodent models of cerebral microinfarct and microhemorrhage. *Stroke* 49, 803–810. doi: 10.1161/STROKEAHA.117.016995

Shimizu, H., Ghazizadeh, M., Sato, S., Oguro, T., and Kawanami, O. (2009). Interaction between β-amyloid protein and heparan sulfate proteoglycans from the cerebral capillary basement membrane in Alzheimer's disease. *J. Clin. Neurosci.* 16, 277–282. doi: 10.1016/j.jocn.2008.04.009

Shimotori, M., Maruyama, H., Nakamura, G., Suyama, T., Sakamoto, F., Itoh, M., et al. (2008). Novel mutations of the GLA gene in Japanese patients with Fabry disease and their functional characterization by active site specific chaperone. *Hum. Mutat.* 29:331. doi: 10.1002/humu.9520

Shoamanesh, A., Preis, S. R., Beiser, A. S., Vasan, R. S., Benjamin, E. J., Kase, C. S., et al. (2015). Inflammatory biomarkers, cerebral microbleeds and small vessel disease: framingham heart study. *Neurology* 84, 825–832. doi: 10.1212/WNL.0000000000001279

Sims, K., Politei, J., Banikazemi, M., and Lee, P. (2009). Stroke in Fabry disease frequently occurs before diagnosis and in the absence of other clinical events: natural history data from the Fabry registry. *Stroke* 40, 788–794. doi: 10.1161/STROKEAHA.108.526293

Singh-Bains, M. K., Linke, V., Austria, M. D. R., Tan, A. Y. S., Scotter, E. L., Mehrabi, N. F., et al. (2019). Altered microglia and neurovasculature in the Alzheimer's disease cerebellum. *Neurobiol. Dis.* 132:104589. doi: 10.1016/j.nbd.2019.104589

Skrobot, O. A., Black, S. E., Chen, C., DeCarli, C., Erkinjuntti, T., Ford, G. A., et al. (2018). Progress toward standardized diagnosis of vascular cognitive impairment: guidelines from the vascular impairment of cognition classification consensus study. *Alzheimers Dement.* 14, 280–292. doi: 10.1016/j.jalz.2017.09.007

Smith, E. E., Schneider, J. A., Wardlaw, J. M., and Greenberg, S. M. (2012). Cerebral microinfarcts: the invisible lesions. *Lancet Neurol.* 11, 272–282. doi: 10.1016/S1474-4422(11)70307-6

Song, B., Ao, Q., Niu, Y., Shen, Q., Zuo, H., Zhang, X., et al. (2013). Amyloid β-peptide worsens cognitive impairment following cerebral ischemia-reperfusion injury. *Neural Regen. Res.* 8, 2449–2457. doi: 10.3969/j.issn.1673-5374.2013.26.006

Soontornniyomkij, V., Lynch, M. D., Mermash, S., Pomakian, J., Badkoobehi, H., Clare, R., et al. (2010). Cerebral microinfarcts associated with severe cerebral β-amyloid angiopathy. *Brain Pathol.* 20, 459–467. doi: 10.1111/j.1750-3639.2009.00322.x

Spangenberg, E., Severson, P. L., Hohsfield, L. A., Crapser, J., Zhang, J., Burton, E. A., et al. (2019). Sustained microglial depletion with CSF1R inhibitor impairs parenchymal plaque development in an Alzheimer's disease model. *Nat. Commun.* 10:3758. doi: 10.1038/s41467-019-11674-z

Spann, N. J., Garmire, L. X., McDonald, J. G., Myers, D. S., Milne, S. B., Shibata, N., et al. (2012). Regulated accumulation of desmosterol integrates macrophage lipid metabolism and inflammatory responses. *Cell* 151, 138–152. doi: 10.1016/j.cell.2012.06.054

Srinivasan, K., Friedman, B. A., Etxeberria, A., Huntley, M. A., van der Brug, M. P., Foreman, O., et al. (2020). Alzheimer's patient microglia exhibit enhanced aging and unique transcriptional activation. *Cell Rep.* 31:107843. doi: 10.1016/j.celrep.2020.107843

Stam, A. H., Kothari, P. H., Shaikh, A., Gschwendter, A., Jen, J. C., Hodgkinson, S., et al. (2016). Retinal vasculopathy with cerebral leukoencephalopathy and systemic manifestations. *Brain* 139, 2909–2922. doi: 10.1093/brain/aww217

Staszewski, J., Piusińska-Macoch, R., Brodacki, B., Skrobowska, E., Macek, K., and Stepień, A. (2017). Risk of vascular events in different manifestations of cerebral small vessel disease: a 2-year follow-up study with a control group. *Heliyon* 3:e00455. doi: 10.1016/j.heliyon.2017.e00455

Stemme, S., Faber, B., Holm, J., Wiklund, O., Witztum, J. L., and Hansson, G. K. (1995). T lymphocytes from human atherosclerotic plaques recognize oxidized low density lipoprotein. *Proc. Natl. Acad. Sci. U S A* 92, 3893–3897. doi: 10.1073/pnas.92.9.3893

Stomrud, E., Björkqvist, M., Janciauskiene, S., Minthon, L., and Hansson, O. (2010). Alterations of matrix metalloproteinases in the healthy elderly with increased risk of prodromal Alzheimer's disease. *Alzheimers Res. Ther.* 2:20. doi: 10.1186/alzrt44

Su, J. H., Cummings, B. J., and Cotman, C. W. (1992). Localization of heparan sulfate glycosaminoglycan and proteoglycan core protein in aged brain and Alzheimer's disease. *Neuroscience* 51, 801–813. doi: 10.1016/0306-4522(92)90521-3

Summers, P. M., Hartmann, D. A., Hui, E. S., Nie, X., Deardorff, R. L., McKinnon, E. T., et al. (2017). Functional deficits induced by cortical microinfarcts. *J. Cereb. Blood Flow Metab.* 37, 3599–3614. doi: 10.1177/0271678X16685573

Sweeney, M. D., Sagare, A. P., Pachicano, M., Harrington, M. G., Joe, E., Chui, H. C., et al. (2020). A novel sensitive assay for detection of a biomarker of pericyte injury in cerebrospinal fluid. *Alzheimers Dement.* 16, 821–830. doi: 10.1002/alz.12061

Szarmach, A., Halena, G., Kaszubowski, M., Piskunowicz, M., Studniarek, M., Lass, P., et al. (2017). Carotid artery stenting and blood-brain barrier permeability in subjects with chronic carotid artery stenosis. *Int. J. Mol. Sci.* 18:1008. doi: 10.3390/ijms18051008

Tabas, I., García-Cardeña, G., and Owens, G. K. (2015). Recent insights into the cellular biology of atherosclerosis. *J. Cell Biol.* 209, 13–22. doi: 10.1083/jcb.201412052

Tabas, I., Williams, K. J., and Borén, J. (2007). Subendothelial lipoprotein retention as the initiating process in atherosclerosis: update and therapeutic implications. *Circulation* 116, 1832–1844. doi: 10.1161/CIRCULATIONAHA.106.676890

Tan, R. Y. Y., and Markus, H. S. (2016). CADASIL: migraine, encephalopathy, stroke and their inter-relationships. *PLoS One* 11:e0157613. doi: 10.1371/journal.pone.0157613

Tan, R., Traylor, M., Rutten-Jacobs, L., and Markus, H. (2017). New insights into mechanisms of small vessel disease stroke from genetics. *Clin. Sci.* 131, 515–531. doi: 10.1042/CS20160825

Tancredi, V., D'Antuono, M., Cafè, C., Giovedì, S., Buè, M. C., D'Arcangelo, G., et al. (2000). The inhibitory effects of interleukin-6 on synaptic plasticity in the rat hippocampus are associated with an inhibition of mitogen-activated protein kinase ERK. *J. Neurochem.* 75, 634–643. doi: 10.1046/j.1471-4159.2000.0750634.x

Tariq, S., and Barber, P. A. (2018). Dementia risk and prevention by targeting modifiable vascular risk factors. *J. Neurochem.* 144, 565–581. doi: 10.1111/jnc.14132

Tarkowski, E., Issa, R., Sjögren, M., Wallin, A., Blennow, K., Tarkowski, A., et al. (2002). Increased intrathecal levels of the angiogenic factors VEGF and TGF-β in Alzheimer's disease and vascular dementia. *Neurobiol. Aging* 23, 237–243. doi: 10.1016/s0197-4580(01)00285-8

Taylor, X., Cisternas, P., You, Y., You, Y., Xiang, S., Marambio, Y., et al. (2020). A1 reactive astrocytes and a loss of TREM2 are associated with an early stage of pathology in a mouse model of cerebral amyloid angiopathy. *J. Neuroinflammation* 17:223. doi: 10.1186/s12974-020-01900-7

Tennstaedt, A., Pöpsel, S., Truebestein, L., Hauske, P., Brockmann, A., Schmidt, N., et al. (2012). Human high temperature requirement serine protease A1 (HTRA1) degrades tau protein aggregates. *J. Biol. Chem.* 287, 20931–20941. doi: 10.1074/jbc.M111.316232

Ter Telgte, A., van Leijsen, E. M. C., Wiegertjes, K., Klijn, C. J. M., Tuladhar, A. M., and de Leeuw, F.-E. (2018). Cerebral small vessel disease: from a focal to a global perspective. *Nat. Rev. Neurol.* 14, 387–398. doi: 10.1038/s41582-018-0014-y

Thal, D. R., Ghebremedhin, E., Orantes, M., and Wiestler, O. D. (2003). Vascular pathology in Alzheimer disease: correlation of cerebral amyloid angiopathy and arteriosclerosis/lipohyalinosis with cognitive decline. *J. Neuropathol. Exp. Neurol.* 62, 1287–1301. doi: 10.1093/jnen/62.12.1287

Thériault, P., ElAli, A., and Rivest, S. (2015). The dynamics of monocytes and microglia in Alzheimer's disease. *Alzheimers Res. Ther.* 7:41. doi: 10.1186/s13195-015-0125-2

Thiel, A., Cechetto, D. F., Heiss, W.-D., Hachinski, V., and Whitehead, S. N. (2014). Amyloid burden, neuroinflammation and links to cognitive decline after ischemic stroke. *Stroke* 45, 2825–2829. doi: 10.1161/STROKEAHA.114.004285

Thomson, E. M., Kumarathasan, P., Calderón-Garcidueñas, L., and Vincent, R. (2007). Air pollution alters brain and pituitary endothelin-1 and inducible nitric oxide synthase gene expression. *Environ. Res.* 105, 224–233. doi: 10.1016/j.envres.2007.06.005

Tiaden, A. N., and Richards, P. J. (2013). The emerging roles of HTRA1 in musculoskeletal disease. *Am. J. Pathol.* 182, 1482–1488. doi: 10.1016/j.ajpath.2013.02.003

Toth, P., Tarantini, S., Csiszar, A., and Ungvari, Z. (2017). Functional vascular contributions to cognitive impairment and dementia: mechanisms and consequences of cerebral autoregulatory dysfunction, endothelial impairment and neurovascular uncoupling in aging. *Am. J. Physiol. Heart Circ. Physiol.* 312, H1–H20. doi: 10.1152/ajpheart.00581.2016

Tuominen, S., Miao, Q., Kurki, T., Tuisku, S., Pöyhönen, M., Kalimo, H., et al. (2004). Positron emission tomography examination of cerebral blood flow and glucose metabolism in young CADASIL patients. *Stroke* 35, 1063–1067. doi: 10.1161/01.STR.0000124124.69842.2d

Uemura, M. T., Ihara, M., Maki, T., Nakagomi, T., Kaji, S., Uemura, K., et al. (2018). Pericyte-derived bone morphogenetic protein 4 underlies white matter damage after chronic hypoperfusion. *Brain Pathol.* 28, 521–535. doi: 10.1111/bpa.12523

Uemura, M. T., Maki, T., Ihara, M., Lee, V. M. Y., and Trojanowski, J. Q. (2020). Brain microvascular pericytes in vascular cognitive impairment and dementia. *Front. Aging Neurosci.* 12:80. doi: 10.3389/fnagi.2020.00080

Ueno, M., Tomimoto, H., Akiguchi, I., Wakita, H., and Sakamoto, H. (2002). Blood-brain barrier disruption in white matter lesions in a rat model of chronic cerebral hypoperfusion. *J. Cereb. Blood Flow Metab.* 22, 97–104. doi: 10.1097/00004647-200201000-00012

Ukraintseva, S., Sloan, F., Arbeev, K., and Yashin, A. (2006). Increasing rates of dementia at time of declining mortality from stroke. *Stroke* 37, 1155–1159. doi: 10.1161/01.STR.0000217971.88034.e9

Underly, R. G., Levy, M., Hartmann, D. A., Grant, R. I., Watson, A. N., and Shih, A. Y. (2017). Pericytes as inducers of rapid, matrix metalloproteinase-9-dependent capillary damage during ischemia. *J. Neurosci.* 37, 129–140. doi: 10.1523/JNEUROSCI.2891-16.2016

Vahedi, K., and Alamowitch, S. (2011). Clinical spectrum of type IV collagen (COL4A1) mutations: a novel genetic multisystem disease. *Curr. Opin. Neurol.* 24, 63–68. doi: 10.1097/WCO.0b013e32834232c6

Vahedi, K., Chabriat, H., Levy, C., Joutel, A., Tournier-Lasserve, E., and Bousser, M.-G. (2004). Migraine with aura and brain magnetic resonance imaging abnormalities in patients with CADASIL. *Arch. Neurol.* 61, 1237–1240. doi: 10.1001/archneur.61.8.1237

Valenti, R., Pescini, F., Antonini, S., Castellini, G., Poggesi, A., Bianchi, S., et al. (2011). Major depression and bipolar disorders in CADASIL: a study using the DSM-IV semi-structured interview. *Acta Neurol. Scand.* 124, 390–395. doi: 10.1111/j.1600-0404.2011.01512.x

Valenti, R., Poggesi, A., Pescini, F., Inzitari, D., and Pantoni, L. (2008). Psychiatric disturbances in CADASIL: a brief review. *Acta Neurol. Scand.* 118, 291–295. doi: 10.1111/j.1600-0404.2008.01015.x

van der Flier, W. M., van Straaten, E. C. W., Barkhof, F., Verdelho, A., Madureira, S., Pantoni, L., et al. (2005). Small vessel disease and general cognitive function in nondisabled elderly: the LADIS study. *Stroke* 36, 2116–2120. doi: 10.1161/01.STR.0000179092.59909.42

van Veluw, S. J., Shih, A. Y., Smith, E. E., Chen, C., Schneider, J. A., Wardlaw, J. M., et al. (2017). Detection, risk factors and functional consequences of cerebral microinfarcts. *Lancet Neurol.* 16, 730–740. doi: 10.1016/S1474-4422(17)30196-5

Venkat, P., Chopp, M., and Chen, J. (2015). Models and mechanisms of vascular dementia. *Exp. Neurol.* 272, 97–108. doi: 10.1016/j.expneurol.2015.05.006

Verdura, E., Hervé, D., Bergametti, F., Jacquet, C., Morvan, T., Prieto-Morin, C., et al. (2016). Disruption of a miR-29 binding site leading to COL4A1 upregulation causes pontine autosomal dominant microangiopathy with leukoencephalopathy. *Ann. Neurol.* 80, 741–753. doi: 10.1002/ana.24782

Verghese, P. B., Castellano, J. M., Garai, K., Wang, Y., Jiang, H., Shah, A., et al. (2013). ApoE influences amyloid-β (Aβ) clearance despite minimal apoE/Aβ association in physiological conditions. *Proc. Natl. Acad. Sci. U S A* 110, E1807–E1816. doi: 10.1073/pnas.1220484110

Vidal, R., Barbeito, A. G., Miravalle, L., and Ghetti, B. (2009). Cerebral amyloid angiopathy and parenchymal amyloid deposition in transgenic mice expressing the Danish mutant form of human BRI2. *Brain Pathol.* 19, 58–68. doi: 10.1111/j.1750-3639.2008.00164.x

Vidal, R., Frangione, B., Rostagno, A., Mead, S., Révész, T., Plant, G., et al. (1999). A stop-codon mutation in the BRI gene associated with familial British dementia. *Nature* 399, 776–781. doi: 10.1038/21637

Vidal, R., Revesz, T., Rostagno, A., Kim, E., Holton, J. L., Bek, T., et al. (2000). A decamer duplication in the 3′ region of the BRI gene originates an amyloid

peptide that is associated with dementia in a Danish kindred. *Proc. Natl. Acad. Sci. U S A* 97, 4920–4925. doi: 10.1073/pnas.080076097

Wang, B.-R., Shi, J.-Q., Ge, N.-N., Ou, Z., Tian, Y.-Y., Jiang, T., et al. (2018). PM2.5 exposure aggravates oligomeric amyloid β-induced neuronal injury and promotes NLRP3 inflammasome activation in an *in vitro* model of Alzheimer's disease. *J. Neuroinflammation* 15:132. doi: 10.1186/s12974-018-1178-5

Wang, T., Wang, L., Moreno-Vinasco, L., Lang, G. D., Siegler, J. H., Mathew, B., et al. (2012). Particulate matter air pollution disrupts endothelial cell barrier *via* calpain-mediated tight junction protein degradation. *Part. Fibre Toxicol.* 9:35. doi: 10.1186/1743-8977-9-35

Wang, L., Yang, J.-W., Lin, L.-T., Huang, J., Wang, X.-R., Su, X.-T., et al. (2020). Acupuncture attenuates inflammation in microglia of vascular dementia rats by inhibiting miR-93-mediated TLR4/MyD88/NF-κB signaling pathway. *Oxid. Med. Cell. Longev.* 2020:8253904. doi: 10.1155/2020/8253904

Wardlaw, J. M., Smith, E., Biessels, G. J., Cordonnier, C., Fazekas, F., Frayne, R., et al. (2013). Neuroimaging standards for research into small vessel disease and its contribution to ageing and neurodegeneration. *Lancet Neurol.* 12, 822–838. doi: 10.1016/S1474-4422(13)70124-8

Weber, C., and Noels, H. (2011). Atherosclerosis: current pathogenesis and therapeutic options. *Nat. Med.* 17, 1410–1422. doi: 10.1038/nm.2538

Weller, R. O., Subash, M., Preston, S. D., Mazanti, I., and Carare, R. O. (2008). Perivascular drainage of amyloid-β peptides from the brain and its failure in cerebral amyloid angiopathy and Alzheimer's disease. *Brain Pathol.* 18, 253–266. doi: 10.1111/j.1750-3639.2008.00133.x

Woodward, N. C., Levine, M. C., Haghani, A., Shirmohammadi, F., Saffari, A., Sioutas, C., et al. (2017a). Toll-like receptor 4 in glial inflammatory responses to air pollution *in vitro* and *in vivo*. *J. Neuroinflammation* 14:84. doi: 10.1186/s12974-017-0858-x

Woodward, N. C., Pakbin, P., Saffari, A., Shirmohammadi, F., Haghani, A., Sioutas, C., et al. (2017b). Traffic-related air pollution impact on mouse brain accelerates myelin and neuritic aging changes with specificity for CA1 neurons. *Neurobiol. Aging* 53, 48–58. doi: 10.1016/j.neurobiolaging.2017.01.007

Wu, Y.-C., Lin, Y.-C., Yu, H.-L., Chen, J.-H., Chen, T.-F., Sun, Y., et al. (2015). Association between air pollutants and dementia risk in the elderly. *Alzheimers Dement.* 1, 220–228. doi: 10.1016/j.dadm.2014.11.015

Wyss-Coray, T., Lin, C., Sanan, D. A., Mucke, L., and Masliah, E. (2000). Chronic overproduction of transforming growth factor-β1 by astrocytes promotes Alzheimer's disease-like microvascular degeneration in transgenic mice. *Am. J. Pathol.* 156, 139–150. doi: 10.1016/s0002-9440(10)64713-x

Yamada, M., and Naiki, H. (2012). Cerebral amyloid angiopathy. *Prog. Mol. Biol. Transl. Sci.* 107, 41–78. doi: 10.1016/B978-0-12-385883-2.00006-0

Yamamoto, Y., Craggs, L., Baumann, M., Kalimo, H., and Kalaria, R. N. (2011). Review: molecular genetics and pathology of hereditary small vessel diseases of the brain. *Neuropathol. Appl. Neurobiol.* 37, 94–113. doi: 10.1111/j.1365-2990.2010.01147.x

Yamamoto, Y., Craggs, L. J. L., Watanabe, A., Booth, T., Attems, J., Low, R. W. C., et al. (2013). Brain microvascular accumulation and distribution of the NOTCH3 ectodomain and granular osmiophilic material in CADASIL. *J. Neuropathol. Exp. Neurol.* 72, 416–431. doi: 10.1097/NEN.0b013e31829020b5

Yang, C., Hawkins, K. E., Doré, S., and Candelario-Jalil, E. (2019). Neuroinflammatory mechanisms of blood-brain barrier damage in ischemic stroke. *Am. J. Physiol. Cell Physiol.* 316, C135–C153. doi: 10.1152/ajpcell.00136.2018

Yang, Y., and Rosenberg, G. A. (2011). Blood-brain barrier breakdown in acute and chronic cerebrovascular disease. *Stroke* 42, 3323–3328. doi: 10.1161/STROKEAHA.110.608257

Yang, J., Zhang, R., Shi, C., Mao, C., Yang, Z., Suo, Z., et al. (2017). AQP4 association with amyloid deposition and astrocyte pathology in the Tg-arcswe mouse model of Alzheimer's disease. *J. Alzheimers Dis.* 57, 157–169. doi: 10.3233/JAD-160957

Yeh, F. L., Wang, Y., Tom, I., Gonzalez, L. C., and Sheng, M. (2016). TREM2 binds to apolipoproteins, including APOE and CLU/APOJ and thereby facilitates uptake of amyloid-β by microglia. *Neuron* 91, 328–340. doi: 10.1016/j.neuron.2016.06.015

Yin, F., Lawal, A., Ricks, J., Fox, J. R., Larson, T., Navab, M., et al. (2013). Diesel exhaust induces systemic lipid peroxidation and development of dysfunctional pro-oxidant and pro-inflammatory high-density lipoprotein. *Arterioscler. Thromb. Vasc. Biol.* 33, 1153–1161. doi: 10.1161/ATVBAHA.112.300552

Youmans, K. L., Tai, L. M., Nwabuisi-Heath, E., Jungbauer, L., Kanekiyo, T., Gan, M., et al. (2012). APOE4-specific changes in Aβ accumulation in a new transgenic mouse model of Alzheimer disease. *J. Biol. Chem.* 287, 41774–41786. doi: 10.1074/jbc.M112.407957

Zhan, X., Cox, C., Ander, B. P., Liu, D., Stamova, B., Jin, L.-W., et al. (2015). Inflammation combined with ischemia produces myelin injury and plaque-like aggregates of myelin, amyloid-β and AβPP in adult rat brain. *J. Alzheimers Dis.* 46, 507–523. doi: 10.3233/JAD-143072

Zhang, F., Eckman, C., Younkin, S., Hsiao, K. K., and Iadecola, C. (1997). Increased susceptibility to ischemic brain damage in transgenic mice overexpressing the amyloid precursor protein. *J. Neurosci.* 17, 7655–7661. doi: 10.1523/JNEUROSCI.17-20-07655.1997

Zhang, D., Li, S., Hou, L., Jing, L., Ruan, Z., Peng, B., et al. (2021). Microglial activation contributes to cognitive impairments in rotenone-induced mouse Parkinson's disease model. *J. Neuroinflammation* 18:4. doi: 10.1186/s12974-020-02065-z

Zhang, L., Lim, S. L., Du, H., Zhang, M., Kozak, I., Hannum, G., et al. (2012). High temperature requirement factor A1 (HTRA1) gene regulates angiogenesis through transforming growth factor-β family member growth differentiation factor 6. *J. Biol. Chem.* 287, 1520–1526. doi: 10.1074/jbc.M111.275990

Zhang, L.-Y., Pan, J., Mamtilahun, M., Zhu, Y., Wang, L., Venkatesh, A., et al. (2020). Microglia exacerbate white matter injury *via* complement C3/C3aR pathway after hypoperfusion. *Theranostics* 10, 74–90. doi: 10.7150/thno.35841

Zhang, C. E., Wong, S. M., van de Haar, H. J., Staals, J., Jansen, J. F. A., Jeukens, C. R. L. P. N., et al. (2017). Blood-brain barrier leakage is more widespread in patients with cerebral small vessel disease. *Neurology* 88, 426–432. doi: 10.1212/WNL.0000000000003556

Zhong, C., Bu, X., Xu, T., Guo, L., Wang, X., Zhang, J., et al. (2018). Serum matrix metalloproteinase-9 and cognitive impairment after acute ischemic stroke. *J. Am. Heart Assoc.* 7:e007776. doi: 10.1161/JAHA.117.007776

Zhong, C., Yang, J., Xu, T., Xu, T., Peng, Y., Wang, A., et al. (2017). Serum matrix metalloproteinase-9 levels and prognosis of acute ischemic stroke. *Neurology* 89, 805–812. doi: 10.1212/WNL.0000000000004257

Zhao, S.-C., Ma, L.-S., Chu, Z.-H., Xu, H., Wu, W.-Q., and Liu, F. (2017). Regulation of microglial activation in stroke. *Acta Pharmacol. Sin.* 38, 445–458. doi: 10.1038/aps.2016.162

Zhao, B.-Q., Wang, S., Kim, H.-Y., Storrie, H., Rosen, B. R., Mooney, D. J., et al. (2006). Role of matrix metalloproteinases in delayed cortical responses after stroke. *Nat. Med.* 12, 441–445. doi: 10.1038/nm1387

Zlokovic, B. V. (2008). The blood-brain barrier in health and chronic neurodegenerative disorders. *Neuron* 57, 178–201. doi: 10.1016/j.neuron.2008.01.003

Zlokovic, B. V. (2011). Neurovascular pathways to neurodegeneration in Alzheimer's disease and other disorders. *Nat. Rev. Neurosci.* 12, 723–738. doi: 10.1038/nrn3114

Conflict of Interest: The authors declare that the research was conducted in the absence of any commercial or financial relationships that could be construed as a potential conflict of interest.

Publisher's Note: All claims expressed in this article are solely those of the authors and do not necessarily represent those of their affiliated organizations, or those of the publisher, the editors and the reviewers. Any product that may be evaluated in this article, or claim that may be made by its manufacturer, is not guaranteed or endorsed by the publisher.

frontiers in Aging Neuroscience

ORIGINAL RESEARCH
published: 06 October 2021
doi: 10.3389/fnagi.2021.728007

Neurovascular Coupling Is Impaired in Hypertensive and Diabetic Subjects Without Symptomatic Cerebrovascular Disease

Ana Monteiro[1,2]*, *Pedro Castro*[1,3], *Gilberto Pereira*[1,3], *Carmen Ferreira*[1,3], *Farzaneh Sorond*[4], *Andrew Milstead*[4], *James P. Higgins*[5], *Jorge Polónia*[6,7] and *Elsa Azevedo*[1,3]

[1] Department of Clinical Neurosciences and Mental Health, Faculty of Medicine of University of Porto, Porto, Portugal, [2] Department of Neurology, Unidade Local de Saúde de Matosinhos, Matosinhos, Portugal, [3] Department of Neurology, Centro Hospitalar Universitário de São João, Porto, Portugal, [4] Department of Neurology, Division of Stroke and Neurocritical, Northwestern University Feinberg School of Medicine, Chicago, IL, United States, [5] Department of Radiology, Northwestern University Feinberg School of Medicine, Chicago, IL, United States, [6] Hypertension Unit, Unidade Local de Saúde de Matosinhos, Matosinhos, Portugal, [7] Department of Medicine, Faculty of Medicine of University of Porto, Porto, Portugal

The mechanistic link between hypertension, diabetes and cerebral small vessel disease (CSVD) is still poorly understood. We hypothesized that hypertension and diabetes could impair cerebrovascular regulation prior to irreversibly established cerebrovascular disease. In this study, 52 hypertensive patients [54% males; age 64 ± 11 years; 58% with comorbid diabetes mellitus (DM)] without symptomatic cerebrovascular disease underwent transcranial Doppler (TCD) monitoring in the middle (MCA) and posterior (PCA) cerebral arteries, to assess vasoreactivity to carbon dioxide ($VRCO_2$) and neurovascular coupling (NVC). 1.5T magnetic resonance imaging was also performed and white matter hyperintensity volume was automatically segmented from FLAIR sequences. TCD data from 17 healthy controls were obtained for comparison (47% males; age 60 ± 16 years). Hypertensive patients showed significant impairment of NVC in the PCA, with reduced increment in cerebral blood flow velocity during visual stimulation (22.4 ± 9.2 vs. 31.6 ± 5.7, $p < 0.001$), as well as disturbed NVC time-varying properties, with slower response (lower rate time: 0.00 ± 0.02 vs. 0.03 ± 6.81, $p = 0.001$), and reduced system oscillation (reduced natural frequency: 0.18 ± 0.08 vs. 0.22 ± 0.06, $p < 0.001$), when compared to controls. $VRCO_2$ remained relatively preserved in MCA and PCA. These results were worse in hypertensive diabetic patients, with lower natural frequency ($p = 0.043$) than non-diabetic patients. White matter disease burden did not predict worse NVC. These findings suggest that hypertensive diabetic patients may have a precocious impairment of NVC, already occurring without symptomatic CSVD. Future research is warranted to evaluate whether NVC assessment could be useful as an early, non-invasive, surrogate marker for CSVD.

Keywords: hypertension, diabetes mellitus, neurovascular coupling (NVC), transcranial doppler (TCD), cerebral small vessel disease

OPEN ACCESS

Edited by:
Anusha Mishra, Oregon Health and Science University, United States

Reviewed by:
Eszter Farkas, University of Szeged, Hungary
Kazuto Masamoto, The University of Electro-Communications, Japan

***Correspondence:**
Ana Monteiro
up201308689@up.pt

Received: *20 June 2021*
Accepted: *31 August 2021*
Published: *06 October 2021*

Citation:
Monteiro A, Castro P, Pereira G, Ferreira C, Sorond F, Milstead A, Higgins JP, Polónia J and Azevedo E (2021) Neurovascular Coupling Is Impaired in Hypertensive and Diabetic Subjects Without Symptomatic Cerebrovascular Disease. Front. Aging Neurosci. 13:728007. doi: 10.3389/fnagi.2021.728007

INTRODUCTION

Cerebral small vessel disease (CSVD) has an enormous impact on public health worldwide (GBD 2017 Causes of Death Collaborators, 2018). It accounts for 25% of ischemic strokes and most hemorrhagic strokes and is the second leading cause for cognitive decline (Sudlow and Warlow, 1997; Iadecola et al., 2019).

Hypertension (HT) is the major vascular risk factor (VRF) for CSVD. Alongside HT, diabetes mellitus (DM) is a recognized VRF implicated in CSVD (Brundel et al., 2012; Liu et al., 2018).

While other etiologies for stroke are fairly well-studied, the pathophysiology and causality of CSVD are still poorly understood. Many of its manifestations are clinically silent until the development of clinical consequences, with stroke, cognitive decline, and gait impairment, limiting disease-specific preventive strategies (Pantoni, 2010). Also, CSVD radiological markers and clinical manifestations seem to be dissociated, for reasons not fully explained (Sorond et al., 2011; Jokumsen-Cabral et al., 2019). Biomarkers for the events predating irreversible damage could be key for better clinical management and pre-symptomatic preventive measures.

There is evidence of neurovascular dysfunction in CSVD and it may precede clinical and imaging manifestations (Wardlaw, 2010; Freeze et al., 2018; Castro et al., 2020). Very few studies have investigated neurovascular coupling (NVC) in HT, mostly using imaging modalities. Transcranial Doppler (TCD) is a non-invasive method that allows the monitoring of microvascular hemodynamic functional integrity (Claassen et al., 2016; Malojcic et al., 2017).

We aimed to study cerebrovascular regulation by TCD in hypertensive and diabetic patients without major CSVD-related impairment as a possible surrogate marker for the future development of symptomatic CSVD, to help guide therapies aimed at the cerebral microcirculation and neurovascular unit.

MATERIALS AND METHODS

Study Subjects

A cross-sectional observational study was conducted in a University Hospital. Hypertensive patients were recruited from the hospital's Hypertension Unit. Exclusion criteria were previous stroke or other significant brain pathology (dementia by clinical criteria, brain tumor, traumatic brain injury, previous cerebral infection or neurodegenerative disease), severe/unstable disease, contraindication for magnetic resonance imaging (MRI), inadequate acoustic temporal bone window, extra- or intracranial artery stenosis >50% and incapability to collaborate or to give informed consent. TCD data from healthy controls of similar age and gender were obtained from previous studies performed with the same protocol (Jokumsen-Cabral et al., 2019).

The local ethics committee approved the study protocol, which followed the tenets of the Declaration of Helsinki. Written informed consent was obtained.

Clinical Evaluation

Participant's clinical and demographic data were recorded. Vascular comorbidities were summarized into a vascular comorbidity score (VCS), including HT, DM, dyslipidemia, tobacco usage, chronic heart failure, coronary heart disease, arrhythmias, peripheral artery disease, and nephropathy. These conditions were scored as present (1 point) or absent (0 points), for a score ranging from 0 to 9 (Mossello et al., 2015). All participants underwent cervical and transcranial Doppler ultrasound (Philips iu22, The Nederlands) to exclude hemodynamically significant vessel pathology. The patients underwent routine 24-h ambulatory blood pressure monitoring (Spacelabs 90207, Redmond, Washington, USA). The mini-mental state examination (MMSE) and the Montreal cognitive assessment (MoCA) were used to screen for dementia. The patients were evaluated by an ophthalmologist, and all had normal binocular visual acuity, allowing for the TCD dynamic testing.

Monitoring Protocol

Evaluations were conducted in a dim-lighted, quiet room ($\simeq$22°C), in a supine position. Cerebral blood flow velocity (CBFV) was continuously recorded in the M1 segment of the right middle cerebral artery (MCA) and the P2 segment of the left posterior cerebral artery (PCA), with 2-MHz TCD probes secured with a headframe (Doppler BoxX, DWL, Singen, Germany), in order to simultaneously obtain data from both arterial territories (Azevedo et al., 2012). Continuous non-invasive arterial blood pressure (BP) was measured with the Finometer (FMS, Amsterdam, The Netherlands). Heart rate was assessed with a three-lead electrocardiogram. End-tidal carbon dioxide ($EtCO_2$) was recorded by capnography (Respsense Nonin, Amsterdam, The Netherlands). Data was synchronized and digitally stored at 400 Hz with Powerlab (AD Instruments, Oxford, UK) for offline analysis. After resting for 20 min, the vasoreactivity to carbon dioxide ($VRCO_2$) and NVC protocols were performed, as described below. CBFV envelopes were continuously registered and analyzed offline.

$VRCO_2$

Participants were monitored through successive 2-min steps of resting, inhalation of a mixture of 5% CO_2 and 95% O_2 mixture ($EtCO_2$ 7–10 mmHg above baseline), resting (room air, until normocapnia) and hyperventilation ($EtCO_2$ 7–10 mmHg below baseline). $VRCO_2$ was calculated as the slope of the relationship between $EtCO_2$ average values plotted against those of relative CBFV achieved at the three stages, expressed as % mean CBFV per mmHg $EtCO_2$ (Madureira et al., 2017).

NVC

NVC was assessed in the PCA territory by a visual paradigm consisting of 10 cycles, each with a 20s resting phase (eyes closed) and 40 s stimulating phase (flickering checkerboard) at 10 Hz (Rosengarten et al., 2001a). The 5s of stable measurement prior to stimulation were used as the baseline (Rosengarten et al., 2001a). All cycles were synchronized and averaged. Peak systolic data was used because it is less prone to artifacts (Rosengarten

et al., 2001b). Maximal systolic CBFV change was obtained to calculate the overshoot parameter as $\frac{maximumCBFV-baselineCBFV}{baselineCBFV} \times 100\%$.[12] The systolic CBFV curve was modeled into a second order linear system to describe the dynamics of NVC response in time according to the equation $G(s) = \frac{K \times (1+Tvs)}{\frac{s2}{\omega 2}+2\xi*\frac{s}{\omega}+1}$, where "K" stands for gain, "Tv" for rate time, "ω" for natural frequency, and "ξ" for attenuation (Rosengarten et al., 2001a). All the parameters of the equation were determined by the least squares method. The sum of the squared residuals and the χ2 were also calculated to ensure the goodness of fit into the real measured values, as provided by the lsqnonlin function. Gain describes the relative

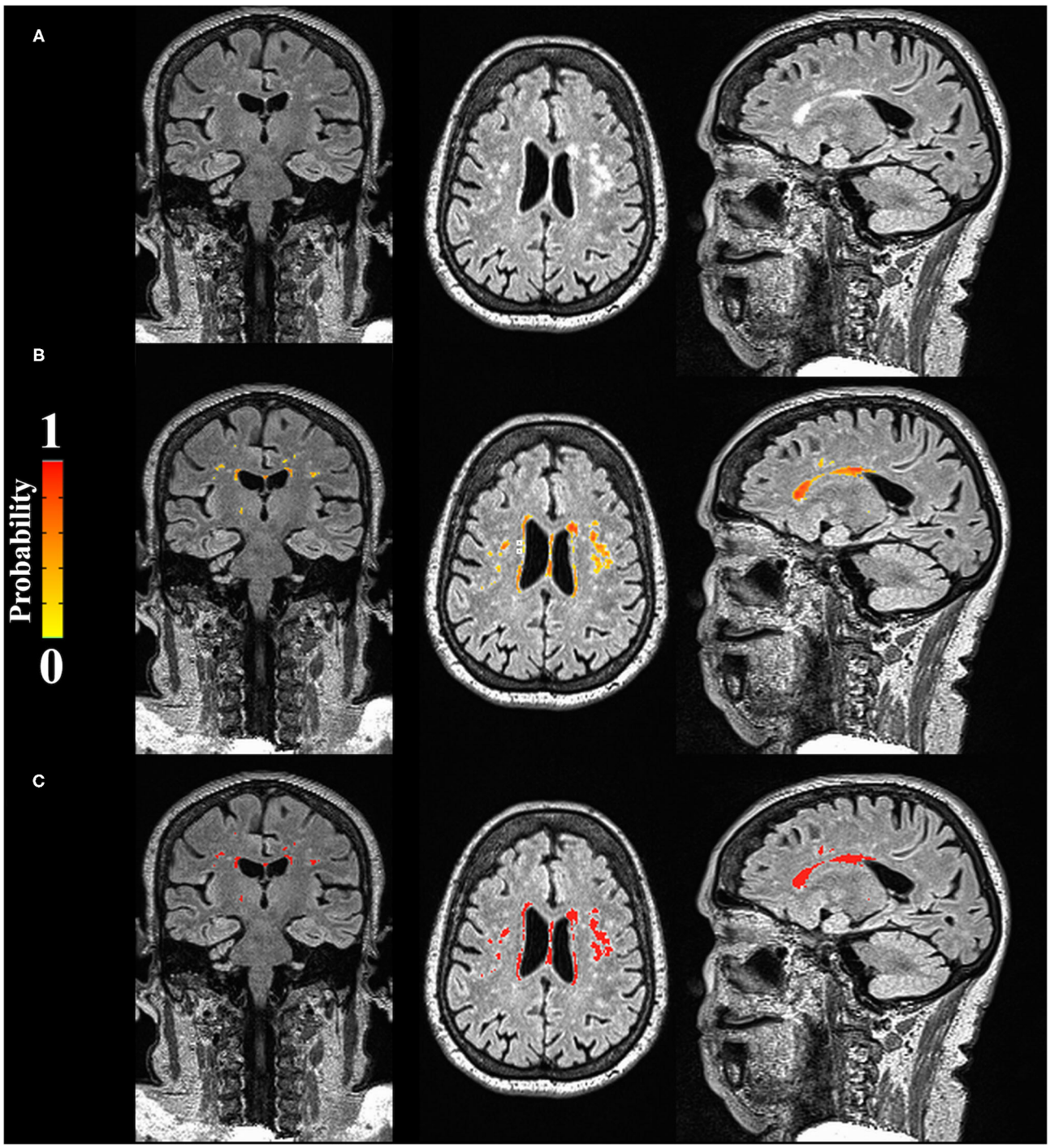

FIGURE 1 | Automatic segmentation of WMH **(A)** Raw data; **(B)** Probability map of WMH; **(C)** Binarized results of WMH (values above 0 were considered WMH).

CBFV difference between rest and steady-state level during visual stimulation; rate time indicates the initial steepness of the CBFV increase; natural frequency represents the oscillatory properties of the system; and attenuation describes dampening and tonus features, such as elastic properties of the vessel wall (Rosengarten et al., 2003). For this specific test, the MCA recordings were used as a control to detect non-specific changes in CBFV during the visual stimulation task.

MRI Imaging

Forty-six patients were eligible and agreed to undergo cerebral MRI (Siemens Aera 1.5T). Of these, data from 6 patients were excluded for lack of quality for the evaluations. White matter hyperintensity (WMH) volumes normalized by intracranial volume were derived from the T2-weighted fluid-attenuated inversion recovery sequences collected in the sagittal plane. Voxels resolution was 1 x 1 x 1, slices = 256, FOV = 256 mm, TR = 5000 ms, TE = 336 ms, TI = 1800 ms (**Figure 1**). Briefly, WMH masks were created using the Lesion Segmentation Algorithm (LPA, 1) from the Lesion Segmentation Toolbox for SPM12 in MATLAB R2018a. Following an initial segmentation of the FLAIR image, probability maps were binarized using AFNI (2,3, v21.0.15) command 3dcalc. Resulting segmentations were quality-checked for sufficient accuracy and volumes were calculated using Freesurfer (v7.1) command mri_segstats.

Additional signs of CSVD were evaluated by an experienced vascular Neurologist to further characterize the CSVD in the patient cohort. Enlarged perivascular spaces (PVS) were defined as small (<0.3 mm) punctate or linear (if perpendicular or longitudinal to the plane of the scan, respectively) hyperintensities on T2 images in the basal ganglia (BG) and centrum semiovale (CS) (Potter et al., 2015). The PVS burden was then stratified into three groups: <11, 11–20 and >20 (Lau et al., 2017). Lacunes were defined as rounded or ovoid lesions >3 mm and <20 mm in diameter in the BG, internal capsule, CS or brainsteam, with CSF density on T2 images (Wardlaw et al., 2013). Cerebral microbleeds were defined as round, hypodense lesions <10 mm on susceptibility weighted imaging collected in the axial plane (slice thickness 2 mm, slices = 256, FOV = 230 mm, TR = 49 ms, TE = 40 ms), according to the guidelines (Greenberg et al., 2009).

Statistical Analysis

Normality was determined using the Shapiro–Wilk test and analysis of skewness. Data with high asymmetry was normalized using logarithmic transformation. Homogeneity of variances was tested for each analysis. Baseline characteristics were compared using the independent sample *t*-test and $\chi 2$-test. Mixed ANOVA or ANCOVA (for PCA) were used to compare hemodynamic data. Subgroup analyses were performed using univariate ANOVA, with Bonferroni *post-hoc* tests. The partial eta squared (ηp^2) was used as a measure of effect size: $\eta p^2 > 0.14$ indicates a large effect, $\eta p^2 > 0.06$ indicates a medium effect and $\eta p^2 > 0.01$ indicates a small effect (Cohen, 1998). Age and gender were used as covariates in the ANOVA and ANCOVA comparisons. Supplemental analysis using body mass index (BMI) and VCS as covariates (plus age and gender) were also performed. Patients were dichotomized by the median value of WMH volume to compare the results of $VRCO_2$ and NVC in the PCA between the two WMH burden groups. Subgroups were compared using the independent sample *t*-test.

Values of $p < 0.05$ were considered significant.

RESULTS

Fifty-two hypertensive patients were evaluated and TCD data from 17 healthy controls were used. Baseline characteristics are reported in **Table 1**. **Supplementary File 1** depicts the burden of

TABLE 1 | Demographics and baseline characteristics.

Participant characteristics	Patients	Controls	*p* value*
Age, years (mean ± SD)	64 ± 11	60 ± 16	0.376
Male, n (%)	28 (54)	8 (47)	0.627
BMI, kg/m^2 (median ± IQR)	29 ± 5	25 ± 4	**<0.001**
Diabetes Mellitus, n (%)	30 (58)	0 (0)	
VCS, n (%)			
0	0 (0)	17 (100)	
1	2 (4)	0 (0)	
2	5 (10)	0 (0)	
3	22 (42)	0 (0)	
4	13 (25)	0 (0)	
5	8 (15)	0 (0)	
6	2 (4)	0 (0)	
HT duration, years (median ± IQR)	17 ± 6	0 (0)	
Chronic medication			
No. antihypertensives (median ± IQR)	3 ± 2	0 (0)	
ACEI/ARB, n (%)	48 (92)	0 (0)	
Diuretics, n (%)	39 (75)	0 (0)	
CCB, n (%)	37 (71)	0 (0)	
BB, n (%)	14 (27)	0 (0)	
Alpha2-agonists, n (%)	4 (8)	0 (0)	
Antiplatelets, n (%)	14 (27)	0 (0)	
Statins, n (%)	40 (77)	0 (0)	
Cognitive parameters (median ± IQR)			
Education, years	4 ± 5		
MMSE	28 ± 3		
MoCA	22 ± 5		
ABPM, mmHg (median ± IQR)			
24-h systolic BP	130 ± 15	-	-
24-h diastolic BP	78 ± 13	-	-
24-h pulse pressure	57 ± 16	-	-
Finapres BP, 5 min (mean ± SD)			
Systolic BP	136 ± 24	109 ± 25	**<0.001**
Diastolic BP	62 ± 17	50 ± 14	**0.035**
Mean BP SP, mmHg$_2$ (median ± IQR)	9 ± 24	7 ± 8	**0.007**
$EtCO_2$, mmHg (median ± IQR)	36 ± 4	38 ± 3	0.553

**Values were obtained using the t-test or the $\chi 2$-test. ABPM, ambulatory blood pressure monitoring; BMI, body mass index; BP: blood pressure; $EtCO_2$, end-tidal carbon dioxide; IQR, interquartile range; SD, standard deviation; SP, spectral power; VCS, vascular comorbidity score. Bold values of statistically significant p values ($p < 0.05$).*

PVS, microbleeds and lacunes in the patient group. Most patients had low burden of PVS in the BG (55.0%) and CS (65.0%). Nine patients (22.5%) presented lacunes and four patients (10%) presented microbleeds.

Cerebral Hemodynamics and $VRCO_2$

Baseline CBFV and CBFV variability (spectral power) were similar in patients and controls (**Table 2**). $VRCO_2$ in either territory (PCA or MCA) was similar between groups and showed no change after adjusting for both VCS and BMI (**Supplementary File 2**).

There were no differences in $VRCO_2$ between hypertensive non-diabetics (HT-nDM), hypertensive diabetics (HT-DM) and controls (**Table 3**). Those results did not change significantly after controlling for BMI or VCS (**Supplementary File 3**).

NVC

NVC in the PCA territory was significantly altered in HT patients, with smaller increases in CBFV during visual

TABLE 2 | Cerebral hemodynamics, $VRCO_2$ and NVC: patients vs. controls, controlling for age and gender.

	Patients		Controls		Artery	Group	Interaction
	MCA	**PCA**	**MCA**	**PCA**	***p* value***	***p* value***	***p* value***
Cerebral hemodynamics							
Mean CBFV (cm/s)	47.6 ± 13.4†	31.4 ± 8.2†	52.4 ± 16.5†	29.1 ± 10.1†	0.044	0.925	0.161
MFV SP (cm/s^2)	3.3 ± 5.0‡	2.5 ± 4.7‡	3.8 ± 4.3‡	2.3 ± 3.1‡	0.976	0.770	0.119
$VRCO_2$ (%/mmHg CO_2)	1.4 ± 0.5†	0.9 ± 0.4‡	1.7 ± 0.6†	1.0 ± 0.7‡	0.107	0.588#	0.437
Neurovascular coupling							
Overshoot§ systolic CBFV (%)		22.4 ± 9.2†		31.6 ± 5.7†		**<0.001**	
Modeled parameters							
Gain (%)		14.0 ± 7.1†		17.3 ± 4.8†		0.118	
Natural frequency (Hz)		0.18 ± 0.08‡		0.22 ± 0.06‡		**<0.001**	
Attenuation (a.u)		0.4 ± 0.4‡		0.4 ± 0.4‡		0.374	
Rate time (s)		0.00 ± 0.02‡		0.03 ± 6.81‡		**0.001#**	

**Two-factor mixed-design ANOVA for the interaction between group variable (patients vs. controls) and arterial territory (MCA vs. PCA), controlling for age and gender. For NVC, values were obtained using an ANCOVA. Effect size: rate time $\eta p^2 = 0.174$, natural frequency $\eta p^2 = 0.237$ and overshoot systolic CBFV $\eta p^2 = 0.186$. ||gender significantly interfered with the model; #age significantly interfered with the model; †Values are presented as mean ± standard deviation. ‡Values are presented as median ± interquartile range. §Maximal CBFV increase during visual stimulation. a.u., arbitrary units; CBFV, cerebral blood flow velocity; $VRCO_2$, vasoreactivity to carbon dioxide; MFV SP, median flow velocity spectral power; MCA, middle cerebral artery; PCA, posterior cerebral artery. Bold values of statistically significant p values ($p < 0.05$).*

TABLE 3 | Cerebral hemodynamics, $VRCO_2$ and NVC: controls vs. HT-nDM vs. HT-DM patients, controlled for age and gender.

	HT-nDM		HT-DM		Controls		Group	HT-nDM vs. Controls	HT-DM vs. Controls	HT-nDM vs. HT-DM
	MCA	**PCA**	**MCA**	**PCA**	**MCA**	**PCA**	***p* value***	***p* value***	***p* value***	***p* value***
Cerebral hemodynamics										
Mean CBFV (cm/s)†	47.0 ± 14.1	33.4 ± 8.4	48.0 ± 13.2	30.0 ± 7.8	52.4 ± 16.5	29.1 ± 10.1	0.993			
MFV SP (cm/s^2)‡	3.1 ± 4.7	2.6 ± 5.0	3.7 ± 7.0	2.5 ± 5.0	3.8 ± 4.3	2.3 ± 3.1	0.921			
$VRCO_2$ (%/mmHg CO_2)†	1.4 ± 0.6	1.2 ± 0.7	1.4 ± 0.5	0.8 ± 0.3	1.7 ± 0.6	1.1 ± 0.4	0.676#			
Neurovascular coupling										
Overshoot§ systolic CBFV (%)†		25.1 ± 8.6		20.7 ± 9.3		31.6 ± 5.7	**<0.001**	0.080	**<0.001**	0.248
Modeled parameters										
Gain (%)†		13.9 ± 5.1		14.1 ± 8.2		17.3 ± 4.8	0.283			
Natural frequency (Hz) †		0.19 ± 0.04		0.16 ± 0.05		0.23 ± 0.06	**<0.001#**	0.052	**<0.001**	**0.043**
Attenuation (a.u)†		0.4 ± 0.3		0.4 ± 0.3		0.5 ± 0.2	0.327#			
Rate time (s)‡		0.00 ± 0.00		0.00 ± 0.26		0.03 ± 6.81	**0.005#**	**0.012**	**0.011**	1.000

**Two-factor mixed-design ANOVA for the interaction between group variable (HT-DM vs. HT-nDM vs. controls) and arterial territory (MCA vs. PCA), controlling for age and gender, with Bonferroni post-hoc. For NVC, values were obtained using an ANCOVA. Effect size: rate time $\eta p^2 = 0.174$, natural frequency $\eta p^2 = 0.313$ and overshoot systolic CBFV $\eta p^2 = 0.22$. †Values are presented as mean ± standard deviation. ‡Values are presented as median ± interquartile range. §Maximal CBFV increase during visual stimulation. ||gender significantly interfered with the model. #age significantly interfered with the model. a.u., arbitrary units; CBFV, cerebral blood flow velocity; HT-DM, hypertensive diabetic; HT-nDM, hypertensive non-diabetic; MCA, middle cerebral artery; MFV SP, median flow velocity spectral power; PCA, posterior cerebral artery; $VRCO_2$, vasoreactivity to carbon dioxide. Bold values of statistically significant p values ($p < 0.05$).*

stimulation ($p < 0.001$) and disturbed NVC time-varying properties, with lower natural frequency ($p < 0.001$) and lower rate time ($p = 0.001$) (**Table 2**; **Figure 2**). These results remained similar when adjusting for BMI and VCS, although the overshoot systolic CBFV was over the limit of statistical significance when adjusting for the VCS ($p = 0.065$) (**Supplementary File 2**).

NVC results were worse in HT-DM than HT-nDM (**Table 3**). For the overshoot systolic CBFV and for natural frequency, only patients with both comorbidities showed significant differences when comparing to controls. HT-DM showed lower natural frequency than non-diabetic patients ($p = 0.043$). When controlling for VCS, natural frequency was also worse in both HT-nDM ($p = 0.020$) and HT-DM ($p = 0.002$) when comparing to controls, with the worst results for HT-DM (HT-nDM vs. HT-DM, p=0.011) (**Supplementary File 3**).

Figure 3 represents the evoked systolic CBFV responses in the PCA and MCA during the visual stimulation in one HT subject, to demonstrate the individual NVC responses.

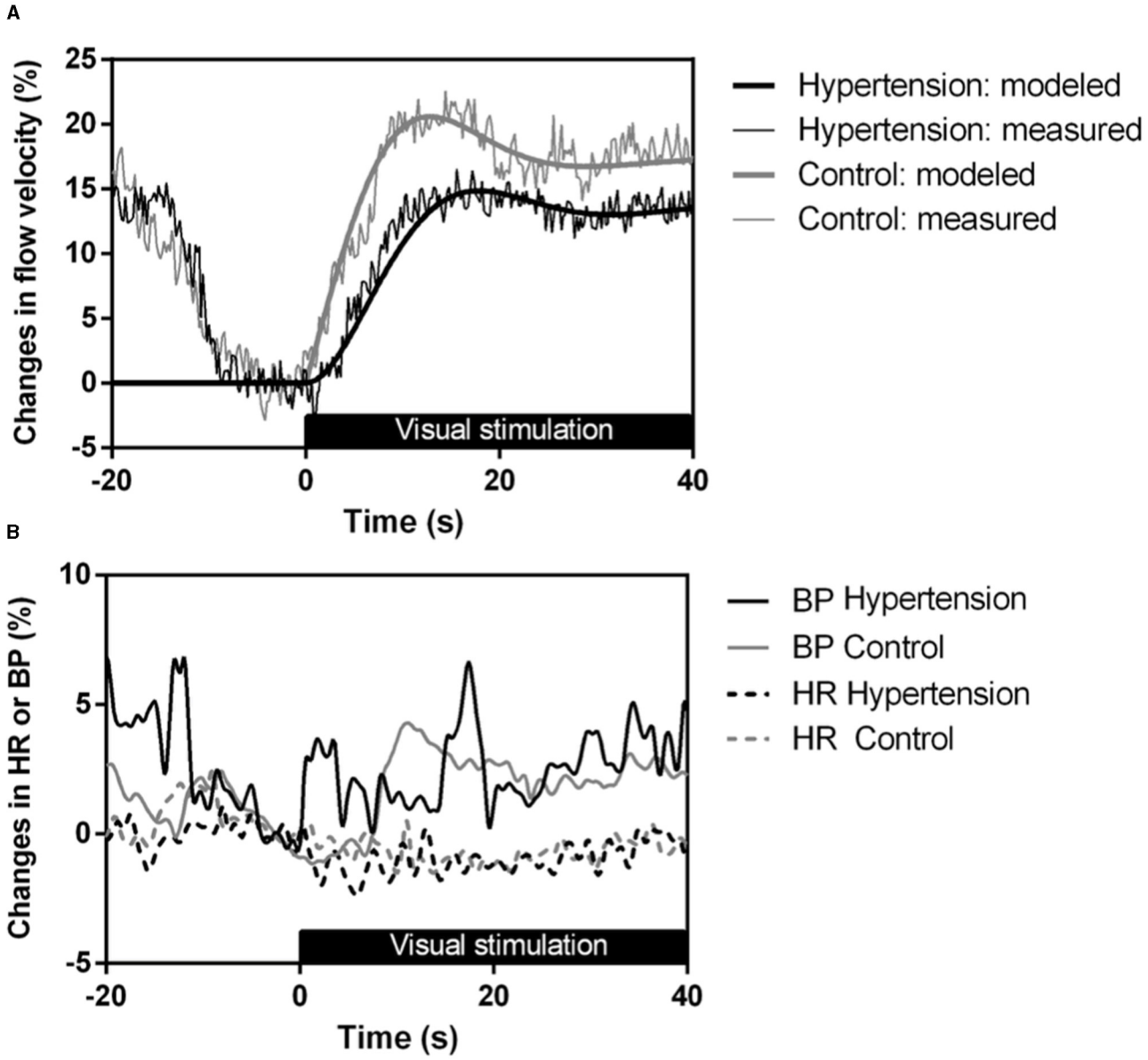

FIGURE 2 | (A) Group-averaged evoked systolic CBFV responses during visual stimulation with the flickering checkerboard; **(B)** Blood pressure (BP) and heart rate (HR) during visual stimulation with the flickering checkerboard. Gray lines represent healthy controls and black lines represent HT patients (thin lines: measured responses, thick lines: modeled blood flow data).

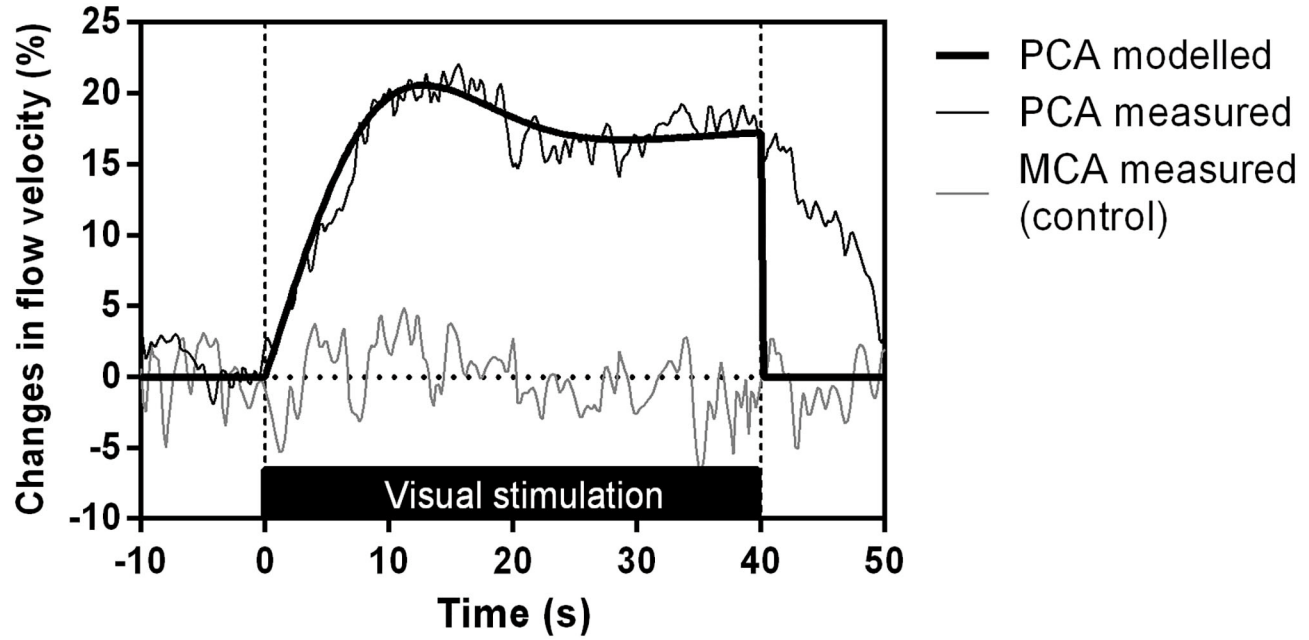

FIGURE 3 | Evoked systolic CBFV responses in the PCA and MCA during visual stimulation with the flickering checkerboard in one HT patient. The black lines represent the PCA response (thin lines: measured responses, thick lines: modeled blood flow data) and the gray lines represent the MCA measured response, used as a control.

TABLE 4 | NVC and $VRCO_2$ in relation to the WMH volume in hypertensive patients.

	WMH volume*					
	MCA			**PCA**		
	≤ 0.14	**> 0.14**	***p* value**	**≤ 0.14**	**> 0.14**	***p* value**
$VRCO_2$ (%/mmHg CO_2)	1.6 ± 0.5	1.2 ± 0.5	**0.004**	1.0 ± 0.6‡	0.8 ± 0.5‡	**0.006**
Neurovascular coupling						
Overshoot§ systolic CBFV, (%)	-	-	-	23.4 ± 10.0†	21.8 ± 8.8†	0.573
Gain (%)	-	-	-	11.7 ± 11.1‡	14.6 ± 7.9‡	0.297
Natural frequency (Hz)	-	-	-	0.2 ± 0.0†	0.2±0.1†	0.432
Attenuation (a.u)	-	-	-	0.4 ± 0.3†	0.4 ± 0.2†	0.891
Rate time (s)	-	-	-	0.0 ± 1.2‡	0.0 ± 0.0‡	0.169

**Dichotomized by median values. p values were obtained using the t-test. †Values are presented as mean ± standard deviation; ‡Values are presented as median ± interquartile range. §Maximal CBFV increase during visual stimulation. a.u., arbitrary units; CBFV, cerebral blood flow velocity; MCA, median cerebral artery; PCA, posterior cerebral artery; $VRCO_2$, vasoreactivity to carbon dioxide; WMH, white matter hyperintensities. Bold values of statistically significant p values ($p < 0.05$).*

Association With White Matter Hyperintensities

As shown in **Table 4**, $VRCO_2$ was lower in the higher burden group in both the MCA ($p = 0.004$) and the PCA ($p = 0.007$). NVC parameters did not differ in both groups.

DISCUSSION

Our study shows that NVC was significantly impaired in hypertensive patients, with reduced CBFV increase and altered time behavior hemodynamic evoked response during visual stimulation. Moreover, NVC tended to be worse in the DM subgroup. $VRCO_2$ remained relatively preserved. These results did not change when adjusting for other vascular risk factors. The novel finding is that the natural frequency seems to be the most sensitive parameter for discriminating abnormal NVC in these patients. Rosengarten and colleagues reported that this parameter had the lowest SD of the modeled parameters, thus having the potential for better differentiating between normal and abnormal NVC, but its capacity to identify vascular response dysfunction in disease settings needed to be studied (Rosengarten et al., 2001a). Our results seem to point toward natural frequency as a possible marker for NVC dysfunction in hypertension and diabetes.

Overall, the white matter disease (WMD) burden was low in the patient cohort. The NVC results were similar between

higher and lower WMD burden groups, while higher burden patients showed worse $VRCO_2$. It has been recently reported that reduced $VRCO_2$ precedes the development of WMH (Sam et al., 2016), which could help explain the difference between the disease burden groups. Similar NVC with higher and lower WMH volume has been previously reported (Sorond et al., 2013). Although WMH volume predicts an increased risk of stroke and cognitive decline, the clinical expression seems to vary (Sorond et al., 2011). Moreover, silent markers of CSVD are frequently detected on the MRI of older individuals without cognitive impairment (Vernooij et al., 2009; Debette and Markus, 2010). Thus, besides macrostructural changes, other modalities reflecting microstructural integrity and function, such as TCD dynamic studies, may provide additional information to further stratify patients at risk.

Neurovascular Unit at the Core of Target Brain Damage in Hypertension

Our results showed a significantly reduced PCA CBFV magnitude response and altered time behavior of reactive hyperemia during visual stimulation in HT patients, especially when diabetes was an added comorbidity. These findings indicate disturbed NVC in these patients' PCA cortical territory, independently of established WMD, as was observed by other groups (Birns et al., 2009; Purkayastha et al., 2014). The decreased CBFV during visual stimulation reflects less robust functional hyperemia, causing failure to meet the metabolic demands and neuronal damage (Iadecola et al., 2019).

The reduced overshoot systolic CBFV in the patient group was not accompanied by a reduction in the modeled parameter gain. This could reflect lack of statistical power to detect the differences between the groups, since the mean gain was lower in the patient group. In addition, it has been demonstrated that the overshoot of systolic CBFV is significantly influenced by not only gain, but also rate time and attenuation (Rosengarten et al., 2001a). Hence, the parameter gain and the overshoot systolic CBFV may not be perfectly matched.

These results are in line with studies on genetically determined CSVD. CADASIL patients demonstrated less robust functional hyperemia in the PCA during visual stimulation, with changes in time dynamics, very similar to our findings (Jokumsen-Cabral et al., 2019). Comparable NVC dysfunction in the posterior circulation was shown in Fabry patients (Azevedo et al., 2012; Castro et al., 2020). Both diseases are characterized by abnormal material deposition in the vessel walls (Baudrimont et al., 1993; Rombach et al., 2010). Interestingly, amyloid deposition also seems to cause NVC impairment (Iadecola and Davisson, 2008; Brickman et al., 2015), and HT appears to have a role in promoting amyloid deposition, thus working synergistically to worsen CSVD and cognitive decline (Iadecola and Davisson, 2008).

Chronic HT leads to structural (mal)adaptations in the cerebral circulation, with remodeling of the cerebral arteries and arterioles. This remodeling involves smooth muscle cell hypertrophy and hyperplasia, increased deposition of extracellular matrix components and degenerated smooth muscle (lipohyalinosis) and fibrinoid necrosis, leading to arterial stiffening and loss of elasticity (Iadecola and Gottesman, 2019). These changes in the proximal resistance arteries cause substantial burden on the vulnerable downstream microcirculation, promoting pressure-induced oxidative stress to the endothelial cells and neuroinflammation (Ungvari et al., 2021). In experimental models, HT results in impairment of endothelium mediated neurovascular coupling responses, in part resulting from this oxidative stress and neuroinflammation (Iadecola and Gottesman, 2019; Ungvari et al., 2021). Hence, the structural changes induced by HT play an important role in the loss of functional integrity of the neurovascular unit. Natural frequency is assumed to represent the tonus and the speed of the system (Rosengarten et al., 2003), which would be altered by the increased rigidity of the vessels and endothelial dysfunction, and our results show that this parameter was the most sensitive in differentiating patients from controls.

Less effective NVC in the MCA territory has been associated with significant cognition, balance, and walking velocity changes in the elderly (Sorond et al., 2011; Purkayastha et al., 2014). Despite the presence and burden of WMD, normal NVC was associated with preserved walking speed, while slower walking is one of the earliest manifestations of CSVD. Further prospective work could use NVC for predicting symptomatic CSVD. Curiously, cocoa and deferoxamine have been demonstrated to reverse some of these changes suggesting the possibility for pharmacological modulation of the neurovascular function (Sorond et al., 2013, 2015).

Additional Contribute From Diabetes Mellitus

Comorbid diabetes associated with increased cerebrovascular dysfunction. NVC was worse in this subgroup of hypertensive patients, particularly in its oscillatory properties (natural frequency), in accordance to previous studies in early type 1 DM (Rosengarten et al., 2002). This might signify higher rigidity of the small arteries due to the accumulation of advanced glycated by-products. In fact, type 2 DM patients have particularly high incidence of lacunar stroke (van Harten et al., 2006; Brundel et al., 2014). Diabetes induced chronic vascular changes include not only macrovascular disorders, such as cardiovascular and cerebrovascular large vessel disease, but also microvascular disorders, with nephropathy, retinopathy and neuropathy (Chawla et al., 2016). Furthermore, studies have implicated DM as a risk factor for cognitive impairment, which may be related to CSVD. However, the mechanism by which cognitive decline occurs and whether it can be explained by dysfunction of the neurovascular unit remains to be elucidated (Mogi and Horiuchi, 2011). The sympathetic nervous system seems to attenuate the cerebrovascular response to hypercapnia, suggesting a direct effect on the cerebral vasculature (Jordan et al., 2000). NVC is also affected by autonomic dysfunction (Azevedo et al., 2011). Thus, differences in DM vs. nDM hypertensive patients could be related to DM associated dysautonomia in CSVD.

Overall, our study further supports cerebrovascular dynamics dysfunction as a major player in explaining the relationship between increased VRF burden and CSVD manifestations, independently of macroscopic white matter lesions.

Limitations

We acknowledge several methodological limitations. Due to the cross-section design, our study cannot provide evidence to support cerebrovascular dysfunction as an early predictor of CSVD. However, these patients had well-controlled HT, based on average ABPM values, with no clinical manifestations of cerebrovascular disease. All the patients were referred to the Hypertension Unit due to severe or difficult to manage HT, and we do not know the duration of the untreated disease, which could impact the degree of microvascular dysfunction.

Although the patient group's sample size is relatively large for hemodynamic physiology studies, this is an exploratory study and must be validated in larger, multicenter cohorts. Also, the control group is relatively small, not exactly age- and gender-matched, and the differences in comorbidities between the two groups can be potential confounders to the observed differences. Besides HT and DM, already discussed, other vascular comorbidities have been associated with the development of CSVD. Dyslipidemia plays an important role in the development of large vessel disease and stroke, but its role in CSVD is still controversial (Tsai et al., 2018). However, animal studies have demonstrated cerebral autoregulation impairment with hyperlipidemia and a relationship between hyperlipidemia and the development of CSVD (Ayata et al., 2013; Kraft et al., 2017). Obesity has been demonstrated to have an impact in the development of CSVD (Yamashiro et al., 2014), and it has been shown to affect cerebral vasoreactivity (Selim et al., 2008). Smoking appears to worsen the effects of hypertension in the cerebral microvasculature (Hara et al., 2019), and there is impaired neurovascular coupling in the PCA of young chronic smokers (Olah et al., 2008). Chronic heart failure can affect cerebral autoregulation, reduce cerebral blood flow (CBF) and has been shown to affect NVC in the PCA (Aires et al., 2020; Ovsenik et al., 2021). The prevalence of CSVD is higher in patients with coronary artery disease (Berry et al., 2019), and it has been identified as an independent risk factor for vascular dementia (Gorelick et al., 2011). It was recently demonstrated that aTrial fibrillation reduces cerebral autoregulation and impairs neurovascular coupling responses to visual stimulation (Junejo et al., 2020). There is evidence that peripheral artery disease is associated with white matter disease and the development of vascular dementia (Bots et al., 1993; Gorelick et al., 2011). In patients with ischemic stroke, impaired renal function correlated with worse dCA and associated with an increased risk of hemorrhagic transformation (Castro et al., 2018). However, in addition to adjusting for age and gender, adjusting for the vascular comorbidities did not modify the results significantly.

Hypertension affects cerebral small vessels heterogeneously, and MRI seems the logical choice for its superior spatial resolution. However, MRI $VRCO_2$ protocols are more prone to failure (Moreton et al., 2018), expensive and not as standardized as TCD (Malojcic et al., 2017). Moreover, TCD offers extraordinary time resolution (∼5 ms) for studying the time behavior of CBFV activation in downstream cortical microvasculature. There are also inherent limitations for continuous blood flow monitoring by TCD, namely, providing a measure of blood flow velocity and not flow. However, the former is an adequate surrogate for the latter as long as the insonated artery diameter remains constant. Since data were acquired in a supine position and relied on spontaneous measurements, changes in artery diameter are not anticipated for NVC. Nevertheless, it has been demonstrated that with increasing partial pressure of arterial CO_2 there is noticeable increase in vessel diameter, which could lead to underestimation of cerebral blood flow in the $VRCO_2$ protocol (Coverdale et al., 2014).

We did not report the presence of cortical microinfarcts (CMI) in this study, despite having been found in cohorts of hypertensive patients (although not consistently) and despite their importance in cognitive decline (van Veluw et al., 2017). We did not detect CMI upon visual inspection of the MRI scans. However, the protocols for detecting CMI are mostly validated in 3T MRI scanners (Coverdale et al., 2014), and our 1.5T scan protocol is underpowered for their detection.

In conclusion, neurovascular coupling, and more specifically the modeled parameter natural frequency, seems to be particularly affected in hypertension and diabetes and could be useful as an early biomarker for microvascular dysfunction, future irreversible vascular damage, and cognitive decline. Additionally, our study supports TCD dynamic tests as useful tools for better understating microvascular damage associated with these diseases, but future research is warranted to confirm these results.

DATA AVAILABILITY STATEMENT

The raw data supporting the conclusions of this article may be made available by the authors upon request, without undue reservation.

ETHICS STATEMENT

The studies involving human participants were reviewed and approved by Comissão de Ética da U. L. S. Matosinhos, Hospital de Pedro Hispano, EPE, Unidade Local de Saúde de Matosinhos, Portugal. The patients/participants provided their written informed consent to participate in this study.

AUTHOR CONTRIBUTIONS

AM: conception and design, data collection, literature search, drafting the manuscript, and critical revision of the manuscript. PC: conception and design, data collection, critical revision of the manuscript, and supervision. GP, CF, and JP: data collection and critical revision of the manuscript. FS, AM, and JH: critical revision of the manuscript. EA: conception and design, critical revision of the manuscript, and supervision. All authors contributed to the article and approved the submitted version.

FUNDING

This study received financial support from Associação para o Estudo das Doenças Neurovasculares for performing MRI studies.

ACKNOWLEDGMENTS

We would like to acknowledge the support received from Associação para o Estudo das Doenças Neurovasculares and we wish to thank the participants who volunteered to be part of this study.

SUPPLEMENTARY MATERIAL

The Supplementary Material for this article can be found online at: https://www.frontiersin.org/articles/10.3389/fnagi.2021.728007/full#supplementary-material

REFERENCES

Aires, A., Andrade, A., Azevedo, E., Gomes, F., Araujo, J. P., and Castro, P. (2020). Neurovascular coupling impairment in heart failure with reduction ejection fraction. *Brain Sci*. 10:714. doi: 10.3390/brainsci10100714

Ayata, C., Shin, H. K., Dilekoz, E., Atochin, D. N., Kashiwagi, S., Eikermann-Haerter, K., et al. (2013). Hyperlipidemia disrupts cerebrovascular reflexes and worsens ischemic perfusion defect. *J. Cereb. Blood Flow Metab*. 33, 954–962. doi: 10.1038/jcbfm.2013.38

Azevedo, E., Castro, P., Santos, R., Freitas, J., Coelho, T., Rosengarten, B., et al. (2011). Autonomic dysfunction affects cerebral neurovascular coupling. *Clin. Auton. Res*. 21, 395–403. doi: 10.1007/s10286-011-0129-3

Azevedo, E., Mendes, A., Seixas, D., Santos, R., Castro, P., Ayres-Basto, M., et al. (2012). Functional transcranial doppler: presymptomatic changes in Fabry disease. *Eur. Neurol*. 67, 331–337. doi: 10.1159/000337906

Baudrimont, M., Dubas, F., Joutel, A., Tournier-Lasserve, E., and Bousser, M. G. (1993). Autosomal dominant leukoencephalopathy and subcortical ischemic stroke. *A clinicopathological study. Stroke* 24, 122–125. doi: 10.1161/01.STR.24.1.122

Berry, C., Sidik, N., Pereira, A. C., Ford, T. J., Touyz, R. M., Kaski, J. C., et al. (2019). Small-vessel disease in the heart and brain: current knowledge, unmet therapeutic need, and future directions. *J. Am. Heart Assoc*. 8:e011104. doi: 10.1161/JAHA.118.011104

Birns, J., Jarosz, J., Markus, H. S., and Kalra, L. (2009). Cerebrovascular reactivity and dynamic autoregulation in ischaemic subcortical white matter disease. *J. Neurol. Neurosurg. Psychiatry* 80, 1093–1098. doi: 10.1136/jnnp.2009.174607

Bots, M. L., van Swieten, J. C., Breteler, M. M., de Jong, P. T., van Gijn, J., Hofman, A., et al. (1993). Cerebral white matter lesions and atherosclerosis in the rotterdam study. *Lancet* 341, 1232–1237. doi: 10.1016/0140-6736(93)91144-B

Brickman, A. M., Guzman, V. A., Gonzalez-Castellon, M., Razlighi, Q., Gu, Y., Narkhede, A., et al. (2015). Cerebral autoregulation, beta amyloid, and white matter hyperintensities are interrelated. *Neurosci. Lett*. 592, 54–58. doi: 10.1016/j.neulet.2015.03.005

Brundel, M., Kappelle, L. J., and Biessels, G. J. (2014). Brain imaging in type 2 diabetes. *Eur. Neuropsychopharmacol*. 24, 1967–1981. doi: 10.1016/j.euroneuro.2014.01.023

Brundel, M., van den Berg, E., Reijmer, Y. D., de Bresser, J., Kappelle, L. J., Biessels, G. J., et al. (2012). Cerebral haemodynamics, cognition and brain volumes in patients with type 2 diabetes. *J. Diabetes Complications* 26, 205–209. doi: 10.1016/j.jdiacomp.2012.03.021

Castro, P., Azevedo, E., Rocha, I., Sorond, F., and Serrador, J. M. (2018). Chronic kidney disease and poor outcomes in ischemic stroke: is impaired cerebral autoregulation the missing link? *BMC Neurol*. 18:21. doi: 10.1186/s12883-018-1025-4

Castro, P., Gutierres, M., Pereira, G., Ferreira, S., Oliveira, J. P., and Azevedo, E. (2020). Evaluation of cerebral microvascular regulatory mechanisms with transcranial doppler in fabry disease. *Brain Sci* 10:528. doi: 10.3390/brainsci10080528

Chawla, A., Chawla, R., and Jaggi, S. (2016). Microvasular and macrovascular complications in diabetes mellitus: distinct or continuum? *Indian J. Endocrinol. Metab*. 20, 546–551. doi: 10.4103/2230-8210.183480

Claassen, J. A., Meel-van den Abeelen, A. S., Simpson, D. M., Panerai, R. B., and International Cerebral Autoregulation Research, N. (2016). Transfer function analysis of dynamic cerebral autoregulation: a white paper from the International cerebral autoregulation research network. *J. Cereb. Blood Flow Metab*. 36, 665–680. doi: 10.1177/0271678X15626425

Cohen, J. (1998). *Statistical Power Analysis for the Behavioral Sciences, 2nd Edn*. Hillsdale, NJ: Erlbaum.

Coverdale, N. S., Gati, J. S., Opalevych, O., Perrotta, A., and Shoemaker, J. K. (2014). Cerebral blood flow velocity underestimates cerebral blood flow during modest hypercapnia and hypocapnia. *J. Appl. Physiol*. 117, 1090–1096. doi: 10.1152/japplphysiol.00285.2014

Debette, S., and Markus, H. S. (2010). The clinical importance of white matter hyperintensities on brain magnetic resonance imaging: systematic review and meta-analysis. *BMJ* 341:c3666. doi: 10.1136/bmj.c3666

Freeze, W. M., Jacobs, H. I. L., Schreuder, F., van Oostenbrugge, R. J., Backes, W. H., Verhey, F. R., et al. (2018). Blood-brain barrier dysfunction in small vessel disease related intracerebral hemorrhage. *Front. Neurol*. 9:926. doi: 10.3389/fneur.2018.00926

GBD 2017 Causes of Death Collaborators (2018). Global, regional, and national age-sex-specific mortality for 282 causes of death in 195 countries and territories, 1980-2017: a systematic analysis for the Global Burden of Disease Study 2017. *Lancet* 392, 1736–1788. doi: 10.1016/S0140-6736(18)32203-7

Gorelick, P. B., Scuteri, A., Black, S. E., Decarli, C., Greenberg, S. M., Iadecola, C., et al. (2011). Vascular contributions to cognitive impairment and dementia: a statement for healthcare professionals from the american heart association/american stroke association. *Stroke* 42, 2672–2713. doi: 10.1161/STR.0b013e3182299496

Greenberg, S. M., Vernooij, M. W., Cordonnier, C., Viswanathan, A., Al-Shahi Salman, R., Warach, S., et al. (2009). Cerebral microbleeds: a guide to detection and interpretation. *Lancet Neurol*. 8, 165–174. doi: 10.1016/S1474-4422(09)70013-4

Hara, M., Yakushiji, Y., Suzuyama, K., Nishihara, M., Eriguchi, M., Noguchi, T., et al. (2019). Synergistic effect of hypertension and smoking on the total small vessel disease score in healthy individuals: the Kashima scan study. *Hypertens. Res*. 42, 1738–1744. doi: 10.1038/s41440-019-0282-y

Iadecola, C., and Davisson, R. L. (2008). Hypertension and cerebrovascular dysfunction. *Cell Metab*. 7, 476–484. doi: 10.1016/j.cmet.2008.03.010

Iadecola, C., Duering, M., Hachinski, V., Joutel, A., Pendlebury, S. T., Schneider, J. A., et al. (2019). Vascular cognitive impairment and dementia: JACC scientific expert panel. *J. Am. Coll. Cardiol*. 73, 3326–3344. doi: 10.1016/j.jacc.2019.04.034

Iadecola, C., and Gottesman, R. F. (2019). Neurovascular and cognitive dysfunction in hypertension. *Circ. Res*. 124, 1025–1044. doi: 10.1161/CIRCRESAHA.118.313260

Jokumsen-Cabral, A., Aires, A., Ferreira, S., Azevedo, E., and Castro, P. (2019). Primary involvement of neurovascular coupling in cerebral autosomal-dominant arteriopathy with subcortical infarcts and leukoencephalopathy. *J. Neurol*. 266, 1782–1788. doi: 10.1007/s00415-019-09331-y

Jordan, J., Shannon, J. R., Diedrich, A., Black, B., Costa, F., Robertson, D., et al. (2000). Interaction of carbon dioxide and sympathetic nervous system activity in the regulation of cerebral perfusion in humans. *Hypertension* 36, 383–388. doi: 10.1161/01.HYP.36.3.383

Junejo, R. T., Braz, I. D., Lucas, S. J., van Lieshout, J. J., Phillips, A. A., Lip, G. Y., et al. (2020). Neurovascular coupling and cerebral autoregulation in atrial fibrillation. *J. Cereb. Blood Flow Metab*. 40, 1647–1657. doi: 10.1177/0271678X19870770

Kraft, P., Schuhmann, M. K., Garz, C., Jandke, S., Urlaub, D., Mencl, S., et al. (2017). Hypercholesterolemia induced cerebral small vessel disease. *PLoS ONE* 12:e0182822. doi: 10.1371/journal.pone.0182822

Lau, K. K., Li, L., Schulz, U., Simoni, M., Chan, K. H., Ho, S. L., et al. (2017). Total small vessel disease score and risk of recurrent stroke: validation in 2 large cohorts. *Neurology* 88, 2260–2267. doi: 10.1212/WNL.0000000000004042

Liu, J., Rutten-Jacobs, L., Liu, M., Markus, H. S., and Traylor, M. (2018). Causal impact of type 2 diabetes mellitus on cerebral small vessel disease: a mendelian randomization analysis. *Stroke* 49, 1325–1331. doi: 10.1161/STROKEAHA.117.020536

Madureira, J., Castro, P., and Azevedo, E. (2017). Demographic and systemic hemodynamic influences in mechanisms of cerebrovascular regulation in healthy adults. *J. Stroke Cerebrovasc. Dis.* 26, 500–508. doi: 10.1016/j.jstrokecerebrovasdis.2016.12.003

Malojcic, B., Giannakopoulos, P., Sorond, F. A., Azevedo, E., Diomedi, M., Oblak, J. P., et al. (2017). Ultrasound and dynamic functional imaging in vascular cognitive impairment and Alzheimer's disease. *BMC Med.* 15:27. doi: 10.1186/s12916-017-0799-3

Mogi, M., and Horiuchi, M. (2011). Neurovascular coupling in cognitive impairment associated with diabetes mellitus. *Circ. J.* 75, 1042–1048. doi: 10.1253/circj.CJ-11-0121

Moreton, F. C., Cullen, B., Delles, C., Santosh, C., Gonzalez, R. L., Dani, K., et al. (2018). Vasoreactivity in CADASIL: comparison to structural MRI and neuropsychology. *J. Cereb. Blood Flow Metab.* 38, 1085–1095. doi: 10.1177/0271678X17710375

Mossello, E., Pieraccioli, M., Nesti, N., Bulgaresi, M., Lorenzi, C., Caleri, V., et al. (2015). Effects of low blood pressure in cognitively impaired elderly patients treated with antihypertensive drugs. *JAMA Intern. Med.* 175, 578–585. doi: 10.1001/jamainternmed.2014.8164

Olah, L., Raiter, Y., Candale, C., Molnar, S., Rosengarten, B., Bornstein, N. M., et al. (2008). Visually evoked cerebral vasomotor response in smoking and nonsmoking young adults, investigated by functional transcranial doppler. *Nicotine Tob. Res.* 10, 353–358. doi: 10.1080/14622200701825874

Ovsenik, A., Podbregar, M., and Fabjan, A. (2021). Cerebral blood flow impairment and cognitive decline in heart failure. *Brain Behav.* 11:e02176. doi: 10.1002/brb3.2176

Pantoni, L. (2010). Cerebral small vessel disease: from pathogenesis and clinical characteristics to therapeutic challenges. *Lancet Neurol.* 9, 689–701. doi: 10.1016/S1474-4422(10)70104-6

Potter, G. M., Chappell, F. M., Morris, Z., and Wardlaw, J. M. (2015). Cerebral perivascular spaces visible on magnetic resonance imaging: development of a qualitative rating scale and its observer reliability. *Cerebrovasc. Dis.* 39, 224–231. doi: 10.1159/000375153

Purkayastha, S., Fadar, O., Mehregan, A., Salat, D. H., Moscufo, N., Meier, D. S., et al. (2014). Impaired cerebrovascular hemodynamics are associated with cerebral white matter damage. *J. Cereb. Blood Flow Metab.* 34, 228–234. doi: 10.1038/jcbfm.2013.180

Rombach, S. M., Twickler, T. B., Aerts, J. M., Linthorst, G. E., Wijburg, F. A., and Hollak, C. E. (2010). Vasculopathy in patients with Fabry disease: current controversies and research directions. *Mol. Genet. Metab.* 99, 99–108. doi: 10.1016/j.ymgme.2009.10.004

Rosengarten, B., Aldinger, C., Kaufmann, A., and Kaps, M. (2001b). Comparison of visually evoked peak systolic and end diastolic blood flow velocity using a control system approach. *Ultrasound Med. Biol.* 27, 1499–1503. doi: 10.1016/S0301-5629(01)00464-1

Rosengarten, B., Budden, C., Osthaus, S., and Kaps, M. (2003). Effect of heart rate on regulative features of the cortical activity-flow coupling. *Cerebrovasc. Dis.* 16, 47–52. doi: 10.1159/000070115

Rosengarten, B., Dost, A., Kaufmann, A., Gortner, L., and Kaps, M. (2002). Impaired cerebrovascular reactivity in type 1 diabetic children. *Diabetes Care* 25, 408–410. doi: 10.2337/diacare.25.2.408-a

Rosengarten, B., Huwendiek, O., and Kaps, M. (2001a). Neurovascular coupling in terms of a control system: validation of a second-order linear system model. *Ultrasound Med. Biol.* 27, 631–635. doi: 10.1016/S0301-5629(01)00355-6

Sam, K., Crawley, A. P., Conklin, J., Poublanc, J., Sobczyk, O., Mandell, D. M., et al. (2016). Development of white matter hyperintensity is preceded by reduced cerebrovascular reactivity. *Ann. Neurol.* 80, 277–285. doi: 10.1002/ana.24712

Selim, M., Jones, R., Novak, P., Zhao, P., and Novak, V. (2008). The effects of body mass index on cerebral blood flow velocity. *Clin. Auton. Res.* 18, 331–338. doi: 10.1007/s10286-008-0490-z

Sorond, F. A., Hurwitz, S., Salat, D. H., Greve, D. N., and Fisher, N. D. (2013). Neurovascular coupling, cerebral white matter integrity, and response to cocoa in older people. *Neurology* 81, 904–909. doi: 10.1212/WNL.0b013e3182a351aa

Sorond, F. A., Kiely, D. K., Galica, A., Moscufo, N., Serrador, J. M., Iloputaife, I., et al. (2011). Neurovascular coupling is impaired in slow walkers: the MOBILIZE Boston study. *Ann. Neurol.* 70, 213–220. doi: 10.1002/ana.22433

Sorond, F. A., Tan, C. O., LaRose, S., Monk, A. D., Fichorova, R., Ryan, S., et al. (2015). Deferoxamine, cerebrovascular hemodynamics, and vascular aging: potential role for hypoxia-inducible transcription factor-1-regulated pathways. *Stroke* 46, 2576–2583. doi: 10.1161/STROKEAHA.115.009906

Sudlow, C. L., and Warlow, C. P. (1997). Comparable studies of the incidence of stroke and its pathological types: results from an international collaboration. International Stroke Incidence Collaboration. *Stroke* 28, 491–499. doi: 10.1161/01.STR.28.3.491

Tsai, H. H., Kim, J. S., Jouvent, E., and Gurol, M. E. (2018). Updates on prevention of hemorrhagic and lacunar strokes. *J. Stroke* 20, 167–179. doi: 10.5853/jos.2018.00787

Ungvari, Z., Toth, P., Tarantini, S., Prodan, C. I., Sorond, F., Merkely, B., et al. (2021). Hypertension-induced cognitive impairment: from pathophysiology to public health. *Nat. Rev. Nephrol.* 1–16. doi: 10.1038/s41581-021-00430-6

van Harten, B., de Leeuw, F. E., Weinstein, H. C., Scheltens, P., and Biessels, G. J. (2006). Brain imaging in patients with diabetes: a systematic review. *Diabetes Care* 29, 2539–2548. doi: 10.2337/dc06-1637

van Veluw, S. J., Shih, A. Y., Smith, E. E., Chen, C., Schneider, J. A., Wardlaw, J. M., et al. (2017). Detection, risk factors, and functional consequences of cerebral microinfarcts. *Lancet Neurol.* 16, 730–740. doi: 10.1016/S1474-4422(17)30196-5

Vernooij, M. W., Ikram, M. A., Vrooman, H. A., Wielopolski, P. A., Krestin, G. P., Hofman, A., et al. (2009). White matter microstructural integrity and cognitive function in a general elderly population. *Arch. Gen. Psychiatry* 66, 545–553. doi: 10.1001/archgenpsychiatry.2009.5

Wardlaw, J. M. (2010). Blood-brain barrier and cerebral small vessel disease. *J. Neurol. Sci.* 299, 66–71. doi: 10.1016/j.jns.2010.08.042

Wardlaw, J. M., Smith, E. E., Biessels, G. J., Cordonnier, C., Fazekas, F., Frayne, R., et al. (2013). Neuroimaging standards for research into small vessel disease and its contribution to ageing and neurodegeneration. *Lancet Neurol.* 12, 822–838. doi: 10.1016/S1474-4422(13)70124-8

Yamashiro, K., Tanaka, R., Tanaka, Y., Miyamoto, N., Shimada, Y., Ueno, Y., et al. (2014). Visceral fat accumulation is associated with cerebral small vessel disease. *Eur. J. Neurol.* 21, 667–673. doi: 10.1111/ene.12374

Conflict of Interest: The authors declare that the research was conducted in the absence of any commercial or financial relationships that could be construed as a potential conflict of interest.

Publisher's Note: All claims expressed in this article are solely those of the authors and do not necessarily represent those of their affiliated organizations, or those of the publisher, the editors and the reviewers. Any product that may be evaluated in this article, or claim that may be made by its manufacturer, is not guaranteed or endorsed by the publisher.

frontiers in Aging Neuroscience

ORIGINAL RESEARCH
published: 20 October 2021
doi: 10.3389/fnagi.2021.727832

Cerebral Vasoreactivity Changes Over Time in Patients With Different Clinical Manifestations of Cerebral Small Vessel Disease

Jacek Staszewski[1], *Aleksander Dębiec*[1]*, *Ewa Skrobowska*[2] *and Adam Stępień*[1]

[1] *Military Institute of Medicine, Clinic of Neurology, Warsaw, Poland,* [2] *Department of Radiology, Military Institute of Medicine, Warsaw, Poland*

Objectives: Endothelial dysfunction (ED) has been linked to the pathogenesis of cerebral small vessel disease (SVD). We aimed to assess ED and cerebrovascular reactivity (CVR) in the patients with a diverse manifestation of SVD, with similar and extensive white matter lesions (WMLs, modified Fazekas scale grade ≥2), compared with a control group (CG) without the MRI markers of SVD, matched for age, gender, hypertension, diabetes, and to evaluate the change of CVR following 24 months.

Methods: We repeatedly measured the vasomotor reactivity reserve (VMRr) and breath-holding index (BHI) of the middle cerebral artery (MCA) by the transcranial Doppler ultrasound (TCD) techniques in 60 subjects above 60 years with a history of lacunar stroke (LS), vascular dementia (VaD), or parkinsonism (VaP) (20 in each group), and in 20 individuals from a CG.

Results: The mean age, frequency of the main vascular risk factors, and sex distribution were similar in the patients with the SVD groups and a CG. The VMRr and the BHI were more severely impaired at baseline (respectively, 56.7 ± 18% and 0.82 ± 0.39) and at follow-up (respectively, 52.3 ± 16.7% and 0.71 ± 0.38) in the patients with SVD regardless of the clinical manifestations (ANOVA, $p > 0.1$) than in the CG (respectively, baseline VMRr 77.2 ± 15.6%, BHI 1.15 ± 0.47, $p < 0.001$; follow-up VMRr 74.3 ± 17.6%, BHI 1.11 ± 0.4, $p < 0.001$). All the assessed CVR measures (VMRr and BHI) significantly decreased over time in the subjects with SVD (Wilcoxon's signed-rank test $p = 0.01$), but this was not observed in the CG ($p > 0.1$) and the decrease of CVR measures was not related to the SVD radiological progression ($p > 0.1$).

Conclusions: This study provided evidence that the change in CVR measures is detectable over a 24-month period in patients with different clinical manifestations of SVD. Compared with the patients in CG with similar atherothrombotic risk factors, all the CVR measures (BMRr and BHI) significantly declined over time in the subjects with SVD. The reduction in CVR was not related to the SVD radiological progression.

Keywords: neurovascular unit (NVU), cerebral small vessel disease, cerebrovascular reactivity (CVR), endothelial dysfunction, neurovascular coupling

OPEN ACCESS

Edited by:
Shereen Nizari,
University College London,
United Kingdom

Reviewed by:
Michael S. Stringer,
University of Edinburgh,
United Kingdom
Rita Moretti,
University of Trieste, Italy

***Correspondence:**
Aleksander Dębiec
adebiec@wim.mil.pl

Received: *19 June 2021*
Accepted: *13 September 2021*
Published: *20 October 2021*

Citation:
Staszewski J, Dębiec A, Skrobowska E and Stępień A (2021) Cerebral Vasoreactivity Changes Over Time in Patients With Different Clinical Manifestations of Cerebral Small Vessel Disease. Front. Aging Neurosci. 13:727832. doi: 10.3389/fnagi.2021.727832

BACKGROUND

Small vessel disease (SVD) is one of the most important cerebral microangiopathy, responsible for the majority of lacunar stroke (LS), vascular dementia (VaD), and parkinsonism (VaP) cases (Pantoni, 2010). The basic mechanism of the cerebral vessels alterations in the SVD is linked to endothelial dysfunction (ED), but whether ED only reflects the load of atherothrombotic risk factors or if it is specific to SVD has not been clearly defined (Forsberg et al., 2018). The neurovascular unit (NVU) concept accentuates the symbiotic association between brain cells, cerebral blood vessels, and subsequently cerebral blood flow (CBF) (Muoio et al., 2014). The endothelium and vascular smooth muscle within the NVU forms the basis of blood-brain-barrier (BBB), and contribute to the neurovascular coupling that is the response of the cerebral vessel to the changes in neural activity (Attwell et al., 2010). The SVD is a dynamic and progressive pathology involving variable components of NVU and BBB, however, the long-term clinical effects and outcomes usually differ between patients (Kisler et al., 2017). The recent studies have shown that the signaling pathways in the NVU control diverse processes, e.g., blood clotting and CBF, nevertheless it is not known precisely how CBF dysregulation translate to the disorders associated with neurovascular dysfunction, such as SVD. Cerebrovascular reactivity (CVR) is a measure of the capability of adaptive changes to vasodilatory stimuli (e.g., change in pCO_2 due to CO_2 inhalation, voluntary apnea, hyperventilation, or acetazolamide), and reflects the compensation of the collateral flow, therefore it can be used to indirectly assess and monitor the sequences of cerebral ED and the progression of vascular disease (Lavi et al., 2006). The reduced CVR indicates the impairment of NVU and regulatory mechanisms of CBF which result in neurovascular uncoupling. There are no biological markers to accurately assess brain vasoreactivity; however, CVR can be evaluated by various tools, such as single photon emission computed tomography (SPECT), PET, various MRI techniques, and transcranial Doppler ultrasound (TCD) (Terborg et al., 2000). Currently, one of the most widely used methods to measure the CVR is MRI, and it offers advantages over the use of radiolabeled products while maintaining regional specificity (Sleight et al., 2021). Though no direct anatomical information can be obtained, TCD permits for the evaluation of mean flow velocity (MFV) changes in the major cerebral arteries after a vasodilative stimulus and it provides complementary information of the brain hemodynamics (Ringelstein et al., 1988; Ebrahim et al., 2019; Burley et al., 2021a). The results of the TCD examination (MFV and pulsatility index) and the ventilation tests correlate with those obtained by other methods, and the value of TCD in the evaluation of CVR impairment, e.g., in the asymptomatic or symptomatic individuals with the brain white matter lesions (WMLs) has been established (Maeda et al., 1993; Marcos et al., 1997; Ghorbani et al., 2015; Fu et al., 2019). The assessment of CVR can be achieved with the bilateral recording of MFV in the middle cerebral artery (MCA) with acceptable reproducibility and inter-rater reliability using carbogen inhalation (McDonnell et al., 2013). Recently, we have found that the cerebral vasodilator responses to breath hold and hyperventilation were abnormal in the patients with VaD, LS, and VaP caused by SVD, and they were severely impaired when compared with the controls matched for the main vascular risk factors and free from the cerebrovascular events (Staszewski et al., 2019). Most of the studies assessing CVR in SVD did not evaluate the CVR changes over time or had unmatched control groups (CGs) (Thrippleton et al., 2018). Therefore, our study aimed to investigate the CVR changes over 24 months in the subjects with diverse manifestations of SVD (LS, VaD, and VaP), with similar and extensive radiological burdens of the disease and compare with a carefully selected CG without MRI markers of SVD, free of cerebrovascular events, and matched for major vascular comorbidities.

MATERIALS AND METHODS

Participants

We analyzed the patients from the SHEF-CSVD Study in which the baseline and follow-up CVR and MRI imaging could be evaluated (Staszewski et al., 2013). The study protocol with detailed selection criteria and methodology has been described previously (Staszewski et al., 2019).

In brief: the SVD group consisted of ambulatory subjects above 60 years, enrolled between December 2011 and September 2015, with established LS (according to the OCSP criteria), VaP, or VaD (according to the Hurtig or NINDS-AIREN criteria) (Chui et al., 1992; Hurtig, 1993; Zijlmans et al., 2004). The patients with MRI contraindications, non-SVD-related WMLs, strategic single-infarct dementia, or post-stroke VaP or VaD, recurrent LS, carotid artery stenosis $\geq$50%, atrial fibrillation, chronic kidney disease (CKD) requiring dialysis, life expectancy $<$6 months, and recent head trauma were not included. To maximize the statistical power, we decided to analyze the equal groups of subjects and we recruited the consecutive patients with VaP and matched them in a 1:1 ratio with VaD, LS patients, and CG (without known cerebrovascular disease or dementia) according to sex, age ($\pm$5 years), and the presence of diabetes and hypertension. The signs of SVD are often seen in MRI in cognitively healthy elderly, and they are highly age-related. The studies showed that the WMLs are detected in 30–90% of cognitively healthy elderly (mean 72–74 years), therefore to maximize the homogeneity of the studied groups, we included only controls with no radiological signs of SVD in MRI (Fazekas 0) and the patients with SVD with extensive WMLs (Fazekas grade 2 or 3) (Longstreth et al., 2005; Gustavsson et al., 2015).

Of the 139 screened subjects (101 patients with SVD and 38 controls), 59 were excluded (18 controls, 15 LS, 9 VaD, and 17 VaP) due to inadequate acoustical bone window at the baseline ($n = 16$), the radiological markers of SVD in controls at baseline MRI examination ($n = 3$), withdrawal of consent during follow-up ($n = 7$), lack of follow-up MRI ($n = 22$), or TCD examination ($n = 11$). The patients with SVD and incomplete follow-up data ($n = 30$) had similar mean age (70.2 ± 7.6 vs. 72.6 ± 6.9, $p = 0.14$) and the baseline SVD score (2.1 ± 0.6 vs. 2 ± 0.6, $p = 0.6$) comparing with those included to the final analysis, however, more men dropped-out in comparison with women (48 vs. 9%, $p < 0.01$). The most common reported reason for lack of follow-up

was that the subjects felt asymptomatic or did not tolerate well to the baseline MRI or TCD examination. Finally, the study group comprised 60 patients with newly diagnosed symptomatic SVD (20 per group: VaP, VaD, and LS) and 20 controls. All the patients were functionally independent (modified Rankin Scale, mRS $\leq$ 3 and total Barthel Index $\geq$ 80) and without severe dementia (Mini-Mental State Examination, MMSE $\geq$ 12) (Schulc et al., 2015).

Study Procedures

All the patients signed informed consent before entering the study. The consent has been obtained prior to any study specific procedures. All the patients had TCD and MRI examinations performed at baseline and the 24-month follow-up visit (mean 23.1 $\pm$ 4 months; LS 22.5 $\pm$ 3; VaP 21.5 $\pm$ 4.6; VaD 23.3 $\pm$ 3.4; CG 23.6 $\pm$ 2; and ANOVA $p = 0.28$).

Ultrasound Examinations

The determination of the cerebrovascular reserve capacity is based on the ability of the intracranial arterioles to dilate. The CO_2 tests assume the correlation among the CBF, the CO_2 partial pressure, and the flow velocity in the basal cerebral arteries, and the reduction or elevation of pCO_2 leads to a decrease or increase in MFV. Since TCD measures flow velocity in the large arteries, this reflects flow in the combined gray and white matter. The TCD study included evaluation of both the MCAs with 2-MHz probes (Companion III, Nicolet) in fixed positions according to the standard protocol (Settakis et al., 2002). The MFV values were averaged, and the interhemispheric differences for mean MFV did not exceed 15%. The recordings were considered acceptable when the velocities of blood flow could be detected bilaterally, and with a clear envelope of the MFV spectrum during the entire cardiac cycle. The CVR was measured as the breath-holding index (BHI), the ratio of the percentage MFV increase during hypercapnia, and vasomotor reactivity reserve (VMRr), the percentage change in MFV from hypo- to hypercapnia (Tsivgoulis and Alexandrov, 2008). Basing on the Markus and Harrison procedure, we measured the baseline MFV (baseMFV) following 10 min of rest with normal breathing (normocapnia), the minimal MFV value (minMFV) following 2 min of hyperventilation (hypocapnia), and the MFV value (maxMFV) subsequent to 30 s of breath holding (hypercapnia) and followed by a period of 4 min of normal breathing of room air (Markus and Harrison, 1992). To achieve the most reproducible results before proceeding to the definitive recording, the participants were trained to perform all the procedures correctly. All of them were able to hyperventilate and hold their breath for the required period. The exact length of breath-holding ranged from 29.8 to 30.5 s at the baseline and 30.1 to 30.3 s at follow-up, and it did not differ between the study groups (ANOVA, $p > 0.1$). The end-tidal CO_2 ($etCO_2$) concentration was monitored by capnograph (PC900A, Creative Medical, Shenzhen, China) during the examination. Blood pressure (BP) and heart rate (HR) were measured prior to and following the tests. Although McDonnell et al. found higher intra-rater reliability for the TCD measurements taken while the patients were sitting, we performed TCD examination in all the subjects in the supine position in accordance with our standard protocol (McDonnell et al., 2013). Ultrasound examination was performed under the standardized conditions (same quiet room and time of the day; no sleep deprivation and no medication intake for at least 6 h were allowed) by a single experienced TCD sonographer unaware of the diagnosis of the subjects. All the patients with LS had the study procedures performed at least 3 weeks (mean 24 $\pm$ 2 days) after their index strokes.

MRI Evaluation (GE Healthcare 1.5 T Scanner, IL, USA)

The images were evaluated for the presence of acute LS, lacunes, deep WMLs (dWMLs), or periventricular (pWMLs), microbleeds (MBs), and enlarged perivascular spaces (PVS) according to the STRIVE guidelines and visual SVD scale (Wardlaw et al., 2013; Staals et al., 2014). The simple modified Fazekas rating scale was used to estimate the extent of pWMLs and dWMLs (Fazekas et al., 1987; Inzitari et al., 2009). The mild white matter lesions (Fazekas grade 1) were defined as the punctate lesions in the deep white matter with a maximum diameter of 9 mm for every single lesion and 20 mm for grouped lesions. The moderate white matter lesions (grade 2) were defined as early confluent lesions of 10–20 mm for single lesions and >20 mm for grouped lesions in any diameter, with no more than connecting bridges between the individual lesions. Severe white matter lesions (grade 3) were defined as single lesions or confluent areas of hyperintensity of 20 mm or greater in any diameter. The presence of each of the four MRI markers for SVD (WMH, lacunes, cerebral microbleeds, and perivascular spaces) was counted to retrieve a total SVD score (ranging from 0 to 4). One point on the visual SVD scale was awarded if confluent deep WMLs (Fazekas grade 2 and 3) or irregular periventricular hyperintensities extending into the deep white matter (Fazekas grade 3) were present or when one or more lacunes or MBs were present; 1 point was awarded if moderate (10–25) to extensive (>25) enlarged PVS were present (Kim et al., 2008). The presence of each marker produced a score of a minimum 0 and a maximum of 4, representing the total MRI load of SVD. At baseline MRI assessment, all the patients with SVD had at least Fazekas grade 2 WMLs, and controls did not have radiological markers of SVD in MRI. The visual rating of SVD radiological progression expressed by the WMLs progression or development of new lacunes was performed at a follow-up visit. As proposed by Prins et al., the WMLs progression and lacunes were rated on the FLAIR images and the presence or absence of progression was rated in the three periventricular regions, basal ganglia, infratentorial region, and four subcortical white matter regions (Prins et al., 2004). The images were reviewed by a neuroradiologist (E.S.) blinded to the clinical data.

Atherothrombotic Risk Evaluation

The vascular comorbidities were defined according to the current standards and evaluated based on the available medical data, physical examinations, widespread histories, and routine laboratory tests performed at baseline (Alberti et al., 2009; Goblirsch et al., 2013).

Statistical Analysis

All the demographic data were summarized, tabulated, and verified for normality with the Shapiro–Wilk test, and the homogeneity of the variances was assured by Levene's test. Categorical and continuous data are presented as frequencies or means ± SD and analyzed using Fisher's exact tests, the chi-square test, paired *t*-tests, or non-parametric tests where appropriate.

The associations between MRI progression with CVR changes over time in the studied groups were compared using a linear mixed model. The model included study group (SVD, CG), Time (Baseline, Follow-up), MRI (progression, no progression), and a Time*Group*MRI interaction for fixed effects. The subject variable was specified to assess possible individual variability. Per group, the Wilcoxon's signed-rank test was performed to evaluate the differences between CVR and other hemodynamic measures at the baseline and at follow-up visits. One-way ANOVA and chi-square tests were used to compare data between the study groups with *post-hoc* Tukey's honestly significant difference (HSD) tests for comparisons among the SVD subgroups. The effect sizes for the group differences were analyzed with partial eta squared (η_p^2) reflecting the proportion of the total variance attributable to the effect (and considered small if 0.01, moderate around 0.06, and high if >0.13). A probability value of $p < 0.05$ was

TABLE 1 | Main characteristics of the study population at baseline.

Variable	SVD ($n = 60$)	LS ($n = 20$)	VaP ($n = 20$)	VaD ($n = 20$)	CG ($n = 20$)	$p^{\#}$
Demographics						
Age (y)*	72.6 (±6.9)	71.7(±7.7)	73.8 (±6.2)	72.2 (±6.8)	71.9 (±3.2)	0.7
Female gender (%)*	30 (50)	10 (50)	10 (50)	10 (50)	10 (50)	1
Vascular risk factors						
Hypertension (%)*	54 (89)	18 (90)	18 (90)	18 (90)	18 (90)	1
Diabetes (%)*	30 (50)	10 (50)	10 (50)	10 (50)	10 (50)	1
CAD (%)	22 (37)	8 (40)	7 (35)	7 (35)	7 (35)	0.2
Current smoking (%)	22 (37)	7 (35)	6 (30)	9 (45)	8 (40)	0.5
Hyperlipidemia (%)	45 (75)	15 (75)	16 (80)	14 (70)	15 (75)	0.8
CKD (%)	8 (13)	2 (10)	2 (10)	4 (20)	3 (15)	0.3
PS (%)	28 (46)	10 (50)	10 (50)	8 (40)	8 (40)	0.8
Obesity (BMI>30)	17 (28)	6 (30)	6 (30)	5 (25)	6 (30)	0.8
Examination findings						
Homocysteine (μmol/l)	14.4 ± 6.1	13.2 ± 3.7	18.1 ± 8.3	12.03 ± 3.5	13.1 ± 2.7	0.01
hsCRP (mg/dL)	0.55 ± 0.9	0.56 ± 1.02	0.64 ± 0.9	0.46 ± 0.8	0.16 ± 0.17	0.2
Uric acid (mg/dL)	5.4 ± 1.5	5.8 ± 1.6	5.5 ± 1.3	4.8 ± 1.5	4.6 ± 1.3	0.05
eGFR (ml/min/1.73 m^2)	78.8 ± 24.1	77.1 ± 29	72.3 ± 22.8	87 ± 17.2	95 ± 16	0.01
HbA1c (%)	6.2 ± 1.03	6.3 ± 1.2	5.9 ± 0.5	6.3 ± 1.2	5.9 ± 0.1	0.26
FG (mg/dL)	120.1 ± 43.2	128.8 ± 48.6	112.8 ± 32.3	120.6 ± 47.2	106.3 ± 18.7	0.21
LDL (mg/dL)	108.4 ± 37.8	97.1 ± 35.5	110.6 ± 36.6	116.5 ± 40.4	122.8 ± 41.8	0.22
HDL (mg/dL)	52.2 ± 17	46.7 ± 10	55.2 ± 16.9	54.1 ± 22.5	60.9 ± 19.3	0.12
TG (mg/dL)	124.5 ± 57.9	125.6 ± 60.1	132.1 ± 64.2	115.5 ± 50	115.1 ± 39	0.7
TC (mg/dL)	185.2 ± 48.1	166.8 ± 39.5	194.4 ± 54.7	193.4 ± 54.7	198.7 ± 31.7	0.1
BMI	26.4 ± 5.6	27.7 ± 7.6	25.1 ± 4	26.3 ± 4.5	27.8 ± 3.8	0.3
MRI examination						
SVD score (mean ± SD)	2 ± 0.6	2.2 ± 0.7	2 ± 0.6	2.1 ± 0.6	0	<0.01
Fazekas pWMLs (mean ± SD)	1.45 ± 0.9	1.5 ± 1.1	1.4 ± 1	1.5 ± 0.7	0	<0.01
Fazekas dWMLs (mean ± SD)	1.6 ± 0.9	1.7 ± 1.1	1.5 ± 0.8	1.7 ± 0.9	0	<0.01
Vascular treatment						
Statin treatment (%)	45 (75)	15 (75)	16 (80)	14 (70)	15 (75)	0.8
ACEI (%)	15 (25)	6 (30)	4 (20)	5 (25)	7 (35)	0.6
Beta blocker (%)	22 (37)	8 (40)	7 (35)	7 (35)	7 (35)	0.2
ARB (%)	19 (32)	6 (30)	7 (35)	6 (30)	7 (35)	0.4
Calcium channel blocker (%)	23 (38)	9 (40)	7 (35)	7 (35)	7 (35)	0.4
Diuretics (%)	12 (20)	4 (20)	3 (15)	5 (25)	4 (20)	0.2

Values represent the means (± SD) for continuously distributed data or the numbers (%) for categorical data.

**Matched factors; #ANOVA and χ^2 difference between the groups $p < 0.05$ compared with CG according to Tukey's honestly significant difference (HSD) test.*

SVD, cerebral small vessel disease; LS, lacunar stroke; VaD, vascular dementia; VaP, vascular parkinsonism; CG, control group; CAD, coronary artery disease; BMI, body mass index; FG, fasting glucose; PS, polymetabolic syndrome; CKD, chronic kidney disease; IMT, intima-media thickness; ACEI, angiotensin-converting-enzyme inhibitors, ARB, angiotensin receptor blockers.

considered significant, all the analyses were made using the PQStat 1.8.0 software.

The study has been approved by the Internal Revision Board (Wojskowy Instytut Medyczny, 46/WIM/2010) and it was conducted in accordance with the Declaration of Helsinki.

RESULTS

The studied cohort consisted of 80 older adults (mean 72.4 ± 6.2 years) of both sexes (50% women). The baseline characteristic of the studied cohort is provided in **Table 1**. The prevalence of the main comorbidities was similar in groups, but there were some differences in the laboratory examination findings: the CG had lower concentrations of homocysteine, showed a trend toward lower concentration of uric acid, and had higher levels of estimated glomerular filtration rate (eGFRs) comparing with other subjects. The SVD subgroups had a similar prevalence of vascular risk factors and treatment use, laboratory, and MRI findings (Fazekas grade 3 was scored by 80% LS, 80% VaD, and 75% VaP subjects; $p = 0.7$). The mean $etCO_2$ concentrations and systolic blood pressure (SBP), diastolic blood pressure (DBP), and heart rate (HR) measures during hyperventilation and breath holding did not differ between the CG and the SVD group, and they were also similar between the SVD subgroups. In addition, these variables did not significantly differ between the baseline and follow-up assessments (Wilcoxon's sign rank test, $p > 0.1$). The reproducibility measurements of VMRr and BHI were performed in a sample of 12 individuals (four from CG, eight with LS). The intraclass correlation coefficient for the two consecutive measurements was 0.90; $p < 0.01$ for VMRr and 0.88; $p < 0.01$ for BHI.

Vasomotor reactivity reserve and the BHI were more severely impaired at the baseline and at follow-up assessments in the patients in the SVD groups (regardless of the clinical spectrum of the disease) than in the CG (**Table 2**). The size effect of the difference was similar in all comparisons (eta-squared ranged between 0.25 and 0.29). For better visualization, the CVR change in the individual subjects is shown in (**Supplementary Figures 1, 2**).

Vasomotor reactivity reserve and the BHI were significantly lower in diabetic patients with SVD vs. diabetic controls at the two timepoints (baseline VMRr: 55.8 ± 16 vs. 74 ± 18%, respectively, $p < 0.001$; BHI: 0.79 ± 0.39 vs. 1.1 ± 0.3, $p = 0.02$; follow-up VMRr 52.7 ± 15 vs. 71.2 ± 20, $p < 0.01$; BHI: 0.72 ± 0.4 vs. 1.04 ± 0.5, $p < 0.01$ and the difference was also significant between the non-diabetic subjects from SVD group vs. CG (respectively; baseline VMRr: 54.2 ± 18.4 vs. 79.9 ± 13.7, $p < 0.001$; BHI: 0.78 ± 0.39 vs. 1.16 ± 0.55, $p = 0.01$; follow-up VMRr 52.1 ± 18 vs. 76.8 ± 14.9%, $p < 0.01$; BHI: 0.70 ± 0.35 vs. 1.15 ± 0.2; $p < 0.001$).

Both the assessed CVR measures (VMRr and the BHI) significantly declined over time in the subjects with SVD (Wilcoxon's signed-rank test, $p = 0.01$), however, there was no significant decline of VMRr and BHI in CG over 24 months of observation (Wilcoxon's signed-rank test $p > 0.1$) (**Figure 1**). The mean VMRr and BHI values were also similar at the baseline and follow-up measurements

TABLE 2 | Basal and follow-up characteristics and vasodilatation responses of cerebral arteries in all the subjects.

Variable	SVD ($n = 60$)	LS ($n = 20$)	VaP ($n = 20$)	VaD ($n = 20$)	CG ($n = 20$)	$p^{\#}$
Baseline measures						
MFV (cm/s)	41.5 ± 12*	43.9 ± 15	42 ± 9.5	38.4 ± 10.4*	46.8 ± 8.7	0.03
VMRr (%)	56.7 ± 18.4*	55.4 ± 18.6*	55.1 ± 15.2*	54.2 ± 18.7*	77.2 ± 15.6	<0.001
BHI	0.82 ± 0.39*	0.86 ± 0.4*	0.77 ± 0.28*	0.71 ± 0.4*	1.15 ± 0.47	<0.001
Resting SBP, mmHg	127.2 ± 17.2	130.1 ± 16.2	126.1 ± 11.1	125.2 ± 16	124 ± 19	0.2
Resting DBP, mmHg	73.4 ± 10.1	72.4 ± 13.2	73.2 ± 12.4	74.4 ± 11	74.1 ± 8	0.7
Resting HR, beats/min	76.8 ± 6.6	76.8 ± 4.7	75.2 ± 8.2	78.3 ± 6.6	72.1 ± 6.1	0.8
Delta $etCO_2$ HV (%)	1.3 ± 0.15	1.4 ± 0.4	1.3 ± 0.2	1.1 ± 0.7	1.4 ± 0.5	0.6
Delta $etCO_2$ BH (%)	1.2 ± 0.1	1.3 ± 0.2	1.3 ± 0.6	1.1 ± 0.6	1.2 ± 0.4	0.8
Follow-up measures						
MFV (cm/sek)	35.2 ± 11.2*	37.1 ± 15.6	34.3 ± 9.2*	34.2 ± 8.3*	43.1 ± 8.2	0.06
VMRr (%)	52.3 ± 16.7*	54.4 ± 17.9*	49.3 ± 11.5*	53.2 ± 19.7*	74.3 ± 17.6*	<0.001
BHI	0.71 ± 0.38*	0.72 ± 0.5*	0.71 ± 0.24*	0.69 ± 0.4*	1.11 ± 0.4*	<0.001
Resting SBP, mmHg	124.8 ± 13.9	127.2 ± 17.1	125.3 ± 9.8	122.1 ± 15	127 ± 9	0.3
Resting DBP, mmHg	76.3 ± 11	74.1 ± 14.1	78.1 ± 7.7	76.7 ± 11	74.2 ± 10	0.6
Resting HR, beats/min	73.9 ± 2.2	72.6 ± 3	75.2 ± 1.2	74.1 ± 2.4	70 ± 10.5	0.2
Delta $etCO_2$ HV (%)	1.23 ± 0.6	1.3 ± 0.7	1.2 ± 0.5	1.2 ± 0.6	1.9 ± 0.7	0.3
Delta $etCO_2$ BH (%)	1.16 ± 0.7	1.1 ± 0.8	1.1 ± 0.4	1.3 ± 0.4	1.2 ± 0.7	0.8

*$^{\#}$ANOVA difference between the groups, *$p < 0.05$ compared with the CG.*

SVD, cerebral small vessel disease; LS, lacunar stroke; VaD, vascular dementia; VaP, vascular parkinsonism; CG, control group; MFV, mean flow velocity; BHI, breath holding index; VMRr, vasomotor reactivity reserve; PI, pulsatile index; RI, resistance index; SBP, systolic blood pressure; DBP, diastolic blood pressure; HR, heart rate.

Δ $etCO_2$HV, Δ end-tidal CO_2 during hyperventilation; Δ $etCO_2$ BH, Δ end-tidal CO_2 during breath holding.

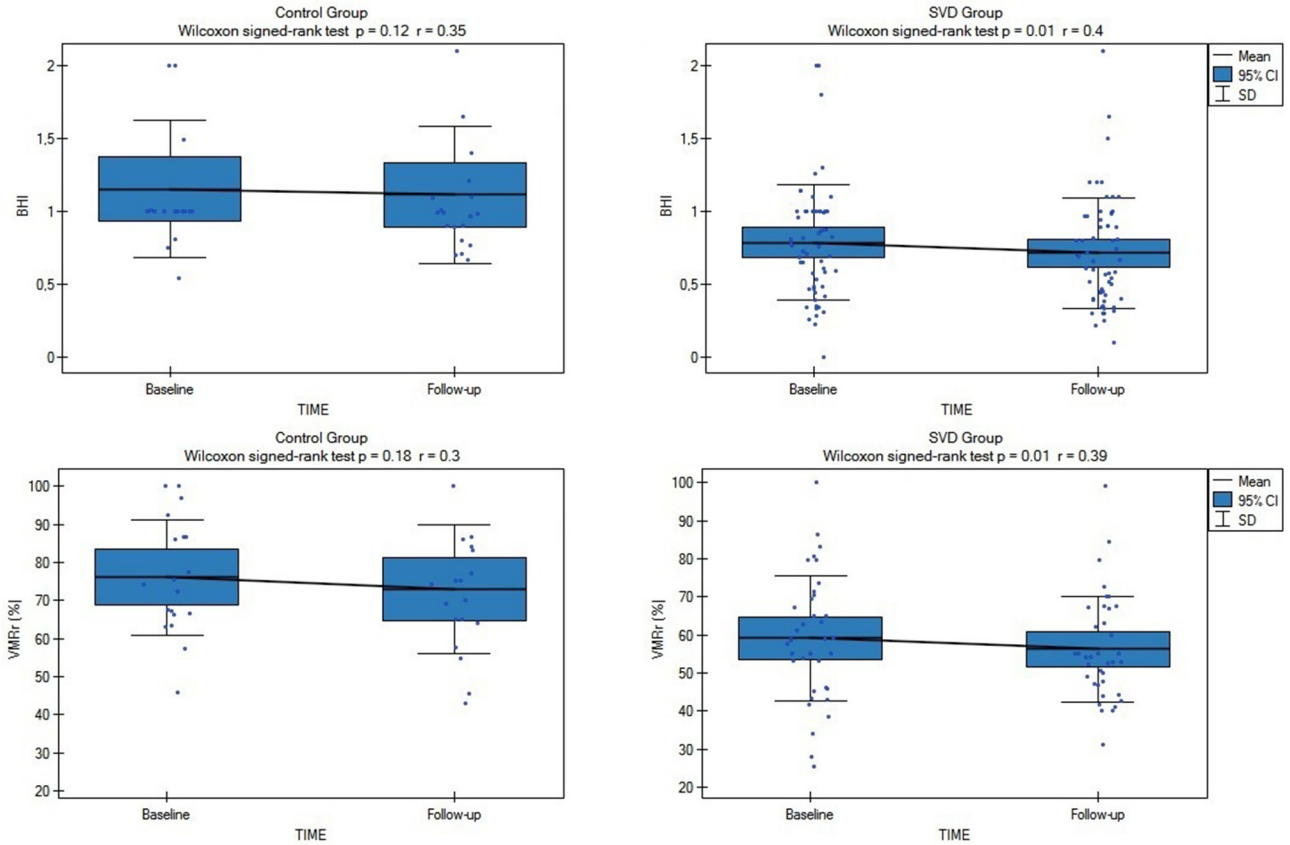

FIGURE 1 | Comparison of baseline and follow-up cerebrovascular reactivity (CVR) measures (VMRr [vasomotor reactivity reserve] and breath-holding index [BHI]) in all subjects from cerebral small vessel disease (SVD) and control group (CG). SVD, cerebral small vessel disease; VMRr, vasomotor reactivity reserve; BHI, breath-holding index.

among the patients with LS, VaD, and VaP (ANOVA, $p > 0.1$).

Radiological progression during the study was observed in 28 of the 80 subjects (35%): significantly more often ($p = 0.03$) in the SVD subjects ($n = 25$ [42%]: eight subjects from LS [40%] group, eight with VaD [40%], and nine with VaP [45%], with no difference between the SVD groups [ANOVA $p > 0.1$]) than in the CG ($n = 3$; 15%). During the follow-up, only 4/80 patients (5%) experienced lacunar stroke (two patients from LS group and two from VaD group), no other vascular events were observed. Although in patients with SVD who experienced radiological progression, all the CVR measures were considerably impaired at the baseline and follow-up assessments compared with the no progression group (respectively, baseline VMRr 43.3 ± 13.2% vs. 63.3 ± 14.9%, $p < 0.001$; eta-square 0.33; baseline BHI 0.63 ± 0.39 vs. 0.9 ± 0.36, $p < 0.001$; eta-square 0.12; follow-up VMRr 41.2 ± 13.4% vs. 60.3 ± 14%, $p < 0.001$; eta-square 0.32; BHI 0.52 ± 0.24 vs. 0.84 ± 0.39, $p < 0.001$; eta-square 0.19), no significant decrease of CVR measures was observed during 24 months of observation (Wilcoxon's signed-rank test, $p > 0.1$) (**Figure 2**). These data did not change significantly when we analyzed all the patients (SVD and CG) with the radiological progression vs. no progression group (respectively, baseline VMRr 45.4 ± 14.1% vs. 68.6 ± 16.9%, $p < 0.001$; baseline BHI 0.65 ± 0.37 vs. 1.0 ± 0.42, $p < 0.001$; follow-up VMRr 43.1 ± 14.3% vs. 65.7 ± 16.9%, $p < 0.001$; BHI 0.55 ± 0.24 vs. 1.0 ± 0.47, $p < 0.001$) and there was also no significant decrease of CVR measures over time of observation (Wilcoxon's signed-rank test, $p > 0.1$). No interaction between CVR measures, time of assessment, and radiological progression in the SVD group were observed in the fixed linear analysis (**Table 3**).

DISCUSSION

This prospective study performed in symptomatic SVD has shown that the change in CVR measures is detectable following a 24-month period and that 42% of patients with SVD demonstrated radiological progression. We also confirmed that the cerebral vasoreactivity measures decreased in SVD regardless of the clinical manifestation of the disease. On the opposite, we did not demonstrate a significant CVR decrease in the subjects from CG who were neurologically asymptomatic, had no radiological markers of SVD in the baseline MRI, but who shared similar atherothrombotic risk factors as the SVD group. Although patients with SVD and radiological progression had

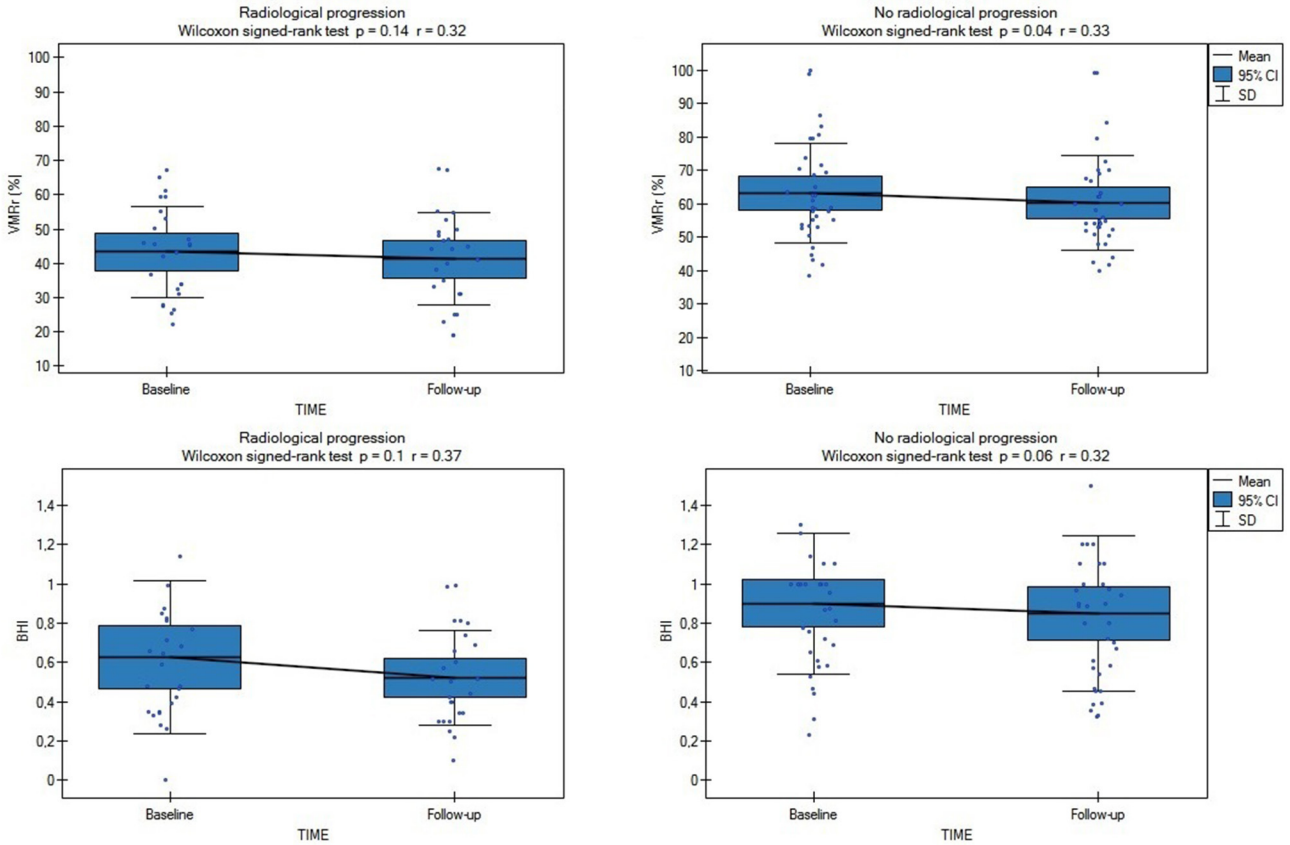

FIGURE 2 | Comparison of baseline and follow-up CVR measures (VMRr and BHI) in SVD subjects with ($n = 25$) and without radiological progression ($n = 35$). VMRr, vasomotor reactivity reserve; BHI, breath-holding index.

TABLE 3 | Association among the cerebral small vessel disease (SVD), assessment time point, and MRI progression on the cerebrovascular reactivity (CVR) measures.

						95% CI	
Dependent variable	**Fixed factor(s)**	**B**	**SE**	***t***	***P****	**Lower limit**	**Upper limit**
BHI							
	Time	−0.01	0.05	−0.01	0.90	−0.11	0.11
	SVD	−0.47	0.11	−4.26	<0.01	−0.69	−0.25
	MRI progression	−0.60	0.22	−2.70	0.01	−1.04	−0.16
	Time*SVD	0.05	0.07	0.55	0.50	−0.20	0.38
	Time*MRI progression	0.08	0.18	1.20	0.24	−0.15	0.59
	SVD*MRI progression	0.29	0.24	1.23	0.22	−0.18	0.77
	Time*SVD*MRI progression	−0.02	0.16	−0.13	0.80	−0.34	0.30
VMRr							
	Time	−3.90	2.60	−1.40	0.20	−9.20	1.30
	SVD	−27.10	4.34	−6.20	<0.01	−35.70	−18.50
	MR progression	−28.80	9.20	−3.10	0.01	−47.10	−10.50
	Time*SVD	7.05	3.23	2.13	0.20	−0.20	5.97
	Time*MRI progression	9.04	6.80	1.32	0.20	−4.50	22.60
	SVD*MRI progression	9.80	9.90	0.90	0.30	−9.98	29.60
	Time*SVD*MRI progression	−10.07	7.40	−1.35	0.17	−24.80	6.70

**Linear mixed effects model.*

BHI, breath holding index; VMRr, vasoreactivity reserve; SVD, small vessel disease.

TABLE 4 | Major transcranial Doppler ultrasound (TCD) studies assessing CVR in sporadic small vessel disease populations.

References	Study population	CVR assessment	Results
Molina et al. (1999)	46 patients with lacunar stroke and 46 CG	Acetazolamide test	Significant CVR reduction in SVD group
Terborg et al. (2000)	46 patients with SVD and 13 CG	Ventilation tests; NIRS	Significantly reduced VMR in TCD and NIRS assessments in severe SVD; a good correlation between the validity of TCD and NIRS
Kidwell et al. (2001)	55 patients with SVD	PI	Correlation between PI and severity of SVD ; PI cut points allowed discrimination of PVH with 89% sensitivity and 86% specificity and discrimination of DWMH with 70% sensitivity and 73% specificity.
Pánczél et al. (2002)	25 patients with lacunar stroke, 20 patients with leukoaraiosis and 35 CG	Tilting, ventilation, and acetazolamide tests	CVR in BA and MCA territory was impaired in hypercapnia in SVD; no significant differences between CVR measures in BA and MCA territory in acetazolamide test; significantly higher $VRCO_2$ in MCA vs BA measurements
Ghorbani et al. (2015)	56 patients with SVD and 48 CG	PI	Good correlation between PI and SVD radiological manifestations: - In PVH with PI cut-off = 0.83, the sensitivity 90% and specificity 98% - In DWMH with PI = 0.79, the sensitivity 75% specificity 87.5% - In lacunar stroke with PI = 0.80, the sensitivity 73% and specificity 90%. - In PH with PI = 0.69, the sensitivity 92% and specificity 87.5%. - In PVH+ DWMH+ lacunar with PI = 0.83, the sensitivity 90% and specificity 96%.
Nam et al. (2020)	206 patients with lacunar stroke	PI	PI was positively associated with the WMHs volume and the presence of old lacunar infarcts.

TCD, transcranial Doppler ultrasound; PI, pulsatile index; MRI, magnetic resonance imaging; SVD, cerebral small vessel disease; CG, control group; PVH, preventricular hyperintensity; DWMH, deep white matter hyperintensity; CVR, cerebrovascular reactivity; BA, basilar artery; MCA, middle cerebral artery; VRCO, ventilatory response to CO_2; PH, pontin hyperintensity; NIRS, near-infrared spectroscopy; CT, computed tomography.

severely impaired CVR at the baseline and follow-up comparing with the subjects with no MRI progression, there was no significant interaction between that CVR decline and risk of radiological progression.

Besides of growing evidence of MRI techniques which increasingly play a more important role as a non-invasive tool capable to assess the cerebral reserve capacity in combination with a vascular challenge, the vasomotor reactivity testing with TCD is still a gold diagnostic standard and it has been proved to assess CBF and indirectly monitor the function of ED in patients with cerebral microangiopathy (Kozera et al., 2009; D'Andrea et al., 2016). The TCD studies demonstrated that CVR is negatively correlated with the duration of hypertension, patient age, and history of cerebrovascular events (Fujishima et al., 2001; Kozera et al., 2010). Some older studies using SPECT or Xenon CT techniques revealed that LS, particularly with leukoaraiosis was associated with the reduced CBF in the white matter and cortex in the subjects with severe WMLs, while the studies on VaD consistently showed reductions in both the white and gray matter (Markus et al., 2000). Many studies investigated CBF in the patients with SVD using TCD techniques, and in line with our data, the majority of them revealed impaired CBF comparing with the healthy controls in the patients with symptomatic and asymptomatic LS, more marked in multiple comparing with single infarcts and a reduction in reactivity that was correlated with the degree of leukoaraiosis (**Table 4**) (Maeda et al., 1993; Molina et al., 1999; Terborg et al., 2000). There is, however, a lack of studies on the dynamic CVR changes over time, especially in SVD, and in well-characterized SVD populations, e.g., in rarely studied patients with VaD and VaP. As SVD is a wide term and it is used to describe the different disease processes ranging from asymptomatic WMLs in normal individuals through to the symptomatic SVD subjects, as we aimed in the presented report, our data added some further evidence that cerebral ED occurs and progresses in patients with LS, VaD, or VaP due to SVD, even if they had well-controlled hypertension (according to the baseline and follow-up BP measurements). Interestingly, a similar trend was not observed in CG with comparable atherothrombotic risk factors (age, sex, diabetes, hypertension, obesity, and smoking), and this may suggest that other vascular factors or duration of exposure to vascular risk factors in SVD are more important and responsible for a continuous decline in the CVR (Muoio et al., 2014). For example, the studies on patients with cerebrovascular disease showed that the reduction in vasodilatory capacity in asymptomatic carotid disease can predispose for the development of cerebrovascular disease (Silvestrini et al., 2000). In 2020, Soman et al. (2020) using arterial spin labeling MRI to evaluate which cardiovascular risk factors alter the CVR found that higher SBP, chronic kidney disease, history of past stroke, and hypercholesterolemia are responsible for the impaired CVR. Although the controls and patients with SVD in our study were well-balanced with the main comorbidities, we did not control other important risk factors of SVD. For instance, chronic poor sleep patterns, depression, prediabetes, and unhealthy diet (dietary salt) can impact the endothelial function through immune influences (Hakim, 2019). Of notice, the Oxford Vascular (OXVASC) Study importantly showed that premorbid hypertension in midlife correlated more strongly with the global SVD burden than a single blood pressure measurement or a known history of hypertension (Lau et al., 2018).

Whether the progressive decrease of CVR is specific to the progressive nature of SVD is unknown (Stevenson et al., 2010). Importantly, we showed that there was no difference in the CVR at the baseline and follow-up assessments between the SVD clinical subgroups and this finding possibly could be related to similar WMLs burden or comparable prevalence of comorbidities. We also observed that the subjects with radiological progression had the most impaired CVR at baseline which, however, did not significantly decrease over time. These findings may indicate that MRI progression in that group may be related to the baseline severe CVR impairment or other factors, e.g., inflammatory or prothrombotic. It is also possible that the TCD measures are less sensitive to the more subtle changes, particularly in the white matter flow. Our results are, however, opposite to a large study in 628 asymptomatic individuals (mean 69 years) with WMLs which showed a progressive reduction in the CBF velocity measured using TCD as WMLs severity increased (Tzourio et al., 2001). Some similar data were demonstrated by Sam et al., who established areas of reduced CVR that preceded the development of WMLs by advanced MRI techniques, suggesting that CVR impairment contributes to the development and progression of SVD (Sam et al., 2016). On the opposite, in a PROSPER trial of statin therapy that investigated 390 individuals with cardiovascular risk factors, there was no association between CBF and the prevalence of WMLs at baseline, a decline of CBF, and risk of development of deep WMLs (Ten Dam et al., 2007). Our results are also in line with the study that showed significantly reduced CVR in LS than in the CG, which, however, could not be explained by the main atherothrombotic risk factors (Deplanque et al., 2013). It is important to appreciate that cerebral reactivity and autoregulation are not fully understood, although the neurogenic, metabolic, or myogenic factors were proposed. Of notice, CO_2-CVR is only one of the several mechanisms of cerebral autoregulation, thus preserved CO_2-CVR does not imply intact cerebral autoregulation (Klinzing et al., 2021). Therefore, CVR impairment could be due to different mechanisms, e.g., related to genetic factors or BBB dysfunction, resulting in microvascular dysfunction (Zlokovic, 2011). Some important aspects of the present study related to the patients with VaD and VaP should be underlined as these subjects probably share SVD pathology with neurodegenerative disease, and it is not established whether the microvascular changes reflect the diminished demand caused by the advanced neurodegeneration or whether SVD precedes and contributes to the neurodegeneration. For example, impaired cerebrovascular reserve capacity and vasoreactivity (identified using TCD along with the BHI) was found in the patients with mild cognitive impairment, Alzheimer's disease, and Parkinson's disease without severe underlying atherosclerosis (Shim et al., 2015; Urbanova et al., 2018). Although the contribution of CVR impairment to the pathogenesis of neurodegenerative diseases is not certain, it might be suspected that a reduced cerebrovascular reserve is an additional deteriorating factor in the neurodegeneration (Ojeda et al., 2017). One unanswered key question is that whether any reductions in the CBF are primary, or merely occurs secondary to the brain damage as due to vaso-neuronal coupling, the reductions in brain metabolism are associated with reduced CBF (Markus et al., 2014).

Most studies in the literature have demonstrated the differences in CBF between the groups of patients with SVD and controls, with very few studies addressing the sensitivity and specificity of these parameters in TCD and MRI examinations (Panerai, 2009). The large variations in CVR across the patients and between different sessions of the same subject are often observed in the TCD and MRI studies, which hamper the ability of these measures in monitoring disease progression (Hou et al., 2020). It should be especially stressed that there are concerns with the application of the BHI as the relationship between breath-hold length and the pCO_2 stimulus remains unclear and this test has low reproducibility and high variability (Alwatban et al., 2018; Koep et al., 2020). The latest studies showed that the blood oxygenation level dependent MRI (BOLD-MRI) method is most reliable and reproducible because it has the advantage of mapping the whole brain with good spatial resolution, allowing investigation of CVR regional distribution (Leoni et al., 2012). Despite the relationships between the baseline CBF measures from TCD and MRI, the current studies showed no direct correlations between the CVR metrics calculated from TCD and MRI-BOLD measures during a 5%CO_2 challenge (Burley et al., 2021b). These variations in the CVR measures in different imaging modalities are important as they significantly reduce the statistical power to detect the pathology-related differences, preclude personalized determination of abnormalities, and challenge the validity of comparing CVR metrics across the studies.

Our study has several limitations, and the data should be cautiously interpreted owing to the single-center design and a small number of subjects included that may introduce bias. Even if we analyzed a relatively homogeneous cohort and highly selected SVD sample of patients, it should be considered a hypothesis-generating pilot study, because it may be less representative of the overall SVD population. However, the majority of the TCD studies on CVR in subjects with SVD had low patient numbers or controls (**Table 4**). Although the patients were prohibited from taking any drugs before the examinations, some medications could have affected the dilatory responses of the arteries. In future studies, additional research may be needed to determine the effect of treatment as a function of CBF on the prognosis of patients. The other limitations are that we used 1.5 Tesla MRI which potentially limited the accuracy of the radiological assessment, and we did not account for $etCO_2$ for calculating the CVR. This could have influenced the results and limit the generalizability and reproducibility of the study, since $PaCO_2$ has a marked influence on CBF and autoregulation, evaluations could be compromised in situations where significant changes in $PaCO_2$ are undetected (Panerai et al., 1999). However, in our study, no significant difference between the subgroups and between the baseline and follow-up $etCO_2$ measures were noticed. Despite the multitude of alternatives to the gas challenges, existing literature lacks definitive conclusions regarding the best practices for the vasoactive modulation and associated analysis protocols for the TCD studies resulting in numerous metrics of cerebral

autoregulation (Valdueza et al., 2008; Sanders et al., 2018). Regardless of methodology, an assessment of cerebrovascular autoregulation is prone to moderate noise and artifact, with low reliability and reproducibility (Lee et al., 2020). In our study, CVR was assessed using TCD which additionally suffers from a limited field of view comparing with the MRI techniques and thus it may be less reflective of the local changes in the tissue blood supply. However, due to limited access and the high cost of MRI examination, the non-invasive, bedside, and acceptable repeatable assessments using TCD, it remains still the most utilized tool to study the CBF regulation in humans. As different techniques have low correlations and target different parts of the vascular tree, they should, however, be regarded as complementary and they are recommended to be used together (Purkayastha and Sorond, 2012; Burley et al., 2021b). Another important limiting factor is that the hemodynamic effect of breath holding is lower than that of CO_2 inhalation or acetazolamide injection, therefore the validity of our results should be confirmed in the future (Marcic et al., 2021). The TCD measurements are limited to the large basal arteries and can only provide an index of global rather than local CBF velocity, and it is highly operator dependent. However, all the TCD tests in our study were carried out by a single certified examiner who has 15 years of experience working with TCD, and thus we have minimized a possible interpersonal difference depending on the experience of the examiner.

The present study has, however, some important strengths. To the best of our knowledge, no data have been published on repeatedly assessed CVR measures over 24 months of observation in a well-phenotyped cohort of patients with SVD with extensive radiological markers of SVD. Ours is the first study to investigate all CVR by TCD in a wide range of participants, such as normal controls and patients with LS, VaD, and VaP. Our findings of impaired and progressive CVR alterations in the SVD subjects are important as this mechanism could contribute to exacerbating the clinical condition and may constitute a potential line of research for the treatment. A better understanding of the variations in CVR is of importance in both clinical and basic science applications (Hou et al., 2020). The majority of data on CVR are derived from the studies on individuals with asymptomatic WMLs, therefore, our study, which included homogenous groups of symptomatic SVD subjects, is important (Blair et al., 2016).

In conclusion, we provided further evidence that cerebral ED occurs and progresses over time in the patients with different clinical manifestations of SVD, however, we did not observe a significant CVR difference between the subjects with SVD and radiological progression comparing with no progression group and no significant CVR alterations over time in the CG who were neurologically asymptomatic and who shared similar comorbidities to the SVD group. The longitudinal studies with larger sample sizes are needed to definite the causal conclusions and confirm these findings.

DATA AVAILABILITY STATEMENT

The raw data supporting the conclusions of this article will be made available by the authors, without undue reservation.

ETHICS STATEMENT

The studies involving human participants were reviewed and approved by Local Medical Ethics Committee, Military Institute of Medicine, Warsaw, Poland (46/WIM/2010). The patients/participants provided their written informed consent to participate in this study.

AUTHOR CONTRIBUTIONS

JS: conceptualization, methodology, validation, data curation, and project administration. JS and ES: investigation. JS and AD: writing—original draft preparation. JS and AS: supervision. All authors have read and agreed to the published version of the manuscript.

FUNDING

This study was supported by the Polish Ministry of Science and Higher Education as a research project of the Military Institute of Medicine (Warsaw, Poland, study number N N402 473840).

SUPPLEMENTARY MATERIAL

The Supplementary Material for this article can be found online at: https://www.frontiersin.org/articles/10.3389/fnagi.2021.727832/full#supplementary-material

REFERENCES

Alberti, K. G., Eckel, R. H., Grundy, S. M., Zimmet, P. Z., Cleeman, J. I., Donato, K. A., et al. (2009). Harmonizing the metabolic syndrome: a joint interim statement of the International Diabetes Federation Task Force on Epidemiology and Prevention; National Heart, Lung, and Blood Institute; American Heart Association; World Heart Federation; International Atherosclerosis Society; and International Association for the Study of Obesity. *Circulation* 120, 1640–1645. doi: 10.1161/CIRCULATIONAHA.109.192644

Alwatban, M., Truemper, E. J., Al-Rethaia, A., Murman, D. L., Bashford, G. R. (2018). The breath-hold acceleration index: a new method to evaluate cerebrovascular reactivity using transcranial Doppler. *J. Neuroimaging* 28, 429–435. doi: 10.1111/jon.12508

Attwell, D., Buchan, A. M., Charpak, S., Lauritzen, M., Macvicar, B. A., and Newman, E. A. (2010). Glial and neuronal control of brain blood flow. *Nature* 468, 232–243. doi: 10.1038/nature09613

Blair, G. W., Doubal, F. N., Thrippleton, M. J., Marshall, I., and Wardlaw, J. M. (2016). Magnetic resonance imaging for assessment of cerebrovascular reactivity in cerebral small vessel disease: a systematic review. *J. Cereb. Blood Flow Metab.* 36, 833–841. doi: 10.1177/0271678X16631756

Burley, C. V., Francis, S. T., Thomas, K. N., Whittaker, A. C., Lucas, S. J. E., and Mullinger, K. J. (2021b). Contrasting measures of cerebrovascular reactivity

between MRI and Doppler: a cross-sectional study of younger and older healthy individuals. *Front. Physiol.* 12:656746. doi: 10.3389/fphys.2021.656746

Burley, C. V., Francis, S. T., Whittaker, A. C., Mullinger, K. J., and Lucas, S. J. E. (2021a). Measuring resting cerebral haemodynamics using MRI arterial spin labelling and transcranial Doppler ultrasound: comparison in younger and older adults. *Brain Behav.* 11:e02126. doi: 10.1002/brb3.2126

Chui, H. C., Victoroff, J. I., Margolin, D., Jagust, W., Shankle, R., and Katzman, R. (1992). Criteria for the diagnosis of ischemic vascular dementia proposed by the State of California Alzheimer's disease diagnostic and treatment centers. *Neurology* 42, 473–480. doi: 10.1212/WNL.42.3.473

D'Andrea, A., Conte, M., Cavallaro, M., Scarafile, R., Riegler, L., Cocchia, R., et al. (2016). Transcranial Doppler ultrasonography: from methodology to major clinical applications. *World J. Cardiol.* 8, 383–400 doi: 10.4330/wjc.v8.i7.383

Deplanque, D., Lavallee, P. C., Labreuche, J., Gongora-Rivera, F., Jaramillo, A., Brenner, D., et al. (2013). Cerebral and extracerebral vasoreactivity in symptomatic lacunar stroke patients: a case-control study. *Int. J. Stroke* 8, 413–421. doi: 10.1111/j.1747-4949.2011.00755.x

Ebrahim, M. H., Khalil, S. H. M., Elbaghdady, M. M. T., and Ata Ata Shaaban, A. E. (2019). Transcranial Doppler assessment of patients with cerebral small vessel disease. *J. Med. Sci. Res.* 2, 75–82. doi: 10.4103/JMISR.JMISR_15_19

Fazekas, F., Chawluk, J. B., Alavi, A., Hurtig, H. I., and Zimmerman, R. A. (1987). MR signal abnormalities at 1.5T in Alzheimer's dementia and normal aging. *AJNR Am. J. Neuroradiol.* 8, 421–426. doi: 10.2214/ajr.149.2.351

Forsberg, K. M. E., Zhang, Y., Reiners, J., Ander, M., Niedermayer, A., Fang, L., et al. (2018). Endothelial damage, vascular bagging and remodeling of the microvascular bed in human microangiopathy with deep white matter lesions. *Acta Neuropathol. Commun.* 6:128. doi: 10.1186/s40478-018-0632-z

Fu, S., Zhang, J., Zhang, H., and Zhang, S. (2019). Predictive value of transcranial doppler ultrasound for cerebral small vessel disease in elderly patients. *Arq. Neuropsiquiatr.* 77, 310–314. doi: 10.1590/0004-282x20190050

Fujishima, S., Ohya, Y., Sugimori, H., Kitayama, J., Kagiyama, S., Ibayashi, S., et al. (2001). Transcranial doppler sonography and ambulatory blood pressure monitoring in patients with hypertension. *Hypertens. Res.* 24, 345–351. doi: 10.1291/hypres.24.345

Ghorbani, A., Ahmadi, M. J., and Shemshaki, H. (2015). The value of transcranial Doppler derived pulsatility index for diagnosing cerebral small-vessel disease. *Adv. Biomed. Res.* 4:54. doi: 10.4103/2277-9175.151574

Goblirsch, G., Bershow, S., Cummings, K., Hayes, R., Kokoszka, M., Lu, Y., et al. (2013). *Stable Coronary Artery Disease*. Vol. 5. Bloomington, MN: Institute for Clinical Systems Improvement (ICSI), 71.

Gustavsson, A. M., Stomrud, E., Abul-Kasim, K., Minthon, L., Nilsson, P. M., Hansson, O., et al. (2015). Cerebral *Cerebrovasc. Dis.* microbleeds and white matter hyperintensities in cognitively healthy elderly: a cross-sectional cohort study evaluating the effect of arterial stiffness. *Extra* 5, 41–51. doi: 10.1159/000377710

Hakim, A. M. (2019). Small vessel disease. *Front. Neurol.* 10:1020. doi: 10.3389/fneur.2019.01020

Hou, X., Liu, P., Li, Y., Jiang, D., De Vis, J. B., Lin, Z., et al. (2020). The association between BOLD-based cerebrovascular reactivity (CVR) and end-tidal CO2 in healthy subjects. *Neuroimage* 207:116365. doi: 10.1016/j.neuroimage.2019.116365

Hurtig, H. I. (1993). "Vascular parkinsonism," in *Parkinsonian Syndromes*, eds M. B. Stern and W. C. Koller (New York, NY: Marcel Dekker), 81–83.

Inzitari, D., Pracucci, G., Poggesi, A., Carlucci, G., Barkhof, F., Chabriat, H., et al. (2009). Changes in white matter as determinant of global functional decline in older independent outpatients: three year follow-up of LADIS (leukoaraiosis and disability) study cohort. *BMJ* 339:b2477. doi: 10.1136/bmj.b2477

Kidwell, C. S., el-Saden, S., Livshits, Z., Martin, N. A., Glenn, T. C., and Saver, J. L. (2001). Transcranial Doppler pulsatility indices as a measure of diffuse small-vessel disease. *J. Neuroimaging* 11, 229–235. doi: 10.1111/j.1552-6569.2001.tb00039.x

Kim, K. W., MacFall, J. R., and Payne, M. E. (2008). Classification of white matter lesions on magnetic resonance imaging in elderly persons. *Biol. Psychiatry* 64, 273–280. doi: 10.1016/j.biopsych.2008.03.024

Kisler, K., Nelson, A. R., Montagne, A., and Zlokovic, B. V. (2017). Cerebral blood flow regulation and neurovascular dysfunction in Alzheimer disease. *Nat. Rev. Neurosci.* 18, 419–434. doi: 10.1038/nrn.2017.48

Klinzing, S., Stretti, F., Pagnamenta, A., Bèchir, M., and Brandi, G. (2021). Transcranial color-coded duplex sonography assessment of cerebrovascular reactivity to carbon dioxide: an interventional study. *BMC Neurol.* 21:305. doi: 10.1186/s12883-021-02310-9

Koep, J. L., Barker, A. R., Banks, R., Banger, R. R., Sansum, K. M., Weston, M. E., et al. (2020). The reliability of a breath-hold protocol to determine cerebrovascular reactivity in adolescents. *J. Clin. Ultrasound* 48, 544–552. doi: 10.1002/jcu.22891

Kozera, G. M., Dubaniewicz, M., Zdrojewski, T., Madej-Dmochowska, A., Mielczarek, M., Wojczal, J., et al. (2010). Cerebral vasomotor reactivity and extent of white matter lesions in middle-aged men with arterial hypertension: a pilot study. *Am. J. Hypertens*. 23, 1198–1203. doi: 10.1038/ajh.2010.152

Kozera, G. M., Wolnik, B., Kunicka, K. B., Szczyrba, S., Wojczal, J., Schminke, U., et al. (2009). Cerebrovascular reactivity, intima-media thickness, and nephropathy presence in patients with type 1 diabetes. *Diabetes Care* 32, 878–882. doi: 10.2337/dc08-1805

Lau, K. K., Li, L., Simoni, M., Mehta, Z., Küker, W., and Rothwell, P. M., Oxford Vascular Study (2018). Long-term premorbid blood pressure and cerebral small vessel disease burden on imaging in transient ischemic attack and ischemic stroke. *Stroke* 49, 2053–2060. doi: 10.1161/STROKEAHA.118.021578

Lavi, S., Gaitini, D., Milloul, V., and Jacob, G. (2006). Impaired cerebral CO2 vasoreactivity: association with endothelial dysfunction. *Am. J. Physiol. Heart Circ. Physiol.* 291, H1856–H1861. doi: 10.1152/ajpheart.00014.2006

Lee, Y. K., Rothwell, P. M., Payne, S. J., and Webb, A. J. S. (2020). Reliability, reproducibility and validity of dynamic cerebral autoregulation in a large cohort with transient ischaemic attack or minor stroke. *Physiol. Meas.* 41:095002. doi: 10.1088/1361-6579/abad49

Leoni, R. F., Mazzetto-Betti, K. C., Silva, A. C., et al. (2012). Assessing cerebrovascular reactivity in carotid steno-occlusive disease using MRI BOLD and ASL techniques. *Radiol. Res. Pract*. 2012:268483. doi: 10.1155/2012/268483

Longstreth, W. T. Jr., Arnold, A. M., Beauchamp, N. J. Jr., Manolio, T. A., Lefkowitz, D., Jungreis, C., et al. (2005). Incidence, manifestations, and predictors of worsening white matter on serial cranial magnetic resonance imaging in the elderly: the Cardiovascular Health Study. *Stroke* 36, 56–61. doi: 10.1161/01.STR.0000149625.99732.69

Maeda, H., Matsumoto, M., Handa, N., Hougaku, H., Ogawa, S., Itoh, T., et al. (1993). Reactivity of cerebral blood flow to carbon dioxide in various types of ischemic cerebrovascular disease: evaluation by the transcranial Doppler method. *Stroke* 24, 670–675. doi: 10.1161/01.STR.24.5.670

Marcic, M., Marcic, L.,Marcic, B., Capkun, V., and Vukojevic, K. (2021). Cerebral vasoreactivity evaluated bytranscranial color doppler and breath-holding test in patients after SARS-CoV-2 infection. *J. Pers. Med*. 11:379. doi: 10.3390/jpm11050379

Marcos, A., Egido, J. A., Barquero, M., Fernandez, C., and de Seijas, E. V. (1997). Full range of vasodilatation tested by transcranial Doppler in the differential diagnosis of vascular and Alzheimer types of dementia. *Cerebrovasc. Dis.* 7, 14–18. doi: 10.1159/000108157

Markus, H., Allan, C., and Ebmeier, K. (2014). "Cerebral hemodynamics in cerebral small vessel disease," in *Cerebral Small Vessel Disease*, eds L. Pantoni and P. Gorelick (Cambridge: Cambridge University Press), 180–191. doi: 10.1017/CBO9781139382694.016

Markus, H. S., and Harrison, M. J. (1992). Estimation of cerebrovascular reactivity using transcranial Doppler, including the use of breath-holding as the vasodilatory stimulus. *Stroke* 23. 668–673. doi: 10.1161/01.STR.23.5.668

Markus, H. S., Lythgoe, D. J., Ostegaard, L., O'Sullivan, M., and Williams, S. C. (2000). Reduced CBF in white matter in ischemic leukoaraiosis demonstrated using quantitative exogenous contrast based perfusion MRI. *J. Neurol. Neurosurg. Psychiatry* 69, 48–53. doi: 10.1136/jnnp.69.1.48

McDonnell, M. N., Berry, N. M., Cutting, M. A., Keage, H. A., Buckley, J. D., and Howe, P. R. (2013). Transcranial Doppler ultrasound to assess cerebrovascular reactivity: reliability, reproducibility and effect of posture. *PeerJ* 1:e65. doi: 10.7717/peerj.65

Molina, C., Sabin, J. A., Montaner, J., Rovira, A., Abilleira, S., and Codina, A. (1999). Impaired cerebrovascular reactivity as a risk marker for first-ever lacunar infarction: a case-control study. *Stroke* 30, 2296–2301. doi: 10.1161/01.STR.30.11.2296

Muoio, V., Persson, P. B., and Sendeski, M. M. (2014). The neurovascular unit - concept review. *Acta Physiol.* 210, 790–798. doi: 10.1111/apha.12250

Nam, K. W., Kwon, H. M., and Lee, Y. S. (2020). Distinct association between cerebral arterial pulsatility and subtypes of cerebral small vessel disease. *PLoS ONE* 15:e0236049. doi: 10.1371/journal.pone.0236049

Ojeda, A. E., Martinez, H. R., Rivera, F. G., Garza, J. M. E., and Medina, H. C. (2017). Cerebral vasoreactivity in Parkinson's Disease: a cross-sectional pilot study in a hispanic cohort. *J. Alzheimers. Dis. Parkinsonism* 7:336. doi: 10.4172/2161-0460.1000336

Pánczél, G., Bönöczk, P., and Nagy, Z. (2002). A vazoreaktivitás zavara agytörzsi és hemisphaerialis kisérbetegségben: összehasonlító vizsgálat [Impairment of vasoreactivity in brainstem and hemispheral small vessel disease: comparative study]. *Ideggyogy Sz* 55, 95–101.

Panerai, R. B. (2009). Transcranial Doppler for evaluation of cerebral autoregulation. *Clin. Auton. Res.* 19, 197–211. doi: 10.1007/s10286-009-0011-8

Panerai, R. B., Deverson, S. T., Mahony, P., Hayes, P., and Evans, D. H. (1999). Effects of CO2 on dynamic cerebral autoregulation measurement. *Physiol. Meas.* 20, 265–275. doi: 10.1088/0967-3334/20/3/304

Pantoni, L. (2010). Cerebral small vessel disease: from pathogenesis and clinical characteristics to therapeutic challenges. *Lancet Neurol.* 9, 689–701. doi: 10.1016/S1474-4422(10)70104-6

Prins, N. D., van Straaten, E. C., van Dijk, E. J., Simoni, M., van Schijndel, R. A., Vrooman, H. A., et al. (2004). Measuring progression of cerebral white matter lesions on MRI: visual rating and volumetrics. *Neurology* 62, 1533–1539. doi: 10.1212/01.WNL.0000123264.40498.B6

Purkayastha, S., and Sorond, F. (2012). Transcranial Doppler ultrasound: technique and application. *Semin. Neurol.* 32, 411–420. doi: 10.1055/s-0032-1331812

Ringelstein, E. B., Sievers, C., Ecker, S., Schneider, P. A., and Otis, S. M. (1988). Noninvasive assessment of CO2-induced cerebral vasomotor response in normal individuals and patients with internal carotid artery occlusions. *Stroke* 19, 963–969. doi: 10.1161/01.STR.19.8.963

Sam, K., Crawley, A. P., Conklin, J., Poublanc, J., Sobczyk, O., Mandell, D. M., et al. (2016). Development of white matter hyperintensity is preceded by reduced cerebrovascular reactivity. *Ann. Neurol.* 80, 277–285. doi: 10.1002/ana.24712

Sanders, M. L., Claassen, J. A. H. R., Aries, M., Bor-Seng-Shu, E., Caicedo, A., Chacon, M., et al. (2018). Reproducibility of dynamic cerebral autoregulation parameters: a multi-centre, multi-method study. *Physiol. Meas.* 39:125002. doi: 10.1088/1361-6579/aae9fd

Schulc, E., Pallauf, M., Mueller, G., Wildbahner, T., and Them, C. (2015). Is the barthel index an adequate assessment tool for identifying a risk group in elderly people living at home? *Int. J. Nurs. Clin. Pract.* 2:140. doi: 10.15344/2394-4978/2015/140

Settakis, G., Lengyel, A., Molnár, C., Bereczki, D., Csiba, L., and Fülesdi, B. (2002). Transcranial Doppler study of the cerebral hemodynamic changes during breath-holding and hyperventilation tests. *J. Neuroimaging* 12, 252–258. doi: 10.1111/j.1552-6569.2002.tb00129.x

Shim, Y., Yoon, B., Shim, D. S., Kim, W., An, J.-Y., and Yang, D.-W. (2015). Cognitive correlates of cerebral vasoreactivity on transcranial doppler in older adults. *J. Stroke Cerebrovasc. Dis.* 24, 1262–1269. doi: 10.1016/j.jstrokecerebrovasdis.2015.01.031

Silvestrini, M., Vernieri, F., Pasqualetti, P., Matteis, M., Passarelli, F., Troisi, E., et al. (2000). Impaired cerebral vasoreactivity and risk of stroke in patients with asymptomatic carotid artery stenosis. *JAMA* 283, 2122–2127. doi: 10.1001/jama.283.16.2122

Sleight, E., Stringer, M. S., Marshall, I., Wardlaw, J. M., and Thrippleton, M. J. (2021). Cerebrovascular reactivity measurement using magnetic resonance imaging: a systematic review. *Front. Physiol.* 12:643468. doi: 10.3389/fphys.2021.643468

Soman, S., Dai, W., Dong, L., Hitchner, E., Lee, K., Baughman, B. D., et al. (2020). Identifying cardiovascular risk factors that impact cerebrovascular reactivity: an ASL MRI study. *J. Magn. Reson. Imaging* 51, 734–747. doi: 10.1002/jmri.26862

Staals, J., Makin, S. D., Doubal, F. N., Dennis, M. S., and Wardlaw, J. M. (2014). Stroke subtype, vascular risk factors, and total MRI brain small-vessel disease burden. *Neurology* 83, 1228–1234. doi: 10.1212/WNL.0000000000000837

Staszewski, J., Piusińska-Macoch, R., Skrobowska, E., Brodacki, B., Pawlik, R., Dutkiewicz, T., et al. (2013). Significance of haemodynamic and haemostatic factors in the course of different manifestations of cerebral small vessel disease: the SHEF-CSVD Study-study rationale and protocol. *Neurosci. J.* 2013:424695. doi: 10.1155/2013/424695

Staszewski, J., Skrobowska, E., Piusińska-Macoch, R., Brodacki, B., and Stepień, A. (2019). Cerebral and extracerebral vasoreactivity in patients with different clinical manifestations of cerebral small-vessel disease: data from the significance of hemodynamic and hemostatic factors in the course of different manifestations of cerebral small-vessel disease study. *J. Ultrasound Med.* 38, 975–987. doi: 10.1002/jum.14782

Stevenson, S. F., Doubal, F. N., Shuler, K., and Wardlaw, J. M. (2010). A systematic review of dynamic cerebral and peripheral endothelial function in lacunar stroke versus controls. *Stroke* 41, e434–e442. doi: 10.1161/STROKEAHA.109.569855

Ten Dam, V. H., van den Heuvel, D. M., de Craen, A. J., Bollen, E. L., Murray, H. M., Westendorp, R. G., et al. (2007). Decline in total cerebral blood flow is linked with increase in periventricular but not deep white matter hyperintensities. *Radiology*. 243, 198–203. doi: 10.1148/radiol.2431052111

Terborg, C., Gora, F., Weiller, C., and Röther, J. (2000). Reduced vasomotor reactivity in cerebral microangiopathy: a study with near-infrared spectroscopy and transcranial Doppler sonography. *Stroke* 31, 924–929. doi: 10.1161/01.STR.31.4.924

Thrippleton, M. J., Shi, Y., Blair, G., Hamilton, I., Waiter, G., Schwarzbauer, C., et al. (2018). Cerebrovascular reactivity measurement in cerebral small vessel disease: rationale and reproducibility of a protocol for MRI acquisition and image processing. *Int. J. Stroke* 13, 195–206. doi: 10.1177/1747493017730740

Tsivgoulis, G., and Alexandrov, A. V. (2008). Cerebral hemodynamics in acute stroke: pathophysiology and clinical implications. *J. Vasc. Interv. Neurol.* 1, 65–69.

Tzourio, C., Levy, C., Dufouil, C., Touboul, P. J., Ducimetière, P., Alpérovitch, A., et al. (2001). Low cerebrl blood flow velocity and risk of white matter hyperintensities. *Ann. Neurol.* 49, 411–414. doi: 10.1002/ana.82

Urbanova, B. S., Schwabova, J. P., Magerova, H., Jansky, P., Markova, H., Vyhnalek, M., et al. (2018). Reduced cerebrovascular reserve capacity as a biomarker of microangiopathy in Alzheimer's disease and mild cognitive impairment. *J. Alzheimer's Dis.* 63, 465–477. doi: 10.3233/JAD-170815

Valdueza, J. M., Schreiber, S. J., Roehl, J.-E., and Klingebiel, R. (2008). "Intracranial hemodynamics and functional tests," in *Neurosonology and Neuroimaging of Stroke*, ed J. M. Valdueza (New York, NY: Thieme), 79–88.

Wardlaw J. M., Smith E. E., Biessels G. J., Cordonnier, C., Fazekas, F., Frayne, R., et al. (2013). Neuroimaging standards for research into small vessel disease and its contribution to ageing and neurodegeneration. *Lancet Neurol.* 12, 822–838. doi: 10.1016/S1474-4422(13)70124-8

Zijlmans, J. C. M., Daniel, S. E., Hughes, A. J., Révész, T., and Lees, A. J. (2004). Clinicopathological investigation of vascular parkinsonism, including clinical criteria for diagnosis. *Mov. Disord.* 19, 630–640. doi: 10.1002/mds.20083

Zlokovic, B. V. (2011). Neurovascular pathways to neurodegeneration in Alzheimer's disease and other disorders. *Nat. Rev. Neurosci.* 12, 723–738. doi: 10.1038/nrn3114

Conflict of Interest: The authors declare that the research was conducted in the absence of any commercial or financial relationships that could be construed as a potential conflict of interest.

Publisher's Note: All claims expressed in this article are solely those of the authors and do not necessarily represent those of their affiliated organizations, or those of the publisher, the editors and the reviewers. Any product that may be evaluated in this article, or claim that may be made by its manufacturer, is not guaranteed or endorsed by the publisher.

frontiers in Aging Neuroscience

REVIEW
published: 20 October 2021
doi: 10.3389/fnagi.2021.749026

From Neurodevelopmental to Neurodegenerative Disorders: The Vascular Continuum

Julie Ouellette[1,2] *and Baptiste Lacoste*[1,2,3]*

[1] Ottawa Hospital Research Institute, Neuroscience Program, Ottawa, ON, Canada, [2] Department of Cellular and Molecular Medicine, Faculty of Medicine, University of Ottawa, Ottawa, ON, Canada, [3] University of Ottawa Brain and Mind Research Institute, Ottawa, ON, Canada

Structural and functional integrity of the cerebral vasculature ensures proper brain development and function, as well as healthy aging. The inability of the brain to store energy makes it exceptionally dependent on an adequate supply of oxygen and nutrients from the blood stream for matching colossal demands of neural and glial cells. Key vascular features including a dense vasculature, a tightly controlled environment, and the regulation of cerebral blood flow (CBF) all take part in brain health throughout life. As such, healthy brain development and aging are both ensured by the anatomical and functional interaction between the vascular and nervous systems that are established during brain development and maintained throughout the lifespan. During critical periods of brain development, vascular networks remodel until they can actively respond to increases in neural activity through neurovascular coupling, which makes the brain particularly vulnerable to neurovascular alterations. The brain vasculature has been strongly associated with the onset and/or progression of conditions associated with aging, and more recently with neurodevelopmental disorders. Our understanding of cerebrovascular contributions to neurological disorders is rapidly evolving, and increasing evidence shows that deficits in angiogenesis, CBF and the blood-brain barrier (BBB) are causally linked to cognitive impairment. Moreover, it is of utmost curiosity that although neurodevelopmental and neurodegenerative disorders express different clinical features at different stages of life, they share similar vascular abnormalities. In this review, we present an overview of vascular dysfunctions associated with neurodevelopmental (autism spectrum disorders, schizophrenia, Down Syndrome) and neurodegenerative (multiple sclerosis, Huntington's, Parkinson's, and Alzheimer's diseases) disorders, with a focus on impairments in angiogenesis, CBF and the BBB. Finally, we discuss the impact of early vascular impairments on the expression of neurodegenerative diseases.

Keywords: cerebrovascular abnormalities, neurodevelopment and intellectual disabilities, aging, neurodegeneration, cerebral blood flow, angiogenesis, blood-brain barrier

OPEN ACCESS

Edited by:
Anusha Mishra,
Oregon Health and Science University, United States

Reviewed by:
Barbara Lykke Lind,
University of Copenhagen, Denmark
Ravi L. Rungta,
Université de Montréal, Canada
Vanessa Coelho-Santos,
Seattle Children's Research Institute, United States

***Correspondence:**
Baptiste Lacoste
blacoste@uottawa.ca

Received: *28 July 2021*
Accepted: *13 September 2021*
Published: *20 October 2021*

Citation:
Ouellette J and Lacoste B (2021) From Neurodevelopmental to Neurodegenerative Disorders: The Vascular Continuum. Front. Aging Neurosci. 13:749026. doi: 10.3389/fnagi.2021.749026

INTRODUCTION

The human brain contains approximately 100 billion vessels (∼600 km), all of which are critical for the delivery of nutrients and oxygen to neural cells (Quaegebeur et al., 2011). Although the brain accounts for only 2% of the body's mass, it consumes about a quarter of the body energy produced at rest (Attwell et al., 2010). This colossal energy consumption is elemental to maintain normal functioning of the brain. Such energy requirements make the brain heavily reliant on key vascular features: (i) a dense vasculature to sustain adequate perfusion, (ii) a functional blood-brain barrier (BBB) to maintain brain homeostasis, and (iii) the proper regulation of cerebral blood flow (CBF) to match metabolic demands (**Figure 1**). Thus, a healthy brain vasculature is essential to support neural cells and ensure normal brain maturation, function and aging (Attwell and Laughlin, 2001; Girouard and Iadecola, 2006; Andreone et al., 2015; Lacoste and Gu, 2015). This is accomplished in part via neurovascular coupling (NVC) mechanisms that regulate CBF to support energetic demands of brain cells (Hamel, 2006; Attwell et al., 2010; Kaplan et al., 2020). While most studies are describing neurovascular signaling at the level of the microvasculature, other vascular segments have received very little attention. There is evidence suggesting that different vascular segments play different roles during vascular responses which is involved in maintaining brain homeostasis. The concept of heterogeneous vascular modules has been extensively reviewed in Schaeffer and Iadecola (2021).

The close anatomical apposition between the nervous and vascular systems supports a functionally integrated network (Attwell et al., 2010; Lecrux and Hamel, 2011; Hillman, 2014; Huneau et al., 2015; Kaplan et al., 2020). This involves modulating vascular tone by secretion of vasoconstrictor and vasodilator molecules. Initially, it was proposed that local metabolic factors released by neurons modulate local CBF (Sherrington, 1890; Friedland and Iadecola, 1991). Since then, several studies have introduced other cellular mediators of NVC which altogether form the neurovascular unit (NVU). This anatomical substrate of NVC indeed involves a multicellular system consisting of neurons, pericytes, smooth muscle cells, astrocytes, microglia and endothelial cells (ECs) that together orchestrate CBF, and thus brain function (Attwell et al., 2010; Andreone et al., 2015; Grubb et al., 2021; **Figure 1**). The cerebral cortex is innervated by projection neurons that release neurotransmitters including, but not limited to, acetylcholine, noradrenaline, serotonin and glutamate, involved in the regulation of vessel diameter (Sandoo et al., 2010). Pericytes, while having debated roles in NVC, possess contractile properties and regulate blood flow around capillaries (Attwell et al., 2010, 2016; Fernandez-Klett and Priller, 2015; Sweeney et al., 2018; Watson et al., 2020; Hartmann et al., 2021). Capillary pericytes are α-smooth muscle actin (SMA)-negative and only partially cover the vessel, while ensheathing pericytes are α-SMA-positive, occupy proximal branches of penetrating arteriole offshoots, and fully cover the vessels. However, they are classified as different from smooth muscle cells as they display an ovoid cell body (Grant et al., 2019). Vascular smooth muscle cells (SMCs), found on intracerebral arterioles and arteries, are absent from intracerebral capillaries. These cells are short, densely packed, ring-shaped, and essential for regulating vessel tone (Lacoste and Gu, 2015; Frosen and Joutel, 2018; Grant et al., 2019). Astrocytes occupy a critical position between blood vessels and neurons. They can modulate vessel tone via receptor-mediated increase in astrocytic Ca^{2+}, resulting in the release of astrocyte-derived prostaglandins (PGE_2), nitric oxide (NO), epoxyeicosatrienoic acids (EETs), glutamate, or adenosine, all of which can alter vascular diameter and tone (Attwell et al., 2010; Cauli and Hamel, 2010; Filosa and Iddings, 2013; Harada et al., 2015; Haidey et al., 2021), as reviewed in detailed elsewhere (Filosa and Iddings, 2013; Howarth, 2014; MacVicar and Newman, 2015; Mishra, 2017; McConnell et al., 2019; Stackhouse and Mishra, 2021). Whereas microglia are the main regulators of inflammatory processes in the brain, their role in NVC is not well defined. However, recently, they were suggested as essential in regulating CBF during neural activation (Császár et al., 2021). Brain ECs have unique morphological and functional features such as a lack of fenestration, the presence of tight junctions between cells, a low number of pinocytic vesicles that limit transcytosis, hence forming the first limiting layer of the BBB (Reese and Karnovsky, 1967; Stamatovic et al., 2008; Rizzo and Leaver, 2010; Salmina et al., 2014; Andreone et al., 2015). This highly selective barrier promotes a tightly regulated brain homeostasis to ensure proper neuronal function, protecting the brain from toxins, pathogens, inflammation, and injury (Weiss et al., 2009; Larsen et al., 2014; Daneman and Prat, 2015; Van Dyken and Lacoste, 2018). Furthermore, brain ECs regulate vascular tone by releasing vasodilators including endothelial-derived NO, endothelium-derived EETs, PGE_2 and prostacyclin, as well as vasoconstrictors such as endothelin-1, thromboxane A_2 and prostaglandin $F_{2\alpha}$ (Mohan et al., 2012; Filosa and Iddings, 2013; Andreone et al., 2015; Kisler et al., 2016, 2017; Dabertrand et al., 2021). While the endothelium regulates vascular permeability and tone, it is also the main target of small vessel disease (SVD), which refers to a pathological process that damages arterioles, venules and brain capillaries. SVD has a major impact on CBF and cognition (Hakim, 2019). The NVU as a whole is also responsible for maintaining BBB integrity (Abbott et al., 2006; Zlokovic, 2008; Daneman, 2012; Kadry et al., 2020). Alterations in vascular patterning, CBF and BBB, either during development or later in life, contribute to the onset and/or progression of early- or late-onset neurological disorders (**Figure 2**).

Well-balanced vascular and neuronal interactions are required to support brain function from early life. The shared spatial and temporal patterns of vascular and neuronal networks suggest an integrative role for vessels in neural development, and *vice versa* (Gu et al., 2005; Carmeliet and Jain, 2011; Andreone et al., 2015; Lacoste and Gu, 2015). Neurovascular crosstalk, which initially takes place during embryogenesis, supports the rising oxygen and nutrient demand of immature neurons as they require extensive energy to maintain normal course of development (De Filippis and Delia, 2011). The increased energy consumption by neurons creates a hypoxic environment acting as a signal for boosting blood vessel production to upsurge delivery of oxygen and metabolic substrates to the brain (Stone et al., 1995;

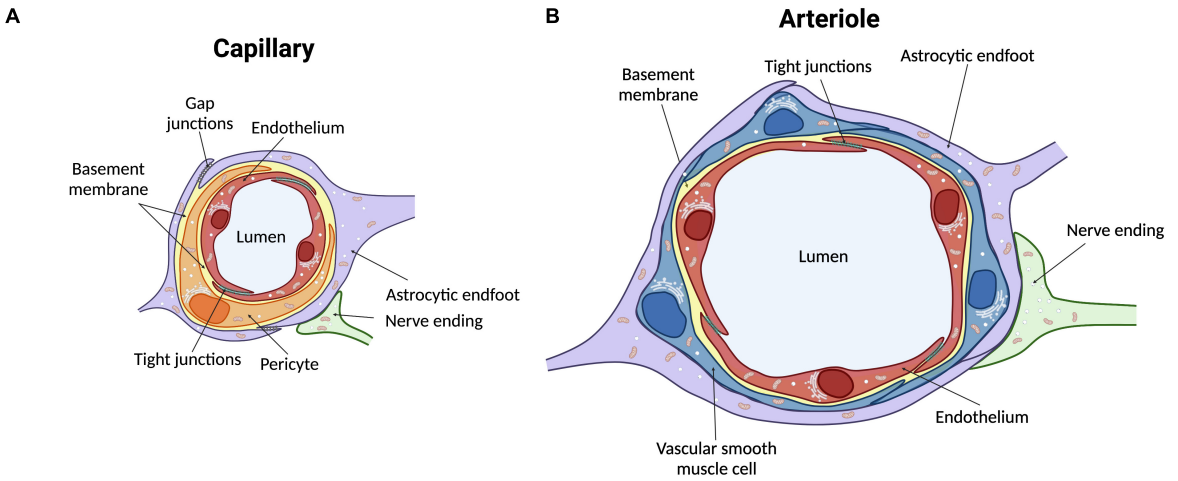

FIGURE 1 | Summary of structures and functions of the neurovascular unit (NVU). The anatomical substrate for regulation of cerebral blood flow and the blood-brain barrier is a multicellular system consisting of neurons, pericytes, smooth muscle cells, astrocytes and endothelial cells known as the NVU. **(A)** Intracerebral capillaries lack vascular smooth muscle cells but are partly covered by contractile pericytes. **(B)** At the level of intracerebral arterioles, the endothelium is fully covered by a single layer of vascular smooth muscle cells, which provide contractile properties to the arteriole. Astrocytes send their processes called endfeet around both capillaries and arterioles, providing support as well as a functional connection to surrounding parenchyma. **(C)** Summary of functions of the blood-brain barrier and neurovascular coupling. Arrows point to neurovascular unit components. *Figure made using BioRender*.

Lacoste and Gu, 2015; Peguera et al., 2021). Hypoxia initiates vessel ingression into deep brain structures, followed by usage of vascular patterning cues (Lacoste and Gu, 2015; Tata et al., 2015; Tata and Ruhrberg, 2018; Okabe et al., 2020). Comparably, ECs instruct neural progenitors into dividing, differentiating or migrating through release of paracrine signals that regulate neuronal development in vascular niches (Hogan et al., 2004; Shen et al., 2004; Daneman et al., 2009; Goldman and Chen, 2011; Delgado et al., 2014; Lacoste and Gu, 2015; Licht and Keshet, 2015; Walchli et al., 2015; Tata and Ruhrberg, 2018; Peguera et al., 2021). Moreover, neuronal activity plays important roles in modulating postnatal brain angiogenesis (Lacoste et al., 2014; Whiteus et al., 2014; Biswas et al., 2020). As the brain matures, vascular networks remodel until the system consists of an extensive network that actively regulates blood flow to adequately sustain energy demands. The functional relationships between neurons and blood vessels ensures that NVC mechanisms progressively develop (Lacoste and Gu, 2015; Coelho-Santos and Shih, 2020). NVC becomes fully functional ∼3–4 weeks after birth in rodents, and 7–8 weeks in humans (Yamada et al., 2000; Muramuto et al., 2002; Kozberg et al., 2016).

These vascular features can become defective early in life, affecting brain maturation. Vascular susceptibilities can also emerge later in life, taking part in neurodegenerative processes. Indeed, NVU deficits play a role in both early- and late-onset neurological disorders (**Figure 2**). Mounting evidence shows that vascular impairments contribute to the pathophysiology of neurological conditions throughout life, including neurodevelopmental, metabolic, and neurodegenerative disorders (Nicolakakis and Hamel, 2011; Van Dyken and Lacoste, 2018; McConnell et al., 2019; Ouellette et al., 2020; Sharma and Brown, 2021). This suggests the existence of a vascular continuum between developmental conditions and illnesses of aging, which will be the focus of this review (**Figure 3**). A better understanding of mechanisms and key players involved in cerebrovascular impairments may lead to transformative therapeutic strategies at different stages of life.

CEREBROVASCULAR DEFICITS ASSOCIATED WITH NEURODEVELOPMENTAL DISORDERS

Neurodevelopmental disorders are considered a group of conditions with onset/diagnosis during infancy, childhood, or adolescence (Morris-Rosendahl and Crocq, 2020). They are

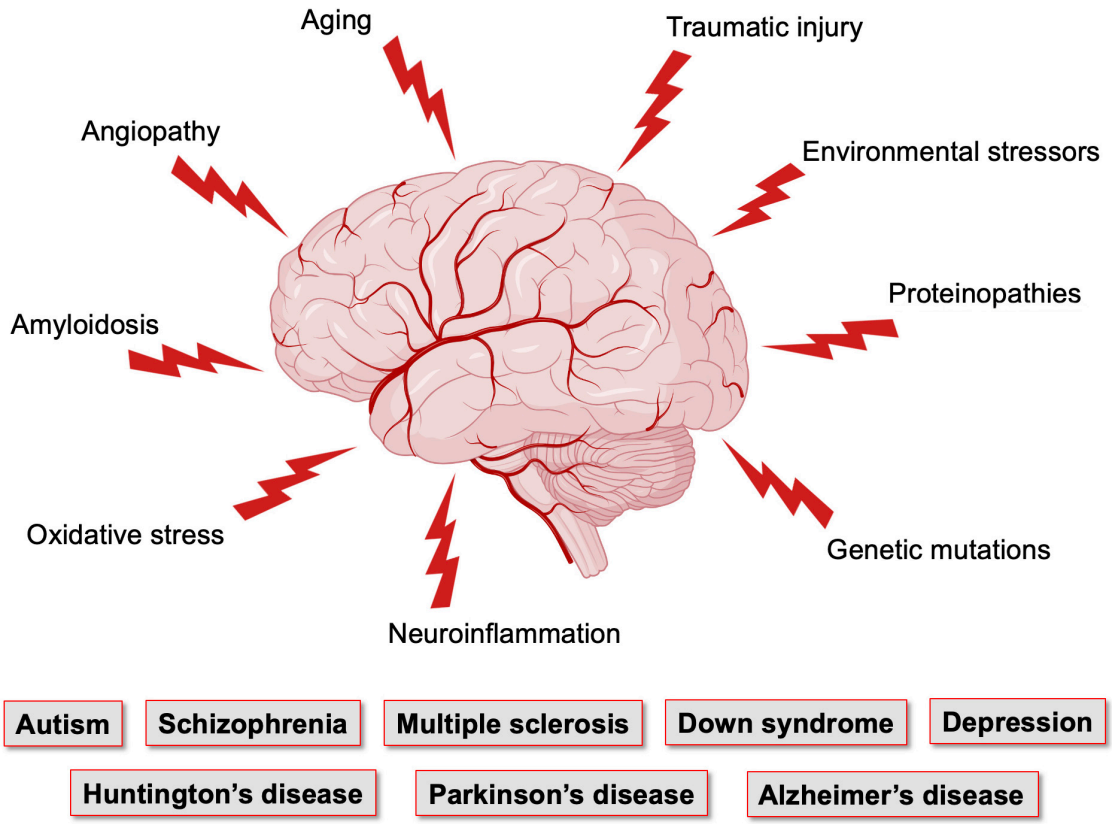

FIGURE 2 | Factors affecting the brain vasculature and leading to neurological conditions. The brain, which has elevated metabolic needs but poor energy storage, is highly dependent on a continuous supply of nutrients and oxygen from the blood stream, and is thus dependent on the integrity of its vasculature. Vasculature of the brain is the most complex and dense in the human body. Yet, it is maintaining a very fragile equilibrium and is the target of numerous pathological conditions that affect neuronal maturation and function. *Figure made using BioRender*.

defined by impairments in motor, social, cognitive, academic, and/or occupational functioning. Most studies focused on the neuronal contributions to these disorders; however, concomitant vascular impairments are starting to emerge (Ouellette et al., 2020). Here, we highlight vascular impairments identified in autism spectrum disorders (ASD) and schizophrenia.

Vascular Links to Autism Spectrum Disorders

ASD are pervasive neurodevelopmental disorders associated with social interaction deficits, speech and language impairments, as well as repetitive behaviors and restricted interests (Vijayakumar and Judy, 2016). These disorders have a prevalence of 1–2% in the general population and affect four times more boys than girls (Hogan et al., 2004; Daneman et al., 2009). Individuals with ASD show atypical behaviors associated with visual attention, imitation, social responses, and motor control by 12 months of age. By the age of 3, a child can be efficiently diagnosed with ASD (Park et al., 2016). While the underlying causes of ASD are enigmatic, both environmental and genetic origins have been found, leading to the identification of gene mutations within the ASD population (Hogan et al., 2004; James et al., 2009; Emerson et al., 2017). Although most studies have been neurocentric, ASD are now being associated with vascular vulnerabilities.

Altered Cerebral Blood Flow in Autism Spectrum Disorders

Neuroimaging techniques can map changes in CBF or blood oxygenation during various activities. Morphological and functional investigations using functional magnetic resonance imaging (fMRI), positron emission tomography (PET), single-photon emission computed tomography (SPECT), or Arterial Spin Labeling (ASL) are used to measure CBF changes in ASD children. CBF disruptions have been demonstrated in ASD patients when compared to healthy controls in different regions of the brain (Bjørklund et al., 2018). It has also been suggested that perfusion alterations are more pronounced in older children diagnosed with ASD. Cerebral hypoperfusion has been detected in nearly 75% of ASD children (Zilbovicius et al., 2000). As CBF impacts the delivery of oxygen and nutrients to neurons, hypoperfusion in ASD children has been associated with key ASD-related behaviors such as language deficits, impaired executive function and abnormal responses to sensory stimuli, as well as difficulty in facial perception (Siegel et al., 1992;

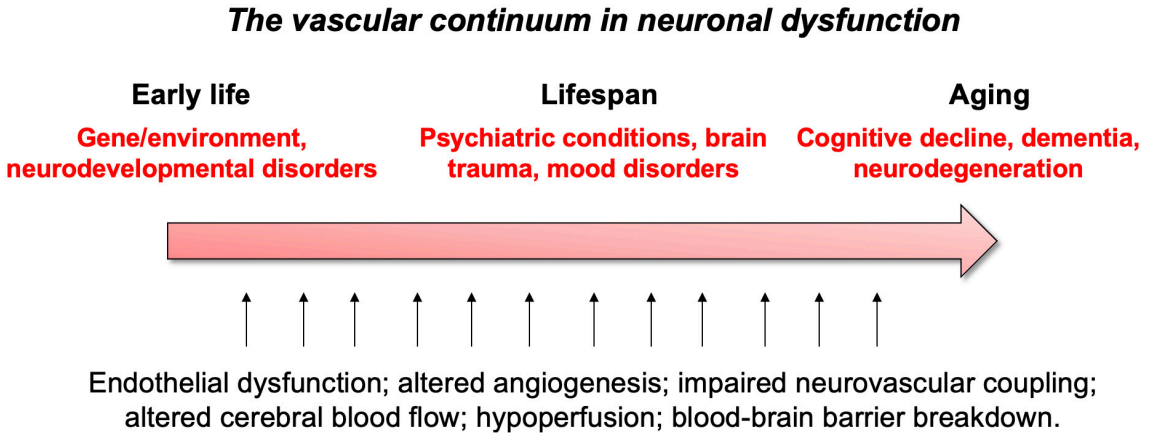

FIGURE 3 | Summary of vascular links to neurological disease throughout life.

Chiron et al., 1995; Ohnishi et al., 2000; Burroni et al., 2008; Reynell and Harris, 2013; Bjørklund et al., 2018; Yerys et al., 2018). These behaviors correlate with abnormal regional cerebral blood flow (rCBF) in the bilateral insula, superior temporal gyri and left prefrontal cortices, medial temporal lobe, supramarginal gyrus, right fusiform gyrus, and dorsal anterior cingulate cortex (Ohnishi et al., 2000; Zilbovicius et al., 2000; Burroni et al., 2008; Jann et al., 2015; Yerys et al., 2018). Studies are attempting to ameliorate these behavioral abnormalities using hyperbaric oxygen treatment (HBOT) to counteract cerebral hypoperfusion in children with ASD. There is some evidence that children who undertook 40 HBOT sessions of 60 min each showed improvements on selected psychosomatic parameters in the Autism Treatment Evaluation Checklist (ATEC) and Childhood Autism Rating Scale (CARS) (Kostiukow and Samborski, 2020). Currently, there is insufficient evidence to support the use of HBOT to treat children with ASD as there are many contradicting studies claiming no improvement in behaviors. Nevertheless, each study followed different protocols, consisted of patients with a large spectrum of behavioral impairments, and some lacked proper control groups, which could explain discrepancies. More research is required to determine if specific groups of children could benefit from HBOT treatment (Rossignol et al., 2012; Sakulchit et al., 2017).

ASL-based measurements of cerebral perfusion showed that children with ASD presented a pattern of widespread hyperperfusion in frontotemporal regions including medial orbitofrontal cortex, bilateral inferior frontal operculum, left inferior/middle temporal gyrus and the right precentral gyrus (Jann et al., 2015). The medial orbitofrontal cortex is known to have extensive connections with the limbic system involved in socio-emotional cognition. Furthermore, hyperperfusion was detected throughout the frontal white matter and subcortical gray matter in ASD children, which correlated positively with severity of social deficits (Peterson et al., 2019). As shown by these studies, CBF abnormalities appear linked to clinical manifestations. Although opposing observations of CBF in ASD patients were reported, these further support the complexity of these disorders (Jann et al., 2015).

Neurovascular coupling alterations were also observed in ASD patients. Hemodynamic responses in children with ASD during a color-word task were significantly lower than the control group, especially in the dorsolateral prefrontal cortex (Uratani et al., 2019). Conversely, children displayed no difference in hemoglobin concentrations in the prefrontal cortex during a letter fluency task, while adults showed reduced responses (Kawakubo et al., 2009). Despite inter-study variability, there seems to be a consensus on the impact of altered CBF on the expression of behavioral impairments (Zilbovicius et al., 2000; Jann et al., 2015). But as ASD are heterogeneous, with various behavioral traits, genetic causes, medical co-morbidities and medications, these variables may have impacted neuroimaging results, which led to inconsistencies. Importantly, these studies take an important step toward the identification of key players in ASD pathophysiology, opening new opportunities for early diagnosis and treatment.

The relationship between CBF alterations and symptom profiles in ASD children provides insight into disease mechanisms that can be tested in animal models. As most pre-clinical studies have also focused on the neuronal aspects of ASD, very few have considered vascular contributions to these disorders in laboratory models. Recent studies using different ASD mouse models have reported alteration in CBF. A study by Abookasis et al. (2018) using inbred Black and Tan Brachyury (BTBR) *T+tf/J* reported decreased CBF in mutant mice using laser speckle imaging and laser Doppler flowmetry (LDF). Subsequently, work by Ouellette et al. (2020) using the 16p11.2 deletion mouse model of ASD (*16p11.2*$^{df/+}$; Horev et al., 2011) demonstrated an increase in resting CBF as well as neurovascular uncoupling in adult (P50) *16p11.2*$^{df/+}$ mice compared to WT littermates using a combination of ultrasound imaging and LDF. No difference in CBF or NVC were observed between younger (P14) mutant and control mice (Ouellette et al., 2020). Results from this study in *16p11.2*$^{df/+}$ mice revealed the cause of these functional cerebrovascular impairments: an endothelial

deficit. While normal vascular smooth muscle cell function was measured, defective endothelium-dependent vasodilation was found *ex vivo* following exposure to specific vasomodulators (Ouellette et al., 2020). This suggests that endothelial health plays an important role in the etiology of the 16p11.2 deletion ASD syndrome. Understanding the molecular and cellular factors that mediate CBF alterations in ASD could help design rescue approaches in animal models, as well as therapeutic approaches down the line.

Since MRI studies rely on Blood Oxygen Level Dependent (BOLD) signals as surrogates for neuronal activity (Hillman, 2014; Howarth et al., 2021; Moon et al., 2021), it is possible that changes in rCBF reflect changes in underlying neuronal activity. For instance, cerebral cortex hypoperfusion in ASD patients could reflect lower metabolic demands (Schifter et al., 1994). In the case *16p11.2*$^{df/+}$ mice, however, it is interesting to note that a neurovascular uncoupling was measured, with enhanced neuronal activation yet reduced vascular responses to whisker stimulations, which led to the discovery of endothelium-dependent deficits (Ouellette et al., 2020).

Altered Blood-Brain Barrier and Angiogenesis in Autism Spectrum Disorders

Cerebral vessels are central for the maintenance of brain homeostasis, sustaining proper neuronal function, and providing an effective protection against toxins and pathogens (Profaci et al., 2020). The BBB consists of specialized ECs lining the vessel wall to separate the peripheral blood from cerebral tissue. Brain (central) ECs are distinct from peripheral ECs, as they produce specific proteins to control the flux (entry and exit) of metabolites across vessels, to maintain low rates of trans-endothelial vesicular transport, and to form tight junctions to limit the para-cellular flow of material between adjacent ECs (Andreone et al., 2015; Chow and Gu, 2015; Kealy et al., 2020). Alterations in the BBB are at the core of the onset and/or progression of numerous neurological disorders (Daneman and Prat, 2015; Van Dyken and Lacoste, 2018; Profaci et al., 2020). Only few studies have investigated the components of the BBB in the context of ASD. Children diagnosed with ASD have been associated with reduced levels of adhesion molecules such as soluble Platelet Endothelial Cell Adhesion Molecule-1 (PECAM-1, or CD31) and P-selectin. Since these molecules are essential to modulate BBB permeability through signaling and leukocyte infiltration, it suggests that crucial BBB components may be at play in ASD pathophysiology (Onore et al., 2012). Furthermore, a post-mortem study, with a small sample size, demonstrated altered BBB integrity in ASD with increased gene expression of matrix metalloproteinase (MMP)-9 (Fiorentino et al., 2016). Studies have shown that MMP-9 regulates cell proliferation, adhesion, degradation of laminin and collagen, angiogenesis, oxidative injury, and is implicated in BBB breakdown (Lepeta and Kaczmarek, 2015; Turner and Sharp, 2016). Additionally, important components of BBB integrity displayed altered expression in ASD patients, including claudin-5 (*CLDN5*) and claudin-12 (*CLDN12*), as well as tricellulin (*MARVD2*), a component of tight junctions involved in decreased permeability to macromolecules in brain ECs (Fiorentino et al., 2016). In an older study, a small subset of ASD participants demonstrated higher levels of autoantibodies against brain ECs in the serum compared to typically developing individuals, suggesting an impact on the BBB (Connolly et al., 1999). Animal models have facilitated the study of BBB integrity in ASD. In a valproic acid rat model of autism, increased BBB permeability to Evans blue was found in the cerebellum, a phenotype attenuated by treatment with memantine, an NMDA receptor modulator. This BBB alteration was also attenuated using minocycline (antibiotic) and agomelatine (melatonin receptor) treatment (Kumar et al., 2015; Kumar and Sharma, 2016). Animal studies have investigated transendothelial transport mechanisms in ASD mouse models. Tarlungeanu et al. (2016) demonstrated that the large neutral amino acid transporter (LAT1, *Slc7a5*) localized at the BBB to maintain normal levels of brain branched chain amino acid (BCAA) was required for neurotypical development. Mice harboring an endothelial-specific deletion of *Slc7a5* (*Slc7a5*$^{\Delta EC}$) displayed behaviors reminiscent of ASD, including motor dysfunctions consistent with a study in human patients harboring the constitutive mutation (Novarino et al., 2012; Tarlungeanu et al., 2016). Interestingly, administration of BCAA rescued ASD-like behaviors in *Slc7a5*$^{\Delta EC}$ mice (Tarlungeanu et al., 2016).

Recently, a post-mortem analysis of brain tissue from individuals diagnosed with ASD revealed significantly higher levels of markers associated with pericytes, as well as increased vascular tortuosity, indirectly suggesting impairments in angiogenesis, a process through which new blood vessels are formed (Azmitia et al., 2016). A more recent study in *16p11.2*$^{df/+}$ mice revealed impaired cerebral angiogenesis in young (P14) *16p11.2*$^{df/+}$ male mice compared to sex-/age-matched littermates, a phenotype which was absent in adult mice. Defective angiogenic activity was also measured using primary brain ECs from P14 *16p11.2*$^{df/+}$ males or ECs derived from human-induced pluripotent stem cells (hiPSCs) of 16p11.2 deletion carriers (Ouellette et al., 2020). Moreover, RNA-sequencing analysis of *16p11.2*$^{df/+}$ mouse brain EC transcriptome revealed changes in the expression of genes involved in angiogenesis (e.g., *Grem1*, *Apln*, *Angpt2*), while key genes involved in BBB regulation (e.g., *Pecam1*, *Mfsd2a*, *Cldn5*, *Slc2a1*) were not affected by the 16p11.2 deletion (Ouellette et al., 2020). Finally, this study generated a mouse model with endothelial-specific 16p11.2 haploinsufficiency which recapitulated ASD-related phenotypes, revealing a causal relationship between endothelial dysfunction and neuronal aspects of the 16p11.2 deletion syndrome (Ouellette et al., 2020).

Overall, these studies allude to the contribution (structural and functional) of a defective BBB and NVU in ASD, with an important role for endothelial impairments.

Vascular Links to Schizophrenia

Schizophrenia is a debilitating neurodevelopmental disorder affecting ∼1% of the population. It is associated with behavioral and cognitive symptoms that arise progressively. Memory and attention deficits appear in childhood, while positive symptoms (psychotic episodes) and negative symptoms (social and motivational deficits) emerge later in adolescence or early adulthood (Stachowiak et al., 2013). Although the incidence of

schizophrenia is higher in men, women have a slightly later disease onset (Gogtay et al., 2011; Ochoa et al., 2012). While the behavioral aspects of schizophrenia have been described, the causes of this disorder are poorly known. As in ASD, both genetic and environmental origins are involved. Schizophrenia has been associated with genes essential for a wide range of functions including neuronal connectivity and patterning of brain structures, cell proliferation and differentiation, as well as cytoskeleton reorganization (Stachowiak et al., 2013; Clifton et al., 2019). As in most neurological disorders, the implication of neuronal alterations has been extensively studied, but research on vascular impairments in schizophrenia is starting to emerge.

Altered Cerebral Blood Flow in Schizophrenia

Cognitive impairments are often present before the first psychotic episode in patients with schizophrenia (Keefe and Harvey, 2012; Schuepbach et al., 2016) and deficits in executive functions are often parallel to changes in CBF. Several studies have linked altered CBF with schizophrenia-related symptoms (Sabri et al., 1997; Malaspina et al., 1999, 2004; Pinkham et al., 2011; Fujiki et al., 2013; Schuepbach et al., 2016; Stegmayer et al., 2017; Zhu et al., 2017). Interestingly, the manifestations of negative or positive symptoms correlate with different rCBF changes. In a study by Pinkham et al. (2011), CBF of 30 schizophrenia patients was measured using ASL perfusion MRI, which revealed a positive correlation between increased severity of positive symptoms and higher CBF in the cingulate and superior frontal gyri, but decreased CBF in precentral and middle frontal gyri. Patients who presented with severe negative symptoms also displayed reduced CBF in the superior temporal gyrus bilaterally, cingulate and left middle frontal gyri (Malaspina et al., 2004; Scheef et al., 2010; Pinkham et al., 2011; Liu et al., 2012). Most studies investigating CBF alterations in schizophrenia considered perfusion rates from medicated patients, and a small number of studies have measured CBF rates in neuroleptic-naïve patients. Using ASL in non-medicated patients, the schizophrenia group displayed resting-state hypoperfusion in the frontal lobes, anterior and medial cingulate gyri, as well as in the parietal lobes, while increased perfusion was measured in the cerebellum, brainstem and thalamus (Scheef et al., 2010). Sabri et al. (1997) measured rCBF using SPECT in non-medicated patients that have experienced positive symptoms, revealing that rCBF values varied depending on the severity of positive symptoms. Hyperperfusion was detected in the frontal, anterior cingulate as well as in both parietal and temporal cortices in patients who had scored high in severity for formal thought disorder (disturbance of the organization and expression of thought). In contrast, patients who scored high for delusions, hallucinations or distrust, with low scores for formal thought, displayed hypoperfusion in the same brain regions. No difference in rCBF was identified between control and schizophrenia groups after treatment (Andreasen et al., 1997; Sabri et al., 1997; Horn et al., 2009). Recent studies have detected hyperperfusion and hypoperfusion in brain regions from individuals with hallucinations. For instance, CBF increase was found in the right superior temporal gyrus and caudate nucleus, while CBF decrease was found bilaterally in the occipital and left parietal cortices (Zhuo et al., 2017). In another study, patients were classified based on the severity of three behavioral dimensions (language, affectivity, and motor) according to the Bern Psychopathology scale. Patients with altered affectivity were associated with increased CBF in the amygdala, while changes in language dimension were linked to increased CBF in Heschl's gyrus (Stegmayer et al., 2017). While schizophrenia is classified as a neurodevelopmental disorder, its symptoms persist with age. Studies have identified significant bilateral temporal hypoperfusion related to aging and disease course. It has been suggested that this decrease in CBF with aging is paralleled with the degenerative changes observed in patients with schizophrenia (Schultz et al., 2002; Kawakami et al., 2014).

The polygenic risk of schizophrenia is an important dimension of this syndrome, and changes in CBF have been identified in patients diagnosed for either familial or sporadic schizophrenia. Sporadic schizophrenia patients were associated with hypofrontality (left frontal gyrus, orbitofrontal cortex, anterior cingulate, and paracingulate cortices), while familial schizophrenia patients had left temporoparietal hypoperfusion (posterior Sylvian fissure at the superior and inferior parietal lobules, angular, and supramarginal gyri). In both groups, positive symptoms are often associated with increased rCBF in the parahippocampal gyrus, cerebellum, and pons (Malaspina et al., 2004). Sporadic patients showed additional hyperperfusion in the fusiform gyrus, and familial patients the hippocampus, dentate, amygdala, thalamus, and putamen (Malaspina et al., 2004). In addition, the prefrontal cortex in schizophrenia has been associated with deficits of pericapillary oligodendrocytes, which could contribute to changes in CBF (Vostrikov et al., 2008; Uranova et al., 2010). Altogether, these studies support the idea that altered CBF is involved in schizophrenia pathophysiology.

In addition to studies investigating resting state CBF, there is evidence of altered NVC in schizophrenia whereby many reports demonstrate reduced hemodynamic response, reflecting reduced neuronal activity during processing of cognitive tasks, especially in the lateral prefrontal cortex and temporal regions (Ford et al., 1999, 2005; Mathalon et al., 2000; Carter et al., 2001; Hanlon et al., 2016; Pu et al., 2016). As with CBF reports, there are inconsistent hemodynamic responses associated with schizophrenia since increased hemodynamic responses in hippocampus, thalamus and prefrontal cortex have been identified (Tregellas et al., 2007). These conflicting results are translating to rodent models of schizophrenia whereby some models have revealed overall hypofrontality, hypoperfusion in the hippocampus or hyperperfusion in the somatosensory cortex (Finnerty et al., 2013; Song et al., 2013; Drazanova et al., 2019).

Altogether, these studies support the idea that altered CBF regulation is involved in schizophrenia pathophysiology. Moreover, it appears critical to consider the polygenic risk of disease, the category and severity of symptoms, as well as the age of patients when comparing CBF rates in schizophrenia. Although many studies have detected altered CBF using various methods, results thus far remain conflicting based on various stages of disease and pharmacological treatment (Drazanova et al., 2019).

Altered Blood-Brain Barrier and Angiogenesis in Schizophrenia

A dysfunctional BBB has been reported in schizophrenia, with increased permeability to damaging proteins (Müller and Ackenheil, 1995; Shcherbakova et al., 1999; Crockett et al., 2021). Studies are starting to decipher changes in cells associated with the BBB (for a detailed review, see Carrier et al., 2020). Briefly, evidence of schizophrenia-associated microvascular abnormalities in the neocortex include thickening and deformation of basal lamina, vacuolation of cytoplasm in ECs, basal lamina and astrocytic end-feet, swelling of astrocyte end-feet, activation of microglial cells in the prefrontal and visual cortex, as well as atypical vascular arborization (Uranova et al., 2010; Carrier et al., 2020).

Moreover, specific mutations are associated with schizophrenia, including alterations in the 22q11.2 deletion syndrome (22qDS) -strongest monogenic risk allele for this disorder, and polymorphisms in claudin-5, a densely expressed tight junction molecule (Gur et al., 2017; Greene et al., 2018; Carrier et al., 2020) altogether revealing barrier dysfunction in schizophrenia patients (Greene et al., 2018; Crockett et al., 2021). Post-mortem brain sections from 22qDS patients and animal models of 22qDS both demonstrate reduced claudin-5 expression in the BBB, which in turn compromised BBB function (Nishiura et al., 2017; Guo et al., 2020; Crockett et al., 2021; Usta et al., 2021). Additionally, altered levels of vascular endothelial (VE)-cadherin and occludin in ECs were identified in schizophrenia. These molecules regulate adherence of ECs and restrict movement of substances across the BBB (Cai et al., 2020). Furthermore, BBB hyperpermeability has been associated with another risk allele for schizophrenia. *NDST3*, expressed in the brain, encodes an enzyme involved in the metabolism of heparan sulfate, a component of basal lamina extracellular matrix that is required for BBB integrity (Khandaker et al., 2015).

Studies have documented primary vascular endothelial dysfunction in schizophrenia. Individuals carrying *MTHER T* and/or *COMT Val* risk allele have been associated with cerebrovascular endotheliopathy, as well as lower frontal executive functions (Grove et al., 2015). While endothelial dysfunction is possibly associated with schizophrenia, many studies are using peripheral endotheliopathy as a surrogate marker for endothelial dysfunction. For example, studies are using non-invasive peripheral arterial tonometry (RH-PAT) to assess peripheral arteriole endothelial-dependent vasodilation and revealed impaired peripheral arterial vasodilation in schizophrenia (Ellingrod et al., 2011; Burghardt et al., 2014). Notably, brain ECs have unique properties to maintain BBB integrity and brain homeostasis. Although altered endothelial function was found in the periphery, it does not represent a definite marker of brain (central) endothelial dysfunction. A critical regulator of angiogenesis, *vascular endothelial growth factor* (VEGF), and its receptor (VEGFR2) have been found upregulated in the prefrontal cortex of individuals diagnosed with schizophrenia (Hino et al., 2016). Findings of elevated VEGF could also be linked to vascular hyperpermeability, as VEGF not only regulates angiogenesis but increases BBB leakage (Mayhan, 1999; Zhang et al., 2000). Conversely, a different group revealed that a decreased production of VEGF predisposed individuals to develop this disorder and contributed to the severity of symptoms (Saoud et al., 2021). Another study investigated the impact of hiPSC-derived neural stem cells from schizophrenia patients on angiogenesis (Casas et al., 2018). This study found an imbalance in the expression and secretion of several angiogenic factors and non-canonical neuro-angiogenic guidance cues from neural stem cells from schizophrenic patients. Conditioned media from these cells induced impaired angiogenesis as evidenced by reduced number of sprouts and tubes formed in *in vivo* and *in vitro* models, as well as decreased neural stem cell migration compared to control conditioned media (Casas et al., 2018).

CEREBROVASCULAR DEFICITS ASSOCIATED WITH NEURODEGENERATIVE DISORDERS

CNS disorders are dichotomized as early onset neurodevelopmental disorders and late-onset neurodegenerative diseases (Taoufik et al., 2018). Neurodegenerative diseases consist of a group of heterogeneous disorders characterized by the progressive degeneration of structure and function in the CNS (Gitler et al., 2017). Although neurodegenerative and neurodevelopmental disorders are differentially classified, an accumulating body of work demonstrates significant similarities between these two groups of conditions. Here below, we cover cerebrovascular impairments reported in four neurodegenerative diseases that emerge throughout lifespan: multiple sclerosis (MS), Huntington's disease (HD), Parkinson's disease (PD), and Alzheimer's disease (AD).

Vascular Links to Multiple Sclerosis

MS is a chronic autoimmune disease of the CNS, occurring when the immune system attacks its own nerve fibers and myelin sheaths (D'Haeseleer et al., 2013). The pathological hallmark of MS consists of perivenular inflammatory lesions, leading to demyelinating plaques and diffuse axonal degeneration throughout the CNS (Dobson and Giovannoni, 2019). It is characterized by the infiltration of T cells reactive against myelin in the CNS (Schwartz and Kipnis, 2005). This demyelinating disease has key features including inflammation, BBB disruption and neurodegeneration. MS has a prevalence of 0.5–1.5 per 100,000 individuals, whereby women are three times more affected than men (Harbo et al., 2013). The age of MS onset is situated between 20 and 40 years of age (Ortiz et al., 2014). General symptoms related to MS include, but are not limited to, tremors, lack of coordination as well as weakness in limbs. There are various types of MS including relapsing-remitting MS (RR-MS), secondary progressive MS (SP-MS) and primary progressive MS (PP-MS). RR-MS consists of unpredictable relapses or inflammatory flare-ups during which new symptoms appear or existing ones worsen (Adhya et al., 2006). Most people with RR-MS, transition to a disease phase known as SP-MS. In this phase, there is progressive worsening and fewer relapses. Active lesions with profound lymphocytic inflammation are mostly found in RR-MS (Dobson and Giovannoni, 2019). PP-MS is

considered as a slow accumulation of disability without defined relapses. In this case, PP-MS is associated with an inactive lesion core surrounded by activated microglia and macrophages (Dobson and Giovannoni, 2019).

Altered Cerebral Blood Flow in Multiple Sclerosis

MS has been associated with functional cerebrovascular abnormalities including decreased cerebral perfusion and reduced CNS venous blood drainage, known as chronic cerebrospinal venous insufficiency (D'Haeseleer et al., 2011). SPECT, PET, and ASL imaging studies have reported decreased CBF in both gray and white matter of MS patients (Ge et al., 2005; D'Haeseleer et al., 2011). Widespread cerebral hypoperfusion has been revealed in SP-MS, RR-MS and PP-MS patients, while an ischemic threshold was not reached (Adhya et al., 2006; Ota et al., 2013; Monti et al., 2018). Gray matter hypoperfusion in MS suggests a reduction of metabolism due to the loss of cortical neurons (Peruzzo et al., 2013). Furthermore, studies have reported that CBF is globally impaired in normal appearing white matter (NAWM) of patients with early RR-MS (Law et al., 2004; Adhya et al., 2006). Of note, CBF was generally lower in PP-MS than in RR-MS in the periventricular and frontal white matter (Adhya et al., 2006). In the contrary, other studies have measured elevation of CBF and cerebral blood volume (CBV) in NAWM of patients with early RR-MS several weeks before signs of increased BBB permeability (Wuerfel et al., 2004). Although studies on different types of MS revealed changes in CBF, general active demyelinating lesion regions are associated with hyperperfusion while the more stable forms show hypoperfusion (Monti et al., 2018). Decreased CBF in cerebral NAWM, thalamus, and putamen was identified in patients whose symptoms emerged within the first 5 years of onset. This suggests that CBF alterations are present in the very early stages of the disease (Varga et al., 2009). Different mechanisms have been proposed to explain hypoperfusion in MS. A study suggested that decreased CBF is secondary to axonal degeneration, which leads to a decreased metabolic demand (Saindane et al., 2007). However, this hypothesis is yet to receive experimental support. A second mechanism that has been proposed is an impaired energy metabolism of astrocytes (De Keyser et al., 1999). In MS, astrocytes are deficient in β2-adrenergic receptors which regulate high energy-consuming activities, such as glycogenolysis and phosphocreatine metabolism (De Keyser et al., 1999). Reduced energy production in astrocytes could be contributing to altered CBF. A third mechanism suggested was increased release of vasoconstrictor endothelin-1 (ET-1) from reactive astrocytes, found in a post-mortem study on white matter samples of RR-MS patients (D'Haeseleer et al., 2013; Hostenbach et al., 2019). Hence, elevated levels of ET-1 could be involved in dysregulating CBF in MS. Interestingly, administration of ET-1 antagonist Bosentan restored CBF to control levels in MS patients (D'Haeseleer et al., 2013).

Impaired cerebral vascular reactivity was evidenced in MS patients exposed to hypercapnia, which has been suggested to contribute to neuronal death identified in this disorder (Marshall et al., 2014). This global deficit is thought to be associated with elevated levels of NO reported in MS (Trapp and Stys, 2009; Juurlink, 2013). These studies suggest that the overproduction of NO may desensitize endothelial and smooth muscle cell function, causing decreased vasodilatory capacity and limited blood supply for neurons that perform demanding tasks. Increased NO in MS may lead to neuronal activity-induced hypoxia leading to neurodegeneration (Marshall et al., 2014). Interestingly, high inflammatory MS lesion load has been associated with increased CBF. Therefore, perfusion changes may be sensitive to active inflammation (Bester et al., 2015). However, it remains unclear whether abnormal perfusion in MS is a precursor of lesions or occurs independently of lesion development (Marshall et al., 2014).

Notably, MS has been associated with cerebral SVD. It was demonstrated that younger MS cases are more severely impacted by cerebral SVD compared to older individuals (Geraldes et al., 2020). This suggests that the interaction between MS and cerebral SVD is affected by age, an assumption still under investigation (Geraldes et al., 2020).

Altered Blood-Brain Barrier and Angiogenesis in Multiple Sclerosis

BBB dysfunction is considered a major hallmark of MS and is deemed a trigger of disease onset (McQuaid et al., 2009; Cramer et al., 2014). Intense focal disruption of the BBB associated with inflammation (identified by gadolinium-enhanced MRI at acute and chronic MS lesion sites; Saade et al., 2018) and diffuse extensive BBB disruption with a long-term pathological activity, are both found in MS patients (Bennett et al., 2010). Hyperpermeability of the BBB was evidenced by leukocyte passage across the BBB (Cramer et al., 2014). Increased BBB leakage was associated with decreased expression of tight junction proteins in brain capillary ECs in patients with active lesions, inactive lesions, as well as NAWM associated with fibrinogen leakage (Kirk et al., 2003; McQuaid et al., 2009; Bennett et al., 2010). More specifically, dysregulation of tight junction adaptor protein ZO-1, occludin and claudin-5 have been reported in both primary progressive and secondary progressive disease states (Kirk et al., 2003; Leech et al., 2007). Experimental autoimmune encephalomyelitis (EAE) in rodents is a disease model with clinical and pathological characteristics relevant to the study of MS. This model revealed reorganization of ZO-1 and actin in the presence of inflammatory factors *in vitro*, associated with increased permeability of an endothelial monolayer (Bennett et al., 2010). The EAE model also revealed increased expression of VEGF in ECs, astrocytes, monocytes and activated TH1 lymphocytes, all of which contribute to BBB permeability during the early phase of disease, while decreased expression VEGF was evident in the late phase (Girolamo et al., 2014). The increase in VEGF expression was also found in the brain of MS patients (Girolamo et al., 2014). Furthermore, junctional adhesion molecule-A, a component of tight junctions, was found abnormally distributed in active and inactive MS lesions, although adherent junction proteins were normally expressed and localized in MS tissue (Padden et al., 2007). In addition, levels of PECAM-1 were found increased in active gadolinium-enhancing MS lesions (Ortiz et al., 2014). While BBB leakage is evident in MS, the complex network of cellular

and molecular players that lead to this dysfunction have yet to be fully understood. Targeting BBB defects in MS represent a therapeutic opportunity, for instance with MMP inhibitors, interferons, and corticosteroids (Minn et al., 2002; Ross et al., 2004; Pardridge, 2012; Ortiz et al., 2014). However, no current therapy addresses BBB deficits (Ortiz et al., 2014). For more details on BBB dysfunction in MS, the following reviews can be consulted (Girolamo et al., 2014; Kamphuis et al., 2015; Xiao et al., 2020).

ECs proliferation as well as an increase in vascular network density has been reported (Ludwin, 2006; Holley et al., 2010). Increased angiogenesis was suggested to contribute to disease progression as well as remission after relapses (Papadaki et al., 2014). In addition to increased VEGF levels, VEGFR2 is also expressed on ECs in active MS lesions (Seabrook et al., 2010). Other molecules, such as basic fibroblast growth factor, were increased in MS patients and involved in angiogenesis (Su et al., 2006). MS patients with activated lesions and NAWM show blood vessels with a glomeruloid morphology, hemorrhages and vessel wall hyalinization (Girolamo et al., 2014). Immunosuppressive therapies have been used in aggressive MS as they not only impact neuroinflammation but also have an anti-angiogenic effect. Further research is warranted to elucidate the vascular links to MS and identify new therapeutic targets, as disease modifying drugs have unfortunately little to no impact on MS progression (Girolamo et al., 2014).

Vascular Links to Huntington's Disease

HD is an hereditary, autosomal dominant and neurodegenerative disorder (Davenport, 1915; Wasmuth et al., 1988; Bano et al., 2011) leading to altered muscle coordination and declined mental abilities (Paulsen, 2011; Ha and Fung, 2012). An expansion of trinucleotide CAG repeats on chromosome 4 within the Huntingtin gene (*HTT)* results in the production of an altered Huntingtin (Htt) protein which accumulates in specific brain regions. Aggregation of mutant Htt (mHtt) leads to increased neurotoxicity (Zheng and Diamond, 2012), particularly in subcortical brain structures such as the neostriatum (caudate and putamen) where GABAergic medium-spiny neurons are particularly vulnerable (Sieradzan and Mann, 2001; Walker, 2007; Ross and Tabrizi, 2011; Drouin-Ouellet et al., 2015; McColgan and Tabrizi, 2018). At the cellular level, mHtt results in neuronal dysfunction and death through disrupted mechanisms involved in proteostasis, transcription and mitochondrial function as well as toxicity from the mutant protein (McColgan and Tabrizi, 2018). Worldwide, 2.71 per 100,000 individuals suffer from HD (Rawlins et al., 2016; Kounidas et al., 2021). Both men and women are affected equally, and heterogeneous symptoms emerge at around 40 years of age. However, functional and structural brain alterations emerge a decade before symptoms manifest (Snowden, 2017). Carriers of CAG repeat expansions in *HTT* can be identified decades before clinical manifestation, allowing researchers to identify possible biomarkers in the premanifest stage of HD (preHD). With this comes the increasing interest to study cerebrovascular abnormalities in HD (Snowden, 2017).

Altered Cerebral Blood Flow in Huntington's Disease

HD-related perfusion deficits have been mostly associated with cerebral hypoperfusion (Reid et al., 1988; Sotrel et al., 1991; Hasselbalch et al., 1992; Harris et al., 1999; Deckel and Duffy, 2000; Wild and Fox, 2009). There is evidence of reduced CBF in the basal ganglia in early HD, prior to gross structural changes and to motor symptoms. In these cases, severity of cortical hypoperfusion correlated with decreased functional capabilities (Sax et al., 1996; Harris et al., 1999). In preHD patients, classified as either near or far from motor symptom onset, displayed altered rCBF by MR-based perfusion imaging. Participants with preHDfar and preHDnear had lower rCBF in the medial prefrontal cortex and increased rCBF in the left precuneus. Of note, structure and function of the precuneus and hippocampus can be abnormal in very early HD (Feigin et al., 2006). PreHDnear participants had additional regions showing altered rCBF, including hypoperfusion in the medial and lateral prefrontal cortex and hyperperfusion in the right hippocampus (Wolf et al., 2011).

While resting CBF is affected, early manifest and premanifest HD patients also display altered neurovascular coupling during visual stimulation (Klinkmueller et al., 2021). After HD onset, a significant hypoperfusion in the HD group was identified in most of the cerebral cortex. During problem-solving activities, such as solving a maze or resting their eyes open while looking at a modified maze, patients with HD showed increased CBF in the caudate nucleus (Deckel and Duffy, 2000; Deckel et al., 2000). Following physical activity, HD patients were associated with CBF hyperperfusion compared to the control group (Steventon et al., 2020).

Animal models of HD (e.g., gene knock-in of a human exon 1 CAG_{140} expansion repeat) also revealed altered rCBF. In mice as in humans, different brain regions displayed either hypoperfusion (basal ganglia motor circuit, hippocampus and prefrontal area) or hyperperfusion (cerebellar-thalamic and somatosensory regions). This altered CBF was apparent at a presymptomatic stage (Wang et al., 2016).

While CBF is starting to emerge as a biomarker for HD, mounting evidence supports the utilization of CBV as an additional metric. Several studies have reported elevated CBV in preHD patients (Hua et al., 2014; Liu et al., 2020). In addition, there is evidence of increased CBV in cortical gray matter after HD onset (Drouin-Ouellet et al., 2015), suggesting that arteriolar CBV may be a sensitive biomarker for premanifest HD (Hua et al., 2014; Liu et al., 2020). From these studies it was suggest that imaging of CBF may be used to detect widespread functional abnormalities in HD, and possibly predict HD symptoms onset during premanifest stages.

Altered Blood-Brain Barrier and Angiogenesis in Huntington's Disease

Increases in vessel density, BBB permeability and VEGF-A release were observed in HD patients and animal models of HD (Steventon et al., 2020). There is evidence that BBB leakage increases alongside disease progression (Drouin-Ouellet et al., 2015). Despite these observations, there seems to be discrepancies between mouse models of HD. For instance, the BACHD

transgenic mice, a well-known model of HD expressing the full-length mutant human *HTT*, failed to develop BBB breakdown at 12 months of age despite robust motor deficits (Lin et al., 2013; Mantovani et al., 2016). BBB dysfunction in HD patients has been associated with decreased tight junction molecules such as occludin and claudin-5 (Drouin-Ouellet et al., 2015). Moreover, other markers associated with BBB permeability, including hepatocyte growth factor, interleukin-8 and tissue inhibitor of MMP-1, were found elevated in HD patients (Drouin-Ouellet et al., 2015). A transgenic mouse model of HD (R6/2 mice) confirmed elevated tight junction molecules similar to HD patients. The R6/2 mouse model of HD is the most commonly studied and harbors a mutant *Htt* with CAG repeat expansion in exon 1 (Li et al., 2005). R6/2 mice also displayed increased transcytosis and paracellular transport across the brain endothelium compared to control mice (Drouin-Ouellet et al., 2015). In R6/2 mice, tight junction imbalance and perturbed BBB homeostasis were perceptible at very early stage of the disease, in absence of symptoms (Di Pardo et al., 2017). At the structural level, mHtt aggregates were found in the basal membrane of cerebral blood vessels in HD patients (Drouin-Ouellet et al., 2015). Interestingly, mHtt aggregates were localized in ECs, smooth muscle cells and perivascular macrophages, consistent with observations in R6/2 mice.

Further research is needed to determine BBB impairments in preHD patients. Lim et al. (2017) reported that iPSCs-derived brain microvascular endothelial cells (BMECs) from HD patients exhibit increased angiogenesis and altered barrier properties associated with elevated transcytosis and paracellular permeability. An increased and unregulated angiogenic activity may lead blood vessels to become more permeable with a potential role in neurovascular dysfunction in HD. RNA-seq analysis revealed a significant number of affected gene that regulate both clathrin- and caveolin- mediated endocytosis, which could lead to changes in endo- and transcytosis across the brain endothelium. These genes include *FABP4*, *DYNAMIN*, and *FILAMIN* that play a role in vesicle formation and scission. In addition, higher levels of transcytosis-related genes such as *CAV1* was detected in HD iPSCs-derived BMECs that also displayed impaired Wnt/β-catenin signaling (Lim et al., 2017). The Wnt/β-catenin pathway is essential for regulation of cell proliferation, cell determination and tissue homeostasis (Silva-Garcia et al., 2019). Furthermore, astrocytes from both HD patients and mouse models were associated with higher levels of VEGF-A, which may trigger proliferation of ECs and contributes to neurovascular changes in HD (Hsiao et al., 2015). Of note, sustained delivery of VEGF into the rat striatum via injectable hydrogels was neuroprotective in a lesioned model of HD; VEGF implants significantly protected against the quinolinic acid-induced loss of striatal neurons (Emerich et al., 2010). Moreover, neuroprotection induced by inhibition of hypoxia inducible factor (HIF) prolyl-4-hydroxylases in HD mice has been correlated with enhanced VEGF expression (Niatsetskaya et al., 2010). In post-mortem tissue, cerebral blood vessel density was greater in HD patients while no differences in diameter of small- or medium sized blood vessels have been observed (Drouin-Ouellet et al., 2015). Post-mortem tissue of HD patients revealed a higher proportion of small compared to medium-sized blood vessels in the putamen, an effect occurring in parallel with putamen degeneration. Notably, altered density of small blood vessels in HD patients was consistent with the R6/2 mouse model when brain vascular anomalies were restricted to smaller vessels (Drouin-Ouellet et al., 2015; St-Amour et al., 2015).

Vascular Links to Parkinson's Disease

PD is the second most common neurodegenerative disorder after AD (Antony et al., 2013). It is characterized by the progressive degeneration of the nigrostriatal system, resulting in rigidity, bradykinesia, postural instability, and resting tremor (Antony et al., 2013; Pagano et al., 2016). The most affected cells are dopaminergic neurons from the substantia nigra pars compacta (SNc). The pathological hallmark of PD is the formation of Lewy bodies containing aggregated α-synuclein (Hijaz and Volpicelli-Daley, 2020). While increasing age is a risk factor for PD, the average age of onset is after 60 years old (Hindle, 2010; Parkinson Canada, 2010). The etiology of PD is multifactorial where genetics (familial PD) and environmental (sporadic PD) factors take part in disease onset (Klein and Westenberger, 2012). Familial PD accounts for 10–15% of all PD cases whereas the remainder is classified as sporadic PD (Verstraeten et al., 2015). Genetically linked PD is inherited in an autosomal dominant or recessive fashion (Ball et al., 2019). Research has identified seven causal genes for familial PD including phosphatase and tensing homolog-induced Kinase-1 (PINK1), Parkinson protein 7 (PARK7), parkin RBR E3 ubiquitin protein ligase (PARK2), vacuolar protein sorting-associated protein 35 (VPS35), alpha-synuclein (SNCA), glucocerebrosidase (GBA) and leucine-rich repeat Kinase 2 (LRRK2) (Verstraeten et al., 2015; Kalinderi et al., 2016; Ball et al., 2019). Conversely, sporadic PD may develop from gene-environment interactions (Benmoyal-Segal and Soreq, 2006). Environmental factors associated with PD includes but are not limited to pesticides, heavy metals, and illicit drugs (Kwakye et al., 2017). Notably, individuals may respond differently to environmental factors which results in diverse symptomology of PD, thus adding to the complexity of the disease (Ball et al., 2019).

Altered Cerebral Blood Flow in Parkinson's Disease

Using non-invasive MRI in an heterogeneous PD patient population, studies revealed decreased CBF in the frontal, parietal and occipital areas, more specifically the posterior parieto-occipital cortex, cuneus, middle frontal gyri, putamen, anterior cingulate and post- and pre-central gyri (Kamagata et al., 2011; Melzer et al., 2011; Fernandez-Seara et al., 2012; Madhyastha et al., 2015). A study by Fernandez-Seara et al. (2012) reported a 20–40% decrease in CBF in PD patients compared to a control group. Studies are trying to determine if CBF changes are related to the presence of dementia in PD, or if it can be considered as a biomarker. Derejko et al. (2006) used SPECT in PD patients with dementia and demonstrated left temporo-parietal hypoperfusion compared to the group without dementia. This suggested that CBF differences between PD patients with or without dementia could represent a clinical biomarker for discriminating PD patients (Derejko et al., 2006). Another study revealed hypoperfusion in PD patients without dementia in posterior

cortical regions (posterior cingulate/precuneus) compared to healthy individuals (Syrimi et al., 2017). Hypoperfusion was positively correlated with global cognitive performance and the level of motor impairment (Madhyastha et al., 2015; Syrimi et al., 2017). Melzer et al. (2011) and Fernandez-Seara et al. (2012) reported CBF reduction with parietal cortex thinning in mild PD patients without dementia and proposed that CBF alterations occur in the early stages of PD.

Although studies have identified hypoperfusion in PD patients, the mechanisms underlying these changes are unknown (Biju et al., 2020). One study used a mouse model of PD (α-synuclein transgenic mice), which overexpress human WT α-synuclein. α-synuclein pathology develops before clinical symptoms and is present in both sporadic and familial forms. Using ASL-MRI analysis in this PD mouse model, authors reported a 36.6% reduction in cortical CBF in mutant mice accompanied by motor coordination impairments and olfactory bulb atrophy/dysfunction (Biju et al., 2020).

Altered Blood-Brain Barrier and Angiogenesis in Parkinson's Disease

The association of PD with altered vascular function has led studies to investigate possible players contributing to BBB (Al-Bachari et al., 2020). In animal studies, BBB disruption in the SNc has been reported (Barcia et al., 2005; Rite et al., 2007; Chao et al., 2009). While human studies investigating BBB in PD patients are sparse, there is evidence of BBB dysfunction with increased permeability in the post commissural putamen of PD patients (Kortekaas et al., 2005; Gray and Woulfe, 2015). Wardlaw et al. (2008) and Al-Bachari et al. (2020) revealed increased leakage of the BBB in PD using ASL and dynamic contrast enhanced -MRI (DCE-MRI). Authors compared PD patients with two other control groups: one with and one without known cerebrovascular disease. This comparison could determine if BBB changes are attributable to co-existing cerebrovascular disease in an aging population, or if a pattern of BBB alteration is specific to PD. Authors reported increased BBB leakage in the group with cerebrovascular disease compared to the group without cerebrovascular disease in regions previously associated with PD, including the substantia nigra, white matter, and posterior cortical regions (Al-Bachari et al., 2020).

Accumulation of α-synuclein in ECs may also contribute to BBB dysfunction and increased permeability (Elabi et al., 2021). Higher number of EC nuclei was found in the SNc of PD patients (Faucheux et al., 1999). Other EC dysfunctions were reported, such as down regulation of tight junction proteins (Kuan et al., 2016). In the 1-methyl-4-phenyl-1,2,3,6-tetrahydropyridine (MPTP) mouse model of PD, down-regulation of tight junction protein ZO-1 and BBB leakage were measured in the substantia nigra (Patel et al., 2011). There is also evidence of string vessel formation in brain capillaries from human PD. String vessels are described as collapsed basement membrane without endothelium and no circulatory function. An altered basement membrane was also observed in PD mice (Yang et al., 2015). VEGF, a prominent growth factor promoting angiogenesis and BBB permeability, was upregulated in the substantia nigra, but not the striatum, of PD patients, while animal models of PD displayed parkinsonian traits following administration of exogenous VEGF into the substantia nigra (Barcia et al., 2005; Wada et al., 2006; Rite et al., 2007).

Guan et al. (2013) reported vascular degeneration in human PD, with formation of endothelial clusters, capillary network damage, and loss of capillary connections in the substantia nigra and brain stem nuclei. Authors found a larger vessel size in PD patients, while capillaries were shorter in average length, less in number and had fewer branches. These observations were also confirmed in an MPTP mouse model of PD (Guan et al., 2013; Sarkar et al., 2014). Furthermore, ultrastructural abnormalities were identified in cerebro-cortical microvessels of PD patients, including basement membrane thickening, vacuolization and pericyte degradation (Farkas et al., 2000). Structural alterations of the basement membrane can lead to pathophysiological consequences including compromised nutrient transport and cognitive disturbances (Farkas et al., 2000). Recently, a PD mouse model of α-synuclein overexpression was associated with altered vascular density at different stages of the disease (Elabi et al., 2021). The study reported that 8 month-old animals had increased vessel density compared to control mice, while 13 month-old PD mice displayed decreased vessel density, suggesting compensatory angiogenesis in the younger group (Elabi et al., 2021). Increased angiogenesis is considered an adaptative response to pathological conditions and is regulated by basement membrane proteins and their integrin receptors. These studies postulate that immature nascent vessels in PD could contribute to increased BBB permeability, as reviewed recently (Bogale et al., 2021).

Vascular Links to Alzheimer's Disease

AD accounts for 60–80% of all diagnoses of dementia (Alzheimer's Association, 2021). This progressive and debilitating neurodegenerative disease manifests with memory, attention, executive, visuospatial and perceptual impairments. AD is not only characterized by amyloid deposition, neuroinflammation, neurodegeneration and cognitive deficits, but also by cerebrovascular pathology. Indeed, an inadequate brain perfusion has been identified as an early event in the development and progression of AD (Nicolakakis and Hamel, 2011). The risk of developing AD is increased by age-associated vascular diseases such as hypercholesterolemia, hypertension, ischemic stroke, and diabetes (Kalaria, 1996; Roher et al., 2003; Casserly and Topol, 2004; Gorelick, 2004; Luchsinger et al., 2005). The AD brain is characterized by increased levels of soluble and insoluble amyloid-beta peptide (Aβ), derived from the amyloid protein precursor (APP), neurofibrillary tangles of hyperphosphorylated *tau* protein, neurodegeneration and neuroinflammation, and also linked with a cerebrovascular pathology (Selkoe, 2002; Iadecola, 2004; Querfurth and LaFerla, 2010). The latter is identified post-mortem by Aβ deposition in brain vessels (cerebral amyloid angiopathy, CAA), Aβ-induced oxidative stress, and alterations of the vessel wall that included fibrosis and degeneration of ECs (Buee et al., 1994; Vinters et al., 1994; Zarow et al., 1997; Farkas and Luiten, 2001; Humpel and Marksteiner, 2005). Various mouse models of AD have been developed, most mimicking

the overproduction of Aβ through transgene expression of mutated human APP (hAPP) combined or not with the amyloidogenic presenilin (PS1) or the pathologic *tau* (Mucke et al., 2000; Oddo et al., 2003; Gotz and Ittner, 2008). These models recapitulate AD's cerebrovascular pathology in addition to the cognitive deficits, senile plaques, Aβ-induced oxidative stress, neuroinflammation, cholinergic denervation, synaptic failure, and cerebral hypometabolism (Hsia et al., 1999; Palop et al., 2003; Aucoin et al., 2005; Tong et al., 2005; Nicolakakis et al., 2008; Iturria-Medina et al., 2016; Love and Miners, 2016; Liu et al., 2018; Czako et al., 2020). It is in fact estimated that up to 45% of all dementias worldwide are partly, or wholly, due to age-related SVD of the brain (Montagne et al., 2016; Clancy et al., 2021). This suggests that AD and vascular dementia share common grounds, which complicates their stratification. As such, it is of utmost importance to improve our understanding of vascular underpinnings of AD (Willis and Hakim, 2013). Clinical studies that attempted to reduce plaque load by blocking Aβ production, removing Aβ with antibodies, or preventing tau phosphorylation, have all failed to alleviate AD symptoms (Korte et al., 2020). However, mounting evidence demonstrates that the brain vasculature is the missing link (Sweeney et al., 2019). Early cerebrovascular dysfunction in AD leads to decreased Aβ clearance, vascular oxidative stress, inflammatory damage and impaired BBB function (Zlokovic, 2005). Here below we will succinctly describe vascular underpinnings of AD, from alterations in CBF to BBB dysfunction, topics that have been extensively reviewed elsewhere (Bell and Zlokovic, 2009; Zlokovic, 2011; Hamel, 2015; Hays et al., 2016; Nelson et al., 2016; Kisler et al., 2017; Korte et al., 2020; Solis et al., 2020; Soto-Rojas et al., 2021).

Cerebral Blood Flow Alterations in Alzheimer's Disease

Numerous investigations on individuals diagnosed with AD observed reduced CBF (Prohovnik et al., 1988; Montaldi et al., 1990; Bressi et al., 1992; O'Brien et al., 1992; Smith et al., 1992; Minoshima et al., 1997; Mattsson et al., 2014; Mielke et al., 2014; Smith and Verkman, 2018). CBF decline can be detected prior to cognitive decline, but also before plaque deposition. The accumulation of soluble Aβ prior to plaque deposition has early pathogenic consequences in AD (Suo et al., 1998). Studies have demonstrated increased levels of soluble amyloid species including $A\beta_{1-40}$ and $A\beta_{1-42}$ in AD cases compared to age-matched controls (Suo et al., 1998; Smith and Greenberg, 2009). Both soluble $A\beta_{1-40}$ and $A\beta_{1-42}$ have been associated to abnormal vascular reactivity in the absence of plaque deposition or vessel wall dysfunction (Smith and Greenberg, 2009; Dietrich et al., 2010). In particular, studies have revealed that application of exogenous $A\beta_{1-40}$ to mouse neocortex *in vivo,* or to healthy bovine blood vessels *ex vivo,* leads to endothelium-dependent vasoconstriction (Thomas et al., 1996; Niwa et al., 2000). In addition, increased levels of soluble amyloid species ($A\beta_{1-40}$ and $A\beta_{1-42}$) are associated with significantly reduced CBF, increased cerebral vascular resistance, decrease myogenic and vasodilator responses (Suo et al., 1998; Dietrich et al., 2010), where $A\beta_{1-42}$ is equally potent to $A\beta_{1-40}$ except at a higher concentration (Dietrich et al., 2010). Soluble Aβ impacts vascular function through increased production of reactive oxygen species (ROS). The reaction of ROS superoxide and excess NO produces peroxynitrite. Peroxynitrite is commonly known as a toxic oxidant which contributes to endothelial dysfunction, a mechanism relevant to AD but also to other neuroinflammatory and metabolic conditions (Beckman et al., 1990; Paris et al., 1998; Tan et al., 2004; Dietrich et al., 2010; Kelleher and Soiza, 2013; Salisbury and Bronas, 2015; Incalza et al., 2018). Both $A\beta_{1-40}$ and $A\beta_{1-42}$ have been shown to acutely increase ROS production in cultured rat cerebral microvascular endothelial and smooth muscle cells in a dose dependent manner (Dietrich et al., 2010). Interestingly, this response was inhibited by the ROS scavenger MnTBAP (Dietrich et al., 2010). Notably, $A\beta_{1-40}$ is the predominant isoform found in cerebral vessel walls and is commonly associated with vascular deposits in CAA, which will be discussed later, while $A\beta_{1-42}$ is the major isoform deposited in senile plaques (Suo et al., 1998). Although this concept is still controversial, it is thought that $A\beta_{1-42}$ acts as a "seed" which initiates the formation of vascular Aβ deposit in CAA (McGowan et al., 2005; Gireud-Goss et al., 2020).

Following Aβ deposition, reduction of CBF was found in the frontal, parietal and temporal cortices from individuals carrying Apolipoprotein E4 (*APOE4*) gene, most prevalent genetic risk factor for AD (Thambisetty et al., 2010; Michels et al., 2016). In addition, ApoE4 allele carriers displayed early impairments in cerebrovascular reactivity to a memory task (Suri et al., 2015). BOLD-fMRI, which uses blood flow changes as a surrogate to neuronal activity, detected decreased activation in areas engaged during naming and fluency tasks in AD patients compared to individuals with no risk factors (Smith et al., 1999). Decreased BOLD-fMRI responses to different cognitive tasks in early stage of AD are region-specific (Kisler et al., 2017). Most studies investigating perfusion in AD reported either CBF or CBV alterations. However, CBF alterations appear before CBV deficits during AD progression (Lacalle-Aurioles et al., 2014).

Decreased CBF is associated with poor cognitive function, and evidence suggested that lower CBF is linked with faster cognitive decline in patients with AD (Benedictus et al., 2017). Zheng et al. (2019) investigated rCBF, functional activity and connectivity in AD by combining resting-state BOLD fMRI and ASL techniques. ASL revealed decreased rCBF in AD patients in the left posterior cingulate cortex, bilateral dorsolateral prefrontal cortex, left interior parietal lobule, right middle temporal gyrus, left middle occipital gyrus and left precuneus. In addition, they revealed decreased connectivity between regions in AD patients, which was associated with impaired cognitive performances (Alsop et al., 2000; Zheng et al., 2019). Brain regions affected by a reduction of CBF in AD patients (parietal, frontal, temporal and occipital cortices) are associated with cognitive impairment in all domains (language, global cognition, memory, attention, executive functioning and visuospatial functioning) (Leeuwis et al., 2017).

Blood flow reductions have also been identified in early preclinical AD, before Aβ plaque deposition (Nicolakakis and Hamel, 2011; Iturria-Medina et al., 2016; Szu and Obenaus, 2021).

Early reduction of CBF has been reported in mouse models of AD, such as mice overexpressing mutant forms of APP (Niwa et al., 2002; Ongali et al., 2010; Lacoste et al., 2013) and in mice expressing the *ApoE4* gene allele (Lin et al., 2017). In some brain areas, CBF reduction can reach over 50%. This CBF reduction has been associated with cognitive changes in mice, including a loss of ability to sustain attention (Marshall et al., 2001). Both *ApoE4* transgenic and APP/PS1 mice revealed CBF reduction prior to neuronal and synaptic dysfunctions (Guo et al., 2019; Montagne et al., 2021).

While decreased CBF in AD is widely accepted, studies are only starting to identify underlying mechanisms, for example the involvement of pericytes. Pericytes have been linked to hypoperfusion and increased capillary constriction in AD (Bell et al., 2010; Korte et al., 2020). Pericyte-deficient transgenic mice with no Aβ pathology develop early CBF reduction in the gray matter, even with normal neuronal activity, endothelial-dependent vasodilation, astrocyte number and blood vessels coverage (Bell et al., 2010; Kisler et al., 2017). As these pericyte-deficient mice age, neuronal dysfunction and degeneration start to emerge. Another underlying mechanism was reported by Cruz Hernandez et al. (2019), demonstrating that capillaries become blocked by neutrophils, while another study revealed increased formation of occlusive thrombi in AD mice (Cortes-Canteli et al., 2019). Inhibiting neutrophils adhesion using an antibody against neutrophil-specific protein Ly6G in the APP/PSI mouse model led to rapid improvements in CBF (Cruz Hernandez et al., 2019). In a follow-up study, the same group assessed the impact of one treatment of anti-Ly6G on short-term memory function and reported increased CBF by 17% in 21–22 months old APP/PSI mice. Furthermore, they suggested that increased CBF improved cognition into late stages of AD mice (Bracko et al., 2020). Reduced neurovascular coupling and cerebrovascular reactivity have also been reported in AD mice (Girouard and Iadecola, 2006; Tong et al., 2019). Recently, impaired capillary endothelial inward rectifying Kir2.1 channel, playing a role in mediating blood delivery, has been associated with AD (Mughal et al., 2021). In a model of familial AD (5xFAD) where Kir2.1 channel function is impaired, systemic administration of the co-factor phosphatidylinositol 4,5-bisphosphate (PIP_2), required for Kir2.1 activity, led to increased CBF and functional neurovascular coupling in 5xFAD mice (Mughal et al., 2021).

AD patients are often (80–90%) diagnosed with CAA, a vessel disorder (Gireud-Goss et al., 2020) and an important risk factor for intracerebral hemorrhage and cognitive impairment (Reijmer et al., 2016). CAA consist of vascular amyloid deposits similar to senile plaques in AD (Kumar-Singh et al., 2005). Neuropathological studies have revealed that CAA affects the outer leptomeningeal vessels on the surface of the brain as well as distal intraparenchymal arteries, arterioles, and capillaries (Gireud-Goss et al., 2020; Howe et al., 2020). APP23 mouse model and human AD brain revealed an association between CAA-related capillary occlusion with CBF disturbances, hypoperfusion, detected by magnetic resonance angiopathy (MRA), which could explain in part the changes in CBF measured in AD patients (Thal et al., 2009; Milner et al., 2014). As in AD, patients with CAA have been linked to altered hemodynamics during visual stimulation as evidenced by reduced amplitude of BOLD response (Smith et al., 2008; Dumas et al., 2012; Switzer et al., 2020).

Altered Blood-Brain Barrier and Angiogenesis in Alzheimer's Disease

Early signs of BBB leakage in AD have been detected before dementia onset (Montagne et al., 2016). Neuroimaging techniques have evidenced BBB breakdown in AD in gray and white matter brain regions (Montagne et al., 2016; van de Haar et al., 2016). Aβ and tau pathologies contribute to increased BBB permeability in AD patients and mouse models (Park et al., 2011; Sagare et al., 2013; Alata et al., 2015). Several players involved in Aβ clearance, and closely related to the BBB, are reduced in AD patients, including phosphatidylinositol-binding clathrin assembly protein (PICALM, allows for Aβ exocytosis across the luminal part of the BBB), P-glycoprotein (expressed on both sided of the BBB) and glucose transporter (GLUT)1 (Mooradian et al., 1997; Chiu et al., 2015; Zhao et al., 2015). AD brain microvessel show diminished expression of LRP1, a major Aβ clearance receptor at the BBB (Deane et al., 2004; Donahue et al., 2006). LRP1 is an ApoE receptor and is expressed at the abluminal side of brain ECs and mediates the internalization of soluble Aβ (Deane et al., 2004). Endothelium-specific deletion of LRP1 leads to the acceleration of Aβ pathology in APP-overexpressing $APP_{sw/0}$ mice (Storck et al., 2016). Moreover, studies have demonstrated low levels of GLUT1 in AD brain endothelium, which alters glucose transport (Kalaria and Harik, 1989; Simpson et al., 1994).

Several features lead to increased BBB permeability in AD, including reduced expression of tight junctions, perivascular accumulation of blood-derived products, degeneration of pericytes and ECs, as well as infiltration of circulating leukocytes (Sweeney et al., 2018; Huang et al., 2020). It was demonstrated that Aβ disrupts tight junctions and increases vascular permeability by suppressing expression of ZO-1, claudin-5 and occludin while increasing expression of MMP-2 and MMP-9 (Kook et al., 2012; Blair et al., 2015; Wan et al., 2015; Huang et al., 2020). Isolated rat cerebral cortical ECs treated with $A\beta_{1-42}$ displayed decreased expression of occludin and redistribution of claudin-5 and ZO-2 in the cytoplasm while in untreated cells, both claudin-5 and ZO-2 were distributed along the plasma membrane at cell-cell contacts (Marco and Skaper, 2006). In addition, studies have reported leakage of blood-derived proteins (fibrinogen, thrombin, albumin, and IgG) around capillaries from post-mortem brain tissue in the prefrontal and entorhinal cortex as well as in hippocampus of AD patients (Ryu and McLarnon, 2009; Hultman et al., 2013; Sengillo et al., 2013). Furthermore, animal studies revealed that lacking pericyte-derived soluble factors, required for a healthy endothelium, can contribute to endothelial degeneration in AD (Bell et al., 2010). Finally, mouse models of AD have demonstrated that pericyte reduction is associated with BBB dysfunction as well as accelerated buildup of Aβ and tau pathology (Sagare et al., 2013). In human studies, there is also evidence of pericyte loss in the hippocampus and cortex of AD

patients due in part to prolonged exposure to Aβ peptides (Sagare et al., 2013; Sengillo et al., 2013; Huang et al., 2020). Of note, pericytes play a role in Aβ clearance by internalizing different Aβ peptides using the LRP1 pathway (Sagare et al., 2013).

Evidence of reduced capillary length and basement membrane changes in AD patients have been reported (Salloway et al., 2002; Sengillo et al., 2013; Halliday et al., 2016). It was shown that AD patients display abnormal angiogenesis due to low expression of MEOX2, a regulator of vascular differentiation, as well as premature pruning of capillary networks resulting in reductions of CBF (Wu et al., 2005; Grammas, 2011). Endothelial degeneration including reduction of EC thickness, length and density of blood vessels were reported in brain tissue from AD patients (Sweeney et al., 2018). An increase of pro-angiogenic factors in the AD brain, without the increase in vasculature, was also reported (Grammas, 2011). Notably, the increased Aβ species and plaques in AD have anti-angiogenic effects (Parodi-Rullan et al., 2020), and impaired angiogenesis was identified in transgenic AD mice (Grammas, 2011). Emerging evidence suggest that dysfunction of the VEGF-A/VEGFR2 pathway may play an aggravating role in neurodegeneration and AD. For instance, sustained brain delivery of VEGF via injectable hydrogels was protective against quinolinic acid-induced neurodegeneration (Emerich et al., 2010), and low VEGF levels have been associated to another debilitating neurological disorder, spinocerebellar ataxia type 1 (Cvetanovic et al., 2011). Aβ acts as an antagonist of VEGF signaling via sequestration of VEGF-A in senile plaques, and also via inhibition of VEGFR2 tyrosine phosphorylation (Patel et al., 2010). Moreover, implantation of VEGF secreting microcapsules on the cerebral cortex of APP/PS1 mice attenuated both brain Aβ burden and cognitive impairments (Spuch et al., 2010). Whether impaired neural perfusion and increased neurotoxicity in AD correlate to a loss of VEGF function, and whether VEGF overexpression is neuroprotective in transgenic AD mice remains to be explored.

CAA is associated with increased BBB permeability and arterial stiffness (Magaki et al., 2018; Gireud-Goss et al., 2020). Aβ deposition in CAA has been found to occur on the cerebrovascular basement membrane of arteries, arterioles and on the basal lamina of capillaries as shown by electron microscopy (Gireud-Goss et al., 2020). Moreover, ultrastructural studies of CAA demonstrated a thinned endothelium, shrinkage and degeneration of ECs, as well as vessel occlusion, all of which can lead to CBF disturbances and microinfarcts (Attems and Jellinger, 2004; Thal et al., 2009; Magaki et al., 2018). Tight junction proteins in CAA-laden vessels are found decreased (Tai et al., 2010). After exposure to exogenous Aβ, human ECs showed decreased expression of occludin, while post-mortem brain tissue of CAA patients revealed decreased expression of claudin-5, ZO-1, CD31 and basement protein collagen IV (Tai et al., 2010; Carrano et al., 2011; Magaki et al., 2018). In addition, CAA patients displayed increased expression of MMP-2 and MMP-9, which may lead to basement membrane degradation and increased BBB permeability (Carrano et al., 2011). In the Tg2576 mouse model of CAA, BBB integrity was compromised due to decreased expression of claudin-5 and claudin-1 (Carrano et al., 2011). Moreover, TgSwDI mice, another model of CAA, revealed spontaneous hemorrhage and loss of BBB integrity (Davis et al., 2004). Soluble $A\beta_{1-40}$, predominant amyloid isoform in vessel walls, also leads to tight junction redistribution at the BBB and decreased transendothelial electric resistance (Hartz et al., 2012; Gireud-Goss et al., 2020). Understanding the impact of Aβ in CAA and AD is essential for slowing cerebrovascular disease progression.

ADDITIONAL REMARKS: VASCULAR DEFICITS IN DOWN SYNDROME, TRAUMATIC BRAIN INJURY AND DEPRESSION

In addition to neurodevelopmental disorders discussed earlier in this review, Down syndrome (DS), which results from trisomy of human chromosome 21, is a cause of early onset Alzheimer's disease-dementia (AD-DS) (Ballard et al., 2016; Tosh et al., 2021). Two-thirds of individuals with DS will develop dementia by the age of 65 (Tosh et al., 2021). The onset of AD in DS patients parallels the development of the classic brain pathological lesions seen in AD patients without DS (Salehi et al., 2016). DS and AD disorders have genetic similarities, as individuals with DS possess a triplication of the gene encoding APP, while patients with familial AD have an extra copy of the APP gene (Salehi et al., 2016). In rodent studies of DS-AD, triplication of chromosome 21 genes other than *APP* demonstrated increased Aβ aggregation deposition and cognitive deficits (Wiseman et al., 2018). A recent study, focused on a model of DS comprising of a mutation in a Down syndrome critical region (Hsa21) on chromosome 21 encompassing 21q21–21q22.3 (Li et al., 2016; Tosh et al., 2021). This study crossed an Hsa21 mouse model of DS with partial trisomies other than *APP* with a transgenic APP mouse model and revealed that an additional copy of genes of the Hsa21 region modulates APP/Aβ biology, including Aβ aggregation and mortality (Tosh et al., 2021). Despite striking similarities between AD and DS in terms of genetics and symptoms onset, neurovascular impairments in DS have been largely overlooked. As such, studies aimed at elucidating vascular abnormalities in DS represent an unmet clinical need.

Early vascular insults following a traumatic brain injury (TBI) can also increase the risk of late-onset neurological diseases (Brett et al., 2021). TBI is a significant public health problem associated with long-term disabilities. Early chronic TBI may lead to secondary injury with pathophysiological changes similar to those observed in neurodegenerative diseases (Impellizzeri et al., 2016). For instance, neuroinflammation plays a fundamental role in TBI, including reactive microglia and astrocytes, as well as release of pro-inflammatory cytokines and chemokines that may hinder the brain's ability to repair itself and lead to neurodegeneration following prolonged activation of these processes (Impellizzeri et al., 2016; Brett et al., 2021). Severe or repeated mild TBI can initiate long-term neurodegeneration with signs of AD (Mendez, 2017). For example, various contact-sport players developed TBI-associated dementia or parkinsonism years after retiring. TBI can induce acute BBB disruption through

TABLE 1 | Major altered features associated with CBF, BBB, and angiogenesis in neurodevelopmental and neurodegenerative disorders.

Disorder	Key features	Selected references
ASD		
Altered CBF	– Widespread cerebral hypoperfusion in 75% of ASD children associated with language deficits, impaired executive function and abnormal response to sensory stimuli. – Hyperperfusion identified in frontotemporal regions. – Reduced hemodynamic responses. – Cerebral hypoperfusion also identified in rodent models of ASD. – Increased resting CBF and decreased NVC in an adult mouse model of ASD associated with endothelial dysfunction.	Ohnishi et al., 2000; Zilbovicius et al., 2000; Burroni et al., 2008; Reynell and Harris, 2013; Jann et al., 2015; Ouellette et al., 2020; Uratani et al., 2019
Altered BBB and angiogenesis	– Reduced level of adhesion molecules (CD31 and P-selectin). – Increased MMP-9 which regulates cell proliferation, adhesion, angiogenesis, oxidative injury and BBB breakdown. – Altered expression of claudin-5 and claudin-12. – Increased BBB permeability and impaired angiogenesis in animal models. – Reduced angiogenesis found in a mouse model of ASD.	Onore et al., 2012; Kumar et al., 2015; Azmitia et al., 2016; Fiorentino et al., 2016; Turner and Sharp, 2016; Ouellette et al., 2020
Schizophrenia		
Altered CBF	– Increased CBF in the cingulate gyrus and superior frontal gyrus associated with positive symptoms. – Negative symptoms associated with hypoperfusion in the superior temporal gyrus bilaterally and left middle frontal gyrus. – rCBF alterations depend on severity of positive symptoms. – Increased CBF in the right superior temporal gyrus and caudate nucleus. – Decreased CBF in the occipital and left parietal cortices. – Altered NVC including reduced amplitude of response and delayed hemodynamics.	Sabri et al., 1997; Carter et al., 2001; Schultz et al., 2002; Malaspina et al., 2004; Ford et al., 2005; Pinkham et al., 2011; Liu et al., 2012; Kawakami et al., 2014; Pu et al., 2016; Zhuo et al., 2017
Altered BBB and angiogenesis	– Increased BBB permeability. – Thickening and deformation of basal lamina, vacuolation of EC cytoplasm, swelling of astrocyte end-feet, activation of microglial cells and atypical vascular arborization in prefrontal and visual cortices. – Decreased claudin-5 expression, altered level of VE-cadherin and occludin in ECs. – Impaired angiogenesis and VEGF upregulation in the prefrontal cortex linked to vascular hyperpermeability.	Grove et al., 2015; Hino et al., 2016; Casas et al., 2018; Carrier et al., 2020; Cai et al., 2020; Guo et al., 2020; Crockett et al., 2021; Usta et al., 2021
MS		
Altered CBF	– Hypoperfusion in SP-MS, RR-MS and PP-MS patients. – Active demyelinating lesions associated with hyperperfusion and stable lesions linked to hypoperfusion. – CBF alterations present in early stages of disease. – Impaired cerebral vascular reactivity leads to neuronal death. – Overproduction of NO desensitize EC and smooth muscle cell function, leading to decreased vasodilatory capacity and limited blood supply to neurons.	Ge et al., 2005; Varga et al., 2009; D'Haeseleer et al., 2011; Ota et al., 2013; Marshall et al., 2014; Bester et al., 2015; Monti et al., 2018; Hostenbach et al., 2019
Altered BBB and angiogenesis	– BBB hyperpermeability. – Decreased expression of TJ proteins (ZO-1, occludin and claudin-5) in ECs in patients with active and inactive lesions. – Rodent model of MS show increased expression of VEGF in ECs, astrocytes and monocytes. – Increased vascular network density and angiogenesis.	Kirk et al., 2003; Bennett et al., 2010; Holley et al., 2010; Cramer et al., 2014; Girolamo et al., 2014; Papadaki et al., 2014
HD		
Altered CBF	– Altered CBF prior to structural changes and motor symptoms. – Cerebral hypoperfusion in the basal ganglia, medial and lateral prefrontal cortex. – Cerebral hyperperfusion in the cerebellar-thalamic and somatosensory regions. – Altered neurovascular coupling during visual stimulation.	Hasselbalch et al., 1992; Sax et al., 1996; Deckel and Duffy, 2000; Wang et al., 2016; Klinkmueller et al., 2021

(Continued)

TABLE 1 | (Continued)

Disorder	Key features	Selected references
Altered BBB and angiogenesis	– Increased vessel density, BBB leakage and VEGF-A release. – Decreased TJ molecules including occludin and claudin-5. – Rodent model of HD revealed increased transcytosis and paracellular transport in brain ECs with TJ imbalance. – mHtt aggregates localized in ECs, smooth muscle cells and perivascular macrophages. – iPSCs-derived HD BMECs show increased angiogenesis, altered barrier properties and impaired Wnt/β-catenin signaling.	Steventon et al., 2020; Drouin-Ouellet et al., 2015; Di Pardo et al., 2017; Lim et al., 2017
PD		
Altered CBF	– Decreased CBF in frontal, parietal and occipital areas. – PD patients with dementia show left temporo-parietal hypoperfusion. – PD patients without dementia display hypoperfusion in the posterior cortical regions. – Hypoperfusion is positively correlated with cognitive performance and motor impairment.	Derejko et al., 2006; Kamagata et al., 2011; Fernandez-Seara et al., 2012; Madhyastha et al., 2015; Syrimi et al., 2017
Altered BBB and angiogenesis	– BBB disruption in the SNc with increased permeability in the post-commissural putamen. – Down regulation of TJ proteins (ZO-1) and higher number of EC nuclei in the SNc. – String vessel formation in brain capillary networks. – Upregulation of VEGF, and parkinsonian traits following VEGF administration in rodent models. – Formation of endothelial clusters, capillary network damage, loss of capillary connections in the SN, basement membrane thickening, vacuolization, and pericyte degradation.	Farkas et al., 2000; Barcia et al., 2005; Kortekaas et al., 2005; Wada et al., 2006; Rite et al., 2007; Chao et al., 2009; Patel et al., 2011; Guan et al., 2013; Yang et al., 2015; Kuan et al., 2016
AD		
Altered CBF	– Reduced CBF prior to cognitive decline and plaque deposition. – Soluble $A\beta_{1-40}$ and $A\beta_{1-42}$ are associated with abnormal vascular reactivity and decreased myogenic responses in absence of plaque deposition. – Hypoperfusion detected following Aβ deposition in the frontal, parietal and temporal cortices and poor cognitive function. – BOLD-fMRI detected decreased activation in regions involved in naming and fluency tasks. – Hypoperfusion identified in rodent models overexpressing mutant forms of APP. – Rodent models show reduced NVC and cerebrovascular reactivity. – Parallel diagnosis of CAA linked with altered hemodynamics, capillary occlusion and hypoperfusion.	Montaldi et al., 1990; Bressi et al., 1992; Smith et al., 1999; Marshall et al., 2001; Girouard and Iadecola, 2006; Smith and Greenberg, 2009; Dietrich et al., 2010; Ongali et al., 2010; Dumas et al., 2012; Lacoste et al., 2013; Mattsson et al., 2014; Milner et al., 2014; Benedictus et al., 2017; Smith and Verkman, 2018
Altered BBB and angiogenesis	– Aβ and tau pathologies contribute to BBB breakdown, reduced expression of TJ (ZO-1, claudin-5, occludin) and degeneration of pericytes and ECs. – Brain microvessel with diminished expression of LRP1. – Reduced level of GLUT1 in brain endothelium. – Reduced capillary length with basement membrane alterations. – Abnormal angiogenesis related to low expression of MEOX2. – Reduced EC thickness, and lower length/density of blood vessels. – Dysfunction of the VEGF-A/VEGFR2 pathway aggravates neurodegeneration. – Rodent models show pericyte loss. – Aβ deposition in CAA linked to decreased TJ proteins, increased expression of MMP-2 and MMP-9, thinned endothelium, degeneration of ECs and leaky BBB.	Kalaria and Harik, 1989; Simpson et al., 1994; Emerich et al., 2010; Tai et al., 2010; Grammas, 2011; Carrano et al., 2011; Sagare et al., 2013; Halliday et al., 2016; Montagne et al., 2016; van de Haar et al., 2016; Magaki et al., 2018; Sweeney et al., 2018; Huang et al., 2020

Selected references are displayed. Aβ, β-amyloid peptide; AD, Alzheimer's disease; APP, amyloid precursor protein; ASD, autism spectrum disorders; BBB, blood brain barrier; BMECs, brain microvascular endothelial cells; BOLD-FMRI, blood oxygen level dependent imaging-functional magnetic resonance imaging; CAA, cerebral amyloid angiopathy; CBF, cerebral blood flow; ECs, endothelial cells; GLUT1, glucose transporter 1; HD, Huntington's disease; iPSC, induced pluripotent stem cells; LRP1, low-density lipoprotein receptor-related protein 1; MEOX2, Mesenchyme Homeobox 2; mHtt, mutant huntingtin; MMP, matrix metalloproteinases; MS, multiple sclerosis; NO, nitric oxide; NVC, neurovascular coupling; PD, Parkinson's disease; PP-MS, primary progressive-multiple sclerosis; rCBF, regional cerebral blood flow; RR-MS, relapsing remitting-multiple sclerosis; SN, substantia nigra; SNc, substantia nigra pars compacta; SP-MS, secondary progressive-multiple sclerosis; TJ, tight junctions; VE-cadherin, vascular endothelial cadherin; VEGF, vascular endothelial growth factor; VEGFR2, vascular endothelial growth factor receptor 2; Wnt/β-catenin, Wingless-related integration site β- catenin; ZO-1, Zonula occludens-1.

vascular shear stress, hemorrhages, edema, alterations in CBF and chronic inflammation, which is known to contribute to Aβ deposition and tau pathology (Iadecola, 2013; De Silva and Faraci, 2016). Autopsies of TBI patients show diffuse Aβ plaques similar to those identified in AD, as reviewed by Perry et al. (2016). The formation of Aβ in perivascular spaces following TBI may lead to an injury cascade consisting of cerebrovascular damage, oxidative stress and ECs dysfunction (Ramos-Cejudo et al., 2018). Interestingly, alterations in EC survival, BBB integrity and neuroinflammation are considered early events after TBI, all of which are characteristic of cerebrovascular damage involved in the progression of AD and impairment of Aβ clearance. Thus, these early vascular impairments promote the onset of neurodegenerative diseases (Ramos-Cejudo et al., 2018). Considering early vascular injuries in TBI, biomarker studies are integrating a variety of neuroimaging and molecular techniques to better understand the incidence of cerebrovascular dysfunction and the onset of neurodegenerative diseases, and therapeutic investigations have looked at ways to improve cerebrovascular function (Graham and Sharp, 2019; Martinez and Stabenfeldt, 2019).

One of the leading causes of mental illness worldwide, depression, has a tremendous impact on psychosocial behaviors and vascular health (Knight and Baune, 2017; Menard et al., 2017). Chronic stress is the primary environmental risk factor for depression. The nucleus accumbens (NAc) is one of the main players in regulating stress response (Russo and Nestler, 2013). Menard et al. (2017) have demonstrated that chronic social stress induces BBB leakiness in the NAc of mice, which leads to circulating proinflammatory mediators and depression-like behaviors such as helplessness, social avoidance and anhedonia. As seen in neurodevelopmental and neurodegenerative disorders, the increase in BBB permeability in the rodent model of chronic social stress was facilitated by the loss of tight junction protein claudin-5 (Menard et al., 2017). Furthermore, stress-induced BBB permeability has been linked to inflammation of the endothelium and up-regulation of an epigenetic repressor, *hdac1*, which is involved in reducing claudin-5 expression and loosening of tight junctions (Dudek et al., 2020). Consequently, these studies are highlighting mechanisms by which chronic stress impacts vascular health, which could have long-term consequences on brain maturation and aging.

The vascular system, as any other system, undergoes aging. It has been hypothesized that vascular aging leads to a progressive functional deterioration (Grunewald et al., 2021). During aging, the brain vasculature undergoes several changes including decreased capillary density, attenuation of neovascularization potential, increased BBB permeability and decreased CBF as reviewed in Watanabe et al. (2020) and Banks et al. (2021). A suggested mechanism of typical vascular aging consist of the inability of VEGF to replenish vessel loss. The mechanisms by which VEGF is involved in vascular aging are unknown. However, mice treated with VEGF have been shown to live longer, with extended multiorgan functionality (Grunewald et al., 2021). Furthermore, aging is associated with several vascular changes including aortic stiffness which has been linked to reduced blood flow in tissues leading to increased neuroinflammation and neurodegeneration later in life (Moore et al., 2021). Therefore, age-related changes in key vascular features may predispose to age-associated diseases (Banks et al., 2021). Improving early pathological conditions by protecting the brain vasculature is essential in preventing or modulating disease progression.

CONCLUSION

Vascular risk factors and co-morbidities take part in disease onset and/or exacerbate disease progression (Sweeney et al., 2018; Clancy et al., 2021). When it comes to alterations in CBF, BBB, and vascular patterning, neurodevelopmental and neurodegenerative disorders share interesting similarities (**Table 1**). While these disorders are siloed, mainly due to the age of onset, the commonalities in vascular alterations force to question the implication of early life vascular impairments on the expression of age-related neurodegenerative diseases. The vascular implications in middle-aged autistic adults have been largely overlooked, 10% of individuals diagnosed with ASD age between 40 and 60 years old will develop dementia, including AD within 15 years (Plana-Ripoll et al., 2019). In addition, there is a high frequency of parkinsonism among older ASD patients (Starkstein et al., 2015). The impact of altered brain perfusion and BBB integrity in ASD may contribute to the onset of neurodegenerative diseases due to the continuous vascular impairments associated with these diseases. Likewise, schizophrenia is associated with an elevated risk for developing Alzheimer's and Parkinson's diseases as they share core features including white matter abnormalities and cognitive deficits (Ribe et al., 2015; Kochunov et al., 2021; Kuusimaki et al., 2021).

Since fast-growing evidence demonstrates the role of early vascular impairments in the onset and/or progression of numerous neurological conditions, more work is needed to identify therapeutic targets to promote healthy cerebrovascular maturation and aging, as well as hinder the progression of age-related dementia and neurodegeneration. This is primordial considering recent findings that ECs show limited turnover compared to other cells in the human body (Sender and Milo, 2021). For instance, it was estimated that the turnover rate of ECs is 0.1% per day, as opposed to much higher rates for erythrocytes (65%), neutrophils (18%) or gastrointestinal epithelial cells (12%). In addition, the turnover rates of cellular mass in the human body were estimated at 0.4% for ECs, 4% for skin cells and adipocytes, and 42% for gastrointestinal epithelial cells (Sender and Milo, 2021). Hence, as ECs are long-lived, they may carry on early structural and functional impairments into adulthood and throughout aging, altering organ function in the long term. This concept emphasizes the importance of infant screening for cerebrovascular abnormalities, and of continuous management of vascular risk factors during lifespan. As such, the vascular continuum between neurodevelopmental and neurodegenerative disease should represent a growing focus in modern neuroscience (**Figure 3**).

AUTHOR CONTRIBUTIONS

JO wrote the draft following BL's instructions. BL chose the theme and edited the manuscript. Both authors contributed to the article and approved the submitted version.

FUNDING

This publication was possible thanks to funding by the Canadian Institutes for Health Research (grant #388805) to BL and a Canadian Vascular Network scholarship to JO.

REFERENCES

Abbott, N. J., Ronnback, L., and Hansson, E. (2006). Astrocyte-endothelial interactions at the blood-brain barrier. *Nat. Rev. Neurosci.* 7, 41–53. doi: 10.1038/nrn1824

Abookasis, D., Lerman, D., Roth, H., Tfilin, M., and Turgeman, G. (2018). Optically derived metabolic and hemodynamic parameters predict hippocampal neurogenesis in the BTBR mouse model of autism. *J. Biophotonics* 11:e201600322. doi: 10.1002/jbio.201600322

Adhya, S., Johnson, G., Herbet, J., Jaggi, H., Babb, J. S., Grossman, R. I., et al. (2006). Pattern of hemodynamic impairment in multiple sclerosis: dynamic susceptibility contrast perfusion MR imaging at 3.0 T. *Neuroimage* 33, 1029–1035. doi: 10.1016/j.neuroimage.2006.08.008

Al-Bachari, S., Naish, J. H., Parker, G. J. M., Emsley, H. C. A., and Parkes, L. M. (2020). Blood-Brain Barrier Leakage Is Increased in Parkinson's Disease. *Front. Physiol.* 11:593026. doi: 10.3389/fphys.2020.593026

Alata, W., Ye, Y., St-Amour, I., Vandal, M., and Calon, F. (2015). Human apolipoprotein E varepsilon4 expression impairs cerebral vascularization and blood-brain barrier function in mice. *J. Cereb. Blood Flow Metab.* 35, 86–94. doi: 10.1038/jcbfm.2014.172

Alsop, D. C., Detre, J. A., and Grossman, M. (2000). Assessment of cerebral blood flow in Alzheimer's disease by spin-labeled magnetic resonance imaging. *Ann. Neurol.* 47, 93–100.

Alzheimer's Association (2021). 2021 Alzheimer's disease facts and figures. *Alzheimers Dement.* 17, 327–406. doi: 10.1002/alz.12328

Andreasen, N. C., O'Leary, D. S., Flaum, M., Nopoulos, P., Watkins, G. L., Boles Ponto, L. L., et al. (1997). Hypofrontality in schizophrenia: distributed dysfunctional circuits in neuroleptic-naïve patients. *Lancet* 349, 1730–1734. doi: 10.1016/s0140-6736(96)08258-x

Andreone, B. J., Lacoste, B., and Gu, C. (2015). Neuronal and vascular interactions. *Annu. Rev. Neurosci.* 38, 25–46. doi: 10.1146/annurev-neuro-071714-033835

Antony, P. M., Diederich, N. J., Kruger, R., and Balling, R. (2013). The hallmarks of Parkinson's disease. *FEBS J.* 280, 5981–5993. doi: 10.1111/febs.12335

Attems, J., and Jellinger, K. A. (2004). Only cerebral capillary amyloid angiopathy correlates with Alzheimer pathology–a pilot study. *Acta Neuropathol.* 107, 83–90. doi: 10.1007/s00401-003-0796-9

Attwell, D., Buchan, A. M., Charpak, S., Lauritzen, M., Macvicar, B. A., and Newman, E. A. (2010). Glial and neuronal control of brain blood flow. *Nature* 468, 232–243. doi: 10.1038/nature09613

Attwell, D., Mishra, A., Hall, C. N., O'Farrell, F. M., and Dalkara, T. (2016). What is a pericyte? *J. Cereb. Blood Flow Metab.* 36, 451–455. doi: 10.1177/0271678X15610340

Attwell, D. A., and Laughlin, S. (2001). An energy budget for signaling in the grey matter of the brain. *J. Cereb. Blood Flow Metab.* 21, 1133–1145.

Aucoin, J. S., Jiang, P., Aznavour, N., Tong, X. K., Buttini, M., Descarries, L., et al. (2005). Selective cholinergic denervation, independent from oxidative stress, in a mouse model of Alzheimer's disease. *Neuroscience* 132, 73–86. doi: 10.1016/j.neuroscience.2004.11.047

Azmitia, E. C., Saccomano, Z. T., Alzoobaee, M. F., Boldrini, M., and Whitaker-Azmitia, P. M. (2016). Persistent angiogenesis in the autism brain: an immunocytochemical study of postmortem cortex, brainstem and cerebellum. *J. Autism Dev. Disord.* 46, 1307–1318. doi: 10.1007/s10803-015-2672-6

Ball, N., Teo, W. P., Chandra, S., and Chapman, J. (2019). Parkinson's disease and the environment. *Front. Neurol.* 10:218. doi: 10.3389/fneur.2019.00218

Ballard, C., Mobley, W., Hardy, J., Williams, G., and Corbett, A. (2016). Dementia in Down's syndrome. *Lancet Neurol.* 15, 622–636. doi: 10.1016/s1474-4422(16)00063-6

Banks, W. A., Reed, M. J., Logsdon, A. F., Rhea, E. M., and Erickson, M. A. (2021). Healthy aging and the blood-brain barrier. *Nat. Aging* 1, 243–254. doi: 10.1038/s43587-021-00043-5

Bano, D., Zanetti, F., Mende, Y., and Nicotera, P. (2011). Neurodegenerative processes in Huntington's disease [Review]. *Cell Death Dis.* 2:e228. doi: 10.1038/cddis.2011.112

Barcia, C., Bautista, V., Sanchez-Bahillo, A., Fernandez-Villalba, E., Faucheux, B., Poza y Poza, M., et al. (2005). Changes in vascularization in substantia nigra pars compacta of monkeys rendered parkinsonian. *J Neural Transm. (Vienna)* 112, 1237–1248. doi: 10.1007/s00702-004-0256-2

Beckman, J. S., Beckman, T. W., Chen, J., Marshall, P. A., and Freeman, B. A. (1990). Apparent hydroxyl radical production by peroxynitrite: implications for endothelial injury from nitric oxide and superoxide. *Proc. Natl. Acad. Sci. U.S.A.* 87, 1620–1624. doi: 10.1073/pnas.87.4.1620

Bell, R. D., Winkler, E. A., Sagare, A. P., Singh, I., LaRue, B., Deane, R., et al. (2010). Pericytes control key neurovascular functions and neuronal phenotype in the adult brain and during brain aging. *Neuron* 68, 409–427. doi: 10.1016/j.neuron.2010.09.043

Bell, R. D., and Zlokovic, B. V. (2009). Neurovascular mechanisms and blood-brain barrier disorder in Alzheimer's disease. *Acta Neuropathol.* 118, 103–113. doi: 10.1007/s00401-009-0522-3

Benedictus, M. R., Leeuwis, A. E., Binnewijzend, M. A., Kuijer, J. P., Scheltens, P., Barkhof, F., et al. (2017). Lower cerebral blood flow is associated with faster cognitive decline in Alzheimer's disease. *Eur. Radiol.* 27, 1169–1175. doi: 10.1007/s00330-016-4450-z

Benmoyal-Segal, L., and Soreq, H. (2006). Gene-environment interactions in sporadic Parkinson's disease. *J. Neurochem.* 97, 1740–1755. doi: 10.1111/j.1471-4159.2006.03937.x

Bennett, J., Basivireddy, J., Kollar, A., Biron, K. E., Reickmann, P., Jefferies, W. A., et al. (2010). Blood-brain barrier disruption and enhanced vascular permeability in the multiple sclerosis model EAE. *J. Neuroimmunol.* 229, 180–191. doi: 10.1016/j.jneuroim.2010.08.011

Bester, M., Forkert, N. D., Stellmann, J. P., Sturner, K., Aly, L., Drabik, A., et al. (2015). Increased perfusion in normal appearing white matter in high inflammatory multiple sclerosis patients. *PLoS One* 10:e0119356. doi: 10.1371/journal.pone.0119356

Biju, K. C., Shen, Q., Hernandez, E. T., Mader, M. J., and Clark, R. A. (2020). Reduced cerebral blood flow in an alpha-synuclein transgenic mouse model of Parkinson's disease. *J. Cereb. Blood Flow Metab.* 40, 2441–2453. doi: 10.1177/0271678X19895432

Biswas, S., Cottarelli, A., and Agalliu, D. (2020). Neuronal and glial regulation of CNS angiogenesis and barriergenesis. *Development* 147:dev182279. doi: 10.1242/dev.182279

Bjørklund, G., Kern, J. K., Urbina, M. A., Saad, K., El-Houfey, A. A., Geier, D. A., et al. (2018). Cerebral hypoperfusion in autism spectrum disorder. *Acta Neurobiol. Exp.* 78, 21–29. doi: 10.21307/ane-2018-005

Blair, L. J., Frauen, H. D., Zhang, B., Nordhues, B. A., Bijan, S., Lin, Y. C., et al. (2015). Tau depletion prevents progressive blood-brain barrier damage in a mouse model of tauopathy. *Acta Neuropathol. Commun.* 3:8. doi: 10.1186/s40478-015-0186-2

Bogale, T. A., Faustini, G., Longhena, F., Mitola, S., Pizzi, M., and Bellucci, A. (2021). Alpha-Synuclein in the regulation of brain endothelial and perivascular cells: gaps and future perspectives. *Front. Immunol.* 12:611761. doi: 10.3389/fimmu.2021.611761

Bracko, O., Njiru, B. N., Swallow, M., Ali, M., Haft-Javaherian, M., and Schaffer, C. B. (2020). Increasing cerebral blood flow improves cognition into late stages in Alzheimer's disease mice. *J. Cereb. Blood Flow Metab.* 40, 1441–1452. doi: 10.1177/0271678X19873658

Bressi, S., Volontè, M. A., Alberoni, M., Canal, N., and Franceschi, M. (1992). Transcranial doppler sonography in the early phase of Alzheimer's disease. *Dement. Geriatr. Cogn. Disord.* 3, 25–31. doi: 10.1159/000106990

Brett, B. L., Gardner, R. C., Godbout, J., Dams-O'Connor, K., and Keene, C. D. (2021). Traumatic brain injury and risk of neurodegenerative disorder. *Biol. Psychiatry* (in press). doi: 10.1016/j.biopsych.2021.05.025

Buee, L., Hof, P. R., Bouras, C., Delacourte, A., Perl, D. P., Morrison, J. H., et al. (1994).). Pathological alterations of the cerebral microvasculature in Alzheimer's disease and related dementing disorders [Research Support, Non-U.S. Gov't Research Support, U.S. Gov't, P.H.S.]. *Acta Neuropathol.* 87, 469–480.

Burghardt, K., Grove, T., and Ellingrod, V. (2014). Endothelial nitric oxide synthetase genetic variants, metabolic syndrome and endothelial function in schizophrenia. *J. Psychopharmacol.* 28, 349–356. doi: 10.1177/0269881113516200

Burroni, L., Orsi, A., Monti, L., Hayek, Y., Rocchi, R., and Vattimo, A. (2008). Regional cerebral blood flow in childhood autism: a SPET study with SPM evaluation. *Nucl. Med. Commun.* 29, 150–156. doi: 10.1097/MNM.0b013e3282f1bb8e

Cai, H. Q., Catts, V. S., Webster, M. J., Galletly, C., Liu, D., O'Donnell, M., et al. (2020). Increased macrophages and changed brain endothelial cell gene expression in the frontal cortex of people with schizophrenia displaying inflammation. *Mol. Psychiatry* 25, 761–775. doi: 10.1038/s41380-018-0235-x

Carmeliet, P., and Jain, R. K. (2011). Molecular mechanisms and clinical applications of angiogenesis. *Nat. Review* 473, 298–307. doi: 10.1038/nature10144REVIEWDLL4

Carrano, A., Hoozemans, J., van der Vies, S., Rozemuller, A., van Horssen, J., and de Vries, H. E. (2011). Amyloid beta induces oxidative stress-mediated blood–brain barrier changes in capillary amyloid angiopathy. *Antioxid. Redox Signal.* 15, 1167–1178. doi: 10.1089/ars.2011.3895

Carrier, M., Guilbert, J., Levesque, J. P., Tremblay, M. E., and Desjardins, M. (2020). Structural and functional features of developing brain capillaries, and their alteration in schizophrenia. *Front. Cell. Neurosci.* 14:595002. doi: 10.3389/fncel.2020.595002

Carter, C. S., MacDonald, A. W., Ross, L. L., and Stenger, V. A. (2001). Anterior cingulate cortex activity and impaired self-monitoring of performance in patients with schizophrenia: an event-related fMRI study. *Am. J. Psychiatry* 158, 1423–1428. doi: 10.1176/appi.ajp.158.9.1423

Casas, B. S., Vitoria, G., do Costa, M. N., Madeiro da Costa, R., Trindade, P., Maciel, R., et al. (2018). hiPSC-derived neural stem cells from patients with schizophrenia induce an impaired angiogenesis. *Transl. Psychiatry* 8:48. doi: 10.1038/s41398-018-0095-9

Casserly, I., and Topol, E. (2004). Convergence of atherosclerosis and Alzheimer's disease: inflammation, cholesterol, and misfolded proteins [Review]. *Lancet* 363, 1139–1146. doi: 10.1016/S0140-6736(04)15900-X

Cauli, B., and Hamel, E. (2010). Revisiting the role of neurons in neurovascular coupling. *Front. Neuroenergetics* 2:9. doi: 10.3389/fnene.2010.00009

Chao, Y.-X., He, B.-P., and Wah Tay, S. S. (2009). Mesenchymal stem cell transplantation attenuates blood brain barrier damage and neuroinflammation and protects dopaminergic neurons against MPTP toxicity in the substantia nigra in a model of Parkinson's disease. *J. Neuroimmunol.* 216, 39–50. doi: 10.1016/j.jneuroim.2009.09.003

Chiron, C., Leboyer, M., Leon, F., Jambaque, L., Nuttin, C., and Syrota, A. (1995). SPECT of the Brain in childhood autism: evidence for a lack of normal hemispheric asymmetry. *Dev. Med. Child Neurol.* 37, 849–860. doi: 10.1111/j.1469-8749.1995.tb11938.x

Chiu, C., Miller, M. C., Monahan, R., Osgood, D. P., Stopa, E. G., and Silverberg, G. D. (2015). P-glycoprotein expression and amyloid accumulation in human aging and Alzheimer's disease: preliminary observations. *Neurobiol. Aging* 36, 2475–2482. doi: 10.1016/j.neurobiolaging.2015.05.020

Chow, B. W., and Gu, C. (2015). The molecular constituents of the blood-brain barrier. *Trends Neurosci.* 38, 598–608. doi: 10.1016/j.tins.2015.08.003

Clancy, U., Gilmartin, D., Jochems, A. C. C., Knox, L., Doubal, F. N., and Wardlaw, J. M. (2021). Neuropsychiatric symptoms associated with cerebral small vessel disease: a systematic review and meta-analysis. *Lancet Psychiatry* 8, 225–236. doi: 10.1016/S2215-0366(20)30431-4

Clifton, N. E., Hannon, E., Harwood, J. C., Di Florio, A., Thomas, K. L., Holmans, P. A., et al. (2019). Dynamic expression of genes associated with schizophrenia and bipolar disorder across development. *Transl. Psychiatry* 9:74. doi: 10.1038/s41398-019-0405-x

Coelho-Santos, V., and Shih, A. Y. (2020). Postnatal development of cerebrovascular structure and the neurogliovascular unit. *Wiley Interdiscip. Rev. Dev. Biol.* 9:e363. doi: 10.1002/wdev.363

Connolly, A. M., Chez, M. G., Pestronk, A., Arnold, S. T., Mehta, S., and Deuel, R. K. (1999). Serum autoantibodies to brain in Landau-Kleffner variant, autism, and other neurologic disorders. *J. Pediatr.* 134, 607–613. doi: 10.1016/s0022-3476(99)70248-9

Cortes-Canteli, M., Kruyer, A., Fernandez-Nueda, I., Marcos-Diaz, A., Ceron, C., Richards, A. T., et al. (2019). Long-Term dabigatran treatment delays Alzheimer's disease pathogenesis in the tgcrnd8 mouse model. *J. Am. Coll. Cardiol.* 74, 1910–1923. doi: 10.1016/j.jacc.2019.07.081

Cramer, S. P., Simonsen, H., Frederiksen, J. L., Rostrup, E., and Larsson, H. B. (2014). Abnormal blood-brain barrier permeability in normal appearing white matter in multiple sclerosis investigated by MRI. *Neuroimage Clin.* 4, 182–189. doi: 10.1016/j.nicl.2013.12.001

Crockett, A. M., Ryan, S. K., Vasquez, A. H., Canning, C., Kanyuch, N., Kebir, H., et al. (2021). Disruption of the blood-brain barrier in 22q11.2 deletion syndrome. *Brain* 144, 1351–1360. doi: 10.1093/brain/awab055

Cruz Hernandez, J. C., Bracko, O., Kersbergen, C. J., Muse, V., Haft-Javaherian, M., Berg, M., et al. (2019). Neutrophil adhesion in brain capillaries reduces cortical blood flow and impairs memory function in Alzheimer's disease mouse models. *Nat. Neurosci.* 22, 413–420. doi: 10.1038/s41593-018-0329-4

Császár, E., Lénárt, N., Cserép, C., Környei, Z., Fekete, R., Pósfai, B., et al. (2021). Microglia control cerebral blood flow and neurovascular coupling via P2Y12R-mediated actions. *bioRXiv* [Preprint] doi: 10.1101/2021.02.04.429741

Cvetanovic, M., Patel, J. M., Marti, H. H., Kini, A. R., and Opal, P. (2011). Vascular endothelial growth factor ameliorates the ataxic phenotype in a mouse model of spinocerebellar ataxia type 1 [Research Support, N.I.H., Extramural Research Support, Non-U.S. Gov't]. *Nat. Med.* 17, 1445–1447. doi: 10.1038/nm.2494

Czako, C., Kovacs, T., Ungvari, Z., Csiszar, A., Yabluchanskiy, A., Conley, S., et al. (2020). Retinal biomarkers for Alzheimer's disease and vascular cognitive impairment and dementia (VCID): implication for early diagnosis and prognosis. *Geroscience* 42, 1499–1525. doi: 10.1007/s11357-020-00252-7

D'Haeseleer, M., Beelen, R., Fierens, Y., Cambron, M., Vanbinst, A. M., Verborgh, C., et al. (2013). Cerebral hypoperfusion in multiple sclerosis is reversible and mediated by endothelin-1. *Proc. Natl. Acad. Sci. U.S.A.* 110, 5654–5658. doi: 10.1073/pnas.1222560110

D'Haeseleer, M., Cambron, M., Vanopdenbosch, L., and De Keyser, J. (2011). Vascular aspects of multiple sclerosis. *Lancet Neurol.* 10, 657–666. doi: 10.1016/s1474-4422(11)70105-3

Dabertrand, F., Harraz, O. F., Masayo, K., Longden, T. A., Rosehart, A. C., Hill-Eubanks, D., et al. (2021). PIP 2 corrects cerebral blood flow deficits in small vessel disease by rescuing capillary Kir2.1 activity. *Proc. Natl. Acad. Sci. U.S.A.* 118:e2025998118. doi: 10.1073/pnas.2025998118

Daneman, R. (2012). The blood–brain barrier in health and disease. *Ann. Neurol.* 72, 648–672. doi: 10.1002/ana.23648

Daneman, R., Agalliu, D., Zhou, L., Kuhnert, F., Kuo, C., and Barres, B. (2009). Wnt/ -catenin signaling is required for CNS, but not non-CNS, angiogenesis. *Proc. Natl. Acad. Sci. U.S.A.* 106, 641–646.

Daneman, R., and Prat, A. (2015). The blood-brain barrier. *Cold Spring Harb. Perspect. Biol.* 7:a020412. doi: 10.1101/cshperspect.a020412

Davenport, C. B. (1915). Huntington's Chorea in relation to heredity and eugenics. *Proc. Natl. Acad. Sci. U.S.A.* 1, 283–285.

Davis, J., Xu, F., Deane, R., Romanov, G., Previti, M. L., Zeigler, K., et al. (2004). Early-onset and robust cerebral microvascular accumulation of amyloid beta-protein in transgenic mice expressing low levels of a vasculotropic Dutch/Iowa mutant form of amyloid beta-protein precursor. *J. Biol. Chem.* 279, 20296–20306. doi: 10.1074/jbc.M312946200

De Filippis, L., and Delia, D. (2011). Hypoxia in the regulation of neural stem cells. *Cell. Mol. Life Sci.* 68, 2831–2844. doi: 10.1007/s00018-011-0723-5

De Keyser, J., Wilczak, N., Leta, R., and Streetland, C. (1999). Astrocytes in multiple sclerosis lack beta-2 adrenergic receptors. *Neurology* 53, 1628–1633. doi: 10.1212/WNL.53.8.1628

De Silva, T. M., and Faraci, F. M. (2016). Microvascular dysfunction and cognitive impairment. *Cell. Mol. Neurobiol.* 36, 241–258. doi: 10.1007/s10571-015-0308-1

Deane, R., Wu, Z., Sagare, A., Davis, J., Du Yan, S., Hamm, K., et al. (2004). LRP/amyloid beta-peptide interaction mediates differential brain efflux of Abeta isoforms. *Neuron* 43, 333–344. doi: 10.1016/j.neuron.2004.07.017

Deckel, A. W., and Duffy, J. D. (2000). Vasomotor hyporeactivity in the anterior cerebral artery during motor activation in Huntington's disease patients. *Brain Res.* 872, 258–261. doi: 10.1016/S0006-8993(00)02506-3

Deckel, A. W., Weiner, R., Szigeti, D., Claark, V., and Vento, J. (2000). Altered patterns of regional cerebral blood flow in patients with Huntington's disease: a SPECT study during rest and cognitive or motor activation. *J. Nucl. Med.* 41, 773–780.

Delgado, A. C., Ferron, S. R., Vicente, D., Porlan, E., Perez-Villalba, A., Trujillo, C. M., et al. (2014). Endothelial NT-3 delivered by vasculature and CSF promotes quiescence of subependymal neural stem cells through nitric oxide induction. *Neuron* 83, 572–585. doi: 10.1016/j.neuron.2014.06.015

Derejko, M., Sławek, J., Wieczorek, D., Brockhuis, B., Dubaniewicz, M., and Lass, P. (2006). Regional cerebral blood flow in Parkinson's disease as an indicator of cognitive impairment. *Nucl. Med. Commun.* 27, 945–951. doi: 10.1097/01.mnm.0000243370.18883.62

Di Pardo, A., Amico, E., Scalabri, F., Pepe, G., Castaldo, S., Elifani, F., et al. (2017). Impairment of blood-brain barrier is an early event in R6/2 mouse model of Huntington Disease. *Sci. Rep.* 7:41316. doi: 10.1038/srep41316

Dietrich, H. H., Xiang, C., Han, B. H., Zipfel, G. J., and Holtzman, D. M. (2010). Soluble amyloid-beta, effect on cerebral arteriolar regulation and vascular cells. *Mol. Neurodegener.* 5:15. doi: 10.1186/1750-1326-5-15

Dobson, R., and Giovannoni, G. (2019). Multiple sclerosis – a review. *Eur. J. Neurol.* 26, 27–40. doi: 10.1111/ene.13819

Donahue, J. E., Flaherty, S. L., Johanson, C. E., Duncan, J. A. III, Silverberg, G. D., Miller, M. C., et al. (2006). RAGE, LRP-1, and amyloid-beta protein in Alzheimer's disease. *Acta Neuropathol.* 112, 405–415. doi: 10.1007/s00401-006-0115-3

Drazanova, E., Ruda-Kucerova, J., Kratka, L., Stark, T., Kuchar, M., Maryska, M., et al. (2019). Different effects of prenatal MAM vs. perinatal THC exposure on regional cerebral blood perfusion detected by Arterial Spin Labelling MRI in rats. *Sci. Rep.* 9:6062. doi: 10.1038/s41598-019-42532-z

Drouin-Ouellet, J., Sawiak, S. J., Cisbani, G., Lagace, M., Kuan, W. L., Saint-Pierre, M., et al. (2015). Cerebrovascular and blood-brain barrier impairments in Huntington's disease: potential implications for its pathophysiology. *Ann. Neurol.* 78, 160–177. doi: 10.1002/ana.24406

Dudek, K. A., Dion-Albert, L., Lebel, M., LeClair, K., Labrecque, S., Tuck, E., et al. (2020). Molecular adaptations of the blood-brain barrier promote stress resilience vs. depression. *Proc. Natl. Acad. Sci. U.S.A.* 117, 3326–3336. doi: 10.1073/pnas.1914655117

Dumas, A., Dierksen, G. A., Gurol, M. E., Halpin, A., Martinez-Ramirez, S., Schwab, K., et al. (2012). Functional magnetic resonance imaging detection of vascular reactivity in cerebral amyloid angiopathy. *Ann. Neurol.* 72, 76–81. doi: 10.1002/ana.23566

Elabi, O., Gaceb, A., Carlsson, R., Padel, T., Soylu-Kucharz, R., Cortijo, I., et al. (2021). Human alpha-synuclein overexpression in a mouse model of Parkinson's disease leads to vascular pathology, blood brain barrier leakage and pericyte activation. *Sci. Rep.* 11:1120. doi: 10.1038/s41598-020-80889-8

Ellingrod, V. L., Taylor, S. F., Brook, R. D., Evans, S. J., Zollner, S. K., Grove, T. B., et al. (2011). Dietary, lifestyle and pharmacogenetic factors associated with arteriole endothelial-dependent vasodilatation in schizophrenia patients treated with atypical antipsychotics (AAPs). *Schizophr. Res.* 130, 20–26. doi: 10.1016/j.schres.2011.03.031

Emerich, D. F., Mooney, D. J., Storrie, H., Babu, R. S., and Kordower, J. H. (2010). Injectable hydrogels providing sustained delivery of vascular endothelial growth factor are neuroprotective in a rat model of Huntington's disease. *Neurotox. Res.* 17, 66–74. doi: 10.1007/s12640-009-9079-0

Emerson, R. W., Adams, C., Nishino, T., Hazlett, H. C., Wolff, J. J., Zwaigenbaum, L., et al. (2017). Functional neuroimaging of high-risk 6-month-old infants predicts a diagnosis of autism at 24 months of age. *Sci. Transl. Med.* 9:eaag2882. doi: 10.1126/scitranslmed.aag2882

Farkas, E., De Jong, G. I., de Vos Ernst, R. A. I., Steur, J. N. H., and Luiten, P. G. M. (2000). Pathological features of cerebral cortical capillaries are doubled in Alzheimer's disease and Parkinson's disease. *Acta Neuropathol.* 100, 395–402. doi: 10.1007/s004010000195

Farkas, E., and Luiten, P. G. (2001). Cerebral microvascular pathology in aging and Alzheimer's disease [Review]. *Prog. Neurobiol.* 64, 575–611.

Faucheux, B. A., Agid, Y., Hirsch, E. C., and Bonnet, A.-M. (1999). Blood vessels change in the mesencephalon of patients with Parkinson's disease. *Lancet* 353, 981–982. doi: 10.1016/s0140-6736(99)00641-8

Feigin, A., Ghilardi, M. F., Huang, C., Ma, Y., Carbon, M., Guttman, M., et al. (2006). Preclinical Huntington's disease: compensatory brain responses during learning. *Ann. Neurol.* 59, 53–59. doi: 10.1002/ana.20684

Fernandez-Klett, F., and Priller, J. (2015). Diverse functions of pericytes in cerebral blood flow regulation and ischemia. *J. Cereb. Blood Flow Metab.* 35, 883–887. doi: 10.1038/jcbfm.2015.60

Fernandez-Seara, M. A., Mengual, E., Vidorreta, M., Aznarez-Sanado, M., Loayza, F. R., Villagra, F., et al. (2012). Cortical hypoperfusion in Parkinson's disease assessed using arterial spin labeled perfusion MRI. *Neuroimage* 59, 2743–2750. doi: 10.1016/j.neuroimage.2011.10.033

Filosa, J. A., and Iddings, J. A. (2013). Astrocyte regulation of cerebral vascular tone. *Am. J. Physiol. Heart Circ. Physiol.* 305, H609–H619. doi: 10.1152/ajpheart.00359.2013

Finnerty, N. J., Bolger, F. B., Palsson, E., and Lowry, J. P. (2013). An investigation of hypofrontality in an animal model of schizophrenia using real-time microelectrochemical sensors for glucose, oxygen, and nitric oxide. *ACS Chem. Neurosci.* 4, 825–831. doi: 10.1021/cn4000567

Fiorentino, M., Sapone, A., Senger, S., Camhi, S. S., Kadzielski, S. M., Buie, T. M., et al. (2016). Blood-brain barrier and intestinal epithelial barrier alterations in autism spectrum disorders. *Mol. Autism* 7:49. doi: 10.1186/s13229-016-0110-z

Ford, J. M., Johnson, M. B., Whitfield, S. L., Faustman, W. O., and Mathalon, D. H. (2005). Delayed hemodynamic responses in schizophrenia. *Neuroimage* 26, 922–931. doi: 10.1016/j.neuroimage.2005.03.001

Ford, J. M., Roth, W. T., Menon, V., and Pfefferbaum, A. (1999). Failures of automatic and strategic processing in schizophrenia: comparisons of event-related brain potential and startle blink modification. *Schizophr. Res.* 37, 149–163. doi: 10.1016/s0920-9964(98)00148-0

Friedland, R. P., and Iadecola, C. (1991). Roy and Sherrington (1890): a centennial reexamination of "On the regulation of the blood-supply of the brain". *Neurology* 41, 10–14. doi: 10.1212/wnl.41.1.10

Frosen, J., and Joutel, A. (2018). Smooth muscle cells of intracranial vessels: from development to disease. *Cardiovasc. Res.* 114, 501–512. doi: 10.1093/cvr/cvy002

Fujiki, R., Morita, K., Sato, M., Kamada, Y., Kato, Y., Inoue, M., et al. (2013). Reduced prefrontal cortex activation using the Trail Making Test in schizophrenia. *Neuropsychiatr. Dis. Treat.* 9, 675–685. doi: 10.2147/NDT.S43137

Ge, Y., Law, M., Johnson, G., Herbert, J., Babb, J. S., Mannon, L. J., et al. (2005). Dynamic susceptibility contrast perfusion MR imaging of multiple sclerosis lesions: characterizing hemodynamic impairment and inflammatory activity. *AJNR Am. J. Neuroradiol.* 26, 1539–1547.

Geraldes, R., Esiri, M. M., Perera, R., Yee, S. A., Jenkins, D., Palace, J., et al. (2020). Vascular disease and multiple sclerosis: a post-mortem study exploring their relationships. *Brain* 143, 2998–3012. doi: 10.1093/brain/awaa255

Gireud-Goss, M., Mack, A. F., McCullough, L. D., and Urayama, A. (2020). Cerebral amyloid angiopathy and blood-brain barrier dysfunction. *Neuroscientist* doi: 10.1177/1073858420954811 [Epub ahead of print].

Girolamo, F., Coppola, C., Ribatti, D., and Trojano, M. (2014). Angiogenesis in multiple sclerosis and experimental autoimmune encephalomyelitis. *Acta Neuropathol. Commun.* 2:84. doi: 10.1186/s40478-014-0084-z

Girouard, H., and Iadecola, C. (2006). Neurovascular coupling in the normal brain and in hypertension, stroke, and Alzheimer disease. *J. Appl. Physiol. (1985)* 100, 328–335. doi: 10.1152/japplphysiol.00966.2005

Gitler, A. D., Dhillon, P., and Shorter, J. (2017). Neurodegenerative disease: models, mechanisms, and a new hope. *Dis. Model. Mech.* 10, 499–502. doi: 10.1242/dmm.030205

Gogtay, N., Vyas, N. S., Testa, R., Wood, S. J., and Pantelis, C. (2011). Age of onset of schizophrenia: perspectives from structural neuroimaging studies. *Schizophr. Bull.* 37, 504–513. doi: 10.1093/schbul/sbr030

Goldman, S. A., and Chen, Z. (2011). Perivascular instruction of cell genesis and fate in the adult brain. *Nat. Neurosci.* 14, 1382–1389. doi: 10.1038/nn.2963

Gorelick, P. B. (2004). Risk factors for vascular dementia and Alzheimer disease. *Stroke* 35(11 Suppl. 1), 2620–2622.

Gotz, J., and Ittner, L. M. (2008). Animal models of Alzheimer's disease and frontotemporal dementia. *Nat. Rev. Neurosci.* 9, 532–544.

Graham, N. S., and Sharp, D. J. (2019). Understanding neurodegeneration after traumatic brain injury: from mechanisms to clinical trials in dementia. *J. Neurol. Neurosurg. Psychiatry* 90, 1221–1233. doi: 10.1136/jnnp-2017-317557

Grammas, P. (2011). Neurovascular dysfunction, inflammation and endothelial activation: implications for the pathogenesis of Alzheimer's disease. *J. Neuroinflammation* 8:26. doi: 10.1186/1742-2094-8-26

Grant, R. I., Hartmann, D. A., Underly, R. G., Berthiaume, A. A., Bhat, N. R., and Shih, A. Y. (2019). Organizational hierarchy and structural diversity of microvascular pericytes in adult mouse cortex. *J. Cereb. Blood Flow Metab.* 39, 411–425. doi: 10.1177/0271678X17732229

Gray, M. T., and Woulfe, J. M. (2015). Striatal blood-brain barrier permeability in Parkinson's disease. *J. Cereb. Blood Flow Metab.* 35, 747–750. doi: 10.1038/jcbfm.2015.32

Greene, C., Kealy, J., Humphries, M. M., Gong, Y., Hou, J., Hudson, N., et al. (2018). Dose-dependent expression of claudin-5 is a modifying factor in schizophrenia. *Mol. Psychiatry* 23, 2156–2166. doi: 10.1038/mp.2017.156

Grove, T., Taylor, S., Dalack, G., and Ellingrod, V. (2015). Endothelial function, folate pharmacogenomics, and neurocognition in psychotic disorders. *Schizophr. Res.* 164, 115–121. doi: 10.1016/j.schres.2015.02.006

Grubb, S., Lauritzen, M., and Aalkjaer, C. (2021). Brain capillary pericytes and neurovascular coupling. *Comp. Biochem. Physiol. A Mol. Integr. Physiol.* 254:110893. doi: 10.1016/j.cbpa.2020.110893

Grunewald, M., Kumar, S., Sharife, H., Volinsky, E., Gileles-Hillel, A., Licht, T., et al. (2021). Counteracting age-related VEGF signaling insufficiency promotes healthy aging and extends life span. *Science* 373:eabc8479. doi: 10.1126/science.abc8479

Gu, C., Yoshida, Y., Livet, J., Reimert, D., Mann, F., Merte, J., et al. (2005). Semaphorin 3E and Plexin-D1 control vascular pattern independently of neuropilins. *Science* 307, 265–268. doi: 10.1126/science.1105416

Guan, J., Pavlovic, D., Dalkie, N., Waldvogel, H., O'Carroll, S. J., Green, C. R., et al. (2013). Vascular degeneration in Parkinson's disease. *Brain Pathol.* 23, 154–164. doi: 10.1111/j.1750-3639.2012.00628.x

Guo, Y., Li, X., Zhang, M., Chen, N., Wu, S., Lei, J., et al. (2019). Age and brain regionassociated alterations of cerebral blood flow in early Alzheimer's disease assessed in AbetaPPSWE/PS1DeltaE9 transgenic mice using arterial spin labeling. *Mol. Med. Rep.* 19, 3045–3052. doi: 10.3892/mmr.2019.9950

Guo, Y., Singh, L. N., Zhu, Y., Gur, R. E., Resnick, A., Anderson, S. A., et al. (2020). Association of a functional Claudin-5 variant with schizophrenia in female patients with the 22q11.2 deletion syndrome. *Schizophr. Res.* 215, 451–452. doi: 10.1016/j.schres.2019.09.014

Gur, R. E., Bassett, A. S., McDonald-McGinn, D. M., Bearden, C. E., Chow, E., Emanuel, B. S., et al. (2017). A neurogenetic model for the study of schizophrenia spectrum disorders: the International 22q11.2 Deletion Syndrome Brain Behavior Consortium. *Mol. Psychiatry* 22, 1664–1672. doi: 10.1038/mp.2017.161

Ha, A. D., and Fung, V. S. (2012). Huntington's disease. *Curr. Opin. Neurol.* 25, 491–498. doi: 10.1097/WCO.0b013e3283550c97

Haidey, J. N., Peringod, G., Institoris, A., Gorzo, K. A., Nicola, W., Vandal, M., et al. (2021). Astrocytes regulate ultra-slow arteriole oscillations via stretch-mediated TRPV4-COX-1 feedback. *Cell Rep.* 36:109405. doi: 10.1016/j.celrep.2021.109405

Hakim, A. M. (2019). Small vessel disease. *Front. Neurol.* 10:1020. doi: 10.3389/fneur.2019.01020

Halliday, M. R., Rege, S. V., Ma, Q., Zhao, Z., Miller, C. A., Winkler, E. A., et al. (2016). Accelerated pericyte degeneration and blood-brain barrier breakdown in apolipoprotein E4 carriers with Alzheimer's disease. *J. Cereb. Blood Flow Metab.* 36, 216–227. doi: 10.1038/jcbfm.2015.44

Hamel, E. (2006). Perivascular nerves and the regulation of cerebrovascular tone. *J. Appl. Physiol.* 100, 1059–1064. doi: 10.1152/japplphysiol.00954.2005

Hamel, E. (2015). Cerebral circulation function and dysfunction in Alzheimer's disease. *J. Cardiovasc. Pharmacol.* 65, 317–324. doi: 10.1097/FJC.0000000000000177

Hanlon, F. M., Shaff, N. A., Dodd, A. B., Ling, J. M., Bustillo, J. R., Abbott, C. C., et al. (2016). Hemodynamic response function abnormalities in schizophrenia during a multisensory detection task. *Hum. Brain Mapp.* 37, 745–755. doi: 10.1002/hbm.23063

Harada, K., Kamiya, T., and Tsuboi, T. (2015). Gliotransmitter release from astrocytes: functional, developmental, and pathological implications in the brain. *Front. Neurosci.* 9:499. doi: 10.3389/fnins.2015.00499

Harbo, H. F., Gold, R., and Tintore, M. (2013). Sex and gender issues in multiple sclerosis. *Ther. Adv. Neurol. Disord.* 6, 237–248. doi: 10.1177/1756285613488434

Harris, G. J., Codoris, A. M., Lewis, R. F., Schmidt, E., Bedi, A., and Brandt, J. (1999). Reduced basal ganglia blood flow and volume in pre-sympotmatic, gene-tested persons at-risk for Huntington's disease. *Brain* 122, 1667–1678. doi: 10.1093/brain/122.9.1667

Hartmann, D. A., Berthiaume, A. A., Grant, R. I., Harrill, S. A., Koski, T., Tieu, T., et al. (2021). Brain capillary pericytes exert a substantial but slow influence on blood flow. *Nat. Neurosci.* 24, 633–645. doi: 10.1038/s41593-020-00793-2

Hartz, A. M., Bauer, B., Soldner, E. L., Wolf, A., Boy, S., Backhaus, R., et al. (2012). Amyloid-beta contributes to blood-brain barrier leakage in transgenic human amyloid precursor protein mice and in humans with cerebral amyloid angiopathy. *Stroke* 43, 514–523. doi: 10.1161/STROKEAHA.111.627562

Hasselbalch, S. G., Øberg, G., Sørensen, S. A., Andersen, A. R., Waldemar, G., Schmidt, J. F., et al. (1992). Reduced regional cerebral blood flow in Huntington's disease studied by SPECT. *J. Neurol. Neurosurg. Psychiatry* 55, 1018–1023. doi: 10.1136/jnnp.55.11.1018

Hays, C. C., Zlatar, Z. Z., and Wierenga, C. E. (2016). The utility of cerebral blood flow as a biomarker of preclinical Alzheimer's disease. *Cell. Mol. Neurobiol.* 36, 167–179. doi: 10.1007/s10571-015-0261-z

Hijaz, B. A., and Volpicelli-Daley, L. A. (2020). Initiation and propagation of alpha-synuclein aggregation in the nervous system. *Mol. Neurodegener.* 15:19. doi: 10.1186/s13024-020-00368-6

Hillman, E. M. (2014). Coupling mechanism and significance of the BOLD signal: a status report. *Annu. Rev. Neurosci.* 37, 161–181. doi: 10.1146/annurev-neuro-071013-014111

Hindle, J. V. (2010). Ageing, neurodegeneration and Parkinson's disease. *Age Ageing* 39, 156–161. doi: 10.1093/ageing/afp223

Hino, M., Kunii, Y., Matsumoto, J., Wada, A., Nagaoka, A., Niwa, S., et al. (2016). Decreased VEGFR2 expression and increased phosphorylated Akt1 in the prefrontal cortex of individuals with schizophrenia. *J. Psychiatry Res.* 82, 100–108. doi: 10.1016/j.jpsychires.2016.07.018

Hogan, K. A., Ambler, C. A., Chapman, D. L., and Bautch, V. L. (2004). The neural tube patterns vessels developmentally using the VEGF signaling pathway. *Development* 131, 1503–1513. doi: 10.1242/dev.01039

Holley, J. E., Newcombe, J., Whatmore, J. L., and Gutowski, N. J. (2010). Increased blood vessel density and endothelial cell proliferation in multiple sclerosis cerebral white matter. *Neurosci. Lett.* 470, 65–70. doi: 10.1016/j.neulet.2009.12.059

Horev, G., Ellegood, J., Lerch, J. P., Son, Y. E., Muthuswamy, L., Vogel, H., et al. (2011). Dosage-dependent phenotypes in models of 16p11.2 lesions found in autism. *Proc. Natl. Acad. Sci. U.S.A.* 108, 17076–17081. doi: 10.1073/pnas.1114042108

Horn, H., Federspiel, A., Wirth, M., Muller, T. J., Wiest, R., Wang, J. J., et al. (2009). Structural and metabolic changes in language areas linked to formal thought disorder. *Br. J. Psychiatry* 194, 130–138. doi: 10.1192/bjp.bp.107.045633

Hostenbach, S., Pauwels, A., Michiels, V., Raeymaekers, H., Van Binst, A. M., Van Merhaeghen-Wieleman, A., et al. (2019). Role of cerebral hypoperfusion in multiple sclerosis (ROCHIMS): study protocol for a proof-of-concept randomized controlled trial with bosentan. *Trials* 20:164. doi: 10.1186/s13063-019-3252-4

Howarth, C. (2014). The contribution of astrocytes to the regulation of cerebral blood flow. *Front. Neurosci.* 8:103. doi: 10.3389/fnins.2014.00103

Howarth, C., Mishra, A., and Hall, C. N. (2021). More than just summed neuronal activity: how multiple cell types shape the BOLD response. *Philos. Trans. R. Soc. Lond. B Biol. Sci.* 376:20190630. doi: 10.1098/rstb.2019.0630

Howe, M. D., McCullough, L. D., and Urayama, A. (2020). The role of basement membranes in cerebral amyloid angiopathy. *Front. Physiol.* 11:601320. doi: 10.3389/fphys.2020.601320

Hsia, A. Y., Masliah, E., McConlogue, L., Yu, G. Q., Tatsuno, G., Hu, K., et al. (1999). Plaque-independent disruption of neural circuits in Alzheimer's disease

mouse models [Research Support, Non-U.S. Gov't Research Support, U.S. Gov't, P.H.S.]. *Proc. Natl. Acad. Sci. U.S.A.* 96, 3228–3233.

Hsiao, H.-Y., Chen, Y.-C., Huang, C.-H., Chen, C.-C., Hsu, Y.-H., Chen, H.-M., et al. (2015). Aberrant astrocytes impair vascular reactivity in Huntington disease. *Ann. Neurol.* 78, 178–192. doi: 10.1002/ana.24428

Hua, J., Unschuld, P. G., Margolis, R. L., van Zijl, P. C., and Ross, C. A. (2014). Elevated arteriolar cerebral blood volume in prodromal Huntington's disease. *Mov. Disord.* 29, 396–401. doi: 10.1002/mds.25591

Huang, Z., Wong, L. W., Su, Y., Huang, X., Wang, N., Chen, H., et al. (2020). Blood-brain barrier integrity in the pathogenesis of Alzheimer's disease. *Front. Neuroendocrinol.* 59:100857. doi: 10.1016/j.yfrne.2020.100857

Hultman, K., Strickland, S., and Norris, E. H. (2013). The APOE varepsilon4/varepsilon4 genotype potentiates vascular fibrin(ogen) deposition in amyloid-laden vessels in the brains of Alzheimer's disease patients. *J. Cereb. Blood Flow Metab.* 33, 1251–1258. doi: 10.1038/jcbfm.2013.76

Humpel, C., and Marksteiner, J. (2005).). Cerebrovascular damage as a cause for Alzheimer's disease [Research Support, Non-U.S. Gov't Review]. *Curr. Neurovasc. Res.* 2, 341–347.

Huneau, C., Benali, H., and Chabriat, H. (2015). Investigating human neurovascular coupling using functional neuroimaging: a critical review of dynamic models. *Front. Neurosci.* 9:467. doi: 10.3389/fnins.2015.00467

Iadecola, C. (2004). Neurovascular regulation in the normal brain and in Alzheimer's disease. *Nat. Rev. Neurosci.* 5, 347–360. doi: 10.1038/nrn1387

Iadecola, C. (2013). The pathobiology of vascular dementia. *Neuron* 80, 844–866. doi: 10.1016/j.neuron.2013.10.008

Impellizzeri, D., Campolo, M., Bruschetta, G., Crupi, R., Cordaro, M., Paterniti, I., et al. (2016). Traumatic brain injury leads to development of Parkinson's disease related pathology in mice. *Front. Neurosci.* 10:458. doi: 10.3389/fnins.2016.00458

Incalza, M. A., D'Oria, R., Natalicchio, A., Perrini, S., Laviola, L., and Giorgino, F. (2018). Oxidative stress and reactive oxygen species in endothelial dysfunction associated with cardiovascular and metabolic diseases. *Vascul. Pharmacol.* 100, 1–19. doi: 10.1016/j.vph.2017.05.005

Iturria-Medina, Y., Sotero, R. C., Toussaint, P. J., Mateos-Perez, J. M., Evans, A. C., and Alzheimer's Disease Neuroimaging Initiative (2016). Early role of vascular dysregulation on late-onset Alzheimer's disease based on multifactorial data-driven analysis. *Nat. Commun.* 7:11934. doi: 10.1038/ncomms11934

James, J. M., Gewolb, C., and Bautch, V. L. (2009). Neurovascular development uses VEGF-A signaling to regulate blood vessel ingression into the neural tube. *Development* 136, 833–841. doi: 10.1242/dev.028845

Jann, K., Hernandez, L. M., Beck-Pancer, D., McCarron, R., Smith, R. X., Dapretto, M., et al. (2015). Altered resting perfusion and functional connectivity of default mode network in youth with autism spectrum disorder. *Brain Behav.* 5:e00358. doi: 10.1002/brb3.358

Juurlink, B. H. (2013). The evidence for hypoperfusion as a factor in multiple sclerosis lesion development. *Mult. Scler. Int.* 2013:598093. doi: 10.1155/2013/598093

Kadry, H., Noorani, B., and Cucullo, L. (2020). A blood-brain barrier overview on structure, function, impairment, and biomarkers of integrity. *Fluids Barriers CNS* 17:69. doi: 10.1186/s12987-020-00230-3

Kalaria, R. N. (1996). Cerebral vessels in ageing and Alzheimer's disease [Research Support, Non-U.S. Gov't Research Support, U.S. Gov't, P.H.S. Review]. *Pharmacol. Ther.* 72, 193–214.

Kalaria, R. N., and Harik, S. I. (1989). Reduced glucose transporter at the blood-brain barrier and in cerebral cortex in Alzheimer disease. *J. Neurochem.* 53, 1083–1088. doi: 10.1111/j.1471-4159.1989.tb07399.x

Kalinderi, K., Bostantjopoulou, S., and Fidani, L. (2016). The genetic background of Parkinson's disease: current progress and future prospects. *Acta Neurol. Scand.* 134, 314–326. doi: 10.1111/ane.12563

Kamagata, K., Motoi, Y., Hori, M., Suzuki, M., Nakanishi, A., Shimoji, K., et al. (2011). Posterior hypoperfusion in Parkinson's disease with and without dementia measured with arterial spin labeling MRI. *J. Magn. Reson. Imaging* 33, 803–807. doi: 10.1002/jmri.22515

Kamphuis, W. W., Derada Troletti, C., Reijerkerk, A., Romero, I. A., and de Vries, H. E. (2015). The blood-brain barrier in multiple sclerosis: microRNAs as key regulators. *CNS Neurol. Disord. Drug Targets* 14, 157–167. doi: 10.2174/1871527314666150116125246

Kaplan, L., Chow, B. W., and Gu, C. (2020). Neuronal regulation of the blood-brain barrier and neurovascular coupling. *Nat. Rev. Neurosci.* 21, 416–432. doi: 10.1038/s41583-020-0322-2

Kawakami, K., Wake, R., Miyaoka, T., Furuya, M., Liaury, K., and Horiguchi, J. (2014). The effects of aging on changes in regional cerebral blood flow in schizophrenia. *Neuropsychobiology* 69, 202–209. doi: 10.1159/000358840

Kawakubo, Y., Kuwabara, H., Watanabe, K., Minowa, M., Someya, T., Minowa, I., et al. (2009). Impaired prefrontal hemodynamic maturation in autism and unaffected siblings. *PLoS One* 4:e6881. doi: 10.1371/journal.pone.0006881

Kealy, J., Greene, C., and Campbell, M. (2020). Blood-brain barrier regulation in psychiatric disorders. *Neurosci. Lett.* 726:133664. doi: 10.1016/j.neulet.2018.06.033

Keefe, R. S. E., and Harvey, P. D. (2012). *Cognitive Impairment in Schizophrenia*, Vol. 213. Berlin: Springer, doi: 10.1007/978-3-642-25758-2_2

Kelleher, R. J., and Soiza, R. L. (2013). Evidence of endothelial dysfunction in the development of Alzheimer's disease: Is Alzheimer's a vascular disorder? *Am. J. Cardiovasc. Dis.* 3, 197–226.

Khandaker, G. M., Cousins, L., Deakin, J., Lennox, B. R., Yolken, R., and Jones, P. B. (2015). Inflammation and immunity in schizophrenia: implications for pathophysiology and treatment. *Lancet Psychiatry* 2, 258–270. doi: 10.1016/s2215-0366(14)00122-9

Kirk, J., Plumb, J., Mirakhur, M., and McQuaid, S. (2003). Tight junctional abnormality in multiple sclerosis white matter affects all calibres of vessel and is associated with blood–brain barrier leakage and active demyelination. *J. Pathol.* 201, 319–327. doi: 10.1002/path.1434

Kisler, K., Nelson, A. R., Montagne, A., and Zlokovic, B. V. (2017). Cerebral blood flow regulation and neurovascular dysfunction in Alzheimer disease. *Nat. Rev. Neurosci.* 18, 419–434. doi: 10.1038/nrn.2017.48

Kisler, K., Nelson, A. R., Rege, S. V., Ramanathan, A., Wang, Y., Ahuja, A., et al. (2016). Pericyte degeneration leads to neurovascular uncoupling and limits oxygen supply to brain. *Nat. Neurosci.* 20, 406–420. doi: 10.1038/nn.4489A

Klein, C., and Westenberger, A. (2012). Genetics of Parkinson's disease. *Cold Spring Harb. Perspect. Med.* 2:a008888. doi: 10.1101/cshperspect.a008888

Klinkmueller, P., Kronenbuerger, M., Miao, X., Bang, J., Ultz, K. E., Paez, A., et al. (2021). Impaired response of cerebral oxygen metabolism to visual stimulation in Huntington's disease. *J. Cereb. Blood Flow Metab.* 41, 1119–1130. doi: 10.1177/0271678X20949286

Knight, M. J., and Baune, B. T. (2017). Psychosocial dysfunction in major depressive disorder-rationale, design, and characteristics of the cognitive and emotional recovery training program for depression (CERT-D). *Front. Psychiatry* 8:280. doi: 10.3389/fpsyt.2017.00280

Kochunov, P., Zavaliangos-Petropulu, A., Jahanshad, N., Thompson, P. M., Ryan, M. C., Chiappelli, J., et al. (2021). A white matter connection of schizophrenia and Alzheimer's disease. *Schizophr. Bull.* 47, 197–206. doi: 10.1093/schbul/sbaa078

Kook, S. Y., Hong, H. S., Moon, M., Ha, C. M., Chang, S., and Mook-Jung, I. (2012). Abeta(1)(-)(4)(2)-RAGE interaction disrupts tight junctions of the blood-brain barrier via Ca(2)(+)-calcineurin signaling. *J. Neurosci.* 32, 8845–8854. doi: 10.1523/JNEUROSCI.6102-11.2012

Korte, N., Nortley, R., and Attwell, D. (2020). Cerebral blood flow decrease as an early pathological mechanism in Alzheimer's disease. *Acta Neuropathol.* 140, 793–810. doi: 10.1007/s00401-020-02215-w

Kortekaas, R., Leenders, K. L., van Oostrom, J. C. H., Vaalburg, W., Bart, J., Willemsen, A. T. M., et al. (2005). Blood–brain barrier dysfunction in parkinsonian midbrain in vivo. *Ann. Neurol.* 57, 176–179. doi: 10.1002/ana.20369

Kostiukow, A., and Samborski, W. (2020). The effectiveness of hyperbaric oxygen therapy (HBOT) in children with autism spectrum disorders. *Pol. Merkur. Lekarski.* 48, 15–18.

Kounidas, G., Cruickshank, H., Kastora, S., Sihlabela, S., and Miedzybrodzka, Z. (2021). The known burden of Huntington disease in the North of Scotland: prevalence of manifest and identified pre-symptomatic gene expansion carriers in the molecular era. *J. Neurol.* doi: 10.1007/s00415-021-10505-w

Kozberg, M. G., Ma, Y., Shaik, M. A., Kim, S. H., and Hillman, E. M. (2016). Rapid postnatal expansion of neural networks occurs in an environment of altered neurovascular and neurometabolic coupling. *J. Neurosci.* 36, 6704–6717. doi: 10.1523/JNEUROSCI.2363-15.2016

Kuan, W. L., Bennett, N., He, X., Skepper, J. N., Martynyuk, N., Wijeyekoon, R., et al. (2016). α-Synuclein pre-formed fibrils impair tight junction protein expression without affecting cerebral endothelial cell function. *Exp. Neurol.* 285(Pt A), 72–81. doi: 10.1016/j.expneurol.2016.09.003

Kumar, H., and Sharma, B. (2016). Memantine ameliorates autistic behavior, biochemistry & blood brain barrier impairments in rats. *Brain Res. Bull.* 124, 27–39. doi: 10.1016/j.brainresbull.2016.03.013

Kumar, H., Sharma, B. M., and Sharma, B. (2015). Benefits of agomelatine in behavioral, neurochemical and blood brain barrier alterations in prenatal valproic acid induced autism spectrum disorder. *Neurochem. Int.* 91, 34–45. doi: 10.1016/j.neuint.2015.10.007

Kumar-Singh, S., Pirici, D., McGowan, E., Serneels, S., Ceuterick, C., Hardy, J., et al. (2005). Dense-Core plaques in Tg2576 and PSAPP mouse models of Alzheimer's disease are centered on vessel walls. *Am. J. Pathol.* 167, 527–543. doi: 10.1016/S0002-9440(10)62995-1

Kuusimaki, T., Al-Abdulrasul, H., Kurki, S., Hietala, J., Hartikainen, S., Koponen, M., et al. (2021). Increased risk of Parkinson's disease in patients with schizophrenia spectrum disorders. *Mov. Disord.* 36, 1353–1361. doi: 10.1002/mds.28484

Kwakye, G. F., McMinimy, R. A., and Aschner, M. (2017). Disease-Toxicant interactions in Parkinson's disease neuropathology. *Neurochem. Res.* 42, 1772–1786. doi: 10.1007/s11064-016-2052-4

Lacalle-Aurioles, M., Mateos-Perez, J. M., Guzman-De-Villoria, J. A., Olazaran, J., Cruz-Orduna, I., Aleman-Gomez, Y., et al. (2014). Cerebral blood flow is an earlier indicator of perfusion abnormalities than cerebral blood volume in Alzheimer's disease. *J. Cereb. Blood Flow Metab.* 34, 654–659. doi: 10.1038/jcbfm.2013.241

Lacoste, B., Comin, C. H., Ben-Zvi, A., Kaeser, P. S., Xu, X., Costa, L. F., et al. (2014). Sensory-Related neural activity regulates the structure of vascular networks in the cerebral cortex. *Neuron* 83, 1117–1130. doi: 10.1016/j.neuron.2014.07.034

Lacoste, B., and Gu, C. (2015). Control of cerebrovascular patterning by neural activity during postnatal development. *Mech. Dev.* 138(Pt 1), 43–49. doi: 10.1016/j.mod.2015.06.003

Lacoste, B., Tong, X. K., Lahjouji, K., Couture, R., and Hamel, E. (2013). Cognitive and cerebrovascular improvements following kinin B1 receptor blockade in Alzheimer's disease mice. *J. Neuroinflammation* 10:57.

Larsen, J., Martin, D. R., and Byrne, M. (2014). Recent advances in delivery through the blood-brain barrier. *Curr. Top. Med. Chem.* 14, 1148–1160. doi: 10.2174/1568026614666140329230311

Law, M., Saindane, A. M., Ge, Y., Babb, J. S., Johnson, G., Mannon, L. J., et al. (2004). Microvascular abnormality in relapsing-remitting multiple sclerosis: perfusion MR imaging findings in normal-appearing white matter. *Radiology* 231, 645–652. doi: 10.1148/radiol.2313030996

Lecrux, C., and Hamel, E. (2011). The neurovascular unit in brain function and disease. *Acta Physiol. (Oxf.)* 203, 47–59. doi: 10.1111/j.1748-1716.2011.02256.x

Leech, S., Kirk, J., Plumb, J., and McQuaid, S. (2007). Persistent endothelial abnormalities and blood-brain barrier leak in primary and secondary progressive multiple sclerosis. *Neuropathol. Appl. Neurobiol.* 33, 86–98. doi: 10.1111/j.1365-2990.2006.00781.x

Leeuwis, A. E., Benedictus, M. R., Kuijer, J. P. A., Binnewijzend, M. A. A., Hooghiemstra, A. M., Verfaillie, S. C. J., et al. (2017). Lower cerebral blood flow is associated with impairment in multiple cognitive domains in Alzheimer's disease. *Alzheimers Dement.* 13, 531–540. doi: 10.1016/j.jalz.2016.08.013

Lepeta, K., and Kaczmarek, L. (2015). Matrix Metalloproteinase-9 as a Novel Player in Synaptic Plasticity and Schizophrenia. *Schizophr. Bull.* 41, 1003–1009. doi: 10.1093/schbul/sbv036

Li, J. Y., Popovic, N., and Brundin, P. (2005). The use of the R6 transgenic mouse models of Huntington's disease in attempts to develop novel therapeutic strategies. *NeuroTherapeutics* 2, 447–464. doi: 10.1602/neurorx.2.3.447

Li, S. S., Qu, Z., Haas, M., Ngo, L., Heo, Y. J., Kang, H. J., et al. (2016). The HSA21 gene EURL/C21ORF91 controls neurogenesis within the cerebral cortex and is implicated in the pathogenesis of Down Syndrome. *Sci. Rep.* 6:29514. doi: 10.1038/srep29514

Licht, T., and Keshet, E. (2015). The vascular niche in adult neurogenesis. *Mech. Dev.* 138(Pt 1), 56–62. doi: 10.1016/j.mod.2015.06.001

Lim, R. G., Quan, C., Reyes-Ortiz, A. M., Lutz, S. E., Kedaigle, A. J., Gipson, T. A., et al. (2017). Huntington's disease iPSC-derived brain microvascular endothelial cells reveal WNT-mediated angiogenic and blood-brain barrier deficits. *Cell Rep.* 19, 1365–1377. doi: 10.1016/j.celrep.2017.04.021

Lin, A. L., Jahrling, J. B., Zhang, W., DeRosa, N., Bakshi, V., Romero, P., et al. (2017). Rapamycin rescues vascular, metabolic and learning deficits in apolipoprotein E4 transgenic mice with pre-symptomatic Alzheimer's disease. *J. Cereb. Blood Flow Metab.* 37, 217–226. doi: 10.1177/0271678X15621575

Lin, C.-Y., Hsu, Y.-H., Lin, M.-H., Yang, T.-H., Chen, H.-M., Chen, Y.-C., et al. (2013). Neurovascular abnormalities in humans and mice with Huntington's disease. *Exp. Neurol.* 250, 20–30. doi: 10.1016/j.expneurol.2013.08.019

Liu, H., Zhang, C., Xu, J., Jin, J., Cheng, L., Wu, Q., et al. (2020). HTT silencing delays onset and slows progression of Huntington's disease like phenotype: monitoring with a novel neurovascular biomarker. *bioRXiv* [Preprint] doi: 10.1101/2020.11.17.386631

Liu, Y., Braidy, N., Poljak, A., Chan, D. K. Y., and Sachdev, P. (2018). Cerebral small vessel disease and the risk of Alzheimer's disease: a systematic review. *Ageing Res. Rev.* 47, 41–48. doi: 10.1016/j.arr.2018.06.002

Liu, Y., Cao, Y., Zhang, W., Bergmeier, S., Qian, Y., Akbar, H., et al. (2012). A small-molecule inhibitor of glucose transporter 1 downregulates glycolysis, induces cell-cycle arrest, and inhibits cancer cell growth in vitro and in vivo. *Mol. Cancer Ther.* 11, 1672–1682. doi: 10.1158/1535-7163.MCT-12-0131

Love, S., and Miners, J. S. (2016). Cerebral Hypoperfusion and the Energy Deficit in Alzheimer's Disease. *Brain Pathol.* 26, 607–617. doi: 10.1111/bpa.12401

Luchsinger, J. A., Reitz, C., Honig, L. S., Tang, M. X., Shea, S., and Mayeux, R. (2005). Aggregation of vascular risk factors and risk of incident Alzheimer disease [Research Support, N.I.H., Extramural Research Support, Non-U.S. Gov't Research Support, U.S. Gov't, P.H.S.]. *Neurology* 65, 545–551. doi: 10.1212/01.wnl.0000172914.08967.dc

Ludwin, S. K. (2006). The pathogenesis of multiple sclerosis: relating human pathology to experimental studies. *J. Neuropathol. Exp. Neurol.* 65, 305–318. doi: 10.1097/01.jnen.0000225024.12074.80

MacVicar, B. A., and Newman, E. A. (2015). Astrocyte regulation of blood flow in the brain. *Cold Spring Harb. Perspect. Biol.* 7:a020388. doi: 10.1101/cshperspect.a020388

Madhyastha, T. M., Askren, M. K., Boord, P., Zhang, J., Leverenz, J. B., and Grabowski, T. J. (2015). Cerebral perfusion and cortical thickness indicate cortical involvement in mild Parkinson's disease. *Mov. Disord.* 30, 1893–1900. doi: 10.1002/mds.26128

Magaki, S., Tang, Z., Tung, S., Williams, C. K., Lo, D., Yong, W. H., et al. (2018). The effects of cerebral amyloid angiopathy on integrity of the blood-brain barrier. *Neurobiol. Aging* 70, 70–77. doi: 10.1016/j.neurobiolaging.2018.06.004

Malaspina, D., Harkavy-Friedman, J., Corcoran, C., Mujica-Parodi, L., Printz, D., Gorman, J. M., et al. (2004). Resting neural activity distinguishes subgroups of schizophrenia patients. *Biol. Psychiatry* 56, 931–937. doi: 10.1016/j.biopsych.2004.09.013

Malaspina, D., Storer, S., Furman, V., Esser, P., Printz, D., Berman, A., et al. (1999). SPECT study of visual fixation in schizophrenia and comparison subjects. *Soc. Biol. Psychiatry* 46, 89–93. doi: 10.1016/s0006-3223(98)00306-0

Mantovani, S., Gordon, R., Li, R., Christie, D. C., Kumar, V., and Woodruff, T. M. (2016). Motor deficits associated with Huntington's disease occur in the absence of striatal degeneration in BACHD transgenic mice. *Hum. Mol. Genet.* 25, 1780–1791. doi: 10.1093/hmg/ddw050

Marco, S., and Skaper, S. D. (2006). Amyloid beta-peptide1-42 alters tight junction protein distribution and expression in brain microvessel endothelial cells. *Neurosci. Lett.* 401, 219–224. doi: 10.1016/j.neulet.2006.03.047

Marshall, O., Lu, H., Brisset, J. C., Xu, F., Liu, P., Herbert, J., et al. (2014). Impaired cerebrovascular reactivity in multiple sclerosis. *JAMA Neurol.* 71, 1275–1281. doi: 10.1001/jamaneurol.2014.1668

Marshall, R. S., Lazar, R. M., Pile-Spellman, J., Young, W. L., Hoang Duong, D., Joshi, S., et al. (2001). Recovery of brain function during induced cerebral hypoperfusion. *Brain* 124, 1208–1217. doi: 10.1093/brain/124.6.1208

Martinez, B. I., and Stabenfeldt, S. E. (2019). Current trends in biomarker discovery and analysis tools for traumatic brain injury. *J. Biol. Eng.* 13:16. doi: 10.1186/s13036-019-0145-8

Mathalon, D. H., Ford, J. M., and Pfefferbaum, A. (2000). Trait and state aspects of P300 amplitude reduction in schizophrenia: a retrospective longitudinal study. *Biol. Psychiatry* 47, 434–449. doi: 10.1016/s0006-3223(99)00277-2

Mattsson, N., Tosun, D., Insel, P. S., Simonson, A., Jack, C. R. Jr., Beckett, L. A., et al. (2014). Association of brain amyloid-beta with cerebral perfusion and structure in Alzheimer's disease and mild cognitive impairment. *Brain* 137(Pt 5), 1550–1561. doi: 10.1093/brain/awu043

Mayhan, W. G. (1999). VEGF increases permeability of the blood-brain barrier via a nitric oxide synthase/cGMP-dependent pathway. *Am. J. Physiol.* 276, C1148–C1153. doi: 10.1152/ajpcell.1999.276.5.C1148

McColgan, P., and Tabrizi, S. J. (2018). Huntington's disease: a clinical review. *Eur. J. Neurol.* 25, 24–34. doi: 10.1111/ene.13413

McConnell, H. L., Li, Z., Woltjer, R. L., and Mishra, A. (2019). Astrocyte dysfunction and neurovascular impairment in neurological disorders: correlation or causation? *Neurochem. Int.* 128, 70–84. doi: 10.1016/j.neuint.2019.04.005

McGowan, E., Pickford, F., Kim, J., Onstead, L., Eriksen, J., Yu, C., et al. (2005). Aβ42 is essential for parenchymal and vascular amyloid deposition in mice. *Neuron* 47, 191–199. doi: 10.1016/j.neuron.2005.06.030

McQuaid, S., Cunnea, P., McMahon, J., and Fitzgerald, U. (2009). The effects of blood–brain barrier disruption on glial cell function in multiple sclerosis. *Biochem. Soc. Trans.* 37(Pt 1), 329–331. doi: 10.1042/BST0370329

Melzer, T. R., Watts, R., MacAskill, M. R., Pearson, J. F., Rueger, S., Pitcher, T. L., et al. (2011). Arterial spin labelling reveals an abnormal cerebral perfusion pattern in Parkinson's disease. *Brain* 134(Pt 3), 845–855. doi: 10.1093/brain/awq377

Menard, C., Pfau, M. L., Hodes, G. E., Kana, V., Wang, V. X., Bouchard, S., et al. (2017). Social stress induces neurovascular pathology promoting depression. *Nat. Neurosci.* 20, 1752–1760. doi: 10.1038/s41593-017-0010-3

Mendez, M. F. (2017). What is the relationship of traumatic brain injury to dementia? *J. Alzheimers Dis.* 57, 667–681. doi: 10.3233/JAD-161002

Michels, L., Warnock, G., Buck, A., Macauda, G., Leh, S. E., Kaelin, A. M., et al. (2016). Arterial spin labeling imaging reveals widespread and Abeta-independent reductions in cerebral blood flow in elderly apolipoprotein epsilon-4 carriers. *J. Cereb. Blood Flow Metab.* 36, 581–595. doi: 10.1177/0271678X15605847

Mielke, M. M., Vemuri, P., and Rocca, W. A. (2014). Clinical epidemiology of Alzheimer's disease: assessing sex and gender differences. *Clin. Epidemiol.* 6, 37–48. doi: 10.2147/CLEP.S37929

Milner, E., Zhou, M. L., Johnson, A. W., Vellimana, A. K., Greenberg, J. K., Holtzman, D. M., et al. (2014). Cerebral amyloid angiopathy increases susceptibility to infarction after focal cerebral ischemia in Tg2576 mice. *Stroke* 45, 3064–3069. doi: 10.1161/STROKEAHA.114.006078

Minn, A., Leclerc, S., Heydel, J.-M., Minn, A.-L., Denizcot, C., Cattarelli, M., et al. (2002). Drug transport into the mammalian brain: the nasal pathway and its specific metabolic barrier. *J. Drug Target* 10, 285–296. doi: 10.1080/713714452

Minoshima, S., Giordani, B., Berent, S., Frey, K. A., Foster, N. L., and Kuhl, D. E. (1997). Metabolic reduction in the posterior cingulate cortex in very early Alzheimer's disease. *Ann. Neurol.* 42, 85–94. doi: 10.1002/ana.410420114

Mishra, A. (2017). Binaural blood flow control by astrocytes: listening to synapses and the vasculature. *J. Physiol.* 595, 1885–1902. doi: 10.1113/JP270979

Mohan, S., Ahmad, A. S., Glushakov, A. V., Chambers, C., and Dore, S. (2012). Putative role of prostaglandin receptor in intracerebral hemorrhage. *Front. Neurol.* 3:145. doi: 10.3389/fneur.2012.00145

Montagne, A., Nation, D. A., Pa, J., Sweeney, M. D., Toga, A. W., and Zlokovic, B. V. (2016). Brain imaging of neurovascular dysfunction in Alzheimer's disease. *Acta Neuropathol.* 131, 687–707. doi: 10.1007/s00401-016-1570-0

Montagne, A., Nikolakopoulou, A. M., Huuskonen, M. T., Sagare, A. P., Lawson, E. J., Lazic, D., et al. (2021). APOE4 accelerates advanced-stage vascular and neurodegenerative disorder in old Alzheimer's mice via cyclophilin A independently of amyloid-β. *Nat. Aging* 1, 506–520. doi: 10.1038/s43587-021-00073-z

Montaldi, D., Brooks, D. N., McColl, J. H., Wyper, D., Patterson, J., Barron, E., et al. (1990). Measurement of regional cerebral blood flow and cognitive performance in Alzheimer's disease. *J. Neurol. Neurosurg. Psychiatry* 53, 33–38. doi: 10.1136/jnnp.53.1.33

Monti, L., Morbidelli, L., and Rossi, A. (2018). Impaired cerebral perfusion in multiple sclerosis: relevance of endothelial factors. *Biomark. Insights* 13, 1–10. doi: 10.1177/1177271918774800

Moon, H. S., Jiang, H., Vo, T. T., Jung, W. B., Vazquez, A. L., and Kim, S. G. (2021). Contribution of excitatory and inhibitory neuronal activity to BOLD fMRI. *Cereb. Cortex* 31, 4053–4067. doi: 10.1093/cercor/bhab068

Mooradian, A. D., Chung, H. C., and Shah, G. N. (1997). GLUT-1 expression in the cerebra of patients with Alzheimer's disease. *Neurobiol. Aging* 18, 469–474. doi: 10.1016/s0197-4580(97)00111-5

Moore, E. E., Liu, D., Li, J., Schimmel, S. J., Cambronero, F. E., Terry, J. G., et al. (2021). Association of aortic stiffness with biomarkers of neuroinflammation, synaptic dysfunction, and neurodegeneration. *Neurology* 97, e329–e340. doi: 10.1212/WNL.0000000000012257

Morris-Rosendahl, D. J., and Crocq, M. A. (2020). Neurodevelopmental disorders-the history and future of a diagnostic concept. *Dialogues Clin. Neurosci.* 22, 65–72. doi: 10.31887/DCNS.2020.22.1/macrocq

Mucke, L., Masliah, E., Yu, G. Q., Mallory, M., Rockenstein, E. M., Tatsuno, G., et al. (2000). High-level neuronal expression of abeta 1-42 in wild-type human amyloid protein precursor transgenic mice: synaptotoxicity without plaque formation. *J. Neurosci.* 20, 4050–4058.

Mughal, A., Harraz, O. F., Gonzales, A. L., Hill-Eubanks, D., and Nelson, M. T. (2021). PIP2 improves cerebral blood flow in a mouse model of Alzheimer's disease. *Function (Oxf)* 2:zqab010. doi: 10.1093/function/zqab010

Müller, N., and Ackenheil, M. (1995). Immunoglobulin and albumin content of cerebrospinal fluid in schizophrenic patients: relationship to negative symptomatology. *Schizophr. Res.* 14, 223–228. doi: 10.1016/0920-9964(94)00045-a

Muramuto, S., Yamada, H., Sadato, N., Kimura, H., Konishi, Y., Kimura, K., et al. (2002). Age-dependent change in metabolic re- sponse to photic stimulation of the primary visual cortex in infants: functional mag- netic resonance imaging study. *J. Comput. Assist. Tomogr.* 26, 894–901.

Nelson, A. R., Sweeney, M. D., Sagare, A. P., and Zlokovic, B. V. (2016). Neurovascular dysfunction and neurodegeneration in dementia and Alzheimer's disease. *Biochim. Biophys. Acta* 1862, 887–900. doi: 10.1016/j.bbadis.2015.12.016

Niatsetskaya, Z., Basso, M., Speer, R. E., McConoughey, S. J., Coppola, G., Ma, T. C., et al. (2010). HIF prolyl hydroxylase inhibitors prevent neuronal death induced by mitochondrial toxins: therapeutic implications for Huntington's disease and Alzheimer's disease [Research Support, N.I.H., Extramural Research Support, Non-U.S. Gov't]. *Antioxid. Redox Signal.* 12, 435–443. doi: 10.1089/ars.2009.2800

Nicolakakis, N., Aboulkassim, T., Ongali, B., Lecrux, C., Fernandes, P., Rosa-Neto, P., et al. (2008). Complete rescue of cerebrovascular function in aged Alzheimer's disease transgenic mice by antioxidants and pioglitazone, a peroxisome proliferator-activated receptor gamma agonist. *J. Neurosci.* 28, 9287–9296.

Nicolakakis, N., and Hamel, E. (2011). Neurovascular function in Alzheimer's disease patients and experimental models. *J. Cereb. Blood Flow Metab.* 31, 1354–1370. doi: 10.1038/jcbfm.2011.43

Nishiura, K., Ichikawa-Tomikawa, N., Sugimoto, K., Kunii, Y., Kashiwagi, K., Tanaka, M., et al. (2017). PKA activation and endothelial claudin-5 breakdown in the schizophrenic prefrontal cortex. *Oncotarget* 7, 93382–93391. doi: 10.18632/oncotarget.21850

Niwa, K., Carlson, G. A., and Iadecola, C. (2000). Exogenous Ab1-40 reproduces cerebrovascular alterations resulting from amyloid precursor protein overexpression in mice. *J. Cereb. Blood Flow Metab.* 20, 1659–1668. doi: 10.1097/00004647-200012000-00005

Niwa, K., Kazama, K., Younkin, S. G., Carlson, G. A., and Iadecola, C. (2002). Alterations in cerebral blood flow and glucose utilization in mice overexpressing the amyloid precursor protein. *Neurobiol. Dis.* 9, 61–68. doi: 10.1006/nbdi.2001.0460

Novarino, G., El-Fishawy, P., Kayserili, H., Meguid, N. A., Scott, E. M., Schroth, J., et al. (2012). Mutations in BCKD-kinase lead to a potentially treatable form of autism with epilepsy. *Science* 338, 394–397. doi: 10.1126/science.1224631

O'Brien, J. T., Eagger, S., Syed, G. M., Sahakian, B. J., and Levy, R. (1992). A study of regional cerebral blood flow and cognitive performance in Alzheimer's disease. *J. Neurol. Neurosurg. Psychiatry* 55, 1182–1187. doi: 10.1136/jnnp.55.12.1182

Ochoa, S., Usall, J., Cobo, J., Labad, X., and Kulkarni, J. (2012). Gender differences in schizophrenia and first-episode psychosis: a comprehensive literature review. *Schizophr. Res. Treat.* 2012:916198. doi: 10.1155/2012/916198

Oddo, S., Caccamo, A., Shepherd, J. D., Murphy, M. P., Golde, T. E., Kayed, R., et al. (2003). Triple-transgenic model of Alzheimer's disease with plaques and tangles: intracellular Abeta and synaptic dysfunction [Comparative Study Research Support, Non-U.S. Gov't Research Support, U.S. Gov't, P.H.S.]. *Neuron* 39, 409–421.

Ohnishi, T., Matsuda, H., Hashimoto, T., Kunihiro, T., Nishikawa, M., Uema, T., et al. (2000). Abnormal regional cerebral blood flow in childhood autism. *Brain* 123(Pt 9), 1838–1844.

Okabe, K., Fukada, H., Tai-Nagara, I., Ando, T., Honda, T., Nakajima, K., et al. (2020). Neuron-derived VEGF contributes to cortical and hippocampal development independently of VEGFR1/2-mediated neurotrophism. *Dev. Biol.* 459, 65–71. doi: 10.1016/j.ydbio.2019.11.016

Ongali, B., Nicolakakis, N., Lecrux, C., Aboulkassim, T., Rosa-Neto, P., Papadopoulos, P., et al. (2010). Transgenic mice overexpressing APP and transforming growth factor-beta1 feature cognitive and vascular hallmarks of Alzheimer's disease. *Am. J. Pathol.* 177, 3071–3080. doi: 10.2353/ajpath.2010.100339

Onore, C., Careaga, M., and Ashwood, P. (2012). The role of immune dysfunction in the pathophysiology of autism. *Brain Behav. Immun.* 26, 383–392. doi: 10.1016/j.bbi.2011.08.007

Ortiz, G. G., Pacheco-Moises, F. P., Macias-Islas, M. A., Flores-Alvarado, L. J., Mireles-Ramirez, M. A., Gonzalez-Renovato, E. D., et al. (2014). Role of the blood-brain barrier in multiple sclerosis. *Arch. Med. Res.* 45, 687–697. doi: 10.1016/j.arcmed.2014.11.013

Ota, T., Sato, N., Nakata, Y., Ito, K., Kamiya, K., Maikusa, N., et al. (2013). Abnormalities of cerebral blood flow in multiple sclerosis: a pseudocontinuous arterial spin labeling MRI study. *Magn. Reson. Imaging* 31, 990–995. doi: 10.1016/j.mri.2013.03.016

Ouellette, J., Toussay, X., Comin, C. H., Costa, L. D. F., Ho, M., Lacalle-Aurioles, M., et al. (2020). Vascular contributions to 16p11.2 deletion autism syndrome modeled in mice. *Nat. Neurosci.* 23, 1090–1101. doi: 10.1038/s41593-020-0663-1

Padden, M., Leech, S., Craig, B., Kirk, J., Brankin, B., and McQuaid, S. (2007). Differences in expression of junctional adhesion molecule-A and beta-catenin in multiple sclerosis brain tissue: increasing evidence for the role of tight junction pathology. *Acta Neuropathol.* 113, 177–186. doi: 10.1007/s00401-006-0145-x

Pagano, G., Ferrara, N., Brooks, D. J., and Pavese, N. (2016). Age at onset and Parkinson disease phenotype. *Neurology* 86, 1400–1407. doi: 10.1212/WNL.0000000000002461

Palop, J. J., Jones, B., Kekonius, L., Chin, J., Yu, G. Q., Raber, J., et al. (2003). Neuronal depletion of calcium-dependent proteins in the dentate gyrus is tightly linked to Alzheimer's disease-related cognitive deficits. *Proc. Natl. Acad. Sci. U.S.A.* 100, 9572–9577.

Papadaki, E. Z., Simos, P. G., Mastorodemos, V. C., Panou, T., Maris, T. G., Karantanas, A. H., et al. (2014). Regional MRI perfusion measures predict motor/executive function in patients with clinically isolated syndrome. *Behav. Neurol.* 2014:252419. doi: 10.1155/2014/252419

Pardridge, W. M. (2012). Drug transport across the blood-brain barrier. *J. Cereb. Blood Flow Metab.* 32, 1959–1972. doi: 10.1038/jcbfm.2012.126

Paris, D., Parker, T. A., Suo, Z., Fang, C., Humphrey, J., Crawford, F., et al. (1998). Role of peroxynitrite in the vasoactive and cytotoxic effects of Alzheimer's beta-amyloid1-40 peptide. *Exp. Neurol.* 152, 116–122. doi: 10.1006/exnr.1998.6828

Park, H. R., Lee, J. M., Moon, H. E., Lee, D. S., Kim, B. N., Kim, J., et al. (2016). A short review on the current understanding of autism spectrum disorders. *Exp. Neurobiol.* 25, 1–13. doi: 10.5607/en.2016.25.1.1

Park, L., Wang, G., Zhou, P., Zhou, J., Pitstick, R., Previti, M. L., et al. (2011). Scavenger receptor CD36 is essential for the cerebrovascular oxidative stress and neurovascular dysfunction induced by amyloid-beta. *Proc. Natl. Acad. Sci. U.S.A.* 108, 5063–5068. doi: 10.1073/pnas.1015413108

Parkinson Canada (2010). *A Manual for People Living with Parkinson's Disease*. Available online at: https://www.parkinson.ca/gated/parkinsons-disease-an-introductory-guide/ (accessed July 5, 2021).

Parodi-Rullan, R., Ghiso, J., Cabrera, E., Rostagno, A., and Fossati, S. (2020). Alzheimer's amyloid beta heterogeneous species differentially affect brain endothelial cell viability, blood-brain barrier integrity, and angiogenesis. *Aging Cell* 19:e13258. doi: 10.1111/acel.13258

Patel, A., Toia, G. V., Colletta, K., Bradaric, B. D., Carvey, P. M., and Hendey, B. (2011). An angiogenic inhibitor, cyclic RGDfV, attenuates MPTP-induced dopamine neuron toxicity. *Exp. Neurol.* 231, 160–170. doi: 10.1016/j.expneurol.2011.06.004

Patel, N. S., Mathura, V. S., Bachmeier, C., Beaulieu-Abdelahad, D., Laporte, V., Weeks, O., et al. (2010). Alzheimer's beta-amyloid peptide blocks vascular endothelial growth factor mediated signaling via direct interaction with VEGFR-2. *J. Neurochem.* 112, 66–76. doi: 10.1111/j.1471-4159.2009.06426.x

Paulsen, J. S. (2011). Cognitive impairment in Huntington disease: diagnosis and treatment [Research Support, N.I.H., Extramural Research Support, Non-U.S. Gov't Review]. *Curr. Neurol. Neurosci. Rep.* 11, 474–483. doi: 10.1007/s11910-011-0215-x

Peguera, B., Segarra, M., and Acker-Palmer, A. (2021). Neurovascular crosstalk coordinates the central nervous system development. *Curr. Opin. Neurobiol.* 69, 202–213. doi: 10.1016/j.conb.2021.04.005

Perry, D. C., Sturm, V. E., Peterson, M. J., Pieper, C. F., Bullock, T., Boeve, B. F., et al. (2016). Association of traumatic brain injury with subsequent neurological and psychiatric disease: a meta-analysis. *J. Neurosurg.* 124, 511–526. doi: 10.3171/2015.2.JNS14503

Peruzzo, D., Castellaro, M., Calabrese, M., Veronese, E., Rinaldi, F., Bernardi, V., et al. (2013). Heterogeneity of cortical lesions in multiple sclerosis: an MRI perfusion study. *J. Cereb. Blood Flow Metab.* 33, 457–463. doi: 10.1038/jcbfm.2012.192

Peterson, B. S., Zargarian, A., Peterson, J. B., Goh, S., Sawardekar, S., Williams, S. C. R., et al. (2019). Hyperperfusion of frontal white and subcortical gray matter in autism spectrum disorder. *Biol. Psychiatry* 85, 584–595. doi: 10.1016/j.biopsych.2018.11.026

Pinkham, A., Loughead, J., Ruparel, K., Wu, W. C., Overton, E., Gur, R., et al. (2011). Resting quantitative cerebral blood flow in schizophrenia measured by pulsed arterial spin labeling perfusion MRI. *Psychiatry Res.* 194, 64–72. doi: 10.1016/j.pscychresns.2011.06.013

Plana-Ripoll, O., Pedersen, C. B., Holtz, Y., Benros, M. E., Dalsgaard, S., de Jonge, P., et al. (2019). Exploring comorbidity within mental disorders among a danish national population. *JAMA Psychiatry* 76, 259–270. doi: 10.1001/jamapsychiatry.2018.3658

Profaci, C. P., Munji, R. N., Pulido, R. S., and Daneman, R. (2020). The blood-brain barrier in health and disease: important unanswered questions. *J. Exp. Med.* 217:e20190062. doi: 10.1084/jem.20190062

Prohovnik, I., Mayeux, R., Sackeim, H. A., Smith, G., Stern, Y., and Alderson, P. O. (1988). Cerebral perfusion as a diagnostic marker of early Alzheimer's disease. *Neurology* 38, 931–937. doi: 10.1212/WNL.38.6.931

Pu, S., Nakagome, K., Yamada, T., Itakura, M., Yamanashi, T., Yamada, S., et al. (2016). Social cognition and prefrontal hemodynamic responses during a working memory task in schizophrenia. *Sci. Rep.* 6:22500. doi: 10.1038/srep22500

Quaegebeur, A., Lange, C., and Carmeliet, P. (2011). The neurovascular link in health and disease: molecular mechanisms and therapeutic implications. *Neuron* 71, 406–424. doi: 10.1016/j.neuron.2011.07.013

Querfurth, H. W., and LaFerla, F. M. (2010). Alzheimer's disease. *N. Engl. J. Med.* 362, 329–344.

Ramos-Cejudo, J., Wisniewski, T., Marmar, C., Zetterberg, H., Blennow, K., de Leon, M. J., et al. (2018). Traumatic brain injury and Alzheimer's disease: the cerebrovascular link. *EBioMedicine* 28, 21–30. doi: 10.1016/j.ebiom.2018.01.021

Rawlins, M. D., Wexler, N. S., Wexler, A. R., Tabrizi, S. J., Douglas, I., Evans, S. J., et al. (2016). The prevalence of Huntington's disease. *Neuroepidemiology* 46, 144–153. doi: 10.1159/000443738

Reese, T. S., and Karnovsky, M. (1967). Fine structural localization of a blood-brain barrier to exogenous peroxidase. *J. Cell Biol.* 34, 207–217. doi: 10.1083/jcb.34.1.207

Reid, I. C., Besson, J. A. O., Best, P. V., Sharp, P. F., Gemmell, H. G., and Smith, F. W. (1988). Imaging of cerebral blood flow markers in Huntington's disease

using single photon emission computed tomography. *J. Neurol. Neurosurg. Psychiatry* 51, 1264–1268. doi: 10.1136/jnnp.51.10.1264

Reijmer, Y. D., van Veluw, S. J., and Greenberg, S. M. (2016). Ischemic brain injury in cerebral amyloid angiopathy. *J. Cereb. Blood Flow Metab.* 36, 40–54. doi: 10.1038/jcbfm.2015.88

Reynell, C., and Harris, J. J. (2013). The BOLD signal and neurovascular coupling in autism. *Dev. Cogn. Neurosci.* 6, 72–79. doi: 10.1016/j.dcn.2013.07.003

Ribe, A. R., Laursen, T. M., Charles, M., Katon, W., Fenger-Gron, M., Davydow, D., et al. (2015). Long-term Risk of dementia in persons with Schizophrenia: a Danish population-based cohort study. *JAMA Psychiatry* 72, 1095–1101. doi: 10.1001/jamapsychiatry.2015.1546

Rite, I., Machado, A., Cano, J., and Venero, J. L. (2007). Blood-brain barrier disruption induces in vivo degeneration of nigral dopaminergic neurons. *J. Neurochem.* 101, 1567–1582. doi: 10.1111/j.1471-4159.2007.04567.x

Rizzo, M. T., and Leaver, H. A. (2010). Brain endothelial cell death: modes, signaling pathways, and relevance to neural development, homeostasis, and disease. *Mol. Neurobiol.* 42, 52–63. doi: 10.1007/s12035-010-8132-6

Roher, A. E., Esh, C., Kokjohn, T. A., Kalback, W., Luehrs, D. C., Seward, J. D., et al. (2003). Circle of willis atherosclerosis is a risk factor for sporadic Alzheimer's disease. *Arterioscler. Thromb. Vasc. Biol.* 23, 2055–2062.

Ross, C. A., and Tabrizi, S. J. (2011). Huntington's disease: from molecular pathogenesis to clinical treatment. *Lancet Neurol.* 10, 83–98. doi: 10.1016/S1474-4422(10)70245-3

Ross, T. M., Martinez, P. M., Renner, J. C., Thorne, R. G., Hanson, L. R., and Frey, W. H. II (2004). Intranasal administration of interferon beta bypasses the blood–brain barrier to target the central nervous system and cervical lymph nodes: a non-invasive treatment strategy for multiple sclerosis. *J. Neuroinflammation* 151, 66–77. doi: 10.1016/j.jneuroim.2004.02.011

Rossignol, D. A., Bradstreet, J. J., Van Dyke, K., Schneider, C., Freedenfeld, S. H., O'Hara, N., et al. (2012). Hyperbaric oxygen treatment in autism spectrum disorders. *Med. Gas Res.* 2:16.

Russo, S. J., and Nestler, E. J. (2013). The brain reward circuitry in mood disorders. *Nat. Rev. Neurosci.* 14, 609–625. doi: 10.1038/nrn3381

Ryu, J. K., and McLarnon, J. G. (2009). A leaky blood-brain barrier, fibrinogen infiltration and microglial reactivity in inflamed Alzheimer's disease brain. *J. Cell. Mol. Med.* 13, 2911–2925. doi: 10.1111/j.1582-4934.2008.00434.x

Saade, C., Bou-Fakhredin, R., Yousem, D. M., Asmar, K., Naffaa, L., and El-Merhi, F. (2018). Gadolinium and multiple sclerosis: vessels, barriers of the brain, and glymphatics. *AJNR Am. J. Neuroradiol.* 39, 2168–2176. doi: 10.3174/ajnr.A5773

Sabri, O., Erkwoh, R., Schreckenberger, M., Owega, A., Sass, H., and Buell, U. (1997). Correlation of positive symptoms exclusively to hyperperfusion or hypoperfusion of cerebral cortex in never-treated schizophrenics. *Lancet* 349, 1735–1739. doi: 10.1016/s0140-6736(96)08380-8

Sagare, A. P., Bell, R. D., Zhao, Z., Ma, Q., Winkler, E. A., Ramanathan, A., et al. (2013). Pericyte loss influences Alzheimer-like neurodegeneration in mice. *Nat. Commun.* 4:2932. doi: 10.1038/ncomms3932

Saindane, A. M., Law, M., Ge, Y., Johnson, G., Babb, J. S., and Grossman, R. I. (2007). Correlation of diffusion tensor and dynamic perfusion MR imaging metrics in normal- appearing corpus callosum: support for primary hypoperfusion in multiple sclerosis. *Am. J. Neuroradiol.* 28, 767–772.

Sakulchit, T., Ladish, C., and Goldman, R. D. (2017). Hyperbaric oxygen therapy for children with autism spectrum disorder. *Can. Fam. Physician* 63, 446–448.

Salehi, A., Ashford, J. W., and Mufson, E. J. (2016). The link between Alzheimer's disease and down syndrome. a historical perspective. *Curr. Alzheimer Res.* 13, 2–6. doi: 10.2174/1567205012999151021102914

Salisbury, D., and Bronas, U. (2015). Reactive oxygen and nitrogen species: impact on endothelial dysfunction. *Nurs. Res.* 64, 53–66. doi: 10.1097/NNR.0000000000000068

Salloway, S., Gur, T., Berzin, T., Zipser, B., Correia, S., Hovanesian, V., et al. (2002). Effect of APOE genotype on microvascular basement membrane in Alzheimer's disease. *J. Neurol. Sci.* 203-204, 183–187. doi: 10.1016/s0022-510x(02)00288-5

Salmina, A. B., Morgun, A. V., Kuvacheva, N. V., Pozhilenkova, E. A., Solonchuk, Y. R., Lopatina, O. L., et al. (2014). Endothelial progenitor cells in cerebral endothelium development and repair. *Curr. Technol. Med.* 6, 213–221. doi: 10.1186/s13041-016-0193-7

Sandoo, A., Veldhuijzen van Zanten, J., Metsios, G., Carroll, D., and Kitas, G. (2010). The endothelium and its role in regulating vascular tone. *Open Cardiovasc. Med. J.* 4, 302–312.

Saoud, H., Aflouk, Y., Ben Afia, A., Gaha, L., and Bel Hadj Jrad, B. (2021). Association of VEGF and KDR polymorphisms with the development of schizophrenia. *medRxiv* [preprint] doi: 10.1101/2021.08.06.21261566

Sarkar, S., Raymick, J., Mann, D., Bowyer, J. F., Hanig, J. P., Schmued, L. C., et al. (2014). Neurovascular changes in acute, sub-acute and chronic mouse models of Parkinson's disease. *Curr. Neurovasc. Res.* 11, 48–61. doi: 10.2174/1567202610666131124234506

Sax, D. S., Powsner, R., Kim, A., Tilak, S., Bhatia, R., Cupples, L. A., et al. (1996). Evidence of cortical metabolic dysfunction in early Huntington's disease by single-photon-emission computed tomography. *Mov. Disord.* 11, 671–677. doi: 10.1002/mds.870110612

Schaeffer, S., and Iadecola, C. (2021). Revisiting the neurovascular unit. *Nat. Neurosci.* 24, 1198–1209. doi: 10.1038/s41593-021-00904-7

Scheef, L., Manka, C., Daamen, M., Kühn, K., Maier, W., Schild, H., et al. (2010). Resting-State perfusion in nonmedicated schizophrenic patients: a continuous arterial spin-labeling 3.0-T MR study. *Radiology* 256, 253–260. doi: 10.1148/radiol.10091224

Schifter, T., Hoffman, J. M., Hatten, P. Jr., Hanson, M. W., Coleman, E., and DeLong, R. (1994). Neuroimaging in infantile autism. *J. Child Neurol.* 9, 155–161. doi: 10.1177/088307389400900210

Schuepbach, D., Egger, S. T., Boeker, H., Duschek, S., Vetter, S., Seifritz, E., et al. (2016). Determinants of cerebral hemodynamics during the Trail Making Test in schizophrenia. *Brain Cogn.* 109, 96–104. doi: 10.1016/j.bandc.2016.09.002

Schultz, S. K., O'Leary, D. S., Boles Ponto, L. L., Arndt, S., Magnotta, V., Leonard Watkins, G., et al. (2002). Age and regional cerebral blood flow in schizophrenia: age effects in anterior cingulate, frontal, and parietal cortex. *J. Neuropsychiatry Clin. Neurosci.* 14, 19–24. doi: 10.1176/jnp.14.1.19

Schwartz, M., and Kipnis, J. (2005). Protective autoimmunity and neuroprotection in inflammatory and noninflammatory neurodegenerative diseases. *J. Neurol. Sci.* 233, 163–166. doi: 10.1016/j.jns.2005.03.014

Seabrook, T. J., Littlewood-Evans, A., Brinkmann, V., Pöllinger, B., Schnell, C., and Hiestand, P. C. (2010). Angiogenesis is present in experimental autoimmune encephalomyelitis and pro- angiogenic factors are increased in multiple sclerosis lesions. *J. Neuroinflammation* 7:95. doi: 10.1186/1742-2094-7-95

Selkoe, D. J. (2002). Alzheimer's disease is a synaptic failure. *Science* 298, 789–791.

Sender, R., and Milo, R. (2021). The distribution of cellular turnover in the human body. *Nat. Med.* 27, 45–48. doi: 10.1038/s41591-020-01182-9

Sengillo, J. D., Winkler, E. A., Walker, C. T., Sullivan, J. S., Johnson, M., and Zlokovic, B. V. (2013). Deficiency in mural vascular cells coincides with blood-brain barrier disruption in Alzheimer's disease. *Brain Pathol.* 23, 303–310. doi: 10.1111/bpa.12004

Sharma, S., and Brown, C. E. (2021). Microvascular basis of cognitive impairment in type 1 diabetes. *Pharmacol. Therap.* 107929. doi: 10.1016/j.pharmthera.2021.107929

Shcherbakova, I., Neshkova, E., Dotsenko, V., Platonova, T., Shcherbakova, E., and Yarovaya, G. (1999). The possible role of plasma kallikrein-kinin system and leukocyte elastase in pathogenesis of schizophrenia. *Immunopharmacology* 43, 273–279. doi: 10.1016/s0162-3109(99)00099-5

Shen, Q., Goderie, S. K., Jin, L., Karanth, N., Sun, Y., Abramova, N., et al. (2004). Endothelial cells stimulate self-renewal and expand neurogenesis of neural stem cells. *Science* 304, 1338–1340. doi: 10.1126/science.1095505

Sherrington, R. A. (1890). On the regulation of the blood-supply of the brain. *Neurology* 41, 10–14.

Siegel, B. V., Tanguay, P., Call, J. D., Abel, L., Ho, A., Lott, I., et al. (1992). Regional cerebral glucose metabolism and attention in adults with a history of childhood autism. *J. Neuropsychiatry Clin. Neurosci.* 4, 406–414. doi: 10.1176/jnp.4.4.406

Sieradzan, K. A., and Mann, D. M. (2001). The selective vulnerability of nerve cells in Huntington's disease [Review]. *Neuropathol. Appl. Neurobiol.* 27, 1–21.

Silva-Garcia, O., Valdez-Alarcon, J. J., and Baizabal-Aguirre, V. M. (2019). Wnt/beta-Catenin signaling as a molecular target by pathogenic bacteria. *Front. Immunol.* 10:2135. doi: 10.3389/fimmu.2019.02135

Simpson, I. A., Chundu, K., Davies-Hill, T., Honer, W., and Davies, P. (1994). Decreased concentrations of GLUT1 and GLUT3 glucose transporters in the brains of patients with Alzheimer's diseas. *Ann. Neurol.* 35, 546–551. doi: 10.1002/ana.410350507

Smith, A. J., and Verkman, A. S. (2018). The "glymphatic" mechanism for solute clearance in Alzheimer's disease: game changer or unproven speculation? *FASEB J.* 32, 543–551. doi: 10.1096/fj.201700999

Smith, C. D., Andersen, A. H., Kryscio, R. J., Schmitt, F. A., Kindy, M. S., Blonder, L. X., et al. (1999). Altered brain activation in cognitively intact individuals at high risk for Alzheimer's disease. *Neurology* 53, 581–595.

Smith, E. E., and Greenberg, S. M. (2009). Beta-amyloid, blood vessels, and brain function. *Stroke* 40, 2601–2606. doi: 10.1161/STROKEAHA.108.536839

Smith, E. E., Vijayappa, M., Lima, F., Delgado, P., Wendell, L., Rosand, J., et al. (2008). Impaired visual evoked flow velocity response in cerebral amyloid angiopathy. *Neurology* 71, 1424–1430. doi: 10.1212/01.wnl.0000327887.64299.a4

Smith, G. S., de Leon, M. J., George, A. E., Kluger, A., Volkow, N. D., McRae, T., et al. (1992). Topography of cross-sectional and longitudinal glucose metabolic deficits in Alzheimer's disease. *Arch. Neurol.* 49, 1142–1150. doi: 10.1001/archneur.1992.00530350056020

Snowden, J. S. (2017). The neuropsychology of Huntington's disease. *Arch. Clin. Neuropsychol.* 32, 876–887. doi: 10.1093/arclin/acx086

Solis, E. Jr., Hascup, K. N., and Hascup, E. R. (2020). Alzheimer's disease: the link between amyloid-beta and neurovascular dysfunction. *J. Alzheimers Dis.* 76, 1179–1198. doi: 10.3233/JAD-200473

Song, C., Schwarzkopf, D. S., Lutti, A., Li, B., Kanai, R., and Rees, G. (2013). Effective connectivity within human primary visual cortex predicts interindividual diversity in illusory perception. *J. Neurosci.* 33, 18781–18791. doi: 10.1523/JNEUROSCI.4201-12.2013

Soto-Rojas, L. O., Pacheco-Herrero, M., Martinez-Gomez, P. A., Campa-Cordoba, B. B., Apatiga-Perez, R., Villegas-Rojas, M. M., et al. (2021). The neurovascular unit dysfunction in Alzheimer's disease. *Int. J. Mol. Sci.* 22:2022. doi: 10.3390/ijms22042022

Sotrel, A., Paskevich, P. A., Kiely, D. K., Bird, E. D., Williams, R. S., and Myers, R. H. (1991). Morphometric analysis of the prefrontal cortex in Huntington's disease. *Neurology* 41, 1117–1123. doi: 10.1212/wnl.41.7.1117

Spuch, C., Antequera, D., Portero, A., Orive, G., Hernandez, R. M., Molina, J. A., et al. (2010). The effect of encapsulated VEGF-secreting cells on brain amyloid load and behavioral impairment in a mouse model of Alzheimer's disease [Research Support, Non-U.S. Gov't]. *Biomaterials* 31, 5608–5618. doi: 10.1016/j.biomaterials.2010.03.042

St-Amour, I., Aubé, B., Rieux, M., and Cicchetti, F. (2015). Targeting cerebrovascular impairments in Huntington's disease: a novel treatment perspective. *Future Med.* 5, 389–393. doi: 10.2217/nmt.15.41

Stachowiak, M. K., Kucinski, A., Curl, R., Syposs, C., Yang, Y., Narla, S., et al. (2013). Schizophrenia: a neurodevelopmental disorder — Integrative genomic hypothesis and therapeutic implications from a transgenic mouse model. *Schizophr. Res.* 143, 367–376. doi: 10.1016/j.schres.2012.11.004

Stackhouse, T. L., and Mishra, A. (2021). Neurovascular coupling in development and disease: focus on astrocytes. *Front. Cell Dev. Biol.* 9:702832. doi: 10.3389/fcell.2021.702832

Stamatovic, S., Keep, R., and Andjelkovic, A. (2008). Brain endothelial cell-cell junctions: how to "open" the blood brain barrier. *Curr. Neuropharmacol.* 6, 179–192. doi: 10.2174/157015908785777210

Starkstein, S., Gellar, S., Parlier, M., Payne, L., and Piven, J. (2015). High rates of parkinsonism in adults with autism. *J. Neurodev. Disord.* 7:29. doi: 10.1186/s11689-015-9125-6

Stegmayer, K., Strik, W., Federspiel, A., Wiest, R., Bohlhalter, S., and Walther, S. (2017). Specific cerebral perfusion patterns in three schizophrenia symptom dimensions. *Schizophr. Res.* 190, 96–101. doi: 10.1016/j.schres.2017.03.018

Steventon, J. J., Furby, H., Ralph, J., O'Callaghan, P., Rosser, A. E., Wise, R. G., et al. (2020). Altered cerebrovascular response to acute exercise in patients with Huntington's disease. *Brain Commun.* 2:fcaa044. doi: 10.1093/braincomms/fcaa044

Stone, J., Itin, A., Alon, T., Pe'er, J., Gnessin, H., Chan-Ling, T., et al. (1995). Development of retinal vasculature is mediated by hypoxia- induced vascular endothelial growth factor (VEGF) expression by neuroglia. *J. Neurosci.* 15, 4738–4747.

Storck, S. E., Meister, S., Nahrath, J., Meissner, J. N., Schubert, N., Di Spiezio, A., et al. (2016). Endothelial LRP1 transports amyloid-beta(1-42) across the blood-brain barrier. *J. Clin. Invest.* 126, 123–136. doi: 10.1172/JCI81108

Su, J. J., Osoegawa, M., Matsuoka, T., Minohara, M., Tanaka, M., Ishizu, T., et al. (2006). Upregulation of vascular growth factors in multiple sclerosis: correlation with MRI findings. *J. Neurol. Sci.* 243, 21–30. doi: 10.1016/j.jns.2005.11.006

Suo, Z., Humphrey, J., Kundtz, A., Sethi, F., Placzek, A., Crawford, F., et al. (1998). Soluble Alzheimers beta-amyloid constricts the cerebral vasculature in vivo. *Neurosci. Lett.* 257, 77–80. doi: 10.1016/s0304-3940(98)00814-3

Suri, S., Mackay, C. E., Kelly, M. E., Germuska, M., Tunbridge, E. M., Frisoni, G. B., et al. (2015). Reduced cerebrovascular reactivity in young adults carrying the APOE epsilon4 allele. *Alzheimers Dement.* 11, 648–657 e641. doi: 10.1016/j.jalz.2014.05.1755

Sweeney, M. D., Kisler, K., Montagne, A., Toga, A. W., and Zlokovic, B. V. (2018). The role of brain vasculature in neurodegenerative disorders. *Nat. Neurosci.* 21, 1318–1331. doi: 10.1038/s41593-018-0234-x

Sweeney, M. D., Montagne, A., Sagare, A. P., Nation, D. A., Schneider, L. S., Chui, H. C., et al. (2019). Vascular dysfunction-The disregarded partner of Alzheimer's disease. *Alzheimers Dement.* 15, 158–167. doi: 10.1016/j.jalz.2018.07.222

Switzer, A. R., Cheema, I., McCreary, C. R., Zwiers, A., Charlton, A., Alvarez-Veronesi, A., et al. (2020). Cerebrovascular reactivity in cerebral amyloid angiopathy, Alzheimer disease, and mild cognitive impairment. *Neurology* 95, e1333–e1340. doi: 10.1212/WNL.0000000000010201

Syrimi, Z. J., Vojtisek, L., Eliasova, I., Viskova, J., Svatkova, A., Vanicek, J., et al. (2017). Arterial spin labelling detects posterior cortical hypoperfusion in non-demented patients with Parkinson's disease. *J. Neural Transm. (Vienna)* 124, 551–557. doi: 10.1007/s00702-017-1703-1

Szu, J. I., and Obenaus, A. (2021). Cerebrovascular phenotypes in mouse models of Alzheimer's disease. *J. Cereb. Blood Flow Metab.* 41, 1821–1841. doi: 10.1177/0271678X21992462

Tai, L. M., Holloway, K. A., Male, D. K., Loughlin, A. J., and Romero, I. A. (2010). Amyloid-beta-induced occludin down-regulation and increased permeability in human brain endothelial cells is mediated by MAPK activation. *J. Cell. Mol. Med.* 14, 1101–1112. doi: 10.1111/j.1582-4934.2009.00717.x

Tan, K. H., Harrington, S., Purcell, W. M., and Hurst, R. D. (2004). Peroxynitrite mediates nitric oxide–induced blood–brain barrier damage. *Neurochem. Res.* 29, 579–587. doi: 10.1023/b:nere.0000014828.32200.bd

Taoufik, E., Kouroupi, G., Zygogianni, O., and Matsas, R. (2018). Synaptic dysfunction in neurodegenerative and neurodevelopmental diseases: an overview of induced pluripotent stem-cell-based disease models. *Open Biol.* 8:180138. doi: 10.1098/rsob.180138

Tarlungeanu, D. C., Deliu, E., Dotter, C. P., Kara, M., Janiesch, P. C., Scalise, M., et al. (2016). Impaired amino acid transport at the blood brain barrier is a cause of autism spectrum disorder. *Cell* 167, 1481–1494 e1418. doi: 10.1016/j.cell.2016.11.013

Tata, M., and Ruhrberg, C. (2018). Cross-talk between blood vessels and neural progenitors in the developing brain. *Neuronal Signal.* 2:NS20170139. doi: 10.1042/NS20170139

Tata, M., Ruhrberg, C., and Fantin, A. (2015). Vascularisation of the central nervous system. *Mech. Dev.* 138(Pt 1), 26–36. doi: 10.1016/j.mod.2015.07.001

Thal, D. R., Capetillo-Zarate, E., Larionov, S., Staufenbiel, M., Zurbruegg, S., and Beckmann, N. (2009). Capillary cerebral amyloid angiopathy is associated with vessel occlusion and cerebral blood flow disturbances. *Neurobiol. Aging* 30, 1936–1948. doi: 10.1016/j.neurobiolaging.2008.01.017

Thambisetty, M., Beason-Held, L., An, Y., Kraut, M. A., and Resnick, S. M. (2010). APOE epsilon4 genotype and longitudinal changes in cerebral blood flow in normal aging. *Arch. Neurol.* 67, 93–98. doi: 10.1001/archneurol.2009.913

Thomas, T., Thomas, G., McLendon, C., Sutton, T., and Mullan, M. (1996). β-Amyloid-mediated vasoactivity and vascular endothelial damage. *Nature* 380, 168–171. doi: 10.1038/380168a0

Tong, X. K., Nicolakakis, N., Kocharyan, A., and Hamel, E. (2005). Vascular remodeling versus amyloid beta-induced oxidative stress in the cerebrovascular dysfunctions associated with Alzheimer's disease. *J. Neurosci* 25, 11165–11174.

Tong, Y., Hocke, L. M., and Frederick, B. B. (2019). Low frequency systemic hemodynamic "noise" in resting state BOLD fMRI: characteristics, causes, implications, mitigation strategies, and applications. *Front. Neurosci.* 13:787. doi: 10.3389/fnins.2019.00787

Tosh, J. L., Rhymes, E. R., Mumford, P., Whittaker, H. T., Pulford, L. J., Noy, S. J., et al. (2021). Genetic dissection of down syndrome-associated alterations in APP/amyloid-beta biology using mouse models. *Sci. Rep.* 11:5736. doi: 10.1038/s41598-021-85062-3

Trapp, B. D., and Stys, P. K. (2009). Virtual hypoxia and chronic necrosis of demyelinated axons in multiple sclerosis. *Lancet Neurol.* 8, 280–291. doi: 10.1016/S1474-4422(09)70043-2

Tregellas, J. R., Davalos, D. B., Rojas, D. C., Waldo, M. C., Gibson, L., Wylie, K., et al. (2007). Increased hemodynamic response in the hippocampus, thalamus and prefrontal cortex during abnormal sensory gating in schizophrenia. *Schizophr. Res.* 92, 262–272. doi: 10.1016/j.schres.2006.12.033

Turner, R. J., and Sharp, F. R. (2016). Implications of MMP9 for blood brain barrier disruption and hemorrhagic transformation following ischemic stroke. *Front. Cell. Neurosci.* 10:56. doi: 10.3389/fncel.2016.00056

Uranova, N. A., Zimina, I. S., Vikhreva, O. V., Krukov, N. O., Rachmanova, V. I., and Orlovskaya, D. D. (2010). Ultrastructural damage of capillaries in the neocortex in schizophrenia. *World J. Biol. Psychiatry* 11, 567–578. doi: 10.3109/15622970903414188

Uratani, M., Ota, T., Iida, J., Okazaki, K., Yamamuro, K., Nakanishi, Y., et al. (2019). Reduced prefrontal hemodynamic response in pediatric autism spectrum disorder measured with near-infrared spectroscopy. *Child Adolesc. Psychiatry Ment. Health* 13:29. doi: 10.1186/s13034-019-0289-9

Usta, A., Kilic, F., Demirdas, A., Isik, U., Doguc, D. K., and Bozkurt, M. (2021). Serum zonulin and claudin-5 levels in patients with schizophrenia. *Eur. Arch. Psychiatry Clin. Neurosci.* 271, 767–773. doi: 10.1007/s00406-020-01152-9

van de Haar, H., Burgmans, S., Jansen, J., van Osch, M., van Buchem, M., Muller, M., et al. (2016). Blood-Brain barrier leakage in patients with early Alzheimer disease. *Radiology* 281, 527–535. doi: 10.1148/radiol.2016152244

Van Dyken, P., and Lacoste, B. (2018). Impact of metabolic syndrome on neuroinflammation and the blood–brain barrier. *Front. Neurosci.* 12:930. doi: 10.3389/fnins.2018.00930

Varga, A. W., Johnson, G., Babb, J. S., Herbert, J., Grossman, R. I., and Inglese, M. (2009). White matter hemodynamic abnormalities precede sub-cortical gray matter changes in multiple sclerosis. *J. Neurol. Sci.* 282, 28–33. doi: 10.1016/j.jns.2008.12.036

Verstraeten, A., Theuns, J., and Van Broeckhoven, C. (2015). Progress in unraveling the genetic etiology of Parkinson disease in a genomic era. *Trends Genet.* 31, 140–149. doi: 10.1016/j.tig.2015.01.004

Vijayakumar, N. T., and Judy, M. V. (2016). Autism spectrum disorders: integration of the genome, transcriptome and the environment. *J. Neurol. Sci.* 364, 167–176. doi: 10.1016/j.jns.2016.03.026

Vinters, H. V., Secor, D. L., Read, S. L., Frazee, J. G., Tomiyasu, U., Stanley, T. M., et al. (1994). Microvasculature in brain biopsy specimens from patients with Alzheimer's disease: an immunohistochemical and ultrastructural study [Research Support, U.S. Gov't, P.H.S.]. *Ultrastruct. Pathol.* 18, 333–348.

Vostrikov, V., Orlovskaya, D. D., and Uranova, N. A. (2008). Deficit of pericapillary oligodendrocytes in the prefrontal cortex in schizophrenia. *World J. Biol. Psychiatry* 9, 34–42. doi: 10.1080/15622970701210247

Wada, K., Arai, H., Takahashi, M., Fukae, J., Oizumi, H., Yasuda, T., et al. (2006). Expression levels of vascular endothelial growth factor and its receptors in Parkinson's disease. *Neuroreport* 17, 705–709. doi: 10.1097/01.wnr.0000215769.71657.65

Walchli, T., Wacker, A., Frei, K., Regli, L., Schwab, M. E., Hoerstrup, S. P., et al. (2015). Wiring the vascular network with neural cues: a CNS perspective. *Neuron* 87, 271–296. doi: 10.1016/j.neuron.2015.06.038

Walker, F. O. (2007). Huntington's disease [Review]. *Lancet* 369, 218–228. doi: 10.1016/S0140-6736(07)60111-1

Wan, W., Cao, L., Liu, L., Zhang, C., Kalionis, B., Tai, X., et al. (2015). Abeta(1-42) oligomer-induced leakage in an in vitro blood-brain barrier model is associated with up-regulation of RAGE and metalloproteinases, and down-regulation of tight junction scaffold proteins. *J. Neurochem.* 134, 382–393. doi: 10.1111/jnc.13122

Wang, T., Zhan, W., Chen, Q., Chen, N., Zhang, J., Liu, Q., et al. (2016). Altered resting-state ascending/descending pathways associated with the posterior thalamus in migraine without aura. *Neuroreport* 27, 257–263. doi: 10.1097/WNR.0000000000000529

Wardlaw, J. M., Farrall, A., Armitage, P. A., Carpenter, T., Chappell, F., Doubal, F., et al. (2008). Changes in background blood-brain barrier integrity between lacunar and cortical ischemic stroke subtypes. *Stroke* 39, 1327–1332. doi: 10.1161/STROKEAHA.107.500124

Wasmuth, J. J., Hewitt, J., Smith, B., Allard, D., Haines, J. L., Skarecky, D., et al. (1988). A highly polymorphic locus very tightly linked to the Huntington's disease gene [Research Support, Non-U.S. Gov't Research Support, U.S. Gov't, P.H.S.]. *Nature* 332, 734–736. doi: 10.1038/332734a0

Watanabe, C., Imaizumi, T., Kawai, H., Suda, K., Honma, Y., Ichihashi, M., et al. (2020). Aging of the vascular system and neural diseases. *Front. Aging Neurosci.* 12:557384. doi: 10.3389/fnagi.2020.557384

Watson, A. N., Berthiaume, A.-A., Faino, A. V., McDowell, K. P., Bhat, N. R., Hartmann, D. A., et al. (2020). Mild pericyte deficiency is associated with aberrant brain microvascular flow in aged PDGFRβ+/- mice. *J. Cereb. Blood Flow Metab.* 40, 2387–2400. doi: 10.1177/0271678X19900543

Weiss, N., Miller, F., Cazaubon, S., and Couraud, P. O. (2009). The blood-brain barrier in brain homeostasis and neurological diseases. *Biochim. Biophys. Acta* 1788, 842–857. doi: 10.1016/j.bbamem.2008.10.022

Whiteus, C., Freitas, C., and Grutzendler, J. (2014). Perturbed neural activity disrupts cerebral angiogenesis during a postnatal critical period. *Nature* 505, 407–411. doi: 10.1038/nature12821

Wild, E. J., and Fox, N. C. (2009). Serial volumetric MRI in Parkinsonian disorders. *Mov. Disord.* 24(Suppl. 2), S691–S698. doi: 10.1002/mds.22500

Willis, K. J., and Hakim, A. M. (2013). Stroke prevention and cognitive reserve: emerging approaches to modifying risk and delaying onset of dementia. *Front. Neurol.* 4:13. doi: 10.3389/fneur.2013.00013

Wiseman, F. K., Pulford, L. J., Barkus, C., Liao, F., Portelius, E., Webb, R., et al. (2018). Trisomy of human chromosome 21 enhances amyloid-beta deposition independently of an extra copy of APP. *Brain* 141, 2457–2474. doi: 10.1093/brain/awy159

Wolf, R. C., Gron, G., Sambataro, F., Vasic, N., Wolf, N. D., Thomann, P. A., et al. (2011). Magnetic resonance perfusion imaging of resting-state cerebral blood flow in preclinical Huntington's disease. *J. Cereb. Blood Flow Metab.* 31, 1908–1918. doi: 10.1038/jcbfm.2011.60

Wu, Z., Guo, H., Chow, N., Sallstrom, J., Bell, R. D., Deane, R., et al. (2005). Role of the MEOX2 homeobox gene in neurovascular dysfunction in Alzheimer disease. *Nat. Med.* 11, 959–965. doi: 10.1038/nm1287

Wuerfel, J., Bellmann-Strobl, J., Brunecker, P., Aktas, O., McFarland, H., Villringer, A., et al. (2004). Changes in cerebral perfusion precede plaque formation in multiple sclerosis: a longitudinal perfusion MRI study. *Brain* 127(Pt 1), 111–119. doi: 10.1093/brain/awh007

Xiao, M., Xiao, Z. J., Yang, B., Lan, Z., and Fang, F. (2020). Blood-Brain barrier: more contributor to disruption of central nervous system homeostasis than victim in neurological disorders. *Front. Neurosci.* 14:764. doi: 10.3389/fnins.2020.00764

Yamada, H., Sadato, N., Konishi, Y., Muramuto, S., Kimura, K., Tanaka, M., et al. (2000). A milestone for normal development of the infantile brain detected by functional MRI. *Neurology* 55, 218–223.

Yang, P., Pavlovic, D., Waldvogel, H., Dragunow, M., Synek, B., Turner, C., et al. (2015). String vessel formation is increased in the brain of Parkinson disease. *J. Parkinsons Dis.* 5, 821–836. doi: 10.3233/JPD-140454

Yerys, B. E., Herrington, J. D., Bartley, G. K., Liu, H. S., Detre, J. A., and Schultz, R. T. (2018). Arterial spin labeling provides a reliable neurobiological marker of autism spectrum disorder. *J. Neurodev. Disord.* 10:32. doi: 10.1186/s11689-018-9250-0

Zarow, C., Barron, E., Chui, H. C., and Perlmutter, L. S. (1997). Vascular basement membrane pathology and Alzheimer's disease. *Ann. N. Y. Acad. Sci.* 826, 147–160.

Zhang, Z. G., Zhang, L., Jiang, Q., Zhang, R., Davies, K., Powers, C., et al. (2000). VEGF enhances angiogenesis and promotes blood-brain barrier leakage in the ischemic brain. *J. Clin. Invest.* 106, 829–838. doi: 10.1172/JCI9369

Zhao, Z., Sagare, A. P., Ma, Q., Halliday, M. R., Kong, P., Kisler, K., et al. (2015). Central role for PICALM in amyloid-beta blood-brain barrier transcytosis and clearance. *Nat. Neurosci.* 18, 978–987. doi: 10.1038/nn.4025

Zheng, W., Cui, B., Han, Y., Song, H., Li, K., He, Y., et al. (2019). Disrupted regional cerebral blood flow, functional activity and connectivity in Alzheimer's disease:

a combined ASL perfusion and resting state fMRI Study. *Front. Neurosci.* 13:738. doi: 10.3389/fnins.2019.00738

Zheng, Z., and Diamond, M. I. (2012). Huntington disease and the huntingtin protein [Review]. *Prog. Mol. Biol. Transl. Sci.* 107, 189–214. doi: 10.1016/B978-0-12-385883-2.00010-2

Zhu, J., Zhuo, C., Xu, L., Liu, F., Qin, W., and Yu, C. (2017). Altered coupling between resting-state cerebral blood flow and functional connectivity in schizophrenia. *Schizophr. Bull.* 43, 1363–1374. doi: 10.1093/schbul/sbx051

Zhuo, C., Zhu, J., Qin, W., Qu, H., Ma, X., and Yu, C. (2017). Cerebral blood flow alterations specific to auditory verbal hallucinations in schizophrenia. *Br. J. Psychiatry* 210, 209–215. doi: 10.1192/bjp.bp.115.174961

Zilbovicius, M., Boddaert, N., Belin, P., Poline, J.-B., Remy, P., Mangin, J.-F., et al. (2000). Temporal lobe dysfunction in childhood autism: a PET study. *Am. J. Psychiatry* 157, 1988–1993.

Zlokovic, B. V. (2005). Neurovascular mechanisms of Alzheimer's neurodegeneration. *Trends Neurosci.* 28, 202–208. doi: 10.1016/j.tins.2005.02.001

Zlokovic, B. V. (2008). The blood-brain barrier in health and chronic neurodegenerative disorders. *Neuron* 57, 178–201. doi: 10.1016/j.neuron.2008.01.003

Zlokovic, B. V. (2011). Neurovascular pathways to neurodegeneration in Alzheimer's disease and other disorders. *Nat. Rev. Neurosci.* 12, 723–738. doi: 10.1038/nrn3114

Conflict of Interest: The authors declare that the research was conducted in the absence of any commercial or financial relationships that could be construed as a potential conflict of interest.

Publisher's Note: All claims expressed in this article are solely those of the authors and do not necessarily represent those of their affiliated organizations, or those of the publisher, the editors and the reviewers. Any product that may be evaluated in this article, or claim that may be made by its manufacturer, is not guaranteed or endorsed by the publisher.

frontiers in Aging Neuroscience

REVIEW
published: 16 November 2021
doi: 10.3389/fnagi.2021.772278

Carbonic Anhydrases as Potential Targets Against Neurovascular Unit Dysfunction in Alzheimer's Disease and Stroke

*Nicole Lemon[1], Elisa Canepa[1], Marc A. Ilies[1,2] and Silvia Fossati[1]**

[1] *Alzheimer's Center at Temple (ACT), Lewis Katz School of Medicine, Temple University, Philadelphia, PA, United States,* [2] *Department of Pharmaceutical Sciences and Moulder Center for Drug Discovery Research, Temple University School of Pharmacy, Temple University, Philadelphia, PA, United States*

The Neurovascular Unit (NVU) is an important multicellular structure of the central nervous system (CNS), which participates in the regulation of cerebral blood flow (CBF), delivery of oxygen and nutrients, immunological surveillance, clearance, barrier functions, and CNS homeostasis. Stroke and Alzheimer Disease (AD) are two pathologies with extensive NVU dysfunction. The cell types of the NVU change in both structure and function following an ischemic insult and during the development of AD pathology. Stroke and AD share common risk factors such as cardiovascular disease, and also share similarities at a molecular level. In both diseases, disruption of metabolic support, mitochondrial dysfunction, increase in oxidative stress, release of inflammatory signaling molecules, and blood brain barrier disruption result in NVU dysfunction, leading to cell death and neurodegeneration. Improved therapeutic strategies for both AD and stroke are needed. Carbonic anhydrases (CAs) are well-known targets for other diseases and are being recently investigated for their function in the development of cerebrovascular pathology. CAs catalyze the hydration of CO_2 to produce bicarbonate and a proton. This reaction is important for pH homeostasis, overturn of cerebrospinal fluid, regulation of CBF, and other physiological functions. Humans express 15 CA isoforms with different distribution patterns. Recent studies provide evidence that CA inhibition is protective to NVU cells *in vitro* and *in vivo*, in models of stroke and AD pathology. CA inhibitors are FDA-approved for treatment of glaucoma, high-altitude sickness, and other indications. Most FDA-approved CA inhibitors are pan-CA inhibitors; however, specific CA isoforms are likely to modulate the NVU function. This review will summarize the literature regarding the use of pan-CA and specific CA inhibitors along with genetic manipulation of specific CA isoforms in stroke and AD models, to bring light into the functions of CAs in the NVU. Although pan-CA inhibitors are protective and safe, we hypothesize that targeting specific CA isoforms will increase the efficacy of CA inhibition and reduce side effects. More studies to further determine specific CA isoforms functions and changes in disease states are essential to the development of novel therapies for cerebrovascular pathology, occurring in both stroke and AD.

Keywords: Alzheimer's disease, stroke, carbonic anhydrase (CA), neurovascular unit (NVU), cerebrovascular pathology, amyloid beta, inflammation, mitochondria

OPEN ACCESS

Edited by:
Cheryl Hawkes,
Lancaster University, United Kingdom

Reviewed by:
Fabrizio Carta,
University of Florence, Italy
Yoon Kyung Choi,
Konkuk University, South Korea

****Correspondence:***
Silvia Fossati
silvia.fossati@temple.edu

Received: *07 September 2021*
Accepted: *20 October 2021*
Published: *16 November 2021*

Citation:
Lemon N, Canepa E, Ilies MA and Fossati S (2021) Carbonic Anhydrases as Potential Targets Against Neurovascular Unit Dysfunction in Alzheimer's Disease and Stroke. Front. Aging Neurosci. 13:772278. doi: 10.3389/fnagi.2021.772278

INTRODUCTION

Neurovascular dysfunction is an important, early and causative event in the pathogenesis of both Alzheimer's disease (AD) and Stroke (Iadecola, 2010, 2017; Hachinski et al., 2019; Sweeney et al., 2019a; Freitas-Andrade et al., 2020; Zlokovic et al., 2020). Indeed, the Neurovascular Unit (NVU) has recently gained a lot of momentum as a pharmacological target in cerebrovascular pathologies and neurodegeneration (Iadecola, 2017; Sweeney et al., 2019a; Zlokovic et al., 2020). The NVU is a functional multicellular structure composed of blood vessels and different cell types surrounding them within the central nervous system (CNS), and is instrumental in regulating CNS homeostasis (Andreone et al., 2015; Iadecola, 2017; Sweeney et al., 2019b; Freitas-Andrade et al., 2020). Important functions of the NVU include regulation of cerebral blood flow (CBF) and immunological surveillance, amongst others (Andreone et al., 2015; Cortes-Canteli and Iadecola, 2020; Freitas-Andrade et al., 2020). NVU dysfunction is observed in aging, AD and following neurological pathologies such as stroke (Iadecola, 2017; Cortes-Canteli and Iadecola, 2020; Freitas-Andrade et al., 2020; Sarvari et al., 2020) and traumatic brain injury (Xing et al., 2012; Lok et al., 2015), among others.

Stroke and dementia are the two most common neurological disorders. They confer risks for each other and share some, mostly modifiable, risk factors. Having a stroke doubles the chance of developing dementia (Savva and Stephan, 2010; Kuźma et al., 2018). Therefore, preventing stroke through management of hypertension and other risk factors could also decrease the incidence of dementia (Kuźma et al., 2018; Hachinski et al., 2019).

AD is the most common form of dementia and has been historically characterized by extracellular amyloid beta (Aβ) plaques and intracellular hyperphosphorylated tau tangles in specific brain regions (Day et al., 2015; Castillo-Carranza et al., 2017; Cortes-Canteli and Iadecola, 2020; Ojo et al., 2021). Interestingly, Aβ and tau intermediate aggregation species, such as oligomers, have been shown to have toxic effects on multiple cell types of the NVU (Fossati et al., 2010, 2012b; Parodi-Rullán et al., 2019; Canepa and Fossati, 2020). This toxicity, in association with the contribution of impaired clearance of undesired material from the brain, may lead to neurodegeneration and cognitive decline (Fossati et al., 2012b; Boland et al., 2018; Da Mesquita et al., 2018; Nortley et al., 2019; Provensi et al., 2019; Braun and Iliff, 2020; Carare et al., 2020; Cortes-Canteli and Iadecola, 2020; Nedergaard and Goldman, 2020; Parodi-Rullán et al., 2020; Quintana et al., 2021). Importantly, up to 90% of AD patients also present with cerebral amyloid angiopathy (CAA), defined as Aβ deposition around the brain vasculature and/or within the vessel walls (Iadecola, 2017; Sweeney et al., 2019a; Zlokovic et al., 2020). CAA is also common in the non-demented elderly population and constitutes an important contributor to NVU dysfunction in both normal aging and AD (Provensi et al., 2019; Cortes-Canteli and Iadecola, 2020; Ojo et al., 2021).

Stroke is classically defined as a neurological damage attributed to an acute focal injury of the CNS by a vascular cause, including cerebral infarction, intracerebral hemorrhage (ICH), and subarachnoid hemorrhage (SAH), and is a major cause of disability and death worldwide (Sacco et al., 2013). The most common type of stroke is Ischemic Stroke (IS) which occurs when atherosclerotic plaques and fatty deposits cause vascular occlusions, interrupting blood flow in the brain. The blood vessel most commonly occluded is the middle cerebral artery (Kuriakose and Xiao, 2020). When IS occurs, it promptly causes multiple detrimental cerebral injuries due to both the lack of oxygen and glucose, as well as the associated pro-inflammatory signaling (Faraco et al., 2007; Freitas-Andrade et al., 2020; Kuriakose and Xiao, 2020; Sarvari et al., 2020). Following this event, there is a reperfusion injury phase, which occurs when oxygen and CBF are restored (Faraco et al., 2007; Freitas-Andrade et al., 2020; Sarvari et al., 2020). Another type of stroke is hemorrhagic stroke (HS), which occurs when a blood vessel, providing blood to the brain, ruptures (Corraini et al., 2017; Sarvari et al., 2020). HS is characterized by greater lesion volume, higher intracranial pressure and induce more severe brain injury than IS. Importantly, IS and HS affect different brain regions (Corraini et al., 2017).

Shared risk factors between AD and stroke are reduced CBF, cardiovascular diseases and age (Sarvari et al., 2020; Ojo et al., 2021). Cardiovascular risk factors like obesity, diabetes, hypertension and atherosclerosis have been observed to exacerbate cerebrovascular pathology as well as neurodegeneration, including AD (Girouard and Iadecola, 2006; de Bruijn and Ikram, 2014; Cortes-Canteli and Iadecola, 2020; Sarvari et al., 2020). The common underlying mechanisms involved in both AD and stroke include neuroinflammation, mitochondrial dysfunction, cell death, and blood brain barrier (BBB) dysregulation, indicating that the NVU is a target for both diseases (Fossati et al., 2012b; Alluri et al., 2014; Sekerdag et al., 2018; Eldahshan et al., 2019; Provensi et al., 2019; Parodi-Rullán et al., 2020). A vast amount of research has been invested into discovering new treatments for AD and stroke. In AD, this has recently led to the controversial FDA-approval of aducanumab (Ferrero et al., 2016; Sevigny et al., 2017; Knopman et al., 2021). However, more research needs to be done to develop successful disease-modifying therapies for both disorders. The scientific community is particularly encouraging the study of repurposed drugs, approved by the FDA for other disorders, which could be beneficial for AD and stroke, while allowing more rapid translation to clinical trials.

This review will introduce the idea of potentially repurposing carbonic anhydrase inhibitors (CAIs), many of which are already FDA-approved for other indications, for prevention of cerebrovascular and neurovascular pathology in AD and stroke and highlight the impact of carbonic anhydrase (CA) modulation in these two dominant neurological disorders.

CAs are a family of zinc metalloenzymes which catalyze the reversible hydration of carbon dioxide to produce bicarbonate and a proton ($CO_2 + H_2O \leftrightarrow HCO_3^- + H^+$) (Supuran, 2011; Mishra et al., 2020). This chemical reaction is essential for many physiological processes, such as pH and ion homeostasis, carbon dioxide transport, electrolyte secretion, gluconeogenesis, lipogenesis, and ureagenesis, water and sodium reabsorption in the kidney, bone reabsorption and calcification, cerebrospinal

fluid formation and turnover, amongst other processes (Provensi et al., 2019; Zamanova et al., 2019; Mishra et al., 2020). CAs have been studied as a well-known pharmacological target for many peripheral and CNS disorders (Bradwell et al., 1992; Ilies et al., 2004; De Simone and Supuran, 2007; Supuran, 2008, 2018; Akocak and Ilies, 2014; Provensi et al., 2019; Zamanova et al., 2019; Mishra et al., 2020). Interestingly, many recent studies revealed a common goal to further elucidate CAs involvement in both AD and stroke.

Humans have 15 CA isoforms, all with different expression patterns at a tissue and cellular level (Supuran, 2011; Provensi et al., 2019; Zamanova et al., 2019; Mishra et al., 2020). Many of these isoforms are expressed within the NVU and it has been hypothesized that each is involved in different functions (Draghici et al., 2014; Rasmussen and Boedtkjer, 2018; Provensi et al., 2019; Zamanova et al., 2019). It is known that some isoforms are extracellular, anchored to the plasma membrane (CA-IV, CA-IX, and CA-XII, CA-XIV), while others are cytosolic (CA-I, CA-II, CA-III, CA-VII, CA-XIII), two are found in the mitochondria (CA-VA and CA-VB) (Boriack-Sjodin et al., 1995; Nishimori et al., 2005), some are acatalytic isoforms (CA-VIII, CA-X, and CA-XI) (Aspatwar et al., 2014), and one isoform is secreted in saliva (CA-VI) (Nishimori et al., 2007; Alterio et al., 2012; Patrikainen et al., 2014; Provensi et al., 2019; Zamanova et al., 2019; Mishra et al., 2020). CA function has been linked to AD pathology as well as stroke, but the specific isoforms and the pathological mechanisms involved are not fully understood (Wang et al., 2009; Draghici et al., 2014; Fossati et al., 2016; Pollard et al., 2016; Solesio et al., 2018; Mishra et al., 2020). The determination of each CA isoforms' role in health and disease should be a priority for the development of novel and effective therapies in cerebrovascular pathology (Provensi et al., 2019; Mishra et al., 2020).

CAIs were developed first as diuretics and have become valuable in treating glaucoma, cerebral edema, epilepsy, as well as high altitude sickness (Mincione et al., 2007; Supuran, 2008; Ritchie et al., 2012; Akocak and Ilies, 2014; Zamanova et al., 2019; Mishra et al., 2020). The FDA-approved CAIs methazolamide (MTZ) and acetazolamide (ATZ) are the most studied pan-CAIs. Their activity in the NVU will be one of the focuses of this review. Other FDA-approved CAIs such as topiramate, which has some selectivity for the mitochondrial CA-VA and CA-VB isoforms, along with compounds with selectivity for CA-IX and CA-XII will also be discussed (Scozzafava et al., 2000; Supuran, 2012; Andring et al., 2020; McDonald et al., 2020). MTZ and ATZ, along with topiramate, have been observed to have protective properties on cerebrovascular pathology, as well as on mitochondria function, an important target for NVU integrity (Wang et al., 2009; Price et al., 2012; Fossati et al., 2016; Solesio et al., 2018; Salameh et al., 2019). A substantial amount of literature on the FDA-approved pan-CAIs indicates that they are safe and can pass the BBB. However, the development of new compounds targeting specific isoforms may improve the efficacy and reduce side effects of the already existing pan-CAIs (Provensi et al., 2019; Mishra et al., 2020).

This review will first illustrate the basic structure and functions of the cells composing the NVU, specifically describing how they become dysfunctional in stroke and AD. We will then discuss the properties of multiple CA isoforms and highlight the available evidence showing how CA inhibition may be protective toward multiple dysregulated mechanisms in NVU-composing cells, pointing to CAs as potential targets for both stroke and AD therapy (Provensi et al., 2019; Mishra et al., 2020).

THE NEUROVASCULAR UNIT: FUNCTION AND DYSFUNCTION IN STROKE AND ALZHEIMER'S DISEASE

The Neurovascular Unit

The cell types that constitute the NVU (depicted in **Figure 1**) and collaborate to perform its functions are endothelial cells (ECs), pericytes, smooth muscle cells (SMCs), astrocytes, and microglia (Iadecola, 2017; Freitas-Andrade et al., 2020), which are functionally or physically connected to neurons (Andreone et al., 2015; Cortes-Canteli and Iadecola, 2020; Freitas-Andrade et al., 2020). The NVU is the morpho-functional unit including the BBB, which is important for the transport of nutrients and oxygen from the systemic circulation to the brain, for the clearance of toxic waste from the CNS, for the connection between blood flow and neuronal function, as well as for forming a physical barrier to prevent the entrance of pathogens and other harmful entities into the CNS (Sarvari et al., 2020).

Endothelial Cells

ECs are essential components of the blood vessel wall. Cerebrovascular ECs form tight and adherent junctions with each other to limit the entry of molecules and cells from the peripheral circulation into the CNS (Reese and Karnovsky, 1967). Transporters expressed on the plasma membrane of ECs specifically regulate what enters and exits the CNS. For example, glucose enters the brain exclusively via transporters, despite the brain being a highly metabolic organ responsible for up to 25% of total glucose consumption in the body (Tang et al., 2017; Parodi-Rullán et al., 2019). ECs also regulate blood flow by releasing vasodilators and vasoconstrictors, such as nitric oxide (NO) and endothelin-1, respectively (Morikawa et al., 1994; Biernaskie et al., 2001; Freitas-Andrade et al., 2020). Due to the fact that mitochondria are very abundant in cerebrovascular ECs (Oldendorf et al., 1977; Sarvari et al., 2020), these cells are particularly sensitive to oxygen deprivation (Pun et al., 2009; Freitas-Andrade et al., 2020). Hence, pathological conditions which cause oxygen-glucose deprivation (OGD) and prompt excessive reactive oxygen species (ROS) production trigger cerebral endothelial dysfunction, cell death and BBB breakdown (Schreibelt et al., 2007; Pun et al., 2009; Lochhead et al., 2010; Ghiso et al., 2014; Fossati et al., 2016; Parodi-Rullán et al., 2019; Freitas-Andrade et al., 2020), pointing to the mitochondria as critical targets for EC function and BBB integrity. Efficient communication and exchange of materials between ECs and other cell types of the NVU is essential for CNS homeostasis (Andreone et al., 2015; Freitas-Andrade et al., 2020; Sarvari et al., 2020).

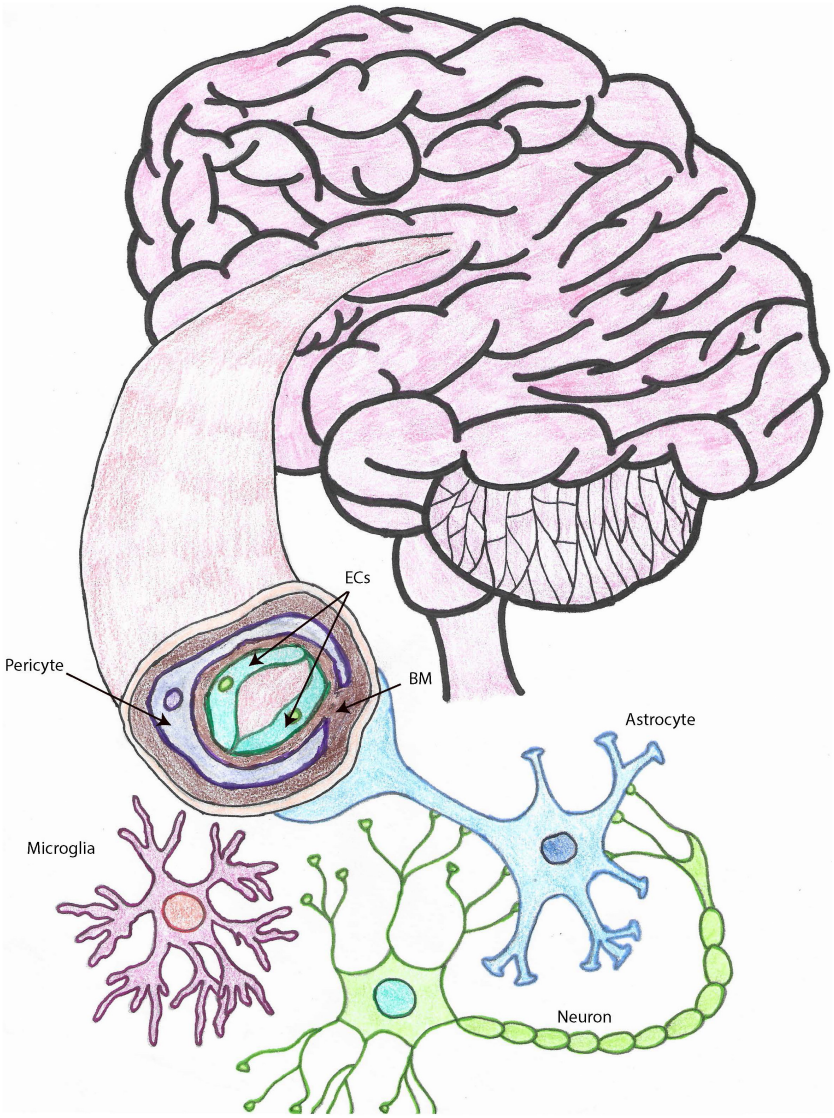

FIGURE 1 | The neurovascular unit. Drawing depicting the cell types that make up the NVU within brain capillaries. Brain capillaries are surrounded by pericytes, as shown in this figure, while arteries and arterioles are surrounded by SMCs. Other important cells associated with blood vessels and important for BBB and neurovascular functions, also represented in this drawing, are astrocytes and microglia. ECs, endothelial cells; SMCs, smooth muscle cells; BBB, blood brain barrier; NVU, neurovascular unit; MCs, microglia cells, BM, basement membrane.

Cerebrovascular dysfunction has been observed in both AD and IS (Fossati et al., 2010, 2012a,b; Guo et al., 2010; Lochhead et al., 2010; Jiao et al., 2011; Shin et al., 2016; Freitas-Andrade et al., 2020; Parodi-Rullán et al., 2020; Quintana et al., 2021). Aging, as well as cardiovascular risk factors, such as hypertension and diabetes, contribute to cerebrovascular pathology (Huang et al., 1995; Girouard and Iadecola, 2006; Price et al., 2012; Cortes-Canteli and Iadecola, 2020; Ojo et al., 2021). The reduction of tight junction proteins such as zona occludin-1 (ZO-1) and occludin is observed in models of stroke and AD (Marco and Skaper, 2006; Jiao et al., 2011; Engelhardt et al., 2014; Freitas-Andrade et al., 2020; Parodi-Rullán et al., 2020). An increase in adhesion molecules expression, such as intercellular adhesion molecule-1 (ICAM-1) and vascular cell adhesion molecule-1 (VCAM-1), is observed in stroke, and recently, has been also associated with AD (Cruz Hernández et al., 2019; Sarvari et al., 2020). The reduction of tight junction proteins and the increase in adhesion molecules triggers the recruitment of peripheral immune cells into the brain and may be due to endothelial activation by danger associated molecular patterns (DAMPs), such as low glucose and oxygen, and aggregated proteins, like Aβ and hyperphosphorylated tau (Canepa and Fossati, 2020; Freitas-Andrade et al., 2020; Sarvari et al., 2020). An increase in BBB permeability allows peripheral substances to enter the CNS, leading to neuroinflammation and oxidative stress (Pun et al., 2009; Turner and Sharp, 2016; Yang et al., 2019). Increased

oxidative stress in ECs exacerbates mitochondrial dysfunction, leading to apoptosis (Lochhead et al., 2010; Fossati et al., 2012b, 2016; Solesio et al., 2018; Parodi-Rullán et al., 2019). During both ischemic injury and AD, ECs have been observed to decrease NO production, causing dysregulation of CBF (Morikawa et al., 1994; Biernaskie et al., 2001; Girouard and Iadecola, 2006; Austin et al., 2013; Parodi-Rullán et al., 2019; Freitas-Andrade et al., 2020). Interestingly, in endothelial nitric oxide synthase (e-NOS) knockout (KO) mice, deficiency of NO reduces the ability of ECs to neutralize ROS enhancing oxidative stress and neuroinflammation, likely exacerbating AD pathology (Austin et al., 2013). Accordingly, in models of AD and stroke, EC dysfunction has been shown to enhance neuroinflammation by increasing the production of ROS and enhancing BBB permeability, amongst other cellular mechanisms (Parodi-Rullán et al., 2019, 2020; Yang et al., 2019).

Pericytes and Smooth Muscle Cells

Pericytes and SMCs surround ECs within the vascular walls, wrapping around capillaries and arterioles/arteries, respectively. Both cell types have a vital role in the regulation of CBF and BBB integrity (Sagare et al., 2013; Hall et al., 2014; Freitas-Andrade et al., 2020). These cells regulate blood flow mainly through their contraction or dilation, which control the diameter of the blood vessel (Hall et al., 2014; Freitas-Andrade et al., 2020). Recently, the role of blood vessels in the clearance of CNS interstitial fluid and proteins has been thoroughly investigated (Aldea et al., 2019; Carare et al., 2020). Intramural periarterial drainage (IPAD) has been hypothesized as a route to drain the brain interstitial fluid and soluble proteins from the CNS into the cervical lymph nodes, by traveling along the capillaries and arterioles in the opposite direction of blood flow, within the basement membrane of the brain vasculature. The contraction of SMCs provides the motive force for IPAD (Carare et al., 2008; Aldea et al., 2019). This system is dysregulated in models of CAA and aging (Ojo et al., 2021). Another brain clearance pathway, the glymphatic system, has been observed to import cerebrospinal fluid along periarterial space and export interstitial fluid along perivenous spaces, in perivascular tunnels, formed by astroglial cells. This pathway has been proposed to be important in the clearance and regulation of toxic proteins in the brain such as tau and Aβ, and to be mediated by astrocytic aquaporin-4 (AQP4) (Braun and Iliff, 2020; Nedergaard and Goldman, 2020). Interestingly, the glymphatic system is most efficient during sleep (Boespflug and Iliff, 2018; Mestre et al., 2020).

During both stroke and AD, pericytes are observed to detach from the BBB (Sagare et al., 2013; Freitas-Andrade et al., 2020). In an AD mouse model, pericyte loss was observed to exacerbate AD pathology (Sagare et al., 2013). The loss of pericytes decreases vascular stability and decreases the ability for the NVU to regulate CBF (Sagare et al., 2013; Hall et al., 2014). On the other hand, a recent study concluded that Aβ induces pericyte-mediated capillary constriction, reducing CBF (Nortley et al., 2019). Pericytes have been observed to endure damage in models of diabetes as well as obesity, which are both risk factors of AD and IS (Price et al., 2012; Shah et al., 2013a). In cats exposed to hypoxia, pericytes exhibited detachment from the microvasculature (Gonul et al., 2002). Along with dysregulation of CBF in models of AD and stroke, pericyte and SMC loss also contribute to impaired clearance in models of AD and CAA (Sagare et al., 2013; Aldea et al., 2019; Carare et al., 2020; Kim et al., 2020; Ojo et al., 2021).

Astrocytes

Astrocytes are essential cells for the NVU and provide a physical connection between blood vessels and neurons (Iadecola and Nedergaard, 2007; Braun and Iliff, 2020). Astrocytic end-feet wrap the blood vessels, helping to stabilize EC tight junctions and regulate CBF (Iadecola and Nedergaard, 2007). Astrocytes play a key role in providing metabolic and physical support to the CNS, along with the regulation of CBF, as well as brain clearance (Freitas-Andrade et al., 2020). AQP4 is a membrane protein that functions in water exchange within the CNS. In healthy individuals, AQP4 is a membrane channel localized at the astrocytic end feet, and it is important for clearance of toxic solutes from the brain (Smith et al., 2019). It is hypothesized that AQP4 is a part of the glymphatic system, mediating fluid exchange and the drainage of proteins, as well as the elimination of liquid from the CNS (Iliff et al., 2012; Boland et al., 2018; Braun and Iliff, 2020; Mestre et al., 2020). Despite the differential contributions of the glymphatic system and the IPAD pathway to the clearance of cerebral fluids and waste material are not completely grasped, it is accepted that astrocytes play a pivotal role in the exchange of fluids, based on studies showing that, in AQP4 KO mice, cerebrospinal fluid influx as well as CNS clearance were decreased (Iliff et al., 2012; Braun and Iliff, 2020). Another essential function of astrocytes is glutamate uptake and release, which is very important for the maintenance of CNS homeostasis (Dejakaisaya et al., 2021; van Putten et al., 2021; Verkerke et al., 2021). Astrocytes also have a critical role in the brain antioxidant system maintenance and in the production of glutathione, an important modulator of oxidative stress and aging (Bains and Shaw, 1997; Venkateshappa et al., 2012; Howarth et al., 2017; Verkerke et al., 2021).

In AD, astrocytes lose their polarization, detach from the BBB, become reactive and release inflammatory cytokines (Liddelow et al., 2017; Sweeney et al., 2019b; Cortes-Canteli and Iadecola, 2020). The crosstalk between astrocytes and microglia needs further understanding, although it has been extensively shown that they modulate each other's activation state (Joshi et al., 2019; McConnell et al., 2019; McAlpine et al., 2021). Astrocytes have also been reported to lose their expression of AQP4 early in AD (Smith et al., 2019). Differently, in stroke, AQP4 expression correlates with cerebral edema, increasing neuronal damage (Manley et al., 2000). In IS, astrogliosis is very significant due to the presence of DAMPs during the initial/acute phase, as well as the secondary/later phase of injury. A major indicator of gliosis is an increase in the expression of glial fibrillary acidic protein (GFAP) by astrocytes, observed in stroke as well as AD models (Pekny and Lane, 2007; Oeckl et al., 2019; Freitas-Andrade et al., 2020). Upon ischemic injury, neurovascular coupling is lost, together with astrocyte mediated CBF (McConnell et al., 2019; Freitas-Andrade et al., 2020). This results in a loop of metabolic stress and inflammation, worsening mitochondrial

dysfunction in vascular cells, and ultimately leading to BBB breakdown (Girouard and Iadecola, 2006; Freitas-Andrade et al., 2020; Radenovic et al., 2020; Sarvari et al., 2020).

Microglia

Although not directly attached to ECs, microglia mediate BBB integrity (Eldahshan et al., 2019; Freitas-Andrade et al., 2020). They are considered the resident immune cells of the CNS, able to phagocytize neurotoxic substances, and, more recently, they have also been reported to participate in a series of cerebral homeostatic functions, including synaptic plasticity and brain development (Badimon et al., 2020; Willis et al., 2020). There are two well-studied activation phenotypes of microglia, referred as M1 and M2, which are classified as being pro-inflammatory and anti-inflammatory, respectively. The M1 phenotype is detrimental to the BBB, causing dysregulation of the NVU, while the M2 facilitates the endocytosis and the clearance of toxic substances and dying cells, limiting the amount of oxidative stress and promoting a more suitable environment for regeneration/healing, following CNS injury (Tang and Le, 2016; Freitas-Andrade et al., 2020; Jiang et al., 2020). Recently, a protein highly expressed in microglia, triggering receptor expressed on myeloid cells-2 (TREM2), has been observed to protect from neurodegeneration in models of AD. TREM2 is hypothesized to be neuroprotective, associated with the M2 phenotype, although there are variants that increase the likelihood of developing AD (Ulland and Colonna, 2018; Gervois and Lambrichts, 2019; Zhou et al., 2020). The protective mechanisms of TREM2 have also been observed in IS (Gervois and Lambrichts, 2019).

Following IS or HS, microglia transition into a reactive state, causing the release of pro-inflammatory cytokines, exacerbating neuroinflammation and neurovascular dysfunction (Eldahshan et al., 2019). Microglia activation is also observed in models of AD and is now considered one of the major hallmarks of the disease (Villegas-Llerena et al., 2016). Inflammasome activation has been observed to occur in aging, neurodegeneration, as well as in stroke (Mohamed et al., 2015; Liddelow et al., 2017; Hu et al., 2019; Yang et al., 2019). In the brain, inflammasome activation occurs in many different cell types. Particularly, microglia, being the most sensitive cells to pathogen associated molecular patterns (PAMPs) and DAMPs, trigger the activation of caspase-1 and the release of cytokines IL-1β along with IL-18 (Hu et al., 2019). The cytokine receptors on vascular cells are then activated, triggering detrimental processes which cause NVU dysfunction and disruption of neurovascular coupling (Eldahshan et al., 2019). Among other cells, microglia have also been observed to secrete metalloproteases (MMPs), such as matrix metallopeptidase-2 (MMP-2) and matrix metallopeptidase-9 (MMP-9), which have been reported to be activated in AD and IS, degrading the basement membrane, therefore increasing BBB permeability and NVU dysfunction (Lorenzl et al., 2003; Hernandez-Guillamon et al., 2010; Yang and Rosenberg, 2015; Turner and Sharp, 2016; Montaner et al., 2019; Freitas-Andrade et al., 2020; Sarvari et al., 2020; Carcel-Marquez et al., 2021).

Basement Membrane

The basement membrane is an essential part of the BBB and is composed of numerous proteins such as laminins, collagen, nidogen, and heparin sulfate proteoglycans (Carare et al., 2020). The different proteins that make up the basement membrane are secreted by the cell types composing the NVU such as ECs, pericytes and astrocytes. These different proteins support cell-cell interactions, and thus BBB integrity (Carare et al., 2020; Freitas-Andrade et al., 2020).

Destruction of the basement membrane is severely apparent after middle cerebral artery occlusion (MCAO) (Sarvari et al., 2020). This degeneration occurs through different mechanisms of neuroinflammation such as ROS production as well as MMP secretion (Mohamed et al., 2015; Yao, 2019; Freitas-Andrade et al., 2020). Furthermore, the secretion and activation of MMPs interferes with the composition of the BBB, causing it to become leaky, and further exacerbating already existing oxidative stress and neuroinflammation (Fujimura et al., 1999; Hernandez-Guillamon et al., 2010; Montaner et al., 2019; Kang and Yao, 2020). Basement membrane composition and structure has also been observed to change in models of CAA (Morris et al., 2014).

Neurons

Blood vessel-coupled-neurons communicate with ECs and other cells of the NVU to modulate vascular structure, dilation or constriction, and to provide nutrients based on neuronal need (Andreone et al., 2015; Iadecola, 2017; Kaplan et al., 2020). Neurovascular coupling is essential to maintain the proper influx of nutrients and the proper efflux of toxic waste from the brain (Girouard and Iadecola, 2006; Andreone et al., 2015; Kaplan et al., 2020). Neuronal activity has been observed to participate in both angiogenesis and neurovascular coupling (Girouard and Iadecola, 2006; Huneau et al., 2015).

Upon CNS injury and cell death of NVU cells, dysregulation of neurovascular coupling occurs (Iadecola, 2017; Sweeney et al., 2019a; Freitas-Andrade et al., 2020; Kaplan et al., 2020). The absence of communication between the CNS and the systemic blood circulation ultimately leads to metabolic failure, oxidative stress, mitochondrial dysfunction and synaptic loss (Freitas-Andrade et al., 2020; Kaplan et al., 2020). It is therefore conceivable that, when cerebrovascular integrity and function are preserved, neurodegeneration is less severe and CNS homeostasis is better maintained.

CARBONIC ANHYDRASES

CAs are a family of zinc metalloenzymes catalyzing the reversible reaction $CO_2 + H_2O \rightleftharpoons HCO_3^- + H^+$. All four species in this chemical reaction are essential for CNS homeostasis. Therefore, it is expected that CAs influence CNS and further NVU function. The CO_2 hydration reaction can occur spontaneously (uncatalyzed), but the reaction rate is too slow for the dynamic of living cells. Consequently, CA is ubiquitously spread in all living organisms, including humans, where it accelerates this reaction millions of times, making the interconversion of CO_2 and HCO_3^- almost instantaneous. In humans, there are 15 CA isoforms, either acatalytic (CA-VIII, CA-X, and CA-XI) with exact function presently unknown, or catalytically active. The latter are found in the subcellular locations where CO_2/HCO_3^- interconversion is required, from the site of production in

the mitochondria (mitochondrial CA-VA and CA-VB), moving into the cytosol (CA-I, CA-II, CA-III, CA-VII, CA-XIII), then to the plasma membrane (CA-IV, CA-IX, CA-XII, CA-XIV) and finally extracellularly (CA-VI secreted in saliva (Supuran, 2008; Zamanova et al., 2019; Mishra et al., 2020). As genetic manipulation and selective inhibitors (Supuran et al., 1998; Ilies et al., 2003; Smaine et al., 2007; Supuran, 2008; Güzel et al., 2009; Winum et al., 2009; Alterio et al., 2012; Akocak et al., 2016; Angeli et al., 2020) have become more available, there has been an increase in studies to determine the cell-specific function of different CA isoforms (Ghandour et al., 1992; Sly and Hu, 1995; Kida et al., 2006; Pan et al., 2006, 2012; Imtaiyaz Hassan et al., 2013; Shah et al., 2013b; Akocak and Ilies, 2014; Angeli et al., 2017; Waheed and Sly, 2017; Haapasalo et al., 2020; Mishra et al., 2020). One of the most ubiquitously expressed and catalytically active isoform is CA-II, having a turnover rate for CO_2 hydration approaching diffusion limit (K_{cat} = 1.4 × 10^6 s^{-1}). It is a cytosolic enzyme and has the widest distribution in the human body, being expressed in cells from virtually every tissue or organ. In the brain, it is found in large amounts in oligodendrocytes and epithelium of the choroid plexus. Subjects suffering from CA-II deficiency syndrome, a human autosomal recessive disorder, display osteopetrosis, bone fragility, renal tubular acidosis, and, importantly, cerebral calcification and cognitive defects, developmental delay and usually a short stature (Sly and Hu, 1995; Supuran, 2008; Zamanova et al., 2019; Mishra et al., 2020). This isoform has been observed to translocate to the mitochondria, upon aging and neurodegeneration in a Purkinje cell degeneration mouse model (Pollard et al., 2016). This study also showed that *C. elegans* exposed to CA-II have a shorter lifespan, suggesting that high CA-II levels are involved in cell life/cycle-limiting mechanisms. Future studies need to further elucidate why and how this occurs.

CA-I isoform was first identified in red blood cells, where is five to six times more abundant than CA-II, although it has only about 15% of the CA-II activity (Supuran, 2008; Zamanova et al., 2019; Mishra et al., 2020). CA-I is the most abundant non-hemoglobin protein in erythrocytes and, together with CA-II, contributes to equilibration of dissolved CO_2/HCO_3^- pools in blood and maintains the pH blood homeostasis, also facilitating the CO_2 transport from brain and metabolizing tissues to lungs (Sly and Hu, 1995; Supuran, 2008; Zamanova et al., 2019; Mishra et al., 2020). CA-I is hypothesized to contribute to cerebral edema due to the observation that CA-I is increased in the brain following HS (Guo et al., 2012). One of the most important cytosolic isozymes in the brain is CA-VII, a fast isozyme (K_{cat} = 9.5 × 10^5 s^{-1}), found especially in the neurons of hippocampus, together with CA-II. Interestingly, CA-VII is not found in glial cells, which contain just CA-II in the cytosol. Besides CNS, CA-VII is found in skeletal muscles, stomach, duodenum, liver, colon (Sly and Hu, 1995; Supuran, 2008; Zamanova et al., 2019; Mishra et al., 2020). In the brain, Kaila's group has shown that CA-VII acts as a molecular switch in hippocampal CA1 pyramidal neurons in the development of synchronous gamma-frequency firing in response to high-frequency stimulation. This finding makes CA-VII an important modulator of long-term potentiation, synaptic plasticity, memory, and learning processes (Ruusuvuori et al., 2004). The same group, using a novel CA-VII (*Car7*) KO mouse model, as well as a CA-II (*Car2*) KO, and a CA-II/VII double KO mouse models, has shown that in mature hippocampal pyramidal neurons CA-VII and CA-II isozymes enhance bicarbonate-driven GABAergic excitation during intense $GABA_A$-receptor activation. The expression of these two cytosolic isozymes was detected at a very early age in the animals (10- and 20-days post-birth), pointing toward CA-VII and CA-II being key molecules in age-dependent neuronal pH regulation (Supuran, 2008; Ruusuvuori et al., 2013; Ruusuvuori and Kaila, 2014; Zamanova et al., 2019; Mishra et al., 2020).

Membrane-bound isozymes also play an important role in the brain, especially for the regulation of extracellular pH (Chesler, 2003; Shah et al., 2005). Thus, the phosphatidylinositol glycan (GPI)-anchored isozymes CA-IV (Stams et al., 1996) is a fast isozyme (K_{cat} = 1.1 × 10^6 s^{-1}) found on the plasma face of the cortical capillaries. It is more resistant to inhibition by halide ions than CA-II, being adapted to perform the CO_2/HCO_3^- interconversion in the extracellular space that contains a higher concentration of Cl^- ions than the cytosol. The isozyme is also expressed in the choriocapillaries of the eye, in skeletal and cardiac muscles, lungs, kidneys, gastrointestinal and reproductive tracts (Sly and Hu, 1995; Supuran, 2008; Zamanova et al., 2019; Mishra et al., 2020). Another isoform localized within the plasma membrane is CA-IX, a transmembrane isozyme, possessing an N-terminal proteoglycan domain, the catalytic domain, a single-pass transmembrane region, and an intracellular tail. It is a dimeric protein with a low expression pattern in most organs, except for the digestive system (largest amount) and CNS, where it can be found mainly in the ventricular-lining cells and in the choroid plexus (Saarnio et al., 1998; Hilvo et al., 2008; Supuran, 2008; Alterio et al., 2009; Pastorek and Pastorekova, 2015; Zamanova et al., 2019; Mishra et al., 2020). The expression of CA-IX is up-regulated in hypoxia by the transcription factor hypoxia inducible factor-1 (HIF1α) and is associated with the Warburg effect in cancer pathology (Ivanov et al., 2001; Supuran, 2008; Pastorek and Pastorekova, 2015; Shabana and Ilies, 2019). In models of glioblastoma, CA-IX has been observed to increase cell migration, motility, and adhesion in monocytes (Huang et al., 2020). Currently, a compound partially selective to inhibit for CA-IX, referred to as SLC-0111, is in clinical trials, and it is likely it would operate as a therapy for multiple cancers, including glioblastoma (Boyd et al., 2017; Ilies and Winum, 2019; Shabana and Ilies, 2019; McDonald et al., 2020). This isoform has also been suggested to be involved in heart fibrosis in a rat cardiac ligation model (Vargas et al., 2016). Interestingly, in humans, CA-IX is expressed also within atherosclerotic plaques, where it is suggested to be a marker of necrotic tissue (Demandt et al., 2021). Recent studies provided evidence that CA-IX likely exacerbates cerebral ischemia outcomes (Mishra et al., 2020). CA-XII is another medium-fast (K_{cat} = 4.2 × 10^5 s^{-1}), membrane-bound isozyme, similar in general structure with CA-IX, but without the proteoglycan domain. It is also dimeric, with the two active sites oriented toward the extracellular milieu

(Ivanov et al., 1998; Türeci et al., 1998; Whittington et al., 2001). It is found in many hypoxic tumors, alongside CA-IX, including gliomas, hemangioblastomas, and meningiomas. However, opposite to CA-IX, CA-XII is highly expressed in many normal tissues including breast epithelium and non-pigmented ciliary epithelial cells of the eye, in brain (small peripheral capillaries), esophagus, pancreas, colon, rectum, kidney, prostate, ovary, testis, endometrium, sweat glands. CA-XII was shown to play a key role in epithelial cell electrolyte homeostasis via activation of the ductal Cl^-/HCO_3^- exchanger AE2, and association with Na^+/HCO_3^- cotransporter kNBC1 (Proescholdt et al., 2005; Purkerson and Schwartz, 2007; Supuran, 2008; Hong et al., 2015; Waheed and Sly, 2017; Zamanova et al., 2019; Mishra et al., 2020). The membrane-bound isozyme CA-XIV possesses an extracellular catalytic domain, a single transmembrane helix, a short intracellular polypeptide segment, and has a moderate catalytic activity. It is highly expressed in the kidney, retina and the heart, as well as in brain, skeletal muscles, liver, and lungs. It was reported that CA-XIV is interacting with bicarbonate transporters and is involved in acid–base balance in muscles and erythrocytes in response to chronic hypoxia, and hyperactivity of the heart (Mori et al., 1999; Supuran, 2008; Mboge et al., 2018; Zamanova et al., 2019; Mishra et al., 2020).

The mitochondrial isoforms CA-VA and CA-VB are isozymes with medium-high activity (K_{catVA} = 2.9 × 10^5 s^{-1}, K_{catVB} = 9.5 × 10^5 s^{-1}), important for gluconeogenesis, lipogenesis, ureagenesis, and other anabolic pathways. They supply HCO_3^- to pyruvate carboxylase during gluconeogenesis and lipogenesis pathways, and to carbamoyl phosphate synthetase in ureagenesis pathway. CA-VA is found mainly in the liver, while CA-VB is found in skeletal and heart muscles, kidneys, pancreas, gastrointestinl tract, brain and spinal cord (Shah et al., 2000; Supuran, 2008; Scozzafava et al., 2013; Zamanova et al., 2019; Mishra et al., 2020). Due to their involvement in these anabolic pathways, they have been studied in models of obesity and type 2 diabetes (De Simone and Supuran, 2007; Supuran, 2012; Scozzafava et al., 2013; Salameh et al., 2019; Mishra et al., 2020). The function of CA-V and the difference between CA-VA and CA-VB isoforms has been examined by analyzing the phenotypical differences between CA-VA and CA-VB KO, as well as the double KO mouse models, indicating their role in ammonia detoxification (Shah et al., 2013b). The function of CA-V in the brain is extremely understudied, however, CA-VA has been reported to be expressed in both neurons and glial cells (Ghandour et al., 2000). Interestingly, the effect of CA-V has been also investigated in cerebral pericytes (Price et al., 2017). It has been observed that silencing of both isoforms protect against high-glucose-induced cell death and ROS production, CA-VA to a more significant degree (Price et al., 2017), confirmed also by increased oxidative stress and apoptosis in models of CA-VA over expression (Price et al., 2017).

Although extensive studies reported the multiple functions of the different CA isoforms in a variety of tissues, further investigation regrading CAs cell-specific expression/activity, especially within the CNS, and in CNS disorders, is needed. In particular, CAs impact on cerebrovascular dysregulation occurring during IS and AD must still be elucidated. It is therefore crucial to identify the cell- and isoform-specific roles, and to design isoform-selective inhibitors, which may be likely to ameliorate the cell/tissue specificity and to decrease the observed side effects of the FDA-approved pan-CAIs (Provensi et al., 2019; Zamanova et al., 2019; Mishra et al., 2020).

Below, we summarize the available literature highlighting the positive effects of CA inhibition on neurovascular dysfunction in stroke-, AD-, CAA-, and diabetes-induced cerebrovascular pathology.

Carbonic Anhydrase Inhibitors and Cerebrovascular Pathology

CAIs have been studied for decades (Maren, 1967; Bertini and Luchinat, 1983; Silverman and Lindskog, 1988; Supuran et al., 2003; Krishnamurthy et al., 2008; Supuran, 2008; Winum et al., 2009; Alterio et al., 2012; Akocak and Ilies, 2014; McKenna and Supuran, 2014; Supuran and Winum, 2015; Ilies and Winum, 2019; Angeli et al., 2020; Supuran and Capasso, 2020). They were first developed as diuretics due to their function on the reabsorption of sodium and water within the kidney (DuBose, 1984; Purkerson and Schwartz, 2007; Supuran, 2018), and are currently used to treat glaucoma as they decrease intraocular pressure, and for the prevention of high altitude sickness (Bradwell et al., 1992; Mincione et al., 2007; Ritchie et al., 2012), as they diminish pulmonary vasoconstriction, increase CBF likely controlling cerebral oxygenation, and reduce cerebral edema (Mishra et al., 2020). However, the molecular mechanism responsible for the effects of CAIs, including some of the most used pan-CAIs such as ATZ and MTZ, are multiple, and still under investigation.

MTZ, for example, was recognized as one of a few compounds that had the ability to inhibit cytochrome c release from the mitochondria under oxidative stress (Wang et al., 2008). Over 1000 compounds of the NINDS drug library were first screened in isolated mitochondria from mouse liver and further confirmed in striatal cells in models of Huntington's disease. MTZ, inhibiting cytochrome c release from challenged mitochondria, also resulted in the reduction of caspase-9 and caspase-3 activation (Wang et al., 2008; Fossati et al., 2016; Sekerdag et al., 2018). Following this study, FDA-approved CAIs such as MTZ, ATZ, topiramate and more recently developed non-FDA approved selective inhibitors, are starting to be applied in models of cerebrovascular pathology, ischemia, CAA and AD, and their positive effects have been attributed, at least in part, to their ability to prevent mitochondrial dysfunction in cerebrovascular cells (Wang et al., 2009; Shah et al., 2013a; Fossati et al., 2016; Solesio et al., 2018).

CA inhibition has been shown to contribute to cerebrovascular tone during transient phases of pH change, but not in steady-state conditions, in rat arteries (Rasmussen and Boedtkjer, 2018). This study used two different CAIs, ATZ and 4-aminomethylbenzenesulfonamide (AMB). It was revealed that only the pan-CAI ATZ, potent against most of intracellular CA isozymes, had an effect on intracellular acidification mechanisms. Based on the observed results, it was concluded that intracellular CAs are responsible for modifying the rate of intracellular pH and vascular tone within the arteries (Rasmussen and Boedtkjer, 2018). Other studies have observed the vasodilator

abilities of ATZ, such as increased NO production leading to increased blood flow in the cortex of rats (Tuettenberg et al., 2001). It is likely that the production of NO is not the only mechanism by which ATZ mediates vasodilation (Kiss et al., 1999). Systemic administration of ATZ has also been widely used as a short test to increase CBF in human studies (Okudaira et al., 1995; Grossmann and Koeberle, 2000; Russell et al., 2008). Interestingly, its stimulatory effect on CBF is reduced in patients with AD or vascular dementia compared to healthy controls (Stoppe et al., 1995; Pavics et al., 1999).

Carbonic Anhydrase Inhibition in Models of Ischemic Stroke

The neuroprotective effects of MTZ, in both *in vitro* and *in vivo* models of ischemic injury, displayed in **Table 1**, were first explored by Wang et al. (2009). Exposing primary cortical neurons to OGD and H_2O_2 resulted in necrosis, which was rescued by MTZ treatment. Similarly, OGD increased cytochrome c release and apoptosis inducing factor (AIF) release from the mitochondria, as well as the activity of caspase-3 (Wang et al., 2009), and MTZ attenuated these effects (Wang et al., 2009), suggesting that MTZ does not only prevent necrosis, but also mitochondria-mediated apoptosis, induced by OGD. In the same study, primary cortical neurons exposed to OGD presented inflammasome activation, measured by the activation of caspase-1 and release of IL-1β. MTZ inhibited both IL-1β release as well as caspase-1 activation *in vitro* (Wang et al., 2009). This finding supports the hypothesis that CAs may mediate both apoptotic and inflammatory mechanisms. In a mouse model of MCAO, MTZ-treated mice (20 mg/kg) had a smaller infarct size, improved neurological score, and decreased cytochrome c release and caspase-3 activation, compared to non-treated mice (Wang et al., 2009). A more recent study performed in rats determined the effectiveness of ATZ alone, as well as in conjugation with head-down tilt, a way to physically promote CBF, in a transient MCAO rat model. The results indicated that ATZ was protective following transient MCAO, significantly decreasing infarct size (Han et al., 2020). Furthermore, ATZ reduced AQP4 expression, compared to rats with no treatment, suggesting a reduction in brain edema (Han et al., 2020). In a rat model of permanent MCAO, ATZ was used in comparison with selective inhibitors for CA-VII, CA-IX, and CA-XII to determine whether these

TABLE 1 | CA inhibition in models of IS.

Model	Mechanism	CA Inhibitor/Isoform	References
Mouse primary cortical neurons	Inhibition of OGD induced necrosis Inhibition of OGD induced mitochondria mediated apoptosis Inhibition of OGD induced inflammasome activation	MTZ	Wang et al., 2009
C57BL/6J Mouse pMCAO	Reduction of infarct size Improvement of neurological score Reduction of caspase 3 activation Decrease of cytochrome C release	MTZ	Wang et al., 2009
Wistar rat tMCAO	Decrease of infarct size Reduction of AQP4 expression Reduction of brain water content and sodium accumulation	ATZ	Han et al., 2020
Sprague dawley rat pMCAO	Improvement of neurological score Reduction of infarct size	CA-VII inhibition, CA-IX/XII inhibition ATZ, CA-IX/XII inhibition	Di Cesare Mannelli et al., 2016
Rat hippocampal slices	Inhibition of OGD induced anoxic depolarization	ATZ, CA-IX inhibition, CA-XII inhibition	Dettori et al., 2021
Wistar rats pMCAO	Reduction of infarct size Improvement of neurological score Attenuation of microglia activation	ATZ, CA-IX/-XII inhibition	Dettori et al., 2021

MTZ, Methazolamide; ATZ, Acetazolamide; HS, hemorrhagic stroke; p/Tmcao, permanent/transient middle cerebral artery occlusion; CA, carbonic anhydrase; AQP4, Aquaporin-4; OGD, oxygen glucose deprivation.

TABLE 2 | CA inhibition in models of HS.

Model	Mechanism	CA Inhibitor/Isoform	References
Sprague-dawley rats intracaudate blood injection	Improvement of neurological outcome Reduction of neuronal death	ATZ	Guo et al., 2012
	Exacerbation of brain water content Increase neurodegeneration	CA-I injection	Guo et al., 2012
Mouse primary cortical neurons	Inhibition of blood/hemoglobin induced cell death Inhibition of blood/hemoglobin induced ROS production	MTZ	Li et al., 2016
C57BL/6J Mice SAH	Reduction in caspase-3 activation and cell death in hippocampus/cortex Improvement in neurological outcome	MTZ	Li et al., 2016
New Zealand White Rabbits SAH	Reduction of neurodegeneration/ apoptosis in hippocampus	Topiramate	Seçkin et al., 2009

ATZ, acetazolamide; MTZ, methazolamide; CA-I, carbonic anhydrase-1; SAH, subarachnoid hemorrhage; ROS, reactive oxygen species.

isoforms are involved in the pathology. Interestingly, the pan-CAI ATZ did not improve neurological score 24 h following occlusion, however, the CAI with selectivity for CA-VII, as well as the compound more selective for membrane isoforms CA-IX and CA-XII, improved the neurological deficits observed in the occluded untreated rats. In the group treated with the CA-IX/CA XII potent and medium selective inhibitor, 6-(benzyloxy)benzo[d]thiazole-2-sulfonamide (BBT), infarct size was significantly reduced, while no reduction was observed in the CA-VII inhibitor group. However, rats treated with 50 mg/kg of ATZ also displayed diminished infarct volume. This study suggests that CA-IX and possibly CA-XII may exacerbate neuronal loss along with neurological and vascular deficits, following ischemic insult (Di Cesare Mannelli et al., 2016). Very recently, another study evaluated different CA-selective inhibitors, in both *in vitro* and *in vivo* models of IS (Dettori et al., 2021). This study analyzed a new generation of CAIs, which are lipophilic and selective for the hypoxia-associated (CA-IX and CA-XII) and cytosolic (CA-II and CA-I) isoforms. Importantly, ATZ was used as a reference compound at a much lower dose in this study (4.4 mg/kg). *In vitro*, the lipophilic CAIs and ATZ protected against OGD-induced anoxic depolarization, providing mechanistic information. *In vivo*, the CAIs reduced infarct volume, neurological deficits, neuronal damage and microglial activation (Dettori et al., 2021). This study also measured TNF-α and Il-10 plasma levels, showing differences between the sham surgery and the occluded groups, without any affect in the treated groups, likely due to the short time window of treatment (24-h). As proposed in the discussion, it is possible that, with a longer treatment, CA inhibition may mediate inflammatory pathways (Bulli et al., 2021; Dettori et al., 2021). Indeed, CAs have been also associated with inflammatory pathologies, such as rheumatoid arthritis and cancer metastasis (Supuran, 2008; Alver et al., 2011; Liu et al., 2012). Overall, both MTZ and ATZ are protective in models of IS, however, the development of CA-IX and potentially CA-XII inhibitors may be beneficial for the treatment of both neurological and vascular disorders, following IS. The protective mechanisms observed following CA inhibition in models of IS, summarized in **Table 2**, seem to be superior with compounds selective for membrane-bound isoforms CA-IX and CA-XII (Bulli et al., 2021).

TABLE 3 | CA inhibition in models of AD and CAA.

Model	Mechanism	CA Inhibitor/Isoform	References
hCMEC/D3	Inhibition of Aβ induced DNA fragmentation Inhibition Aβ induced of cytochrome c release Inhibition of Aβ induced H_2O_2 production Inhibition of Aβ induced caspase-9 activity	MTZ, ATZ	Fossati et al., 2010; Solesio et al., 2018
Human primary brain SMC	Inhibition of Aβ induced DNA fragmentation Inhibition Aβ induced of cytochrome c release	MTZ	Fossati et al., 2010
Normal Human Astrocytes	Inhibition of Aβ induced DNA fragmentation	MTZ	Fossati et al., 2016
Human Glioma M059K	Inhibition of Aβ induced DNA fragmentation Inhibition Aβ induced of cytochrome c release Inhibition of Aβ induced H_2O_2 production Inhibition of Aβ induced caspase-9 activity	MTZ	Fossati et al., 2016
Human Neuroblastoma (SHSY5Y)	Inhibition of Aβ induced DNA fragmentation Inhibition Aβ induced of cytochrome c release Inhibition of Aβ induced H_2O_2 production Inhibition of Aβ induced caspase-9 activity	MTZ, ATZ	Fossati et al., 2016; Solesio et al., 2018
	Activation of Nrf2	MTZ	Sotolongo et al., 2020
Rat primary cortical neurons	Activation of Nrf2	MTZ	Sotolongo et al., 2020
C57BL/6 Mice Aβ hippocampal injection	Inhibition of caspase-3 activation Increase of NeuN expression in hippocampus Reduction of caspase-3 activation in reactive microglia	MTZ	Fossati et al., 2016

hCMEC/D3, human cerebral microvasculature endothelial cells; Aβ, amyloid-beta; MTZ, methazolamide; ATZ, acetazolamide; SMC, smooth muscle cell; SHSY5Y, human neuroblastoma cells; MO59K, glioblastoma cell line; Nrf2, nuclear factor erythroid 2-related factor.

Carbonic Anhydrase Inhibition in Models of Hemorrhagic Stroke

The protective mechanisms of CA inhibition in models of HS are summarized in **Table 2**. Inhibition of CA reduced brain injury after ICH in Sprague-Dawley rats (Guo et al., 2012). This study focused on CA-I, which is highly expressed in red blood cells. Upon intracaudate injection of blood, CA-I levels were increased in the ipsilateral basal ganglia, for as long as 3 days post-injection. Moreover, following intracaudate injection of CA-I, increased brain water content, microglial activation and neuronal cell death were detected, suggesting that CA-I expression may contribute to cerebral edema and neuroinflammation. ATZ-treated rats exhibited reduced perihematomal edema, as well as sodium accumulation, together with decreased neuronal deficits (Guo et al., 2012). However, the cellular mechanisms responsible for the effects of CA-I on BBB integrity require further investigation. Lately, the scientific community is beginning to hypothesize that CA-I, in both the retina and brain, contributes to vascular permeability, suggesting that specific inhibitors of CA-I could be beneficial to minimize NVU dysfunction, and thus neuroinflammation around the barrier (Gao et al., 2007). Furtherly, in a SAH mouse model, mice treated with the pan-CAI, MTZ, had decreased caspase-3 activation and

apoptosis in the hippocampus and cortex, compared to the non-treated group, ameliorating neurological deficits (Li et al., 2016). In primary cortical neurons, MTZ reduced hemoglobin and blood induced cell death along with production of ROS (Li et al., 2016). Topiramate, another CAI active on multiple CA enzymes, including CA-V, reduced SAH injury in rabbits (Seçkin et al., 2009).

Carbonic Anhydrase Inhibition in Models of Alzheimer's Disease and Cerebral Amyloid Angiopathy

Recently, the effects of CA inhibition on mitochondrial and neurovascular cell function have been tested in models of amyloidosis (**Table 3**). In AD and CAA, Aβ toxic aggregates accumulate around and within the cerebral vessel walls, as well as in parenchymal plaques in specific brain regions, such as the hippocampus and cortex (Ghiso et al., 2014; Cortes-Canteli and Iadecola, 2020). Our lab has shown that Aβ oligomers and protofibrils induce cytochrome c release from the mitochondria in multiple cell types of the NVU, including ECs and SMCs, neurons and glial cells, leading to caspase activation and cell death (Fossati et al., 2010, 2012a,b, 2016; Parodi-Rullán et al., 2020). In all of these neurovascular cell types, MTZ reduced mitochondrial mediated cell death triggered by Aβ (Fossati et al., 2010, 2016). Moreover, MTZ attenuated caspase-3 and caspase-9 activation in ECs, neuronal and glial cells *in vitro,* as well as caspase-3 activation *in vivo* (Fossati et al., 2016; Solesio et al., 2018). In an *in vivo* study, Aβ was injected into the hippocampus of wild-type mice, in the presence or absence of a previous intraperitoneal MTZ injection. Interestingly, MTZ treatment attenuated the activation of caspase-3 in microglia and increased the amount of NeuN positive neurons within the hippocampus, indicating that MTZ treatment had a protective effect against neurodegeneration following Aβ-injection (Fossati et al., 2016). To elucidate the specific mechanisms responsible for these protective effects, our group showed that Aβ-induced mitochondrial dysfunction, mitochondrial membrane depolarization, cytochrome C release, and H_2O_2 production were attenuated in neuronal and ECs, not only by MTZ, but also by ATZ, which was effective at lower concentrations (Solesio et al., 2018). Moreover, both ATZ and MTZ inhibited caspase-9 activation caused by Aβ in cerebrovascular EC, and the resulting apoptosis (Solesio et al., 2018). MTZ has been also observed to increase the activation of nuclear factor-related factor 2 (Nrf2), in models of high-altitude sickness and more interestingly, in human neuroblastoma cells and primary cortical neurons challenged with Aβ *in vitro* (Lu et al., 2020; Sotolongo et al., 2020). Nrf2-activation by MTZ increased the activity of antioxidant enzymes, such as superoxide dismutase-1 and heme-oxygenase-1, pointing to the potential downstream effects of MTZ (Sotolongo et al., 2020). These studies support the hypothesis that CA inhibition is protective to multiple cell types of the NVU, in models of amyloidosis, and highlight the necessity to test

TABLE 4 | CA isoforms in CNS and cerebrovascular pathology.

CA isoform	Cellular localization	Cell type/Brain area	Cellular function	Neurological disorder	References
CA-I	Cytosol	Red blood cells	-pH homeostasis in the blood -Edema/sodium accumulation in the brain	IH	Guo et al., 2012
CA-II	Cytosol	-Epithelium of choroid plexus -Glial Cells -Neurons	-Intracellular ion homeostasis -Cell-life/life cycle	Loss of expression associated with cognitive abnormalities	Sly and Hu, 1995; Mishra et al., 2020
CA-III	Cytosol	MCA	N/A	N/A	Rasmussen and Boedtkjer, 2018
CA-IV	Plasma membrane	-Cortical capillaries -MCA	Extracellular pH	N/A	Chesler, 2003; Shah et al., 2005; Rasmussen and Boedtkjer, 2018
CA-VA	Mitochondria	-Cerebrovascular pericytes -Neurons -Glial cells	-High-glucose induced Apoptosis -High-glucose induced ROS production -Cell viability -Biogenesis reactions	Type-2 Diabetes induced cerebrovascular pathology	Ghandour et al., 2000; Patrick et al., 2015; Price et al., 2017
CA-VB	Mitochondria	-Cerebrovascular pericytes -MCA -CNS cells	Cell Viability	Type-2 Diabetes induced cerebrovascular pathology	Price et al., 2017; Rasmussen and Boedtkjer, 2018; Mishra et al., 2020
CA-VII	Cytosol	Hippocampal neurons	-Gamma-frequency firing -Long-term potentiation	Epilepsy	Ruusuvuori et al., 2004, 2013
CA-IX	Plasma membrane	-Glioblastoma -Choroid plexus -Ventricular linings	-Extracellular pH -Monocyte adhesion/cell migration -Tumor progression	Glioblastoma-IS	Di Cesare Mannelli et al., 2016; Huang et al., 2020; Mishra et al., 2020
CA-XII	Plasma membrane	-Glioblastoma -Peripheral capillaries -MCA	Extracellular pH	Glioblastoma	Proescholdt et al., 2005; Rasmussen and Boedtkjer, 2018

CA, carbonic anhydrase; MCA, middle cerebral artery; IH, intracerebral hemorrhage; IS, ischemic stroke.

these and/or isoform-specific compounds in clinical trials for AD and CAA. New studies currently performed in our lab are also confirming the positive effects of CAIs on cognitive performance in mouse models of amyloidosis (Angiulli et al., 2018). Additional studies are in process to investigate chronic treatments with pan-CAIs in multiple models of CAA and AD, in parallel with the assessment of specific isoform inhibitors, to further elucidate the role of different CA isoforms in AD and CAA pathology.

Interestingly, although CAIs are proving to be beneficial in preventing CAA and AD pathology, CA activators have also showed beneficial effects for memory retention in acute models (Ilies et al., 2002; Canto de Souza et al., 2017; Sanku et al., 2018; Provensi et al., 2019; Blandina et al., 2020; Schmidt et al., 2020). These findings point to a relevant role of CA enzymes in the modulation of multiple pathways in contextual fear memory extinction, neurodegenerative and neurovascular pathology. They also highlight the need for a careful and specific modulation of CA enzyme's activity, and for a further understanding of the effects of each isoform in different brain areas, cell types, and pathological conditions.

Carbonic Anhydrase Inhibition in Models of Diabetes-Induced Cerebrovascular Pathology

Some studies have also explored the specific inhibition of the mitochondrial isoforms CA-VA and CA-VB, which recently gained interest for their role in the prevention of cerebrovascular pathology, in different models of diabetes (Price et al., 2012, 2017; Shah et al., 2013a), which contributes to AD and stroke pathogenesis (Kuźma et al., 2018; Cortes-Canteli and Iadecola, 2020; Freitas-Andrade et al., 2020; Zlokovic et al., 2020). In a streptozotocin induced diabetic CD-1 mouse model it was reported that topiramate treatment for 3 weeks increased the levels of glutathione and reduced oxidative stress in the brain. It was also observed that diabetes-induced loss of cerebral pericytes was attenuated by topiramate (Price et al., 2012). The same group confirmed these mechanisms in the brains of CA-V double KO mice, where increased levels of glutathione and decreased oxidative stress was observed compared to wild-type (Price et al., 2012). Hyperglycemia-treated cerebrovascular pericytes increased ROS production, as well as the rate of

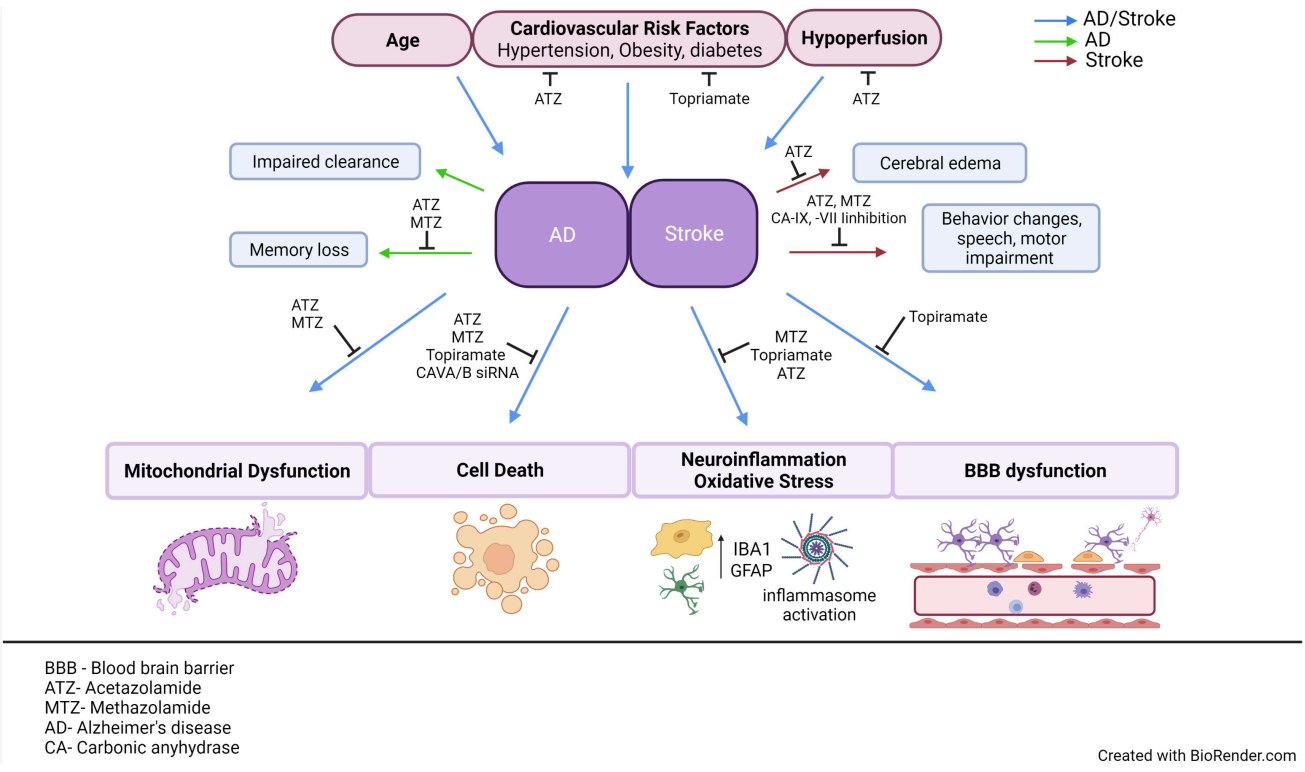

FIGURE 2 | AD and stroke share common risk factors and pathological mechanisms. This figure aims to emphasize the multiple CAIs, as well as point out specific CA isoforms that have been observed to modulate cerebrovascular pathology in models of AD or stroke. Age, cardiovascular risk factors and hypoperfusion are all common risk factors between AD and stroke. Both AD and stroke exhibit NVU dysfunction, accompanied by many common molecular mechanisms, such as mitochondrial dysfunction, vascular, and neuronal cell death, neuroinflammation, and BBB dysfunction. If these mechanisms are causes or effects of neurovascular dysfunction is still a hotly debated issue. Despite the differences in the advanced pathological manifestations of the two diseases, stroke does increase the risk of dementia, suggesting that targeting their common risk factors and molecular mechanisms could ultimately mitigate the development of cerebrovascular pathology in both disorders, protecting brain health and CNS homeostasis. ATZ, Acetazolamide; MTZ, methazolamide; BBB, blood brain barrier; NVU, neurovascular unit; CNS, central nervous system; CA, carbonic anhydrase; AD, Alzheimer's disease; CAIs, carbonic anhydrase inhibitors. This figure was created with BioRender.com.

mitochondrial respiration. The inhibition of CA (particularly CA-V), with topiramate, reduced ROS production (Shah et al., 2013a). Although topiramate has a high inhibitory activity on the CA-V isoforms, it also has affinity for the other isoforms, as well as multiple off-target effects in the brain, as shown by studies that analyzed topiramate's functions on GABA and glutamate receptors (Johnson, 2005; Mao et al., 2015). Ideally, more specific inhibitors should be developed to further investigate the functions of CA-VA/B. The same group used a plasmid to overexpress CA-VA in cerebral pericytes exposed to high-glucose to confirm the hypothesized molecular mechanisms involving CA-VA, such as ROS production and cell death, observing that topiramate was protective against these mechanisms (Patrick et al., 2015). As a proof of concept, the same group genetically knocked down CA-VA and CA-VB in cerebral pericytes (Price et al., 2017). CA-VA and CA-VB knockdown improved cell viability, compared to the control, when exposed to hyperglycemia, although the specific knockdown of CA-VA was even more effective than CA-VB knockdown in decreasing ROS production and apoptosis, in a hyperglycemic environment (Price et al., 2017). These studies reveal potential differences between CA-VA and CA-VB function in brain pericytes, which need further investigation. In a streptozotocin induced diabetic mouse model, cerebrovascular pathology was also characterized using electron microscopy. The breakdown of the BBB and its dysfunction was attenuated by topiramate treatment *in vivo* (Salameh et al., 2016). More recently, a study using a high-fat-induced diabetes mouse model, focused on the disruption of the hippocampal BBB. BBB tight junction proteins, such as ZO-1 and claudin-12, were reduced with a high-fat diet, while topiramate treatment increased their expression, along with the attenuation of oxidative stress (Salameh et al., 2019).

CONCLUSION

The NVU is an important functional structure of the CNS, and its failure participates in the development of AD, vascular dementias, and exacerbates stroke outcomes. Multiple pathological and cellular mechanisms leading to NVU pathology need clarification, and new therapeutic strategies should be further investigated and developed. As scientific techniques improve, the ability to understand the functions of this unit increases. Recent studies support that CA inhibition is protective to the NVU, and the role of these enzymes should be further investigated. **Table 4** emphasizes the CA isoforms that have been discussed throughout the review, their cellular localizations, their association with specific neurological disorders, and their expression in neurovascular cells. Clarifying how the cells of the NVU interact with each other, as well as the roles of CAs within each cell type, is critical for targeting cerebrovascular pathology in IS, AD, as well as other neurogenerative diseases. The pan-CAIs MTZ and ATZ, as well as topiramate, have shown protective effects in models of stroke, cerebrovascular pathology, type II diabetes, and AD, summarized in **Figure 2**. Although these compounds are FDA-approved, facilitating translation to clinical trials, these CAIs are not specific drugs. Isoform-specific CAIs are of increasing interest, as 15 isoforms with different functions and localizations have been identified in humans. Further preclinical and clinical studies to assess the efficacy of CA inhibition in AD as well as IS are essential. To confirm the role of specific CA isoforms as pharmacological targets, genetic studies, such as isoform KO and knock in in different NVU cell types, would be beneficial. Overall, the studies discussed above provide evidence for CAs as important potential mediators and targets in neurovascular pathology for AD, stroke and related cerebrovascular disorders.

AUTHOR CONTRIBUTIONS

NL and SF designed and conceptualized the review. NL wrote the review draft and did the literature search. SF critically revised, edited the manuscript, provided relevant insights, additional literature search, and acquired funding. EC and MI revised the manuscript and provided additional literature search. All authors contributed to the article and approved the submitted version.

FUNDING

This work was supported by NIH R01NS104127 and R01AG062572 grants, the Edward N. and Della L. Thome Memorial Foundation Awards Program in Alzheimer's Disease Drug Discovery Research, the Alzheimer's Association (AARG), the Pennsylvania Department of Heath Collaborative Research on Alzheimer's Disease (PA Cure) Grant, awarded to SF, and by the Karen Toffler Charitable Trust, and the Lemole Center for Integrated Lymphatics research.

ACKNOWLEDGMENTS

We thank Ashley Carey for conceptualizing and drawing **Figure 1** of the review. We also acknowledge that **Figure 2** was created using BioRender.com.

REFERENCES

Akocak, S., Alam, M. R., Shabana, A. M., Sanku, R. K., Vullo, D., Thompson, H., et al. (2016). PEGylated Bis-Sulfonamide Carbonic Anhydrase Inhibitors Can Efficiently Control the Growth of Several Carbonic Anhydrase IX-Expressing Carcinomas. *J. Med. Chem.* 59, 5077–5088. doi: 10.1021/acs.jmedchem.6b00492

Akocak, S., and Ilies, M. A. (2014). "Next-generation primary sulfonamide carbonic anhydrase inhibitors" in *Targeting Carbonic Anhydrases*. (Eds) C. T. Supuran., and C. Cappasso. (London: Future Science Ltd). 34–51. doi: 10.4155/fseb2013.13.22

Aldea, R., Weller, R. O., Wilcock, D. M., Carare, R. O., and Richardson, G. (2019). Cerebrovascular Smooth Muscle Cells as the Drivers of Intramural Periarterial Drainage of the Brain. *Front. Aging Neurosci.* 11:1.

Alluri, H., Stagg, H. W., Wilson, R. L., Clayton, R. P., Sawant, D. A., Koneru, M., et al. (2014). Reactive oxygen species-caspase-3 relationship in mediating blood-brain barrier endothelial cell hyperpermeability following oxygen-glucose deprivation and reoxygenation. *Microcirculation* 21, 187–195.

Alterio, V., Di Fiore, A., D'ambrosio, K., Supuran, C. T., and De Simone, G. (2012). Multiple binding modes of inhibitors to carbonic anhydrases: how to design specific drugs targeting 15 different isoforms? *Chem. Rev.* 112, 4421–4468. doi: 10.1021/cr200176r

Alterio, V., Hilvo, M., Di Fiore, A., Supuran, C. T., Pan, P., Parkkila, S., et al. (2009). Crystal structure of the catalytic domain of the tumor-associated human carbonic anhydrase IX. *Proc. Natl. Acad. Sci. U. S. A.* 106, 16233–16238. doi: 10.1073/pnas.0908301106

Alver, A., Şentürk, A., Çakirbay, H., Menteşe, A., Gökmen, F., Keha, E. E., et al. (2011). Carbonic anhydrase II autoantibody and oxidative stress in rheumatoid arthritis. *Clin. Biochem.* 44, 1385–1389. doi: 10.1016/j.clinbiochem.2011.09.014

Andreone, B. J., Lacoste, B., and Gu, C. (2015). Neuronal and vascular interactions. *Annu. Rev. Neurosci.* 38, 25–46. doi: 10.1146/annurev-neuro-071714-033835

Andring, J. T., Fouch, M., Akocak, S., Angeli, A., Supuran, C. T., Ilies, M. A., et al. (2020). Structural Basis of Nanomolar Inhibition of Tumor-Associated Carbonic Anhydrase IX: X-Ray Crystallographic and Inhibition Study of Lipophilic Inhibitors with Acetazolamide Backbone. *J. Med. Chem.* 63, 13064–13075. doi: 10.1021/acs.jmedchem.0c01390

Angeli, A., Carta, F., Nocentini, A., Winum, J. Y., Zalubovskis, R., Akdemir, A., et al. (2020). Carbonic Anhydrase Inhibitors Targeting Metabolism and Tumor Microenvironment. *Metabolites* 10:412. doi: 10.3390/metabo10100412

Angeli, A., Vaiano, F., Mari, F., Bertol, E., and Supuran, C. T. (2017). Psychoactive substances belonging to the amphetamine class potently activate brain carbonic anhydrase isoforms VA, VB, VII, and XII. *J. Enzyme Inhib. Med. Chem.* 32, 1253–1259. doi: 10.1080/14756366.2017.1375485

Angiulli, F., Solesio, M. E., Debure, L., Cejudo, J. R., Wisniewski, T., and Fossati, S. (2018). P3-464: carbonic anhydrase inhibitors ameliorate neurovascular dysfunction in a mouse model of cerebral amyloid angiopathy. *Alzheimers Dement.* 14, 1296–1296. doi: 10.1016/j.jalz.2018.06.1828

Aspatwar, A., Tolvanen, M. E., Ortutay, C., and Parkkila, S. (2014). Carbonic anhydrase related proteins: molecular biology and evolution. *Subcell. Biochem.* 75, 135–156. doi: 10.1007/978-94-007-7359-2_8

Austin, S. A., Santhanam, A. V., Hinton, D. J., Choi, D. S., and Katusic, Z. S. (2013). Endothelial nitric oxide deficiency promotes Alzheimer's disease pathology. *J. Neurochem.* 127, 691–700. doi: 10.1111/jnc.12334

Badimon, A., Strasburger, H. J., Ayata, P., Chen, X., Nair, A., Ikegami, A., et al. (2020). Negative feedback control of neuronal activity by microglia. *Nature* 586, 417–423. doi: 10.1038/s41586-020-2777-8

Bains, J. S., and Shaw, C. A. (1997). Neurodegenerative disorders in humans: the role of glutathione in oxidative stress-mediated neuronal death. *Brain Res.Rev.* 25, 335–358. doi: 10.1016/S0165-0173(97)00045-3

Bertini, I., and Luchinat, C. (1983). Cobalt(II) as a probe of the structure and function of carbonic anhydrase. *Accounts Chem. Res.* 16, 272–279. doi: 10.1021/ar00092a002

Biernaskie, J., Corbett, D., Peeling, J., Wells, J., and Lei, H. (2001). A serial MR study of cerebral blood flow changes and lesion development following endothelin-1-induced ischemia in rats. *Magn. Reson Med.* 46, 827–830. doi: 10.1002/mrm.1263

Blandina, P., Provensi, G., Passsani, M. B., Capasso, C., and Supuran, C. T. (2020). Carbonic anhydrase modulation of emotional memory. Implications for the treatment of cognitive disorders. *J. Enzyme Inhib. Med. Chem.* 35, 1206–1214. doi: 10.1080/14756366.2020.1766455

Boespflug, E. L., and Iliff, J. J. (2018). The Emerging Relationship Between Interstitial Fluid-Cerebrospinal Fluid Exchange, Amyloid-beta, and Sleep. *Biol. Psychiatry* 83, 328–336. doi: 10.1016/j.biopsych.2017.11.031

Boland, B., Yu, W. H., Corti, O., Mollereau, B., Henriques, A., Bezard, E., et al. (2018). Promoting the clearance of neurotoxic proteins in neurodegenerative disorders of ageing. *Nat. Rev. Drug Discov.* 17, 660–688. doi: 10.1038/nrd.2018.109

Boriack-Sjodin, P. A., Heck, R. W., Laipis, P. J., Silverman, D. N., and Christianson, D. W. (1995). Structure determination of murine mitochondrial carbonic anhydrase V at 2.45-A resolution: implications for catalytic proton transfer and inhibitor design. *Proc. Natl. Acad. Sci. U. S. A.* 92, 10949–10953. doi: 10.1073/pnas.92.24.10949

Boyd, N. H., Walker, K., Fried, J., Hackney, J. R., Mcdonald, P. C., Benavides, G. A., et al. (2017). Addition of carbonic anhydrase 9 inhibitor SLC-0111 to temozolomide treatment delays glioblastoma growth in vivo. *JCI Insight* 2:e92928. doi: 10.1172/jci.insight.92928

Bradwell, A. R., Wright, A. D., Winterborn, M., and Imray, C. (1992). Acetazolamide and high altitude diseases. *Int. J. Sports Med.* 13, S63–S64. doi: 10.1055/s-2007-1024597

Braun, M., and Iliff, J. J. (2020). The impact of neurovascular, blood-brain barrier, and glymphatic dysfunction in neurodegenerative and metabolic diseases. *Int. Rev. Neurobiol.* 154, 413–436. doi: 10.1016/bs.irn.2020.02.006

Bulli, I., Dettori, I., Coppi, E., Cherchi, F., Venturini, M., Di Cesare Mannelli, L., et al. (2021). Role of Carbonic Anhydrase in Cerebral Ischemia and Carbonic Anhydrase Inhibitors as Putative Protective Agents. *Int. J. Mol. Sci.* 22:5029. doi: 10.3390/ijms22095029

Canepa, E., and Fossati, S. (2020). Impact of Tau on Neurovascular Pathology in Alzheimer's Disease. *Front. Neurol.* 11:573324. doi: 10.3389/fneur.2020.573324

Canto de Souza, L., Provensi, G., Vullo, D., Carta, F., Scozzafava, A., et al. (2017). Carbonic anhydrase activation enhances object recognition memory in mice through phosphorylation of the extracellular signal-regulated kinase in the cortex and the hippocampus. *Neuropharmacology* 118, 148–156. doi: 10.1016/j.neuropharm.2017.03.009

Carare, R. O., Aldea, R., Agarwal, N., Bacskai, B. J., Bechman, I., Boche, D., et al. (2020). Clearance of interstitial fluid (ISF) and CSF (CLIC) group-part of Vascular Professional Interest Area (PIA): cerebrovascular disease and the failure of elimination of Amyloid-β from the brain and retina with age and Alzheimer's disease-Opportunities for Therapy. *Alzheimers Dement.* 12:e12053. doi: 10.1002/dad2.12053

Carare, R. O., Bernardes-Silva, M., Newman, T. A., Page, A. M., Nicoll, J. A., Perry, V. H., et al. (2008). Solutes, but not cells, drain from the brain parenchyma along basement membranes of capillaries and arteries: significance for cerebral amyloid angiopathy and neuroimmunology. *Neuropathol. Appl. Neurobiol.* 34, 131–144. doi: 10.1111/j.1365-2990.2007.00926.x

Carcel-Marquez, J., Cullell, N., Muino, E., Gallego-Fabrega, C., Lledos, M., Ibanez, L., et al. (2021). Causal Effect of MMP-1 (Matrix Metalloproteinase-1), MMP-8, and MMP-12 Levels on Ischemic Stroke: a Mendelian Randomization Study. *Stroke* 52, e316–e320. doi: 10.1161/STROKEAHA.120.033041

Castillo-Carranza, D. L., Nilson, A. N., Van Skike, C. E., Jahrling, J. B., Patel, K., Garach, P., et al. (2017). Cerebral Microvascular Accumulation of Tau Oligomers in Alzheimer's Disease and Related Tauopathies. *Aging Dis.* 8, 257–266. doi: 10.14336/AD.2017.0112

Chesler, M. (2003). Regulation and modulation of pH in the brain. *Physiol. Rev.* 83, 1183–1221. doi: 10.1152/physrev.00010.2003

Corraini, P., Henderson, V. W., Ording, A. G., Pedersen, L., Horváth-Puhó, E., and Sørensen, H. T. (2017). Long-Term Risk of Dementia Among Survivors of Ischemic or Hemorrhagic Stroke. *Stroke* 48, 180–186. doi: 10.1161/STROKEAHA.116.015242

Cortes-Canteli, M., and Iadecola, C. (2020). Alzheimer's Disease and Vascular Aging: JACC Focus Seminar. *J. Am. Coll. Cardiol.* 75, 942–951. doi: 10.1016/j.jacc.2019.10.062

Cruz Hernández, J. C., Bracko, O., Kersbergen, C. J., Muse, V., Haft-Javaherian, M., Berg, M., et al. (2019). Neutrophil adhesion in brain capillaries reduces cortical blood flow and impairs memory function in Alzheimer's disease mouse models. *Nat. Neurosci.* 22, 413–420. doi: 10.1038/s41593-018-0329-4

Da Mesquita, S., Louveau, A., Vaccari, A., Smirnov, I., Cornelison, R. C., and Kingsmore, K. M. (2018). Functional aspects of meningeal lymphatics in ageing and Alzheimer's disease. *Nature* 560, 185–191. doi: 10.1038/s41586-018-0368-8

Day, R. J., Mason, M. J., Thomas, C., Poon, W. W., and Rohn, T. T. (2015). Caspase-Cleaved Tau Co-Localizes with Early Tangle Markers in the Human Vascular Dementia Brain. *PLoS One* 10:e0132637. doi: 10.1371/journal.pone.0132637

de Bruijn, R. F., and Ikram, M. A. (2014). Cardiovascular risk factors and future risk of Alzheimer's disease. *BMC Med.* 12:130. doi: 10.1186/s12916-014-0130-5

De Simone, G., and Supuran, C. T. (2007). Antiobesity carbonic anhydrase inhibitors. *Curr. Top. Med. Chem.* 7, 879–884. doi: 10.2174/156802607780636762

Dejakaisaya, H., Kwan, P., and Jones, N. C. (2021). Astrocyte and glutamate involvement in the pathogenesis of epilepsy in Alzheimer's disease. *Epilepsia* 62, 1485–1493. doi: 10.1111/epi.16918

Demandt, J. A. F., Dubois, L. J., Van Kuijk, K., Zaťovičová, M., Jin, H., Parkkila, S., et al. (2021). The hypoxia-sensor carbonic anhydrase IX affects macrophage metabolism, but is not a suitable biomarker for human cardiovascular disease. *Sci. Rep.* 11:425. doi: 10.1038/s41598-020-79978-5

Dettori, I., Fusco, I., Bulli, I., Gaviano, L., Coppi, E., Cherchi, F., et al. (2021). Protective effects of carbonic anhydrase inhibition in brain ischaemia. *J. Enzyme Inhib. Med. Chem.* 36, 964–976. doi: 10.1080/14756366.2021.1907575

Di Cesare Mannelli, L., Micheli, L., Carta, F., Cozzi, A., Ghelardini, C., and Supuran, C. T. (2016). Carbonic anhydrase inhibition for the management of cerebral ischemia: in vivo evaluation of sulfonamide and coumarin inhibitors. *J. Enzyme Inhib. Med. Chem.* 31, 894–899. doi: 10.3109/14756366.2015.1113407

Draghici, B., Vullo, D., Akocak, S., Walker, E. A., Supuran, C. T., and Ilies, M. A. (2014). Ethylene bis-imidazoles are highly potent and selective activators for isozymes VA and VII of carbonic anhydrase, with a potential nootropic effect. *Chem. Commun.* 50, 5980–5983. doi: 10.1039/C4CC02346C

DuBose, T. D. Jr. (1984). Carbonic anhydrase-dependent bicarbonate transport in the kidney. *Ann. N. Y. Acad. Sci.* 429, 528–537. doi: 10.1111/j.1749-6632.1984.tb12382.x

Eldahshan, W., Fagan, S. C., and Ergul, A. (2019). Inflammation within the neurovascular unit: focus on microglia for stroke injury and recovery. *Pharmacol. Res.* 147:104349. doi: 10.1016/j.phrs.2019.104349

Engelhardt, S., Al-Ahmad, A. J., Gassmann, M., and Ogunshola, O. O. (2014). Hypoxia selectively disrupts brain microvascular endothelial tight junction complexes through a hypoxia-inducible factor-1 (HIF-1) dependent mechanism. *J. Cell. Physiol.* 229, 1096–1105. doi: 10.1002/jcp.24544

Faraco, G., Fossati, S., Bianchi, M. E., Patrone, M., Pedrazzi, M., Sparatore, B., et al. (2007). High mobility group box 1 protein is released by neural cells upon different stresses and worsens ischemic neurodegeneration in vitro and in vivo. *J. Neurochem.* 103, 590–603. doi: 10.1111/j.1471-4159.2007.04788.x

Ferrero, J., Williams, L., Stella, H., Leitermann, K., Mikulskis, A., O'gorman, J., et al. (2016). First-in-human, double-blind, placebo-controlled, single-dose escalation study of aducanumab (BIIB037) in mild-to-moderate Alzheimer's disease. *Alzheimers Dement.* 2, 169–176. doi: 10.1016/j.trci.2016.06.002

Fossati, S., Cam, J., Meyerson, J., Mezhericher, E., Romero, I. A., Couraud, P. O., et al. (2010). Differential activation of mitochondrial apoptotic pathways by vasculotropic amyloid-beta variants in cells composing the cerebral vessel walls. *FASEB J.* 24, 229–241. doi: 10.1096/fj.09-139584

Fossati, S., Ghiso, J., and Rostagno, A. (2012a). Insights into caspase-mediated apoptotic pathways induced by amyloid-beta in cerebral microvascular endothelial cells. *Neurodegener. Dis.* 10, 324–328. doi: 10.1159/000332821

Fossati, S., Ghiso, J., and Rostagno, A. (2012b). TRAIL death receptors DR4 and DR5 mediate cerebral microvascular endothelial cell apoptosis induced by oligomeric Alzheimer's Aβ. *Cell Death Dis.* 3, e321. doi: 10.1038/cddis.2012.55

Fossati, S., Giannoni, P., Solesio, M. E., Cocklin, S. L., Cabrera, E., Ghiso, J., et al. (2016). The carbonic anhydrase inhibitor methazolamide prevents amyloid beta-induced mitochondrial dysfunction and caspase activation protecting neuronal and glial cells in vitro and in the mouse brain. *Neurobiol. Dis.* 86, 29–40. doi: 10.1016/j.nbd.2015.11.006

Freitas-Andrade, M., Raman-Nair, J., and Lacoste, B. (2020). Structural and Functional Remodeling of the Brain Vasculature Following Stroke. *Front. Physiol.* 11:948. doi: 10.3389/fphys.2020.00948

Fujimura, M., Gasche, Y., Morita-Fujimura, Y., Massengale, J., Kawase, M., and Chan, P. H. (1999). Early appearance of activated matrix metalloproteinase-9 and blood-brain barrier disruption in mice after focal cerebral ischemia and reperfusion. *Brain Res.* 842, 92–100. doi: 10.1016/S0006-8993(99)01843-0

Gao, B. B., Clermont, A., Rook, S., Fonda, S. J., Srinivasan, V. J., Wojtkowski, M., et al. (2007). Extracellular carbonic anhydrase mediates hemorrhagic retinal and cerebral vascular permeability through prekallikrein activation. *Nat. Med.* 13, 181–188. doi: 10.1038/nm1534

Gervois, P., and Lambrichts, I. (2019). The Emerging Role of Triggering Receptor Expressed on Myeloid Cells 2 as a Target for Immunomodulation in Ischemic Stroke. *Front. Immunol.* 10:1668. doi: 10.3389/fimmu.2019.01668

Ghandour, M. S., Langley, O. K., Zhu, X. L., Waheed, A., and Sly, W. S. (1992). Carbonic anhydrase IV on brain capillary endothelial cells: a marker associated with the blood-brain barrier. *Proc. Natl. Acad. Sci. U. S. A.* 89, 6823–6827. doi: 10.1073/pnas.89.15.6823

Ghandour, M. S., Parkkila, A. K., Parkkila, S., Waheed, A., and Sly, W. S. (2000). Mitochondrial carbonic anhydrase in the nervous system: expression in neuronal and glial cells. *J. Neurochem.* 75, 2212–2220. doi: 10.1046/j.1471-4159.2000.0752212.x

Ghiso, J., Fossati, S., and Rostagno, A. (2014). Amyloidosis associated with cerebral amyloid angiopathy: cell signaling pathways elicited in cerebral endothelial cells. *J. Alzheimers Dis.* 42, S167–S176. doi: 10.3233/JAD-140027

Girouard, H., and Iadecola, C. (2006). Neurovascular coupling in the normal brain and in hypertension, stroke, and Alzheimer disease. *J. Appl. Physiol.* 100, 328–335. doi: 10.1152/japplphysiol.00966.2005

Gonul, E., Duz, B., Kahraman, S., Kayali, H., Kubar, A., and Timurkaynak, E. (2002). Early pericyte response to brain hypoxia in cats: an ultrastructural study. *Microvasc. Res.* 64, 116–119. doi: 10.1006/mvre.2002.2413

Grossmann, W. M., and Koeberle, B. (2000). The dose-response relationship of acetazolamide on the cerebral blood flow in normal subjects. *Cerebrovasc. Dis.* 10, 65–69. doi: 10.1159/000016027

Guo, F., Hua, Y., Wang, J., Keep, R. F., and Xi, G. (2012). Inhibition of carbonic anhydrase reduces brain injury after intracerebral hemorrhage. *Transl. Stroke Res.* 3, 130–137. doi: 10.1007/s12975-011-0106-0

Guo, J., Krause, D. N., Horne, J., Weiss, J. H., Li, X., and Duckles, S. P. (2010). Estrogen-receptor-mediated protection of cerebral endothelial cell viability and mitochondrial function after ischemic insult in vitro. *J. Cereb. Blood Flow Metab.* 30, 545–554. doi: 10.1038/jcbfm.2009.226

Güzel, O., Innocenti, A., Scozzafava, A., Salman, A., and Supuran, C. T. (2009). Carbonic anhydrase inhibitors. Phenacetyl-, pyridylacetyl- and thienylacetyl-substituted aromatic sulfonamides act as potent and selective isoform VII inhibitors. *Bioorg. Med. Chem. Lett.* 19, 3170–3173. doi: 10.1016/j.bmcl.2009.04.123

Haapasalo, J., Nordfors, K., Haapasalo, H., and Parkkila, S. (2020). The Expression of Carbonic Anhydrases II, IX and XII in Brain Tumors. *Cancers* 12:1723. doi: 10.3390/cancers12071723

Hachinski, V., Einhaupl, K., Ganten, D., Alladi, S., Brayne, C., Stephan, B. C. M., et al. (2019). Preventing dementia by preventing stroke: the Berlin Manifesto. *Alzheimers Dement.* 15, 961–984. doi: 10.1016/j.jalz.2019.06.001

Hall, C. N., Reynell, C., Gesslein, B., Hamilton, N. B., Mishra, A., Sutherland, B. A., et al. (2014). Capillary pericytes regulate cerebral blood flow in health and disease. *Nature* 508, 55–60. doi: 10.1038/nature13165

Han, M., Kwon, I., Ha, J., Kim, J., Cha, M. J., Kim, Y. D., et al. (2020). Collateral augmentation treatment with a combination of acetazolamide and head-down tilt in a rat ischemic stroke model. *J. Clin. Neurosci.* 73, 252–258. doi: 10.1016/j.jocn.2020.01.079

Hernandez-Guillamon, M., Mawhirt, S., Fossati, S., Blais, S., Pares, M., Penalba, A., et al. (2010). Matrix metalloproteinase 2 (MMP-2) degrades soluble vasculotropic amyloid-beta E22Q and L34V mutants, delaying their toxicity for human brain microvascular endothelial cells. *J. Biol. Chem.* 285, 27144–27158. doi: 10.1074/jbc.M110.135228

Hilvo, M., Baranauskiene, L., Salzano, A. M., Scaloni, A., Matulis, D., Innocenti, A., et al. (2008). Biochemical characterization of CA IX, one of the most active carbonic anhydrase isozymes. *J. Biol. Chem.* 283, 27799–27809. doi: 10.1074/jbc.M800938200

Hong, J. H., Muhammad, E., Zheng, C., Hershkovitz, E., Alkrinawi, S., Loewenthal, N., et al. (2015). Essential role of carbonic anhydrase XII in secretory gland fluid and HCO3 (-) secretion revealed by disease causing human mutation. *J. Physiol.* 593, 5299–5312. doi: 10.1113/JP271378

Howarth, C., Sutherland, B., Choi, H. B., Martin, C., Lind, B. L., Khennouf, L., et al. (2017). A Critical Role for Astrocytes in Hypercapnic Vasodilation in Brain. *J. Neurosci.* 37, 2403–2414. doi: 10.1523/JNEUROSCI.0005-16.2016

Hu, M. Y., Lin, Y. Y., Zhang, B. J., Lu, D. L., Lu, Z. Q., and Cai, W. (2019). Update of inflammasome activation in microglia/macrophage in aging and aging-related disease. *CNS Neurosci. Ther.* 25, 1299–1307. doi: 10.1111/cns.13262

Huang, B. R., Liu, Y. S., Lai, S. W., Lin, H. J., Shen, C. K., Yang, L. Y., et al. (2020). CAIX Regulates GBM Motility and TAM Adhesion and Polarization through EGFR/STAT3 under Hypoxic Conditions. *Int. J. Mol. Sci.* 21:5838. doi: 10.3390/ijms21165838

Huang, P. L., Huang, Z., Mashimo, H., Bloch, K. D., Moskowitz, M. A., Bevan, J. A., et al. (1995). Hypertension in mice lacking the gene for endothelial nitric oxide synthase. *Nature* 377, 239–242. doi: 10.1038/377239a0

Huneau, C., Benali, H., and Chabriat, H. (2015). Investigating Human Neurovascular Coupling Using Functional Neuroimaging: a Critical Review of Dynamic Models. *Front. Neurosci.* 9:467. doi: 10.3389/fnins.2015.00467

Iadecola, C. (2010). The overlap between neurodegenerative and vascular factors in the pathogenesis of dementia. *Acta Neuropathol.* 120, 287–296. doi: 10.1007/s00401-010-0718-6

Iadecola, C. (2017). The Neurovascular Unit Coming of Age: a Journey through Neurovascular Coupling in Health and Disease. *Neuron* 96, 17–42. doi: 10.1016/j.neuron.2017.07.030

Iadecola, C., and Nedergaard, M. (2007). Glial regulation of the cerebral microvasculature. *Nat. Neurosci.* 10, 1369–1376. doi: 10.1038/nn2003

Ilies, M., Banciu, M. D., Ilies, M. A., Scozzafava, A., Caproiu, M. T., and Supuran, C. T. (2002). Carbonic anhydrase activators: design of high affinity isozymes I, II, and IV activators, incorporating tri-/tetrasubstituted-pyridinium-azole moieties. *J. Med. Chem.* 45, 504–510. doi: 10.1021/jm011031n

Ilies, M. A., Masereel, B., Rolin, S., Scozzafava, A., Câmpeanu, G., Cîmpeanu, V., et al. (2004). Carbonic anhydrase inhibitors: aromatic and heterocyclic sulfonamides incorporating adamantyl moieties with strong anticonvulsant activity. *Bioorg. Med. Chem.* 12, 2717–2726. doi: 10.1016/j.bmc.2004.03.008

Ilies, M. A., Vullo, D., Pastorek, J., Scozzafava, A., Ilies, M., Caproiu, M. T., et al. (2003). Carbonic anhydrase inhibitors. Inhibition of tumor-associated isozyme IX by halogenosulfanilamide and halogenophenylaminobenzolamide derivatives. *J. Med. Chem.* 46, 2187–2196. doi: 10.1021/jm021123s

Ilies, M. A., and Winum, J.-Y. (2019). "Chapter 16 - Carbonic anhydrase inhibitors for the treatment of tumors: therapeutic, immunologic, and diagnostic tools targeting isoforms IX and XII" in *Carbonic Anhydrases*. eds C. T. Supuran and A. Nocentini (United States: Academic Press). 331–365. doi: 10.1016/B978-0-12-816476-1.00016-2

Iliff, J. J., Wang, M., Liao, Y., Plogg, B. A., Peng, W., Gundersen, G. A., et al. (2012). A paravascular pathway facilitates CSF flow through the brain parenchyma and the clearance of interstitial solutes, including amyloid β. *Sci. Transl. Med.* 4, 147ra111. doi: 10.1126/scitranslmed.3003748

Imtaiyaz Hassan, M., Shajee, B., Waheed, A., Ahmad, F., and Sly, W. S. (2013). Structure, function and applications of carbonic anhydrase isozymes. *Bioorg. Med. Chem.* 21, 1570–1582. doi: 10.1016/j.bmc.2012.04.044

Ivanov, S., Liao, S. Y., Ivanova, A., Danilkovitch-Miagkova, A., Tarasova, N., Weirich, G., et al. (2001). Expression of hypoxia-inducible cell-surface transmembrane carbonic anhydrases in human cancer. *Am. J. Pathol.* 158, 905–919. doi: 10.1016/S0002-9440(10)64038-2

Ivanov, S. V., Kuzmin, I., Wei, M.-H., Pack, S., Geil, L., Johnson, B. E., et al. (1998). Down-regulation of transmembrane carbonic anhydrases in renal cell carcinoma cell lines by wild-type von Hippel-Lindau transgenes. *Proc. Natl. Acad. Sci.* 95:12596. doi: 10.1073/pnas.95.21.12596

Jiang, C. T., Wu, W. F., Deng, Y. H., and Ge, J. W. (2020). Modulators of microglia activation and polarization in ischemic stroke (Review). *Mol. Med. Rep.* 21, 2006–2018. doi: 10.3892/mmr.2020.11003

Jiao, H., Wang, Z., Liu, Y., Wang, P., and Xue, Y. (2011). Specific role of tight junction proteins claudin-5, occludin, and ZO-1 of the blood-brain barrier in a focal cerebral ischemic insult. *J. Mol. Neurosci.* 44, 130–139. doi: 10.1007/s12031-011-9496-4

Johnson, B. A. (2005). Recent advances in the development of treatments for alcohol and cocaine dependence: focus on topiramate and other modulators of GABA or glutamate function. *CNS Drugs* 19, 873–896. doi: 10.2165/00023210-200519100-00005

Joshi, A. U., Minhas, P. S., Liddelow, S. A., Haileselassie, B., Andreasson, K. I., Dorn, G. W. II, et al. (2019). Fragmented mitochondria released from microglia trigger A1 astrocytic response and propagate inflammatory neurodegeneration. *Nat. Neurosci.* 22, 1635–1648. doi: 10.1038/s41593-019-0486-0

Kang, M., and Yao, Y. (2020). Basement Membrane Changes in Ischemic Stroke. *Stroke* 51, 1344–1352. doi: 10.1161/STROKEAHA.120.028928

Kaplan, L., Chow, B. W., and Gu, C. (2020). Neuronal regulation of the blood-brain barrier and neurovascular coupling. *Nat. Rev. Neurosci.* 21, 416–432. doi: 10.1038/s41583-020-0322-2

Kida, E., Palminiello, S., Golabek, A. A., Walus, M., Wierzba-Bobrowicz, T., Rabe, A., et al. (2006). Carbonic anhydrase II in the developing and adult human brain. *J. Neuropathol. Exp. Neurol.* 65, 664–674. doi: 10.1097/01.jnen.0000225905.52002.3e

Kim, S. H., Ahn, J. H., Yang, H., Lee, P., Koh, G. Y., and Jeong, Y. (2020). Cerebral amyloid angiopathy aggravates perivascular clearance impairment in an Alzheimer's disease mouse model. *Acta Neuropathol. Commun.* 8:181. doi: 10.1186/s40478-020-01042-0

Kiss, B., Dallinger, S., Findl, O., Rainer, G., Eichler, H. G., and Schmetterer, L. (1999). Acetazolamide-induced cerebral and ocular vasodilation in humans is independent of nitric oxide. *Am. J. Physiol.* 276, R1661–R1667. doi: 10.1152/ajpregu.1999.276.6.R1661

Knopman, D. S., Jones, D. T., and Greicius, M. D. (2021). Failure to demonstrate efficacy of aducanumab: an analysis of the EMERGE and ENGAGE trials as reported by Biogen. December 2019. *Alzheimers Dement.* 17, 696–701. doi: 10.1002/alz.12213

Krishnamurthy, V. M., Kaufman, G. K., Urbach, A. R., Gitlin, I., Gudiksen, K. L., Weibel, D. B., et al. (2008). Carbonic Anhydrase as a Model for Biophysical and Physical-Organic Studies of Proteins and Protein-Ligand Binding. *Chem. Rev.* 108, 946–1051. doi: 10.1021/cr050262p

Kuriakose, D., and Xiao, Z. (2020). Pathophysiology and Treatment of Stroke: present Status and Future Perspectives. *Int. J. Mol. Sci.* 21:7609. doi: 10.3390/ijms21207609

Kuźma, E., Lourida, I., Moore, S. F., Levine, D. A., Ukoumunne, O. C., and Llewellyn, D. J. (2018). Stroke and dementia risk: A systematic review and meta-analysis. *Alzheimers Dement.* 14, 1416–1426. doi: 10.1016/j.jalz.2018.06.3061

Li, M., Wang, W., Mai, H., Zhang, X., Wang, J., Gao, Y., et al. (2016). Methazolamide improves neurological behavior by inhibition of neuron apoptosis in subarachnoid hemorrhage mice. *Sci. Rep.* 6:35055. doi: 10.1038/srep35055

Liddelow, S. A., Guttenplan, K. A., Clarke, L. E., Bennett, F. C., Bohlen, C. J., Schirmer, L., et al. (2017). Neurotoxic reactive astrocytes are induced by activated microglia. *Nature* 541, 481–487. doi: 10.1038/nature21029

Liu, C., Wei, Y., Wang, J., Pi, L., Huang, J., and Wang, P. (2012). Carbonic anhydrases III and IV autoantibodies in rheumatoid arthritis, systemic lupus erythematosus, diabetes, hypertensive renal disease, and heart failure. *Clin. Dev. Immunol.* 2012:354594. doi: 10.1155/2012/354594

Lochhead, J. J., Mccaffrey, G., Quigley, C. E., Finch, J., Demarco, K. M., Nametz, N., et al. (2010). Oxidative stress increases blood-brain barrier permeability and induces alterations in occludin during hypoxia-reoxygenation. *J. Cereb. Blood Flow Metab.* 30, 1625–1636. doi: 10.1038/jcbfm.2010.29

Lok, J., Wang, X. S., Xing, C. H., Maki, T. K., Wu, L. M., Guo, S. Z., et al. (2015). Targeting the neurovascular unit in brain trauma. *CNS Neurosci. Ther.* 21, 304–308. doi: 10.1111/cns.12359

Lorenzl, S., Albers, D. S., Relkin, N., Ngyuen, T., Hilgenberg, S. L., Chirichigno, J., et al. (2003). Increased plasma levels of matrix metalloproteinase-9 in patients with Alzheimer's disease. *Neurochem. Int.* 43, 191–196. doi: 10.1016/S0197-0186(03)00004-4

Lu, H., Zhang, H., and Jiang, Y. (2020). Methazolamide in high-altitude illnesses. *Eur. J. Pharm. Sci.* 148:105326. doi: 10.1016/j.ejps.2020.105326

Manley, G. T., Fujimura, M., Ma, T., Noshita, N., Filiz, F., Bollen, A. W., et al. (2000). Aquaporin-4 deletion in mice reduces brain edema after acute water intoxication and ischemic stroke. *Nat. Med.* 6, 159–163. doi: 10.1038/72256

Mao, X. Y., Cao, Y. G., Ji, Z., Zhou, H. H., Liu, Z. Q., and Sun, H. L. (2015). Topiramate protects against glutamate excitotoxicity via activating BDNF/TrkB-dependent ERK pathway in rodent hippocampal neurons. *Prog. Neuropsychopharmacol. Biol. Psychiatry* 60, 11–17. doi: 10.1016/j.pnpbp.2015.01.015

Marco, S., and Skaper, S. D. (2006). Amyloid beta-peptide1-42 alters tight junction protein distribution and expression in brain microvessel endothelial cells. *Neurosci. Lett.* 401, 219–224. doi: 10.1016/j.neulet.2006.03.047

Maren, T. H. (1967). Carbonic anhydrase: chemistry, physiology, and inhibition. *Physiol. Rev.* 47, 595–781. doi: 10.1152/physrev.1967.47.4.595

Mboge, M. Y., Mahon, B. P., Mckenna, R., and Frost, S. C. (2018). Carbonic Anhydrases: role in pH Control and Cancer. *Metabolites* 8:19. doi: 10.3390/metabo8010019

McAlpine, C. S., Park, J., Griciuc, A., Kim, E., Choi, S. H., Iwamoto, Y., et al. (2021). Astrocytic interleukin-3 programs microglia and limits Alzheimer's disease. *Nature* 595, 701–706. doi: 10.1038/s41586-021-03734-6

McConnell, H. L., Li, Z., Woltjer, R. L., and Mishra, A. (2019). Astrocyte dysfunction and neurovascular impairment in neurological disorders: correlation or causation? *Neurochem. Int.* 128, 70–84. doi: 10.1016/j.neuint.2019.04.005

McDonald, P. C., Chia, S., Bedard, P. L., Chu, Q., Lyle, M., Tang, L., et al. (2020). A Phase 1 Study of SLC-0111, a Novel Inhibitor of Carbonic Anhydrase IX,

in Patients With Advanced Solid Tumors. *Am. J. Clin. Oncol.* 43, 484–490. doi: 10.1097/COC.0000000000000691

McKenna, R., and Supuran, C. T. (2014). Carbonic anhydrase inhibitors drug design. *Subcell. Biochem.* 75, 291–323. doi: 10.1007/978-94-007-7359-2_15

Mestre, H., Mori, Y., and Nedergaard, M. (2020). The Brain's Glymphatic System: current Controversies. *Trends Neurosci.* 43, 458–466. doi: 10.1016/j.tins.2020.04.003

Mincione, F., Scozzafava, A., and Supuran, C. T. (2007). The development of topically acting carbonic anhydrase inhibitors as anti-glaucoma agents. *Curr. Top. Med. Chem.* 7, 849–854. doi: 10.2174/156802607780636735

Mishra, C. B., Tiwari, M., and Supuran, C. T. (2020). Progress in the development of human carbonic anhydrase inhibitors and their pharmacological applications: where are we today? *Med. Res. Rev.* 40, 2485–2565. doi: 10.1002/med.21713

Mohamed, I. N., Ishrat, T., Fagan, S. C., and El-Remessy, A. B. (2015). Role of inflammasome activation in the pathophysiology of vascular diseases of the neurovascular unit. *Antioxid. Redox Signal.* 22, 1188–1206. doi: 10.1089/ars.2014.6126

Montaner, J., Ramiro, L., Simats, A., Hernandez-Guillamon, M., Delgado, P., Bustamante, A., et al. (2019). Matrix metalloproteinases and ADAMs in stroke. *Cell. Mol. Life Sci.* 76, 3117–3140. doi: 10.1007/s00018-019-03175-5

Mori, K., Ogawa, Y., Ebihara, K., Tamura, N., Tashiro, K., Kuwahara, T., et al. (1999). Isolation and characterization of CA XIV, a novel membrane-bound carbonic anhydrase from mouse kidney. *J. Biol. Chem.* 274, 15701–15705. doi: 10.1074/jbc.274.22.15701

Morikawa, E., Moskowitz, M. A., Huang, Z., Yoshida, T., Irikura, K., and Dalkara, T. (1994). L-arginine infusion promotes nitric oxide-dependent vasodilation, increases regional cerebral blood flow, and reduces infarction volume in the rat. *Stroke* 25, 429–435. doi: 10.1161/01.STR.25.2.429

Morris, A. W., Carare, R. O., Schreiber, S., and Hawkes, C. A. (2014). The Cerebrovascular Basement Membrane: role in the Clearance of β-amyloid and Cerebral Amyloid Angiopathy. *Front. Aging Neurosci.* 6:251. doi: 10.3389/fnagi.2014.00251

Nedergaard, M., and Goldman, S. A. (2020). Glymphatic failure as a final common pathway to dementia. *Science* 370, 50–56. doi: 10.1126/science.abb8739

Nishimori, I., Minakuchi, T., Onishi, S., Vullo, D., Scozzafava, A., and Supuran, C. T. (2007). Carbonic anhydrase inhibitors. DNA cloning, characterization, and inhibition studies of the human secretory isoform VI, a new target for sulfonamide and sulfamate inhibitors. *J. Med. Chem.* 50, 381–388. doi: 10.1021/jm0612057

Nishimori, I., Vullo, D., Innocenti, A., Scozzafava, A., Mastrolorenzo, A., and Supuran, C. T. (2005). Carbonic anhydrase inhibitors. The mitochondrial isozyme VB as a new target for sulfonamide and sulfamate inhibitors. *J. Med. Chem.* 48, 7860–7866. doi: 10.1021/jm050483n

Nortley, R., Korte, N., Izquierdo, P., Hirunpattarasilp, C., Mishra, A., Jaunmuktane, Z., et al. (2019). Amyloid β oligomers constrict human capillaries in Alzheimer's disease via signaling to pericytes. *Science* 365:eaav9518. doi: 10.1126/science.aav9518

Oeckl, P., Halbgebauer, S., Anderl-Straub, S., Steinacker, P., Huss, A. M., and Neugebauer, H. (2019). Glial Fibrillary Acidic Protein in Serum is Increased in Alzheimer's Disease and Correlates with Cognitive Impairment. *J. Alzheimers Dis.* 67, 481–488. doi: 10.3233/JAD-180325

Ojo, J. O., Reed, J. M., Crynen, G., Vallabhaneni, P., Evans, J., Shackleton, B., et al. (2021). Molecular Pathobiology of the Cerebrovasculature in Aging and in Alzheimers Disease Cases With Cerebral Amyloid Angiopathy. *Front. Aging Neurosci.* 13:658605. doi: 10.3389/fnagi.2021.658605

Okudaira, Y., Bandoh, K., Arai, H., and Sato, K. (1995). Evaluation of the acetazolamide test. Vasoreactivity and cerebral blood volume. *Stroke* 26, 1234–1239. doi: 10.1161/01.STR.26.7.1234

Oldendorf, W. H., Cornford, M. E., and Brown, W. J. (1977). The large apparent work capability of the blood-brain barrier: a study of the mitochondrial content of capillary endothelial cells in brain and other tissues of the rat. *Ann. Neurol.* 1, 409–417. doi: 10.1002/ana.410010502

Pan, P., Leppilampi, M., Pastorekova, S., Pastorek, J., Waheed, A., Sly, W. S., et al. (2006). Carbonic anhydrase gene expression in CA II-deficient (Car2-/-) and CA IX-deficient (Car9-/-) mice. *J. Physiol.* 571, 319–327. doi: 10.1113/jphysiol.2005.102590

Pan, P. W., Parkkila, A. K., Autio, S., Hilvo, M., Sormunen, R., Pastorekova, S., et al. (2012). Brain phenotype of carbonic anhydrase IX-deficient mice. *Transgenic Res.* 21, 163–176. doi: 10.1007/s11248-011-9520-z

Parodi-Rullán, R., Ghiso, J., Cabrera, E., Rostagno, A., and Fossati, S. (2020). Alzheimer's amyloid β heterogeneous species differentially affect brain endothelial cell viability, blood-brain barrier integrity, and angiogenesis. *Aging Cell.* 19:e13258. doi: 10.1111/acel.13258

Parodi-Rullán, R., Sone, J. Y., and Fossati, S. (2019). Endothelial Mitochondrial Dysfunction in Cerebral Amyloid Angiopathy and Alzheimer's Disease. *J. Alzheimers Dis.* 72, 1019–1039. doi: 10.3233/JAD-190357

Pastorek, J., and Pastorekova, S. (2015). Hypoxia-induced carbonic anhydrase IX as a target for cancer therapy: from biology to clinical use. *Semin. Cancer Biol.* 31, 52–64. doi: 10.1016/j.semcancer.2014.08.002

Patrick, P., Price, T. O., Diogo, A. L., Sheibani, N., Banks, W. A., and Shah, G. N. (2015). Topiramate Protects Pericytes from Glucotoxicity: role for Mitochondrial CA VA in Cerebromicrovascular Disease in Diabetes. *J. Endocrinol. Diabetes* 2, 1–7. doi: 10.15226/2374-6890/2/2/00123

Patrikainen, M., Pan, P., Kulesskaya, N., Voikar, V., and Parkkila, S. (2014). The role of carbonic anhydrase VI in bitter taste perception: evidence from the Car6^{-}/$^{-}$ mouse model. *J. Biomed. Sci.* 21, 82. doi: 10.1186/s12929-014-0082-2

Pavics, L., Grunwald, F., Reichmann, K., Horn, R., Kitschenberg, A., Hartmann, A., et al. (1999). Regional cerebral blood flow single-photon emission tomography with 99mTc-HMPAO and the acetazolamide test in the evaluation of vascular and Alzheimer's dementia. *Eur. J. Nucl. Med.* 26, 239–245. doi: 10.1007/s002590050383

Pekny, M., and Lane, E. B. (2007). Intermediate filaments and stress. *Exp. Cell Res.* 313, 2244–2254. doi: 10.1016/j.yexcr.2007.04.023

Pollard, A., Shephard, F., Freed, J., Liddell, S., and Chakrabarti, L. (2016). Mitochondrial proteomic profiling reveals increased carbonic anhydrase II in aging and neurodegeneration. *Aging* 8, 2425–2436. doi: 10.18632/aging.101064

Price, T. O., Eranki, V., Banks, W. A., Ercal, N., and Shah, G. N. (2012). Topiramate treatment protects blood-brain barrier pericytes from hyperglycemia-induced oxidative damage in diabetic mice. *Endocrinology* 153, 362–372. doi: 10.1210/en.2011-1638

Price, T. O., Sheibani, N., and Shah, G. N. (2017). Regulation of high glucose-induced apoptosis of brain pericytes by mitochondrial CA VA: a specific target for prevention of diabetic cerebrovascular pathology. *Biochim. Biophys. Acta Mol. Basis Dis.* 1863, 929–935. doi: 10.1016/j.bbadis.2017.01.025

Proescholdt, M. A., Mayer, C., Kubitza, M., Schubert, T., Liao, S.-Y., Stanbridge, E. J., et al. (2005). Expression of hypoxia-inducible carbonic anhydrases in brain tumors. *Neurooncology* 7, 465–475. doi: 10.1215/S1152851705000025

Provensi, G., Carta, F., Nocentini, A., Supuran, C. T., Casamenti, F., Passani, M. B., et al. (2019). A New Kid on the Block? Carbonic Anhydrases as Possible New Targets in Alzheimer's Disease. *Int J Mol Sci* 20:4724. doi: 10.3390/ijms20194724

Pun, P. B., Lu, J., and Moochhala, S. (2009). Involvement of ROS in BBB dysfunction. *Free Radic. Res.* 43, 348–364. doi: 10.1080/10715760902751902

Purkerson, J. M., and Schwartz, G. J. (2007). The role of carbonic anhydrases in renal physiology. *Kidney Int.* 71, 103–115. doi: 10.1038/sj.ki.5002020

Quintana, D. D., Anantula, Y., Garcia, J. A., Engler-Chiurazzi, E. B., Sarkar, S. N., Corbin, D. R., et al. (2021). Microvascular degeneration occurs before plaque onset and progresses with age in 3xTg AD mice. *Neurobiol. Aging* 105, 115–128. doi: 10.1016/j.neurobiolaging.2021.04.019

Radenovic, L., Nenadic, M., Ułamek-Kozioł, M., Januszewski, S., Czuczwar, S. J., Andjus, P. R., et al. (2020). Heterogeneity in brain distribution of activated microglia and astrocytes in a rat ischemic model of Alzheimer's disease after 2 years of survival. *Aging* 12, 12251–12267. doi: 10.18632/aging.103411

Rasmussen, J. K., and Boedtkjer, E. (2018). Carbonic anhydrase inhibitors modify intracellular pH transients and contractions of rat middle cerebral arteries during CO. *J. Cereb. Blood Flow Metab.* 38, 492–505. doi: 10.1177/0271678X17699224

Reese, T. S., and Karnovsky, M. J. (1967). Fine structural localization of a blood-brain barrier to exogenous peroxidase. *J. Cell. Biol.* 34, 207–217. doi: 10.1083/jcb.34.1.207

Ritchie, N. D., Baggott, A. V., and Andrew Todd, W. T. (2012). Acetazolamide for the prevention of acute mountain sickness–a systematic review and meta-analysis. *J. Travel Med.* 19, 298–307. doi: 10.1111/j.1708-8305.2012.00629.x

Russell, S. M., Woo, H. H., Siller, K., Panasci, D., and Leroux, P. D. (2008). Evaluating middle cerebral artery collateral blood flow reserve using acetazolamide transcranial Doppler ultrasound in patients with carotid occlusive disease. *Surg. Neurol.* 70, 466–470. doi: 10.1016/j.surneu.2007.10.030

Ruusuvuori, E., Huebner, A. K., Kirilkin, I., Yukin, A. Y., Blaesse, P., Helmy, M., et al. (2013). Neuronal carbonic anhydrase VII provides GABAergic excitatory drive to exacerbate febrile seizures. *Embo J.* 32, 2275–2286. doi: 10.1038/emboj.2013.160

Ruusuvuori, E., and Kaila, K. (2014). Carbonic anhydrases and brain pH in the control of neuronal excitability. *Subcell. Biochem.* 75, 271–290. doi: 10.1007/978-94-007-7359-2_14

Ruusuvuori, E., Li, H., Huttu, K., Palva, J. M., Smirnov, S., Rivera, C., et al. (2004). Carbonic anhydrase isoform VII acts as a molecular switch in the development of synchronous gamma-frequency firing of hippocampal CA1 pyramidal cells. *J. Neurosci.* 24, 2699–2707. doi: 10.1523/JNEUROSCI.5176-03.2004

Saarnio, J., Parkkila, S., Parkkila, A. K., Waheed, A., Casey, M. C., Zhou, X. Y., et al. (1998). Immunohistochemistry of carbonic anhydrase isozyme IX (MN/CA IX) in human gut reveals polarized expression in the epithelial cells with the highest proliferative capacity. *J. Histochem. Cytochem.* 46, 497–504. doi: 10.1177/002215549804600409

Sacco, R. L., Kasner, S. E., Broderick, J. P., Caplan, L. R., Connors, J. J., Culebras, A., et al. (2013). An updated definition of stroke for the 21st century: a statement for healthcare professionals from the American Heart Association/American Stroke Association. *Stroke* 44, 2064–2089. doi: 10.1161/STR.0b013e318296aeca

Sagare, A. P., Bell, R. D., Zhao, Z., Ma, Q., Winkler, E. A., Ramanathan, A., et al. (2013). Pericyte loss influences Alzheimer-like neurodegeneration in mice. *Nat. Commun.* 4:2932. doi: 10.1038/ncomms3932

Salameh, T. S., Mortell, W. G., Logsdon, A. F., Butterfield, D. A., and Banks, W. A. (2019). Disruption of the hippocampal and hypothalamic blood-brain barrier in a diet-induced obese model of type II diabetes: prevention and treatment by the mitochondrial carbonic anhydrase inhibitor, topiramate. *Fluids Barriers CNS* 16:1. doi: 10.1186/s12987-018-0121-6

Salameh, T. S., Shah, G. N., Price, T. O., Hayden, M. R., and Banks, W. A. (2016). Blood-Brain Barrier Disruption and Neurovascular Unit Dysfunction in Diabetic Mice: protection with the Mitochondrial Carbonic Anhydrase Inhibitor Topiramate. *J. Pharmacol. Exp. Ther.* 359, 452–459. doi: 10.1124/jpet.116.237057

Sanku, R. K. K., John, J. S., Salkovitz, M., Ilies, M. A., and Walker, E. A. (2018). Potential learning and memory disruptors and enhancers in a simple, 1-day operant task in mice. *Behav. Pharmacol.* 29, 482–492. doi: 10.1097/FBP.0000000000000400

Sarvari, S., Moakedi, F., Hone, E., Simpkins, J. W., and Ren, X. (2020). Mechanisms in blood-brain barrier opening and metabolism-challenged cerebrovascular ischemia with emphasis on ischemic stroke. *Metab. Brain Dis.* 35, 851–868. doi: 10.1007/s11011-020-00573-8

Savva, G. M., and Stephan, B. C. (2010). Epidemiological studies of the effect of stroke on incident dementia: a systematic review. *Stroke* 41, e41–46. doi: 10.1161/STROKEAHA.109.559880

Schmidt, S. D., Costa, A., Rani, B., Godfried Nachtigall, E., Passani, M. B., Carta, F., et al. (2020). The role of carbonic anhydrases in extinction of contextual fear memory. *Proc. Natl. Acad. Sci. U. S. A.* 117, 16000–16008. doi: 10.1073/pnas.1910690117

Schreibelt, G., Kooij, G., Reijerkerk, A., Van Doorn, R., Gringhuis, S. I., Van Der Pol, S., et al. (2007). Reactive oxygen species alter brain endothelial tight junction dynamics via RhoA. PI3 kinase, and PKB signaling. *FASEB J.* 21, 3666–3676. doi: 10.1096/fj.07-8329com

Scozzafava, A., Briganti, F., Ilies, M. A., and Supuran, C. T. (2000). Carbonic anhydrase inhibitors: synthesis of membrane-impermeant low molecular weight sulfonamides possessing in vivo selectivity for the membrane-bound versus cytosolic isozymes. *J. Med. Chem.* 43, 292–300. doi: 10.1021/jm990479+

Scozzafava, A., Supuran, C. T., and Carta, F. (2013). Antiobesity carbonic anhydrase inhibitors: a literature and patent review. *Expert. Opin. Ther. Pat.* 23, 725–735. doi: 10.1517/13543776.2013.790957

Seçkin, H., Simşek, S., Oztürk, E., Yigitkanli, K., Ozen, O., Beşalti, O., et al. (2009). Topiramate attenuates hippocampal injury after experimental subarachnoid hemorrhage in rabbits. *Neurol. Res.* 31, 490–495. doi: 10.1179/016164108X339369

Sekerdag, E., Solaroglu, I., and Gursoy-Ozdemir, Y. (2018). Cell Death Mechanisms in Stroke and Novel Molecular and Cellular Treatment Options. *Curr. Neuropharmacol.* 16, 1396–1415. doi: 10.2174/1570159X16666180302115544

Sevigny, J., Chiao, P., Bussiere, T., Weinreb, P. H., Williams, L., Maier, M., et al. (2017). Addendum: The antibody aducanumab reduces Abeta plaques in Alzheimer's disease. *Nature* 546:564. doi: 10.1038/nature22809

Shabana, A. M., and Ilies, M. A. (2019). *Drug Delivery to Hypoxic Tumors Targeting Carbonic Anhydrase IX*. United States: American Chemical Society. 223–252. doi: 10.1021/bk-2019-1309.ch010

Shah, G. N., Hewett-Emmett, D., Grubb, J. H., Migas, M. C., Fleming, R. E., Waheed, A., et al. (2000). Mitochondrial carbonic anhydrase CA VB: differences in tissue distribution and pattern of evolution from those of CA VA suggest distinct physiological roles. *Proc. Natl. Acad. Sci. U. S. A.* 97, 1677–1682. doi: 10.1073/pnas.97.4.1677

Shah, G. N., Morofuji, Y., Banks, W. A., and Price, T. O. (2013a). High glucose-induced mitochondrial respiration and reactive oxygen species in mouse cerebral pericytes is reversed by pharmacological inhibition of mitochondrial carbonic anhydrases: implications for cerebral microvascular disease in diabetes. *Biochem. Biophys. Res. Commun.* 440, 354–358. doi: 10.1016/j.bbrc.2013.09.086

Shah, G. N., Rubbelke, T. S., Hendin, J., Nguyen, H., Waheed, A., Shoemaker, J. D., et al. (2013b). Targeted mutagenesis of mitochondrial carbonic anhydrases VA and VB implicates both enzymes in ammonia detoxification and glucose metabolism. *Proc. Natl. Acad. Sci. U. S. A.* 110, 7423–7428. doi: 10.1073/pnas.1305805110

Shah, G. N., Ulmasov, B., Waheed, A., Becker, T., Makani, S., Svichar, N., et al. (2005). Carbonic anhydrase IV and XIV knockout mice: roles of the respective carbonic anhydrases in buffering the extracellular space in brain. *Proc. Natl. Acad. Sci. U. S. A.* 102, 16771–16776. doi: 10.1073/pnas.0508449102

Shin, J. A., Yoon, J. C., Kim, M., and Park, E. M. (2016). Activation of classical estrogen receptor subtypes reduces tight junction disruption of brain endothelial cells under ischemia/reperfusion injury. *Free Radic. Biol. Med.* 92, 78–89. doi: 10.1016/j.freeradbiomed.2016.01.010

Silverman, D. N., and Lindskog, S. (1988). The catalytic mechanism of carbonic anhydrase: implications of a rate-limiting protolysis of water. *Acc. Chem. Res.* 21, 30–36. doi: 10.1021/ar00145a005

Sly, W. S., and Hu, P. Y. (1995). Human carbonic anhydrases and carbonic anhydrase deficiencies. *Annu. Rev. Biochem.* 64, 375–401. doi: 10.1146/annurev.bi.64.070195.002111

Smaine, F. Z., Winum, J. Y., Montero, J. L., Regainia, Z., Vullo, D., Scozzafava, A., et al. (2007). Carbonic anhydrase inhibitors: selective inhibition of the extracellular, tumor-associated isoforms IX and XII over isozymes I and II with glycosyl-thioureido-sulfonamides. *Bioorg. Med. Chem. Lett.* 17, 5096–5100. doi: 10.1016/j.bmcl.2007.07.019

Smith, A. J., Duan, T., and Verkman, A. S. (2019). Aquaporin-4 reduces neuropathology in a mouse model of Alzheimer's disease by remodeling peri-plaque astrocyte structure. *Acta Neuropathol. Commun.* 7:74. doi: 10.1186/s40478-019-0728-0

Solesio, M. E., Peixoto, P. M., Debure, L., Madamba, S. M., De Leon, M. J., Wisniewski, T., et al. (2018). Carbonic anhydrase inhibition selectively prevents amyloid β neurovascular mitochondrial toxicity. *Aging Cell.* 17:e12787. doi: 10.1111/acel.12787

Sotolongo, K., Ghiso, J., and Rostagno, A. (2020). Nrf2 activation through the PI3K/GSK-3 axis protects neuronal cells from Abeta-mediated oxidative and metabolic damage. *Alzheimers Res. Ther.* 12:13. doi: 10.1186/s13195-019-0578-9

Stams, T., Nair, S. K., Okuyama, T., Waheed, A., Sly, W. S., and Christianson, D. W. (1996). Crystal structure of the secretory form of membrane-associated human carbonic anhydrase IV at 2.8-A resolution. *Proc. Natl. Acad. Sci. U. S. A.* 93, 13589–13594. doi: 10.1073/pnas.93.24.13589

Stoppe, G., Schutze, R., Kogler, A., Staedt, J., Munz, D. L., Emrich, D., et al. (1995). Cerebrovascular reactivity to acetazolamide in (senile) dementia of Alzheimer's type: relationship to disease severity. *Dementia* 6, 73–82. doi: 10.1159/000106925

Supuran, C. T. (2008). Carbonic anhydrases: novel therapeutic applications for inhibitors and activators. *Nat. Rev. Drug Discov.* 7, 168–181. doi: 10.1038/nrd2467

Supuran, C. T. (2011). Carbonic anhydrase inhibitors and activators for novel therapeutic applications. *Future Med. Chem.* 3, 1165–1180. doi: 10.4155/fmc.11.69

Supuran, C. T. (2012). Carbonic anhydrase inhibitors as emerging drugs for the treatment of obesity. *Expert Opin. Emerg. Drugs* 17, 11–15. doi: 10.1517/14728214.2012.664132

Supuran, C. T. (2018). Applications of carbonic anhydrases inhibitors in renal and central nervous system diseases. *Expert Opin. Ther. Pat.* 28, 713–721. doi: 10.1080/13543776.2018.1519023

Supuran, C. T., and Capasso, C. (2020). Antibacterial carbonic anhydrase inhibitors: an update on the recent literature. *Expert Opin. Ther. Pat.* 30, 963–982. doi: 10.1080/13543776.2020.1811853

Supuran, C. T., Scozzafava, A., and Casini, A. (2003). Carbonic anhydrase inhibitors. *Med. Res. Rev.* 23, 146–189. doi: 10.1002/med.10025

Supuran, C. T., Scozzafava, A., Ilies, M. A., Iorga, B., Cristea, T., Briganti, F., et al. (1998). Carbonic anhydrase inhibitors — Part 53. Synthesis of substituted-pyridinium derivatives of aromatic sulfonamides: the first non-polymeric membrane-impermeable inhibitors with selectivity for isozyme IV. *Eur. J. Med. Chem.* 33, 577–594. doi: 10.1016/S0223-5234(98)80017-2

Supuran, C. T., and Winum, J. Y. (2015). Carbonic anhydrase IX inhibitors in cancer therapy: an update. *Future Med. Chem.* 7, 1407–1414. doi: 10.4155/fmc.15.71

Sweeney, M. D., Montagne, A., Sagare, A. P., Nation, D. A., Schneider, L. S., Chui, H. C., et al. (2019a). Vascular dysfunction-The disregarded partner of Alzheimer's disease. *Alzheimers Dement.* 15, 158–167.

Sweeney, M. D., Zhao, Z., Montagne, A., Nelson, A. R., and Zlokovic, B. V. (2019b). Blood-Brain Barrier: From Physiology to Disease and Back. *Physiol. Rev.* 99, 21–78. doi: 10.1152/physrev.00050.2017

Tang, M., Gao, G., Rueda, C. B., Yu, H., Thibodeaux, D. N., Awano, T., et al. (2017). Brain microvasculature defects and Glut1 deficiency syndrome averted by early repletion of the glucose transporter-1 protein. *Nat. Commun.* 8:14152. doi: 10.1038/ncomms14152

Tang, Y., and Le, W. (2016). Differential Roles of M1 and M2 Microglia in Neurodegenerative Diseases. *Mol. Neurobiol.* 53, 1181–1194. doi: 10.1007/s12035-014-9070-5

Tuettenberg, J., Heimann, A., and Kempski, O. (2001). Nitric oxide modulates cerebral blood flow stimulation by acetazolamide in the rat cortex: a laser Doppler scanning study. *Neurosci. Lett.* 315, 65–68. doi: 10.1016/S0304-3940(01)02325-4

Türeci, Ö, Sahin, U., Vollmar, E., Siemer, S., Göttert, E., Seitz, G., et al. (1998). Human carbonic anhydrase XII: cDNA cloning, expression, and chromosomal localization of a carbonic anhydrase gene that is overexpressed in some renal cell cancers. *Proc. Natl. Acad. Sci.* 95:7608. doi: 10.1073/pnas.95.13.7608

Turner, R. J., and Sharp, F. R. (2016). Implications of MMP9 for Blood Brain Barrier Disruption and Hemorrhagic Transformation Following Ischemic Stroke. *Front. Cell. Neurosci.* 10:56. doi: 10.3389/fncel.2016.00056

Ulland, T. K., and Colonna, M. (2018). TREM2 - a key player in microglial biology and Alzheimer disease. *Nat. Rev. Neurol.* 14, 667–675. doi: 10.1038/s41582-018-0072-1

van Putten, M., Fahlke, C., Kafitz, K. W., Hofmeijer, J., and Rose, C. R. (2021). Dysregulation of Astrocyte Ion Homeostasis and Its Relevance for Stroke-Induced Brain Damage. *Int. J. Mol. Sci.* 22:5679. doi: 10.3390/ijms22115679

Vargas, L. A., Pinilla, O. A., Díaz, R. G., Sepúlveda, D. E., Swenson, E. R., Pérez, N. G., et al. (2016). Carbonic anhydrase inhibitors reduce cardiac dysfunction after sustained coronary artery ligation in rats. *Cardiovasc. Pathol.* 25, 468–477. doi: 10.1016/j.carpath.2016.08.003

Venkateshappa, C., Harish, G., Mythri, R. B., Mahadevan, A., Bharath, M. M., and Shankar, S. K. (2012). Increased oxidative damage and decreased antioxidant function in aging human substantia nigra compared to striatum: implications for Parkinson's disease. *Neurochem. Res.* 37, 358–369. doi: 10.1007/s11064-011-0619-7

Verkerke, M., Hol, E. M., and Middeldorp, J. (2021). Physiological and Pathological Ageing of Astrocytes in the Human Brain. *Neurochem. Res.* 46, 2662–2675. doi: 10.1007/s11064-021-03256-7

Villegas-Llerena, C., Phillips, A., Garcia-Reitboeck, P., Hardy, J., and Pocock, J. M. (2016). Microglial genes regulating neuroinflammation in the progression of Alzheimer's disease. *Curr. Opin. Neurobiol.* 36, 74–81. doi: 10.1016/j.conb.2015.10.004

Waheed, A., and Sly, W. S. (2017). Carbonic anhydrase XII functions in health and disease. *Gene* 623, 33–40. doi: 10.1016/j.gene.2017.04.027

Wang, X., Figueroa, B. E., Stavrovskaya, I. G., Zhang, Y., Sirianni, A. C., Zhu, S., et al. (2009). Methazolamide and melatonin inhibit mitochondrial cytochrome C release and are neuroprotective in experimental models of ischemic injury. *Stroke* 40, 1877–1885. doi: 10.1161/STROKEAHA.108.540765

Wang, X., Zhu, S., Pei, Z., Drozda, M., Stavrovskaya, I. G., Del Signore, S. J., et al. (2008). Inhibitors of cytochrome c release with therapeutic potential for Huntington's disease. *J. Neurosci.* 28, 9473–9485. doi: 10.1523/JNEUROSCI.1867-08.2008

Whittington, D. A., Waheed, A., Ulmasov, B., Shah, G. N., Grubb, J. H., Sly, W. S., et al. (2001). Crystal structure of the dimeric extracellular domain of human carbonic anhydrase XII, a bitopic membrane protein overexpressed in certain cancer tumor cells. *Proc. Natl. Acad. Sci. U. S. A.* 98, 9545–9550. doi: 10.1073/pnas.161301298

Willis, E. F., Macdonald, K. P. A., Nguyen, Q. H., Garrido, A. L., Gillespie, E. R., and Harley, S. B. R. (2020). Repopulating Microglia Promote Brain Repair in an IL-6-Dependent Manner. *Cell* 180, 833.e–846.e. doi: 10.1016/j.cell.2020.02.013

Winum, J. Y., Poulsen, S. A., and Supuran, C. T. (2009). Therapeutic applications of glycosidic carbonic anhydrase inhibitors. *Med. Res. Rev.* 29, 419–435. doi: 10.1002/med.20141

Xing, C., Hayakawa, K., Lok, J., Arai, K., and Lo, E. H. (2012). Injury and repair in the neurovascular unit. *Neurol. Res.* 34, 325–330. doi: 10.1179/1743132812Y.0000000019

Yang, C., Hawkins, K. E., Doré, S., and Candelario-Jalil, E. (2019). Neuroinflammatory mechanisms of blood-brain barrier damage in ischemic stroke. *Am. J. Physiol. Cell. Physiol.* 316, C135–C153. doi: 10.1152/ajpcell.00136.2018

Yang, Y., and Rosenberg, G. A. (2015). Matrix metalloproteinases as therapeutic targets for stroke. *Brain Res.* 1623, 30–38. doi: 10.1016/j.brainres.2015.04.024

Yao, Y. (2019). Basement membrane and stroke. *J. Cereb. Blood Flow Metab.* 39, 3–19. doi: 10.1177/0271678X18801467

Zamanova, S., Shabana, A. M., Mondal, U. K., and Ilies, M. A. (2019). Carbonic anhydrases as disease markers. *Expert. Opin. Ther. Pat.* 29, 509–533. doi: 10.1080/13543776.2019.1629419

Zhou, Y., Song, W. M., Andhey, P. S., Swain, A., Levy, T., Miller, K. R., et al. (2020). Human and mouse single-nucleus transcriptomics reveal TREM2-dependent and TREM2-independent cellular responses in Alzheimer's disease. *Nat. Med.* 26, 131–142. doi: 10.1038/s41591-019-0695-9

Zlokovic, B. V., Gottesman, R. F., Bernstein, K. E., Seshadri, S., Mckee, A., Snyder, H., et al. (2020). Vascular contributions to cognitive impairment and dementia (VCID): a report from the 2018 National Heart, Lung, and Blood Institute and National Institute of Neurological Disorders and Stroke Workshop. *Alzheimers Dement.* 16, 1714–1733. doi: 10.1002/alz.12157

Conflict of Interest: The authors declare that the research was conducted in the absence of any commercial or financial relationships that could be construed as a potential conflict of interest.

Publisher's Note: All claims expressed in this article are solely those of the authors and do not necessarily represent those of their affiliated organizations, or those of the publisher, the editors and the reviewers. Any product that may be evaluated in this article, or claim that may be made by its manufacturer, is not guaranteed or endorsed by the publisher.

frontiers in Aging Neuroscience

ORIGINAL RESEARCH
published: 23 November 2021
doi: 10.3389/fnagi.2021.751304

Insulin-Like Growth Factor-1 Differentially Modulates Glutamate-Induced Toxicity and Stress in Cells of the Neurogliovascular Unit

*Cellas A. Hayes[1], Brandon G. Ashmore[1], Akshaya Vijayasankar[1], Jessica P. Marshall[1] and Nicole M. Ashpole[1,2]**

[1] Department of BioMolecular Sciences, University of Mississippi School of Pharmacy, University of Mississippi, Oxford, MS, United States, [2] Research Institute of Pharmaceutical Sciences, University of Mississippi School of Pharmacy, University of Mississippi, Oxford, MS, United States

The age-related reduction in circulating levels of insulin-like growth factor-1 (IGF-1) is associated with increased risk of stroke and neurodegenerative diseases in advanced age. Numerous reports highlight behavioral and physiological deficits in blood-brain barrier function and neurovascular communication when IGF-1 levels are low. Administration of exogenous IGF-1 reduces the extent of tissue damage and sensorimotor deficits in animal models of ischemic stroke, highlighting the critical role of IGF-1 as a regulator of neurovascular health. The beneficial effects of IGF-1 in the nervous system are often attributed to direct actions on neurons; however, glial cells and the cerebrovasculature are also modulated by IGF-1, and systemic reductions in circulating IGF-1 likely influence the viability and function of the entire neuro-glio-vascular unit. We recently observed that reduced IGF-1 led to impaired glutamate handling in astrocytes. Considering glutamate excitotoxicity is one of the main drivers of neurodegeneration following ischemic stroke, the age-related loss of IGF-1 may also compromise neural function indirectly by altering the function of supporting glia and vasculature. In this study, we assess and compare the effects of IGF-1 signaling on glutamate-induced toxicity and reactive oxygen species (ROS)-produced oxidative stress in primary neuron, astrocyte, and brain microvascular endothelial cell cultures. Our findings verify that neurons are highly susceptible to excitotoxicity, in comparison to astrocytes or endothelial cells, and that a prolonged reduction in IGFR activation increases the extent of toxicity. Moreover, prolonged IGFR inhibition increased the susceptibility of astrocytes to glutamate-induced toxicity and lessened their ability to protect neurons from excitotoxicity. Thus, IGF-1 promotes neuronal survival by acting directly on neurons and indirectly on astrocytes. Despite increased resistance to excitotoxic death, both astrocytes and cerebrovascular endothelial cells exhibit acute increases in glutamate-induced ROS production and mitochondrial dysfunction when IGFR is inhibited at the time of glutamate stimulation. Together these data highlight

OPEN ACCESS

Edited by:
Shereen Nizari, University College London, United Kingdom

Reviewed by:
Stefano Tarantini, University of Oklahoma Health Sciences Center, United States
Qiaojie Xiong, Stony Brook University, United States

***Correspondence:**
Nicole M. Ashpole
nmashpol@olemiss.edu

Received: *31 July 2021*
Accepted: *08 October 2021*
Published: *23 November 2021*

Citation:
Hayes CA, Ashmore BG, Vijayasankar A, Marshall JP and Ashpole NM (2021) Insulin-Like Growth Factor-1 Differentially Modulates Glutamate-Induced Toxicity and Stress in Cells of the Neurogliovascular Unit. Front. Aging Neurosci. 13:751304. doi: 10.3389/fnagi.2021.751304

that each cell type within the neuro-glio-vascular unit differentially responds to stress when IGF-1 signaling was impaired. Therefore, the reductions in circulating IGF-1 observed in advanced age are likely detrimental to the health and function of the entire neuro-glio-vascular unit.

Keywords: astrocytes, endothelial cells, neurotoxicity, somatomedin C, reactive oxygen species

INTRODUCTION

Aging is a primary risk factor for a number of diseases and pathologies, including stroke, which is recognized as one of the leading causes of death and disability globally (Johnson et al., 2016; Benjamin et al., 2019). Ischemic stroke is particularly devastating as the long-term phenotypic deficits in cognitive behavior and sensorimotor function build in the days following the insult, even if blood flow to the ischemic tissue is restored [as reviewed by George and Steinberg (2015)]. Ischemia precipitates cellular damage in the brain within minutes, as the loss of blood flow induces metabolic and oxidative stress in the energy-demanding neurons, and nearby glial and cerebrovascular cells. Immediate restoration of blood flow is critical, as the length of ischemia correlates with the extent of tissue damage (Terasaki et al., 2014). To date, the most effective ischemic stroke therapy is fibrinolytic breakdown of the clot with administration of tissue plasminogen activator. Unfortunately, this therapy is time-restricted and requires confirmation of ischemic vs hemorrhagic manifestation, which restricts clinical utility and has limited its use to around 5% of stroke patients each year (National Institute of Neurological Disorders and Stroke rt-Pa Stroke Study Group, 1995). Longitudinal observation-based clinical assessments have identified multiple possible biomarkers of stroke risk and severity, including insulin-like growth factor-1 (IGF-1), which may serve as a point of therapeutic intervention in the days surrounding insult (Katzan et al., 2000; California Acute Stroke Pilot Registry Investigators, 2005; Qureshi et al., 2005; Kleindorfer et al., 2008).

Insulin-like growth factor-1 is a pleiotropic neuroendocrine modulator that has been assessed in both clinical and preclinical studies of stroke [as reviewed by Hayes et al. (2021)]. Both humans and rodents exhibit age-related circulating declines of IGF-1 (O'Connor et al., 1998; Sonntag et al., 2013). IGF-1 levels decline in advanced age, and the extent of this decline is associated with increased risk of stroke incidence, increased mortality, and worsened functional outcomes post-stroke in humans (Johnsen et al., 2004; De Smedt et al., 2011; Tang et al., 2014; Armbrust et al., 2017; Saber et al., 2017). Moreover, altered IGF-1 levels are also associated with increased risk of multiple age-related neuropathologies marked by neurovascular distress, excitotoxicity, and oxidative stress (Watanabe et al., 2005; Sonntag et al., 2013; Ghazi Sherbaf et al., 2018; Gubbi et al., 2018). While many studies associate reduced IGF-1 with increased neurodegeneration, some clinical studies of dementias and stroke see increased IGF-1 levels at the start of pathology, which may be an attempted compensatory mechanism designed to protect the brain (Gubbi et al., 2018; Castilla-Cortazar et al., 2020). Preclinical studies suggest that IGF-1 plays a causal role in the stroke risk and recovery processes by directly regulating cell damage during ischemia [as reviewed by Hayes et al. (2021)]. IGF-1 supplementation in rodent models of middle cerebral artery occlusion and photothrombotic stroke reduces the size of infarcted tissue and the accompanying sensorimotor deficits, even when administered in the days after insult (Liu et al., 2001; Bake et al., 2014, 2016; Parker et al., 2017; Serhan et al., 2019; Hayes et al., 2021). Because IGF-1 regulates numerous cells throughout the body, the cellular mechanism by which IGF-1 protects viability and function in the brain remains unclear. It is commonly inferred that the beneficial effects of IGF-1 are mediated by direct regulation of neurons. However, neurons, astrocytes, endothelial cells, and perivascular cells each express the receptor for IGF-1, IGFR. Together, these cells work to compose the neurovascular unit (also known as neuro-glio-vascular unit) which tightly coordinates physiological responses within the nervous system and is a central target for dysfunction in neurodegenerative diseases and pathologies (Stanimirovic and Friedman, 2012). Additional work is needed to tease apart the impact of each cell type when exogenous IGF-1 is administered to protect against the damage induced by stroke and neurodegenerative diseases.

Animal models of circulating IGF-1 deficiency exhibit impaired neurovascular coupling, compromised blood-brain barrier integrity, and increased prevalence of micro hemorrhages (Toth et al., 2015; Tarantini et al., 2016b, 2017, 2021a; Hayes et al., 2021). Increased reactive oxygen species (ROS) production, increased inflammation, and reduced glutamate and glucose handling machinery accompany the loss of circulating IGF-1 in these models (Toth et al., 2015, 2017). Together, these data suggest that the age-related reduction in IGF-1 likely leads to severe consequences on the structure and function of the neuro-glio-vascular unit. Indeed, *in vitro* studies have highlighted roles for IGF-1 in promoting specific functions of each cellular component of the neuro-glio-vascular unit. Pharmacological and genetic manipulations of IGF-1 alter the viability and oxidative stress levels of cultured neurons (Wang et al., 2014; Li et al., 2017; Chen et al., 2019). Additionally, IGF-1 signaling in brain vascular endothelial cell cultures promotes angiogenesis and tight-junction formation/integrity (Lopez-Lopez et al., 2004; Bake et al., 2016; Higashi et al., 2020). Genetic reductions of IGFR specifically in endothelial cells impairs stimulation-induced cerebral blood flow, indicating that the loss of IGF-1 signaling in one component of the neurovascular unit results in phenotypic changes commonly observed in the aged brain (Tarantini et al., 2021b). We recently reported that deficiency in IGF-1 signaling in astrocytes impairs glutamate handling *in vitro* and *in vivo*, by reducing glutamate transporter expression and availability at the cell surface (Prabhu et al., 2019). Although

there are thought to several key drivers to aging pathologies and disease, glutamate over excitation is a central contributor to tissue damage following ischemic stroke (Choi and Rothman, 1990; Moskowitz et al., 2010), it is likely that the age-related loss of IGF-1 may compromise the neuro-glio-vascular unit by weakening the glutamate-buffering capabilities of astrocytes which ultimately exacerbates calcium imbalances, mitochondrial dysfunction, and oxidative stress. While the aforementioned studies highlight the ability of IGF-1 to regulate neurons, astrocytes, and brain-derived endothelial cells, each of these studies was performed under varied conditions. A comparative approach is needed to better-understand how the age-related loss of IGF-1 influences cells within the neuro-glio-vascular unit. Thus, we exposed individual cell cultures and co-cultures to excitotoxic levels of glutamate when IGF-1 signaling was impaired. This approach allows for determination of the cellular mechanism(s) by which IGF-1 exerts its protective effects during ischemic stroke-induced stressors. In addition, it highlights cell-specific responses to a common driver of neuronal dysfunction-glutamate excitotoxicity- which has applications to numerous age-related neurodegenerative disease states.

MATERIALS AND METHODS

Animals

All procedures were approved by the Institutional Animal Use and Care Committees of the University of Mississippi, and performed in accordance with their approved guidelines. Timed-pregnant Sprague Dawley rats (16–18 days postictal plug) were purchased (Envigo) and were temporarily housed in 19 × 11.5 × 11 inch polycarbonate cages until the time of euthanasia. Rats were given access to standard rat chow (Teklad 7001) and water *ad libitum*. At the time of euthanasia, pregnant dams were anesthetized with isoflurane and cervical dislocation was completed. Embryonic pups (E17–19) were excised and rapidly decapitated. Due to the non-proliferative nature of neurons, the number of cells needed seeded per well, and the replication of results across multiple primary cell culture preparations, multiple pregnant dams were needed for these studies (approximately 7). The average litter size of a Sprague Dawley female is 10–11 pups, and cerebral tissues of all pups were pooled at the time of euthanasia. Isolated embryonic rat pups were not separated based on sex; thus, our studies are indicative of cell responses from both sexes combined. To reduce animal number, astrocytes and neurons were both cultured from the pooled tissues at the same time, in varying selection medias, as described below.

Neuron Cultures

Primary rat neuron cultures were established following previously described protocols (Ashpole and Hudmon, 2011). Cell culture dishes and coverslips were coated with Poly-D-Lysine (PDL; Sigma P6407) for at least 2 h at 37°C in a humidified incubator containing 5% CO2. Individual cultures were plated in 96-well plates, while 15 mm glass coverslips were used to plate neurons for the triple co-cultures. Following PDL coating, cell culture surfaces were washed with 1X PBS (Gibco 10010-023) and dried. Primary neuronal cultures were derived from the cortex and hippocampus of E17-19 Sprague Dawley rat pups. External cerebrovasculature was removed, the tissue was minced and subsequently enzymatically and mechanically digested with papain (Worthington Biochemical Corporation, LS003126) and glass-blown pipettes, respectively. Dissociated cells were pelleted with centrifugation (500–1,000 *g*, 5 min) and suspended in neuron growth media [Neurobasal medium (Gibco 21103-049) containing B27 (Life Technologies, 17504044), penicillin/streptomycin (10 units/mL; Life Technologies, 15140122), and 1x L−glutamine (250303-081)] with a target density of 2,500,000/mL. As neurons are non-dividing, the density of cells plated is indicative of the density at the time of experimentation; less than 10% of the cells in these cultures are GFAP + or IBA + positive, indicating they are predominantly neurons (Ashpole and Hudmon, 2011). Partial media changes occurred every 3–4 days post seeding to replenish nutrients and remove debris.

Astrocyte Cultures

Tissue from male and female rat pups was isolated, digested, and pelleted following the methodology described above for neuron cultures, and neurons and astrocytes were derived from the same isolated tissues. To promote astrocyte selection after digested tissue was centrifuged, cell pellets were suspended in astrocyte growth media containing Neurobasal medium (Gibco 21103-049) with 10% fetal bovine serum (Corning 35-010-CV), penicillin/streptomycin (10 units/mL; Life Technologies, 15140122), and 1x L−glutamine (250303-081). Cells were plated on PDL-coated 10 cm dishes and media was completely exchanged the day following plating. To further select for astrocytes, the cells were sub-cultured every 3–4 days (90–100% confluent). For this, the growth media was removed, cells were washed with 1X PBS, and 0.05–0.25% of Trypsin-EDTA 1X (Gibco 25200-072) was added. To avoid excess debris, trypsin was applied twice during the first passage- once for 2 min to dislodge neurons and microglial cells from the upper layer (vacuumed off), and a second time to release the astrocytes underneath. Once the astrocytes dislodged, the cells were centrifuged (1,000 × *g*; 5 min) and suspended in growth medium for further plating. All astrocyte cultures were passaged multiple times prior to experimentation (as described above), and the growth rate was continuously monitored to determine if cells were exhibiting replicative senescence. Cells were not passaged more than 6 times to avoid confounds of senescent phenotypes. The resulting cultures are >90% GFAP+, indicating they are astrocytes (Prabhu et al., 2019).

Endothelial Cell Culture

Rat brain microvascular endothelial cells (RBMVECs) and medium were purchased from Cell Applications Inc. (San Diego) and cultured following the manufacturer's guidelines. A single vial of RBMVEC were used to conduct all included studies. RMBVEC were continually passaged and 20% of cells were frozen at each passage throughout the study for replicate, follow-up, and future studies to reduce variance from a different lot of cells

originally isolated. In brief, cells were grown on a T-75 flasks pre-coated with Cell Attachment Factor Solution (123-100, Cell Applications), in 15 mL of RBMVEC growth medium (R819-500). Growth medium was changed 24 h after initial seeding, and cells were sub-cultured every 4–6 days or when at 80–100% confluency. Media was changed every other day. RBMVECs were passaged using the same protocol as astrocytes, using the proprietary trypsin solution (Cell Applications Inc).

Co-cultures

Triple cultures were developed by plating primary neurons on glass coverslips, RBMVECs on transwell inserts, and astrocytes on the surface of a multi-well plate. Astrocytes were cultured and passaged at least 1 week prior to combination with the other cells, to allow for selection of astrocytes away from neurons and microglial cells. Neurons were also cultured 7–8 days prior to combination and experimentation, to allow for development/expression of ionotropic glutamate receptors (GluNR) responsible for excitotoxic signaling. Coverslips were elevated off the surface of the multi-well plate and astrocytes were seated in the outer 1/3 of the wells. The media on all 3 cell types was exchanged for neuron growth media 24 h prior to combination of the co-cultures to allow for uniformity between media types.

Cells Treatments

Glutamate stimulation was performed using L-glutamic acid and glycine (FisherScientific) in a ratio of 10:1 glutamate:glycine diluted from a PBS stock solution. Increasing concentrations of glutamate were prepared in the appropriate cell growth media, and administered as a 2x solution to the cells plated in their respective media (final concentration 1x upon application). Cells were incubated for 1 h at 37°C. Following treatment, glutamate media was removed, cells were washed in fresh growth media twice, and incubated in new growth media until the designated time point. All cell viability studies were conducted 24 h after cells were stimulated with glutamate. All other study time points are described in the respective sections. In one experimental series, media lacking the B-27 supplement was administered 24 h prior to glutamate stimulation.

Stock solutions of picropodophyllin toxin (PPP; Sigma T-9576) and MK-801 (Sigma M107) were prepared in dimethyl sulfoxide (DMSO; Fisher BP321-100) and administered to cells at concentrations and time-points described. Treatment groups were block randomized to ensure equal sampling. Individual wells in the multi-well plates were treated as independent samples; and assays with neurons and astrocytes were further repeated across multiple tissue preparations to verify reproducibility of findings in cells isolated from separate rat pup litters.

Cell Viability

Following treatments, cell viability/cytotoxicity was quantified using Live:Dead viability/cytotoxicity kit (Thermo Fisher Scientific L3224). Calcien-AM and ethidium homodimer were diluted (1:1000-2000; 1:500-1000) were diluted in PBS. Growth media was removed and cells were washed with 1X PBS prior to adding the live/dead labels. After 20 min of incubation, cells were imaged on the Nikon Ti2-E HCA inverted fluorescent microscope using the JOBS automated image acquisition (Nikon). Magnification was set to 200x (20x, extra-long working distance objective) and samples were excited with the LED Triggered acquisition exposures using excitation/emission filters for 470-FITC and 540-TRITC. The JOBS program selected 6 fields at random per well for imaging, and the total number of live and dead cells were quantified in 2–3 images using the Nikon Elements Cell Analysis plug-in features. The total number of cells and percent toxicity were calculated by observers blinded to treatment groups.

Reactive Oxygen Species Quantification

Following treatment, ROS production was quantified in astrocytes and endothelial cells. Media was removed, and cells were washed with 1X PBS. Cells were then loaded with 3 μM of 2′,7′-dichlorodihydrofluorescein diacetate (DCFDA; Thermofisher, D399) for 20 min and incubated at 37°C in a humidified incubator containing 5% CO^2. DCFDA was then imaged using the FITC filter on the Nikon Ti2-E microscope as described above. Six images at random through the JOBS interface and 4–6 non-adjacent cells per field were selected at random to be quantified by a blinded observer. DCFDA intensity of each cell was normalized to the background of that image.

Seahorse

Cells were seeded on the XFe96 growth plates 2–3 days prior to extracellular efflux assessment. Treatments were administered at the desired time points and mitochondrial response was assessed using the Cell Mito Stress Test, per manufacturer recommendations. The sensor cartridge was hydrated in water overnight at 37°C and then equilibrated with the recommended equilibration buffer. Oligomycin (1.5 μM), FCCP (1 μM), and rotenone (0.5 μM) were loaded into the sensor plates and injected into the wells by the XFe/XF Seahorse system. Basal and maximal respiration, as well as proton leak were auto-calculated by the Seahorse program using an average of 3 readings per stage.

Data Analysis

Statistical analysis and graphical analyses were performed using Sigma Plot version 14 software and R studio. One-way and two-way ANOVAs was used when appropriate (defined in the figure legend). *Post hoc* comparisons were selected based upon the experimental question and fulfillment of normality and equal distribution. Details for each are provided in figure legend. All data were expressed with mean ± standard error. Sample sizes were estimated using previous variance observations with these experimental methodologies. With $\beta = 0.8$, $n = 4–6$ was required to achieve power for most studies. F values for two-way ANOVAs are described in the results and main effects are noted in figures with a pound sign (#). For all studies, $p < 0.05$ was used as the statistical significance value and denoted using an asterisk (*).

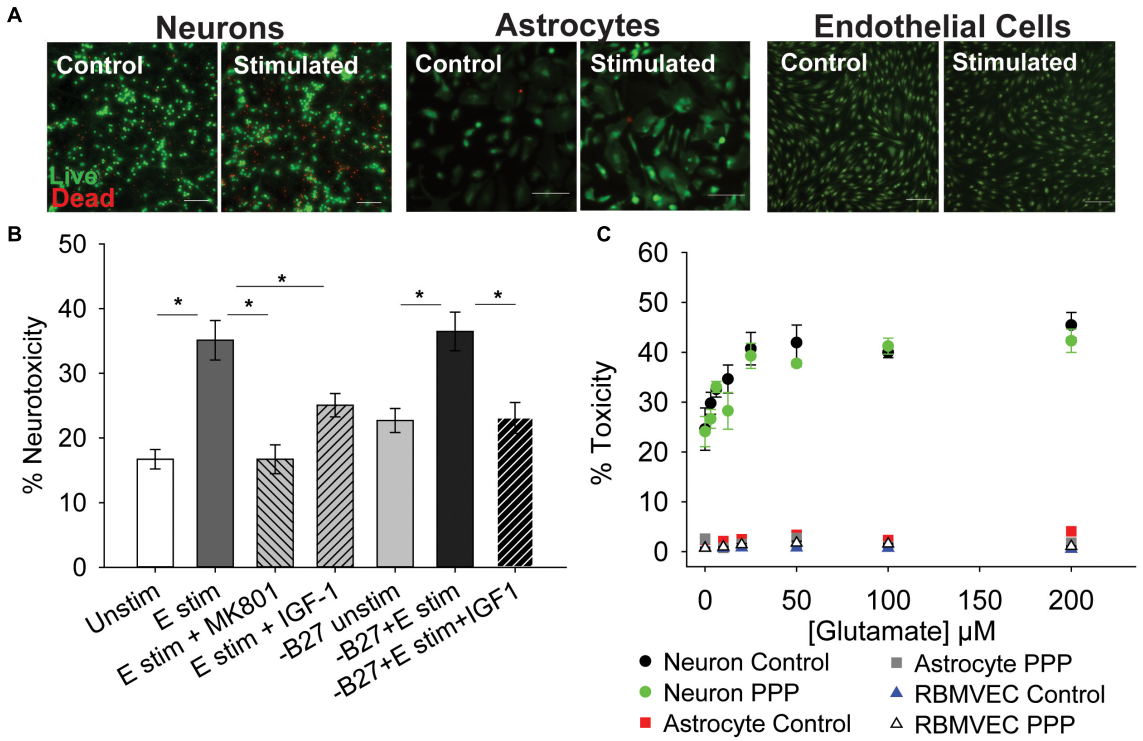

FIGURE 1 | IGF-1 protects against excitotoxicity in glutamate-sensitive neurons. **(A)** Representative images of neurons (left two panels), astrocytes (middle two panels), and rat brain microvascular endothelial cells (right two panels) stained with live (green)/Dead (red) viability/cytotoxicity indicator dyes 24 h after stimulation with control or 100 μM glutamate, as indicated. Scale bar represents 100 μm. **(B)** Average toxicity in neurons 24 h after treatment (n = 8 wells/group). A one-way ANOVA with *post hoc* Bonferroni was used for statistical comparisons; *indicates significant difference between the delineated bars. **(C)** Average toxicity of cells 24 h after acute treatment with both 0.5 μM PPP and increasing concentrations of glutamate (n = 4–8 wells/group). A two-way ANOVA was employed with glutamate concentrations and PPP-treatment serving as factors. No significant differences were observed. Graph color code: black circles = vehicle-treated neurons; green circles = PPP-treated neurons; red boxes = vehicle-treated astrocytes; dark gray boxes = PPP-treated astrocytes; blue triangles = vehicle-treated rat brain microvascular endothelial cells (RBMVEC); and light gray triangles = PPP-treated RBMVEC. All data are presented as mean ± SEM.

RESULTS

Insulin-Like Growth Factor-1 Protects Against Excitotoxicity in Neurons

To determine if inhibition of IGF-1 signaling differentially affects the glutamate sensitivity of cells within the neuro-glio-vascular unit, cultures of neurons, astrocytes, and microvascular endothelial cells were established. Primary cerebral neurons were isolated from embryonic rat pups (male and female combined) and grown in culture for 8–10 days. Primary neurons at this stage of development are sensitive to excitotoxicity when exposed to high concentrations of glutamate and glycine, due to overactivation of ionotropic GluNR. As expected, acute treatment of neurons with 100 μM glutamate/10 μM glycine (termed glutamate stimulation throughout) resulted in a significant increase in cellular toxicity 24 h after stimulation (**Figures 1A,B**; $p < 0.001$ vs unstimulated). Co-administration of the GluNR antagonist MK-801 prevented excitotoxicity (**Figure 1B**; $p < 0.001$ vs glutamate stimulated control). Administration of exogenous 100 nM IGF-1 at the time of stimulation also prevented excitotoxicity ($p = 0.019$ vs glutamate stimulated control), consistent with previous reports. No differences in the total number of neurons per field were noted following treatment (**Supplementary Figure 1A**).

The neuronal growth media contains a supplement (B27) that has a high concentration of insulin, which can cross-talk and activate IGFR. Thus, to better determine the protective effects of IGF-1 signaling, the excitotoxicity profile was again assessed without B27 present. No change in baseline levels of toxicity were observed between control neurons with and without B27, and glutamate stimulation still significantly increased toxicity in the absence of B27 (**Figure 1B**; $p = 0.002$ vs –B27 unstimulated control). Once more, exogenous IGF-1 prevented excitotoxicity (**Figure 1B**; $p = 0.003$ vs –B27 glutamate stimulated control).

To more specifically assess the impact of reducing IGF-1 signaling, the extent of excitotoxicity when IGFR was pharmacologically inhibited was then examined. For this, picropodophyllotoxin (PPP), a known small molecule inhibitor of the IGFR receptor kinase activity, was co-administered at the time of glutamate stimulation and toxicity was measured 24 h later. Surprisingly, PPP did not shift the concentration-dependence or maximal extent of glutamate toxicity in cultured neurons (**Figure 1C**). A two-way ANOVA revealed a significant effect of glutamate concentration ($F = 13.759$, $p < 0.001$), but no

significant effect of PPP treatment (F = 2.598, p = 0.111), and no significant interaction between the two factors (F = 0.506, p = 0.827).

Astrocytes and microvascular endothelial cells are not as sensitive to glutamate as neurons as no change in toxicity was observed across all glutamate concentrations (**Figures 1A–C**). Similarly, no increase in sensitivity was observed with IGFR inhibition at the time of glutamate stimulation (**Figure 1C**).

Prolonged IGFR Inhibition Increases Astrocytic Sensitivity to Glutamate

The lack of effect with pharmacological inhibition of IGFR in **Figure 1C** was inconsistent with the protective effects of exogenous IGF-1 in **Figure 1B**. However, co-administration of PPP at the time of glutamate could have temporal confounds that limit interpretation. Thus, we next administered PPP 24 h prior to glutamate stimulation to better mimic the prolonged loss of IGFR signaling observed in aging. Prolonged IGFR inhibition with 0.5 μM PPP did not lead to difference in neuronal excitotoxicity (F = 0.255, p = 0.615), but did lead to differences in astrocyte viability (F = 6.677, p = 0.011; **Figures 2A,B**). Within group comparisons did not unveil a specific concentration of glutamate that PPP treatment significantly worsened, thus it is assumed that IGFR inhibition led to modest reductions in cell viability across all glutamate treatments.

No changes in endothelial cell viability were observed with prolonged IGFR inhibition; however, a pronounced reduction in total cell number was noted when microvascular endothelial cells were treated with 0.5 μM PPP (F = 117.942, $p < 0.001$; **Figure 2C**). A significant difference within unstimulated controls with PPP pre-treatment was detected ($p < 0.001$), and this effect persisted across all glutamate concentrations. Thus, no main effect of, or interaction with, glutamate concentration was observed in the treated microvascular endothelial cells.

The change in endothelial cell number prompted further analyses of neuron and astrocyte counts with treatment. Similar reductions in astrocyte count were observed with 0.5 μM PPP treatment (F = 73.322, $p < 0.001$; **Figures 2A–C**). Glutamate concentration did not alter astrocyte count nor interact with the PPP effect. Main effects of both glutamate concentration and PPP treatment on total neuron count were detected (F = 3.309, p = 0.004; F = 7.835, p = 0.006, respectively). *Post hoc* comparisons within groups revealed that the only significant difference within the PPP vs vehicle treatments was the drop in total cell number at 200 μM glutamate (p = 0.012), likely an indication of dead cells washed away during the staining process at this high concentration of glutamate.

When the concentration of PPP was increased to 5 μM, significant differences in neuron and astrocyte survival were observed (**Figure 2D**). Both glutamate concentration and PPP treatment had significant main effects on neurotoxicity (F = 4.272, $p < 0.001$; F = 12.565, $p < 0.001$, respectively). However, no interaction between the two factors was detected (F = 0.732; p = 0.646). Within group comparisons revealed significant increases in neurotoxicity when neurons pre-treated with 5 μM PPP were stimulated with 50 and 200 μM glutamate (p = 0.048 and p = 0.006, respectively). No baseline differences in toxicity amongst unstimulated controls treated with vehicle or PPP were observed (p = 0.751). A significant reduction in total neuron number was observed with 5 μM PPP treatment and with glutamate (F = 49.058, $p < 0.001$; F = 2.878, p = 0.009, respectively; **Figure 2E**). No significant interactions between the factors was detected (F = 0.932, p = 0.485). Within factor comparisons showed decreased cell number within PPP-treated neuron cultures stimulated with ≥12.5 μM glutamate, again suggesting potential loss of dead cells during the staining process since neurons are non-mitotic.

Prolonged IGFR inhibition in astrocytes also resulted in main effects of glutamate concentration and PPP treatment on the levels of cytotoxicity (F = 157.321, $p < 0.001$; F = 2.209, p = 0.039, respectively; **Figure 2D**). Moreover, a significant interaction between glutamate concentration and PPP treatment was also observed (F = 2.743, p = 0.011). Within factor comparisons revealed significant increases in PPP-pretreated astrocytes stimulated with ≥6 μM glutamate, suggesting that while astrocytes display increased resistance to glutamate toxicity under control conditions, the loss of IGF-1 signaling predisposes astrocytes to excitotoxic stress. A significant reduction in astrocyte cell number was also observed with 5 μM PPP treatment (F = 257.893, $p < 0.001$), across all glutamate concentrations. Main effect differences for glutamate concentration did not reach significance (F = 1.882, p = 0.079), nor did interactions between factors (F = 2.071, p = 0.052). Prolonged treatment with another IGFR inhibitor, NCP-ADW742, also increased susceptibility to glutamate excitotoxicity and reduced astrocyte cell number (**Supplementary Figures 1B,C**). Baseline toxicity levels and cell numbers were observed with administration of supplemental IGF-1 prior to glutamate stress (**Supplementary Figures 1B–E**), indicating that the prolonged loss of IGF-1 predisposes astrocytes to glutamate toxicity, despite their typical resistance to the stress.

Similar to the before no differences in endothelial cell toxicity were observed across any treatment groups, but 5 μM PPP did reduce cell number across all glutamate concentrations (F = 538.084, $p < 0.001$; **Figure 2E**). Again, this suggests that while IGFR inhibition did not predispose endothelial cells to glutamate toxicity, it likely reduces cell division.

Astrocytes Fail to Protect Neurons When IGFR Is Inhibited

Cells within the neuro-glio-vascular unit coordinate to create an optimal microenvironment, by releasing growth mediators, buffering stressors, and regulating nutrient supply. Thus, we next assessed whether co-cultures of endothelial cells, neurons, and astrocytes would exhibit differences in glutamate sensitivity when IGFR is inhibited. As anticipated, 100 μM glutamate did not significantly increase neurotoxicity in the presence of astrocytes and endothelial cells, nor did acute co-administration of 0.5 μM PPP with 100 μM glutamate (p = 0.139; **Figure 3A**). No differences in astrocyte or endothelial cell toxicity were observed in these acute treatments (**Figures 3B,C**).

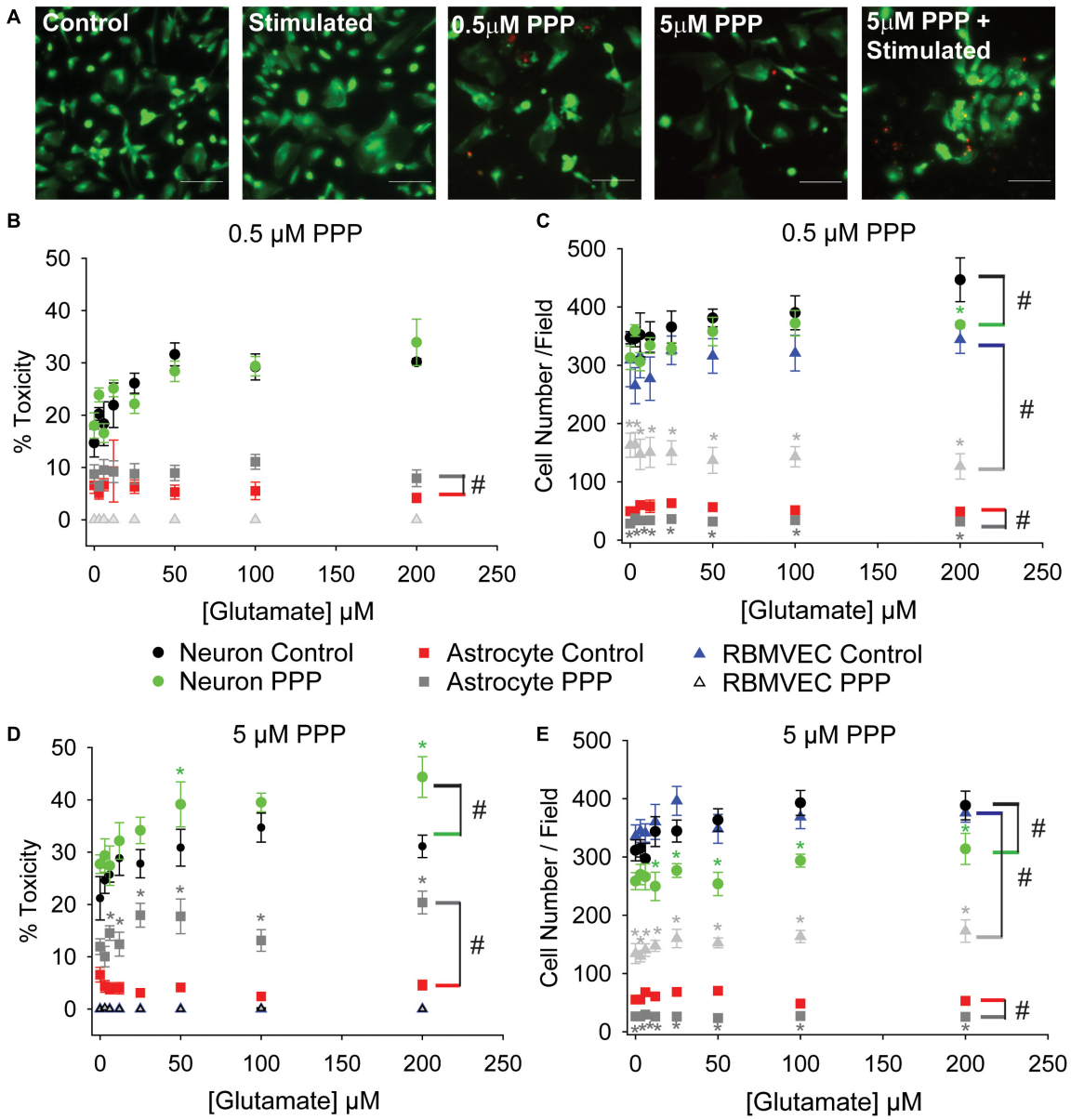

FIGURE 2 | Prolonged IGFR inhibition increases astrocytic sensitivity to glutamate and reduces astrocyte and endothelial cell number. **(A)** Representative images of astrocytes stained with live (green)/Dead (red) viability/cytotoxicity indicator dyes. From left to right: unstimulated control, glutamate-stimulated vehicle-treated, unstimulated 0.5 μM PPP-treated, unstimulated 5 μM PPP, and glutamate-stimulated 5 μM PPP. Scale bar represents 100 μm. **(B)** Average toxicity and **(C)** average cell number per well of cells pre-treated with 0.5 μM PPP, and subsequently stimulated with increasing concentrations of glutamate, 24 h after stimulation. **(D)** Average toxicity and **(E)** average cell number per well of cells pre-treated with 5 μM PPP, and subsequently stimulated with increasing concentrations of glutamate, 24 h after stimulation. All data are presented as mean ± SEM, n = 5–8 wells/treatment group. A two-way ANOVA was employed with glutamate concentrations and PPP-treatment serving as factors. Cell types were each analyzed independently. # indicates a significant main effect within that cell type. *Post hoc* Holm-Sidak tests were used for pairwise multiple comparisons. *indicates a significant difference between PPP-treatment and vehicle-treatment within a given glutamate concentration. Graph color code: black circles = vehicle-treated neurons; green circles = PPP-treated neurons; red boxes = vehicle-treated astrocytes; dark gray boxes = PPP-treated astrocytes; blue triangles = vehicle-treated rat brain microvascular endothelial cells (RBMVEC); and light gray triangles = PPP-treated RBMVEC.

When astrocytes alone were pre-treated with 5 μM PPP and then combined with neurons and endothelial cells for glutamate stimulation, a significant increase in neurotoxicity was observed (p = 0.007 vs control) (**Figure 3D**). No differences in toxicity or cell number were noted in either the astrocytes or endothelial cells within the triple cultures (**Figures 3E,F** and **Supplementary Figures 1D–F**). Together these data suggest that a reduction of IGFR signaling in astrocytes impairs their ability to buffer glutamate and protect neurons from overexcitation, even when in the presence of endothelial cells.

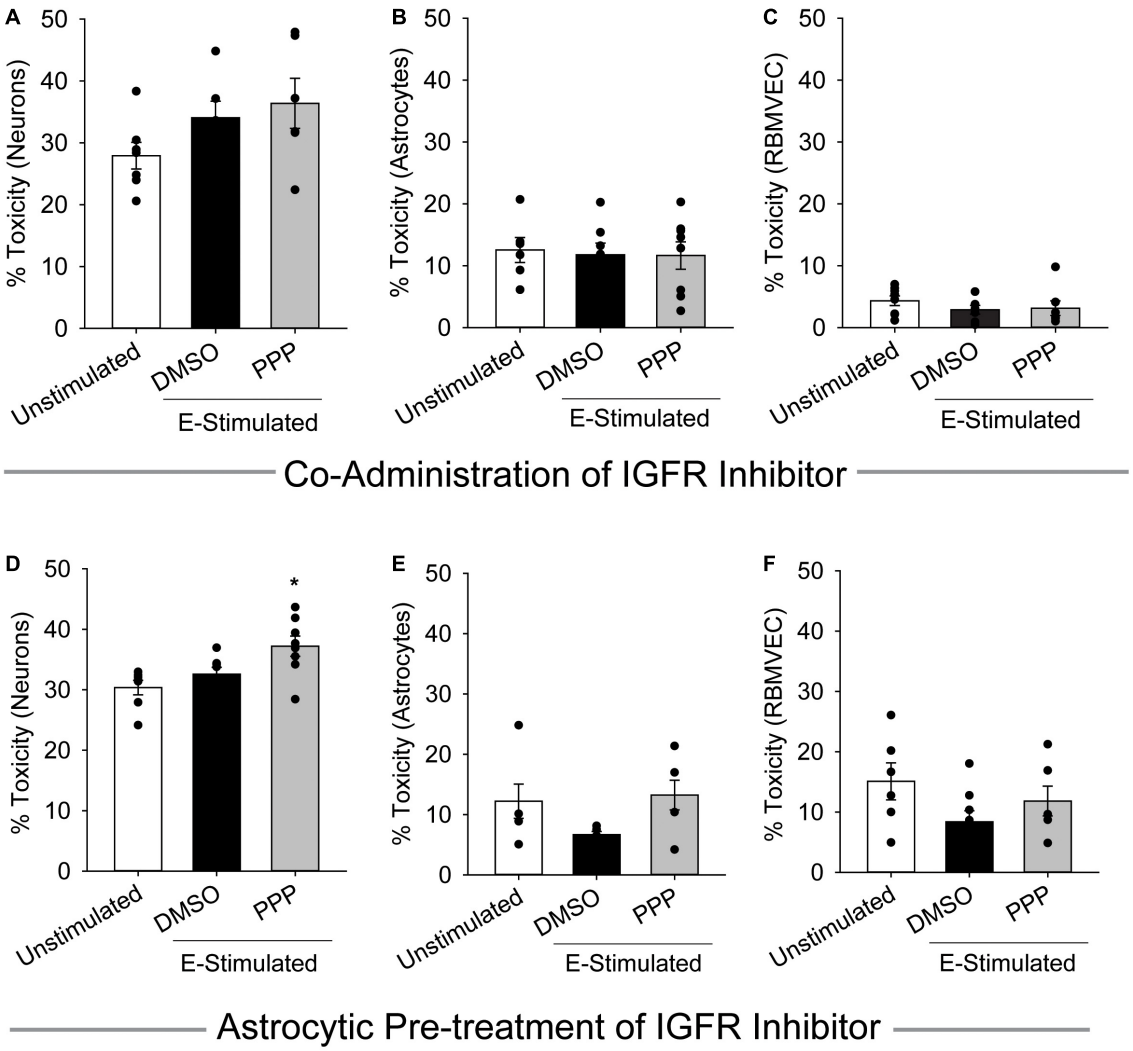

FIGURE 3 | Astrocytes fail to protect against excitotoxicity when IGFR is inhibited. Average cell death 24 h after triple cultures of neurons **(A)**, astrocytes **(B)**, and endothelial cells **(C)** were co-administered 0.5 μM PPP and 100 μM glutamate for 1 h (n = 6–8 wells/group). One-way ANOVA failed to detect differences in any of the treatment groups. **(D–F)** Astrocytes were pre-treated with 5 μM PPP for 24 h prior to combining with endothelial cells and neurons for a triple culture system. Average cell death in the neurons **(D)**, astrocytes **(E)**, and endothelial cells **(F)** after stimulation with 100 μM glutamate for 1 h (n = 5–8 wells/group). One-way ANOVAs with *post hoc* Bonferroni comparison was used for statistical analyses. *indicates significant difference between control and PPP-treated glutamate-stimulated neurons. All data are presented as mean ± SEM, n = 5–8 wells/treatment group.

Astrocytic and Endothelial Reactive Oxygen Species Levels Are Elevated by IGFR Inhibition and Glutamate Stimulation

While acute co-administration of 0.5 μM PPP and glutamate did not increase toxicity in astrocyte or endothelial cultures, alterations in metabolic function and oxidative stress may still occur with this stressor. Thus, astrocytes and endothelial cells were treated with 100 μM glutamate alone, or in conjunction with 0.5 μM PPP, and the production of ROS was quantified at various time points following treatment. Astrocytic ROS production increases in the hours following glutamate stimulation (**Figure 4A**). Significant effects of both time and treatment were observed (F = 185.57, $p < 0.001$; F = 3.187, p = 0.027, respectively), as well as an interaction between both factors (F = 4.586, $p < 0.001$). 5 h post-treatment, vehicle treated and PPP-treated astrocytes stimulated with glutamate showed significant increases in ROS levels over unstimulated controls (both $p < 0.001$ vs unstimulated control). Moreover, co-administration of PPP and glutamate resulted in significantly increased ROS levels than glutamate stimulated controls (p = 0.014), suggesting that the extent of glutamate-induced ROS production was exacerbated by IGFR inhibition. 5 h after glutamate stimulation with another IGFR inhibitor, NVP-ADW742, also significantly increased ROS (**Supplementary Figure 2A**), indicating the effect is not limited to PPP. Additional analysis of mitochondrial bioenergetics at

this time point revealed that glutamate stimulation decreased maximal extracellular acidification rates, while PPP + glutamate decreased extracellular acidification and oxygen consumption rates, suggesting changes in both glycolysis and oxidative phosphorylation (**Supplementary Figure 2B**). No differences in basal respiration rates were noted with any of the treatments (**Supplementary Figure 2B**).

Similar to astrocytes, brain-derived microvascular endothelial cells showed increased ROS production 5 h after 0.5 μM PPP was co-administered with 100 μM glutamate (**Figure 4B**). A main effect treatment was observed (F = 5.287, p = 0.004). While glutamate alone did not increase ROS production in the endothelial cells (p = 0.945), a significant increase in ROS was seen in cells treated with PPP + glutamate vs unstimulated control (p = 0.02), and vs glutamate-stimulated control (p = 0.004).

Additional analyses of ROS levels 24 h following treatment revealed differential recovery from acute IGFR inhibition and glutamate stimulation. Astrocytes do not show increased ROS at 24 h with 100 μM glutamate or 100 μM glutamate + 0.5 μM PPP treatment (**Figure 4C**). In fact, ROS levels were significantly reduced in glutamate-stimulated PPP-treated astrocytes vs unstimulated controls (p = 0.024) and PPP treatment was trending (p = 0.053 vs control). Endothelial cells continue to show increased ROS levels long after the acute exposure to 100 μM glutamate + 0.5 μM PPP (p = 0.013 vs unstimulated control; **Figure 4D**), suggesting that IGFR inhibition at the time of glutamate stimulation increases endothelial ROS levels long-term. Note, this was with acute PPP treatment, at a time point in which no differences in endothelial cell toxicity was observed (**Figure 1C**).

DISCUSSION

The age-related loss of IGF-1 has been linked to cognitive impairment, neurodegeneration, and increased susceptibility ischemic stroke and other neurovascular pathologies (Sonntag et al., 2013; Ashpole et al., 2015b). These deficits often come as a disconnect from the enhanced longevity observed in animal models of IGF-1 deficiency. While early-life reductions in circulating IGF-1 do lead to increased lifespan, reduced IGF-1 in advanced age has multiple consequences in animal models as it increases sarcopenia, bone frailty, learning and memory deficits, and cerebrovascular dysfunction (Ashpole et al., 2015a, 2016, 2017; Toth et al., 2015; Tarantini et al., 2016a, 2021a; Farias Quipildor et al., 2019). For example, IGF-1 deficiency in mice decreases stimulation-evoked cerebral blood flow, blood brain barrier integrity, and the strength and flexibility of cerebral arteries. IGF-1 deficiency also impairs the production and release of vasomediator eicosanoids from astrocytes, alters endothelial nitric oxide production, and increases susceptibility to hypertension-induced microhemorrhages (Toth et al., 2015; Tarantini et al., 2017, 2021a; Fulop et al., 2019). Considering this, it is not surprising that IGF-1 has long-been implicated in the risk and severity of ischemic stroke. As described earlier, clinical and preclinical evidence highlight inverse correlation (and causation in animal models) between IGF-1 and the risk/outcome of ischemic stroke (Hayes et al., 2021).

While recent studies are beginning to shed light on the impact of IGF-1 on neurovascular communication in advanced age, there remains a significant gap in our understanding of how individual cell types that normally coordinate signaling together within the neurovascular unit each respond to reduced IGF-1 signaling. In this study, we aimed to compare the effects of IGF-1 deficiency on the cellular responses to high levels of extracellular glutamate. As the predominant excitatory neurotransmitter in the brain, glutamate induces depolarization and initiates multiple calcium signaling cascades. During periods of ischemia or proteotoxic stress, neurons experience energy imbalances and ionic stressors that ultimately lead to terminal depolarization and the dumping of glutamate stores, inflammatory mediators, and oxidative stressors into the extracellular space, which expands the region of distress and malfunction [as recently reviewed (Choi, 2020)]. This excitotoxic cascade is one of the drivers of neuronal loss and glial activation in ischemic stroke and neurodegenerative diseases. Thus, understanding how the loss of IGF-1 alters the glutamate response of neurons, astrocytes, and endothelial cells within the neurovascular unit provides much-needed information on potential cellular mechanisms by which IGF-1 deficiency in advanced age influences health and function of the brain.

Recent evidence from our laboratory indicated that IGFR inhibition reduced the ability of astrocytes to buffer extracellular glutamate by decreasing glutamate transporter availability (Prabhu et al., 2019). Therefore, in this study, we hypothesized that maintenance of IGF-1 signaling in astrocytes is necessary for neuroprotection from glutamate excitotoxicity. We also hypothesized that maintenance of IGF-1 signaling in neurons was essential for limiting overexcitation, as other studies have shown exogenous IGF-1 can protect against excitotoxicity and oxidative stress (Wang et al., 2014; Li et al., 2017; Chen et al., 2019). Our results indicate that while exogenous IGF-1 can protect neurons from glutamate, acute and prolonged loss of IGFR signaling does not exacerbate neuronal death in cultures of pure neurons. Interestingly, inhibition of IGF-1R not only impairs the neuroprotective capabilities of astrocytes, it predisposes astrocytes to glutamate toxicity as well. It is unclear what the mechanism for this enhanced sensitivity may be. Perhaps the lack of glutamate transporter availability with IGF-1 signaling deficiency resulted in increased GluNR activation in the astrocytes as well, since astrocytes are known to express a variety of ionotropic and metabotropic GluNRs (Serrano et al., 2008; Lalo et al., 2011; Bradley and Challiss, 2012; Ceprian and Fulton, 2019). If this were the case, the astrocytes could be experiencing intracellular calcium imbalances and oxidative stress, which have both been shown to increase astrocyte toxicity in response to other stressors.

As mentioned, reductions in IGF-1 in the brain increase ROS levels and mitochondrial dysfunction. We observed significant increases in ROS production in both astrocytes and endothelial cells when IGFR was inhibited at the time of glutamate stimulation. We chose to focus our experimental design on these two cell types and this acute treatment because it did not lead to any changes in observed toxicity. Oxidative stress is expected in

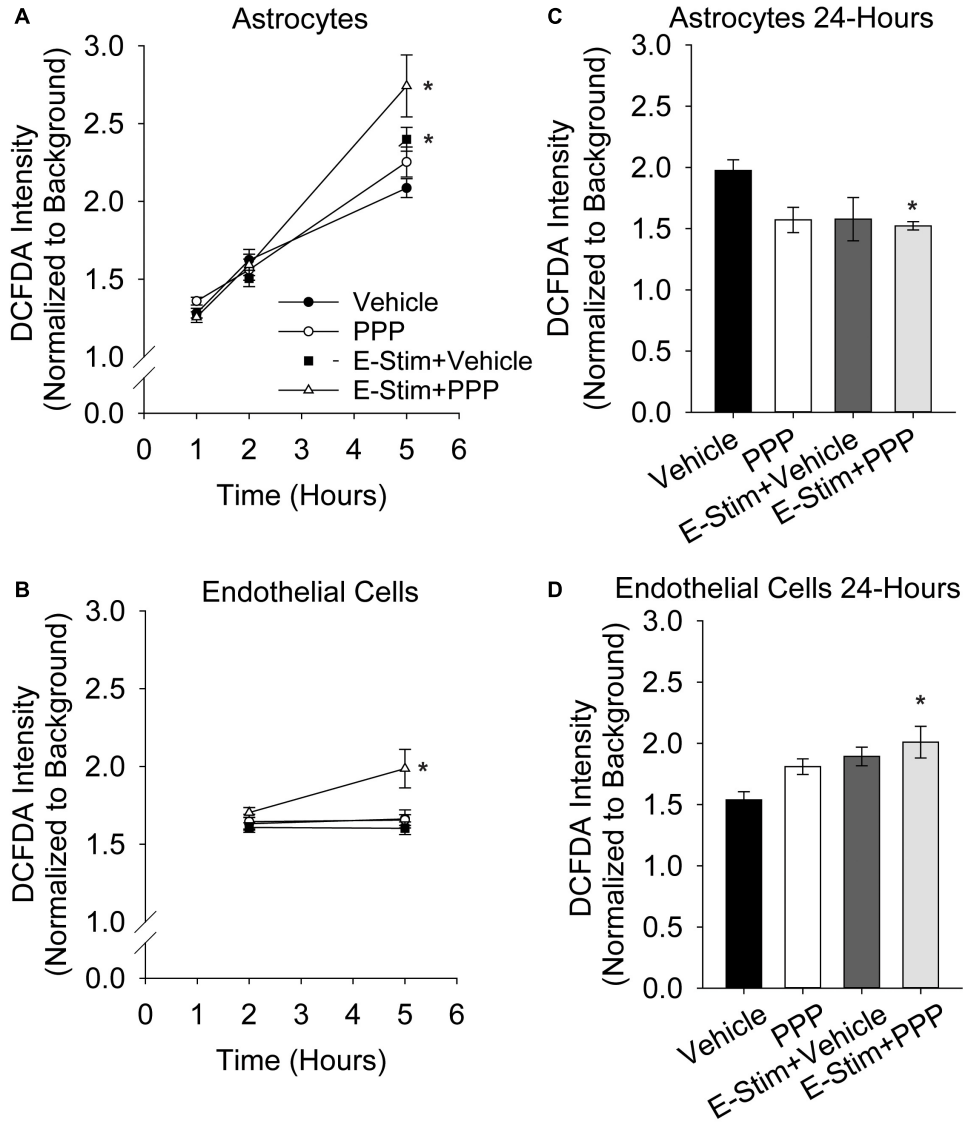

FIGURE 4 | Astrocytic and endothelial ROS levels are elevated by IGFR inhibition and glutamate stimulation. Average ROS levels in pure cultures of astrocytes **(A)** or endothelial cells **(B)** co-treated with 0.5 μM PPP and 100 μM glutamate for 1 h, and subsequently measured 1, 2, and 5 h after treatment. Four cells were selected at random per field, with 3 fields per well, and 8–10 wells per treatment group. Background intensity within each image was measured and used to normalize. A two-way ANOVA was employed with both time and treatment as factors, and a *post hoc* Holm-Sidak was used to compare within groups. * indicates a significant effect of treatment at that time. Average ROS levels in pure cultures of astrocytes **(C)** or endothelial cells **(D)** co-treated with 0.5 μM PPP and 100 μM glutamate for 1 h, and subsequently measured 24 h after treatment. Four cells were selected at random per field, with 3 fields per well, and 4–8 wells per treatment group. A one-way ANOVA with *post hoc* Dunnett's test was used for statistical comparisons to control. * indicates a significant effect vs control. All data are presented as mean ± SEM.

neurons that are dying from excitotoxicity, but neither astrocytes nor endothelial cells were sensitive to glutamate when IGFR was acutely inhibited. The increased ROS levels in both cell types indicates that the cells were indeed undergoing a stress response with the combined treatment. While it could be inferred that the ability of astrocytes to return ROS levels back to baseline by 24 h may contribute to their increased resistance to excitotoxic stress, there is a disconnect in the endothelial cells that likely renders this to be more complicated. Perhaps an increase in endothelial cell toxicity would have been observed at later time points. Further studies on the underlying mechanism(s) and consequence(s) of these observations are needed.

Combined triple cultures of neurons, astrocytes, and endothelial cells highlighted a few distinct responses to glutamate and IGFR inhibition than the individual cultures of each cell type. First, the same concentration of glutamate that led to significant increases in neurotoxicity within pure neuron cultures failed to induce toxicity within the triple culture. This was an expected outcome, as astrocytes are known to buffer glutamate and co-cultures of neurons and astrocytes have

been shown to reduce the extent of neurotoxicity (Choi et al., 1987; Rosenberg et al., 1992). Second, and more interestingly, prolonged IGFR inhibition in astrocytes prior to glutamate stimulation did not increase the toxicity of astrocytes nor decrease the total cell number of astrocytes within the triple cultures. These effects were pronounced in pure astrocyte cultures, suggesting that co-culturing astrocytes with neurons and endothelial cells afforded them protection against the stressors of IGFR deficiency/glutamate stimulation. Additional studies examining ROS levels, inflammatory mediators, and growth factor production and release with triple cultures exposed to these same stressors may be warranted.

In our recent study examining glutamate uptake in astrocytes, we utilized similar concentrations of the pharmacological inhibitor PPP and did not observe a significant reduction in total cell number. Thus, we were surprised to see a reduction in astrocyte count here. However, in that study, cells were treated when at or close to confluence, which was evident in DAPI-stained microscopy images accompanying those data (Prabhu et al., 2019). In the current study, we aimed to treat at 75% confluence in order to avoid stress of over-growth, however, microscopic live/dead staining analysis showed that even the vehicle-treated controls were not at this level of confluence even 24 h after treatment. Thus, the reduction in cell number observed in pure cultures of astrocytes and endothelial cells was likely due to changes in cell division and growth with IGF-1 deficiency. Nevertheless, it is interesting that the reduction in astrocyte number with prolonged IGFR inhibition was restricted to the pure cultures, and not the triple cultures.

The complication of cell proliferation also limited our ability to utilize genetic approaches in our *in vitro* studies. IGF-1 is a primary growth factor with autocrine and paracrine functions, and genetic reductions that alter cell proliferation make it difficult to control studies of neuroendocrine hormones. We originally aimed to include siRNA and/or cell-specific knock-outs using our inducible cell-specific IGFR knock-out lines. However, due to obvious insufficient cell proliferation caused by siRNA transfection/transduction (both approaches were attempted) as well as Cre-recombinase induced knock-outs, we concluded that the significant reductions in cell number would confound results. Astrocyte count following knock-out with siRNA or with 4-OH-tamoxifen-induced recombination was less than 50% of that observed in the control-treated wells (siRNA vector transfected or vehicle-treated). Hence, pharmacological interventions were utilized to address our central question of how the loss of IGF-1 impacts the major cells of the neurogliovascular unit. While exogenous IGF-1 was added in a few studies here, the growth media of the cells contains insulin and IGF-1 at concentrations known to promote growth and development, thus pharmacological inhibitors were selected to more specifically reduce IGFR signaling. Alternative studies could alter the density of seeded cells to account for the loss in proliferation with knock-out, however, compensatory changes in other growth receptors (GH, InsR, etc.) and IGF-1 binding proteins will also need to be examined as they are known to occur with IGF-1 manipulations *in vivo* (Ashpole et al., 2015b).

Our comparative study is limited by not including additional cells found within the brain and blood-brain barrier. For example, pericytes not only serve as a protective layer of the blood brain barrier, they regulate blood capillary diameter within the brain by dilating and relaxing in response to glutamate (Kisler et al., 2017, 2020; Brown et al., 2019). Because of this, pericytes are important during ischemic reperfusion as they can assist with restoring flow of oxygen and glucose to the ischemic tissue (Yang et al., 2017; Khennouf et al., 2018; Sun J. et al., 2020). Little is known about the influence of IGF-1 on pericytes within the brain, and additional studies on how IGF-1 may influence pericytic glutamate response are needed.

Additionally, microglia are known to respond to excitotoxic insult, ischemia, and reperfusion. In fact, microglia have been implicated in the exacerbation of damage following glutamate excitotoxicity and ischemic stroke, due to increased production of ROS and pro-inflammatory mediators (Ma et al., 2017; Qin et al., 2019; Lian et al., 2020). At the same time, microglia also play an important protective role following tissue stroke damage, so the duality of their contribution to physiology/pathophysiology cannot be over-simplified to just a negative contribution to damage (Ma et al., 2017; Qin et al., 2019; Marino Lee et al., 2021). The age-related loss of circulating IGF-1 is associated with increased microglial activation, neuroinflammation, and susceptibility to a compromised blood-brain barrier. The relationship between IGF-1 and microglial activation is not limited to temporal correlations, as there are numerous studies that highlight IGF-1 directly regulates the structure and function of microglia. Exogenous IGF-1 alters phenotypic activation states and reduces microglial-associated production and release of tumor necrosis factor-alpha (TNF-α), interleukin-1 beta (IL-1β), inducible nitric oxide synthase (iNOS), and ROS (Park et al., 2011; Grinberg et al., 2013). Administration of IGF-1 following ischemic and/or hemorrhagic stroke attenuates microglial activation, inflammation, and ROS (Serhan et al., 2020; Sun Z. et al., 2020). Considering this, we expect that reductions in IGF-1 signaling within our cell culture system would also promote pro-inflammatory and oxidative stress phenotypes, which would further neuronal death. However, one study highlights that microglial presence in tri-cultures are neuroprotective and reduces neurons loss and astrocyte hypertrophy even though the presence of microglia increased inflammatory cytokine production compared to cell culture without microglia (Goshi et al., 2020). Future studies of ischemic and excitotoxic stressors should take microglial contributions into account while controlling for the natural migratory phenotype microglia display following activation, as results may be confounded by increased basal levels of neuroinflammatory stress (which often show an activated phenotype in culture).

Transitioning to an *in vivo* system would circumvent concerns regarding the lack of including all cell types present in the cerebral tissue within our co-culture models; however, the intricacies of timed, cell-specific manipulations make *in vivo* models difficult, particularly when trying to assess effects without developmental compensation interference. Inducible transgenic animals for each cell type are needed to rigorously assess the effects of the loss

of IGF-1 in adulthood on each component of the neuro-glio-vascular unit. We previously established an inducible astrocyte-specific transgenic mouse model, and identified that glutamate handling machinery was reduced in the brains of these mice, which served as a rationale for studying glutamate excitotoxicity here (Prabhu et al., 2019). A recent study highlighted changes in neurovascular coupling when IGFR signaling was targeted in adult microvascular endothelial cells (Tarantini et al., 2021b). Thus, inducible models of astrocytic and endothelial cell IGFR knock-outs are available. Our singular and co-culture *in vitro* studies allow us to begin to delineate and compare the responses of specific cells without the confounds of other variables like paracrine compensation or pharmacological drug delivery or metabolism in one cell type over another. Further side-by-side comparisons of excitotoxic or ischemic damage in mice with inducible IGFR knock-out in neurons, astrocytes, endothelial cells, pericytes, and microglia would confirm the role for IGF-1 regulation of each cell, while also revealing other potential changes in physiology and pathophysiological responses in the intact brain.

Together, our study highlights that cell types within the neurovascular unit differentially respond to IGF-1 signaling. Despite differences in baseline susceptibility to glutamate, both neurons and astrocytes are both protected from excitotoxicity by IGF-1. Growth and division of endothelial cells and astrocytes are both influenced by IGF-1, however, endothelial cells remain resistant to glutamate toxicity even when IGF-1 signaling is reduced. The resistance of these supporting cells does not mean there are no consequences of reduced IGF-1 signaling in the time of glutamate stress, as both astrocytes and endothelial cells show signs of oxidative stress in the hours following exposure. The combination of neuron, astrocyte, and endothelial cells in culture afforded astrocytic protection from IGF-1 deficiency/glutamate stress but also highlighted a failure in the ability of astrocytes to protect the nearby neurons. Thus, the age-related loss of IGF-1 likely impairs the function and vitality of the entire neurovascular unit by differentially exerting stressors on neurons, endothelial cells, and astrocytes.

DATA AVAILABILITY STATEMENT

The raw data supporting the conclusions of this article will be made available by the authors, without undue reservation.

ETHICS STATEMENT

The animal study was reviewed and approved by Institutional Animal Use and Care Committee of the University of Mississippi.

AUTHOR CONTRIBUTIONS

CH and NA were responsible for conceptualization, investigation, project administration, and formal statistical analyses. CH, JM, and NA developed and designed methodology. BA, AV, and NA performed blinded image analyses and curated data. CH prepared visualizations. CH, BA, and NA prepared the original draft. All authors reviewed and edited the manuscript.

FUNDING

This work was supported by funds from the National Institutes of Health R15AG059142 and P30GM122733 to NA. Additional financial support for training was provided by the Southern Regional Education Board and the Society for Neuroscience to CH.

SUPPLEMENTARY MATERIAL

The Supplementary Material for this article can be found online at: https://www.frontiersin.org/articles/10.3389/fnagi.2021.751304/full#supplementary-material

Supplementary Figure 1 | Additional assessments of total cell number. **(A)** Average number of neurons per field 24 h after treatment. One-way ANOVA revealed no difference between means. **(B–D)** Astrocytes were pre-treated with 5 μM PPP for 24 h prior to combining with endothelial cells and neurons for a triple culture system. Average number of cells per field in the neurons **(B)**, astrocytes **(C)**, and endothelial cells **(D)** cultures after stimulation with 100 μM glutamate for 1 h (n = 5–8 wells/group). One-way ANOVA revealed no difference between means, and the p value of the ANOVA is listed for each. All data are presented as mean ± SEM. **(E)** Average astrocyte viability 24 h after 100 μM glutamate stimulation. Prior to stimulation, the cells were pre-treated with vehicle, 5 μM NVP-ADW742, or 100 nM IGF-1 for 24 h (n = 6–8 wells/group). **(F)** Average astrocyte cell count following treatment with vehicle, 5 μM NVP-ADW742, or 100 nM IGF-1 (n = 6–8 wells/group).

Supplementary Figure 2 | Astrocyte ROS and mitochondrial stress. **(A)** Average ROS levels 5 h after pure cultures of astrocytes treated with 0.5 μM NVP-ADW742 and 100 μM glutamate. Data were not normally distributed, so a Tukey's *post hoc* comparison was utilized following One-way ANOVA; * indicates a significant difference compared to vehicle (n = 10 wells/group). **(B)** Average oxygen consumption rate (y axis) and extracellular acidification rate (x axis) in astrocytes treated with vehicle control, 100 μM glutamate, or 100 μM glutamate + 0.5 μM PPP for one hor. Measurements occurred 5 h after treatment. Maximal respiration is grouped in the top right 3 points, and basal respiration is grouped in the bottom left 3 points. A one-way ANOVA was used for each comparison of maximal OCR, maximal ECAR, basal OCR, and basal ECAR. *Post hoc* Dunnett's test vs vehicle control was used when relevant. * indicates significant difference in OCR, and # indicates significant difference in ECAR. All data are presented as mean ± SEM, n = 7–8 wells/group.

REFERENCES

Armbrust, M., Worthmann, H., Dengler, R., Schumacher, H., Lichtinghagen, R., Eschenfelder, C. C., et al. (2017). Circulating insulin-like growth factor-1 and insulin-like growth factor binding protein-3 predict three-months outcome after ischemic stroke. *Exp. Clin. Endocrinol. Diab.* 125, 485–491. doi: 10.1055/s-0043-103965

Ashpole, N. M., Herron, J. C., Estep, P. N., Logan, S., Hodges, E. L., Yabluchanskiy, A., et al. (2016). Differential effects of IGF-1 deficiency during the life span on structural and biomechanical properties in the tibia of aged mice. *Age* 38:99025. doi: 10.1007/s11357-016-9902-5

Ashpole, N. M., Sanders, J. E., Hodges, E. L., Yan, H., and Sonntag, W. E. (2015b). Growth hormone, insulin-like growth factor-1 and the aging brain. *Exp. Gerontol.* 68, 76–81. doi: 10.1016/j.exger.2014.10.002

Ashpole, N. M., Herron, J. C., Mitschelen, M. C., Farley, J. A., Logan, S., Yan, H., et al. (2015a). IGF-1 regulates vertebral bone aging through sex-specific and time-dependent mechanisms. *J. Bone Miner Res.* 2015:2689. doi: 10.1002/jbmr.2689

Ashpole, N. M., and Hudmon, A. (2011). Excitotoxic neuroprotection and vulnerability with CaMKII inhibition. *Mol. Cell Neurosci.* 46, 720–730. doi: 10.1016/j.mcn.2011.02.003

Ashpole, N. M., Logan, S., Yabluchanskiy, A., Mitschelen, M. C., Yan, H., Farley, J. A., et al. (2017). IGF-1 has sexually dimorphic, pleiotropic, and time-dependent effects on healthspan, pathology, and lifespan. *Geroscience* 39, 129–145. doi: 10.1007/s11357-017-9971-0

Bake, S., Okoreeh, A. K., Alaniz, R. C., and Sohrabji, F. (2016). Insulin-like growth factor (IGF)-I modulates endothelial blood-brain barrier function in ischemic middle-aged female rats. *Endocrinology* 157, 61–69. doi: 10.1210/en.2015-1840

Bake, S., Selvamani, A., Cherry, J., and Sohrabji, F. (2014). Blood brain barrier and neuroinflammation are critical targets of IGF-1-mediated neuroprotection in stroke for middle-aged female rats. *PLoS One* 9:e91427. doi: 10.1371/journal.pone.0091427

Benjamin, E. J., Muntner, P., Alonso, A., Bittencourt, M. S., Callaway, C. W., Carson, A. P., et al. (2019). Heart disease and stroke statistics-2019 update: a report from the american heart association. *Circulation* 139, e56–e528. doi: 10.1161/CIR.0000000000000659

Bradley, S. J., and Challiss, R. A. (2012). G protein-coupled receptor signalling in astrocytes in health and disease: a focus on metabotropic glutamate receptors. *Biochem. Pharmacol.* 84, 249–259. doi: 10.1016/j.bcp.2012.04.009

Brown, L. S., Foster, C. G., Courtney, J. M., King, N. E., Howells, D. W., and Sutherland, B. A. (2019). Pericytes and neurovascular function in the healthy and diseased brain. *Front. Cell Neurosci.* 13:282. doi: 10.3389/fncel.2019.00282

California Acute Stroke Pilot Registry Investigators (2005). Prioritizing interventions to improve rates of thrombolysis for ischemic stroke. *Neurology* 64, 654–659. doi: 10.1212/01.wnl.0000151850.39648.5

Castilla-Cortazar, I., Aguirre, G. A., Femat-Roldan, G., Martin-Estal, I., and Espinosa, L. (2020). Is insulin-like growth factor-1 involved in Parkinson's disease development? *J. Transl. Med.* 18:70. doi: 10.1186/s12967-020-02223-0

Ceprian, M., and Fulton, D. (2019). Glial Cell AMPA receptors in nervous system health, injury and disease. *Int. J. Mol. Sci.* 20:20102450. doi: 10.3390/ijms20102450

Chen, W., He, B., Tong, W., Zeng, J., and Zheng, P. (2019). Astrocytic insulin-like growth factor-1 protects neurons against excitotoxicity. *Front. Cell Neurosci.* 13:298. doi: 10.3389/fncel.2019.00298

Choi, D. W. (2020). Excitotoxicity: still hammering the ischemic brain in 2020. *Front. Neurosci.* 14:579953. doi: 10.3389/fnins.2020.579953

Choi, D. W., Maulucci-Gedde, M., and Kriegstein, A. R. (1987). Glutamate neurotoxicity in cortical cell culture. *J. Neurosci.* 7, 357–368.

Choi, D. W., and Rothman, S. M. (1990). The role of glutamate neurotoxicity in hypoxic-ischemic neuronal death. *Annu. Rev. Neurosci.* 13, 171–182. doi: 10.1146/annurev.ne.13.030190.001131

De Smedt, A., Brouns, R., Uyttenboogaart, M., De Raedt, S., Moens, M., Wilczak, N., et al. (2011). Insulin-like growth factor I serum levels influence ischemic stroke outcome. *Stroke* 42, 2180–2185. doi: 10.1161/STROKEAHA.110.600783

Farias Quipildor, G. E., Mao, K., Hu, Z., Novaj, A., Cui, M. H., Gulinello, M., et al. (2019). Central IGF-1 protects against features of cognitive and sensorimotor decline with aging in male mice. *Geroscience* 41, 185–208. doi: 10.1007/s11357-019-00065-3

Fulop, G. A., Ramirez-Perez, F. I., Kiss, T., Tarantini, S., Valcarcel Ares, M. N., Toth, P., et al. (2019). IGF-1 Deficiency promotes pathological remodeling of cerebral arteries: a potential mechanism contributing to the pathogenesis of intracerebral hemorrhages in aging. *J. Gerontol. A Biol. Sci. Med. Sci.* 74, 446–454. doi: 10.1093/gerona/gly144

George, P. M., and Steinberg, G. K. (2015). Novel stroke therapeutics: unraveling stroke pathophysiology and its impact on clinical treatments. *Neuron* 87, 297–309. doi: 10.1016/j.neuron.2015.05.041

Ghazi Sherbaf, F., Mohajer, B., Ashraf-Ganjouei, A., Mojtahed Zadeh, M., Javinani, A., Sanjari Moghaddam, H., et al. (2018). Serum insulin-like growth factor-1 in parkinson's disease; study of cerebrospinal fluid biomarkers and white matter microstructure. *Front. Endocrinol.* 9:608. doi: 10.3389/fendo.2018.00608

Goshi, N., Morgan, R. K., Lein, P. J., and Seker, E. (2020). A primary neural cell culture model to study neuron, astrocyte, and microglia interactions in neuroinflammation. *J. Neuroinflam.* 17:155. doi: 10.1186/s12974-020-01819-z

Grinberg, Y. Y., Dibbern, M. E., Levasseur, V. A., and Kraig, R. P. (2013). Insulin-like growth factor-1 abrogates microglial oxidative stress and TNF-alpha responses to spreading depression. *J. Neurochem.* 126, 662–672. doi: 10.1111/jnc.12267

Gubbi, S., Quipildor, G. F., Barzilai, N., Huffman, D. M., and Milman, S. (2018). 40 YEARS of IGF1: IGF1: the Jekyll and Hyde of the aging brain. *J. Mol. Endocrinol.* 61, T171–T185. doi: 10.1530/JME-18-0093

Hayes, C. A., Valcarcel-Ares, M. N., and Ashpole, N. M. (2021). Preclinical and clinical evidence of IGF-1 as a prognostic marker and acute intervention with ischemic stroke. *J. Cereb. Blood Flow Metab.* 2021:894. doi: 10.1177/0271678X211000894

Higashi, Y., Sukhanov, S., Shai, S. Y., Danchuk, S., Snarski, P., Li, Z., et al. (2020). Endothelial deficiency of insulin-like growth factor-1 receptor reduces endothelial barrier function and promotes atherosclerosis in Apoe-deficient mice. *Am. J. Physiol. Heart Circ. Physiol.* 319, H730–H743. doi: 10.1152/ajpheart.00064.2020

Johnsen, S. P., Sorensen, H. T., Thomsen, J. L., Gronbaek, H., Flyvbjerg, A., Engberg, M., et al. (2004). Markers of fetal growth and serum levels of insulin-like growth factor (IGF) I, -II and IGF binding protein 3 in adults. *Eur. J. Epidemiol.* 19, 41–47. doi: 10.1023/b:ejep.0000013396.40006.8f

Johnson, W., Onuma, O., Owolabi, M., and Sachdev, S. (2016). Stroke: a global response is needed. *Bull. World Health Organ.* 94:636. doi: 10.2471/BLT.16.181636

Katzan, I. L., Furlan, A. J., Lloyd, L. E., Frank, J. I., Harper, D. L., Hinchey, J. A., et al. (2000). Use of tissue-type plasminogen activator for acute ischemic stroke: the Cleveland area experience. *JAMA* 283, 1151–1158. doi: 10.1001/jama.283.9.1151

Khennouf, L., Gesslein, B., Brazhe, A., Octeau, J. C., Kutuzov, N., Khakh, B. S., et al. (2018). Active role of capillary pericytes during stimulation-induced activity and spreading depolarization. *Brain* 141, 2032–2046. doi: 10.1093/brain/awy143

Kisler, K., Nelson, A. R., Rege, S. V., Ramanathan, A., Wang, Y., Ahuja, A., et al. (2017). Pericyte degeneration leads to neurovascular uncoupling and limits oxygen supply to brain. *Nat. Neurosci.* 20, 406–416. doi: 10.1038/nn.4489

Kisler, K., Nikolakopoulou, A. M., Sweeney, M. D., Lazic, D., Zhao, Z., and Zlokovic, B. V. (2020). Acute ablation of cortical pericytes leads to rapid neurovascular uncoupling. *Front. Cell Neurosci.* 14:27. doi: 10.3389/fncel.2020.00027

Kleindorfer, D., Lindsell, C. J., Brass, L., Koroshetz, W., and Broderick, J. P. (2008). National US estimates of recombinant tissue plasminogen activator use: ICD-9 codes substantially underestimate. *Stroke* 39, 924–928. doi: 10.1161/STROKEAHA.107.490375

Lalo, U., Pankratov, Y., Parpura, V., and Verkhratsky, A. (2011). Ionotropic receptors in neuronal-astroglial signalling: what is the role of "excitable" molecules in non-excitable cells. *Biochim. Biophys. Acta* 1813, 992–1002. doi: 10.1016/j.bbamcr.2010.09.007

Li, Y., Sun, W., Han, S., Li, J., Ding, S., Wang, W., et al. (2017). IGF-1-Involved negative feedback of NR2B NMDA subunits protects cultured hippocampal neurons against NMDA-Induced Excitotoxicity. *Mol. Neurobiol.* 54, 684–696. doi: 10.1007/s12035-015-9647-7

Lian, L., Zhang, Y., Liu, L., Yang, L., Cai, Y., Zhang, J., et al. (2020). Neuroinflammation in Ischemic Stroke: Focus on MicroRNA-mediated Polarization of Microglia. *Front. Mol. Neurosci.* 13:612439. doi: 10.3389/fnmol.2020.612439

Liu, X. F., Fawcett, J. R., Thorne, R. G., and Frey, W. H. II (2001). Non-invasive intranasal insulin-like growth factor-I reduces infarct volume and improves neurologic function in rats following middle cerebral artery occlusion. *Neurosci. Lett.* 308, 91–94. doi: 10.1016/s0304-3940(01)01982-6

Lopez-Lopez, C., LeRoith, D., and Torres-Aleman, I. (2004). Insulin-like growth factor I is required for vessel remodeling in the adult brain. *Proc. Natl. Acad. Sci. USA* 101, 9833–9838. doi: 10.1073/pnas.0400337101

Ma, Y., Wang, J., Wang, Y., and Yang, G. Y. (2017). The biphasic function of microglia in ischemic stroke. *Prog. Neurobiol.* 157, 247–272. doi: 10.1016/j.pneurobio.2016.01.005

Marino Lee, S., Hudobenko, J., McCullough, L. D., and Chauhan, A. (2021). Microglia depletion increase brain injury after acute ischemic stroke in aged mice. *Exp. Neurol.* 336:113530. doi: 10.1016/j.expneurol.2020.113530

Moskowitz, M. A., Lo, E. H., and Iadecola, C. (2010). The science of stroke: mechanisms in search of treatments. *Neuron* 67, 181–198. doi: 10.1016/j.neuron.2010.07.002

National Institute of Neurological Disorders and Stroke rt-Pa Stroke Study Group (1995). Tissue plasminogen activator for acute ischemic stroke. *N. Engl. J. Med.* 333, 1581–1587. doi: 10.1056/NEJM199512143332401

O'Connor, K. G., Tobin, J. D., Harman, S. M., Plato, C. C., Roy, T. A., Sherman, S. S., et al. (1998). Serum levels of insulin-like growth factor-I are related to age and not to body composition in healthy women and men. *J. Gerontol. A Biol. Sci. Med. Sci.* 53, M176–M182. doi: 10.1093/gerona/53a.3.m176

Park, S. E., Dantzer, R., Kelley, K. W., and McCusker, R. H. (2011). Central administration of insulin-like growth factor-I decreases depressive-like behavior and brain cytokine expression in mice. *J. Neuroinflam* 8:12. doi: 10.1186/1742-2094-8-12

Parker, K., Berretta, A., Saenger, S., Sivaramakrishnan, M., Shirley, S. A., Metzger, F., et al. (2017). PEGylated insulin-like growth factor-I affords protection and facilitates recovery of lost functions post-focal ischemia. *Sci. Rep.* 7:241. doi: 10.1038/s41598-017-00336-z

Prabhu, D., Khan, S. M., Blackburn, K., Marshall, J. P., and Ashpole, N. M. (2019). Loss of insulin-like growth factor-1 signaling in astrocytes disrupts glutamate handling. *J. Neurochem.* 2019:14879. doi: 10.1111/jnc.14879

Qin, C., Zhou, L.-Q., Ma, X.-T., Hu, Z.-W., Yang, S., Chen, M., et al. (2019). Dual functions of microglia in ischemic stroke. *Neurosci. Bull.* 35, 921–933. doi: 10.1007/s12264-019-00388-3

Qureshi, A. I., Suri, M. F., Nasar, A., He, W., Kirmani, J. F., Divani, A. A., et al. (2005). Thrombolysis for ischemic stroke in the united states: data from national hospital discharge Survey 1999-2001. *Neurosurgery* 57, 647–654.

Rosenberg, P. A., Amin, S., and Leitner, M. (1992). Glutamate uptake disguises neurotoxic potency of glutamate agonists in cerebral cortex in dissociated cell culture. *J. Neurosci.* 12, 56–61.

Saber, H., Himali, J. J., Beiser, A. S., Shoamanesh, A., Pikula, A., Roubenoff, R., et al. (2017). Serum insulin-like growth factor 1 and the risk of ischemic stroke: the framingham study. *Stroke* 48, 1760–1765. doi: 10.1161/STROKEAHA.116.016563

Serhan, A., Aerts, J. L., Boddeke, E., and Kooijman, R. (2020). Neuroprotection by insulin-like growth factor-1 in rats with ischemic stroke is associated with microglial changes and a reduction in neuroinflammation. *Neuroscience* 426, 101–114. doi: 10.1016/j.neuroscience.2019.11.035

Serhan, A., Boddeke, E., and Kooijman, R. (2019). Insulin-like growth factor-1 is neuroprotective in aged rats with ischemic stroke. *Front. Aging Neurosci.* 11:349. doi: 10.3389/fnagi.2019.00349

Serrano, A., Robitaille, R., and Lacaille, J. C. (2008). Differential NMDA-dependent activation of glial cells in mouse hippocampus. *Glia* 56, 1648–1663. doi: 10.1002/glia.20717

Sonntag, W. E., Deak, F., Ashpole, N., Toth, P., Csiszar, A., Freeman, W., et al. (2013). Insulin-like growth factor-1 in CNS and cerebrovascular aging. *Front. Aging Neurosci.* 5:27. doi: 10.3389/fnagi.2013.00027

Stanimirovic, D. B., and Friedman, A. (2012). Pathophysiology of the neurovascular unit: disease cause or consequence? *J. Cereb. Blood Flow Metab.* 32, 1207–1221. doi: 10.1038/jcbfm.2012.25

Sun, J., Huang, Y., Gong, J., Wang, J., Fan, Y., Cai, J., et al. (2020). Transplantation of hPSC-derived pericyte-like cells promotes functional recovery in ischemic stroke mice. *Nat. Commun.* 11:5196. doi: 10.1038/s41467-020-19042-y

Sun, Z., Wu, K., Gu, L., Huang, L., Zhuge, Q., Yang, S., et al. (2020). IGF-1R stimulation alters microglial polarization via TLR4/NF-kappaB pathway after cerebral hemorrhage in mice. *Brain Res. Bull.* 164, 221–234. doi: 10.1016/j.brainresbull.2020.08.026

Tang, J. H., Ma, L. L., Yu, T. X., Zheng, J., Zhang, H. J., Liang, H., et al. (2014). Insulin-like growth factor-1 as a prognostic marker in patients with acute ischemic stroke. *PLoS One* 9:e99186. doi: 10.1371/journal.pone.0099186

Tarantini, S., Balasubramanian, P., Yabluchanskiy, A., Ashpole, N. M., Logan, S., Kiss, T., et al. (2021a). IGF1R signaling regulates astrocyte-mediated neurovascular coupling in mice: implications for brain aging. *Geroscience* 43, 901–911. doi: 10.1007/s11357-021-00350-0

Tarantini, S., Nyul-Toth, A., Yabluchanskiy, A., Csipo, T., Mukli, P., Balasubramanian, P., et al. (2021b). Endothelial deficiency of insulin-like growth factor-1 receptor (IGF1R) impairs neurovascular coupling responses in mice, mimicking aspects of the brain aging phenotype. *Geroscience* 2021:4052. doi: 10.1007/s11357-021-00405-2

Tarantini, S., Tucsek, Z., Valcarcel-Ares, M. N., Toth, P., Gautam, T., Giles, C. B., et al. (2016b). Circulating IGF-1 deficiency exacerbates hypertension-induced microvascular rarefaction in the mouse hippocampus and retrosplenial cortex: implications for cerebromicrovascular and brain aging. *Age* 38, 273–289. doi: 10.1007/s11357-016-9931-0

Tarantini, S., Giles, C. B., Wren, J. D., Ashpole, N. M., Valcarcel-Ares, M. N., Wei, J. Y., et al. (2016a). IGF-1 deficiency in a critical period early in life influences the vascular aging phenotype in mice by altering miRNA-mediated post-transcriptional gene regulation: implications for the developmental origins of health and disease hypothesis. *Age* 38, 239–258. doi: 10.1007/s11357-016-9943-9

Tarantini, S., Valcarcel-Ares, N. M., Yabluchanskiy, A., Springo, Z., Fulop, G. A., Ashpole, N., et al. (2017). Insulin-like growth factor 1 deficiency exacerbates hypertension-induced cerebral microhemorrhages in mice, mimicking the aging phenotype. *Aging Cell* 16, 469–479. doi: 10.1111/acel.12583

Terasaki, Y., Liu, Y., Hayakawa, K., Pham, L. D., Lo, E. H., Ji, X., et al. (2014). Mechanisms of neurovascular dysfunction in acute ischemic brain. *Curr. Med. Chem.* 21, 2035–2042. doi: 10.2174/09298673216661312282 23400

Toth, P., Tarantini, S., Ashpole, N. M., Tucsek, Z., Milne, G. L., Valcarcel-Ares, N. M., et al. (2015). IGF-1 deficiency impairs neurovascular coupling in mice: implications for cerebromicrovascular aging. *Aging Cell* 14, 1034–1044. doi: 10.1111/acel.12372

Toth, P., Tarantini, S., Csiszar, A., and Ungvari, Z. (2017). Functional vascular contributions to cognitive impairment and dementia: mechanisms and consequences of cerebral autoregulatory dysfunction, endothelial impairment, and neurovascular uncoupling in aging. *Am. J. Physiol. Heart Circ. Physiol.* 312, H1–H20. doi: 10.1152/ajpheart.00581.2016

Wang, Y., Wang, W., Li, D., Li, M., Wang, P., Wen, J., et al. (2014). IGF-1 alleviates NMDA-induced excitotoxicity in cultured hippocampal neurons against autophagy via the NR2B/PI3K-AKT-mTOR pathway. *J. Cell Physiol.* 229, 1618–1629. doi: 10.1002/jcp.24607

Watanabe, T., Miyazaki, A., Katagiri, T., Yamamoto, H., Idei, T., and Iguchi, T. (2005). Relationship between serum insulin-like growth factor-1 levels and Alzheimer's disease and vascular dementia. *J. Am. Geriatr. Soc.* 53, 1748–1753. doi: 10.1111/j.1532-5415.2005.53524.x

Yang, S., Jin, H., Zhu, Y., Wan, Y., Opoku, E. N., Zhu, L., et al. (2017). Diverse Functions and mechanisms of pericytes in ischemic stroke. *Curr. Neuropharmacol.* 15, 892–905. doi: 10.2174/1570159X15666170112170226

Conflict of Interest: The authors declare that the research was conducted in the absence of any commercial or financial relationships that could be construed as a potential conflict of interest.

Publisher's Note: All claims expressed in this article are solely those of the authors and do not necessarily represent those of their affiliated organizations, or those of the publisher, the editors and the reviewers. Any product that may be evaluated in this article, or claim that may be made by its manufacturer, is not guaranteed or endorsed by the publisher.

frontiers in Aging Neuroscience

BRIEF RESEARCH REPORT
published: 21 December 2021
doi: 10.3389/fnagi.2021.756537

Treadmill Exercise During Cerebral Hypoperfusion Has Only Limited Effects on Cognitive Function in Middle-Aged Subcortical Ischemic Vascular Dementia Mice

*Ryo Ohtomo[1,2], Hidehiro Ishikawa[1], Keita Kinoshita[1,3], Kelly K. Chung[1], Gen Hamanaka[1], Gaku Ohtomo[2], Hajime Takase[1], Christiane D. Wrann[4,5], Hiroshi Katsuki[3], Atsushi Iwata[6], Josephine Lok[1,7], Eng H. Lo[1] and Ken Arai[1]**

[1] Neuroprotection Research Laboratory, Departments of Radiology and Neurology, Massachusetts General Hospital and Harvard Medical School, Charlestown, MA, United States, [2] Department of Neurology, Graduate School of Medicine, The University of Tokyo, Tokyo, Japan, [3] Department of Chemico-Pharmacological Sciences, Graduate School of Pharmaceutical Sciences, Kumamoto University, Kumamoto, Japan, [4] Cardiovascular Research Center, Department of Medicine, Massachusetts General Hospital and Harvard Medical School, Charlestown, MA, United States, [5] McCance Center for Brain Health, Massachusetts General Hospital, Boston, MA, United States, [6] Department of Neurology, Tokyo Metropolitan Geriatric Medical Center Hospital, Tokyo, Japan, [7] Pediatric Critical Care Medicine, Department of Pediatrics, Massachusetts General Hospital, Boston, MA, United States

OPEN ACCESS

Edited by:
Yorito Hattori, National Cerebral and Cardiovascular Center (Japan), Japan

Reviewed by:
Maiko T. Uemura, University of Pennsylvania, United States
Satoshi Saito, National Cerebral and Cardiovascular Center (Japan), Japan

***Correspondence:**
Ken Arai
karai@partners.org

Received: *10 August 2021*
Accepted: *16 November 2021*
Published: *21 December 2021*

Citation:
Ohtomo R, Ishikawa H, Kinoshita K, Chung KK, Hamanaka G, Ohtomo G, Takase H, Wrann CD, Katsuki H, Iwata A, Lok J, Lo EH and Arai K (2021) Treadmill Exercise During Cerebral Hypoperfusion Has Only Limited Effects on Cognitive Function in Middle-Aged Subcortical Ischemic Vascular Dementia Mice. Front. Aging Neurosci. 13:756537. doi: 10.3389/fnagi.2021.756537

Clinical and basic research suggests that exercise is a safe behavioral intervention and is effective for improving cognitive function in cerebrovascular diseases, including subcortical ischemic vascular dementia (SIVD). However, most of the basic research uses young animals to assess the effects of exercise, although SIVD is an age-related disease. In this study, therefore, we used middle-aged mice to examine how treadmill exercise changes the cognitive function of SIVD mice. As a mouse model of SIVD, prolonged cerebral hypoperfusion was induced in 8-month-old male C57BL/6J mice by bilateral common carotid artery stenosis. A week later, the mice were randomly divided into two groups: a group that received 6-week treadmill exercise and a sedentary group for observation. After subjecting the mice to multiple behavioral tests (Y-maze, novel object recognition, and Morris water maze tests), the treadmill exercise training was shown to only be effective in ameliorating cognitive decline in the Y-maze test. We previously demonstrated that the same regimen of treadmill exercise was effective in young hypoperfused-SIVD mice for all three cognitive tests. Therefore, our study may indicate that treadmill exercise during cerebral hypoperfusion has only limited effects on cognitive function in aging populations.

Keywords: aging, behavior, cognitive function, mouse, subcortical ischemic vascular dementia, treadmill exercise

INTRODUCTION

Physical activity helps to promote and maintain brain health, including memory retention and cognitive performance. Research has shown that increased physical activity both prevents and ameliorates multiple brain diseases, including subcortical ischemic vascular dementia (SIVD). SIVD is the most common form of vascular cognitive impairment and dementia (VCID) (Erkinjuntti et al., 2000a,b). SIVD patients typically suffer from peri-ventricular white matter

degeneration that leads to stepwise development of neurological deficits and loss of executive function, such as difficulties with working memory (Roman et al., 2002; Roh and Lee, 2014; Prins and Scheltens, 2015; Wallin et al., 2018). Although SIVD is expected to become more prevalent as the population ages, to date, there are no clinically effective drugs.

There is an emerging body of evidence suggesting that patients with mild VCID perform better at cognitive functioning tests after aerobic exercise (Liu-Ambrose et al., 2016). However, there is a lack of basic data in experimental models that supports the efficacy of exercise for preventing SIVD/VCID progression. Recently, we reported that treadmill exercise improved cognitive function and increased the number of oligodendrocyte precursor cells (OPCs) in the white matter of hypoperfused-SIVD mice (Ohtomo et al., 2020). Nevertheless, an important question remains; although aging is a major risk factor for SIVD, and the majority of SIVD patients are elderly, no reports to date have examined the efficacy of exercise in aged SIVD mice. Therefore, in this study, we asked whether treadmill exercise alleviates cognitive decline by cerebral hypoperfusion in 8-months old mice.

MATERIALS AND METHODS

Overall Experimental Design

In this mouse model of SIVD, cognitive function (working memory, cognitive memory, and special learning) is known to decline in 4 weeks, presumably due to rarefaction of the white matter (Shibata et al., 2004, 2007; Ihara and Tomimoto, 2011; Yang et al., 2016; Ohtomo et al., 2020; Takase et al., 2021). Our intervention was a 6-week treadmill training which, according to our hypothesis, would slow cognitive decline and ameliorate the deterioration in performance over time. We hypothesized this because this treadmill protocol was shown to be effective in multiple CNS disease models, including young hypoperfused-SIVD mice (Ohtomo et al., 2020; Kinoshita et al., 2021). In this study, we conducted two experiments; Experiment 1 was for Y-maze test, and Experiment 2 was for novel object recognition test (NORT) and Morris water maze test (**Figure 1**). In both experiments, after the Sham or bilateral common carotid artery stenosis (BCAS) surgery on day 1, treadmill training occurred from day 8 to day 47 in the training group. Mice in the sedentary group were placed on the treadmill for an equivalent amount of time, but without running. In addition to the memory assessment, we also conducted immunohistological and biochemical analyses using mouse brain sections prepared from the mice in Experiment 1. For Experiment 1, 33 mice were used, and 6 mice (5 mice of the BCAS/Sedentary group and 1 mouse of the BCAS/Treadmill group) were excluded due to death or unhealthy conditions. For Experiment 2, 34 mice were used, and 6 mice were excluded due to dead or unhealthy conditions.

Prolonged Cerebral Hypoperfusion Model (BCAS Mice)

All performed experiments followed an institutionally approved protocol in accordance with the National Institutes of Health Guide for the Care and Use of Laboratory Animals and the law for the humane treatment and management of animals. Eight-month-old male C57BL/6J mice (Jackson Laboratory, United States) were housed in a specific pathogen-free conditioned 12-hour light/dark cycle room with free access to food and water throughout the experiment. After a week-long habituation period in our animal facility, mice were randomly selected to have a microcoil (0.18 mm diameter; Samini, Japan) applied to bilateral common carotid arteries for the induction of chronic cerebral hypoperfusion. The surgical procedure was performed as previously described (Shibata et al., 2004; Ohtomo et al., 2020). A control group received sham operation (after exposing bilateral common carotid arteries, the cervical incision was closed without coil application).

Treadmill Training Protocol

Sham or BCAS-operated mice were randomly divided into a sedentary group and a training group. The training group was forced to run on a treadmill device (Exter 3/6 Treadmill, Columbus Instruments, United States) for 6 weeks (in the early afternoon, 5 days a week on weekdays). Running speed suitable for exercise was determined from our previous studies that demonstrated protective effects against brain injury (Ohtomo et al., 2020; Kinoshita et al., 2021), beginning with a speed of 2 m/min, with an increase of 2 m/min every 2 min, until a maximum speed of 10 m/min was reached. The length of the total exercise was initially set at 20 min and increased daily by 10 min up to 60 min for familiarization, as shown in **Figure 1**. The sedentary group was placed on the device without running for the same amount of time as the training group. Mice were always placed in the same lane throughout the experiment.

Evaluation of the Muscle Fibers of Gastrocnemius Muscles

On day 49, the right gastrocnemius muscle was excised from randomly selected BCAS/Sedentary (N = 10) or BCAS/Treadmill (N = 10) mice from Experiment 1, under anesthesia with isoflurane before transcardial perfusion. Muscles perpendicularly embedded to Cryomold (Sakura Finetek USA, United States) with Tissue-Tek® (Sakura Finetek USA) were quickly frozen by liquid nitrogen and kept at −80°C until use. Five samples were randomly selected from each study group, and 10 μm-thick frozen sections were made using cryostat CM1520 (Leica, Germany). Sections were then fixed with −20°C methanol for 10 min and stained with Hematoxylin 2 (Thermo Fisher Scientific) and Eosin-Y (Thermo Fisher Scientific) according to the manufacturer's instructions. Stained sections were observed with ECLIPSE Ti-S (Nikon, Japan) and scanned with Retiga™ 2000R Fast 1394 Digital Camera (QImaging, Canada). Then, a cross-sectional area of 50 muscle fibers per mouse was measured by using ImageJ[1]. To compare the area distribution of the muscle fibers between the groups, a histogram was drawn using PRISM® 7 (GraphPad Software, United States).

[1]https://imagej.nih.gov/

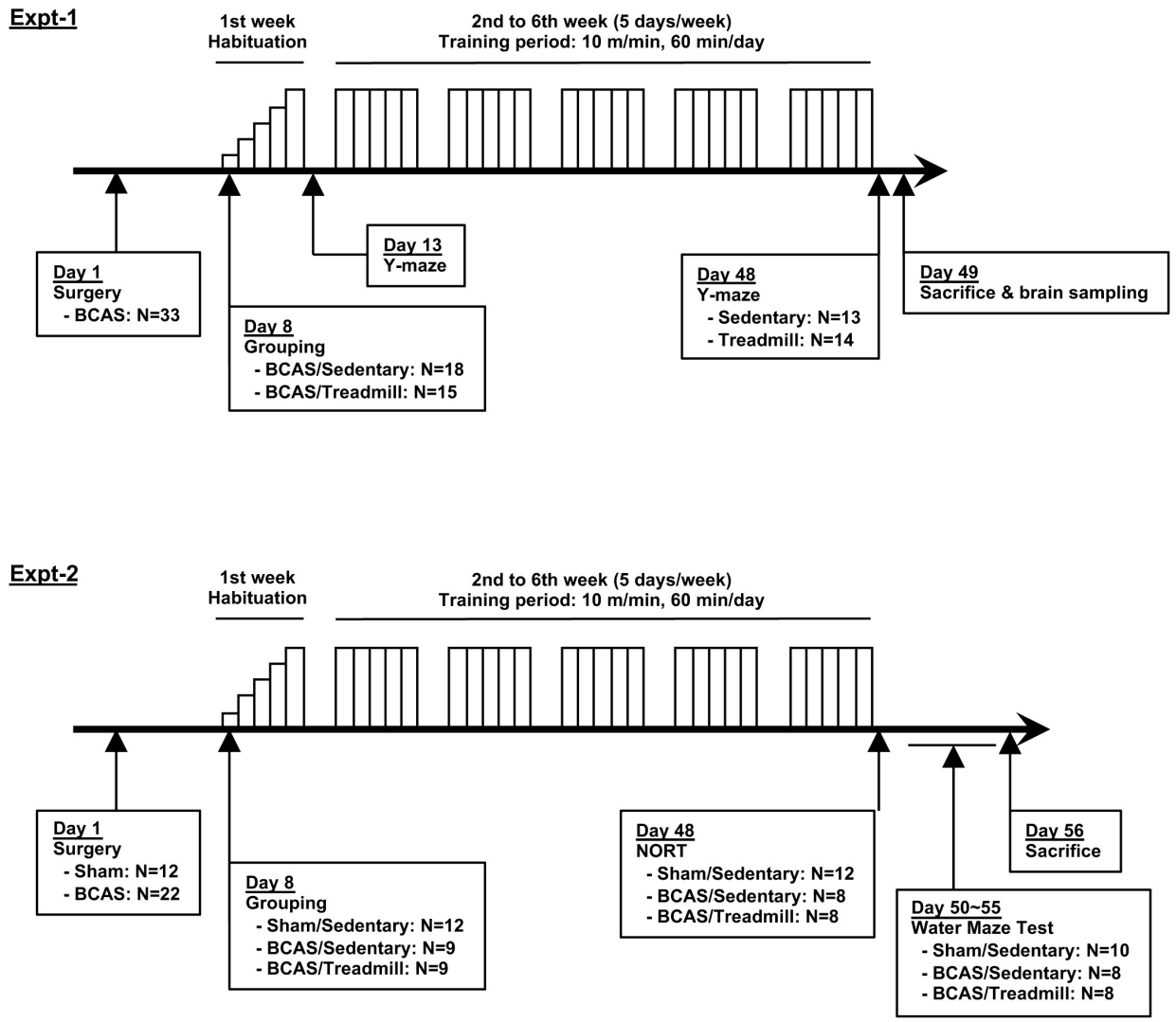

FIGURE 1 | Schematic overview of this study. Two experiments were conducted to examine the effects of treadmill exercise on the cognitive function of middle-aged hypoperfused SIVD-mice. BCAS mice were separated into 2 groups (Sedentary vs. Treadmill) 7 days after the surgery. Following a week-long habituation period (from day 8 to day 12), mice in the treadmill group were placed on a treadmill, on which they were obligated to run for 60 min/day at a maximum speed of 10 m/min on weekdays for 5 weeks. Y-maze was conducted 2 times, on day 13 and day 48 (Experiment 1). NORT was conducted 2 times, on day 48 (Experiment 2). The Morris water maze was conducted between days 50–55 (Experiment 2).

Y-Maze

After the first and sixth week of exercise (day 13 and day 48), mice were tested for spontaneous alternation behavior with Y-maze between 6 AM and 9 AM. Our approach in conducting the Y-maze test multiple times in the same mouse was justified by the papers that the retention memory within the Y-maze task may not last longer than a few hours (Dellu et al., 2000; Fu et al., 2017). Each mouse was placed in the arm of symmetrical Y-maze apparatus to freely explore the maze for 8 min. The task was videotaped, and the sequence and the total number of arm entries were manually recorded later in a blinded manner. An arm entry was confirmed when bilateral hind paws were placed inside the arm. Arms were washed with 70% Ethanol between each test. Percentage of alternation was calculated as follows: number of triads containing entries into 3 different arms/(total number of arms entered -2) $\times$ 100.

NORT

Mice were tested for recognition memory by NORT between 8 AM and 1 PM on day 48. At first, the mice were habituated in an empty cage for 10 min before training. During training, they experienced 5-min exposure to 2 identical plastic blocks 2 times. After 30 min, they were then presented with 2 different plastic blocks (one of the original blocks replaced by a new block) for 5 min. The mouse behavior was videotaped and manually assessed in a blinded manner. Object recognition was scored by the total time spent either sniffing or touching the object. The performance of recognition memory was evaluated by the ratio

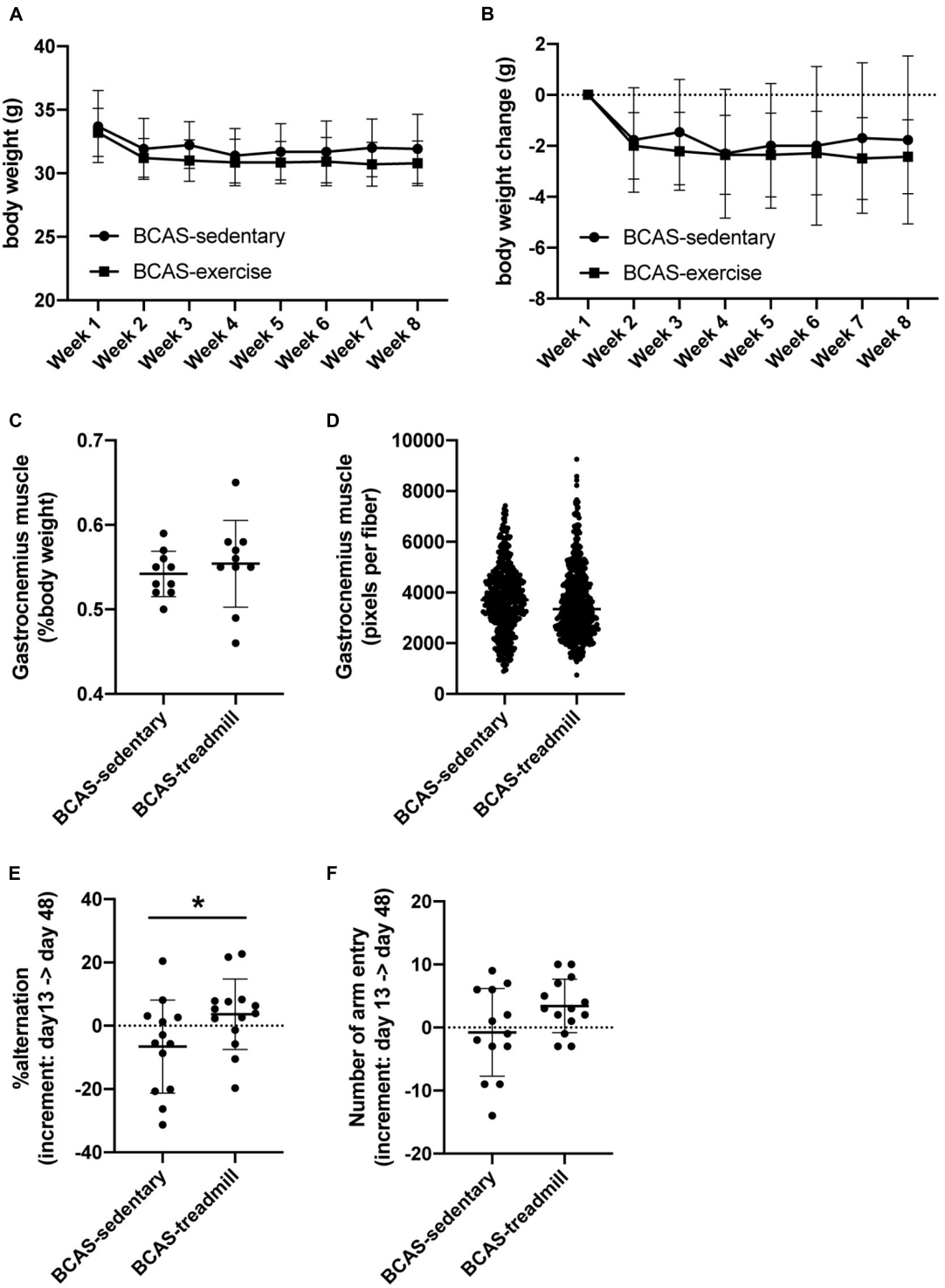

FIGURE 2 | Result of cognitive function test from Experiment 1. **(A,B)** Body weight transition of mice **(A)**, and temporal body weight change of mice **(B)**. There was no significant difference between the 2 groups (BCAS/Sedentary vs. BCAS/Treadmill). Data are expressed as mean ± SD. **(C,D)** Weight of gastrocnemius muscle (percentage of body weight) **(C)** and distribution of the area of muscle fibers **(D)** at day 49. There was no significant difference between the 2 groups (BCAS/Sedentary vs. BCAS/Treadmill). Data are expressed as mean ± SD. **(E,F)** Change in alternation (an index of working memory) in Y-maze test before and after the training period **(E)** and change in the number of arm entries in Y-maze test before and after the training period **(F)**. There was a significant difference in the increment of alteration between the 2 groups (BCAS/Sedentary vs. BCAS/Treadmill) (*$P < 0.05$, Mann-Whitney *U* test). Data are mean ± SD.

of the time spent on the new object to the total time spent on 2 objects (Ohtomo et al., 2020). Five mice were excluded from analysis due to lack of interest toward the objects (e.g., those mice did not sniff or touch the 2 objects).

Morris Water Maze Test

On days 50–55, mice were tested with Morris water maze to evaluate spatial learning and memory as previously described (Ohtomo et al., 2020). In brief, mice had to find a hidden (2 cm under the water surface) escape platform (diameter: 11.5 cm) which was placed in the northeastern quadrant of a circular pool (diameter: 110 cm) filled with opacified water kept at 25°C. In the acquisition phase, mice performed 4 trials per day from a random starting position for 5 consecutive days, with a maximum trial duration of 60 s. To test spatial memory, the platform was removed, and 60-second probe trials were performed on day 54 (4 h after the last acquisition test) and day 55 (4 h after the last acquisition test). Escape latency to find the hidden platform and number of entries into quadrants were examined using ANY-maze video tracking software (Stoelting Co., United States). Due to passive floating behavior in the water, 2 mice were excluded from analysis (one from the BCAS/Sedentary, and the other from the BCAS/Treadmill group). For the Sham/Sedentary group, we randomly picked 10 mice out of 12 Sham/Sedentary mice for the Morris water maze test due to time scheduling issues.

Western Blot Analysis

Mouse brains were removed following transcardial perfusion with 40 mL PBS (0.1 M), quickly frozen in dry ice, and kept at -80°C until use. Frozen brains were thawed to a semi-frozen state, and three 2 mm-thick coronal sections were obtained from the forebrain 1–7 mm anterior to the confluence of sinuses using the mouse brain matrix slicing tool. The brain sections were placed in ice-cold PBS, and the meninges were removed, after which the corpus callosum and cerebral cortex were carefully removed under a microscope with a disposable micro knife (Fine Science Tools, Canada). Four times the amount of PBS with protease inhibitor cocktail (Cytoskeleton, United States) was promptly added to the samples and dismembraned by sonic dismembrator (ThermoFisher Scientific, United States) on ice. After adding Triton X-100 (Sigma-Aldrich, United States) to a final concentration of 1%, samples were frozen at −80°C and thawed on ice. Then, they were centrifuged at 10000 × *g* for 15 min at 4°C to remove cellular debris. Protein concentration was determined by the BCA assay (Thermo Fisher, United States). Collected samples were heated with equal amounts of LDS sample buffer (ThermoFisher Scientific) and sample reducing agent (ThermoFisher Scientific) at 70°C for 10 min. Each sample was equally (30 μg) loaded onto 4–12% Bis-Tris gels (ThermoFisher Scientific) for electrophoresis, followed by transfer to a nitrocellulose membrane (Thermo Fisher Scientific). Membranes were blocked in 5% skim milk (LabScientific, United States) and incubated overnight at 4°C with primary antibodies against PDGFRα (1:500, Sigma-Aldrich, United States), MBP (1:1000, Thermo Fisher Scientific), and β-actin (1:10000, Sigma-Aldrich). Then, membranes were processed with peroxidase-conjugated secondary antibodies [1:1000 for anti-rabbit antibody (GE Healthcare, United States), and 1:2000 for anti-mouse antibody (GE Healthcare, United States)] and visualized by enhanced chemiluminescence (Thermo Fisher Scientific). Visualized bands were semi-quantified with ImageJ.

Immunohistochemistry

Five samples were randomly selected from each study group, and 20 μm-thick coronal sections (corresponding to the area 0–1 mm anterior to bregma) were prepared for immunostaining using cryostat CM1520. Frozen sections were then fixed with −20°C methanol for 10 min. After being washed with PBS containing 0.1% Triton X-100 for 5 min 3 times, they were incubated in PBS/3% BSA solution for 1 h at room temperature. Then, sections were incubated in PBS/3% BSA solution containing primary antibodies anti-PDGFRα (1:100, R&D systems, United States) or anti-nestin (1:100, Abcam, United States) at 4°C overnight. After being washed with PBS 3 times, they were incubated with secondary antibodies (1:1000, Jackson Immunoresearch Laboratories) for 1 h at room temperature. Finally, the sections were washed three times with PBS, and covered with VECTASHIELD® mounting medium with DAPI (Vector Laboratories, United States). Stained sections were observed with ECLIPSE Ti-S and scanned with Retiga™ 2000R Fast 1394 Digital Camera. All brain sections were blinded to the examiner before the evaluation of fluorescence intensity. Immunofluorescence intensity of PDGFRα-positive cells inside the subventricular zone (SVZ) was calculated by ImageJ. Bilateral sides of two coronal sections cut from the area + 0.5 ∼ + 1.0 mm to the bregma were evaluated, and the average of 4 areas was calculated per mouse. The same procedure was conducted for evaluating the fluorescence intensity of nestin-positive cells.

Statistics

Statistical analysis was performed with R version 3.4.0[2] and PRISM® 7. For body weight, data were first tested with two-way analysis of variance (ANOVA), followed by *post hoc* Sidak's multiple comparisons test. For the acquisition phase of the Morris water maze test, data were first tested with two-way ANOVA, followed by *post hoc* Tukey's multiple comparisons test. Data from the probe test were first analyzed with Brown-Forsythe ANOVA, followed by *post hoc* Dunnett's T3 multiple comparisons test. NORT data were first analyzed with one-way ANOVA, followed by *post hoc* Tukey's multiple comparisons test. Mann-Whitney *U* test or Welch's *t*-test was used for other analyses. All values were expressed as mean ± SD. *P*-values less than 0.05 were considered statistically significant.

RESULTS

To examine the effects of treadmill exercise on the cognitive function of middle-aged hypoperfused-SIVD mice, we conducted two sets of experiments (**Figure 1**). Hypoperfused-SIVD mice were prepared by subjecting mice to the BCAS operation.

[2]https://www.r-project.org/

The baseline of cerebral blood flow is lower in aged mice (22 months old), compared to young mice (2–3 months old), thus the decrease of cerebral blood flow by BCAS is less impacted in aged mice (Baik et al., 2021). However, at least in our system, the BCAS operation caused prolonged cerebral blood flow reduction in middle-aged mice (8 months old) (**Supplementary Figure 1**). In the first set of experiments, we prepared two groups (hypoperfused-SIVD mice without exercise treadmill and hypoperfused-SIVD mice with exercise treadmill) to investigate whether exercise treadmill during cerebral hypoperfusion mitigated cognitive decline (e.g., from day 13 to day 48 after BCAS) using Y-maze test. In addition, after the completion of the Y-maze experiment, gastrocnemius muscles and brains were sampled for biochemical analyses. In the second set of experiments, we prepared three groups (sham mice without exercise treadmill, hypoperfused-SIVD mice without exercise treadmill, and hypoperfused SIVD mice with exercise) to examine whether the cognitive function of hypoperfused-SIVD mice with treadmill exercise would be comparable with that of sham mice without treadmill exercise. For both experiments, male C57BL/6J (8 months old) mice were subjected to the 6-week exercise after sham or BCAS operation. One week was spent on habituation exercise, where running speed began at 2 m/min and was increased by 2 m/min every 2 min until a maximum speed of 10 m/min was reached; the duration of the daily exercise was initially set at 20 min and was increased daily by 10 min up to 60 min. In the following 5 weeks, mice were then subjected to running exercise at a speed of 10 m/min for 60 min/day.

In the first set of experiments, both groups (hypoperfused-SIVD mice without exercise and hypoperfused-SIVD mice with exercise) lost body weight after BCAS operation, and over time during the treadmill exercise training, they did not gain body weight regardless of treadmill exercise (**Figures 2A,B**). In addition, there was no significant difference in the right gastrocnemius muscles between the two groups (**Figure 2C** for the percentage of gastrocnemius muscle weight and **Figure 2D** for the distribution of muscle fiber thickness). However, in the Y-maze tests, while hypoperfused-SIVD mice without treadmill exercise showed a decline in cognitive function from day 13 to day 48 after BCAS operation, hypoperfused-SIVD mice with treadmill exercise did not (**Figures 2E,F**).

In the second set of experiments, we assessed cognitive function with the Morris water maze test and NORT. In the Morris water maze test, there was no significant difference in the memory acquisition between the three groups (sham mice without exercise vs. hypoperfused-SIVD mice without exercise vs. hypoperfused-SIVD mice with exercise) (**Figure 3A**). In addition, in the probe tests at 4 and 24 h after the last session of acquisition trial, there were no differences in the memory retention performance between the groups (**Figures 3B–D**). In NORT, as expected, sham mice without exercise showed a preference for the novel object; however, hypoperfused-SIVD mice without exercise showed no preference between the familiar and novel objects (**Figure 3E**). On the other hand, there was no significant difference in the preference between sham mice without exercise and hypoperfused-SIVD mice with exercise (**Figure 3F**).

Finally, we examined whether white matter pathology would be affected by treadmill exercise, because white matter damage is one of the major characteristics of SIVD. Fluoro-myelin staining showed that there was no difference in myelin density in the corpus callosum between hypoperfused-SIVD mice with or without treadmill exercise (**Figure 4A**). Western blotting also confirmed that treadmill exercise did not change the myelin density of corpus callosum, assessed by the level of MBP, which is a major component of the myelin sheath (**Figure 4B**). After white matter damage, compensatory responses would be activated, and OPCs play an important role in increasing the number of myelin-producing oligodendrocytes. However, the number of OPCs was not affected by the treadmill exercise in middle-aged hypoperfused-SIVD mice (**Figures 4B,C**). In addition, there was no significant difference in the Nestin-positive cells, which can differentiate into both neurons and OPCs in the adult brain after brain injury (**Figure 4C**). And finally, we checked if the middle-aged SIVD mice had a significant infarction in the cortical area. It is now well accepted that prolonged cerebral hypoperfusion by BCAS does not cause infarcts in young mice, but little is known about this point in middle-aged mice. But we confirmed no ischemic infarction in the cortex by hematoxylin-eosin staining with randomly selected 10 brain samples from the SIVD mice (**Supplementary Figure 2**).

DISCUSSION

Our current study demonstrated that in middle-aged mice with prolonged cerebral hypoperfusion, treadmill exercise ameliorates the decline of working memory in the Y-maze test. On the other hand, treadmill exercise was limited in its supportive effects on cognitive function in the Morris water maze test and NORT. Previously, we showed that the same regimen of treadmill exercise suppressed cognitive decline, assessed by the three cognitive function tests (Y-maze, Morris water maze test, and NORT), in young mice with cerebral hypoperfusion (Ohtomo et al., 2020). Our previous study also showed that the treadmill exercise during cerebral hypoperfusion increased the number of OPCs within the SVZ region of young hypoperfused-SIVD mice (Ohtomo et al., 2020), although we did not confirm the positive effects of treadmill exercise on OPC function in this study. Therefore, together with our previous data (Ohtomo et al., 2020), our current study may suggest that the efficacy of treadmill exercise in cognitive function would decrease with age, but treadmill exercise still seems effective in supporting cognitive function even in aging populations. This is consistent with past studies that treadmill exercise supported cognitive function in both young and aged AD mice, but the efficacy was smaller in the aged groups (Choi et al., 2021).

An important aspect of our current study is the finding that treadmill exercise is less effective in middle-aged SIVD model mice. To the best of our knowledge, except for our previous report (Ohtomo et al., 2020), there are only two previous studies that evaluate the effectiveness of exercise in preventing/ameliorating cognitive decline caused by chronic cerebral hypoperfusion (Jiang et al., 2017; Lee et al., 2017). These two studies showed

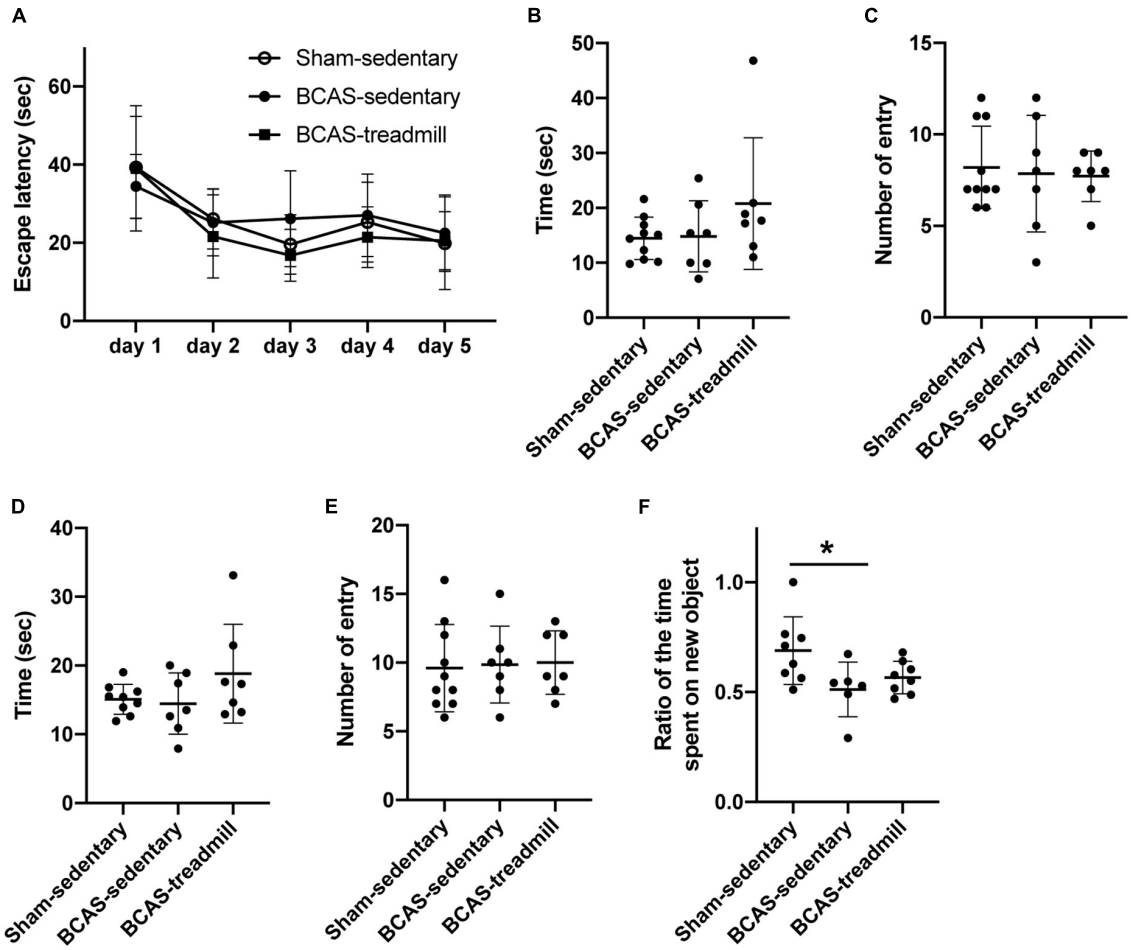

FIGURE 3 | Result of cognitive function test from Experiment 2. **(A)** During the acquisition phase of Morris water maze, no difference was observed in latencies to locate the hidden platform between the 3 groups (Sham/Sedentary vs. BCAS/Sedentary vs. BCAS/Treadmill). Data are mean ± SD. **(B,C)** Result of the probe trial (4 h after the last acquisition session) in the Morris water maze test. There were no significant differences in both **(B)** number of entries into and **(C)** time spent in the quadrant which formerly contained a hidden platform in the acquisition phase. Data are mean ± SD. **(D,E)** Result of the probe trial (24 h after the last acquisition session) in the Morris water maze test. There were no significant differences in both **(D)** number of entries into and **(E)** time spent in the quadrant which formerly contained a hidden platform in the acquisition phase. Data are mean ± SD. **(F)** Compared to the Sham/Sedentary group, the BCAS/Sedentary group showed less preference to the novel object (*$p < 0.05$, one-way ANOVA followed by *post hoc* Tukey's test). However, there was no significant difference between Sham/Sedentary and BCAS/Treadmill groups. Data are mean ± SD.

that treadmill exercise is effective in ameliorating cognitive dysfunction using young SIVD model rats. Our findings further add to this existing literature. The efficacy of treadmill exercise during cerebral hypoperfusion in cognitive function might be less effective in aging populations. This may be partly explained by the fact that compensative responses after brain injury, such as neurogenesis and oligodendrogenesis, are dampened by age (Miyamoto et al., 2013; Liang et al., 2016). While the treadmill exercise increased the number of OPCs within the SVZ region in young SIVD mice (Ohtomo et al., 2020), our current study did not confirm this effect in middle-aged mice. In addition, the body weight loss after cerebral hypoperfusion was not recovered by treadmill exercise in middle-aged mice (**Figures 2A,B**), although the same protocol of treadmill exercise helped young SIVD mice recover their body weight (Ohtomo et al., 2020). In stroke mice, the body weight recovery was associated with an improvement of motor function (Desgeorges et al., 2017; Kinoshita et al., 2021), which may also explain the difference in the efficacy of treadmill exercise between young and middle-aged mice.

Although we have demonstrated that treadmill exercise ameliorates cognitive decline caused by cerebral hypoperfusion to some extent in middle-aged mice, there are some limitations and caveats in this study. First, we used only one protocol of treadmill exercise, which was shown to be effective for young mice (Ohtomo et al., 2020; Kinoshita et al., 2021). In general, in aged populations, the capability of movement and the total volume of muscle is lower compared to younger populations, so the exercise protocol for young mice may not be suitable for middle-aged mice. The optimization of the conditions of treadmill exercise for middle-aged (or even aged) mice would be necessary for

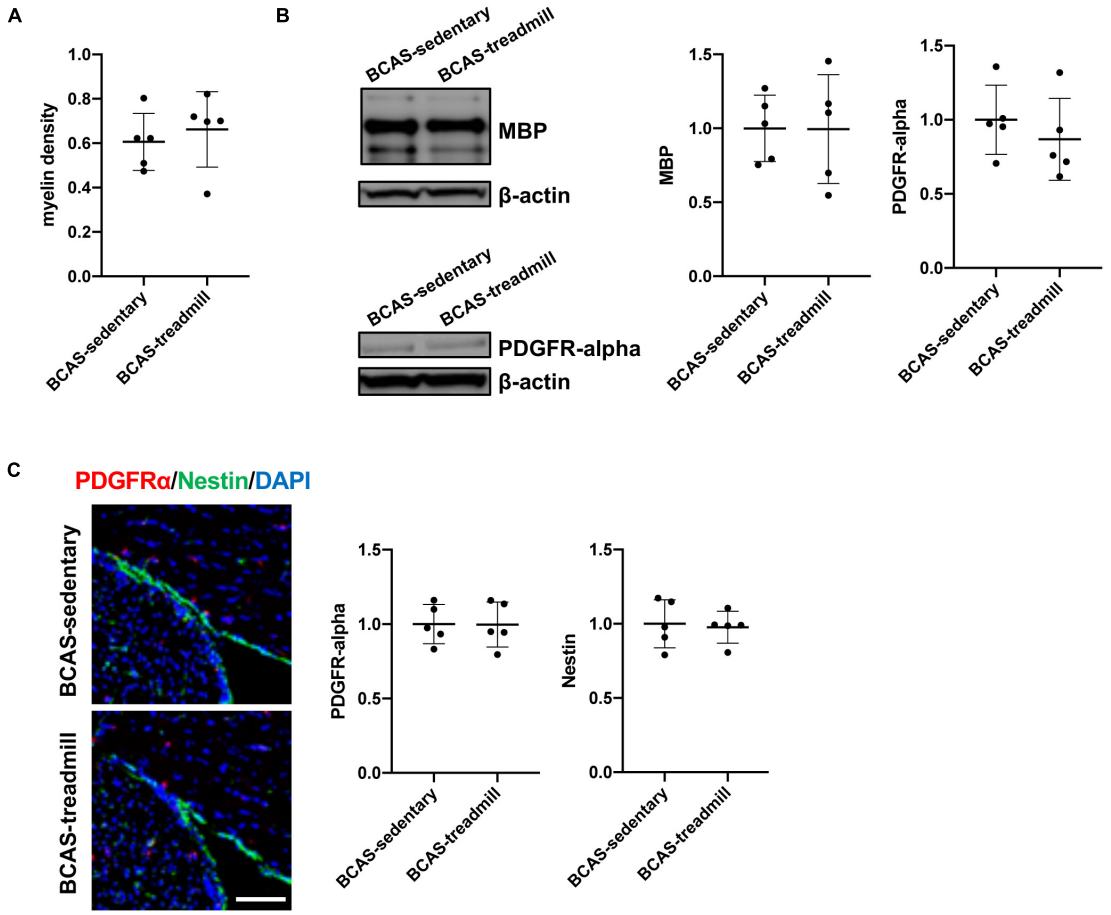

FIGURE 4 | (A) Result of myelin density of the corpus callosum, assessed by fluoromyelin staining. Myelin density was calculated based on the intensity of age-matched male C57/BL6J mice (average of 5 mice). There was no significant difference in myelin density between the 2 groups (BCAS/Sedentary vs. BCAS/Treadmill). Data are expressed as mean ± SD. **(B)** Result of MBP and PDGFRα western blot using samples from the corpus callosum region. Data are expressed as mean ± SD. **(C)** Immunohistochemistry showed that there were no significant differences in both the intensity of PDGFRα-positive cells and the intensity of Nestin-positive cells within the SVZ region. Data are expressed as mean ± SD.

future studies to pursue exercise as a therapeutic option for SIVD and other CNS disease patients. Second, because we focused on the effect of treadmill exercise on middle-aged SIVD mice, our current study did not include a sham-exercise group in our experiments. However, considering that treadmill exercise improves cognitive function in older mice (Maejima et al., 2018), further studies would be needed to answer the question of whether the effect of treadmill exercise is ineffective in middle-aged mice or only in middle-aged SIVD mice in our system. Careful comparison of the effect of treadmill exercise between these two groups may also help us to find a therapeutic target for SIVD. Third, our current study does not address the potential mechanism behind the effects of exercise on cognitive function. In young mice, the activation of compensatory responses, such as an increase of OPC number within the SVZ region, may partially contribute (Ohtomo et al., 2020); however, no OPC activation was observed in middle-aged mice. The hippocampal region plays an important role in cognitive function, including spatial learning and memory, and our pilot study indicated that in the SGZ region of hippocampus, treadmill exercise may increase the number of stem cells (data not shown). Because accumulating evidence now suggests the close relationship between exercise and the neuronal responses in the hippocampus (Moon et al., 2016; Liu and Nusslock, 2018; Lourenco et al., 2019; Baik et al., 2021), it would be helpful to examine the cellular and molecular signaling in the hippocampus after treadmill exercise in middle-aged SIVD mice in future studies. The final caveat of our study is that we used only male mice for our experiment. Since the sex-difference may alter the dynamics of systemic humoral factors as mentioned in the published literature (Herson et al., 2013; McMullan et al., 2016; Stanford et al., 2017), it will be important to determine if our results can be replicated in middle-aged female mice.

In conclusion, we have demonstrated that treadmill exercise has some effect in reducing cognitive decline in middle-aged mice with prolonged cerebral hypoperfusion that mimics the pathophysiology of SIVD. Exercise is a safe behavioral intervention and has the potential to be a non-pharmacological

therapy for several CNS diseases, including SIVD. Because polypharmacy among elderly patients has become a serious social issue around the world (Fried et al., 2014), future studies are warranted to pursue the therapeutic option of exercise as a non-pharmacological approach to decrease the cognitive decline in SIVD or other dementia patients.

DATA AVAILABILITY STATEMENT

The original contributions presented in the study are included in the article/**Supplementary Material**, further inquiries can be directed to the corresponding author/s.

ETHICS STATEMENT

The animal study was reviewed and approved by the Massachusetts General Hospital Institutional Animal Care and Use Committee.

AUTHOR CONTRIBUTIONS

RO, HI, KK, GH, and HT: collection of data. RO, KK, HI, and GO: data analysis. RO, KC, JL, EL, and KA: manuscript writing. RO, KC, GO, CW, HK, AI, JL, EL, and KA: interpretation. RO, GO, EL, and KA: conception and design. EL and KA: funding acquisition. All authors: final approval of manuscript. All authors contributed to the article and approved the submitted version.

FUNDING

This work was supported in part by the National Institutes of Health (R01NS065089, R01NS110818, R01NS113556, and R21AG066478) and JSPS KAKENHI (16H05319).

SUPPLEMENTARY MATERIAL

The Supplementary Material for this article can be found online at: https://www.frontiersin.org/articles/10.3389/fnagi.2021.756537/full#supplementary-material

REFERENCES

Baik, S. H., Selvaraji, S., Fann, D. Y., Poh, L., Jo, D. G., Herr, D. R., et al. (2021). Hippocampal transcriptome profiling reveals common disease pathways in chronic hypoperfusion and aging. *Aging* 13, 14651–14674. doi: 10.18632/aging.203123

Choi, D. H., Kwon, K. C., Hwang, D. J., Koo, J. H., Um, H. S., Song, H. S., et al. (2021). Treadmill Exercise Alleviates Brain Iron Dyshomeostasis Accelerating Neuronal Amyloid-beta Production, Neuronal Cell Death, and Cognitive Impairment in Transgenic Mice Model of Alzheimer's Disease. *Mol. Neurobiol.* 58, 3208–3223. doi: 10.1007/s12035-021-02335-8

Dellu, F., Contarino, A., Simon, H., Koob, G. F., and Gold, L. H. (2000). Genetic differences in response to novelty and spatial memory using a two-trial recognition task in mice. *Neurobiol. Learn Mem.* 73, 31–48. doi: 10.1006/nlme.1999.3919

Desgeorges, M. M., Devillard, X., Toutain, J., Castells, J., Divoux, D., Arnould, D. F., et al. (2017). Pharmacological inhibition of myostatin improves skeletal muscle mass and function in a mouse model of stroke. *Sci. Rep.* 7:14000. doi: 10.1038/s41598-017-13912-0

Erkinjuntti, T., Inzitari, D., Pantoni, L., Wallin, A., Scheltens, P., Rockwood, K., et al. (2000a). Limitations of clinical criteria for the diagnosis of vascular dementia in clinical trials. Is a focus on subcortical vascular dementia a solution? *Ann. N. Y. Acad. Sci.* 903, 262–272. doi: 10.1111/j.1749-6632.2000.tb06376.x

Erkinjuntti, T., Inzitari, D., Pantoni, L., Wallin, A., Scheltens, P., Rockwood, K., et al. (2000b). Research criteria for subcortical vascular dementia in clinical trials. *J. Neural. Transm. Suppl.* 59, 23–30. doi: 10.1007/978-3-7091-6781-6_4

Fried, T. R., O'Leary, J., Towle, V., Goldstein, M. K., Trentalange, M., and Martin, D. K. (2014). Health outcomes associated with polypharmacy in community-dwelling older adults: a systematic review. *J. Am. Geriatr. Soc.* 62, 2261–2272. doi: 10.1111/jgs.13153

Fu, Y., Chen, Y., Li, L., Wang, Y., Kong, X., and Wang, J. (2017). Food restriction affects Y-maze spatial recognition memory in developing mice. *Int. J. Dev. Neurosci.* 60, 8–15. doi: 10.1016/j.ijdevneu.2017.03.010

Herson, P. S., Palmateer, J., and Hurn, P. D. (2013). Biological sex and mechanisms of ischemic brain injury. *Transl. Stroke Res.* 4, 413–419. doi: 10.1007/s12975-012-0238-x

Ihara, M., and Tomimoto, H. (2011). Lessons from a mouse model characterizing features of vascular cognitive impairment with white matter changes. *J. Aging Res.* 2011:978761. doi: 10.4061/2011/978761

Jiang, T., Zhang, L., Pan, X., Zheng, H., Chen, X., Li, L., et al. (2017). Physical Exercise Improves Cognitive Function Together with Microglia Phenotype Modulation and Remyelination in Chronic Cerebral Hypoperfusion. *Front. Cell. Neurosci.* 11:404. doi: 10.3389/fncel.2017.00404

Kinoshita, K., Hamanaka, G., Ohtomo, R., Takase, H., Chung, K. K., Lok, J., et al. (2021). Mature Adult Mice With Exercise-Preconditioning Show Better Recovery After Intracerebral Hemorrhage. *Stroke* 52, 1861–1865. doi: 10.1161/STROKEAHA.120.032201

Lee, J. M., Park, J. M., Song, M. K., Oh, Y. J., Kim, C. J., and Kim, Y. J. (2017). The ameliorative effects of exercise on cognitive impairment and white matter injury from blood-brain barrier disruption induced by chronic cerebral hypoperfusion in adolescent rats. *Neurosci. Lett.* 638, 83–89. doi: 10.1016/j.neulet.2016.12.018

Liang, A. C., Mandeville, E. T., Maki, T., Shindo, A., Som, A. T., Egawa, N., et al. (2016). Effects of Aging on Neural Stem/Progenitor Cells and Oligodendrocyte Precursor Cells After Focal Cerebral Ischemia in Spontaneously Hypertensive Rats. *Cell Transpl.* 25, 705–714. doi: 10.3727/096368916X690557

Liu, P. Z., and Nusslock, R. (2018). Exercise-Mediated Neurogenesis in the Hippocampus via BDNF. *Front. Neurosci.* 12:52.

Liu-Ambrose, T., Best, J. R., Davis, J. C., Eng, J. J., Lee, P. E., Jacova, C., et al. (2016). Aerobic exercise and vascular cognitive impairment: A randomized controlled trial. *Neurology* 87, 2082–2090.

Lourenco, M. V., Frozza, R. L., de Freitas, G. B., Zhang, H., Kincheski, G. C., Ribeiro, F. C., et al. (2019). Exercise-linked FNDC5/irisin rescues synaptic plasticity and memory defects in Alzheimer's models. *Nat. Med.* 25, 165–175. doi: 10.1038/s41591-018-0275-4

Maejima, H., Kanemura, N., Kokubun, T., Murata, K., and Takayanagi, K. (2018). Exercise enhances cognitive function and neurotrophin expression in the hippocampus accompanied by changes in epigenetic programming in senescence-accelerated mice. *Neurosci. Lett.* 665, 67–73. doi: 10.1016/j.neulet.2017.11.023

McMullan, R. C., Kelly, S. A., Hua, K., Buckley, B. K., Faber, J. E., Pardo-Manuel de Villena, F., et al. (2016). Long-term exercise in mice has sex-dependent benefits on body composition and metabolism during aging. *Physiological. Rep.* 2016:4. doi: 10.14814/phy2.13011

Miyamoto, N., Pham, L. D., Hayakawa, K., Matsuzaki, T., Seo, J. H., Magnain, C., et al. (2013). Age-related decline in oligodendrogenesis retards white matter repair in mice. *Stroke* 44, 2573–2578. doi: 10.1161/STROKEAHA.113.001530

Moon, H. Y., Becke, A., Berron, D., Becker, B., Sah, N., Benoni, G., et al. (2016). Running-Induced Systemic Cathepsin B Secretion Is Associated with Memory Function. *Cell Metab.* 24, 332–340. doi: 10.1016/j.cmet.2016.05.025

Ohtomo, R., Kinoshita, K., Ohtomo, G., Takase, H., Hamanaka, G., Washida, K., et al. (2020). Treadmill Exercise Suppresses Cognitive Decline and Increases White Matter Oligodendrocyte Precursor Cells in a Mouse Model of Prolonged Cerebral Hypoperfusion. *Transl Stroke Res.* 11, 496–502. doi: 10.1007/s12975-019-00734-7

Prins, N. D., and Scheltens, P. (2015). White matter hyperintensities, cognitive impairment and dementia: an update. *Nat. Rev. Neurol.* 11, 157–165. doi: 10.1038/nrneurol.2015.10

Roh, J. H., and Lee, J. H. (2014). Recent updates on subcortical ischemic vascular dementia. *J. Stroke* 16, 18–26. doi: 10.5853/jos.2014.16.1.18

Roman, G. C., Erkinjuntti, T., Wallin, A., Pantoni, L., and Chui, H. C. (2002). Subcortical ischaemic vascular dementia. *Lancet Neurol.* 1, 426–436. doi: 10.1016/s1474-4422(02)00190-4

Shibata, M., Ohtani, R., Ihara, M., and Tomimoto, H. (2004). White matter lesions and glial activation in a novel mouse model of chronic cerebral hypoperfusion. *Stroke* 35, 2598–2603.

Shibata, M., Yamasaki, N., Miyakawa, T., Kalaria, R. N., Fujita, Y., Ohtani, R., et al. (2007). Selective impairment of working memory in a mouse model of chronic cerebral hypoperfusion. *Stroke* 38, 2826–2832. doi: 10.1161/STROKEAHA.107.490151

Stanford, K. I., Takahashi, H., So, K., Alves-Wagner, A. B., Prince, N. B., Lehnig, A. C., et al. (2017). Maternal Exercise Improves Glucose Tolerance in Female Offspring. *Diabetes* 66, 2124–2136. doi: 10.2337/db17-0098

Takase, H., Hamanaka, G., Ohtomo, R., Ishikawa, H., Chung, K. K., Mandeville, E. T., et al. (2021). Transcriptome Profiling of Mouse Corpus Callosum After Cerebral Hypoperfusion. *Front. Cell Dev. Biol.* 9:685261.

Wallin, A., Roman, G. C., Esiri, M., Kettunen, P., Svensson, J., Paraskevas, G. P., et al. (2018). Update on Vascular Cognitive Impairment Associated with Subcortical Small-Vessel Disease. *J. Alzheimer's Dis. JAD* 62, 1417–1441. doi: 10.3233/jad-170803

Yang, Y., Kimura-Ohba, S., Thompson, J., and Rosenberg, G. A. (2016). Rodent Models of Vascular Cognitive Impairment. *Transl. Stroke Res.* 7, 407–414. doi: 10.1007/s12975-016-0486-2

Conflict of Interest: The authors declare that the research was conducted in the absence of any commercial or financial relationships that could be construed as a potential conflict of interest.

Publisher's Note: All claims expressed in this article are solely those of the authors and do not necessarily represent those of their affiliated organizations, or those of the publisher, the editors and the reviewers. Any product that may be evaluated in this article, or claim that may be made by its manufacturer, is not guaranteed or endorsed by the publisher.

frontiers in Aging Neuroscience

ORIGINAL RESEARCH
published: 14 February 2022
doi: 10.3389/fnagi.2021.779823

Gradual Not Sudden Change: Multiple Sites of Functional Transition Across the Microvascular Bed

Kira Shaw[1], Katie Boyd[1], Silvia Anderle[1], Matthew Hammond-Haley[2†], Davina Amin[3†], Orla Bonnar[4] and Catherine N. Hall[1]*

[1] Sussex Neuroscience, School of Psychology, University of Sussex, Falmer, United Kingdom, [2] Brighton and Sussex Medical School, Brighton, United Kingdom, [3] Department of Neuroscience, Physiology and Pharmacology, University College London, London, United Kingdom, [4] MassGeneral Institute for Neurodegenerative Disease, Massachusetts General Hospital and Harvard Medical School, Charlestown Navy Yard, MA, United States

OPEN ACCESS

Edited by:
Shereen Nizari,
University College London,
United Kingdom

Reviewed by:
Andy Shih,
Seattle Children's Research Institute,
United States
Changsi Cai,
University of Copenhagen, Denmark

***Correspondence:**
Catherine N. Hall
Catherine.hall@sussex.ac.uk

† Present address:
Matthew Hammond-Haley,
British Heart Foundation Centre of Research Excellence, Kings College London, London, United Kingdom
Davina Amin,
Whittington Hospital, Whittington Health NHS Trust, London, United Kingdom

Specialty section:
This article was submitted to Cellular and Molecular Mechanisms of Brain-aging, a section of the journal Frontiers in Aging Neuroscience

Received: 19 September 2021
Accepted: 20 December 2021
Published: 14 February 2022

Citation:
Shaw K, Boyd K, Anderle S, Hammond-Haley M, Amin D, Bonnar O and Hall CN (2022) Gradual Not Sudden Change: Multiple Sites of Functional Transition Across the Microvascular Bed. Front. Aging Neurosci. 13:779823. doi: 10.3389/fnagi.2021.779823

In understanding the role of the neurovascular unit as both a biomarker and target for disease interventions, it is vital to appreciate how the function of different components of this unit change along the vascular tree. The cells of the neurovascular unit together perform an array of vital functions, protecting the brain from circulating toxins and infection, while providing nutrients and clearing away waste products. To do so, the brain's microvasculature dilates to direct energy substrates to active neurons, regulates access to circulating immune cells, and promotes angiogenesis in response to decreased blood supply, as well as pulsating to help clear waste products and maintain the oxygen supply. Different parts of the cerebrovascular tree contribute differently to various aspects of these functions, and previously, it has been assumed that there are discrete types of vessel along the vascular network that mediate different functions. Another option, however, is that the multiple transitions in function that occur across the vascular network do so at many locations, such that vascular function changes gradually, rather than in sharp steps between clearly distinct vessel types. Here, by reference to new data as well as by reviewing historical and recent literature, we argue that this latter scenario is likely the case and that vascular function gradually changes across the network without clear transition points between arteriole, precapillary arteriole and capillary. This is because classically localized functions are in fact performed by wide swathes of the vasculature, and different functional markers start and stop being expressed at different points along the vascular tree. Furthermore, vascular branch points show alterations in their mural cell morphology that suggest functional specializations irrespective of their position within the network. Together this work emphasizes the need for studies to consider where transitions of different functions occur, and the importance of defining these locations, in order to better understand the vascular network and how to target it to treat disease.

Keywords: neurovascular, pericyte, brain, mural cell, arteriole, capillary, endothelial cell

INTRODUCTION

The human brain has an extensive vascular network essential for supplying the brain's rich energy demands. Oxygen, glucose and other nutrients and signaling molecules are sent to the brain *via* finely regulated cerebral blood flow which is delivered through arteries, arterioles and capillaries. Deoxygenated blood and waste products are then removed *via* capillaries, venules and veins. In the neocortex, large pial vessels run along the surface then dive and penetrate the brain, before branching into smaller vessels to form the dense capillary network (Duvernoy et al., 1981). Pial and parenchymal arterioles and capillaries respond to neuronal nutrient and oxygen demand by dilating and contracting (Iadecola, 2017) to alter blood flow locally, a process called neurovascular coupling (NVC). NVC is controlled by the neurovascular unit (NVU), formed by vascular cells (mural cells - smooth muscle cells and pericytes, and endothelial cells), astrocytes and neurons. In addition to modulating contractile tone and blood flow, the NVU is also fundamental in regulating blood brain barrier (BBB) permeability and nutrient delivery (Hawkins and Davis, 2005; Iadecola, 2017; Sweeney et al., 2018), as well as helping to coordinate the brain's immune response by restricting leukocyte invasion into the tissue.

Different parts of the vascular tree contribute differentially to these various functions, but in many cases, it remains unclear how function changes along the vessel bed. This is partly because of variability in nomenclature and definitions across studies, and partly because of an understandable, but ultimately misleading, tendency to oversimplify the manner in which these functional transitions occur. It is important to better understand these functional transitions, however, in order to identify which cells and vessels need to be targeted to manipulate these various processes therapeutically in conditions such as Alzheimer's disease or stroke.

Here we use existing literature and novel data to consider which components of the vasculature mediate different functions, to better understand functional transitions across the vascular network. We suggest that evidence indicates multiple transition points at different positions in the vascular network, and therefore to gradual, heterogeneous changes in vascular function, rather than sudden transition points between distinct vessel types.

Transitions in Anatomy Across the Cerebral Microvascular Bed

Across the vascular bed, from arteriole to capillary to venule, the diameter of vessels first decreases then increases, and the morphology of their mural cells (smooth muscle cells or pericytes) abluminal to the endothelial tube changes. Penetrating arteries and arterioles are typically between 15 and 40 μm in diameter and are composed of an inner layer of endothelial cells with abundant caveolae. They contain an internal elastic lamina and therefore express elastin in the vessel wall, which can be detected from its binding to the dye Alexa 633 hydrazide (Shen et al., 2012). At the surface, they often have 2-3 outer layers of closely packed ring-shaped smooth muscle cells (SMCs), which are electrically coupled *via* gap junctions (Chow et al., 2020; Garcia and Longden, 2020) and strongly express smooth muscle alpha actin (αSMA). At the pial surface, the blood vessel is separated from the pial membrane by Virchow-Robin space, which narrows after the arteriole enters the brain through a "pial funnel" (Gao et al., 2015). Downstream from this region, SMCs form only one layer before transitioning to a pericyte morphology. Grant et al. (2019) report the first cells with "bump on a log" morphology as always occurring beyond the first branch from the arteriole, and most reports consider the arterioles to be covered with annular SMCs (e.g., Hamilton et al., 2010; Grant et al., 2019; Kisler et al., 2017). However, even near the pial surface, mural cells' morphology changes from a simple annulus to gaining a distinct soma and processes. While these cells are often still termed smooth muscle cells, historically this transitional form would be called a pericyte (Zimmermann, 1923; Attwell et al., 2016).

At the first branch point from penetrating arterioles are precapillary sphincters: contractile mural cells encircling a narrow section of vessel between the penetrating arteriole and first order capillary (Chambers and Zweifach, 1946; Grubb et al., 2020). The first branches off the penetrating arteriole are often termed precapillary arterioles or first order capillaries (where penetrating arterioles are branch order 0). These vessels tend to have a diameter of between 5-15 μm, and are enwrapped with mural cells that express αSMA and have a protruding, distinct soma, and processes that cover the vessel to a large degree, recently termed "ensheathing pericytes" (Hartmann et al., 2015; Grant et al., 2019; but see Hill et al., 2015; Attwell et al., 2016). These first branches are often termed the precapillary arteriole or transitional zone, though these terms sometimes are used to mean only the first vessel branching off the penetrating arteriole (e.g., Thakore et al., 2021), and other times include the 2nd and 3rd branches with larger pericyte coverage and αSMA actin expression (Gonzales et al., 2020).

Downstream of these vessels, after 1-3 branches from the diving arteriole (Grant et al., 2019) pericytes become less dense and their processes cover less of the vessel as branch order increases and vessel diameter decreases (range 3-9 μm). These capillary pericytes have been reported to have low (Bandopadhyay et al., 2001) or absent (Nehls and Drenckhahn, 1991; Grant et al., 2019) expression of αSMA and have been termed mesh and thin strand pericytes (Hartmann et al., 2015). Latterly these have been combined into a single category (capillary pericytes), due to the difficulty in distinguishing a transition point between these two morphologies (Grant et al., 2019). These capillaries with low or absent αSMA expression and low pericyte coverage are often termed mid-capillaries.

In post-capillary venules, pericytes have a stellate morphology, becoming less extended with thicker, more radial processes (Joyce et al., 1985; Hartmann et al., 2015). These post-capillary venules branch to form large venules (> 50 μm), which have weak αSMA labeling, indicating limited contractile potential (Hill et al., 2015). On larger venules, SMCs are circumferential but are less compact and show a less complete coverage of the vasculature and a leaf-like instead of banded appearance compared to arteriolar SMCs (Hill et al., 2015).

Therefore, the anatomy of the vessels and mural cells of the cerebral vasculature, as commonly reported, is used to define the following distinct vascular segments: pial arterioles, penetrating or diving arterioles, precapillary sphincters, pre-capillaries, also termed transitional or low branch order capillaries, mid-capillaries, post-capillaries and venules. These have been recently condensed into 4 categories, arterioles, a transitional zone, capillaries and venules, with distinct mural cells on each (Hartmann et al., 2021a). In some ways this categorization is a helpful way to discuss features of different parts of the vascular bed, as the recent Hartmann et al. review does in a clear and informative manner. Our argument, however, is that it is important to recognize that these categories are overly simplistic because they are superimposed on more gradually changing anatomy and function across the vascular bed. For example, existing literature shows that mural cell morphologies transition gradually not abruptly along the network. This concept was first discussed by Zimmermann (1923) and is evident from more recent work which shows that there is a continuum of cell lengths seen from SMCs through ensheathing to mid-capillary pericytes (Grant et al., 2019). Furthermore, the shift in vessel coverage of pericyte processes argued to mark a boundary between ensheathing and mesh pericytes has a different distribution across branch orders than that of αSMA expression (Grant et al., 2019), i.e., αSMA transitions occur at largely different locations than do transitions in pericyte coverage of the vessel.

Neurovascular Coupling Differences Across the Cerebral Microvascular Bed

This heterogeneity of anatomy across the vascular tree presumably reflects the varying functional roles performed by different vessels. Anatomical transitions have been best mapped onto functional changes in terms of dilatory capacity and involvement in neurovascular coupling (i.e., dilation in response to increased neuronal activity). Disease affects different parts of the vasculature in specific ways, making it important to understand how and where such functional transitions occur to be able to intervene successfully to target pathological mechanisms.

Classically, neuronal activity causes local pial and penetrating arterioles to dilate, causing an increase in blood flow to active brain regions (Attwell et al., 2010). However, different components of the vasculature are now known to play distinct roles in generating this response. Mid-capillary regions, being closer on average than any other vessel segment to most neurons, likely first detect neuronal activity, either *via* the accompanying increase in extracellular potassium concentration (Longden et al., 2017) and/or *via* production of vasoactive signaling molecules such as prostaglandin E2 (Hall et al., 2014; Mishra et al., 2016) or EETs (Mishra et al., 2016; Zhang et al., 2021). This signal then spreads upstream from the capillary bed, causing dilation of upstream low branching order capillaries and arterioles (Hall et al., 2014; Rungta et al., 2018), *via* spread of hyperpolarizing currents carried by inward rectifying potassium channels (Zhang et al., 2011; Longden and Nelson, 2015). Whether mid-capillaries constrict and dilate in response to modulation of neuronal activity remains somewhat controversial. Some studies report that they do not (Hill et al., 2015), but a growing body of evidence supports their contractility (Hall et al., 2014; Kisler et al., 2017; Hartmann et al., 2021b; Shaw et al., 2021), though this may be *via* a different mechanism than in arterioles and lower branching order capillaries (Hartmann et al., 2021b).

The size, frequency and timing of responses to neuronal activity are often reported to vary across vascular compartments though not always in a consistent manner. Arteriole response magnitudes vary along their length, with surface sections of penetrating arterioles dilating more than deeper sections, probably as a result of the mechanical restriction imposed by brain tissue (Gao et al., 2015), though deeper arteriole sections have also been found to dilate more rapidly than shallower sections (Tian et al., 2010). In alpha-chloralose anaesthetized somatosensory cortex, Hall and colleagues found response frequency decreased as branching order increased (i.e., capillaries responded less frequently than arterioles; Hall et al., 2014), though first and second branch order capillaries showed larger and faster dilations than arterioles, a finding subsequently supported by other studies (Zhang et al., 2021). In the olfactory bulb, the region around the branch off the arteriole also dilated first, with slower responses up and downstream (Rungta et al., 2021). However, the same group found much more variable timings in neocortex of ketamine-medetomidine anaesthetized or awake mice, with capillaries or arterioles each being faster on some occasions (Rungta et al., 2021), and in both these reports, mid-capillary dilations were very small (though these data conflate responders and non-responders, unlike some other studies, Hall et al., 2014; Shaw et al., 2021). Precapillary sphincters, where studied, have often shown larger dilations, as a proportion of their diameter, than adjacent arterioles and capillaries (Grubb et al., 2020; Zambach et al., 2021).

In short, there are functional differences between neurovascular coupling responses along the vascular network, with mid-capillaries responding less frequently than upstream vessels to increases in local neuronal activity, and the fastest responses often, but not exclusively, observed in the first and second order capillaries. The physiological mechanisms underlying this heterogeneity in contractile responses are not wholly clear. Pericytes expressing αSMA seem likely to mediate more reliable, often larger and faster changes in vascular tone (Hill et al., 2015; Hartmann et al., 2021b), but as αSMA is commonly expressed in vessels up to and including the 3rd branch from the penetrating arteriole (Grant et al., 2019), variations in αSMA expression alone cannot explain the observed pattern of responses.

Indeed, several vasoactive pathways and mechanisms modulating the diameter of different vascular segments have been found to vary across the vascular network. Vessels beyond the penetrating arteriole were found to dilate *via* ATP-mediated increases in astrocytic calcium and prostaglandin action on EP4 receptors, while diving arterioles dilated *via* NMDA receptor mediated NO production (Mishra et al., 2016). Another functional transition point at the same location was also recently observed, as capillary endothelial cells were found to express MFSD2A, inhibiting caveolae formation,

while arteriolar endothelial cells showed much lower MFSD2A expression, instead having abundant caveolae that were necessary for intact neurovascular coupling (Andreone et al., 2017). Because MFSD2A-mediated reduction in caveolae formation reduces transcytosis to sustain BBB integrity (Ben-Zvi et al., 2014), this suggests a possible transition in both BBB function and neurovascular coupling mechanisms at the same arteriole-to-capillary point.

It is not just the mechanism of vasodilation that is sensitive to the position in the microvasculature: The integration of vascular signals across the vascular network is an area of increasing focus, with many recent papers shedding new insights on how vasoactive signals are propagated upstream of their detection in the mid-capillary bed. Potassium currents (Longden et al., 2017), nitric oxide (Kovacs-Oller et al., 2020), calcium and ATP signals (Thakore et al., 2021) have all recently been shown to be important in the transmission of vasodilatory signals and, by their nature, these signals span vascular segments and may be influenced by functional variations across these sections. While many studies have not explicitly investigated how different vascular segments affect signal transmission, Thakore et al. (2021) recently showed that ATP application or TRPA1 channel activation in the capillary bed produces slowly-propagating calcium signals through capillary endothelial cells that depend on ATP release from Panx1 channels, but are converted, by IK and SK channels in a transitional segment, into rapidly-propagating electrical signals that dilate upstream arterioles. A similarly propagating signal has been shown to be initiated in the capillary bed by PGE2 (Rosehart et al., 2021; this issue). In these papers, the transitional zone was defined as the first branch off the penetrating arteriole, and did not include lower branching order vessels that would be expected to express αSMA, and it is not clear whether these higher branching order vessels also show rapid IK or SK-mediated propagation of dilation.

Perhaps unsurprisingly given the varying vasoactive properties of different vascular segments, their function can be differentially affected by disease. In Alzheimer's disease, capillaries may mediate functionally significant decreases in cerebral blood flow, as capillaries but not arterioles were found to be constricted due to endogenous Aβ-mediated endothelin signaling to pericytes (Nortley et al., 2019), and to be plugged by neutrophils (Cruz Hernández et al., 2019). Similar effects may be seen after stroke, with capillaries constricting in brain slices during ischemia (Hall et al., 2014) and showing stalled flow and constrictions after reperfusion *in vivo* (Yemisci et al., 2009), though the largest constrictions may be seen in αSMA-expressing vessels rather than mid-capillary regions (Hill et al., 2015). Conversely, in mice carrying the main genetic risk factor for Alzheimer's disease, APOE4, capillary function was unaffected, but the large pial vessels were dysfunctional, with vasomotion and dilation frequencies reduced compared to APOE3-expressing controls (Bonnar et al., 2021). However, none of these studies define the precise location of these transitions in disease susceptibility.

To summarize, the contractile properties of the vascular tree, in terms of both capacity and timing of dilations, mechanisms mediating neurovascular signaling and integration, and the sensitivity of these processes to disease states all vary depending on the position in the vascular network. In some cases (e.g., response frequency) function seems to gradually change along the network, while in others (e.g., mechanism of neurovascular coupling), there are more abrupt transitions of function, and in many cases the location of functional transitions remains unknown.

Oxygen Supply

The major function of the brain's blood supply is to provide it with nutrients. These include the energy substrates, oxygen and glucose, as well as nucleosides and amino acids needed for mRNA and protein synthesis. Classically, the dense capillary bed has been thought of as the site of nutrient exchange, but actually measuring where nutrient delivery occurs is not straightforward.

Improved two-photon phosphorescence lifetime imaging of oxygen probes has recently provided insights into the concentration gradients of oxygen across the microvasculature in mouse cortex, and therefore where most oxygen delivery likely takes place. In anaesthetized cortex, arterioles were found to be responsible for 50% of the extracted oxygen (Sakadžić et al., 2014), with capillaries (here defined as vessels two branches downstream of the penetrating arteriole) appearing to provide a reserve for oxygen delivery capacity, taking on a larger role during hypercapnia and, as suggested by modeling, when oxygen consumption rates increased. Indeed, in more recent studies in awake mice (therefore with a larger basal oxygen consumption rate), less oxygen was found to be delivered by the arterioles (34%), with the majority of the remainder expected to be delivered by the capillary bed (Li et al., 2019).

The factors driving oxygen delivery by these different vessels include red blood cell linear density, speed, local oxygen concentration gradients, and intravascular resistance to oxygen diffusion. These differ between cortical layers (Lyons et al., 2016; Schmid et al., 2017; Li et al., 2019) and are differently variable within these layers. For example, red blood cell (RBC) flow was lowest and more homogenous between capillaries and, correspondingly, oxygen extraction was largest in deep cortical layers, with faster flow and less oxygen extraction in superficial capillaries (Schmid et al., 2017; Li et al., 2019). This was in part because blood pressure dropped more in the diving arteriole when feeding deeper layers (Schmid et al., 2017). Furthermore, from arterial to venous capillaries, oxygenation becomes increasingly variable as an increasingly clear relationship between RBC flow and pO2 emerges [more O2 having been extracted from capillaries with slowly moving RBCs (Li et al., 2019)]. Thus, position in the vascular network in terms of both tissue depth and branching order affects how blood delivers oxygen to the tissue.

Nutrient Supply and the BBB

Unlike oxygen, which can diffuse through cell membranes, other nutrients are supplied to the brain *via* specialist transporters which allow their passage across the BBB. The conventional view is that arterioles and arteries control the blood supply to the tissue but do not participate in the exchange of nutrients in the brain, which is instead mediated by capillaries and post-capillary venules (Yuan and Rigor, 2010). The BBB strictly controls the

influx and efflux of molecules across its endothelial layer largely by active transport. In addition to being vital for neuronal function, these proteins can be targeted for drug development to allow drugs to access the brain.

Little work has studied where in the vascular network these transporters are most active, though a recent RNA Seq study showed them to be predominantly expressed in capillary and venule mural cells, in contrast to transcription factors which were overrepresented at the arterial end of the vasculature (Vanlandewijck et al., 2018). A key question to be addressed in future, is whether this myriad of different transporters and transcription factors transition in similar or different locations across the vascular network.

The BBB and Immune Regulation

The BBB is also a key site of regulation of immune access to the brain, which again varies across the vascular tree. Unlike arteriolar and capillary endothelial cells, post-capillary venular endothelial cells are connected by adherens rather than tight junctions, meaning they are more leaky than the capillaries which feed them (Rous and Smith, 1931; Pober and Sessa, 2014). The basement membrane that surrounds them also has a different structure, being lamellar instead of homogenous (Braverman, 1989). Leukocyte infiltration into the surrounding tissue primarily happens in this region, leukocytes migrating through gaps between pericytes and thus being regulated by pericyte morphology (Proebstl et al., 2012). Pericyte contractility may feed into this process, as pericyte relaxation (not contraction) widens the gaps between cells, facilitating leukocyte infiltration (Wang et al., 2012). Once in the parenchyma, leukocytes migrate along NG2-expressing pericytes, which release factors to support their migration (Stark et al., 2013). Thus, an important transition in vascular immune function appears to occur between NG2-positive pericytes on capillaries and the NG2-negative pericytes on veins, though whether this happens to the same extent in brain as in peripheral tissues remains unknown. In addition to regulation of immune cell entry, the vasculature can also transport cytokines into the brain, as well as respond to circulating factors with parenchymal production of cytokines and chemokines (Banks et al., 2009; Rustenhoven et al., 2017), but how this varies across the vascular network is also unknown.

More studies into the site of immune regulation in the brain would be valuable, however, as, perhaps unsurprisingly, these pathways of immune regulation by pericytes and endothelial cells are important for understanding and treating disease. Pericyte damage and increased permeability of the brain vasculature to plasma proteins and immune cells are hallmarks of Alzheimer's disease, multiple sclerosis, and stroke (Daneman, 2012), where infiltrating immune cells have also been shown to induce vascular dysfunction, demyelination, axonal damage, and neurodegeneration (Hochmeister et al., 2006; Ryu et al., 2015). Understanding where in the network structural and functional contributions of the vasculature to the regulation of neural inflammation occur may thus enable us to understand which cells should be best targeted therapeutically.

Vasomotion

As well as nutrients being delivered across the BBB, the vasculature also plays an important role in the removal of potentially neurotoxic substances from the surrounding brain tissue. Vasomotion, a phenomenon first reported in bat wing veins (Jones, 1853), is a spontaneous low frequency oscillation in blood vessel tone (typically centered near 0.1 Hz; Mayhew et al., 1996); and independent of heartbeat or respiration), which is present in vessels (particularly arteries) throughout the body (Aalkjær et al., 2011). This rhythmic pulsing of vessels is thought to contribute substantially to paravascular clearance (Aldea et al., 2019; van Veluw et al., 2020) and tissue oxygenation (Tsai and Intaglietta, 1989; Aalkjær et al., 2011; Thorn et al., 2011; Mateo et al., 2017). In arterioles, oscillations are generated within the vascular wall as a result of local SMC dilations and contractions, possibly *via* phospholipase C and phospholipase A_2 mediated cyclical release of calcium from IP3-sensitive stores (Haddock et al., 2002). Capillaries have not been reported to show these low frequency oscillations in diameter, though RBC flow does show similar fluctuations which may be due to upstream diameter fluctuations (Colantuoni et al., 1994; Biswal and Hudetz, 1996). However, a functional transition in vasomotion of vessel diameters has not yet been pinpointed.

Given the importance of vasomotion as a driving force for paravascular tissue clearance, it is not surprisingly affected by vascular-degenerating diseases. In a mouse model of Alzheimer's disease, arterioles surrounded with Aβ showed impaired vasomotion when driven by neuronal activity, and showed reduced dextran clearance from the parenchyma (van Veluw et al., 2020). Mice carrying the main genetic risk factor for Alzheimer's disease, APOE4, also showed a reduction in pial arteriole vasomotion compared to APOE3 controls (Bonnar et al., 2021). Thus, vasomotion is important for regulating supply and clearance of substances to the brain, and is affected by disease. However, we do not yet know where in the vascular tree the transition point falls in which the vessels cease to show vasomotion.

Summary

Vascular anatomy, contractility, nutrient delivery, immune regulation and clearance all differ across the vascular bed. To a large extent, functions of the vascular network have been assumed to transition broadly with branching anatomy, from vasomotion pial and diving arterioles that show reliable, large neurovascular coupling responses, through fast responding pre-capillaries/low branching order capillaries, to less reliably dilating mid-capillaries. These mid-capillaries are thought to have a stronger role than upstream vessels in BBB regulation and nutrient transport, while further downstream, post-capillary venules regulate immune cell infiltration. While this framework no doubt captures the broad changes that occur over the vascular network, it is by no means clear that the vasculature can be usefully divided into such discrete divisions. Indeed some of the research discussed above points to the existence of additional functional transitions within vascular segments, including the decreasing size of dilations in superficial and deeper diving

arterioles (Gao et al., 2015), and pericyte coverage of vessels continuing to decrease into the capillary bed (Grant et al., 2019). However, most focus on localizing functional changes across the vasculature has fallen on contractile function or mural cell anatomy, so it is unclear whether other functions transition at the same, or different, locations. If different functions show the same transition points as contractile function, we could reasonably consider the vascular segments separated by these transition points as different vessel types. If, however, different vascular functions transition at different locations, it becomes somewhat meaningless to use these shifts in contractile function to define vascular segments.

To test the principle of whether there are clear locations within the vascular network at which transitions occur between multiple functions of the vasculature, we used immunohistochemistry to label different functional markers in brain slices expressing DsRed under the control of the NG2 promoter, as well as *in vivo* two-photon imaging of vascular responses to visual stimuli in awake mice to study the contractile characteristics of the vascular bed at the different functional transition points. There was no single point in the vasculature where the function transitioned from "arteriole-like" to "capillary-like." Classic pericyte markers, NG2 and PDGFRβ were in fact expressed throughout the vascular network, while transitions in markers for contractility, arteriolar compliance, neurovascular coupling and angiogenic potential occurred at different points in the vascular bed. We observed no sudden transitions in mural cell morphology across the vascular network, or at termination points of functional markers, though branch points showed distinct changes in mural cell morphology throughout the vasculature studied (arteriole-capillary). Finally, we also observed transitions of neurovascular and vasomotion function down the depth of arterioles, highlighting that arterioles become more capillary-like further from the pial surface.

MATERIALS AND METHODS

Animals

All experimental procedures were performed in accordance with the 1986 Animal (Scientific Procedures) Act and approved by the United Kingdom Home Office and the University of Sussex or University College London animal welfare ethical review boards. Experiments were performed on mice aged 1-8 months of both sexes (3-8 months for *in vivo* experiments). Mice were all on a C57BL/6J background which were either wild-type, expressed DsRed under the control of the NG2 promoter (Zhu et al., 2008), or for data collected from the 186 vessels recorded for the *in vivo* experiments expressed GCaMP6f under the control of the Thy1 promoter (Dana et al., 2014) or were SST-Cre crossed with floxed GCaMP6f. Food and water were available *ad libitum*, and mice were housed at 22°C in a 12 h light/dark cycle (which was reversed for the mice used in *in vivo* experiments).

Ex vivo Imaging

Each immunohistochemistry experiment used tissue from a minimum of 3 animals, on at least 3 different experimental days. Methods for slicing, fixing and labelling were as described previously (Mishra et al., 2014; Boyd et al., 2021), as follows:

Slicing

NG2 DsRed mice were sacrificed by Schedule 1 approved methods (cervical dislocation followed by decapitation). The brain was then removed from the cranium and anterior and posterior coronal sections were removed, producing a block containing the central portion of the cerebral hemispheres. This block was then mounted onto a chilled slicing block using cyanoacrylate glue, with the inferior surface of the brain facing an agarose block. Using a vibratome, 200 μm coronal brain slices were prepared in ice-cold slicing solution containing (mM): NaCl (124), NaHCO3 (26), glucose (10), KCl (2.5), MgCl2 (2), CaCl2 (2), NaH2PO4 (1), kynurenic acid (1), bubbled with 95% oxygen and 5% CO2. Slices were incubated in a slice storage container containing slicing solution bubbled with 95% oxygen and 5% CO2 at room temperature to recover for > 30 min before fixation. Some slices were incubated in oxygenated slicing solution containing the fluorescent dye AlexaFluor 633 hydrazide (20 μM) to label elastin (Shen et al., 2012).

Fixation, Blocking and Permeabilization

Slices were fixed in 4% paraformaldehyde solution for 30 min in a 24-well plate on a rotary shaker. Slices were then washed (3 × 10 min) in 0.1 M phosphate buffered saline (PBS) on a rotary shaker at room temperature. In preparation for antibody labeling the slices were incubated for 3 h in 0.2% Triton X-100, 10% normal goat serum and 0.2M glycine in 0.1M PBS (blocking and permeabilizing solution) at room temperature to block generalized secondary antibody staining and to permeabilize the tissue.

Immunohistochemical Labeling

The following primary antibodies were used, all at 1:200 dilution in 0.1M PBS: rabbit anti-αSMA (Abcam), chicken anti-nestin (Abcam), rabbit anti-PDGFRβ (Santa Cruz Biotechnologies), rabbit anti-GLUT-1 (Abcam), and chicken anti-GFAP (Abcam). Slices were incubated in primary antibody in PBS overnight (12-16 h) on a rotary shaker at room temperature, washed (3 × 10 min) in 0.1 M PBS, followed by a 6-8 h fluorescently labeled appropriate secondary antibody incubation in 0.1M PBS at room temperature (AlexaFluor 647 goat anti-rabbit IgG or AlexaFluor 488 donkey anti-rabbit IgG - both Life Technologies; Goat anti-chicken CF488 IgY - Sigma). A no-primary control experiment was used for each antibody to check for non-specific binding of secondary antibodies. After labeling, slices were mounted onto microscope slides with Vectashield hard-set mounting medium including DAPI (Vector Laboratories) and covered with a glass cover slip. Cover slip borders were then sealed with nail varnish.

Confocal Imaging

SMCs and pericytes on large and small blood vessels, respectively, were readily identifiable through DsRed expression under the control of the NG2 promoter. Fluorescent labeling of the proteins described previously allowed visualization of the expression of proteins involved in the various functions of the cerebral

vasculature. Fixed slices were imaged using a Leica SP8 or Zeiss LSM780 confocal laser-scanning microscope. Imaging with multiple wavelengths was performed as sequential scans at each wavelength, to minimize "bleed-through" of fluorescence between channels. Z stacks of penetrating arterioles and their downstream capillary bed were obtained using a 20x air objective. These stacks were then projected as 'maximum-intensity projections' and stitched together using the MosaicJ plugin of ImageJ software (NIH, Bethesda, MD, United States). High-power Z-stacks of regions of interest, including the transition point of the various markers, were acquired using a 63x oil immersion objective.

Image Analysis

Image analysis was conducted using FIJI/ImageJ. Intersoma distances and diameters were calculated manually using the measurement tool in ImageJ. Measurements were made in one z-plane by drawing a line from the mid-point of the pericyte soma nearest the transition in labeling, to the mid-point of the closest proximal vascular mural cell on the same vessel. Somata were identified by DsRed expression and confirmed by DAPI stained cell nuclei. Diameters were measured as the distance between the innermost DsRed labeling on either side of the vessel lumen (i.e., the diameters include endothelial cell thickness). Branch points of the vessels were identified from the penetrating arteriole, termed branch order 0, incrementing by 1 at each subsequent branch point.

In vivo Imaging

Surgery and Two-Photon Imaging

Cranial window surgery to insert an optical window over V1 suitable for chronic, awake two-photon imaging was performed on 11 mice (6 female) under isoflurane anesthesia (see Shaw et al., 2021 for full methods). Following a one-week minimum post-surgery recovery period, mice were habituated to head fixation over multiple sessions. The experimental set-up consisted of a cylinder fitted with a Kuebler rotary encoder placed under a two-photon microscope with red and green filters (Scientifica), and in front of two computer screens for visual stimulus presentation. The objective used for two-photon imaging was a water-based 16x aperture (LWD, Nikon) with tissue excited at 940 nm (Chameleon Vision II Ti:Sapphire laser, Coherent). The visual stimulus was a drifting grating (PsychoPy) that varied either by contrast (25, 63, or 100%, all at 315° orientation), size (20° small circular stimulus or 220° full screen stimulus, both at 100% contrast), or spatial frequency (0.04 or 0.2 cycles per degree). As our data selected only the trials where the mouse was not running, chi-square tests were conducted to ensure all vessel segments were subject to the same distribution of stimulus conditions across trials (contrast $p = 0.94$; size $p = 0.99$; spatial frequency $p = 0.99$). Imaging sessions recorded fluorescent blood vessels and calcium activity (in excitatory or somatostatin cells), however, for the purposes of this study only data recorded from vessels was analyzed. To visualize blood vessels (penetrating arterioles and their downstream capillaries) during darkness or visual stimulation whilst the animal was running or resting, mice were injected with 2.5% (w/v) Texas Red Dextran dissolved in saline (70 kDa *via* tail vein or 3 kDa subcutaneously, Fisher Scientific). For the stimulus-dependent vessel dilation data, we looked only at the dilations occurring during rest trials (i.e., to remove locomotion confounds). Imaging sessions were recorded in SciScan software (SciScan v1.2.1, Scientifica), where the imaged vessels ranged between 0 and 729.6 μm in depth (mean: 182.55 μm, SD: 132.65 μm), had an average pixel size of 0.1958 μm (range: 0.1484 - 0.4431 μm, SD: 0.08 μm) and were acquired at speeds of 7.6 Hz.

Vessel Classification

Vessel diameter, vessel depth and branch order were measured for all vessel classifications (see **Table 1**). Because we wanted to look at responses down the penetrating arteriole, in these experiments we separately classified the penetrating arteriole and capillary branching orders. This was therefore different to that used for immunohistochemical analysis, where the penetrating arteriole was always 0, and branch orders always referred to the position in the capillary bed. Here, for penetrating arterioles, branch order started at 0 at the pial surface, and increased by 1 down the length of the diving vessel after a branch offshoot was encountered. For capillaries, the first offshoot protruding off the penetrating arteriole was always given a branch order of 1 and vessel branch order increased by 1 for each bifurcation encountered (see **Supplementary Figure 1**).

Data Extraction

To improve image quality, vessel recordings were subject to several preprocessing steps prior to analysis. Using ImageJ: image type was set at 8 bit, images were despeckled, and light artifacts from the stimulus minimized using the 'stack contrast adjustment' plugin. To correct for motion artifacts (mainly arising from locomotion) vessel recordings were also image registered using Suite2P (Pachitariu et al., 2016). A custom MATLAB script was used to extract vessel diameter along the full width at half maximum (see Shaw et al., 2021). Diameter measurements were averaged along the entire vessel length, leaving an averaged (per frame) continuous diameter trace over time.

Data Analysis

Stimulus-dependent responses: Continuous vessel diameter traces were cut into 30 s trials around the stimulus presentations (stimulation occurred between 5-10 s). Data trials were then normalized to the 5 s pre-stimulus baseline period ($\Delta D/D = (D-Dmin)/(Dmax - Dmin)$), and multiplied by 100 (to present data as a% increase from baseline). Only 'rest' trials were included, meaning there was no significant locomotion occurring in the 2 s prior to or during the stimulus. Locomotion events had a duration $>$ 1/3 s and were distanced from other locomotion epochs by at least 1 s. The locomotion-free stimulus-centered vessel trials were categorized as responsive or non-responsive to stimulation, with responsive trials being those in which the maximum dilation during the stimulus event exceeded 0.5 $\times$ the standard deviation of the 5 s baseline period. The maximum dilation was calculated by finding the peak of the trace during the stimulus. The peak at the cessation of the stimulus was taken

TABLE 1 | Vessel characteristics/responses separated by vascular segment.

Vessel Label	Branch Order	Sample size	Num Trials	Diameter (μm)	Depth (μm)	Pixel size (μm)	Response rate (%)	Peak dilation (%)	Peak dilation (μm)	Power at 0.1Hz
Penetrating Arteriole	0	21 vessels (20 for Welch's)	5-19 (mean: 12.86)	10.14 ± 4.66	74.40 ± 48.31	0.2438 ± 0.096	35.51 ± 25.36	All: 5.59 ± 5.20 R: 12.50 ± 17.80	All: 0.47 ± 0.05 R: 0.66 ± 0.11	0.040 ± 0.05
Penetrating Arteriole	1	22 vessels	2-17 (mean: 11.23)	9.62 ± 4.91	133.39 ± 78.07	0.2351 ± 0.078	26.99 ± 26.95	All: 4.69 ± 3.29 R: 7.90 ± 4.56	All: 0.35 ± 0.03 R: 0.34 ± 0.06	0.025 ± 0.03
Penetrating Arteriole	2	12 vessels	3-17 (mean: 12.33)	8.60 ± 2.35	130.03 ± 90.50	0.2025 ± 0.053	19.66 ± 14.22	All: 3.14 ± 1.48 R: 5.25 ± 2.86	All: 0.43 ± 0.04 R: 0.40 ± 0.07	0.017 ± 0.03
Penetrating Arteriole	3 +	9 vessels (8 for Welch's)	11-17 (mean: 13.78)	11.31 ± 4.65	234.14 ± 62.05	0.2528 ± 0.089	13.87 ± 11.35	All: 3.03 ± 1.90 R: 3.32 ± 3.42	All: 0.75 ± 0.1 R: 0.86 ± 0.15	0.017 ± 0.02
Capillary	1	50 vessels (49 for Welch's)	2-17 (mean: 11.24)	6.72 ± 3.36	161.51 ± 139.57	0.1603 ± 0.026	18.89 ± 18.28	All: 5.47 ± 6.69 R: 9.29 + /8.99	All: 0.37 ± 0.03 R: 0.42 ± 0.07	0.025 ± 0.06
Capillary	2	29 vessels	3-19 (mean: 12.41)	5.84 ± 2.02	161.86 ± 139.19	0.1595 ± 0.022	17.10 ± 16.23	All: 5.22 ± 3.84 R: 7.90 ± 8.79	All: 0.34 ± 0.03 R: 0.36 ± 0.07	0.027 ± 0.05
Capillary	3	22 vessels	4-19 (mean: 12.14)	5.75 ± 1.81	182.96 ± 100.9	0.1541 ± 0.017	25.14 ± 27.40	All: 4.28 ± 2.67 R: 7.00 + /4.98	All: 0.28 ± 0.04 R: 0.24 ± 0.06	0.011 ± 0.02
Capillary	4 +	21 vessels	2-18 (mean: 11.43)	4.84 ± 1.62	219.14 ± 92.02	0.1564 ± 0.020	18.53 ± 22.92	All: 9.04 ± 11.79 R: 7.14 ± 4.56	All: 0.22 ± 0.03 R: 0.14 ± 0.03	0.009 ± 0.01

Values are calculated per individual vessel (presented as mean ± STD between vessels). All: averaged across all trials; Raveraged across responsive trials only. Note that some sample sizes are lower for the Welch's power spectrum comparisons (specified in brackets) as 3 vessels were removed as outliers (see methods for outlier details).

by measuring the value of the vessel dilation trace at 10 s. The onset time of dilation responses was calculated as the time to 10% of the maximum peak (during the stimulation period). Four noisy data trials (from 2222 total trials) were removed from the diameter traces [3 trials from vessel 77 (C5) and 1 trial from vessel 167 (C5)] because dilation shifts were very noisy (high frequency shifts reflective of motion artifacts/signal loss) and peaks exceeded 10x the average (mean dilation peak across all responsive vessels during visual stimulation: 8.43 vs 101.3%, 123.2, 214.3, and 92.4%).

Power Spectra Responses

Welch's power spectral density estimates were computed across all continuous vessel diameter traces. These recordings could be during rest, visual stimulus and/or locomotion, and we included the entire continuous trace in the power analysis as (a) the stimulus presentation occurred for 5 s every 30 s, meaning the power spectrum peak corresponding to stimulus presentation would be at 0.03 Hz (outside our 0.05-0.15 Hz range of interest); and (b) there was no significant difference in the amount of time spent in locomotion between the different vessel categories (mean time spent in locomotion: 13.07%, standard deviation: 6.39%, $p = 0.45$). All continuous data was detrended by subtracting the baseline (the 8th percentile calculated over a 15 s time window; see Bonnar et al., 2021). The MATLAB function "pwelch" was used to conduct discrete Fourier transforms across 60 s time windows. Data plots display raw power spectra and power spectra corrected for 1/f (pink) noise (1/f corrected trace = Welch power spectrum trace * corresponding Welch frequency trace). All data underwent outlier removal based on the maximum value detected between 0-1 Hz (all traces containing peaks greater than 3 * the standard deviation of all the maximum values were removed). This resulted in the removal of 3/186 vessel diameter traces (from categories: PA BO0, PA BO3, and Cap BO1). For comparing power spectra, the power value at 0.1 Hz was extracted. The number of vessels which showed high power at 0.1 Hz was assessed by separating vessel diameter traces by those above and below a set threshold (standard deviation across all detected power values at 0.1 Hz * 0.5).

Statistics

Statistical analyses were conducted in RStudio. Data in graphs are presented as mean ± SEM, and individual dots on bar graphs represent data from individual blood vessels, whereas violin plots were used to represent individual stimulus-presentation trials. For comparing the distribution of vessel responsivity rates or stimulus condition, data was taken from individual stimulus-presentation trials, and tested using a 3D Cochran-Mantel-Haenszel test with Fisher's *post hoc* comparison. For comparing the sizes of vessel dilations or the power in the vasomotion frequency range, where data was non-normal, data was averaged across vessels and a Kruskal-Wallis test with *post hoc* pairwise Wilcoxon rank sum tests were utilized. Branch order and/or vessel categorization (penetrating arteriole/capillary) were set as the independent variable, dilation peak (for all trials during stimulus period or at stimulus cessation), time to 10% of dilation peak, power (value at 0.1 Hz or AUC between 0.05-0.15 Hz)

or locomotion frequency (% time spent in locomotion) as the dependent variable. For comparing the individual vessel diameters and depths, where data was normally distributed, one-way ANOVAs with Tukey's *post hoc* comparisons were used. For *post hoc* tests, for clarity only significant ($p < 0.05$) or trend ($p < 0.1$) level comparisons are shown, but these tests were always carried out, so absence of a displayed p value indicates a non-significant ($p > 0.1$) result.

RESULTS

"Pericyte Markers" Are Expressed Throughout the Microvascular Network

NG2, a chondroitin sulfate proteoglycan, is considered a pericyte marker and has been reported at low levels in smooth muscle cells (Kumar et al., 2017). However, NG2-controlled DsRed labeling is found throughout the microvascular tree, including in smooth muscle cells with a clear banded morphology (**Figure 1**). Immunohistochemical labeling for another pericyte marker, PDGFRβ (Winkler et al., 2010), also reveals protein expression throughout the microvascular tree, including in SMCs on pial vessels as well as penetrating arterioles and capillaries (**Figure 1**).

Markers of Contractility and Elasticity Terminate at Different Positions of the Vascular Tree

As discussed above, a much studied transition across the vascular bed has been that between vascular mural cells expressing high levels of αSMA and those expressing low or no levels of αSMA, which broadly occurs between ensheathing and mesh pericytes, though the distribution of αSMA termination positions is different from that of the change in vessel coverage (Grant et al., 2019). As discussed above, this switch in αSMA expression may coincide with the faster responses observed in low branching order capillaries (Rungta et al., 2018), though contractility of pericytes may extend beyond this transition in αSMA expression, as mid-capillary pericytes also dilate (Hall et al., 2014; Kisler et al., 2017; Hartmann et al., 2021b), presumably using different contractile machinery (Hartmann et al., 2021b). This latter study also found these mid-capillary pericytes to show slower constriction to optogenetic stimulation than did αSMA expressing-pericytes.

Vessels also show a transition in expression of elastin across the vascular bed, representing another flow regulation functional transition. In mammals, the number of layers of elastin expressed in the vessel wall scales with blood pressure and arterial size, being highest in the largest arteries (Cocciolone et al., 2018), but with only one layer, just abluminal to endothelial cells, for most intracerebral arterioles (Shinaoka et al., 2013). Elastin expression terminates before arterioles branch successively to become capillaries, presumably reflecting the lower blood pressures to which these smaller vessels are exposed. Elastin's main role is to increase vessel distensibility, storing energy in the vessel wall during systole, and releasing it during diastole, thus smoothing blood flow across the heart beat and dampening pressure waves, protecting downstream vascular beds from large fluctuations in pressure (Shinaoka et al., 2013). In addition to this biomechanical role, it may also act as a signaling molecule, regulating and attracting smooth muscle and immune cells (Cocciolone et al., 2018).

Elastin can be readily labeled by i.v. injection or incubation of tissue with AlexaFluor 633 hydrazide (Shen et al., 2012), but its role in microvascular regulation remains understudied. Recently, however, it has been used to identify intracortical arterioles in which endothelial caveolae were found to be critical players in neurovascular coupling (Chow et al., 2020), and was found around precapillary sphincters branching off penetrating arterioles that regulate blood flow and pressure into the cortical capillary network (Grubb et al., 2020; Zambach et al., 2021).

To test whether the transitions between αSMA and elastin expression occur at the same location, thus defining two different vessel "types," we used immunolabeling for αSMA combined with AlexaFluor 633 hydrazide labeling of elastin. We found that elastin terminated on vessels of large and small diameters (**Figures 2B,D**) but always upstream from the point of termination of αSMA (**Figures 2A-D,F**; 4/4 double-labeled branches showed non-overlapping termination points).

Nestin Expression in the Capillary Bed Extends Beyond αSMA Labeling

Nestin is an intermediate filament protein, commonly thought to be expressed in proliferating cells (Suzuki et al., 2010), and is associated with cardiovascular remodeling (Calderone, 2018). Recently it has been shown to be expressed in quiescent as well as proliferating endothelial cells and, indeed, may exert an inhibitory effect on endothelial cell proliferation (Dusart et al., 2018). Nestin expression by endothelial cells may therefore not necessarily reflect ongoing angiogenesis, but rather indicate the angiogenic potential of vessels. Double labeling of nestin and αSMA or elastin in NG2-DsRed mice revealed the capillary network to be nestin-positive (**Figure 3**). Nestin labeling extended from the capillary bed into lower branching order capillaries that were also αSMA positive (**Figures 3B-D**), but never overlapped with elastin-labeled vessels (**Figures 3F-H**).

To quantify the expression patterns of nestin, αSMA and elastin across the microvascular network, we next categorized the termination points of each label according to vessel lumen diameter, branching order from the penetrating arteriole (where the penetrating arteriole is 0th order; **Figure 4A**), and the distance between mural cells, or inter-soma distance (ISD). This latter measurement serves as an indicator of the morphology of these cells, as they transition from banded SMCs that are adjacent to each other, to pericytes with distinct soma and processes that become progressively longer along the vascular bed into the capillary network (Grant et al., 2019). Termination points of the different markers occurred at vessels of similar diameters (**Figure 4B**), but at different branch orders (**Figure 4A**) or ISD values (**Figure 4C**), indicative of different positions in the vascular tree. Specifically, elastin termination points were on vessels of significantly lower branch orders than termination points for αSMA or nestin, and mural cells at elastin and

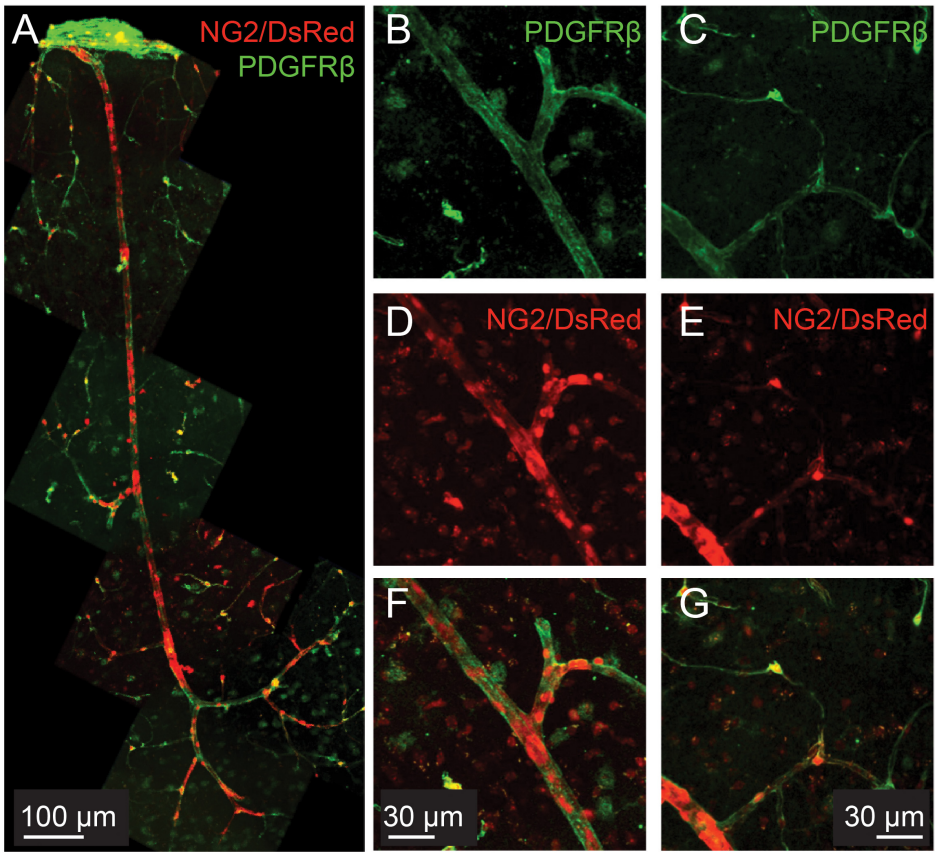

FIGURE 1 | PDGFRβ is expressed in smooth muscle cells as well as pericytes in the cortical microvasculature. Green: immunohistochemical labeling for PDGFRβ. Red: DsRed expressed under the control of the NG2 control promoter. **(A)** Example vascular bed from pial surface (top) to layers V/VI of cortex (bottom). **(B–G)**: Two different example vessels at higher magnification, to show capillary pericyte labeling of both markers.

nestin termination points were significantly closer together than at termination points for αSMA. Furthermore, consistent with our observations from double labeling of elastin and αSMA (**Figure 2**), the ISD at which elastin terminated was always smaller than that where αSMA terminated (**Figure 4D**). Thus, each functional transition occurred at a different point in the vascular tree, as defined by branch order and/or ISD. This means that in addition to the functional transitions between elastin presence and absence, and αSMA presence and absence, there is an additional functional transition point, where nestin terminates, between these two positions.

nNOS Association With Blood Vessels Is Strongest in Low Branching Order Vessels

The vasodilatory signaling molecule nitric oxide (NO) is released by sub-populations of interneurons during synaptic activation, and can mediate or modulate neurovascular coupling (Attwell et al., 2010). In neocortex, if not cerebellum, it seems predominantly involved in regulating arteriole but not capillary diameter, a transition appearing to occur between the diving arteriole and first capillary branch (Hall et al., 2014; Mishra et al., 2016). To investigate whether this reflects neuronal NO sources for vasodilation differing along the vascular tree, we immunohistochemically labeled brain slices for neuronal nitric oxide synthase (nNOS or NOS1) while labeling the vasculature with Alexa647-conjugated isolectin B4, which binds to the basement membrane (Peters and Goldstein, 1979). Consistent with previous studies (Vlasenko et al., 2007), some arterioles showed clear nNOS labeling around (but not within) vessels which extended into the capillary bed, as well as parenchymal signal (**Figures 5A-F**). To assess whether nNOS is preferentially expressed around particular elements of the vascular network, we measured the intensity of labeling immediately around vessels of different branching orders, and at increasing distances from these vessels (**Figure 5G**). Linear mixed modeling (with distance from vessel and branch order as fixed factors and vessel as a random factor) showed nNOS labeling to be significantly more intense at the vessel compared to the parenchyma (F = 7.20, d.f. = 3,30, p = 0.0009), but there was no difference in nNOS labeling around different branches (F = 0.87, d.f. = 3, 30, p = 0.47), nor did branch order affect the drop-off in signal away from the vessel (F = 0.25, d.f. = 9, 30, p = 0.98). When just the labeling at the vessel was considered, branch order was borderline-significant (F = 4.1, d.f. = 3,6, p = 0.068). Together these results suggest

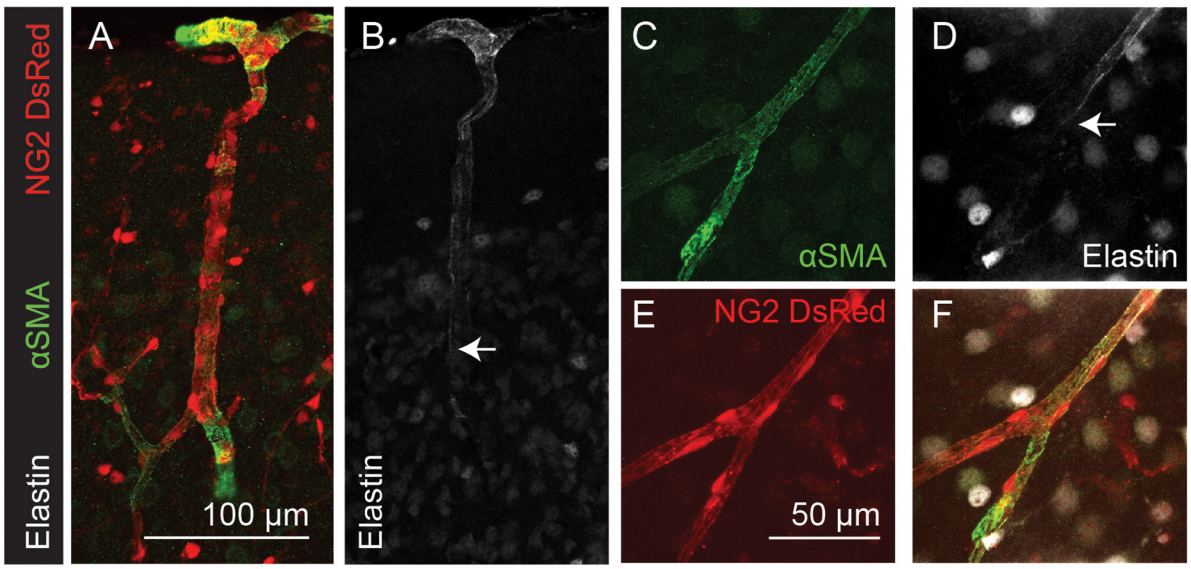

FIGURE 2 | Elastin labeling (white) terminates before αSMA labeling (green) in the cortical microvasculature (arrows). Red: DsRed expressed in NG2-positive mural cells. Panels **(A–F)** show arteriole and capillary example images. Arrows indicate termination point of elastin labeling. Images are representative of 9 (αSMA) and 12 (elastin) vascular trees, which are quantified in **Figure 4**.

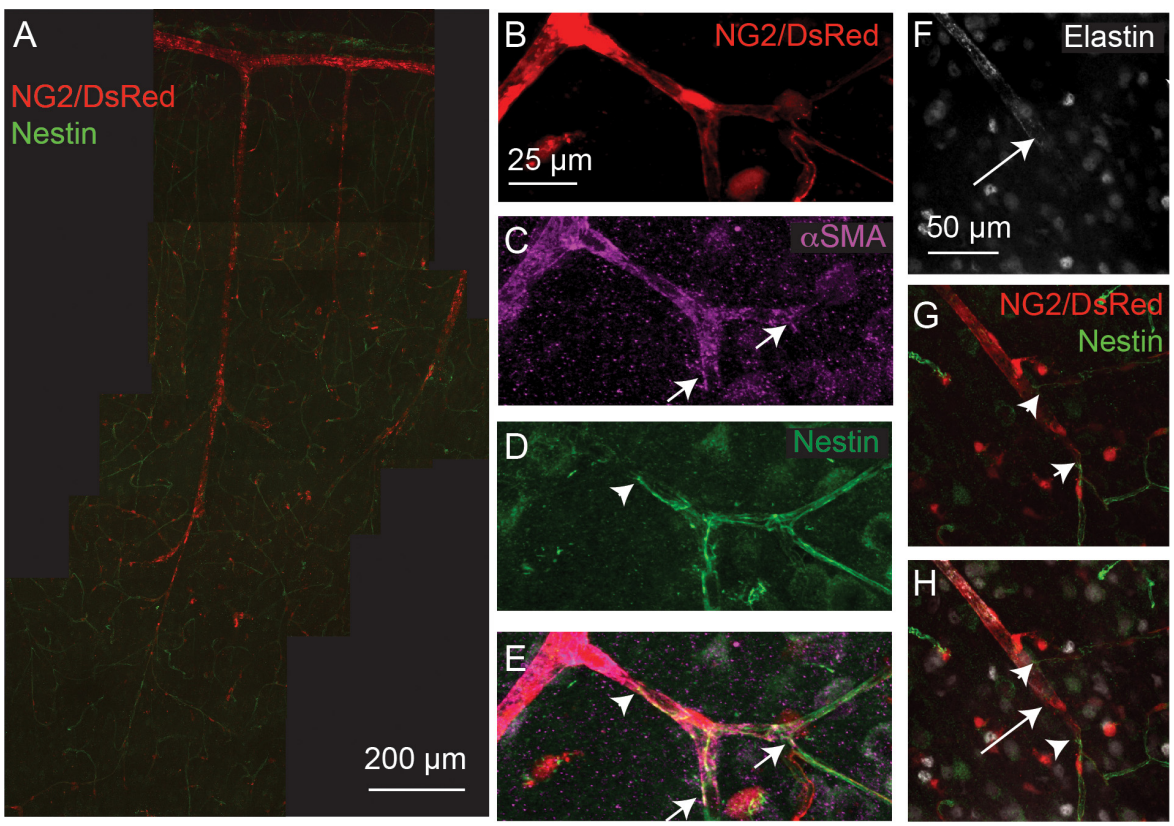

FIGURE 3 | Nestin expression (green) extends from the capillary bed to terminate (arrowheads) on vessels that express αSMA (magenta; termination point showed with small arrows), but does not extend as far as the termination point of elastin (long arrows). Red: DsRed-NG2 positive mural cells. **(A)** Example vascular bed from pia (top) to layer V/VI of cortex. **(B–E)** and **(F–H)** are two other example vessels at higher magnification. Images are representative of 11 vascular trees, which are quantified in **Figure 4**.

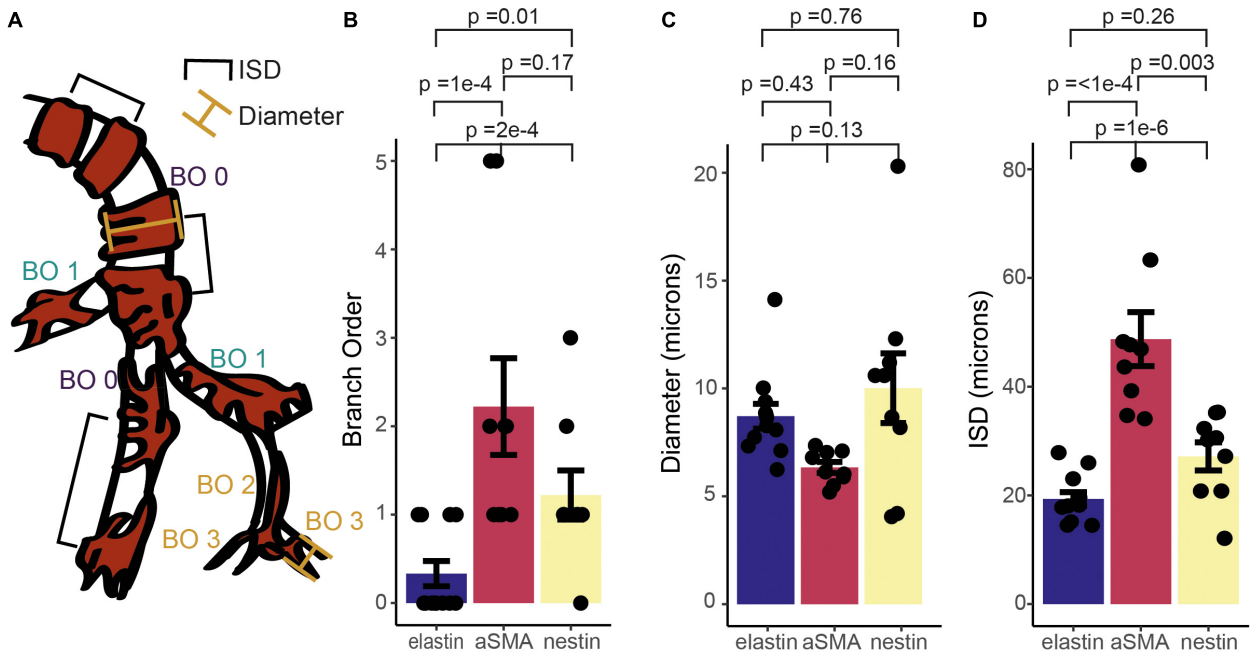

FIGURE 4 | Quantification of relative termination points of three vascular functional markers, assessed from vessel branch order (BO; **A,B**), luminal diameter **(A,C)** and inter-soma distance (ISD; **A,D**). Bars represent mean ± SEM. Each data point represents a vessel (elastin, $n = 12$; αSMA, $n = 9$, nestin, $n = 11$). *P* values are results from independent sample t tests corrected for multiple comparisons using the Holm-Bonferroni method.

that nNOS interneurons do target blood vessels, but that the degree of association is similar between penetrating arterioles and the first few capillary branches from the arteriole. The tendency for marginally stronger labeling at arterioles may contribute to the different dependence of neurovascular coupling reported in capillaries and arterioles (Mishra et al., 2016), but is unlikely to explain it entirely. Interestingly, recent work has shown that NO can modulate the propagation of vasodilation through the vascular network (Kovacs-Oller et al., 2020). It is an open, and important, question if nNOS-derived NO could contribute to neurovascular coupling by modulating the integration of vascular signals across the network in addition to its direct effect on vasodilation, and how such NO release would interact with endothelial (eNOS)-derived NO, which is also an important modulator of neurovascular function (e.g., Toth et al., 2015; Chow et al., 2020). Studying the pattern of targets of NO signaling (e.g., soluble guanylyl cyclase, or cytochrome P450 ω hydroxylase (Sun et al., 2000) should be informative in identifying how different vessels can respond to this perivascular NO production.

Shifts in Functional Expression Are Not Accompanied by Sudden Shifts in Vascular Cell Length

Previous work suggests that mural cell morphology changes in some respects near to the point at which αSMA expression terminates, with αSMA-expressing ensheathing pericytes covering the underlying vessel to a greater degree than mesh pericytes immediately downstream of the αSMA termination point (though the distribution of changes in coverage is shifted to higher branch order vessels than the termination of αSMA; Grant et al., 2019). However, the degree of vessel coverage by processes is not the only morphological change that pericytes undergo across the vascular network, as they change cell length (indicated by ISD), as well as soma orientation and shape, number and orientation of processes and many other descriptors (Zimmermann, 1923). ISD is different across pericyte categories as defined by vessel coverage, with ensheathing pericytes having a lower ISD than mesh pericytes (Grant et al., 2019; Shaw et al., 2021), so we wondered whether any abrupt shifts in ISD would be observed at functional marker transitions, suggestive of a major change in vessel type at this point. We therefore plotted the ISD immediately before and after the termination points of αSMA and elastin, normalized to the ISD at the termination point (**Figures 6A,B**). There was no significant change in ISD at the termination point of either functional marker. We had measured more ISD values on the elastin vessels, so also calculated the ISD two further cells away from the termination point, which also showed no differences compared to the cells nearer the transition point, further emphasizing the lack of an abrupt change (**Figure 6C**).

Mural Cells Are More Densely Spaced at Branch Points Compared With Non-branch Regions

Pericytes are often found at vessel bifurcations (Hartmann et al., 2015), but we also noticed that they appeared to have a different morphology at branch points, cells being clustered with a shorter ISD and greater vessel coverage (**Figure 7A**). Indeed, both

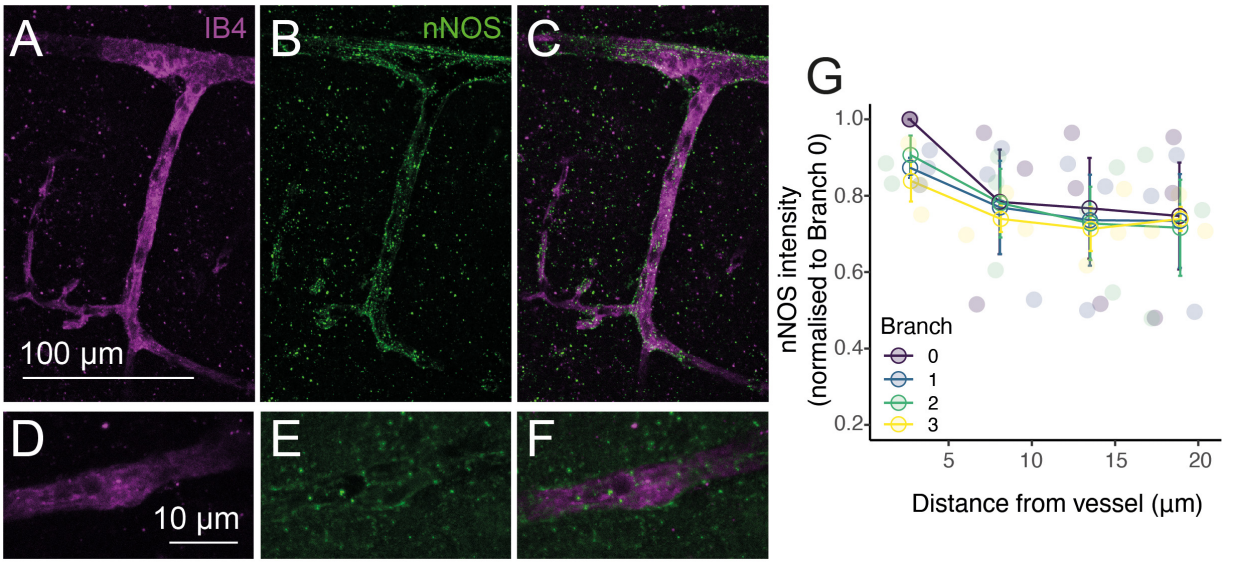

FIGURE 5 | NO production occurs preferentially near vessels. Alexa 647-conjugated Isolectin B4 (IB4; **A,C,D,F**; magenta) and immunohistochemical labeling of nNOS (**B,C,E,F**; green) show increased nNOS expression around vessels. **(G)**: Quantification of nNOS labeling around different vessel branches, expressed by normalizing the intensity of labeling around the vessel to that at the penetrating arteriole (0th order vessel). Data represents mean ± SEM. Individual points show different vessels (n = 3).

vessel diameter and ISD were greater at branch points than expected based on the average of the upstream and downstream values of these parameters (**Figure 7B**). Furthermore, while the increase in diameter was larger at branch points on larger vessels (**Figure 7C**), the change in morphology, indicated by the relative change in ISD, occurred on all vessels irrespective of the vessel diameter or ISD at the branch point (across a range of vessels from 5-20 µm in diameter; **Figures 7D,E**). Because ISD generally increases as vessel diameter decreases into the vascular bed (**Figure 7F**), mural cells at bifurcations therefore, at least in terms of ISD, have a morphology more like larger upstream vessels. This suggests the vascular network shows functional specialization at bifurcations, in addition to classic arteriole-capillary transitions of function. Pericytes at branch points can generate different calcium signals and constriction of different downstream branches, but downstream branch points were less responsive to applied vasoactive agents than upstream vessels (Gonzales et al., 2020). Our data suggest that these downstream bifurcations may still be specialized in some manner, compared to adjacent non-branch capillaries. Pericytes are known to occur frequently at bifurcations (Hartmann et al., 2015). Our analysis reveals that these pericytes at or near branch points are also shorter than expected from the ISD of non-branch pericytes immediately up or downstream.

In vivo Vascular Responses

Functional markers and anatomical changes in mural cell density indicate, therefore, that vascular function changes gradually across the vascular network, with multiple functional transition points corresponding to changes in vascular distensibility, proliferative capacity and contractility. These changes are superimposed on gradually changing mural cell properties that do not show clear alterations (at least in some features) at these transition points, but which do show specializations at branch points that likely reflect functional changes. Furthermore, inspection of the images of DsRed-positive mural cells on arterioles (in **Figures 1A**, **2A**, **3A**, **7A** and **Supplementary Figure 1**) show that, unlike commonly assumed, mural cells on arterioles often lose their annular shape as the arteriole dives into the cortex, forming intermediate pericyte morphologies with a distinct soma and processes in deeper regions.

We wanted to test, where possible, how these transitions reflected alterations in the physiological responses of different components of the vascular bed, so studied three properties of visual cortical microvasculature: frequency and size/timing of dilations in response to visual stimulation, and low frequency oscillations in the vasomotion range. We compared responses of the penetrating arteriole before and after smaller branches had come off the main vessel, as well as comparing responses of the arteriole to increasing branch orders of capillaries (see **Supplementary Figure 2D** for how different vessels' branch order was defined in order to separate vascular responses along the length of the penetrating arteriole). All data is summarized in **Table 1** (and data demographics [cortical depth, diameter] shown in **Supplementary Figure 3**).

Arterioles Dilate the Most Near the Cortical Surface but Deeper Sections Behave More Like Capillaries

Vessel responsiveness was assessed across the microvasculature by testing if visual stimulation led to an increase in vessel diameter (of > 0.5 standard deviations of the baseline). Sections

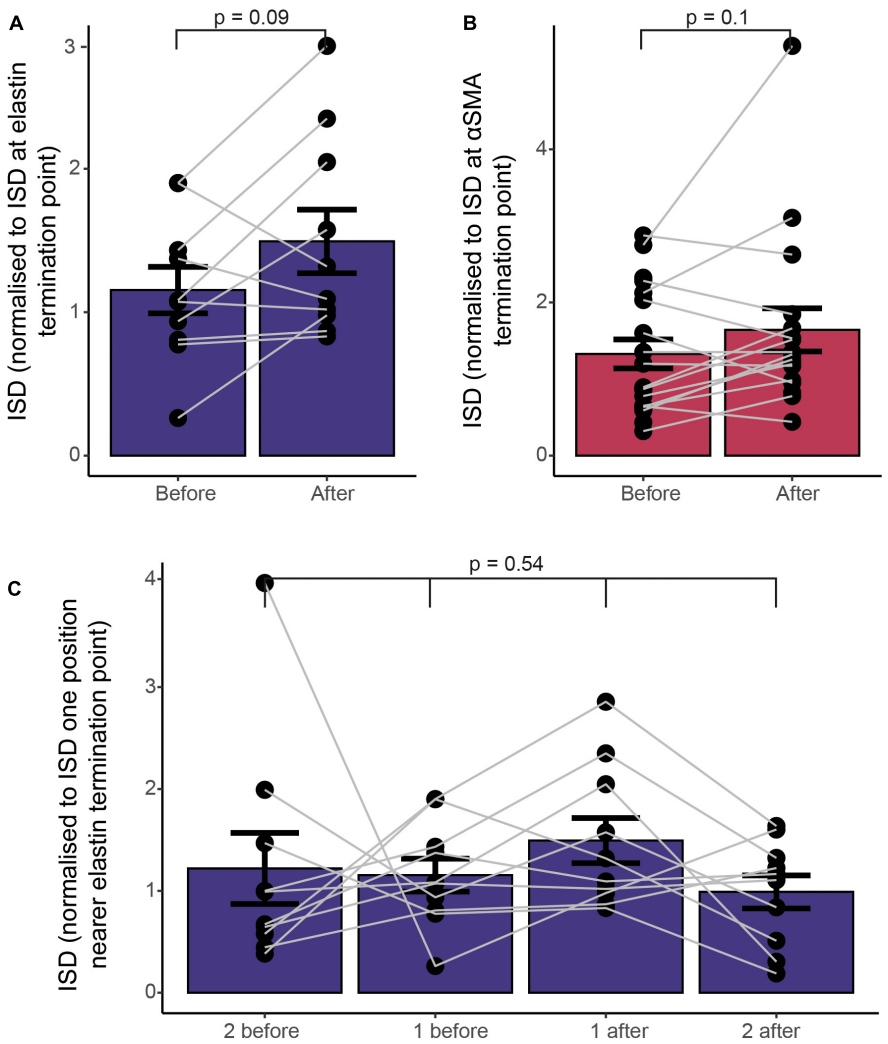

FIGURE 6 | Functional markers terminate at different points along the vascular tree, without a concomitant change in vascular mural cell morphology, as assessed by ISD. **(A)** ISD before or after the termination point normalized to the ISD at the termination point of elastin **(A)** or αSMA **(B)**. Bars show mean ± SEM, with connected data points representing individual vessels (*N* = 9 for αSMA and 11 for elastin). *P* values are from paired *t* tests **(A,B)** or a repeated measures ANOVA **(C)**.

of arterioles near the cortical surface dilated significantly more frequently than either downstream arteriole sections (≥ BO2) or downstream capillaries (**Figure 8** and **Supplementary Figures 4–6**). Specifically, descending the penetrating arteriole, dilations occurred with a similar frequency, and responses when they occurred were of a similar size in the first two sections of the vessel (before the first capillary branch and between the 1st and 2nd branches off the penetrating vessel), but these superficial responses were more frequent and tended to be larger than responses of the deepest sections of the penetrating vessel (**Figure 8**).

Across the capillary bed (i.e., any vessel downstream of the penetrating arteriole, populated by high αSMA ensheathing pericytes or low αSMA mid-capillary pericytes), dilation responses were of a similar frequency and size, with response frequencies being similar to the deep sections of the penetrating vessel (i.e., PA2 + ; **Figure 8**). There were no differences between the speed of dilations across the different vascular segments (**Supplementary Figures 4–6**).

More Arterioles Near the Cortical Surface Show Higher Power in the Vasomotion Range Compared to in Deeper Sections and the Capillary Bed

We next measured vasomotion of the vascular diameter of surface and deep sections of penetrating arterioles and different branches of the capillary bed, finding that vasomotion (power at 0.1Hz) was similar between arteriole sections and between capillaries (**Figures 9A-F**). When we compared arterioles near the cortical surface (PA0-1), to deeper arteriole sections (PA2 +) and capillaries (C1 +), there was some evidence that penetrating arterioles show more vasomotion near the pial surface, as power at 0.1Hz was highest in superficial penetrating arterioles

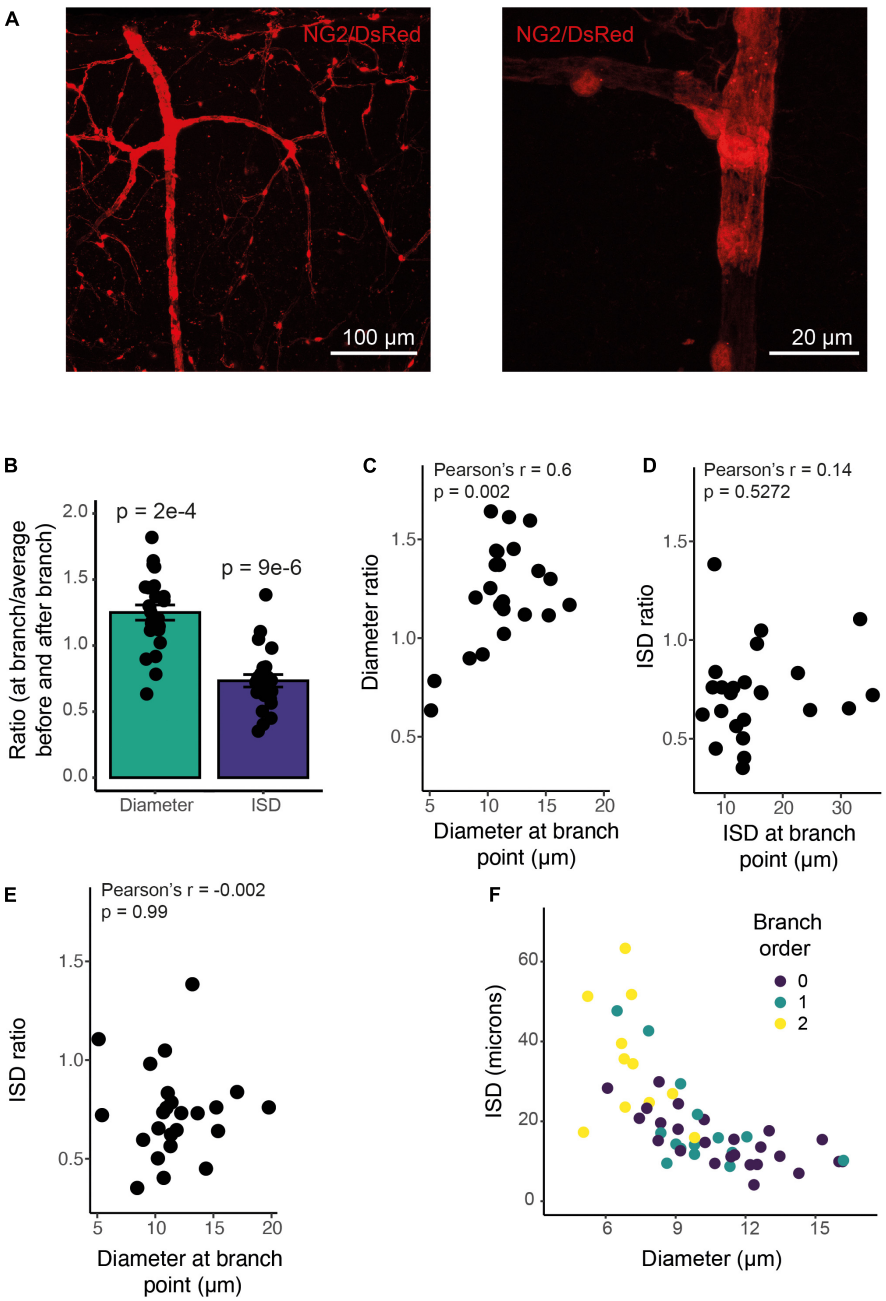

FIGURE 7 | ISD increases along the vessel but is smaller at branch points of any size. **(A)** Example NG2/DsRed labeled cortical vasculature, showing a whole penetrating arteriole and branches (left), and a high-resolution image of a single branch point, with clustered pericytes (right). This whole vascular tree is shown in **Supplementary Figure 1**. **(B)** Branch points have a larger diameter and more densely spaced pericytes than surrounding non-branch regions: The ratio of diameter at a branch point to the average of values immediately up and downstream of that branch point is larger than 1, and the ratio of ISD at a branch point to the average of ISD up and downstream of that branch point is less than one. *N* = 24 branch points. P values are from one sample t tests compared to 1. **(C)** This diameter ratio correlates significantly with the vessel diameter: smaller vessels show a relatively smaller increase in diameter at branch points. ISD ratio (calculated as in B) is uncorrelated with either ISD **(D)** or diameter **(E)**. Thus, smaller vessels show the same proportional increase in pericyte density at branch points as do large vessels. Bars represent mean ± SEM, data points are individual branches from 16 vessels. **(F)** Mural cell ISD increases with decreasing vessel diameter. Dots represent individual ISD values from 20 vessels.

(**Figure 9G**), and significantly more upstream arteriole sections (PA0-1: 33%) showed an increase in power in the vasomotion range compared to capillaries (C1 + : 13%) (0.5 SD above baseline; **Figure 9G,H**).

DISCUSSION

Our results demonstrate the existence of an intermediate transition point in vascular function between the termination

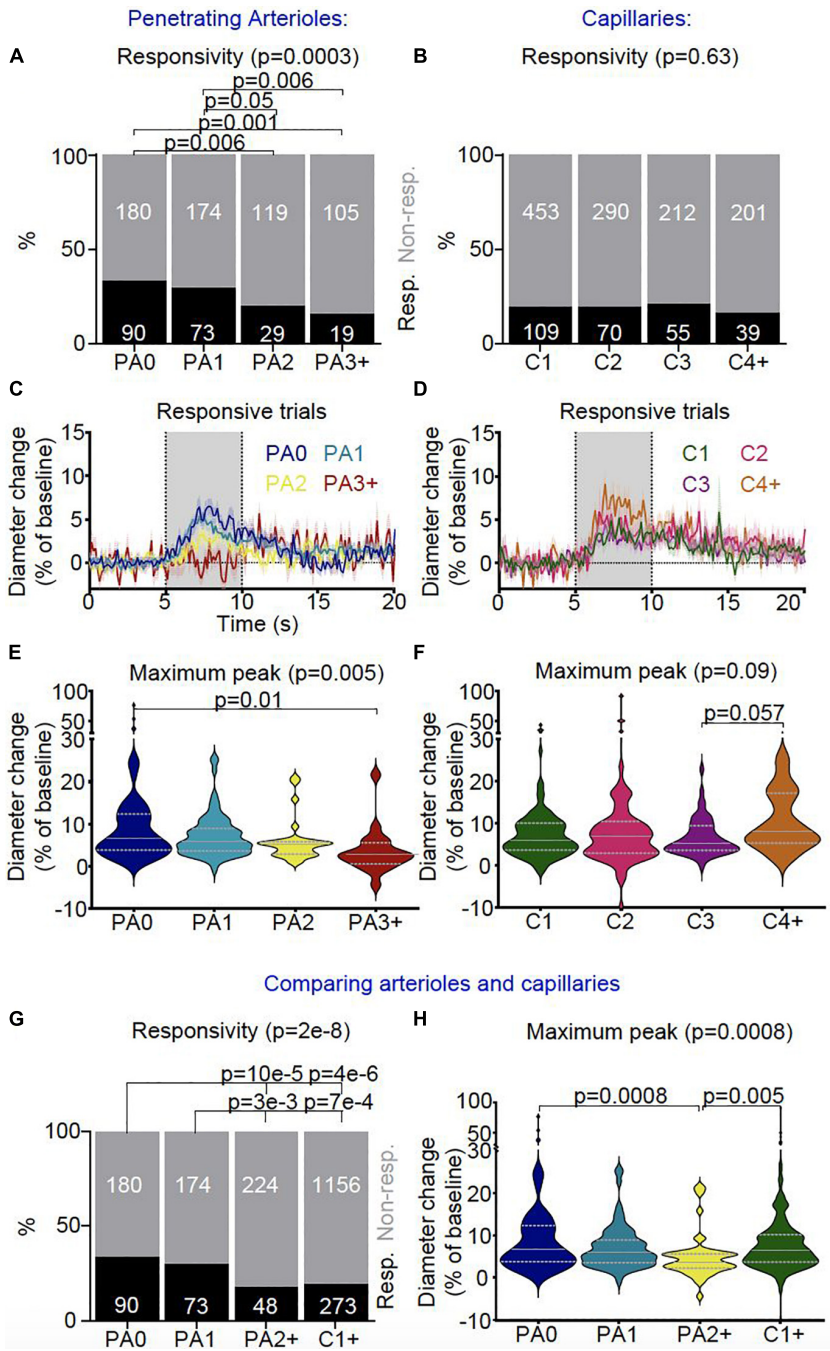

FIGURE 8 | *In vivo* vascular stimulus-dependent responses separated by vessel segment (responsive trials only). Stimulus-induced vascular dilations were classified as responsive (black) or non-responsive across the vascular segments for **(A)** penetrating arterioles (PA0 nTrials = 270, nVessels = 21; PA1 nTrials = 247, nVessels = 22; PA2 nTrials = 148, nVessels = 12; PA3 + nTrials = 124, nVessels = 9) and **(B)** capillaries (C1 nTrials = 562, nVessels = 50; C2 nTrials = 360, nVessels = 29; C3 nTrials = 267, nVessels = 22; C4 + nTrials = 240, nVessels = 21). Lower order (PA0 and PA1) penetrating arterioles were more likely to dilate during stimulus presentation than higher order diving arterioles (PA2, PA3 +), whereas no differences were found in the response rates between capillaries. Vessel responses were plotted for the **(C)** penetrating arteriole (PA0 nTrials = 90, nVessels = 18; PA1 nTrials = 73, nVessels = 15; PA2 nTrials = 29, nVessels = 9; PA3 + nTrials = 19, nVessels = 7) and **(D)** capillary (C1 nTrials = 109, nVessels = 36; C2 nTrials = 70, nVessels = 21; C3 nTrials = 55, nVessels = 17; C4 + nTrials = 39, nVessels = 14) classifications during the stimulus for responsive trials only (traces represent mean ± SEM across trials; data from all trials are shown in **Supplementary Figure 4**). Gray bar (5-10 s) shows when the stimulus was presented. Responsive trials, averaged across individual vessels, and the maximum dilation during the stimulus presentation was compared between branch orders for **(E)** penetrating arterioles and **(F)** capillaries. There were differences in the maximum dilation during stimulus presentation across sections of penetrating arterioles ($p = 0.04$; Kruskal-Wallis test as data is highly skewed), with the largest dilations in the most superficial section (PA0) ($p = 0.06$ vs PA3 +, pairwise comparison with Wilcoxon Rank Sum test), whereas stimulus-induced dilations were not significantly different across the capillary bed. We then compared vessel responses between the superficial and deep sections of penetrating arterioles (PA0 nTrials = 270, nVessels = 21; PA1 nTrials = 247, nVessels = 22; PA2 + nTrials = 272, nVessels = 21) and the capillary network (C1 + nTrials = 1429, nVessels = 122). **(G)** Lower order (more superficial) penetrating

(Continued)

FIGURE 8 | arterioles (PA0-1) were more likely to dilate to visual stimulus than higher order penetrating arterioles (PA2 +) and capillaries (C1 +) (p = 2e-8). **(H)** Stimulus-dependent vascular dilation responses were then averaged across each vessel and superficial and deep penetrating arterioles were compared with the capillary bed (PA0 nTrials = 90, nVessels = 18; PA1 nTrials = 73, nVessels = 15; PA2 + nTrials = 48, nVessels = 16; C1 + nTrials = 277, nVessels = 90; data including non-responsive trials is shown in **Supplementary Figure 6**). The maximum dilation differed across vessel categories (p = 0.05; Kruskal-Wallis test), being borderline significantly smaller in deep PA sections than either superficial arteriolar segments or the capillary bed (p = 0.06 vs PA0-1 and C1 +). Horizontal gray lines on violin plots show median (solid line) and interquartile range (dotted lines), and statistical comparisons of vessel responsivity rates were made using a Chi-square test with Fisher's *post hoc* comparison, and of dilation peaks using a Kruskal-Wallis test with *post hoc* Wilcoxon rank sum tests to assess pairwise comparisons.

points for elastin and αSMA – a transition in nestin expression. Furthermore, pericyte morphology as assessed from ISD does not alter abruptly around these transition points, suggesting that gradual changes in morphology along the vascular network are superimposed upon multiple sharp changes in protein expression levels. In both large and small vessels, branch points are also functionally specialized, having denser pericyte coverage than adjacent up and downstream vessels. Conversely, we did not find any transitions in expression of classic pericyte markers PDGFRβ and NG2, or perivascular nNOS levels, which were expressed from the pia to the mid-capillary bed. Finally, *in vivo*, below their second branch, penetrating arterioles showed similar neurovascular coupling and vasomotion to capillaries, having a lower frequency of dilation or vasomotion compared to the first two segments of the penetrating arterioles.

Thus overall, our data support a view of the vascular network whereby sharp distinctions between different vascular segments do not exist, but rather different functions transition at different positions within the vascular tree, within classic vascular categories such as "arterioles" and "capillaries" as well as between them. This means that vascular function overall changes gradually across the vascular network, including along classically defined single "vessel types" such as diving arterioles.

Expression of Pericyte Markers Throughout the Vascular Network

We found PDGFRβ and NG2 to be expressed throughout the arteriole-capillary vascular network. Both are classically considered to be pericyte markers (Winkler et al., 2010; Armulik et al., 2011), but our results are consistent with the described effects on smooth muscle cells of PDGFRβ gain-of-function mutations, which increase leukocyte accumulation in the aorta (He et al., 2015). Single cell RNA seq analyses also support the more widespread expression of both PDGFRβ and NG2, with mRNA transcripts found in smooth muscle cells as well as pericytes (Vanlandewijck et al., 2018), albeit at moderately lower levels.

The function of these two "marker" proteins may be different depending on their vascular location. NG2 is known to be important for neovascularization and stabilization of newly formed vessels, *via* the interaction of NG2 with integrins and growth factor receptors on the same and other cells (Stallcup, 2018). In capillary pericytes of the mature vasculature, however, it promotes the formation of new capillaries through angiogenesis, whereas in larger vessels it instead may promote arteriogenetic remodeling of vessel diameter (Rundek and Della-Morte, 2015). Such remodeling can occur after decreased tissue oxygen and, consistent with widespread NG2 expression, cells in surface and penetrating arterioles, and the capillary bed, have been found to proliferate after cerebral ischemia (Wei et al., 2001). PDGFRβ also functions differently in arteries compared to smaller vessels. In culture, pericytes but not smooth muscle cells shed PDGFRβ in response to stress (Sagare et al., 2015) and mutations that block PDGFRβ signaling reduce pericyte number and increase capillary leakiness, without affecting smooth muscle cells (Nikolakopoulou et al., 2017). Conversely, inhibition of PDGFRβ pharmacologically or using siRNA preserves cerebral arterial smooth muscle cells and arterial vascular tone after sub-arachnoid hemorrhage (Shiba et al., 2012; Wan et al., 2019), highlighting a potential pathophysiological contribution of PDGFRβ signaling to arterial smooth muscle cells.

Thus both NG2 and PDGFRβ are expressed throughout the cerebral microvasculature, but differ functionally depending on their location, presumably due to differences in expression levels of other proteins that are localized to different parts of the vascular network.

nNOS Is Expressed Around Arterioles and Capillaries

Given the involvement of nNOS-derived NO in arteriole but not capillary neurovascular coupling (Mishra et al., 2016), we expected to observe differential expression of nNOS along the vascular network. However, while nNOS was expressed at greater levels around vessels than in the parenchyma, this occurred to a similar degree for all vessels studied (up to 3rd branch order) and not just the diving arterioles. NO can control the electrical coupling of pericytes in the retina (Kovacs-Oller et al., 2020) as well as the production of other vasoactive molecules such as 20-HETE (Liu et al., 2008; Hall et al., 2014), so neuronally derived NO may be released onto all vessels but play a different role at arterioles than capillaries, generating a dilation in the former and modulating the response in the latter. A gradient of expression of the other constitutive NOS isoform, endothelial NOS, has not been reported, and RNA Seq data suggests it is expressed at similar levels in arterial, capillary and venous endothelial cells (Vanlandewijck et al., 2018).

Correspondence of Elastin and αSMA Labeling to Transitions in Physiological Responses

As previously described, elastin and αSMA labeling in the vascular wall both label arterioles (Shen et al., 2012; Grant et al., 2019) with αSMA labeling extending into the capillary bed (Grant et al., 2019; Chow et al., 2020; Thakore et al., 2021). Here we show these termination points are distinct and non-overlapping, occurring at significantly different branch orders and with different pericyte morphologies as assessed by ISD. The location of elastin labeling quite well matches locations

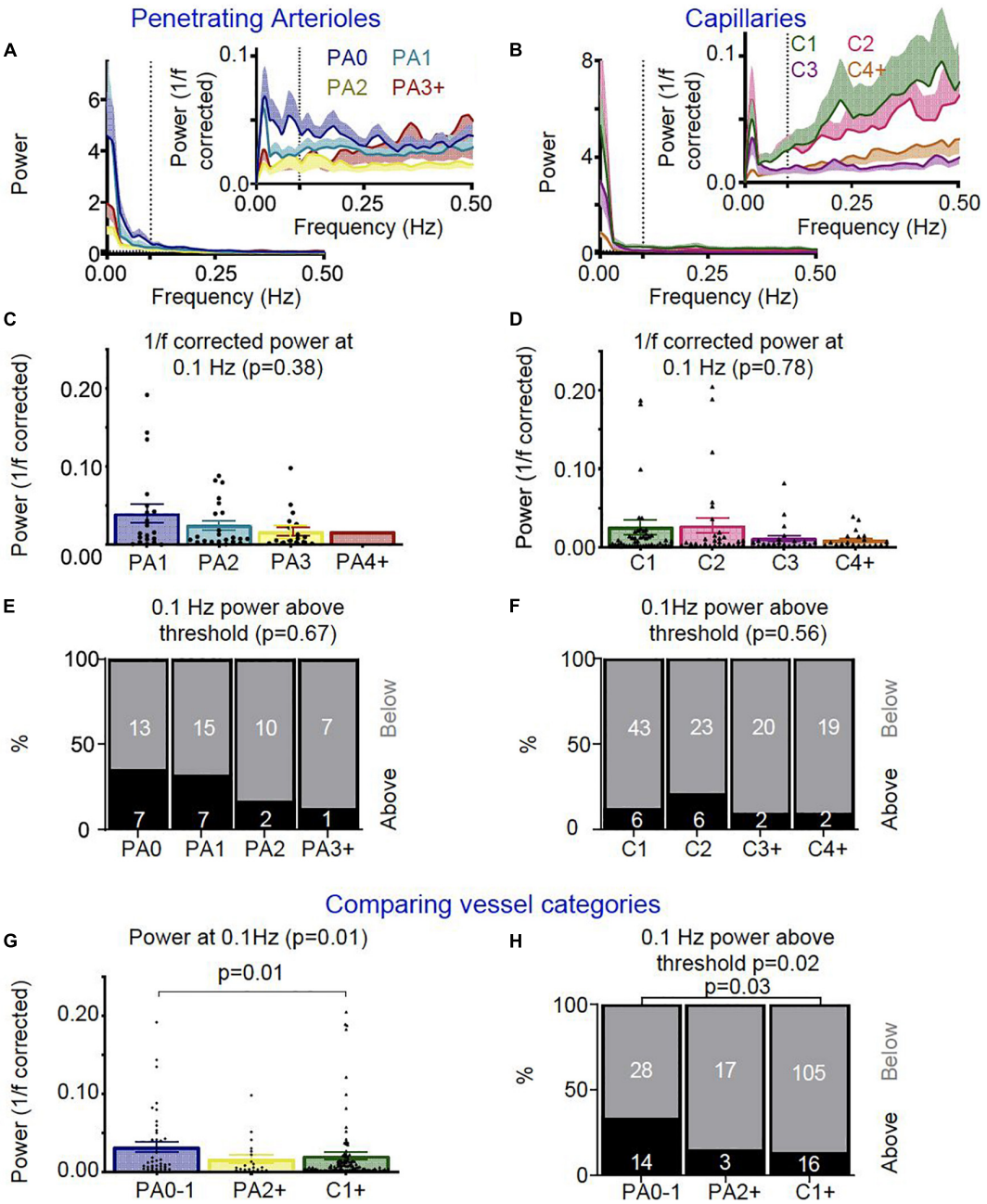

FIGURE 9 | *In vivo* vascular vasomotion responses separated by vessel segment. Average power spectra of **(A)** penetrating arteriole (PA0 nVessels = 20, PA1 nVessels = 22, PA2 nVessels = 12, PA3 + nVessels = 8) and **(B)** capillaries (C1 nVessels = 49, C2 nVessels = 29, C3 nVessels = 22, C4 + nVessels = 21) were separated by branch order for raw traces (left) and 1/f corrected traces (right insert). No significant differences were seen in the 1/f corrected power at 0.1 Hz between **(C)** penetrating arteriole or **(D)** capillary segments. Error bars represent mean ± SEM, and power at 0.1 Hz was compared between individual vessels using a Kruskal Wallis test. **(A)** threshold was set for assessing the number of vessels which showed high 1/f corrected power at 0.1 Hz (threshold: 0.5 * standard deviation across all vessels' 0.1 Hz 1/f corrected power values), and no significant differences were seen between **(E)** penetrating arteriole or **(F)** capillary vascular segments in the ratio of vessels with higher 1/f corrected power at the vasomotion frequency (numbers in bars represent individual vessels). We then compared vessel responses between the penetrating arterioles (PA0-1 nVessels = 42, PA2 + nVessels = 20) and capillary network (nVessels = 120). As for neurovascular coupling responses, superficial (PA0-1) and deep (PA2 +) arterioles were compared with the capillary bed (C1 +). **(G)** Average 1/f corrected power at 0.1 Hz was different across these vessel groups, with superficial arterioles showing significantly more power at 0.1 Hz than capillaries ($p = 0.01$; Wilcoxon rank sum pairwise comparisons). **(H)** The lowest order penetrating arterioles (PA0-1) also had more vessels with higher 1/f corrected power at 0.1 Hz than other categories ($p = 0.01$), specifically when compared to the capillaries ($p = 0.03$). Statistical comparisons of the number of vessels with higher power in the vasomotion range were made using a Chi-square test with Fisher's *post hoc* comparison, and of power at 0.1 Hz using a Kruskal Wallis test with Wilcoxon rank sum pairwise *post hoc* tests.

where we see transitions in physiological responses - the second branch off the diving arteriole - below which responses seem more like those in the capillary bed. Of our 12 elastin-labeled vessels, 8 terminated on the penetrating arteriole (75%), of which 5 (42% of the total) terminated before the first branch from the arteriole, i.e., upstream of where we observe a change in response frequencies. Thus, arteriole elastin labeling broadly, but not tightly, corresponds with the superficial part of the diving arteriole where neurovascular dilations and vasomotion were most frequently observed.

Though associated with contractile ability, the termination point of αSMA does not, however, correlate very well with the size or frequency of neurovascular coupling responses or vasomotion, we observed *in vivo*. αSMA universally terminated beyond the penetrating arteriole, but we found no differences in neurovascular response frequency, dilation size or vasomotion between different capillary branching orders (1-4 +), though many fewer of these smaller vessels express αSMA. Furthermore, responses were equally frequent in αSMA-expressing deep sections of the penetrating arteriole as in the capillary bed, and capillary dilations were actually larger than these deep arteriole dilations. This is at odds with previous findings, where dilations in $\geq$ 4th order vessels were substantially smaller than higher order vessels in whisker barrel cortex of awake mice (Rungta et al., 2021). The reasons for this are unclear. Firstly, we compare both response frequency and response sizes, whereas these two measures are conflated in Rungta et al's paper. However, as we also saw similar response frequencies and sizes across the capillary bed, this cannot explain why we do not see smaller responses in $\geq$ 4th order vessels. The cortical area is different (visual vs. somatosensory), and the degree of neuronal stimulation might be different (whole field drifting gratings vs. a single whisker deflection), which could perhaps have an impact on neurovascular coupling. Another potential cause of these differences is the method of detecting vascular diameter. We used xy images from which we calculate the diameter perpendicular to every point of a small length of a vessel's axis, thus averaging across space (12-109 pixels, or 2.4-22 microns), while Rungta et al. used line scans of vessels to measure vascular diameter at a single position. The spatial smoothing we used in this paper is likely to give us a higher sensitivity to small deflections in diameter.

Previous work in anaesthetized animals, has also found different vascular segments to show different time courses of dilation, with deeper sections of arterioles or first order capillaries responding faster than superficial arteriolar segments (Tian et al., 2010; Hall et al., 2014; Rungta et al., 2018). Our data from awake mice did not show this, with similar response kinetics between vascular segments.

Transitional Segment?

The vascular segment between the penetrating arteriole, or end of elastin labeling, and the end of αSMA labeling has often been termed a "precapillary arteriole" or a "transitional segment" (e.g., Rungta et al., 2021), representing a region where vascular function transitions between arteriole and capillary. However, our *in vivo* data suggests that this segment, corresponding roughly to branch orders 1 to 3, is not (in our hands) where transitions of contractile behavior occur. Other transitions do occur in this zone: We found endothelial expression of the intermediate filament protein nestin extends out of the capillary bed to a position between the termination points of elastin and αSMA. In the retina, calponin, filamentous microtubules, αSMA, filamentous actin and myosin heavy chain were all also found to change expression levels across this section (Gonzales et al., 2020). However, these all transitioned at different positions, calponin terminating on the arteriole, microtubules on branch 1 and αSMA on branch 2, with filamentous actin and myosin heavy chain gradually decreasing in expression levels from branch orders 0 to 4 (beyond which vessels were not studied). These progressive changes in function across a number of markers fit with the gradual changes in mural cell morphology or ISD we observed before and after the termination points of elastin and αSMA, at roughly branch orders 0 and 3, respectively. Thus this "transitional zone" is not uniform, with a single type of vascular cell and, crucially, is not the only region where such transitions of function are occurring, as similar transitions in vasomotion, neurovascular coupling, and mural cell morphology also occur when descending the penetrating arteriole: Neurovascular coupling responses and vasomotion were observed more frequently in superficial segments of diving arterioles than in either downstream capillaries or deep sections of the arterioles, which were similar to each other in response characteristics. Correspondingly, mural cells lost their annular smooth muscle cell morphology to gain a distinct soma and processes at lower reaches of the diving arterioles. This suggests arteriolar mural cells can be pericytes, unlike has been argued (Hartmann et al., 2021a).

This data suggests that the division of the vascular network into four functional segments: arterioles with SMCs, a transitional zone with ensheathing pericytes, capillaries with capillary pericytes and venules with venular SMCs (Hartmann et al., 2021a), while helpful in discussing broad functional changes across the network, is overly simplistic and neglects the gradual transition in functions that occurs. Indeed, multiple other functional transitions occur at other positions in the vascular tree, including between the pial and penetrating arterioles: Penetrating arterioles exhibit higher contractile tone at low intravascular pressures than pial arterioles (Longden et al., 2016). Neurovascular response sizes are also smaller, possibly because of the lower external pressure on the surface vessel compared to penetrating arterioles which are surrounded by brain tissue (Gao et al., 2015).

Branch Points May Be Functionally Specialized

Our data suggest that pericytes exist at a higher density at branch points than on surrounding vessel lengths, and this clustering occurs to a similar degree on small and large microvessels. This suggests some functional specialization at branch points. 90% of branch points in the transitional segment were previously found to have a pericyte at that location

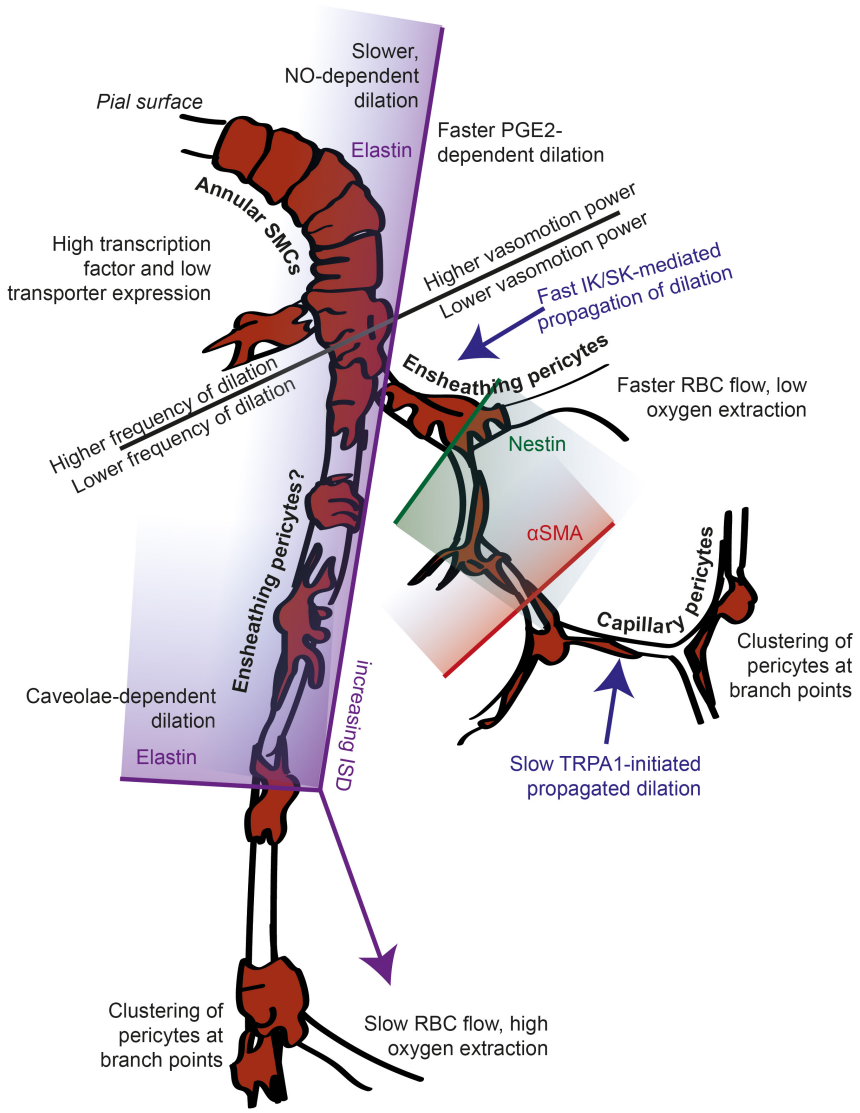

FIGURE 10 | Summary of known functional transition points across the arteriole-capillary axis. The location of many functional transitions remains unknown, indicated by label placement in a general zone, without an arrow (e.g., between slow and fast propagated dilation, and expression levels of transporters vs. transcription factors). Gradient shading shows that the labeled marker is expressed in the vascular zone to the shaded side of the termination point indicated. Current nomenclature for mural cells is indicated, with mural cells on the arteriole suggested to be ensheathing pericytes rather than smooth muscle cells due to their pericyte morphology. This is backed up by the similar behavior of deep arteriole sections compared to the capillary bed, though there are other differences (e.g., elastin labeling, caveloe) as indicated.

compared to only 45% of more distal branch points (Gonzales et al., 2020). This corresponds with the increase in pericyte ISD we report here, but our data suggest that even the distal branch points are functionally specialized, as they have a shorter ISD than surrounding non-branch point regions. The pericytes at proximal branch points had calcium sparks that corresponded with selective constriction of individual branches, suggesting branch points serve to direct blood flow to active neurons (Gonzales et al., 2020). Distal branch points (> 4th branch order) were not found to be contractile, and calcium changes in these pericytes were not reported. As our data suggest these distal capillaries do dilate to a similar degree as the proximal branches, it would be valuable to study whether these branch points' pericyte calcium changes also correspond to changes in vascular diameter of the different downstream branches.

Transcriptomic Gradients Could Illuminate Transitions in Whole Range of Functions

Our data and the wider literature currently support multiple transitions of function at different positions of the vascular bed, including down diving arterioles, and along increasingly

branching capillaries. Contractile function and neurovascular coupling are the functions most widely studied, but transitions at different locations are also seen in oxygen supply as well as expression of transcription factors, transporters, regulators of angiogenesis and immune regulators. However, these studies are all limited by a low capacity to look at different functions. Rather than focusing on individual vascular functions, single cell RNA Seq has the potential to illuminate the whole range of gene expression differences that exist across the vascular network (He et al., 2018). Clustering of vascular endothelial and mural cells has revealed that endothelial gene expression changes gradually, suggesting that there are likely not simultaneous transitions in expression of many genes at the same point on the vessel. More abrupt transitions between smooth muscle cell and pericytes have been reported (Vanlandewijck et al., 2018), which may fit with the sharp transitions observed in some vascular features (e.g., the shift in vessel coverage from ensheathing to mesh pericytes). However, this study also shows large numbers of genes that are expressed in wider zones of the vasculature, e.g., pericytes and arteriolar but not arterial SMCs, supporting the existence of multiple transition points. Indeed, another RNA Seq study identifies multiple pericyte clusters suggestive of multiple functional transition points (Zeisel et al., 2018). Future studies could link single cell RNA seq data to specific spatial locations within the vascular network, to illuminate this issue further. Such data would allow us to better understand the vascular regions to target with pharmacological interventions, given Alzheimer's disease and stroke are vasculature-degenerating conditions that differentially affect the various parts of the vascular network.

CONCLUSION

Our data, and the literature, support the existence of multiple transition points in vascular function, different proteins being expressed at overlapping sections of the vascular network, and properties of neurovascular and vasomotion response rates, sizes and timings varying at different places in the network (summarized in **Figure 10**). These various functional transitions are superimposed on gradually changing mural cell morphologies across the vascular tree, which show specializations at branch points. Thus, while categorization of vessels or mural cells may be a useful simplification in some circumstances, it is important to remember that, for example, an upstream ensheathing pericyte is not identical to a downstream ensheathing pericyte, nor to one on a branch point. Understanding where and how different vascular functions (e.g., oxygen and nutrient supply, waste clearance, immune regulation) are supported across the vascular tree is vital to understand how different sections are impacted, and could be targeted, during disease, but will likely require approaches such as spatially-localized RNA Seq to identify how the transcriptome as a whole alters across the cerebral microvascular network.

DATA AVAILABILITY STATEMENT

The datasets presented in this study can be found at Figshare.com, doi: 10.25377/sussex.17840939.

ETHICS STATEMENT

All experiments were carried out in compliance with the UK Animal Experiments (Scientific Procedures) Act 1986 after approval of the local University of Sussex or UCL Local Ethics Committees and under project or personal licences granted by the UK Home Office.

AUTHOR CONTRIBUTIONS

KB, MH-H, DA, and CH collected the data. KS, KB, MH-H, DA, and CH analyzed the data. KS, SA, OB, and CH wrote the manuscript. All authors contributed to the article and approved the submitted version.

FUNDING

KS, OB, and CH were supported by an MRC Discovery Award (MC_PC_15071; mrc.ukri.org), MRC Project Grants MR/S026495/1 and MR/V036750/1 an Academy of Medical Sciences/Wellcome Trust Springboard Award (acmedsci.ac.uk) all held by CH. An ERC grant (BrainEnergy: 740427) held by David Attwell also supported the work by CH and DA. KB and SA were supported by University of Sussex Ph.D. studentships and MHH by a University of Sussex Junior Research Associate position. The funders had no role in study design, data collection and analysis, decision to publish, or preparation of the manuscript.

ACKNOWLEDGMENTS

We would like to thank David Attwell for comments on the manuscript, support during early data collection and the gift of the NG2-DsRed mice. We would also like to thank Laura Bell and the staff of the Biological Research Facility at the University of Sussex for maintaining the mouse colonies used in these studies. We would also like to thank Dori M. Grijseels for producing the schematic of the *in vivo* experimental set-up (used in **Supplementary Figure 2**) and Luca Biasetti for acquisition of supporting images.

SUPPLEMENTARY MATERIAL

The Supplementary Material for this article can be found online at: https://www.frontiersin.org/articles/10.3389/fnagi.2021.779823/full#supplementary-material

REFERENCES

Aalkjær, C., Boedtkjer, D., and Matchkov, V. (2011). Vasomotion – what is currently thought? *Acta Physiol.* 202, 253–269. doi: 10.1111/j.1748-1716.2011.02320.x

Aldea, R., Weller, R. O., Wilcock, D. M., Carare, R. O., and Richardson, G. (2019). Cerebrovascular smooth muscle cells as the drivers of intramural periarterial drainage of the brain. *Front. Aging Neurosci.* 11:1. doi: 10.3389/fnagi.2019.00001

Andreone, B. J., Chow, B. W., Tata, A., Lacoste, B., Ben-Zvi, A., Bullock, K., et al. (2017). Blood-brain barrier permeability is regulated by lipid transport-dependent suppression of caveolae-mediated transcytosis. *Neuron* 94, 581–594.e5. doi: 10.1016/j.neuron.2017.03.043

Armulik, A., Genové, G., and Betsholtz, C. (2011). Pericytes: developmental, physiological, and pathological perspectives, problems, and promises. *Dev. Cell* 21, 193–215. doi: 10.1016/j.devcel.2011.07.001

Attwell, D., Buchan, A. M., Charpak, S., Lauritzen, M., Macvicar, B. A., and Newman, E. A. (2010). Glial and neuronal control of brain blood flow. *Nature* 468, 232–243. doi: 10.1038/nature09613

Attwell, D., Mishra, A., Hall, C. N., O'Farrell, F. M., and Dalkara, T. (2016). What is a pericyte? *J. Cereb. Blood Flow Metab.* 36, 451–455. doi: 10.1177/0271678X15610340

Bandopadhyay, R., Orte, C., Lawrenson, J. G., Reid, A. R., De Silva, S., and Allt, G. (2001). Contractile proteins in pericytes at the blood-brain and blood-retinal barriers. *J. Neurocytol.* 30, 35–44.

Banks, W. A., Lynch, J. L., and Price, T. O. (2009). "Cytokines and the blood–brain barrier," in *The Neuroimmunological Basis of Behavior and Mental Disorders*, eds A. Siegel and S. S. Zalcman (Boston, MA: Springer US), 3–17. doi: 10.1007/978-0-387-84851-8_1

Ben-Zvi, A., Lacoste, B., Kur, E., Andreone, B. J., Mayshar, Y., Yan, H., et al. (2014). Mfsd2a is critical for the formation and function of the blood-brain barrier. *Nature* 509, 507–511. doi: 10.1038/nature13324

Biswal, B. B., and Hudetz, A. G. (1996). Synchronous oscillations in cerebrocortical capillary red blood cell velocity after nitric oxide synthase inhibition. *Microvasc. Res.* 52, 1–12. doi: 10.1006/mvre.1996.0039

Bonnar, O., Shaw, K., Grijseels, D. M., Clarke, D., Bell, L., Anderle, S., et al. (2021). APOE4 genotype increases neuronal calcium signals and decreases pial arteriole responsivity and vasomotion in visual cortex of awake mice. *bioRxiv* [Preprint]. doi: 10.1101/2021.05.26.445731

Boyd, K., Hammond-Haley, M., Vroman, R., and Hall, C. N. (2021). Imaging pericytes and the regulation of cerebral blood flow. *Methods Mol. Biol.* 2235 89–117

Braverman, I. M. (1989). Ultrastructure and organization of the cutaneous microvasculature in normal and pathologic states. *J. Invest. Dermatol.* 93, 2S–9S. doi: 10.1111/1523-1747.ep12580893

Calderone, A. (2018). The biological role of nestin$^{(+)}$-cells in physiological and pathological cardiovascular remodeling. *Front. Cell Dev. Biol.* 6:15. doi: 10.3389/fcell.2018.00015

Chambers, R., and Zweifach, B. W. (1946). Functional activity of the blood capillary bed, with special reference to visceral tissue. *Ann. N. Y. Acad. Sci.* 46, 683–695. doi: 10.1111/j.1749-6632.1946.tb31697.x

Chow, B. W., Nuñez, V., Kaplan, L., Granger, A. J., Bistrong, K., Zucker, H. L., et al. (2020). Caveolae in CNS arterioles mediate neurovascular coupling. *Nature* 579, 106–110. doi: 10.1038/s41586-020-2026-1

Cocciolone, A. J., Hawes, J. Z., Staiculescu, M. C., Johnson, E. O., Murshed, M., and Wagenseil, J. E. (2018). Elastin, arterial mechanics, and cardiovascular disease. *Am. J. Physiol. Heart Circ. Physiol.* 315, H189–H205. doi: 10.1152/ajpheart.00087.2018

Colantuoni, A., Bertuglia, S., and Intaglietta, M. (1994). Microvascular vasomotion: origin of laser Doppler flux motion. *Int. J. Microcirc. Clin. Exp.* 14, 151–158. doi: 10.1159/000178823

Cruz Hernández, J. C., Bracko, O., Kersbergen, C. J., Muse, V., Haft-Javaherian, M., Berg, M., et al. (2019). Neutrophil adhesion in brain capillaries reduces cortical blood flow and impairs memory function in Alzheimer's disease mouse models. *Nat. Neurosci.* 22, 413–420. doi: 10.1038/s41593-018-0329-4

Dana, H., Chen, T.-W., Hu, A., Shields, B. C., Guo, C., Looger, L. L., et al. (2014). Thy1-GCaMP6 transgenic mice for neuronal population imaging *in vivo*. *PLoS One* 9:e108697. doi: 10.1371/journal.pone.0108697

Daneman, R. (2012). The blood-brain barrier in health and disease. *Ann. Neurol.* 72, 648–672. doi: 10.1002/ana.23648

Dusart, P., Fagerberg, L., Perisic, L., Civelek, M., Struck, E., Hedin, U., et al. (2018). A systems-approach reveals human nestin is an endothelial-enriched, angiogenesis-independent intermediate filament protein. *Sci. Rep.* 8:14668. doi: 10.1038/s41598-018-32859-4

Duvernoy, H. M., Delon, S., and Vannson, J. L. (1981). Cortical blood vessels of the human brain. *Brain Res. Bull.* 7, 519–579. doi: 10.1016/0361-9230(81)90007-1

Gao, Y.-R., Greene, S. E., and Drew, P. J. (2015). Mechanical restriction of intracortical vessel dilation by brain tissue sculpts the hemodynamic response. *Neuroimage* 115, 162–176. doi: 10.1016/j.neuroimage.2015.04.054

Garcia, D. C. G., and Longden, T. A. (2020). Ion channels in capillary endothelium. *Curr. Top. Membr.* 85, 261–300. doi: 10.1016/bs.ctm.2020.01.005

Gonzales, A. L., Klug, N. R., Moshkforoush, A., Lee, J. C., Lee, F. K., Shui, B., et al. (2020). Contractile pericytes determine the direction of blood flow at capillary junctions. *Proc. Natl. Acad. Sci. U.S.A.* 117, 27022–27033. doi: 10.1073/pnas.1922755117

Grant, R. I., Hartmann, D. A., Underly, R. G., Berthiaume, A.-A., Bhat, N. R., and Shih, A. Y. (2019). Organizational hierarchy and structural diversity of microvascular pericytes in adult mouse cortex. *J. Cereb. Blood Flow Metab.* 39, 411–425. doi: 10.1177/0271678X17732229

Grubb, S., Cai, C., Hald, B. O., Khennouf, L., Murmu, R. P., Jensen, A. G. K., et al. (2020). Precapillary sphincters maintain perfusion in the cerebral cortex. *Nat. Commun.* 11:395. doi: 10.1038/s41467-020-14330-z

Haddock, R. E., Hirst, G. D. S., and Hill, C. E. (2002). Voltage independence of vasomotion in isolated irideal arterioles of the rat. *J. Physiol.* 540, 219–229. doi: 10.1113/jphysiol.2001.013698

Hall, C. N., Reynell, C., Gesslein, B., Hamilton, N. B., Mishra, A., Sutherland, B. A., et al. (2014). Capillary pericytes regulate cerebral blood flow in health and disease. *Nature* 508, 55–60. doi: 10.1038/nature13165

Hamilton, N. B., Attwell, D., and Hall, C. N. (2010). Pericyte-mediated regulation of capillary diameter: a component of neurovascular coupling in health and disease. *Front. Neuroenergetics* 2:5. doi: 10.3389/fnene.2010.00005

Hartmann, D. A., Coelho-Santos, V., and Shih, A. Y. (2021a). Pericyte control of blood flow across microvascular zones in the central nervous system. *Annu. Rev. Physiol.* doi: 10.1146/annurev-physiol-061121-040127 Avilable online at: https://www.annualreviews.org/doi/abs/10.1146/annurev-physiol-061121-040127.

Hartmann, D. A., Berthiaume, A.-A., Grant, R. I., Harrill, S. A., Koski, T., Tieu, T., et al. (2021b). Brain capillary pericytes exert a substantial but slow influence on blood flow. *Nat. Neurosci.* 24, 633–645. doi: 10.1038/s41593-020-00793-2

Hartmann, D. A., Underly, R. G., Grant, R. I., Watson, A. N., Lindner, V., and Shih, A. Y. (2015). Pericyte structure and distribution in the cerebral cortex revealed by high-resolution imaging of transgenic mice. *Neurophotonics* 2:041402. doi: 10.1117/1.NPh.2.4.041402

Hawkins, B. T., and Davis, T. P. (2005). The blood-brain barrier/neurovascular unit in health and disease. *Pharmacol. Rev.* 57, 173–185. doi: 10.1124/pr.57.2.4

He, C., Medley, S. C., Hu, T., Hinsdale, M. E., Lupu, F., Virmani, R., et al. (2015). PDGFRβ signalling regulates local inflammation and synergizes with hypercholesterolaemia to promote atherosclerosis. *Nat. Commun.* 6:7770. doi: 10.1038/ncomms8770

He, Y., Wang, M., Chen, X., Pohmann, R., Polimeni, J. R., Scheffler, K., et al. (2018). Ultra-slow single-vessel BOLD and CBV-based fMRI spatiotemporal dynamics and their correlation with neuronal intracellular calcium signals. *Neuron* 97, 925–939.e5. doi: 10.1016/j.neuron.2018.01.025

Hill, R. A., Tong, L., Yuan, P., Murikinati, S., Gupta, S., and Grutzendler, J. (2015). Regional blood flow in the normal and ischemic brain is controlled by arteriolar smooth muscle cell contractility and not by capillary pericytes. *Neuron* 87, 95–110. doi: 10.1016/j.neuron.2015.06.001

Hochmeister, S., Grundtner, R., Bauer, J., Engelhardt, B., Lyck, R., Gordon, G., et al. (2006). Dysferlin is a new marker for leaky brain blood vessels in multiple sclerosis. *J. Neuropathol. Exp. Neurol.* 65, 855–865. doi: 10.1097/01.jnen.0000235119.52311.16

Iadecola, C. (2017). The neurovascular unit coming of age: a journey through neurovascular coupling in health and disease. *Neuron* 96, 17–42. doi: 10.1016/j.neuron.2017.07.030

Jones, T. W. (1853). Discovery that the veins of the bat's wing (Which Are Furnished with Valves) are endowed with rhythmical contractility, and that the

onward flow of blood is accelerated by such contraction. *Edinb. Med. Surg. J.* 79, 367–373.

Joyce, N. C., Haire, M. F., and Palade, G. E. (1985). Contractile proteins in pericytes. I. Immunoperoxidase localization of tropomyosin. *J. Cell Biol.* 100, 1379–1386. doi: 10.1083/jcb.100.5.1379

Kisler, K., Nelson, A. R., Rege, S. V., Ramanathan, A., Wang, Y., Ahuja, A., et al. (2017). Pericyte degeneration leads to neurovascular uncoupling and limits oxygen supply to brain. *Nat. Neurosci.* 20, 406–416. doi: 10.1038/nn.4489

Kovacs-Oller, T., Ivanova, E., Bianchimano, P., and Sagdullaev, B. T. (2020). The pericyte connectome: spatial precision of neurovascular coupling is driven by selective connectivity maps of pericytes and endothelial cells and is disrupted in diabetes. *Cell Discov.* 6:39. doi: 10.1038/s41421-020-0180-0

Kumar, A., D'Souza, S. S., Moskvin, O. V., Toh, H., Wang, B., Zhang, J., et al. (2017). Specification and diversification of pericytes and smooth muscle cells from mesenchymoangioblasts. *Cell Rep.* 19, 1902–1916. doi: 10.1016/j.celrep.2017.05.019

Li, B., Esipova, T. V., Sencan, I., Kılıç, K., Fu, B., Desjardins, M., et al. (2019). More homogeneous capillary flow and oxygenation in deeper cortical layers correlate with increased oxygen extraction. *elife* 8:e42299. doi: 10.7554/eLife.42299

Liu, X., Li, C., Falck, J. R., Roman, R. J., Harder, D. R., and Koehler, R. C. (2008). Interaction of nitric oxide, 20-HETE, and EETs during functional hyperemia in whisker barrel cortex. *Am. J. Physiol. Heart Circ. Physiol.* 295, H619–H631. doi: 10.1152/ajpheart.01211.2007

Longden, T. A., Dabertrand, F., Koide, M., Gonzales, A. L., Tykocki, N. R., Brayden, J. E., et al. (2017). Capillary K^+-sensing initiates retrograde hyperpolarization to increase local cerebral blood flow. *Nat. Neurosci.* 20, 717–726. doi: 10.1038/nn.4533

Longden, T. A., Hill-Eubanks, D. C., and Nelson, M. T. (2016). Ion channel networks in the control of cerebral blood flow. *J. Cereb. Blood Flow Metab.* 36, 492–512. doi: 10.1177/0271678X15616138

Longden, T. A., and Nelson, M. T. (2015). Vascular inward rectifier K^+ channels as external K^+ sensors in the control of cerebral blood flow. *Microcirculation* 22, 183–196. doi: 10.1111/micc.12190

Lyons, D. G., Parpaleix, A., Roche, M., and Charpak, S. (2016). Mapping oxygen concentration in the awake mouse brain. *elife* 5:e12024. doi: 10.7554/eLife.12024

Mateo, C., Knutsen, P. M., Tsai, P. S., Shih, A. Y., and Kleinfeld, D. (2017). Entrainment of arteriole vasomotor fluctuations by neural activity is a basis of blood-oxygenation-level-dependent "Resting-State" connectivity. *Neuron* 96, 936–948.e3. doi: 10.1016/j.neuron.2017.10.012

Mayhew, J. E., Askew, S., Zheng, Y., Porrill, J., Westby, G. W., Redgrave, P., et al. (1996). Cerebral vasomotion: a 0.1-Hz oscillation in reflected light imaging of neural activity. *Neuroimage* 4, 183–193. doi: 10.1006/nimg.1996.0069

Mishra, A., O'Farrell, F. M., Reynell, C., Hamilton, N. B., Hall, C. N., and Attwell, D. (2014). Imaging pericytes and capillary diameter in brain slices and isolated retinae. *Nat. Protoc.* 9, 323–336. doi: 10.1038/nprot.2014.019

Mishra, A., Reynolds, J. P., Chen, Y., Gourine, A. V., Rusakov, D. A., and Attwell, D. (2016). Astrocytes mediate neurovascular signaling to capillary pericytes but not to arterioles. *Nat. Neurosci.* 19, 1619–1627. doi: 10.1038/nn.4428

Nehls, V., and Drenckhahn, D. (1991). Heterogeneity of microvascular pericytes for smooth muscle type alpha-actin. *J. Cell Biol.* 113, 147–154. doi: 10.1083/jcb.113.1.147

Nikolakopoulou, A. M., Zhao, Z., Montagne, A., and Zlokovic, B. V. (2017). Regional early and progressive loss of brain pericytes but not vascular smooth muscle cells in adult mice with disrupted platelet-derived growth factor receptor-β signaling. *PLoS One* 12:e0176225. doi: 10.1371/journal.pone.0176225

Nortley, R., Korte, N., Izquierdo, P., Hirunpattarasilp, C., Mishra, A., Jaunmuktane, Z., et al. (2019). Amyloid β oligomers constrict human capillaries in Alzheimer's disease *via* signaling to pericytes. *Science* 365:eaav9518. doi: 10.1126/science.aav9518

Pachitariu, M., Stringer, C., Schröder, S., Dipoppa, M., Rossi, L. F., Carandini, M., et al. (2016). Suite2p: beyond 10,000 neurons with standard two-photon microscopy. *bioRxiv* [Preprint]. doi: 10.1101/061507

Peters, B. P., and Goldstein, I. J. (1979). The use of fluorescein-conjugated *Bandeiraea simplicifolia* B4-isolectin as a histochemical reagent for the detection of alpha-D-galactopyranosyl groups: their occurrence in basement membranes. *Exp. Cell Res.* 120, 321–334. doi: 10.1016/0014-4827(79)90392-6

Pober, J. S., and Sessa, W. C. (2014). Inflammation and the blood microvascular system. *Cold Spring Harb. Perspect. Biol.* 7:a016345. doi: 10.1101/cshperspect.a016345

Proebstl, D., Voisin, M.-B., Woodfin, A., Whiteford, J., D'Acquisto, F., Jones, G. E., et al. (2012). Pericytes support neutrophil subendothelial cell crawling and breaching of venular walls *in vivo*. *J. Exp. Med.* 209, 1219–1234. doi: 10.1084/jem.20111622

Rosehart, A. C., Longden, T. A., Weir, N., Fontaine, J. T., Joutel, A., and Dabertrand, F. (2021). Prostaglandin E2 dilates intracerebral arterioles when applied to capillaries: implications for small vessel diseases. *Front. Aging Neurosci.* 13:695965. doi: 10.3389/fnagi.2021.695965

Rous, P., and Smith, F. (1931). The gradient of vascular permeability?: III. The gradient along the capillaries and venules of frog skin. *J. Exp. Med.* 53, 219–242. doi: 10.1084/jem.53.2.219

Rundek, T., and Della-Morte, D. (2015). The role of shear stress and arteriogenesis in maintaining vascular homeostasis and preventing cerebral atherosclerosis. *Brain Circ.* 1, 53–62. doi: 10.4103/2394-8108.164993

Rungta, R. L., Chaigneau, E., Osmanski, B.-F., and Charpak, S. (2018). Vascular compartmentalization of functional hyperemia from the synapse to the pia. *Neuron* 99, 362–375.e4. doi: 10.1016/j.neuron.2018.06.012

Rungta, R. L., Zuend, M., Aydin, A.-K., Martineau, É, Boido, D., Weber, B., et al. (2021). Diversity of neurovascular coupling dynamics along vascular arbors in layer II/III somatosensory cortex. *Commun. Biol.* 4:855. doi: 10.1038/s42003-021-02382-w

Rustenhoven, J., Jansson, D., Smyth, L. C., and Dragunow, M. (2017). Brain pericytes as mediators of neuroinflammation. *Trends Pharmacol. Sci.* 38, 291–304. doi: 10.1016/j.tips.2016.12.001

Ryu, J. K., Petersen, M. A., Murray, S. G., Baeten, K. M., Meyer-Franke, A., Chan, J. P., et al. (2015). Blood coagulation protein fibrinogen promotes autoimmunity and demyelination *via* chemokine release and antigen presentation. *Nat. Commun.* 6:8164. doi: 10.1038/ncomms9164

Sagare, A. P., Sweeney, M. D., Makshanoff, J., and Zlokovic, B. V. (2015). Shedding of soluble platelet-derived growth factor receptor-β from human brain pericytes. *Neurosci. Lett.* 607, 97–101. doi: 10.1016/j.neulet.2015.09.025

Sakadžić, S., Mandeville, E. T., Gagnon, L., Musacchia, J. J., Yaseen, M. A., Yucel, M. A., et al. (2014). Large arteriolar component of oxygen delivery implies a safe margin of oxygen supply to cerebral tissue. *Nat. Commun.* 5:5734. doi: 10.1038/ncomms6734

Schmid, F., Tsai, P. S., Kleinfeld, D., Jenny, P., and Weber, B. (2017). Depth-dependent flow and pressure characteristics in cortical microvascular networks. *PLoS Comput. Biol.* 13:e1005392. doi: 10.1371/journal.pcbi.1005392

Shaw, K., Bell, L., Boyd, K., Grijseels, D. M., Clarke, D., Bonnar, O., et al. (2021). Neurovascular coupling and oxygenation are decreased in hippocampus compared to neocortex because of microvascular differences. *Nat. Commun.* 12:3190. doi: 10.1038/s41467-021-23508-y

Shen, Z., Lu, Z., Chhatbar, P. Y., O'Herron, P., and Kara, P. (2012). An artery-specific fluorescent dye for studying neurovascular coupling. *Nat. Methods* 9, 273–276. doi: 10.1038/nmeth.1857

Shiba, M., Suzuki, H., Fujimoto, M., Shimojo, N., Imanaka-Yoshida, K., Yoshida, T., et al. (2012). Imatinib mesylate prevents cerebral vasospasm after subarachnoid hemorrhage *via* inhibiting tenascin-C expression in rats. *Neurobiol. Dis.* 46, 172–179. doi: 10.1016/j.nbd.2012.01.005

Shinaoka, A., Momota, R., Shiratsuchi, E., Kosaka, M., Kumagishi, K., Nakahara, R., et al. (2013). Architecture of the subendothelial elastic fibers of small blood vessels and variations in vascular type and size. *Microsc. Microanal.* 19, 406–414. doi: 10.1017/S1431927612014341

Stallcup, W. B. (2018). The NG2 proteoglycan in pericyte biology. *Adv. Exp. Med. Biol.* 1109, 5–19. doi: 10.1007/978-3-030-02601-1_2

Stark, K., Eckart, A., Haidari, S., Tirniceriu, A., Lorenz, M., von Brühl, M.-L., et al. (2013). Capillary and arteriolar pericytes attract innate leukocytes exiting through venules and "instruct" them with pattern-recognition and motility programs. *Nat. Immunol.* 14, 41–51. doi: 10.1038/ni.2477

Sun, C. W., Falck, J. R., Okamoto, H., Harder, D. R., and Roman, R. J. (2000). Role of cGMP versus 20-HETE in the vasodilator response to nitric oxide in rat cerebral arteries. *Am. J. Physiol. Heart Circ. Physiol.* 279, H339–H350. doi: 10.1152/ajpheart.2000.279.1.H339

Suzuki, S., Namiki, J., Shibata, S., Mastuzaki, Y., and Okano, H. (2010). The neural stem/progenitor cell marker nestin is expressed in proliferative endothelial cells, but not in mature vasculature. *J. Histochem. Cytochem.* 58, 721–730. doi: 10.1369/jhc.2010.955609

Sweeney, M. D., Sagare, A. P., and Zlokovic, B. V. (2018). Blood-brain barrier breakdown in Alzheimer disease and other neurodegenerative disorders. *Nat. Rev. Neurol.* 14, 133–150. doi: 10.1038/nrneurol.2017.188

Thakore, P., Alvarado, M. G., Ali, S., Mughal, A., Pires, P. W., Yamasaki, E., et al. (2021). Brain endothelial cell TRPA1 channels initiate neurovascular coupling. *elife* 10:e63040. doi: 10.7554/eLife.63040

Thorn, C. E., Kyte, H., Slaff, D. W., and Shore, A. C. (2011). An association between vasomotion and oxygen extraction. *Am. J. Physiol. Heart Circ. Physiol.* 301, H442–H449. doi: 10.1152/ajpheart.01316.2010

Tian, P., Teng, I. C., May, L. D., Kurz, R., Lu, K., Scadeng, M., et al. (2010). Cortical depth-specific microvascular dilation underlies laminar differences in blood oxygenation level-dependent functional MRI signal. *Proc. Natl. Acad. Sci. U.S.A.* 107, 15246–15251. doi: 10.1073/pnas.1006735107

Toth, P., Tarantini, S., Davila, A., Valcarcel-Ares, M. N., Tucsek, Z., Varamini, B., et al. (2015). Purinergic glio-endothelial coupling during neuronal activity: role of P2Y1 receptors and eNOS in functional hyperemia in the mouse somatosensory cortex. *Am. J. Physiol. Heart Circ. Physiol.* 309, H1837–45. doi: 10.1152/ajpheart.00463.2015

Tsai, A. G., and Intaglietta, M. (1989). Local tissue oxygenation during constant red blood cell flux: a discrete source analysis of velocity and hematocrit changes. *Microvasc. Res.* 37, 308–322. doi: 10.1016/0026-2862(89)90049-6

van Veluw, S. J., Hou, S. S., Calvo-Rodriguez, M., Arbel-Ornath, M., Snyder, A. C., Frosch, M. P., et al. (2020). Vasomotion as a driving force for paravascular clearance in the awake mouse brain. *Neuron* 105, 549–561e5. doi: 10.1016/j.neuron.2019.10.033

Vanlandewijck, M., He, L., Mäe, M. A., Andrae, J., Ando, K., Del Gaudio, F., et al. (2018). A molecular atlas of cell types and zonation in the brain vasculature. *Nature* 554, 475–480. doi: 10.1038/nature25739

Vlasenko, O. V., Dovgan', A. V., Maisky, V. A., Maznychenko, A. V., and Pilyavskii, A. I. (2007). NADPH-diaphorase reactivity and neurovascular coupling in the basal forebrain and motor cortex. *Neurophysiology* 39, 355–357. doi: 10.1007/s11062-007-0056-z

Wan, W., Ding, Y., Xie, Z., Li, Q., Yan, F., Budbazar, E., et al. (2019). PDGFR-β modulates vascular smooth muscle cell phenotype *via* IRF-9/SIRT-1/NF-κB pathway in subarachnoid hemorrhage rats. *J. Cereb. Blood Flow Metab.* 39, 1369–1380. doi: 10.1177/0271678X18760954

Wang, S., Cao, C., Chen, Z., Bankaitis, V., Tzima, E., Sheibani, N., et al. (2012). Pericytes regulate vascular basement membrane remodeling and govern neutrophil extravasation during inflammation. *PLoS One* 7:e45499. doi: 10.1371/journal.pone.0045499

Wei, L., Erinjeri, J. P., Rovainen, C. M., and Woolsey, T. A. (2001). Collateral growth and angiogenesis around cortical stroke. *Stroke* 32, 2179–2184. doi: 10.1161/hs0901.094282

Winkler, E. A., Bell, R. D., and Zlokovic, B. V. (2010). Pericyte-specific expression of PDGF beta receptor in mouse models with normal and deficient PDGF beta receptor signaling. *Mol. Neurodegener.* 5:32. doi: 10.1186/1750-1326-5-32

Yemisci, M., Gursoy-Ozdemir, Y., Vural, A., Can, A., Topalkara, K., and Dalkara, T. (2009). Pericyte contraction induced by oxidative-nitrative stress impairs capillary reflow despite successful opening of an occluded cerebral artery. *Nat. Med.* 15, 1031–1037. doi: 10.1038/nm.2022

Yuan, S. Y., and Rigor, R. R. (2010). *Regulation of Endothelial Barrier Function*. San Rafael, CA: Morgan & Claypool Life Sciences.

Zambach, S. A., Cai, C., Helms, H. C. C., Hald, B. O., Dong, Y., Fordsmann, J. C., et al. (2021). Precapillary sphincters and pericytes at first-order capillaries as key regulators for brain capillary perfusion. *Proc. Natl. Acad. Sci. U.S.A.* 118:e2023749118. doi: 10.1073/pnas.2023749118

Zeisel, A., Hochgerner, H., Lönnerberg, P., Johnsson, A., Memic, F., van der Zwan, J., et al. (2018). Molecular architecture of the mouse nervous system. *Cell* 174, 999–1014.e22. doi: 10.1016/j.cell.2018.06.021

Zhang, T., Wu, D. M., Xu, G.-Z., and Puro, D. G. (2011). The electrotonic architecture of the retinal microvasculature: modulation by angiotensin II. *J. Physiol.* 589, 2383–2399. doi: 10.1113/jphysiol.2010.202937

Zhang, W., Davis, C. M., Zeppenfeld, D. M., Golgotiu, K., Wang, M. X., Haveliwala, M., et al. (2021). Role of endothelium-pericyte signaling in capillary blood flow response to neuronal activity. *J. Cereb. Blood Flow Metab.* 41, 1873–1885. doi: 10.1177/0271678X211007957

Zhu, X., Bergles, D. E., and Nishiyama, A. (2008). NG2 cells generate both oligodendrocytes and gray matter astrocytes. *Development* 135, 145–157. doi: 10.1242/dev.004895

Zimmermann, K. W. (1923). *Der Feinere bau der Blutcapillaren*. Berlin: Springer. doi: 10.1007/978-3-642-92456-9

Conflict of Interest: The authors declare that the research was conducted in the absence of any commercial or financial relationships that could be construed as a potential conflict of interest.

Publisher's Note: All claims expressed in this article are solely those of the authors and do not necessarily represent those of their affiliated organizations, or those of the publisher, the editors and the reviewers. Any product that may be evaluated in this article, or claim that may be made by its manufacturer, is not guaranteed or endorsed by the publisher.

Advantages of publishing in Frontiers

OPEN ACCESS
Articles are free to read for greatest visibility and readership

FAST PUBLICATION
Around 90 days from submission to decision

HIGH QUALITY PEER-REVIEW
Rigorous, collaborative, and constructive peer-review

TRANSPARENT PEER-REVIEW
Editors and reviewers acknowledged by name on published articles

Frontiers
Avenue du Tribunal-Fédéral 34
1005 Lausanne | Switzerland

Visit us: www.frontiersin.org
Contact us: frontiersin.org/about/contact

REPRODUCIBILITY OF RESEARCH
Support open data and methods to enhance research reproducibility

DIGITAL PUBLISHING
Articles designed for optimal readership across devices

FOLLOW US
@frontiersin

IMPACT METRICS
Advanced article metrics track visibility across digital media

EXTENSIVE PROMOTION
Marketing and promotion of impactful research

LOOP RESEARCH NETWORK
Our network increases your article's readership